THE STRUCTURE AND ORIGIN OF CAMBRO-ORDOVICIAN THROMBOLITES WESTERN NEWFOUNDLAND

JOHN MICHAEL KENNARD, B.Sc.

VOL. 1

NOTICE

The quality of this microform is heavily dependent upon the quality of the original thesis submitted for microfilming. Every effort has been made to ensure the highest quality of reproduction possible.

If pages are missing, contact the university which granted the degree.

Some pages may have indistinct print especially if the original pages were typed with a poor typewriter ribbon or if the university sent us an inferior photocopy.

Reproduction in full or in part of this microform is governed by the Canadian Copyright Act, R.S.C. 1970, c. C-30, and subsequent amendments.

AVIS

La qualité de cette microforme dépend grandement de la qualité de la thèse soumise au microfilmage. Nous avons tout fait pour assurer une qualité supérieure de reproduction.

S'il manque des pages, veuillez communiquer avec l'université qui a conféré le grade.

La qualité d'impression de certaines pages peut laisser à désirer, surtout si les pages originales ont été dactylographiées à l'aide d'un ruban usé ou si l'université nous a fait parvenir une photocopie de qualité inférieure.

La reproduction, même partielle, de cette microforme est soumise à la Loi canadienne sur le droit d'auteur, SRC 1970, c. C-30, et ses amendements subséquents.

THE STRUCTURE AND ORIGIN OF CAMBRO-ORDOVICIAN THROMBOLITES WESTERN NEWFOUNDLAND

by

© John Michael Kennard, B.Sc.

A thesis submitted to the school of Graduate Studies
in partial fulfillment of the requirements for the
degree of Doctor of Philosophy

Department of Earth Sciences
Memorial University of Newfoundland

March 1989

St. John's Newfoundland

ISBN 0-315-59249-4

ABSTRACT

An integrated scheme to systematically analyse the structure and interpret the origin of thrombolites is proposed on the basis of detailed field and petrographic analysis of Cambro-Ordovician thrombolites in western Newfoundland. This scheme utilizes a three-tiered analysis of microbial buildups: 1) megastructure, the overall bed form, 2) mesostructure, the internal fabric, and 3) microstructure, the microscopic fabric. This scheme has proved equally applicable to Cambro-Ordovician thrombolites, stromatolites, *Epiphyton-Renalcis-Girvanella* "microfossil" boundstones, and mixed microbial-metazoan buildups in western Newfoundland, elsewhere in North America and central Australia, and highlights differences between these types of buildups.

Megastructure records the growth relationship between a buildup and its enclosing strata, is independent of meso-structure and microstructure, and reflects the sum of environmental factors acting on the buildup. Mesostructure records the spatial relationship between framework and inter-framework components, is governed by the shape and lateral continuity of the formative microbial community, and reflects a balance between biological and environmental factors. Microstructure is directly controlled by biological factors, and commonly yields clear evidence of specific sediment-forming processes (biologically influenced calcification,

trapping and binding of detritus), and the gross morphologic composition (coccoid or filamentous) of the formative microbial community.

Microstructural analysis indicates that Cambro-Ordovician thrombolites were most commonly constructed by relatively complex coccoid or coccoid-dominated microbial communities, and that the dominant process involved in their formation was *in situ* calcification of the microbial community. This calcified community formed a rigid framework between which autochthonous and allochthonous sediment accumulated. In contrast, co-occurring stromatolites were most commonly constructed by internally well differentiated filamentous or filament-dominated communities, and the dominant process involved in their formation was mechanical trapping and binding of detritus, either alone or in combination with *in situ* calcification of the microbial community. Thrombolites are commonly associated with a diverse and abundant metazoan fauna, whereas metazoans are rarely associated with stromatolites.

Zoned microbial buildups result from ecologic successions of microbial communities, and provide diagnostic evidence of shoaling versus deepening sedimentation; thrombolite or "microfossil" boundstone passing up into stromatolite indicates shoaling (regressive) conditions, and the reverse zonation indicates deepening (transgressive) conditions.

A broad zonation of microbial buildups is evident across Cambro-Ordovician platforms: stromatolites within

intracratonic and inner-platform peritidal environments, thrombolites within intracratonic and platform-interior subtidal environments, and calcified "microfossil" boundstones which are largely restricted to platform margins.

Critical evaluation of the temporal and spatial distribution of thrombolites indicates that they are essentially an Early Cambrian to Early Ordovician "Sauk Sequence" phenomenon, and were restricted to warm sub-equatorial climates. Their appearance can be attributed to the initial calcification of cyanobacteria at the onset of a world-wide marine transgression in latest Proterozoic-earliest Cambrian time, an event that was probably triggered by environmental rather than evolutionary changes. Their abrupt decline in Early Ordovician time, and continued limited occurrence today, probably resulted from niche competition by newly evolved skeletal metazoans, calcareous algae and non-calcareous algae, and increased predation by molluscs.

ACKNOWLEDGEMENTS

This study was funded by a Natural Sciences and Engineering Research Council Grant to Professor N.P. James, and supported by an Australian Commonwealth Postgraduate Overseas Study Award from my employer, the Bureau of Mineral Resources, Geology and Geophysics, Australia. This support is gratefully acknowledged.

I am indebted to my supervisor Noel P. James for providing the opportunity to study the thrombolites in western Newfoundland, and his advice and enthusiasm during the course of this study. Noel's knowledge and generous support have greatly broadened my horizons and interest in carbonate sedimentology.

I wish to thank N. Chow for sharing her knowledge of the Cambrian carbonates on the Port au Port Peninsula in western Newfoundland, and I. Knight, J.D. Aitken, M.N. Rees, A.J. Rowell, J.F. Read, and S.M. Rowland for their assistance to examine other North American thrombolite localities. J.P. Grotzinger kindly enabled me to examine samples of clotted microbialites from the Rocknest Formation, N.W.T., Canada.

I thank M.R. Walter for providing advice and stimulating discussions throughout the study, and for introducing me to the fascinating world of stromatolites and thrombolites.

All aspects of this study benefited from generous support from the Australian Bureau of Mineral Resources, Geology and Geophysics, Australia. I thank P.J. Cook for making this support available, J. Kovacs, M.R. Moffat and J. Mifsud for draughting figures, and C. Zwarko for photographic reproduction of plates.

I greatly appreciate the support and sacrifices made by my wife Margaret during this study, and by my children Alice, Julian and Robin who were born in the midst of this study.

TABLE OF CONTENTS

VOLUME 1 TEXT page

VOLUME 2 PLATES AND APPENDICES page

LIST OF FIGURES

LIST OF TABLES

LIST OF PLATES (VOLUME 2)

CHAPTER 1

INTRODUCTION

1.1 PROLOGUE

Ancient carbonate reefs and organic buildups are important sources of palaeontological, palaeoecological and sedimentological information, and are of considerable economic importance because they contain a disproportionately large amount of oil and gas reserves compared to other types of sedimentary deposits. Prior to Cambrian time, stromatolites (laminated organosedimentary deposits constructed by benthic microbial communities) were the only form of organic buildup. Stromatolites declined both in abundance and diversity in late Proterozoic time (Awramik, 1971; Walter and Heys, 1985), and the first metazoan buildups, constructed by archaeocyaths and calcified microorganisms (*Epiphyton, Renalcis,* and *Girvanella*), appeared in Early Cambrian time. A new type of microbial buildup, **thrombolites** (Aitken, 1967), also appeared in Early Cambrian time.

Definition

Thrombolites are nonlaminated, macroscopically clotted, organosedimentary deposits constructed by benthic microbial communities.

Following the abrupt decline of archaeocyaths at the close of Early Cambrian time (James and Debrenne, 1980; Debrenne

and others, 1984), thrombolites proliferated in subtidal environments until Early Ordovician time. Skeletal metazoan buildups re-appeared in Early to Middle Ordovician time, and throughout the remainder of Phanerozoic time, as well as in marine carbonate environments today, thrombolites and stromatolites are generally subordinate to buildups constructed by metazoans and calcareous algae.

Despite the widespread recognition of thrombolites in Cambro-Ordovician strata for more than twenty years, detailed studies of these buildups are surprisingly few in number. Furthermore, there has been no systematic analysis of thrombolite buildups in the rock record. This contrasts sharply with the large number of detailed investigations and syntheses of stromatolites and metazoan buildups.

The Cambro-Ordovician platformal strata in western Newfoundland, particularly those on the Port au Port Peninsula, contain one of the best exposed, well preserved and easily accessible sequences of thrombolites in North America. This study is an analysis of their structure and origin.

1.2 OBJECTIVES AND SCOPE OF STUDY

The objectives of this study are threefold:

1. To develop an integrated scheme to systematically analyse the structure and interpret the origin of Cambro-Ordovician thrombolites.
2. To compare the structure and origin of thrombolites

to that of associated stromatolites.

3. To critically evaluate the temporal and spatial distribution of thrombolites in the rock record.

A sedimentological rather than palaeontological approach has been adopted throughout this study. This not only reflects the interests of the author, but also reflects a traditional bias in the Earth Sciences (in the Western world, at least); Phanerozoic stromatolites (including thrombolites) have generally been studied by sedimentologists, and Precambrian stromatolites have largely been studied by palaeontologists. This age-dependent emphasis simply results from the relative biostratigraphic importance of stromatolites in Precambrian versus Phanerozoic strata; whereas stromatolites offer the best potential for biostratigraphic correlation of Precambrian strata (Hofmann, 1987), correlation of Phanerozoic strata is best achieved by metazoan biostratigraphy. Adoption of a sedimentological approach places more emphasis on the processes by which stromatolites\thrombolites were generated, as well as their relationship to metazoan buildups, rather than the biological affinity of the microbes that constructed them, or their biostratigraphic potential.

1.3 PREVIOUS STUDIES

Although thrombolites are now recognized as a characteristic component of Cambro-Ordovician platformal

strata, there are few detailed sedimentological studies of these structures. In introducing the term, Aitken (1967) provided an instructive account of their gross external form and lithological association, but only a short, generalized description of their internal fabric.

Brief sedimentological descriptions of thrombolite fabrics have subsequently been published by Ahr (1971), Chafetz (1973), Rubin and Friedman (1977), Monninger (1979), Schmitt (1979), Radke (1980, 1981), Kennard (1981), Read and Pfeil (1983), Owen and Friedman (1984), Demicco (1985), and Bova and Read (1987). More detailed descriptions appear in several unpublished theses on the Cambro-Ordovician carbonates of North America (Mazzullo, 1974; Lohmann, 1977; Markello, 1979; Pratt, 1979; Demicco, 1981; Bova, 1982; Koerschner, 1983). Only two detailed sedimentological studies of thrombolite fabrics have been published: 1) Monty (1976) discussed the origin of several modern thrombolitic fabrics and microstructures, and 2) Pratt and James (1982) described the external morphology and internal fabric (but not the microstructure) of stromatolites, thrombolites and mixed microbial-metazoan bioherms of Early Ordovician age in the St. George Group, western Newfoundland. This latter publication significantly contributed to the current wide usage of the term thrombolite, and, together with a subsequent study of Phanerozoic mud-mounds (Pratt, 1982a), the recognition of hitherto unrecognized thrombolitic fabrics in post Cambro-Ordovician buildups.

Detailed microstructural studies of Cambro-Ordovician thrombolites have not been undertaken, except by Soviet workers (for example Maslov, 1960) who have adopted a palaeontological rather than sedimentological approach.

Two recent publications on thrombolites warrant special mention: 1) Kennard and James (1986a), in which some preliminary results of this investigation were summarized, and 2) Burne and Moore (1987), in which aspects of these preliminary results were discussed in reference to processes that form modern thrombolitic structures. Burne and Moore's study is discussed in detail in Chapter 2 (Section 2.3) and Chapter 6 (Section 6.3).

1.4 APPROACH AND ORGANIZATION

An initial reconnaissance field survey of Cambro-Ordovician strata in western Newfoundland (Fig. 1-1) confirmed earlier observations by N.P. James, N. Chow, I. Knight and B.R. Pratt (various personal communications, 1983-1985) that the best exposed, least dolomitized, and most easily accessible sequence of thrombolites occurs on the coastal rock platforms on the southern shore of the Port au Port Peninsula. Thrombolite horizons within this sequence had previously been identified in detailed lithologic sections measured by Pratt (1979) and Chow (1986). All known thrombolite horizons were briefly examined at the commencement of this study, and representative thrombolites and thrombolites of special

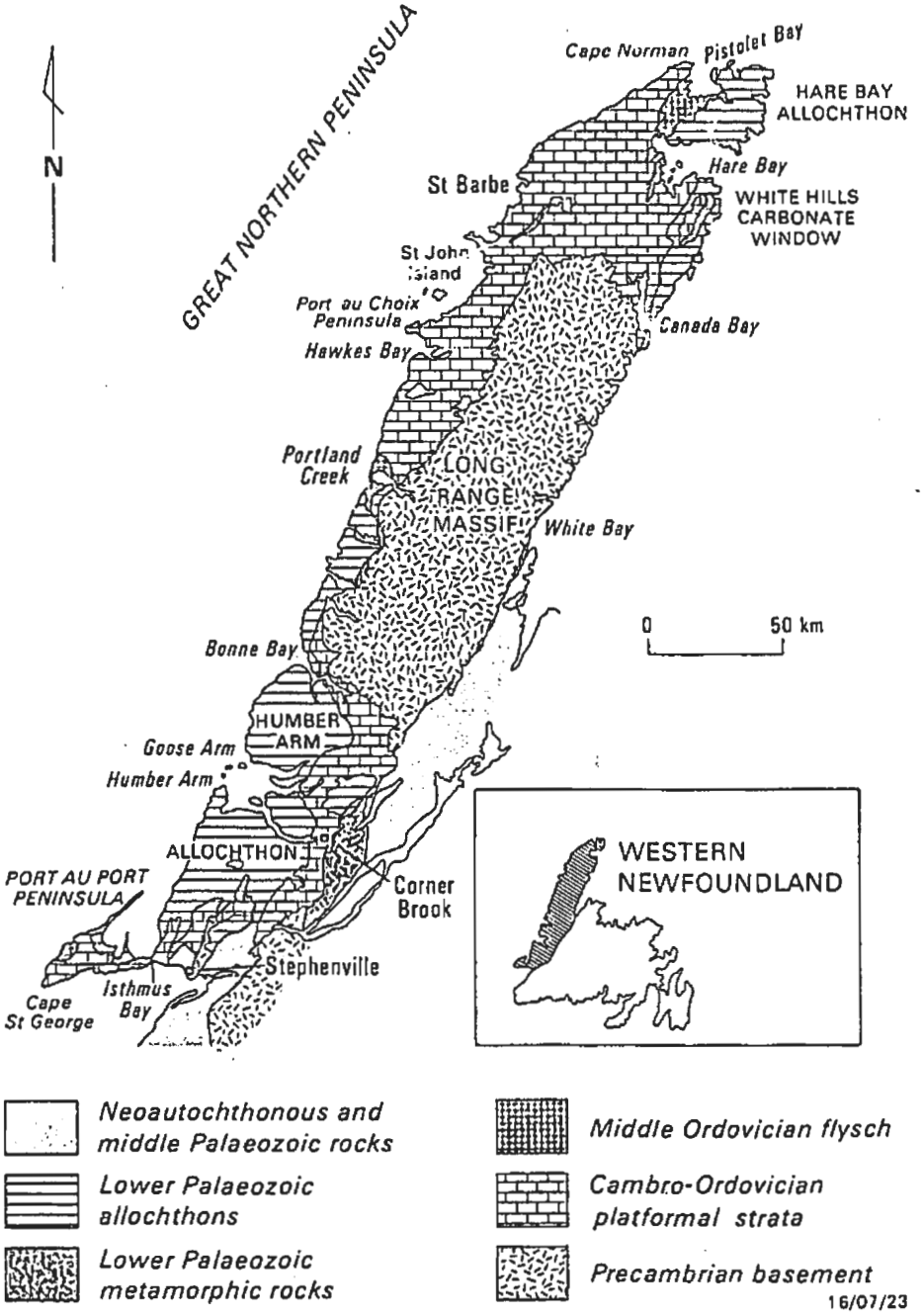

Figure 1-1. Locality and geological map of western Newfoundland (after Knight and James, 1987).

character were subsequently selected for detailed examination.

Initial laboratory examination of these samples confirmed my previous experience (Kennard, 1981) that thrombolites display a complex myriad of unusual, frequently vague, megascopic and microscopic fabrics. It became evident that in order to accurately describe, compare and interpret this somewhat bewildering spectrum of petrographic observations, it was necessary to develop an integrated analytical and classification scheme. This scheme was developed and continuously refined during mesoscopic and microscopic examination of eighty thrombolite\stromatolite lithotypes from the Port au Port Peninsula. This scheme is presented in Chapters 2 and 3, and is utilized in Chapter 4 to document and interpret the origin of eighteen specific thrombolite (and co-occurring stromatolite) horizons on the Port au Port Peninsula.

In order to test the wider applicability of this scheme and these interpretations, Cambro-Ordovician thrombolites identified by other workers in other areas were also analysed (Chapter 5). These regions include the Great Northern Peninsula in western Newfoundland, the Rocky Mountains in Alberta, western Canada, the Appalachian Mountains in Virginia, eastern U.S.A., the Great Basin in Utah and Nevada, western U.S.A., and the Amadeus Basin in central Australia. Data from all areas is synthesized in Chapter 6, and provides the basis for a comparative analysis of the structure and origin of thrombolites and co-occurring stromatolites. The

temporal and spatial distribution of thrombolites in the rock record are examined in Chapter 7.

1.5 METHODS

This investigation integrates field and petrographic studies. Petrographic studies are based on low magnification (1-20 X) examination of slabbed and polished samples (typically 100-500 square centimetres in area, and about one centimetre-thick), and microscopic examination (30-600 X magnification) of large thin sections (75 x 38 mm, or 75 x 50 mm in size). Low to moderate magnification (30-100 X) proved to be routinely more informative than higher magnification (100-600 X) for thin section microscopy and photomicroscopy. A Wild M400 Photomacroscope thus proved to be most suitable for this study. Some acetate peels were also prepared, but were significantly inferior in terms of microstructural detail to thin sections. Standard thin section staining techniques (Alizarin Red-S and Potassium ferricyanide) were also tried, but since these stains generally obscured rather than enhanced microstructural definition, staining was not continued.

1.6 NOMENCLATURE AND GLOSSARY

Aitken (1967) proposed the term **thrombolite** (from the Greek *thrombos*; bloodclot) as a field term for "cryptalgal structures related to stromatolites but lacking lamination

and characterized by a macroscopic clotted fabric". He coined the term **cryptalgal** (from the Greek *kryptos*; hidden, secret) to refer to a group of sedimentary rocks or rock structures (comprising stromatolites, thrombolites, oncolites and cryptalgalaminites) "believed to originate through the sediment-binding and\or carbonate-precipitating activities of nonskeletal algae". In modern usage, however, the term "algae" is restricted to eukaryotic photosynthetic organisms, whereas sediment-forming microbial communities are commonly dominated by photosynthetic prokaryotes, particularly cyanobacteria (formerly called cyanophytes or blue-green algae) and photosynthetic bacteria; eukaryotic algae *senso stricto* (such as diatoms) are generally subordinate (Bauld, 1981a, 1981b, 1984; Krumbein, 1983). Thus, **algae\algal** *sensu* Aitken (1967) is synonymous with **microbe\microbial** which is used as a general term to encompass various types of microorganisms within benthic, sediment-forming communities, regardless of their morphologic or physiologic classification.

Pratt and James (1982) proposed that the term thrombolite be amended to refer to the individual cryptalgal structures (clots, *sensu* Aitken) within thrombolites, rather than the overall rock body or mound composed of cryptalgal clots as proposed by Aitken. This amendment was proposed "to conform with recent customary usage" of the term stromatolite, a term which Pratt and James considered referred to the individual laminated columns within mound structures, not the mound itself. I do not agree that Pratt and James's understanding of the term stromatolite conforms to recent customary usage,

nor does it conform to Kalkowsky's (1908) original definition and usage of the term, a detailed translation and discussion of which is provided by Monty (1977, 1982) and Krumbein (1983). According to Kalkowsky's usage, **stromatoids** are the superimposed layers or laminae within a stromatolite, and **stromatolite** refers to the overall rock body composed of stromatoids and sediment or cement-filled interstices. A parallelism in nomenclature is here proposed for thrombolites; **thromboids** (clots, *sensu* Aitken, 1967; mesoclots, *sensu* Kennard and James, 1986a) are the individual macroscopic clots within a thrombolite, and **thrombolite** refers to the overall rock body composed of thromboids and sediment or cement-filled interstices. I see no merit in Pratt and James's (1982) proposed amendment of the term thrombolite, and urge that Aitken's original usage be retained. The term **microbialite** (Burne and Moore, 1987) refers to all microbial deposits regardless of their internal fabric, including thrombolites and stromatolites.

Carbonate lithologies are herein described according to Dunham's (1962) textural classification (comprising **grainstone, packstone, wackestone, mudstone** and **boundstone**), and all particle and crystal sizes are based on the scale of Wentworth (1922). **Microcrystalline** refers to crystals finer than sand-size (less than 0.0625 mm), **fine-microcrystalline** refers to crystals less than 0.016 mm (16 μm), and **cryptocrystalline** refers to crystals too small to be resolved under a standard petrographic microscope, approximately 0.004 mm (4 μm) and less.

Other terms commonly used in this study are defined in the following glossary. An asterix (*) denotes new terms defined in this study.

Bioherm: A lens or mound-like carbonate buildup derived largely from the *in situ* production or activities of organisms, and which has a width to thickness ratio of less than or equal to thirty (after Cummings, 1932; Nelson and others, 1962).

Biostrome: A stratiform or sheet-like carbonate buildup derived largely from the *in situ* production or activities of organisms, and which has a width to thickness ratio of more than thirty (Nelson and others, 1962).

Calcareous microfossil*: Calcareous metabolised skeleton or metabolized remains of a microorganism (for example calcareous remains of red and green algae, calcareous coccoliths and foraminifera); syn. calcareous skeletal microfossil (see Monty, 1981).

Calcified "microfossil"*: Calcareous remains of a microorganism which is not an obligate calcifier (that is, the calcified remains of a non-skeletal microorganism; for example *Girvanella, Renalcis, Epiphyton*.

Carbonate buildup: A circumscribed body of carbonate rock which formed *in situ*, possessed topographic relief above equivalent, typically thinner, deposits, and differs from surrounding, underlying and overlying rocks (after Heckel, 1974; Wilson, 1975).

Column: A discrete laminated stromatolitic structure elongated in the direction of growth (after Walter, 1976b).

Carbonate Corpuscle*: A discrete carbonate particle or grain of either detrital or *in situ* origin.

Cryptomicrobial fabric*: A vague sediment fabric attributable to the constructional activities of microbes, and which cannot be unequivocally categorized as either a stromatoid or a thromboid (after Kennard and James, 1986a).

Fenestrae: Primary or contemporaneous gaps in a rock framework that are larger than the grain-supported interstices (Tebbutt and others, 1965).

Lobate microstructure*: A microfabric consisting of multiple lobate calcareous bodies attributed to the remains or activities of microorganisms.

Microbialite: An organosedimentary deposit that has accreted as a result of a benthic microbial community trapping and binding detrital sediment and\or forming the locus of mineral precipitation (Burne and Moore, 1987); this term embraces thrombolites, stromatolites, cryptomicrobial mounds and most tufas.

Mucilage, Mucilaginous sheath: Soft and amorphous extracellular gelatinous matter (Golubic, 1976b).

Mudrock: Siliciclastic rock in which greater than 50 percent of the constituent particles are finer than sand size (after Blatt and others, 1972; Lundeguard and Samuels, 1980); distinct from lime mudstone.

Parted limestone: Thinly interbedded limestone and dolostone, or limestone and\or dolostone and shale (Aitken, 1966; Chow, 1986).

Pellet: Subrounded to ellipsoidal, coarse silt to fine sand-sized peloid of probable faecal origin (after Folk, 1959).

Peloid: A microcrystalline or cryptocrystalline allochemical grain of unspecified size or origin (after McKee and Gutschick, 1969; Bathurst, 1975).

Peritidal: Refers to tidal and near tidal sediments or environments.

Reef: A wave-resistant or potentially wave-resistant carbonate buildup stabilized syndepositionally by organic growth and\or submarine cementation (Geldsetzer, 1986).

Ribboned limestone: Synonym of parted limestone (Demicco, 1983).

Synoptic relief: The relief of a structure (bioherm, biostrome, column, thromboid, skeletal organism etc.) above the substrate at the time of its formation or growth (after Hofmann, 1969; Walter, 1976b).

Stromatoid: Superimposed layers or laminae within a stromatolite (after Kalkowsky, 1908; see discussions in Hofmann, 1969, 1973; Monty, 1977; Krumbein, 1983).

Thromboid*: Macroscopic clot within a thrombolite (cf. clot *sensu* Aitken, 1967; mesoclot *sensu* Kennard and James, 1986a).

1.7 SPELLING

British spelling has been utilized in preference to American spelling throughout this study.

CHAPTER 2

SYSTEMATIC ANALYSIS AND INTERPRETATION OF THROMBOLITES

This chapter presents an integrated scheme to systematically analyse the structure and interpret the origin of thrombolites. This scheme is similar to the hierachical procedure used to analyse and classify stromatolites (Hofmann, 1969; Walter, 1972; Preiss, 1976), and to the approach used by sedimentologists and palaeontologists to study modern and ancient reefs. It is considered to be equally applicable to thrombolites of all ages. A brief outline of the scheme was presented by Kennard and James (1986b).

The scheme is based on a three-tiered analysis of the structure of microbial buildups (Fig. 2-1):

1. **Megastructure** - the overall bed form as determined from field exposures. These megascopic features have a scale of tens of metres to a few decimetres.
2. **Mesostructure** - the internal fabric of the thrombolite as determined by detailed inspection of outcrops and polished slabbed specimens. These mesoscopic features have a scale of a few decimetres to a few millimetres.
3. **Microstructure** - the microscopic fabric of the thrombolite as determined by their study in thin sections, peels or scanning electron microscopy.

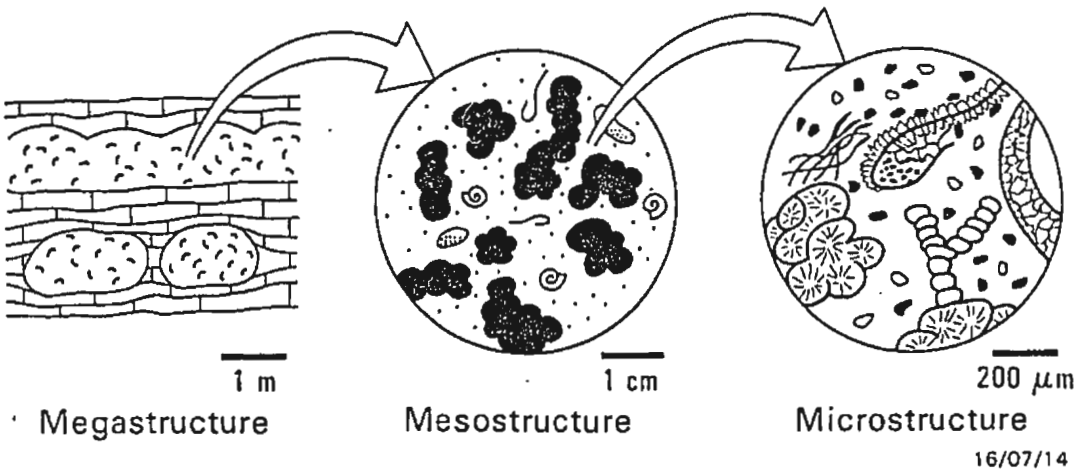

Figure 2-1. Schematic illustration of 3-tiered analysis of microbial buildups.

2.1 MEGASTRUCTURE

Thrombolites display a wide spectrum of bed forms which can be readily classified into various types of bioherms and biostromes in a similar manner to the schemes developed for stromatolites (see Walter, 1972; Preiss, 1976). These stromatolite-based schemes need to be expanded, however, since many thrombolites have a greater thickness to width ratio than stromatolites. Thus pedestal, club and egg-shaped thrombolite bioherms are common. The complete range of thrombolite megastructures is shown in Fig. 2-2.

In describing the megastructure of thrombolites it is important to define the relationship between the thrombolite and the enclosing strata, since such a relationship is commonly the only means available to assess the gross synoptic relief of the structure. Several relationships are recognised (listed in order of implied greater synoptic relief): intertonguing, onlapping, abutting and draping. Subsequent differential compaction, however, commonly modifies or obscures these relationships. In the case of stromatolites, synoptic relief can simply be determined by tracing the profile of individual laminae (Hofmann, 1969).

Within a given horizon, the base or bases of thrombolite(s) generally rest on a single stratigraphic plane, and are commonly established on a foundation layer of pebble conglomerate. The fabric of this conglomerate may be either flat-lying or edgewise, and in some cases the pebbles

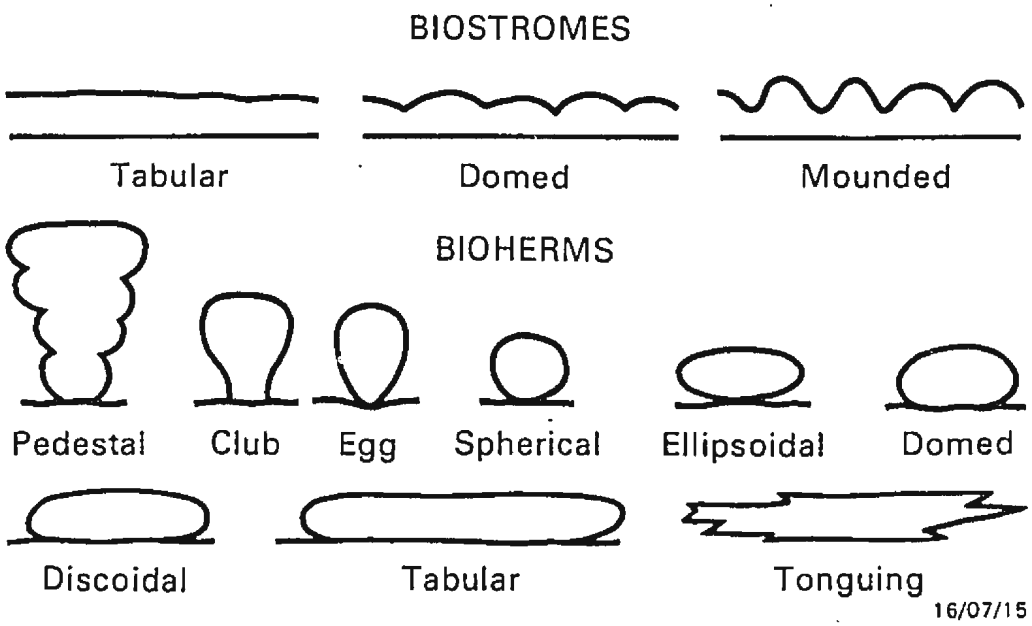

Figure 2-2. Megastructure of thrombolites.

are arranged in a series of fan-like arrays (examples are shown in Plates 27-B, 32-A). These conglomerates are generally interpreted to be subtidal storm lag deposits (Sepkoski, 1982; Grotzinger, 1986b; Whisonant, 1987) or beach rock (Donaldson and Ricketts, 1979), and their minor topographic relief evidently favoured the establishment of thrombolite-forming (or stromatolite-forming) microbial communities. The fan-like pebble arrays are similar to the radiating edgewise pebbles and shells found on some modern wave-cut platforms and beaches (Bluck, 1967; Dionne, 1971; Sanderson and Donovan, 1974), and their distinctive fabric is thought to result from oscillating wave-induced currents.

Horizontal spacing of bioherms tends to be regular within a given horizon, and individual bioherms usually have a common shape and size, and terminate at a common stratigraphic plane. In some instances, however, bioherms and biostromes are superimposed on top of one another, thus forming complex reef-like structures which display an ecologic zonation of microbial, and in some cases metazoan, communities (such examples are described in Chapter 4, Horizons A and L, respectively).

2.2 MESOSTRUCTURE

It is the complex clotted internal fabric of thrombolites that distinguishes them from stromatolites, but this is perhaps the most difficult aspect of thrombolites to

systematically analyse and classify. As with most other carbonate buildups, however, thrombolites are composed of three types of components:

1. **Framework** - those components that form the structural frame of the thrombolite.
2. **Inter-framework** - those components that passively infill the structural frame.
3. **Diagenetic** - those components that overprint or replace framework and inter-framework components.

2.2.1 FRAMEWORK COMPONENTS.

The framework of thrombolites, as well as other microbial buildups, comprises one or more of the following components: 1) thromboids, 2) stromatoids, 3) undifferentiated crypto-microbial fabrics, 4) marine cement, 5) pebble aggregates, and 6) skeletal metazoans and\or calcareous algae.

The relative volumetric proportion of these frame-building components provides the basis for the field classification of microbial buildups presented in Chapter 3.

1 Thromboids

Thromboids are here defined as the individual, non-laminated, mesoscopic clot-like structures (cryptalgal clots *sensu* Aitken, 1967; mesoclots *sensu* Kennard and James, 1986a) that result from the activities of microbial communities. They are the essential frame-building component of all thrombolites. They are typically dark coloured, have a

microcrystalline texture, and range from about 1 mm to several centimetres in size. They display a variety of geometric shapes and arrangements which form the basis for their classification as shown in Figure 2-3. These classes are further subdivided according to the degree of interconnection of the thromboids (isolated, partially interconnected, anastomosing and coalesced). Thromboids are commonly disrupted by metazoan burrows.

2 Stromatoids

Kalkowsky (1908) used the term stromatoid to refer to superimposed carbonate layers or laminae within stromatolites. Superimposed stromatolitic laminae also occur within some thrombolites, and are hence designated stromatoids. By definition, thrombolites comprise a greater volume of thromboids than stromatoids; if stromatoids are volumetrically predominant, then the buildup is classified a stromatolite (see Chapter 3).

Stromatoids occur within thrombolites either as isolated to partially interconnected frame-building structures, or else they encrust, and are in turn encrusted by, thromboids. They are generally centimetre-sized and occur in several geometric arrangements (Fig. 2-4). Their detailed geometric attributes (shape, size, profile, linkage, spacing, relief, and degree of inheritance) are described in an identical manner to the laminae\stromatoids within stromatolites (see Hofmann, 1969; Walter, 1972; Preiss, 1976).

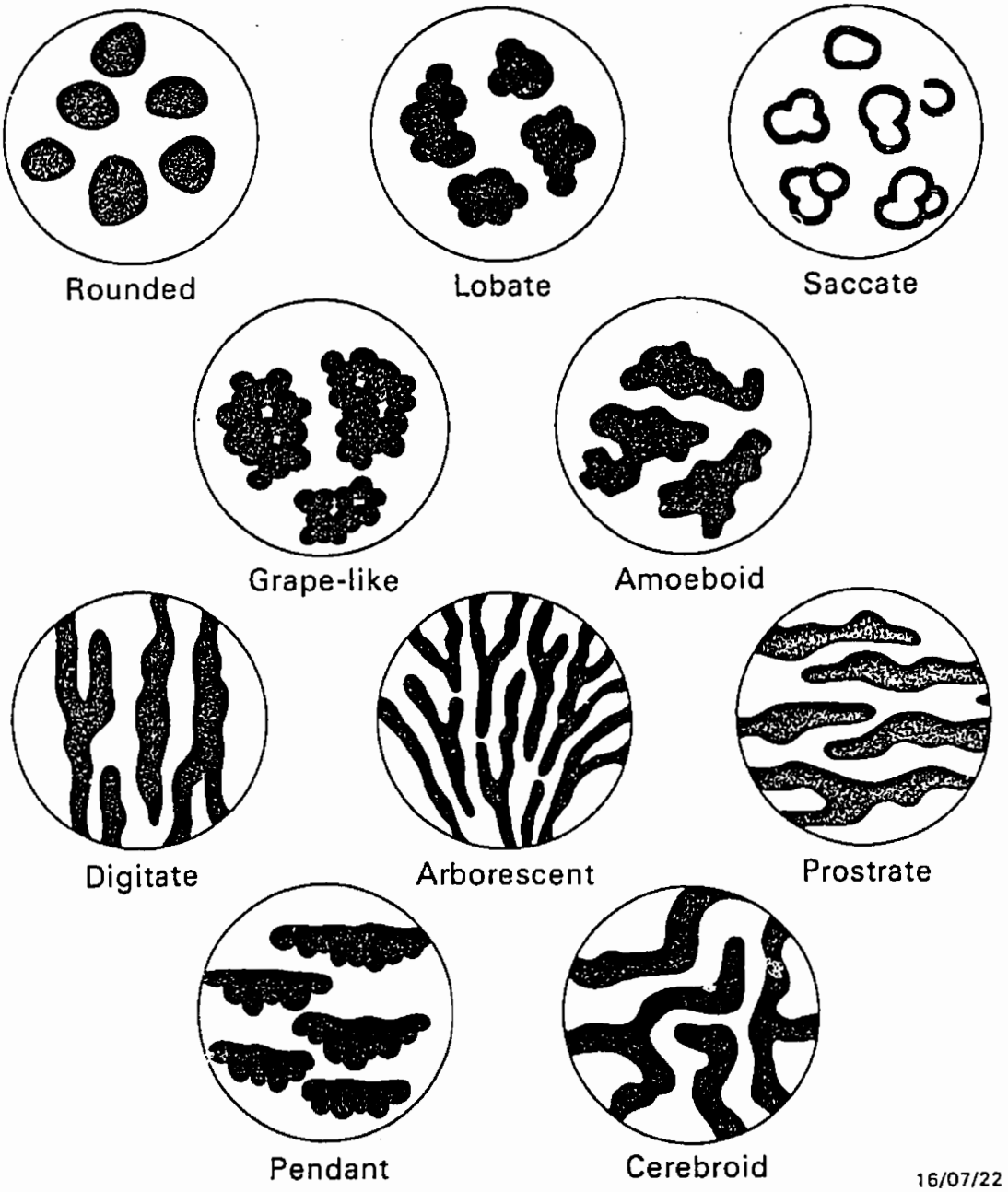

Figure 2-3. Schematic illustration of thromboids.

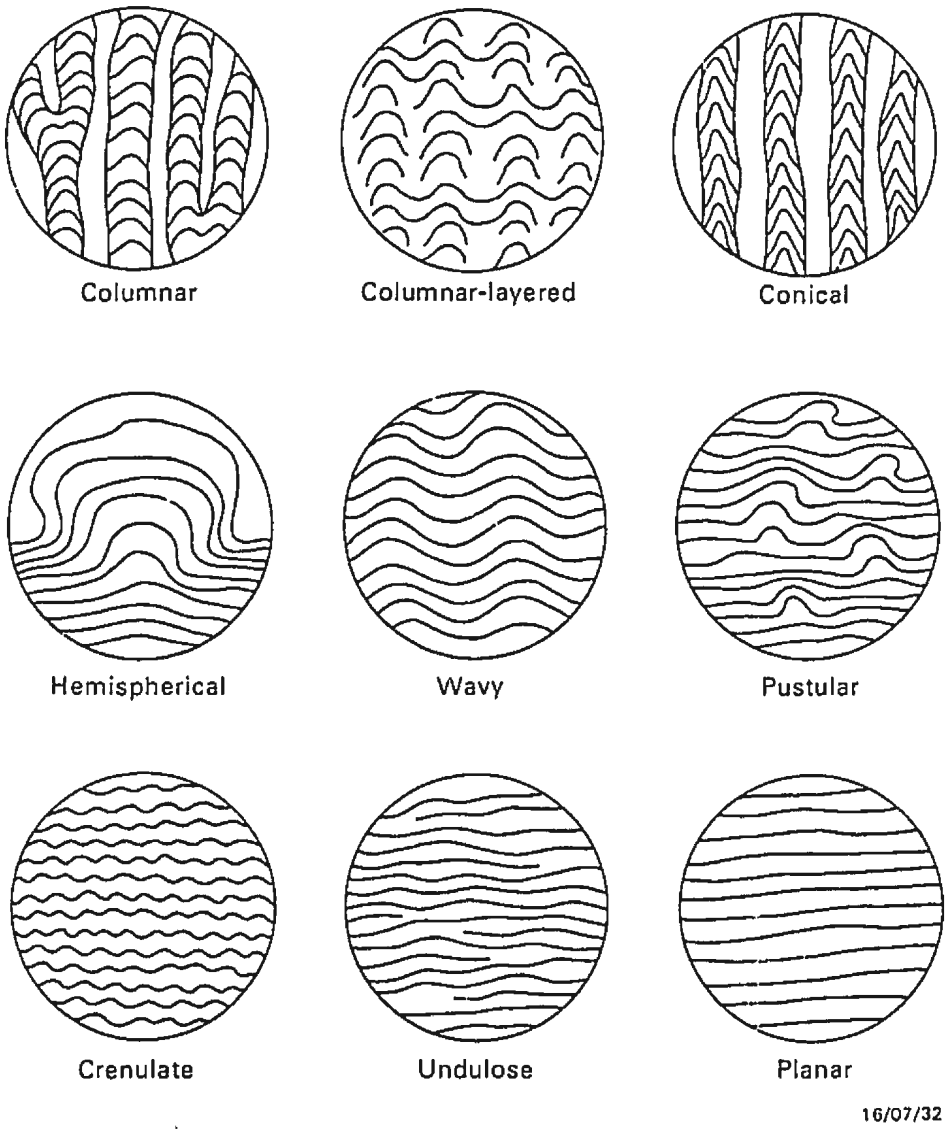

Figure 2-4. Schematic illustration of stromatoids.

3 Undifferentiated Cryptomicrobial Fabrics

Vague microbial fabrics that cannot be strictly categorised as either thromboids or stromatoids are here defined as cryptomicrobial fabrics. This term is a modification of Aitken's (1967) term cryptalgal, and signifies that a microbial (algal, *sensu* Aitken) origin is generally inferred rather than directly observed.

These fabrics typically have a vague mottled or patchy texture which defies objective classification. In some instances, microstructural analysis indicates that such fabrics result from the disruption, modification or replacement of precursor thromboids or stromatoids. Several such processes are possible: oxidation and decay of organic matter, displacive growth of early diagenetic minerals, bioturbation, neomorphism, dissolution, dolomitization, silicification, and stylolitization. If these processes are incipient, then the original character of the fabric (thromboid or stromatoid) can commonly be determined. In many buildups, however, no vestige of the original fabric is evident, and it may not be possible to distinguish framework and inter-framework components. That is, the buildups have a pervasive cryptomicrobial fabric.

4 Marine Cement

Marine cement is locally a minor frame-building component of thrombolites, and in rare instances it is a major or dominant frame-building component. Usually, however, marine

cement passively fills framework voids, in which case it is categorised an inter-framework component (see section 2.2.2).

Frame-building marine cement occurs either as individual and coalesced mammelons of fibrous fan-like habit (designated botryoidal cements by Ginsburg and James, 1976), or thin fibrous crusts, both of which grew naked on the surface of the thrombolite. This cement encrusts, and is commonly encrusted by, thromboids and stromatoids, or is buried by inter-framework detrital sediment. It appears black in hand specimen, and thus is frequently difficult to differentiate from thromboids and, in some cases, stromatoids. In thin section, however, it has a diagnostic amber coloured, turbid appearance due to numerous micro-inclusions. The micro-fabric of this cement is described in section 2.3.14.

This cement is analogous to the fibrous botryoidal marine cements within modern coralgal reefs (Schroeder, 1972; Ginsburg and Schroeder, 1973; Ginsburg and James, 1976), and some middle Palaeozoic reefs (Davies, 1977; Babcock, 1977; Mazzullo and Cys, 1977, 1979; Mazzullo, 1980; Toomey and Babcock, 1983).

5 Pebble Aggregates

As noted in Section 2.1, many thrombolites are established on a foundation layer of pebble conglomerate. These pebbles typically form an integral part of the thrombolite bed, and can be regarded as an initial self-supporting framework which was encrusted by other frame-building components (thromboids, stromatoids or marine cement). Pebbles also commonly occur

lodged between framework components, but in such instances they clearly represent inter-framework, rather than framework, components.

6 Skeletal Metazoans and Calcareous Algae

Some thrombolites contain *in situ*, frame-building, skeletal metazoans or calcareous algae such as corals, sponges, bryozoans, serpulid worms, stromatoporoids, *Pulchrilamina* or *Calathium*. These skeletons form part of the framework of the thrombolite, and they encrust and are themselves encrusted by microbial frame-building components (thromboids, stromatoids or cryptomicrobial fabrics). Two examples of composite microbial-metazoan buildups are described in Chapter 4 (Horizons L and P) and their classification is discussed in Chapter 3.

2.2.2 INTER-FRAMEWORK COMPONENTS

There are two types of inter-framework components in thrombolites: detrital sediment, and void-filling cement.

1 Detrital Sediment

Detrital sediment accumulates between the framework components and typically shows no evidence of microbial binding. These sediments exhibit a wide range of textures (grainstone, packstone, wackestone or mudstone), and are commonly bioturbated. They comprise a diverse range of autochthonous and\or allochthonous material; that is material

generated within the buildup, or material derived elsewhere and washed into the buildup, respectively. Typical autochthonous material includes: irregular peloids and corpuscles eroded from the framework, fragments of calcified filaments, ?faecal pellets, and debris of metazoans that inhabited the buildup (trilobites, gastropods, pelmatozoans, brachiopods and cephalopods). Typical allochthonous material includes: rounded and abraded peloids, intraclasts, ooids, skeletal particles and terrigenous silt. Autochthonous and allochthonous grains can generally be differentiated on the basis of their texture, shape and degree of sorting. The source of the carbonate mud within this sediment is generally difficult to determine, but much of it is probably produced within the buildup by the disintergration of calcified microbial matter (Wolf, 1965a, 1965b, 1965c; Klement and Toomey, 1967; Kobluk and Risk, 1977c; Coniglio and James, 1985), or possibly by *in situ* precipitation (Tsein, 1985).

Inter-framework sediment provides important information about the depositional environment (turbulence, water depth and generation and influx of detritus) and metazoan palaeo-ecology of thrombolites.

2 Void-filling Cement

This cement occludes open void spaces within both framework and inter-framework components such as fenestrae, shelter cavities, intra- and inter-particle voids, burrows, grain moulds, secondary vugs and fractures. It provides an important record of the diagenetic history of thrombolites,

but detailed diagenetic analysis is beyond the scope of this study. Four main types of void-filling carbonate cement are recognised within thrombolites:

1. Common isopachous fringes of fibrous, generally inclusion-rich, microcrystalline calcite 20-100 μm thick. These fringes are volumetrically minor and are typically the first generation of void-filling cement. They are interpreted as syn-sedimentary marine cement (Longman, 1980; James and Choquette, 1983; Harris and others, 1985).
2. Rare clear prismatic calcite within inter-particle voids, fossil moulds and burrows. The prismatic crystals are a few to several hundred microns long, and generally have straight intercrystalline boundaries, scalenohedral terminations and uniform extinction. They are either the first generation of cement or succeed isopachous fibrous cement, and commonly syntaxially overgrow trilobite fragments. This prismatic cement is interpreted as an early diagenetic, syn-sedimentary to meteoric to shallow burial precipitate (cf. James and Klappa, 1983; Chow, 1986).
3. Common monocrystalline syntaxial calcite which is ubiquitously associated with pelmatozoan fragments. The syntaxial overgrowths are early diagenetic, either syn-sedimentary or early meteoric (cf. Meyers and Lohmann, 1978; Wilkinson and others, 1982; James and Klappa, 1983).
4. Rare radiaxial fibrous calcite (Bathurst, 1959, 1975) which occludes shelter cavities beneath trilobite fragments. This cement, characterized by a distally-

divergent subcrystal pattern and a cross-cutting distally-convergent pattern of fast-vibration (optic axis or C-axis) directions, syntaxially overgrows the prismatic microfabric of the sheltering trilobite skeleton, and grew downward into the cavity (see Plate 20-C). This cement has not been observed in association with other types of void-filling cement. Although the origin of radiaxial fibrous cement has long been controversial (see synthesis of ideas by Kendall and Tucker, 1973), recent studies indicate it is probably a primary, synsedimentary or shallow burial, precipitate (Sandberg, 1985; Kendall, 1985; Saller, 1986), and not a neomorphic replacement of an acicular cement (Kendall and Tucker, 1973). The present occurrence is consistent with either a synsedimentary or shallow burial origin.

5. Mosaics of clear blocky calcite. This is generally the last generation of cement and occludes all remaining primary and secondary voids. The blocky crystals range from about 50-500 μm in size and characteristically increase in size away from their substrate. This is volumetrically the most dominant type of cement and is a relatively late diagenetic, meteoric or burial precipitate (cf. Grover and Reid, 1983; James and Klappa, 1983; Chow, 1986; Choquette and James, 1987).

2.2.3 DIAGENETIC COMPONENTS

Neomorphic spar, dolomite, quartz and stylolites may selectively or randomly replace framework and inter-framework components, and thereby enhance the complexity of the thrombolite fabric. Wherever possible the effects of these processes need to be considered in order to determine the original mesostructure. Analysis of these diagenetic fabrics is otherwise beyond the scope of this study.

2.3 MICROSTRUCTURE

The microstructure is undoubtedly the most challenging and, by the same token, most rewarding aspect of the analysis of thrombolites. Since the microstructure records the sediment building activities of the formative microbial community, microstructural analysis can determine the origin of a thrombolite in terms of: 1) the specific types of sediment forming processes, and 2) the gross morphologic composition (coccoid or filamentous) of the microbial community. The interpretation of microstructure is not always inherently obvious, however, and it can commonly only be interpreted by comparison with modern microbial microstructures.

Several types of sediment forming processes can occur within benthic microbial communities (Krumbein, 1978; Lyons and others, 1984; Burne and Moore, 1987): trapping and binding of detrital particles, inorganic calcification,

biologically influenced calcification, and skeletal calcification. All of these processes may operate within thrombolite-forming communities, either singly or in unison, but skeletal calcification *sensu stricto* can generally be discounted for most microbial buildups.

Trapping and binding of detrital particles : Black (1933) demonstrated that microbial communities can readily trap detrital sediment introduced into the environment. Filamentous microbes appear to be the dominant sediment trapping element of microbial communities. They can achieve this in two distinct ways (Monty, 1967): 1) infiltration and entrapment of detritus between relatively large and robust erect filaments, such as *Rivularia, Dichothrix, Scytonema* and *Lyngbyra*, and 2) agglutination of fine-grained detritus onto the sticky mucilaginous surface of masses of very fine filaments which are too small to entrap detrital grains, for example *Phormidium* (formerly *Schizothrix sensu* Monty, 1967, subsequently reidentified by Golubic and Focke, 1978). The motility of cyanobacteria in response to variations in light intensity, combined with upward migration necessary to keep pace with sediment accumulation, are considered important aspects of a communities ability to trap and bind detritus (Monty, 1976). Coccoid cyanobacteria, diatoms and other eukaryotic microalgae may also actively trap and bind detritus, either by agglutination or simply the overgrowth of detritus mechanically deposited on the surface of a mat; these microbes are important sediment trapping agents within

the subtidal colloform mats in Shark Bay, Western Australia (Playford and Cockbain, 1976; Bauld, 1984).

Inorganic Calcification : Microbes and microbial communities, as well as the detrital particles that they trap, can provide a foundation for inorganic precipitates (cements). Inorganic precipitation may be promoted by either the evaporation of saturated solutions, or the loss of CO_2 (degassing) from supersaturated solutions. In marine environments, degassing can result from turbulence (such as wave action on reefs), increased temperature, or upwelling (reduced pressure). The resulting precipitates encrust the microbes (which themselves may or may not be preserved) and\or the entrapped sediments, and form lithified deposits variously referred to as tufa, travertine, sinter or coniatolite.

Modern examples of inorganic precipitates associated with microbial communites occur in many freshwater environments (caves, springs, waterfalls, and lakes; Pentecost, 1978, 1985), and appear to be important in the formation of at least some marine deposits, such as the oolitic hardgrounds on the Eleuthera Bank, Bahamas (Dravis, 1979), the subtidal lithified pavement and club-shaped stromatolites in Shark Bay (Playford and Cockbain, 1976; Burne and James, 1986), the coniatolites in the Persian Gulf (Purser and Loreau, 1973), a proportion of the carbonate precipitates within the Solar Lake mats, Sinai (Lyons and others, 1984), and perhaps the deep-water lithoherms in the Straits of Florida (Neumann and others, 1977).

Ancient examples of probable inorganic precipitates associated with marine microbial mats are the uniformly laminated tiny "digitate stromatolites" and "tufas" that characterize many Lower Proterozoic sequences (Donaldson, 1963; Hoffman, 1975; Hofmann, 1977; Grotzinger and Hoffman, 1983; Grey, 1984; Hofmann and Jackson, 1987; Grotzinger, in press). These deposits lack microfossils, although many contain dark organic-rich layers and are silicified, and their overall fabric and structure may well be due to abiogenic processes (Walter, personal communication, 1987). Grotzinger and Read (1983) and Grotzinger (1986a), for example, considered that the tiny arborescent stromatolites and tufas in the Rocknest Formation were precipitated when waters supersaturated with respect to aragonite were blown, either as wind or storm driven tides, over supratidal microbial mats and evaporated.

Several examples of botryoidal cements established on microbial elements occur in the microbial buildups of western Newfoundland (Chapter 4): the micro-fabric of these cements is described in section 2.3.14.

Biologically influenced calcification : Pentecost and Riding (1986) recently reviewed the subject of cyanobacterial calcification, and concluded that although cyanobacteria commonly participate in processes of calcification, and many exhibit specificity for calcification, none is an obligate calcifier. Such biologically influenced calcification (Burne and Moore, 1987) is only partly within the influence of the

organism; it requires suitable environmental conditions favouring precipitation of carbonate, together with the presence of a suitable site for nucleation. Pentecost (1985) considers that the ionizable carboxylic acid groups within the polysaccharide sheaths of cyanobacteria provide such a site for nucleation, and that the mineralogy and composition of the precipitated carbonate is consistent with that to be expected from essentially inorganic precipitation; that is, it is not dictated by the organism. Calcification may occur either within the sheath (impregnation) or upon it (encrustation) (Riding, 1977b), and although the sheaths of filamentous cyanobacteria may be calcified during their life, calcification of coccoid forms is probably a post-mortem process (Golubic, 1983; Pentecost and Riding, 1986).

Calcified cyanobacteria are relatively common in modern non-marine environments, but are relatively scarce in modern marine environments (Monty, 1973; Golubic, 1983). The change from fresh-water to marine environments is associated with a change in the composition of calcified cyanobacteria from low-magnesium to high-magnesium calcite, a reflection of the greater concentration of magnesium ions in sea water. In contrast to modern environments, marine calcified cyanobacteria are abundant in Palaeozoic and Mesozoic microbial buildups. They are virtually absent, however, in the Precambrian and become less common after the mid-Cretaceous (Riding, 1982; Pentecost and Riding, 1986). The temporal distribution of calcified cyanobacteria is discussed in more detail in Chapter 7.

Bacteria also induce the precipitation of calcium carbonate (Lalou, 1957; Oppenheimer, 1961; Greenfield, 1963; McCallum and Guhathakurta, 1970; Deelman, 1975; Krumbein and Cohen, 1977; Krumbein, 1978, 1979; Chafetz and Folk, 1984). Within sea water, these precipitates (under both natural and laboratory conditions) generally comprise aragonite or high magnesium calcite, and most commonly form dumbbell-shaped, rosette-shaped, or spherulitic aggregates of needles and encrusted rods. Extensive sedimentological, mineralogical, microbiological, isotopic, and pore water studies of microbial mats and associated sediments in Solar Lake, Sinai (Friedman and others, 1973; Krumbein and Cohen, 1977; Krumbein and others, 1977; Cohen and others, 1977a, 1977b, 1977c; Jorgensen and Cohen, 1977; Aharon and others, 1977; Lyons and others, 1984) indicate that degradation of cyanobacteria by sulfate reducing bacteria is largely responsible for the calcification of these shallow water mats. Thermodynamic modelling of these pore waters (Lyons and others, 1984) suggests that as sulfate reduction proceeds, biogenic HCO_3^- is produced from the oxidized cyanobacteria, and reacts with Ca^+ to precipitate carbonate minerals. Authigenic aragonite, low- and high-magnesium calcite, monohydrocalcite, and dolomite have all been observed in the Solar Lake mats.

Furthermore, Chafetz (1986) concluded that the nuclei of many modern, silt-sized, marine peloids probably originate as a fine grained precipitate of high magnesium carbonate within and around active clumps of bacteria, and that the vital

activity of the bacteria influences the precipitation of the calcite. This finding has particular significance for thrombolites and stromatolites since they are commonly dominated by micro-clotted fabrics (grumous or *structure grumeleuse*; see Section 2.3.3) that are strikingly similar to the "peloidal textures" described within modern reef micro-cavities and lithified submarine substrates (Land and Goreau, 1970; Land, 1971; Alexandersson, 1972; Ginsburg and Schroeder, 1973; James and others, 1976; James and Ginsburg, 1979; Macintyre, 1977, 1978, 1984, 1985; Marshall, 1983; Chafetz, 1986). Bacterial precipitates are thus probably equally significant within ancient reefs and microbial buildups (cf. Cross and Lightly, 1986; Reid, 1987).

Skeletal calcification : Obligate calcifiers, those organisms whose metabolic processes produce an organized calcareous structure, are generally minor constituents of modern, and by inference ancient, microbial communities (Monty, 1981; Pentecost and Riding, 1986; Burne and Moore, 1987). The only common constituent of modern benthic microbial communities that produces metabolised skeletons are diatoms, which are siliceous; their remains, however, form only a minor component of the resulting microbial buildup, and are unknown in pre-Cretaceous sediments. Eukaryotic red and green algae and metazoans are the only significant organisms that secrete calcareous skeletons within, and thereby contribute to the construction of, ancient microbial buildups.

Numerous distinct types of microstructure are recognised within the microbial framework (thromboids, stromatoids, cryptomicrobial fabrics) of thrombolites:

1. Calcified "microfossils"
2. Lobate microstructure
3. Grumous microstructure
4. Peloidal microstructure
5. Vermiform microstructure
6. Filamentous microstructure
7. Spongeous microstructure
8. Tubiform microstructure
9. Mottled microstructure
10. Massive microstructure
11. Laminated microstructure
12. Compound microstructure
13. Variegated microstructure

Whilst some of these microstructures occur in all types of microbial frameworks (thromboids, stromatoids and cryptomicrobial fabrics), others are predominantly or exclusively restricted to thromboids (microstructural types 1 and 2), stromatoids (types 4, 5, 6 and 11) or cryptomicrobial fabrics (type 9). Although intergradations commonly occur between many of these microstructures, each type represents a distinct end member within the observed spectrum. The structure and origin of each microstructure is discussed below.

2.3.1 CALCIFIED "MICROFOSSILS"

Several types of morphologically distinct calcareous microbial forms or "microfossils" occur within thrombolites. Although these "microfossils" have been assigned specific Linnaean names, most are not the deliberately secreted skeletons of genetically discrete organisms, but rather appear to result from the synsedimentary calcification of dead and decaying cyanobacteria or cyanobacterial colonies (Pratt, 1984; Pentecost and Riding, 1986; Burne and Moore, 1987). This calcification is most likely a biologically influenced process related to either: 1) the photosynthetic removal of carbon dioxide by cyanobacteria, with consequent elevation of pH and precipitation of calcium carbonate (Golubic, 1973), 2) the degradation of cyanobacteria by sulfate reducing bacteria (Krumbein, 1979), or 3) the heterogeneous nucleation of carbonate crystals on or within the polysaccharide sheath of cyanobacteria (Pentecost, 1985). These "microfossils" may well represent taxa that displayed specificity for calcification, a feature displayed by some extant cyanobacteria taxa (Pentecost and Riding, 1986).

The following calcified "microfossils" occur within thrombolites (Fig. 2-5): *Renalcis* and related forms, *Girvanella*, and rarely *Nuia*, calcispheres and calcareous algae. These "microfossils" are typically framework components, but they also occur as reworked detrital particles within the inter-framework sediment (this is the most common occurrence for *Nuia* and calcispheres).

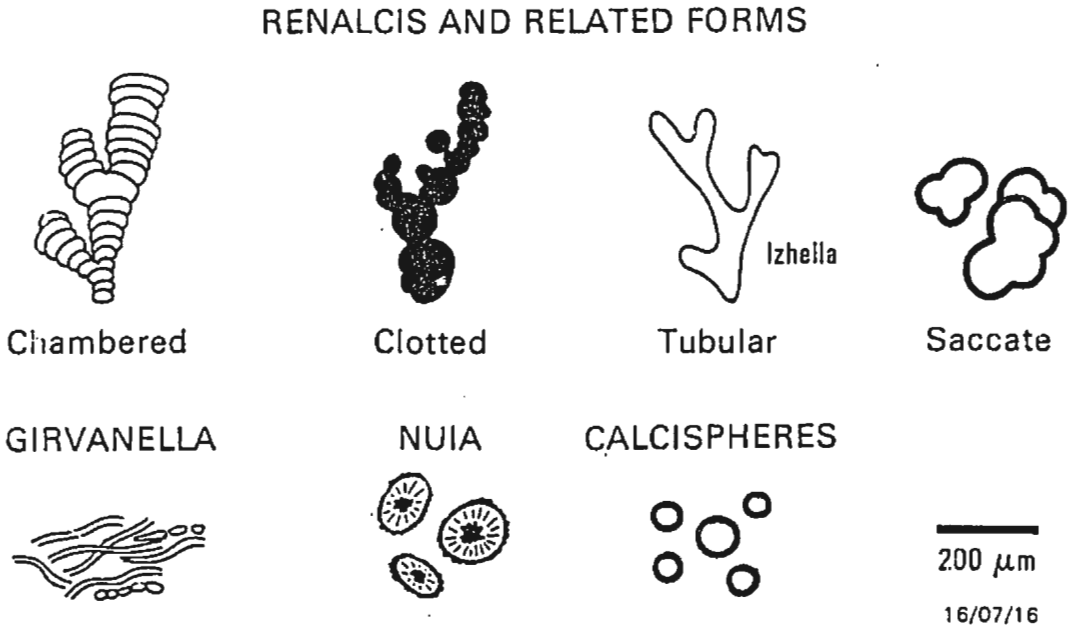

Figure 2-5. Calcified "microfossils" that occur within thrombolites.

1 *Renalcis* and related forms

Renalcis is a common constituent of thromboids, but seldom occurs within stromatoids. It displays a spectrum of clotted, saccate, chambered, and rarely tubular morphologies (Fig. 2-5, terminology of Pratt, 1984), equivalent to part of the "*Renalcis-Epiphyton* morphological series" of Riding and Voronova (1985). Dendritic *Epiphyton*-like morphotypes, however, are rarely observed within thrombolites (see section 5.4.3). The individual clots, sacs and chambers are generally 20-500 μm in diameter, although some saccate forms are over 1 mm in diameter, and they form arborescent or grape-like aggregates (thalli) up to several millimetres in size.

Renalcis is interpreted as a calcified colony of coccoid cyanobacteria (Hofmann, 1975a; Pratt, 1984). Calcification is thought to have occurred soon after the death of the colony or in repeated steps during successive growth phases of the colony. Pratt (1984) related the different morphotypes to variations in the size and shape of the colony, the frequency of calcification, and whether the entire colony or only its outer musilaginous sheath was calcified. Thus clotted morphotypes result from the intermittent growth and pervasive calcification of successively encrusting sub-colonies; chambered morphotypes result from the intermittent growth and selective calcification of the outer sheath of successively encrusting sub-colonies; and saccate and tubular morphotypes result from the selective calcification of the outer sheath of entire colonies after they ceased to grow. Examples of *Renalcis* are shown in Plates 25-A,E, 46, 70-B,C and 74.

2 *Girvanella*

Girvanella is locally abundant in some thrombolites and stromatolites, but is generally uncommon within thromboids. However, fine *Girvanella* fragments or *Girvanella* clasts are common within the inter-framework sediments of many thrombolites, thus suggesting that *Girvanella* may have formed part of the framework of these thrombolites. Within frame-building components, *Girvanella* forms a network of loosely to tightly intertwined calcareous tubules which generally have a preferred substrate parallel orientation. The tubules have an external diameter of approximately 10-30 μm, generally range up to 200 μm in length, and are unbranched. The walls of the tubules are composed of cryptocrystalline calcite and are generally less than 5 μm thick. Branching, fan or bush-like tubular morphotypes (*Ortonella, Hedstroemia* and other members of Riding and Voronova's (1985) "*Botomaella-Solenopora* morphological series") are rarely observed within thrombolites.

Calcareous *Girvanella* tubules are believed to represent the impregnated and\or encrusted sheaths of filamentous cyanobacteria (Riding, 1975, 1977b; Danielli, 1981). Similar calcified microbial filaments occur within many modern microbial mats and stromatolites (Monty, 1967, Plate 6-1; Monty and Hardie, 1976, Figs. 9, 10; Halley, 1976, Figs. 5, 6, 7; Hardie and Ginsburg, 1977, Figs. 48, 53B; Riding, 1977b, Plate 11; Krumbein and Potts, 1978). Examples of *Girvanella* within Cambro-Ordovician microbialites are shown in Plates 25-B, 29-B,E and 62-C,D.

3 *Nuia*

Nuia is a rare constituent of thrombolites. It consists of a diffuse cryptocrystalline centre surrounded by radial-fibrous calcite, is circular to ovoid in cross-section, and 100-500 μm in diameter. It occurs as isolated detrital grains that accumulated within the inter-framework sediments or, less commonly, that are bound within thromboids and stromatoids. Elongate tubular forms such as those illustrated by Mamet and Roux (1982) have not been observed within thrombolites or stromatolites. *Nuia* is a microfossil of uncertain affinity, probably a green alga (Toomey and Klement, 1966; Mamet and Roux, 1982).

4 Calcispheres

Calcareous calcispheres are a rare constituent of some thrombolites, and have been observed within thromboids, stromatoids and inter-framework detrital sediments. These spherical bodies consist of a thin cryptocrystalline calcite wall and a hollow cement-filled centre, and are 100-300 μm in diameter. They occur as isolated o. scattered detrital particles that were trapped within the thrombolite.

The origin of calcispheres is uncertain, but they most likely represent the reproduction cysts of dasycladacean algae (Marszalek, 1975; Wray, 1977). An example is shown in Plate 52-B.

5 ?Green Algae

In rare instances fragments of codiacean or dasycladacean algae occur within thrombolites. Although their idendity remains uncertain, some of these fragments are similar to *Calcifolium* (Plate 38-D,E; compare with Wray, 1977, Fig. 84).

2.3.2 LOBATE MICROSTKUCTURE

Lobate microstructure is here defined as a microfabric consisting of microscopic, multiple lobate calcareous bodies which are attributed to the activities or remains of micro-organisms. The lobate bodies range from about 200 μm to a few millimetres in size, and individual lobes have a diameter of 100-500 μm. In some aspects these lobate bodies superficially resemble *Renalcis* or related forms, but they are significantly larger and exhibit a spectrum of distinct fabrics. An important point to note here is that although lobate microstructures appear as dark coloured constituents in hand specimens, in thin section they are typically light coloured; the reverse situation generally holds for *Renalcis*.

Lobate microstructures are widespread within thromboids but are uncommon within stromatoids. They also occur as reworked detrital grains (referred to herein as microbial corpuscles) within the inter-framework sediment of thrombolites.

Several intergradational types of lobate microstructures are recognized within thrombolites (Fig. 2-6): saccate, cellular, spherulitic and (not illustrated) massive.

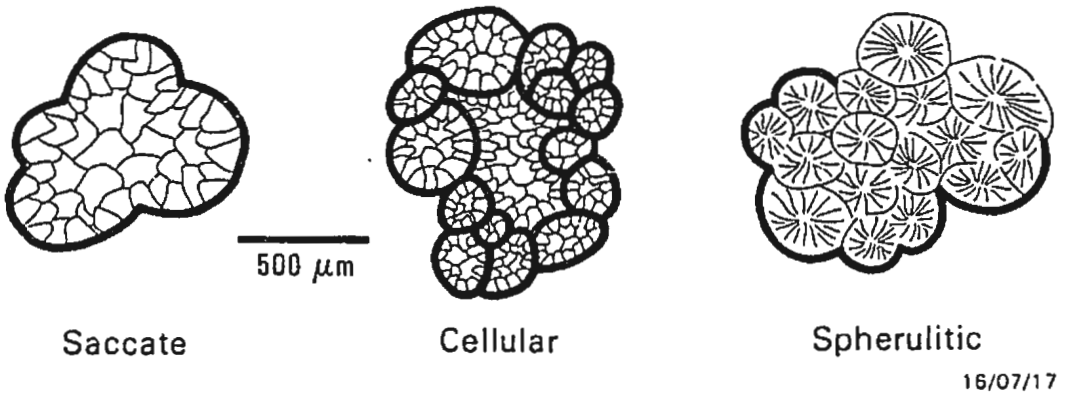

Figure 2-6. Schematic illustration of lobate microstructures.

Saccate lobate microstructure consists of lobate bodies that have dark, 20-60 μm thick cryptocrystalline walls and clear centres infilled by a mosaic of microcrystalline cement or microspar. Examples are shown in Plates 5-B, 19-A,B, 36-D, 58-B, 79-C and 84-B,C,D.

Cellular lobate microstructure consists of lobate bodies that contain numerous individually walled sub-bodies or "cells" which are infilled by a mosaic of microcrystalline cement or microspar. The individual cells are generally 100-500 μm in diameter. Examples are shown in Plates 19-A, 39-E and 68-F.

Spherulitic lobate microstructure consists of lobate bodies that contain numerous spherulitic sub-bodies which have a radial-fibrous texture. The individual spherulites are generally 150-300 μm in diameter, and are characterized by a "Maltese-like" extinction cross when viewed under cross-polarised light. They contain numerous sub-micron-sized inclusions which impart a characteristic amber-coloured appearance and commonly delineate individual fibrous crystallites approximately 2 μm wide. Spherulitic bodies generally lack cryptocrystalline walls, or else the walls are incomplete. Examples are shown in Plates 38-C, 39-A,B,C,D, 55-B,C, 66-B, 84-C,D and 85-A,B.

Massive lobate microstructure consists of lobate bodies that have an homogeneous micro- or crypto-crystalline texture. Examples are shown in Plates 5-A, 26-B,C, 47-D, 84-A, 85-C.

Modern analogues of saccate and cellular lobate microstructures occur in the stromatolite crusts in Laguna Figueroa (formerly known as Laguna Mormona), Baja California (Horodyski and Vonder Haar, 1975). These modern aragonitic crusts are composed of incipiently permineralized, sub-millimetre to millimetre-sized, spherical to mamillate (lobate) colonies of the coccoid cyanobacterium *Pleurocapsa* (originally identified as *Entophysalis* by Horodyski and Vonder Haar, 1975, but subsequently re-identified by Stolz, 1983). The colonies consist of a few to several hundred individual cells which are enclosed within multiple gelatinous sheaths. Within the interior of the colonies these sheaths are relatively thin, but they become progressively thicker towards the margin of the colony. Degradation and subsequent permineralization of the colonies is selective; intracellular material rapidly decomposes and is rarely preserved within the aragonite crust; thin inner sheaths that enclose single cells and small groups of cells are relatively more resistant to degradation and are occasionally permineralized; and the thick outer sheath that encloses the entire colony is most resistant to decomposition and is extensively permineralized. These incipiently permineralized colonies bear a striking resemblance to the saccate and cellular lobate microstructures prevalent within thrombolites (compare Plates 19-A,B, 36-D, 39-E, 79-C and 84-B,C,D with Horodyski and Vonder Haar, 1975, Figs. 7, 8). Thus ancient saccate and cellular microstructures are similarly interpreted as variously degraded and calcified coccoid

colonies (presumably cyanabacteria), and by extrapolation, massive lobate microstructures are interpreted as pervasively calcified coccoid colonies. Degradation and calcification of the microbial community is probably controlled by bacterial sulfate reduction (Krumbein and Cohen, 1977; Krumbein and others, 1977; Lyons and others, 1984). Soudry (1987) and Soudry and Southgate (in press) illustrate analogous cellular microstructures within ancient phosphatized microbial mats, and a modern calcareous example is illustrated by Monty (1967, Pl. 8-1,2) from Andros Island, Bahamas.

Spherulitic microstructures, on the other hand, are probably analogous to the aragonite spherulites described by Monty (1976) within the pustular coccoid microbial mats at Shark Bay, Western Australia, as well as the probable bacterial mats at Mono Lake, California. They are also similar to the spherulitic microstructures within Pleistocene stromatolites in the precursor Dead Sea, Israel (Buchbinder, 1981). At Shark Bay, the spherulites range from about 40 to 100 μm in diameter, and the individual spherulites or clusters of spherulites are precipitated within hollow organic shells (Monty, 1976, Fig. 27). Their precipitation is probably triggered by bacterial activity within degraded coccoid communities (communication by Monty, 1979, cited in Buchbinder, 1981, p.192). At Mono Lake the spherulites are about 40 μm in diameter and their juxtaposition and superposition generates knobbly, sub-millimetric to millimetric bodies (Monty, 1976, Fig. 29). They are precipitated within

or beneath (?)bacterial mats. These modern analogues thus suggest that comparable spherulitic bodies within ancient thrombolites represent bacterial precipitates within degraded coccoid colonies. Similar spherulitic bacterial precipitates have been produced experimentally in sea water by Lalou (1957), Oppenheimer (1961), McCallum and Guhathakurta (1970), Deelman (1975), Krumbein and Cohen, (1977) and Krumbein (1974, 1979).

The interpretation that saccate, cellular and massive lobate microstructures owe their origin to the selective degradation and calcification of coccoid cyanobacterial colonies is analogous to the origin proposed by Hofmann (1975a) and Pratt (1984) for *Renalcis*. In this latter case, however, calcification generated architectures of relative limited variability which are amenable to Linnaean classification.

2.3.3 GRUMOUS MICROSTRUCTURE

Grumous microstructure, derived from the french "grumeau" meaning clot or lump, comprises irregular dark clots of extremely fine (usually cryptocrystalline) carbonate separated by patches of clear coarser grained (usually microcrystalline) carbonate (modified after Walter, 1972). Grumous microstructure is thus simply a synonym of clotted micro-fabric. The individual micritic clots within such a fabric are referred to as "microclots" in order to avoid confusion with mesoscopic clots (thromboids).

The individual microclots exhibit a spectrum of shapes, sizes and degree of interconnection, although sub-equidimensional, partially interconnected, 10-100 μm size microclots are predominant. They may be either sharply defined (distinct, Hofmann, 1969) or poorly defined (diffuse, Hofmann, 1969). As the microclots become more distinct and separate from one another they intergrade with peloids, and thus grumous microstructure commonly intergrades with peloidal microstructure (Fig. 2-7). A common variant of grumous microstructure is that in which the microclots have a diffuse, coarse silt-sized (about 50 μm) globular form (Bathurst, 1975, 511-513); this microstructure was originally designated *structure grumeleuse* by Cayeux (1935). Grumous fabrics are also commonly referred to by a plethora of terms such as pseudo-pelletal, pelleted micrite, micro-peloidal, pelletoidal or pelletal.

Grumous microstructures are prevalent in most thrombolites, either within thromboids, stromatoids or undifferentiated cryptomicrobial fabrics. They are also widespread within stromatolites (Walter, 1972) and "Waulsortian" mud mounds (Wilson, 1975; Pratt, 1982b; James, 1983; James and Macintyre, 1985).

The origin of grumous microstructures is uncertain. Within thrombolites, and microbial buildups in general, the following mechanisms are feasible: 1) *in situ* inorganic or biologically influenced precipitation, 2) neomorphism of homogenous micrite (Cayeux, 1935), and 3) merging of detrital peloids (Beales, 1956, 1958, 1965; Bathurst, 1975). In some

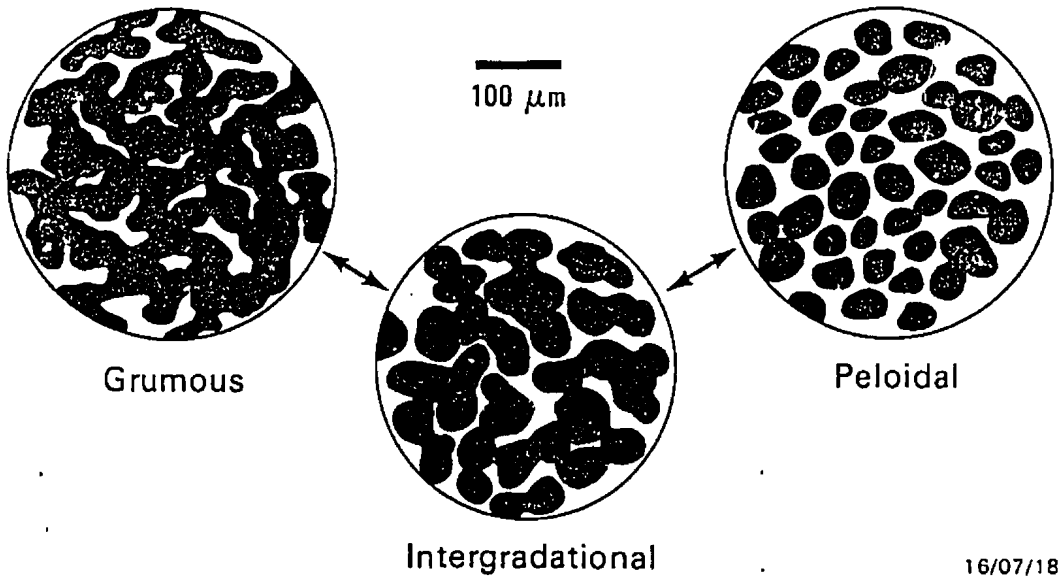

Figure 2-7 Schematic illustration of grumous and peloidal microstructures.

cases it may be possible to differentiate between these options, but this is probably the exception rather than the rule. For example, thromboids with grumous microstructure which are surrounded by silt-rich inter-framework micrite, but which are themselves devoid of terrigenous silt, probably represent *in situ* precipitates. Similarly, grumous microstructures in which the microclots have lobate or irregular thread-like forms, probably represent permineralized coccoid and filamentous microbes, respectively. Conversely, if definitive detrital grains such as terriginous silt or metazoan debris are common within grumous microstructures, the microclots may well represent merged detrital peloids. In many cases, however, the microclots may be polygenetic.

Grumous microstructures occur within many modern microbial mats and deposits including;

1. The "clotty structure" described by Monty (1967, p.74, Plate 8-3,4) within the supratidal mats of Andros Island, Bahamas. This structure is generated by two means: erratic precipitation of fine-grained carbonate around and within loose mucilaginous masses of coccoid or filamentous microbes, and fragmentation and collapse of delicate calcified filaments.
2. The "clotted mud" generated by the pustular, coccoid-dominated mats on the Trucial Coast, Persian Gulf (Kinsman and Park, 1976).
3. The clotted muddy layers on the Andros Island tidal flats (Hardie and Ginsburg, 1977, Fig. 38B). This clotted fabric is thought to be due to merging of soft muddy

peloids that were originally deposited as well sorted silt-sized grains on sticky *Schizothrix (Phormidium)* mats.

4. The "peloidal" crusts and micro-cavity fillings within modern reefs (Land and Goreau, 1970; Land, 1971; Alexandersson, 1972; Ginsburg and Schroeder, 1973; James and others, 1976; James and Ginsburg, 1979; Macintyre, 1977, 1978, 1984, 1985; Marshall, 1983; Chafetz, 1986). The origin of these peloidal textures has been a subject of controversy, and several explanations have been presented (see review by Macintyre, 1985): faecal pellets, detrital grains, broken calcified filaments and inorganic precipitates). Most recently Chafetz (1986) concluded that the peloids probably originate as bacterial precipitates.

Examples of grumous microstructures within Cambro-Ordovician microbialites are shown in Plates 12-E, 29-C, 52-D, 66-C, 67-D, and 75-C,D.

2.3.4 PELOIDAL MICROSTRUCTURE

Peloidal microstructure consists of aggregates of discrete detrital grains, predominantly peloids, without significant development of fenestrae. Although the peloids may appear to have a grain-supported fabric, at the time of their accumulation they were either trapped or agglutinated and then bound by organic matter. Direct microstructural evidence of such binding may not be present, but one or more lines of

indirect evidence are indicative of binding: 1) non-uniform packing of the grains (Neumann and others, 1970), 2) selective grain size sorting, typically the finer-size fraction, of the available detritus (Black, 1933; Gebelein, 1969; Frost, 1974; Hardie and Ginsburg, 1977), 3) crestal thickening of convex layers of detrital grains (Gebelein, 1969), 4) layers of detrital grains inclined at angles greater than the angle of repose of unattached free grains (Golubic, 1973; Hardie and Ginsburg, 1977), and, in all cases, 5) the occurrence of the grains within mesoscopic frame-building microbial components, either thromboids or stromatoids.

Detrital grains other than peloids also frequently occur within peloidal microstructures: terrigenous silt and sand, metazoan debris, ooids and intraclasts. Such grain types are rarely predominant, in which case the microstructure is said to be silty, bioclastic, oolitic etc..

Peloidal microstructures are common in thrombolites, and are particularly profuse within stromatolites. Within thrombolites, they are generally much more abundant in stromatoids than in thromboids.

The origin of peloidal microstructures has been well documented in several studies of modern microbial mats and stromatolites, and in every case it is generated by filamentous or filament-dominated microbial communities (Black, 1933; Monty, 1967, 1976; Gebelein, 1969; Neumann and others, 1970; Hardie and Ginsburg, 1977; Golubic and Focke, 1978). The detrital peloids are either entrapped between

individual filaments or agglutinated to the sticky surface of filamentous masses (Monty, 1967), and continued upward growth of the filaments binds the detrital grains and thereby generates a peloidal microstructure. These filaments are generally motile phototactic oscillatoriaceans (cyanobacteria) (Monty, 1976), but equivalent microstructures could probably also be generated by motile filamentous bacteria (see Doemel and Brock, 1974). Peloidal microstructures in ancient thrombolites and stromatolites are thus similarly interpreted to result from the trapping or agglutination and binding of detrital grains by filamentous microbes.

Modern examples of peloidal microstructure are the peloid-rich layers of the Andros Island tidal flats (Black, 1933; Hardie and Ginsburg, 1977, Figs. 35, 37, 53). Modern oolitic and bioclastic peloidal microstructures occur within the subtidal columnar stromatolites at Shark Bay (Logan and others, 1974; Logan, 1974, Figs. 10A, 13C, 13D; Monty, 1976, Figs. 12, 13; Playford and Cockbain, 1976, Fig. 11; Burne and James, personal communication, 1988), on the Eleuthera Bank, Bahamas (Dravis, 1982), and between the Exuma Islands, Bahamas (Dill and others, 1986). Modern sandy microstructures occur on the Massachusetts coast (Cameron and others, 1985), and on the tidal flats of Mauritania, West Africa (Schwarz and others, 1975). Examples of peloidal microstructures within Cambro-Ordovician microbialites are shown in Plates 6-E, 38-A,B, 53-A,B, and 56-B,C.

2.3.5 VERMIFORM MICROSTRUCTURE

Vermiform microstructure (Walter, 1972) consists of a network of fine sinuous tubules composed of clear microcrystalline carbonate, separated by darker coloured finer grained, usually cryptocrystalline, carbonate. The tubules are 20-60 μm wide, up to two millimetre long, and commonly branch and coalesce in T and Y shaped patterns. Within any one sample they tend to have a relatively uniform diameter, and may have a preferred prostrate, erect or random reticulate orientation (Fig. 2-8). The distance between tubules is typically several times greater than their width, but in some cases the tubules are closely spaced or intertwined. The texture of the clear microcrystalline carbonate within the tubules suggests that it is either pore-filling cement or neomorphic microspar. The cryptocrystalline carbonate between the tubules may be either massive (simple vermiform microstructure) or clotted (compound vermiform-grumous microstructure). With slight neomorphism, vermiform microstructure may intergrade with grumous microstructure (Walter, 1972, p.160).

Vermiform microstructures are relatively scarce within thromboids, and hence thrombolites in general, but are common within the Cambro-Ordovician stromatolites of western Newfoundland. Walter (1972) similarly concluded that vermiform microstructures are abundant within Lower Palaeozoic stromatolites, and in view of the fact that this microstructure is unique amongst described Australian

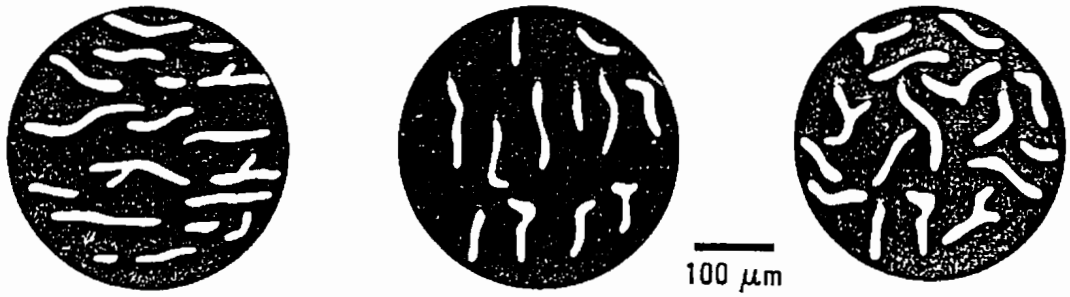

Figure 2-8. Schematic illustration of vermiform microstructures.

stromatolites, he considered it to be of taxonomic importance, and proposed it as the main diagnostic feature of the stromatolite group *Madiganites* (see Hofmann, 1975b, for a criticism of this taxonomic procedure). Vermiform microstructures have also been recorded in Carboniferous stromatolites (*Spongiostromes*) (Gürich, 1906).

The clear sinuous tubules within vermiform microstructure are reminiscent of the calcified filamentous tubules of *Girvanella*, but they lack the dark cryptocrystalline wall of that form. They probably represent moulds of relatively large filaments between which micritic sediment was either trapped or precipitated. Walter (1972, p.87) suggested that upward gliding trichomes, a consequence of positive phototaxis, would generate a network of abandoned mucilaginous sheaths, and subsequent oxidation or calcification of these sheaths would result in a vermiform microstructure. In the samples examined in the course of this study, however, there is no evidence of a calcified wall around the sinuous tubules; such calcification could be expected to generate microstructures intermediate to *Girvanella*, but this was never observed. The tubules are thus interpreted as moulds of oxidized sheaths and\or trichomes. Sinuous tubules of similar size are also formed by endolithic (boring) microbes (see Golubic and others, 1975; Kobluk and Risk, 1977a, 1977b; Hoffman, E.J., 1985), but as pointed out by Walter (1972, p.87) it is unlikely that such borings would have a uniform distribution within stromatoid laminae, and they would tend to disrupt (rather than construct) stromatoids as well as thromboids.

Examples of modern vermiform microstructure are illustrated by Davies (1970, Fig. 13A,B), Monty (1976, Figs. 24, 25), and Hardie and Ginsburg, 1977, Figs. 39A, 50B), and in each case the network of sinuous tubules is attributed to the oxidation of relatively large filaments. Examples of vermiform microstructures within Cambro-Ordovician microbialites are shown in Plates 42-A,B,C, 55-C, 56-B,C,D, 66-D, and 87.

2.3.6 FILAMENTOUS MICROSTRUCTURE

Filamentous microstructure consists of a network of fine micritic threads separated by clear microcrystalline carbonate. The threads are 5-30 μm wide, up to several hundred microns long, and occur in four arrangements (Fig. 2-9): 1) prostrate, horizontally oriented parallel threads, 2) erect, vertically oriented parallel threads, 3) reticulate randomly oriented threads, and 4) radiating tufts. The preservation of the threads may be variable, ranging from distinct, to diffuse linear arrays of micritic microclots. Filamentous microstructures are uncommon within thromboids but are locally prominent within stromatoids.

This microstructure is closely related to vermiform and *Girvanella* microstructures, but in this case the former filamentous microbes are preserved as calcified threads rather than tubular filament moulds or impregnated and encrusted sheaths. The micritic carbonate that forms the threads may be precipitated in one of two ways (Wright and Wright, 1985): 1) precipitation within the vacated sheaths

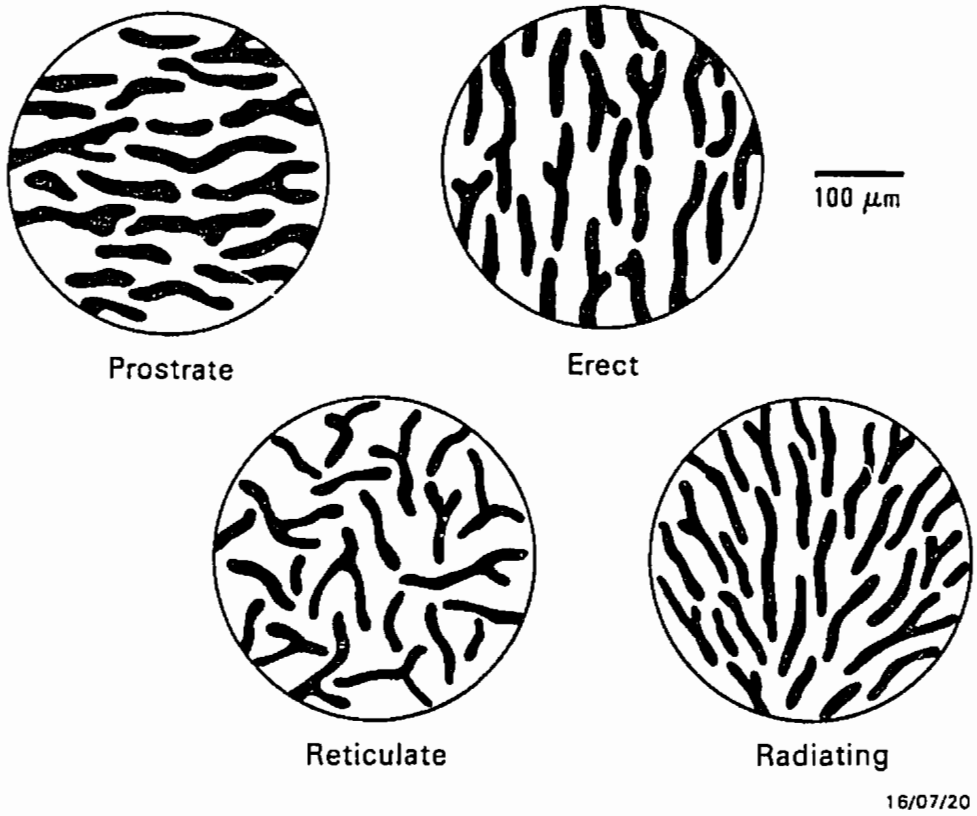

Figure 2-9. Schematic illustration of filamentous microstructures.

after the trichomes have moved or decayed, and 2) calcification of the actual trichome, but this situation rarely occurs in modern examples (communication by Monty, 1980, cited in Wright and Wright, 1985, p.48). The diameter of the calcified filaments is of little or no taxonomic significance since the micritic precipitates typically enlarge the size of the original filaments. For example, the diameter of calcified *Phormidium* filaments within modern stromatolites range from 10 to 50 μm (Monty and Mas, 1981), yet the living filaments are only a few microns in diameter (Golubic and Focke, 1978).

Examples of modern filamentous microstructure are the calcified filaments of *Scytonema* within the freshwater marshes of Andros Island, Bahamas (Monty, 1967, Plates 5, 6, 11-2; Monty 1976, Figs. 3, 4E; Monty and Hardie 1976, Fig. 2a). Examples of filamentous microstructures within Cambro-Ordovician microbialites are shown in Plates 6-D, 14-D,E, 40-C,D,E, and 55-D.

2.3.7 SPONGEOUS MICROSTRUCTURE

Spongeous microstructure consists of a network of microscopic fenestrae*. The micro-fenestrae generally have a laminoid or amoeboid shape, may be isolated or interconnected, and range from a few to tens of microns in size.

* For the purpose of this study, a distinction is made between mesoscopic fenestrae (greater than 100 μm wide and hundreds of microns long) and microscopic fenestrae (microfenestrae) which are only visible under high magnification.

They may remain as open voids or, more commonly, they are occluded by a mosaic of clear microcrystalline cement. In some cases the micro-fenestrae contain internal sediment such as micrite or silt-sized peloids. The carbonate material between the micro-fenestrae may have one of several fabrics: in the simple case it consists of homogeneous micrite or microspar, whilst in more complex cases it consists of grumous, peloidal, vermiform or filamentous microstructures. These complex cases are said to have a compound micro-structures (section 2.3.12) and are designated spongeous-grumous, spongeous-peloidal, etc..

Micro-fenestrae are generally ubiquitous within thromboids and stromatoids, and occur in most types of microbial buildups (Logan and others, 1974; Monty, 1976). They can form in several ways directly analogous to larger mesoscopic fenestrae (see Logan, 1974; Monty, 1976; Grover and Read, 1978; and Shinn, 1968, 1983). Processes likely to be particularly relevant to the formation of micro-fenestrae within thrombolites include: 1) oxidation of non-calcified microbes or colonies, 2) desiccation and consequent shrinkage of organic matter, and 3) accumulation of gas generated by photosynthesis or bacterial degradation.

Typical examples of modern spongeous microstructures are illustrated by Monty (1976, Figs. 19, 28), Monty and Hardie (1976, Fig. 14b) and Hardie and Ginsburg (1977, Figs. 44, 54B). Examples of spongeous microstructures within Cambro-Ordovician microbialites are shown in Plates 46, 48-B, 52, 58-C,D, 59-B, 66-C, 69-E and 77-C.

2.3.8 TUBIFORM MICROSTRUCTURE

Tubiform microstructure consists of isolated or interconnected tubular fenestrae. It is differentiated from vermiform microstructure by the greater size of the tubes (greater than 60 μm in diameter, typically 100-1000 μm), and from spongeous microstructures by the tubular shape of the fenestrae. The tubes may remain as open voids, or more commonly are occluded by sparry cement and\or internal sediment. The material between the tubes may have various microstructures: massive, grumous, peloidal, vermiform etc..

Tubiform microstructures are relatively uncommon in thromboids and stromatoids. The tubular fenestrae could have several origins: 1) oxidation of bundles of filamentous microbes, 2) desiccation and shrinkage of organic matter or bound sediment, 3) generation and upward migration of gas bubbles, 4) dewatering, 5) metazoan burrows and borings, and, at least in late Palaeozoic and younger buildups, 6) root moulds. Modern examples of tubiform microstructures are the gas filled tubular fenestrae within the cinder microbial mats of Abu Dhabi, Persian Gulf (Kendall and Skipwith, 1968), halophyte and mangrove root moulds within the microbial mats of Shark Bay, Western Australia (Logan, 1974), and oligochaete burrows and moulds of vertical tufts of *Scytonema* filaments within the tidal mats of Andros Island (Hardie and Ginsburg, 1977, Figs. 36, 45). Examples of tubiform microstructures within Cambro-Ordovician microbialites are shown in Plates 56-A, 73-B, and 88-D.

2.3.9 MOTTLED MICROSTRUCTURE

Mottled microstructure consists of irregular patches of texturally and\or colour differentiated carbonate, typically tens to hundreds of microns in size. The individual patches have either cryptocrystalline, neomorphic microcrystalline, or replacement (for example dolomite) textures. Their boundaries are typically diffuse and gradational, or else they are marked by stylolites. Pore-filling textures are either absent or very poorly defined.

Mottled microstructures commonly occur within both thromboids and stromatoids, and are ubiquitous within cryptomicrobial fabrics. They are attributed to the disruption and modification of precursor microstructures by bioturbation or subsequent diagenesis (neomorphism, stylolitization and dolomitization). Examples are shown in Plates 9-E,D, 53-C, and 73-B.

2.3.10 MASSIVE MICROSTRUCTURE

Massive microstructure (Hofmann, 1969) consists of homogenous micrite or neomorphic microspar. It is relatively uncommon within thromboids, but individual stromatoid laminae frequently comprise massive micrite.

Massive microstructures could be generated in several ways: 1) trapping and binding of carbonate mud by microbes that have no preserved remains, 2) pervasive calcification of organic matter, and 3) aggrading neomorphism of grumous

microstructures. Examples are shown in Plates 14-A, 30-B,C, 38-A,B, 42-A,C, and 63-E.

2.3.11 LAMINATED MICROSTRUCTURE

Within thrombolites, laminated microbial microstructures are, by definition, restricted to stromatoids. Whilst the internal structure of these laminae may consist of any one of the previously described microstructures, the successive stacking or alternation of these laminae generates various types of laminated microstructure: film, banded, streaky, striated, and tussock (Hofmann, 1969; Walter, 1972; Bertrand-Sarfati, 1976). It is important to realize that these laminated microstructure are defined on the basis of the size, shape, continuity and inter-relationship of the laminae, and not necessarily on the internal fabric (microstructure *senso stricto*) of the individual laminae. Thus in order to fully classify the microstructure of stromatoids, a compound term is generally required, such as banded vermiform or streaky peloidal.

Film microstructure (Bertrand-Sarfati, 1976) consists of regularly banded very thin dark micritic films. In most cases the dark micritic films alternate with thicker clear microcrystalline laminae. Bertrand-Sarfati states that the films have an average thickness of 3 microns, yet cites ancient and modern examples in which the films are 3-5 μm and 5-10 μm thick, respectively. Since the internal fabric of

laminae thinner than about 10 μm cannot be resolved in standard thin section microscopy, an upper thickness of 10 μm is suggested for film microstructure. Modern examples of film microstructure are the calcified *Phormidium* (formerly *Schizothrix*) films within the supratidal fresh water marshes of eastern Andros Island, Bahamas (Monty, 1967, Pl. 7) and the fine siliceous laminae within conical stromatolites (*Conophyton weedi*) from the hot springs and geysers in Yellowstone National Park, Wyoming (Walter and others, 1976). Film microstructure is rare within Cambro-Ordovician microbialites.

Banded microstructure (Walter, 1972) consists of very distinct continuous laminae which have abrupt, more or less parallel boundaries. Banded microstructure is synonymous with ribboned microstructure (Hofmann, 1969), and is differentiated from film microstructure by the thickness of the laminae (greater than 10 μm) and their internal texture (either microcrystalline, cryptocrystalline, or a combination of both). Modern examples of banded microstructure are the smooth mats of Gladstone Embayment, Shark Bay (Davies, 1970, Figs. 9, 10, 11) and Abu Dhabi, Persian Gulf (Kinsman and Park, 1976, Fig.7; Monty, 1976, Fig. 11), the supratidal mats of eastern Andros Island (Monty's, 1967, type 2 mats), the stromatolites in Marion Lake, South Australia (von der Borch and others, 1977), and the flat-topped and conical columns within hot springs in Yellowstone National Park, Wyoming (Walter and others, 1976, Figs. 2-4, 20-28). These modern

banded microstructures were all constructed by filament-dominated microbial communities. In the case of the Yellowstone National Park examples, Walter and others (1976) demonstrated that the banding results from the phototactic alignment of filaments either parallel to laminae (conical forms) or alternatively parallel to and perpendicular to laminae (flat-topped forms). Examples within Cambro-Ordovician microbialites are shown in Plates 21, 42-D, and 88-A.

Streaky microstructure (Walter, 1972) consists of moderately distinct and continuous laminae, and is synonymous with the platy microstructure of Russian workers. The darker laminae are usually the most distinct and frequently grade vertically into less distinct pale laminae. Modern examples of streaky microstructure are the tufted mats of Shark Bay (Logan and others, 1974, Fig. 8D; Logan, 1974, Fig. 17A) and, on Andros Island, the crinkled fenestral mats composed of alternating non-calcified (hyaline) and calcified detrital-rich layers of *Scytonema* filaments (Monty, 1967, Plate 12-1; Hardie and Ginsburg, 1977, Fig. 43), and the laminated domes constructed of alternating erect and prostrate *Phormidium* (formerly *Schizothrix*) filaments (Monty, 1967, Plate 19-1; Monty, 1976, Fig. 2). Examples within Cambro-Ordovician microbialites are shown in Plates 6-A, 19-C, 40-A, 73, and 88-B.

Striated microstructure (Hofmann, 1969; Walter, 1972) consists of laminae formed of a series of lenses. The lenses

may be separate or joined, and some laminae have widely spaced lenticular thickenings. Modern examples of striated microstructure are the lenticular peloidal laminae within the smooth flat *Phormidium* (formerly *Schizothrix*) mats of Andros Island (Hardie and Ginsburg, 1977, Figs. 37, 38A). Examples within Cambro-Ordovician microbialites are shown in Plate 53-A,B.

Tussock microstructure (Bertrand-Sarfati, 1976) consists of a series of juxtaposed hemispheroidal tussocks which have an internal radiating filamentous microstructure. Successive stacking of the tussocks generates a sub-parallel mamillate lamination. Although this microstructure has not been observed in microbialites examined in this study, it is included here since it is somewhat similar to fabrics here interpreted as botryoidal marine cement (see section 2.3.14).

Laminated microstructures are interpreted on the basis of the microstructure of the individual laminae. In the absence of diagnostic microstructural types, however, the shape of the laminae may indicate the composition of the formative mats. For example modern pimpled, pustular and mamillate mats are dominated by coccoid rather than filamentous microbes, whereas uniformly well laminated mats are commonly (but by no means always) constructed by filamentous microbes (Hofmann, 1973; Gebelein, 1974; Awramik, 1984).

2.3.12 COMPOUND MICROSTRUCTURE

Compound microstructure consists of a combinatation of two or more types of microstructure. For example, a microstructure consisting of micro-tubules separated by micro-clotted carbonate is designated a vermiform-grumous microstructure, and one in which the micro-tubules are separated by detrital peloids is designated a vermiform-peloidal microstructure (Plates 56-B,C, 64). Other examples of compound microstructure that commonly occur within Cambro-Ordovician microbialites are spongeous-grumous and spongeous-peloidal microstructures (Plates 48-B, 52-D, 59-B, and 68-E). Several types of modern compound microstructure are illustrated by Hardie and Ginsburg (1977) from Andros Island: spongeous-grumous (their Fig. 44), vermiform-grumous (their Fig. 50B), and vermiform-peloidal (their Figs. 35, 39A).

2.3.13 VARIEGATED MICROSTRUCTURE

Many thromboids comprise a complex arrangement of several microstructural types, each type occurring as a discrete mass adjacent to, or encased within, other microstructural types. These complex microstructural arrangements are designated variegated microstructure; for example, variegated lobate, grumous, massive, and peloidal microstructure (Plate 38-A,B). Other examples of variegated microstructures are shown in Plates 55-B,C, 58-A,C, 61-A,B, and 66-B.

2.3.14 MICROSTRUCTURE OF FRAME-BUILDING MARINE CEMENT

Several types of frame-building botryoidal marine cement, differentiated on the basis of habit and micro-fabric, are recognized within Cambro-Ordovician thrombolites and stromatolites in western Newfoundland (Fig. 2-10). They are all composed of calcite and have a characteristic turbid, weakly pseudo-pleochroic, amber-coloured appearance in thin section due to numerous sub-micron sized inclusions. The botryoids have three main types of occurrence: 1) they encrust, and are in turn encrusted by, individual microbial framework components, such as thromboids or stromatoids, 2) interlayered with stromatoids and detrital sediment, and 3) enveloping crusts around the margins and flanks of entire bioherms.

1 Fascicular-Optic Botryoids

These botryoids are comprised of a single fan-shaped crystal of turbid calcite in which curved cross-twin lamellae have a convex outward arrangement with respect to the basal apex of the fan (Fig. 2-10A; Plates 5-D and 7-C,D). The fast-vibration direction (C axis) of the crystal diverges outward from the apex of the fan, such that when the microscope stage is rotated under cross-polarized light, an extinction cross sweeps across the crystal as if it were a bundle of discrete fibers. This type of fabric is defined as fascicular-optic (Kendall, 1977). In addition to the ubiquitous sub-micron-sized inclusions, the crystals commonly contain scattered

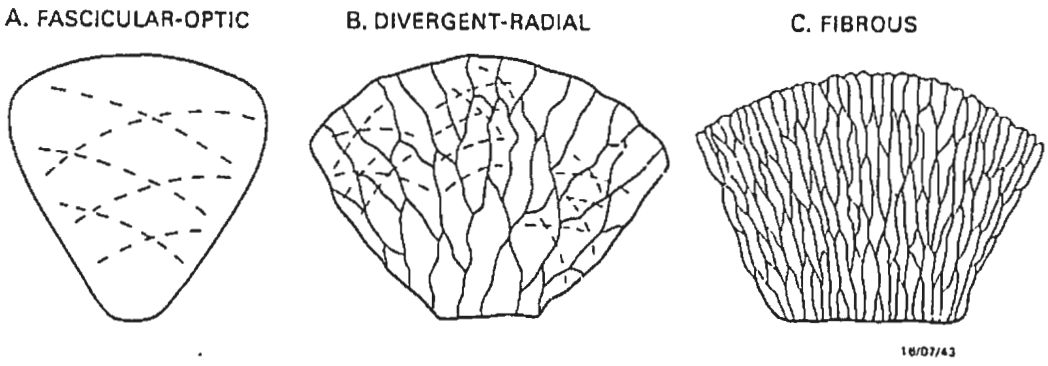

Figure 2-10. Micro-fabrics of botryoidal marine cement.

inclusions of clear rhombic dolomite, about 1-5 μm is size, which are in optic continuity with the host calcite (Plate 7-E). The crystals have a broad open-fan to elongate closed-fan shape, are 0.3-1 mm high and 0.2-1 mm wide, and have irregular non-planar margins. They occur either as single botryoids separated by detrital sediment, or layers of nested botryoids.

Kendall (1977) concluded that fascicular-optic calcite is a neomorphic crystal fabric in which a precursor bundle of radiating acicular crystals is replaced by a single crystal of fascicular-optic calcite, and that the former outline of these acicular crystals is commonly recorded by linear arrays of micro-inclusions. Although such inclusion-defined outlines have not been observed within the present fascicular-optic botryoids, their distinctive fabric nevertheless implies that they were probably also formed by the neomorphic coalescence of precursor acicular bundles. The presence of micro-dolomite inclusions suggests that the acicular crystals were originally composed of high-magnesium calcite (Lohmann and Meyers, 1977). Similar fan-shaped crystals of fascicular-optic calcite cement occur within the Lower Cambrian archaeocyathan buildups in southern Labrador, Canada (James and Klappa, 1983, their Type 2 fibrous spar).

2 Divergent-Radial Botryoids

These botryoids consist of a radial array of irregular poorly defined elongate crystals and sub-crystals which have length to width ratios of 5:1 or more (Fig. 2-10B; Plates

7-A,B and 8-C,D). The individual sub-crystals are 10-100 μm wide and 150-500 μm long, have concertal boundaries, and slight undulose extinction approximately coincident with their elongation (angle of extinction less than 10 degrees). Curved cross-twin lamellae are commonly present, generally extend across several adjacent sub-crystals, and have a convex outward arrangement. In some examples, however, the cross-twin lamellae are planar. Scattered micro-dolomite inclusions occur in optical continuity with the sub-crystals, and the ubiquitous sub-micron sized inclusions sometimes define the linear outline of precursor acicular crystals 5-10 μm wide. The botryoids range from 1 to 3 mm in diameter, and the radial arrangement of sub-crystals within each botryoid generates an erratic sweeping extinction pattern with an overall divergent arrangement of fast-vibration directions. The botryoids occur either singly or coalesce to form mamillate layers. In oblique cross-section, the botryoids appear as an irregular mosaic of very fine to finely crystalline xenotopic calcite. Such mosaics can readily be distinguished from later void-filling cements since the constituent crystals or sub-crystals 1) do not progressively increase in size towards the centre of the mosaic, 2) comprise turbid, pseudo-pleochroic inclusion-rich (rather than clear) calcite, 3) commonly contain micro-dolomite inclusions, 4) have curved twin lamellae, and 5) have concertal boundaries.

The divergent-radial botryoids are similar to the dark coloured botryoidal cements within the Permian Capitan Reef

complex and the Pennsylvanian-Permian phylloid algal mounds of New Mexico and Texas. These younger cements have been the subject of much of the controversy concerning the nature and origin of the shelf margin carbonates of the Permian Reef Complex (Toomey and Babcock, 1983), but there is now a consensus that they represent precursor acicular marine cements, probably originally aragonite (Mazzullo and Cys, 1977, 1979; Mazzullo, 1980; Cross and Klosterman, 1981b). Mazzullo (1980) presented the following neomorphic evolution of their fabric: 1) precipitation of acicular aragonite crystals with inter-crystal inclusions, entrapped particulates, and square-tipped terminations, 2) formation of calcitic "ray-crystals" by the conversion of the aragonite fibres to calcite and the lateral coalescence and syntaxial overgrowth of individual calcitic fibres, and 3) the formation of "composite crystals", the most conspicuous and abundant fabric, by the aggrading recrystallization of the calcitic ray-crystals. The fabric of these Pennyslvanian-Permian cements, termed "divergent-radial pseudospar" by Mazzullo (1980) and "fan-arrays" by Cross and Klosterman (1981b), is very similar to the divergent-radial botryoids within the microbial buildups of western Newfoundland, except that: 1) square tipped relics of acicular crystals have not been observed, 2) micro-dolomite inclusions are present, and 3) curved twin lamellae (absent in the Pennyslvanian-Permian cements) are common. Thus although these divergent-radial botryoids probably also formed by the neomorphic coalescence of acicular fibrous cement, the absence of square-tipped

relics and the presence of micro-dolomite inclusions (Lohmann and Meyers, 1977) suggest that this precursor acicular cement was most likely high-magnesium calcite rather than aragonite.

Divergent-radial botryoids are the dominant type of marine cement within the microbialites of western Newfoundland, and commonly occur in gradational association with fascicular-optic botryoids. As the individual sub-crystals become larger and better defined, they form a series of nested fan-shaped crystals otherwise indistinguishable from larger fascicular-optic crystals. Thus, whereas monocrystalline fascicular-optic botryoids result from the uniform lateral coalescence of single radiating bundles of fibrous calcite, poly-crystalline divergent-radial botryoids most probably result from the incomplete coalescence of single or, more likely, composite bundles of fibrous calcite.

3 Fibrous Botryoids

These botryoids comprise parallel to slightly divergent arrays of poorly defined fibrous crystals, typically 5-30 μm wide and 50-500 μm long, which frequently contain linear trains of sub-micron sized inclusions spaced about 5 μm apart (Fig. 2-10C; Plate 22). Cross-twin lamellae do not occur within these botryoids. The botryoids generally have a slightly feathery upper margin and coalesce to form relatively continuous, sub-isopachous, mamillate crusts. They may be superimposed one on top of each other, in which case they are separated by thin bands of cryptocrystalline

carbonate, or occur interlayered with detrital sediments or stromatoid laminae (Plate 6-E).

Fibrous botryoids clearly represent fibrous cements which have undergone minimal subsequent neomorphism. The original fibres are commonly delineated by linear trains of inclusions (Plate 22-D,E), and the feathery upper margins of the botryoids most likely mimic the original scalenohedral terminations of these fibres. The presence of micro-dolomite inclusions (Plate 22-C) suggests that they were originally composed of high-magnesium calcite (Lohmann and Meyers, 1977).

These fibrous botryoids are similar to the Type 4 fibrous cements described by James and Klappa (1983) except that the fibrous crystals (prismatic domains of James and Klappa) are slightly shorter, and neomorphic microcrystalline calcite does not occur at the boundary between crystals, within crystals, or in bands across crystals. James and Klappa similarly considered this cement type to represent neomorphosed fibrous high-magnesium calcite.

4 Fibrous-Concentric Botryoids

This rare type of botryoidal cement has only been observed within one microbial buildup (Horizon A, Chapter 4). It comprises successive 20-60 μm thick layers of fibrous calcite separated by dark concentric bands of cryptocrystalline calcite, a fabric very similar to radial-concentric ooids (Plate 8-A,B). Although the individual fibrous crystallites are too small to be differentiated in thin section, they

generate a smooth sweeping extinction cross under cross-polarized light. In contrast to fascicular-optic, divergent-radial and fibrous botryoids, micro-dolomite inclusions have not been observed within this type of botryoidal cement.

The fibrous-concentric botryoids form pendant crusts on the flanks and undersides of thromboids, and they are commonly overgrown by divergent-radial botryoids. This mode of occurrence rules out the possibility that the dark crypto-crystalline bands represent layers of detrital sediment interlayered with fibrous precipitates. It is thus suggested that the fibrous-concentric botryoids were formed by the alternating precipitation of layers of fibrous and micritic cement. However, just as the inorganic versus organic influence on the origin of ooid cortical layers remains a matter of great uncertainty (Bathurst, 1975), organic (microbial) processes may well have also been involved in the formation of these botryoids.

Model for Generation of Botryoidal Fabrics

The various types of botryoidal fabrics, with the exception of the rare fibrous-concentric fabric, can be modelled as a spectrum of neomorphic fabrics which, with increasing degree of neomorphism, grade from: 1) fibrous, to 2) divergent-radial, to 3) fascicular-optic fabrics. In this model, fibrous botryoidal fabrics result from the inversion (high-magnesium to low-magnesium calcite) and incipient coalescence (aggrading neomorphism) of the original cement fibres to generate a fabric of moderately well defined fibrous

crystals. The outlines of the original fibres are commonly delineated by linear trains of inclusions, and the original (?)scalenohedral terminations of the fibres result in the feathery upper margin of the botryoids. Polycrystalline divergent-radial fabrics result from inversion and more complete lateral coalescence of small groups of adjacent fibres to form irregular elongate sub-crystals with planar and\or curved cross-twin lamellae, and inclusion-defined outlines of the original fibres are less commonly preserved. Monocrystalline fascicular-optic fabrics result from inversion and the complete lateral coalescence of discrete bundles of fibres to form a single relatively large fan-shaped crystal with prominant curved cross-twin lamellae, and no trace of the original fibres. The presence of micro-dolomite inclusions is apparently not effected by the degree of neomorphic coalescence of the fibres, since they are commonly observed within fibrous, divergent-radial and fascicular-optic fabrics. Since the original fibres within these botryoids appear to have had scalenohedral rather than square-tipped terminations, they were probably originally composed of high-magnesium calcite. A low-magnesium calcite precursor appears unlikely since ordinary calcite is seldom, if ever, fibrous (Folk, 1974; James and Klappa, 1983). Similarly, the presence of micro-dolomite inclusions suggests a primary high-magnesium calcite composition (Lohmann and Meyers, 1977).

An example of the probable original fabric of the fibrous, divergent-radial, and fascicular-optic botryoids is

illustrated by Chow (1986, Plate 9D) from the thick thrombolite-stromatolite complex in the Cape Anne Member of the March Point Formation, western Newfoundland (Horizon A, Chapter 4), although other examples of this fabric were not observed in the present study. The illustrated example consists of a radiating fan-like array of inclusion-rich elongate prismatic crystals, each 20-30 μm wide and 150-250 μm long, with prominant scalenohedral terminations delineated by infiltrated inter-crystalline micrite (Fig. 2-11). Although micro-dolomite inclusions are not present in these crystals, they are strikingly similar to, but considerably larger than, the nucleated splays of bladed magnesium-calcite in the Belize barrier reef (James and Ginsburg, 1979).

Alternative Microbial Origin of Botryoids

In the foregoing discussion it was proposed that the observed spectrum of botryoidal fabrics was related to the progressive neomorphic alteration of primary inorganic marine cement. Although an inorganic origin for these sparry radial fabrics is consistent with current thinking, and has a firm basis in terms of modern analogues, it is conceivable that such fabrics could also result from the neomorphic alteration of primary organic (microbial) structures. Such a case has been argued for some, apparently a relatively minor number, of the fibrous botryoids within the Lower Permian phylloid algal mounds in the Laborcita Formation, New Mexico (Cross and Klosterman, 1981b), and for radial sparitic fabrics

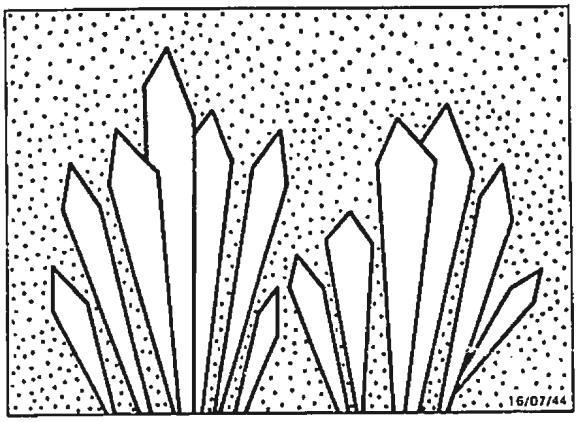

Figure 2-11. Radiating fan-like prismatic marine cement (after Chow, 1986, Fig. 5.1) which may represent the precursor of the observed neomorphic series of botyroidal marine cements in thrombolites.

in Lower Cretaceous oncolites and stromatolites in eastern Spain (Monty and Mas, 1981).

Cross and Klosterman's (1981b, p.68-69) proposal, however, is not convincing; it is predominantly based on speculation rather than hard petrographic evidence, as well as an apparent lack of evidence for open cavities into which the botryoids grew, an aspect subsequently soundly rejected by Shinn and others (1983). Monty and Mas's (1981) argument, on the other hand, is considerably more credible; based on a comparison of radial fabrics within Cretaceous and modern freshwater oncolites and stromatolites, they demonstrated that bundles of calcified filaments can serve as templates for the precipitation of arrays of fibrous calcite, which with "slight reorganization of the crystals ... could possibly yield crystalline fabrics" like the Lower Cretaceous radial fan arrays (Monty and Mas, 1981, p.111-112). These Lower Cretaceous fabrics are very similar to the divergent-radial botryoids within the microbial buildups of western Newfoundland, but in contrast to the Cretaceous examples, delicate calcified filaments or streaks of organic matter are not evident within these botryoids. Furthermore, the occurrence of perfectly straight inclusion-defined outlines strongly suggests a radial crystalline, rather than filamentous, precursor fabric for these botryoids. Finally, since non-radial calcified filaments are elsewhere commonly preserved within these microbial buildups, there is no obvious reason why radial clusters of calcified filaments, such as those illustrated from Precambrian stromatolites by

Bertrand-Sarfati (1972, 1976), should be selectively destroyed within these buildups. A primary microbial origin is thus rejected for these botryoids in favour of the earlier presented neomorphic inorganic origin.

CHAPTER 3

FIELD CLASSIFICATION OF MICROBIAL BUILDUPS

In the course of field studies of Palaeozoic platform carbonates, one is repeatedly confronted with the problems of objectively describing, classifying, and differentiating the somewhat bewildering spectrum of observed microbial buildups. This is particularly true for Cambro-Ordovician carbonates which record the first appearance of thrombolites, a substantial decline in the abundance and diversity of stromatolites, the appearance and demise of archaeocyathan buildups, and the appearance of complex metazoan reefs. Many of these buildups are characterized by composite, zoned, or transitional fabrics of thrombolitic, stromatolitic, and metazoan affinity, and all too frequently they defy classification by any existing scheme, including that of Dunham (1962), Aitken (1967), Embry and Klovan (1971) and Cuffey (1985). Furthermore, the terms cryptalgal, thrombolitic, and stromatolitic have recently been applied to a wide range of buildups of various ages (Pratt, 1982a; Grotzinger and Hoffman, 1983; Ellis and others, 1985; Clough and Blodgett, 1985; Noble, 1985; Feary, 1986), the precise nature of which is impossible to determine in the absence of lengthy descriptions and good quality photographs. Hence there is a need for a simple field classification of microbial and mixed microbial-metazoan buildups, regardless

of their age, such that a given designation will convey a concise understanding of their composition and fabric. Such a scheme is presented below, an outline of which was presented in Kennard and James (1986a).

The proposed classification is based on the relative volumetric proportion of mesoscopic organic frame-building components: stromatoids (S), thromboids (T), cryptomicrobial fabrics (C), and skeletal metazoans and calcareous algae (SKEL). In the case of solely microbial buildups, that is microbialites, the relative abundance of these components can be portrayed by reference to a S-T-C triangular diagram (Fig. 3-1). In this scheme buildups composed predominantly of stromatoids are designated stromatolites, buildups composed predominantly of thromboids are designated thrombolites, and buildups dominated by cryptomicrobial fabrics are simple designated undifferentiated microbial boundstones (microbialites). Buildups composed of a combination of thromboids and stromatoids are designated stromatolitic thrombolites if thromboids are predominant, and thrombolitic stromatolites if stromatoids are predominant. These latter designations are not equivalent to the designations proposed by Aitken (1967), since they specifically refer to buildups comprised of stromatoids and thromboids rather than transitional structures intermediate to stromatoids and thromboids. Buildups composed of undifferentiated crypto-microbial fabrics and minor thromboids or stromatoids are designated disrupted thrombolites or disrupted stromatolites, because they are considered to have been originally composed

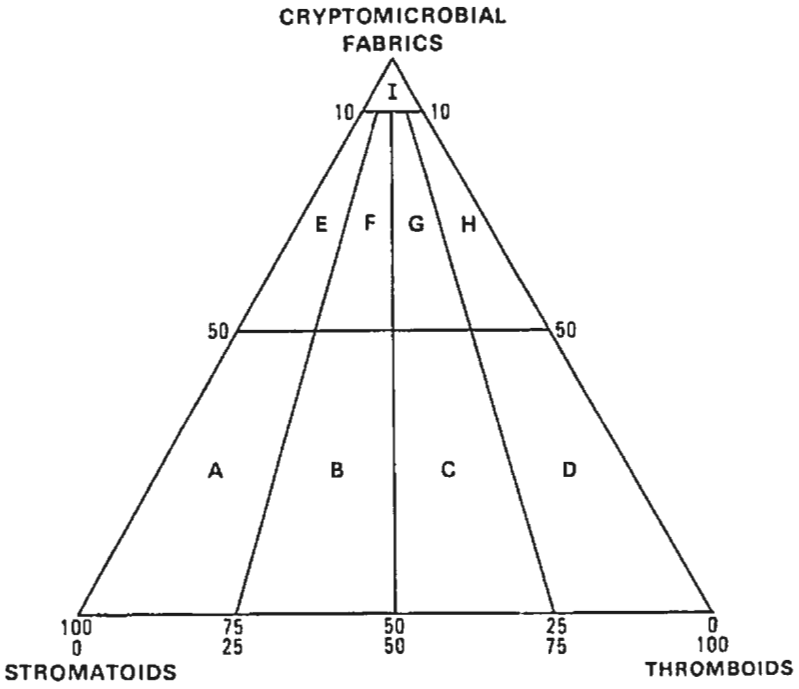

A *Stromatolite*
B *Thrombolitic Stromatolite*
C *Stromatolitic Thrombolite*
D *Thrombolite*
E *Disrupted Stromatolite*
F *Disrupted Thrombolitic Stromatolite*
G *Disrupted Stromatolitic Thrombolite*
H *Disrupted Thrombolite*
I *Undifferentiated Microbial Boundstone*

11/2

Figure 3-1. Classification of microbial buildups (microbialites) based on the volumetric proportion of frame-building mesoscopic constituents.

of thromboids or stromatoids that have since been obscured by either organic or inorganic processes (see previous discussion of undifferentiated cryptomicrobial fabrics in section 2.2.1).

Two simple modifications of this tripartite classification are useful. Firstly, if specific calcified "microfossils" such as *Renalcis, Girvanella, Epiphyton* etc. form distinct mesoscopic constituents, then the buildup is designated a *Renalcis* thrombolite, *Girvanella*-thrombolitic stromatolite etc., in accordance with the relative abundance of each constituent. If these microfossils are the dominant or sole framework constituent, however, then the buildup is best designated a *Renalcis* boundstone, *Girvanella* boundstone etc.. These calcified microbial boundstones are of special significance because they are largely restricted to platform-margin buildups (McIlreath, 1977; Pfeil and Reid, 1980; Playford, 1980a; James, 1981; Kepper, 1981; Demicco and Hardie, 1981; Demicco, 1985; Read and Pfeil, 1983; Coniglio and James, 1985; see Section 5.4.3 for further discussion). Secondly, buildups which comprise a significant proportion of inorganic frame-building components (marine cement or pebble aggregates) are designated cement-bearing or pebble-bearing buildups. When these modifying terms are used to classify a particular buildup, they specifically refer to the presence of frame-building marine cement or pebbles, and not inter-framework marine cement or pebbles.

Buildups constructed jointly by frame-building microbial components and mesoscopic skeletal metazoans or calcareous

algae are classified by reference to a S-T-C-SKEL tetrahedral diagram (Fig. 3-2). In this quadri-partite scheme, buildups are designated metazoan-bearing microbial (or calcareous algal-bearing microbial), or microbial-bearing metazoan buildups (or microbial-bearing calcareous algal buildups) depending on whether microbial or metazoan\calcareous algal frame-building components are volumetrically dominant; again it is stressed that these modifying terms only refer to the presence of that component within the framework of the buildup, and have no bearing on their presence or absence within inter-framework components. Microbial-metazoan and microbial-calcareous algal buildups are similarly given designations in accordance with the relative abundance of each microbial, metazoan or calcareous algal constituent. For example, a structure composed of thromboids, *Renalcis*, and minor corals and stromatoids (Pratt and James, 1982, Fig. 20) is designated a *Renalcis*-coral-stromatolitic thrombolite. Other examples of previously described microbial-metazoan and microbial-calcareous algal buildups of Ordovician age are given in Table 3-1, and several examples are described in Chapter 4 (Horizons L and P) and Chapter 5 (section 5.1.3).

This fabric-based classification of microbial buildups compliments the process-based classification recently presented by Burne and Moore (1987, Figs. 1, 2), and is necessitated by the fact that formative processes are commonly very difficult to interpret for ancient microbialites.

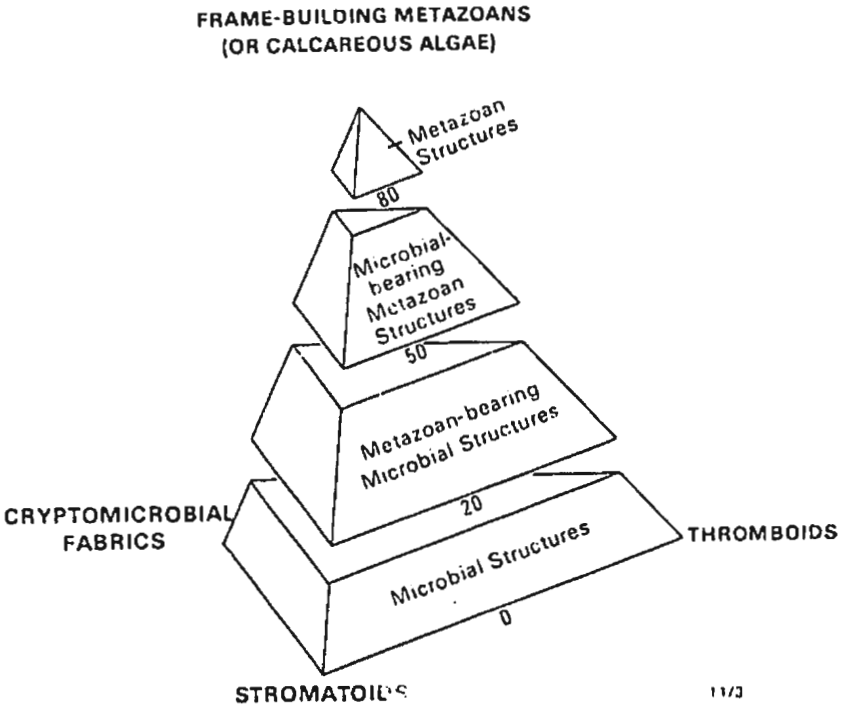

Figure 3-2. Classification of mixed metazoan-microbial buildups based on the volumetric proportion of frame-building mesoscopic constituents.

TABLE 3-1

EXAMPLES OF ORDOVICIAN STROMATOLITIC AND THROMBOLITIC METAZOAN\CALCAREOUS ALGAL BUILDUPS

FORMATION	AGE	DOMINANT FRAMEWORK\BAFFLING COMPONENTS	CLASSIFICATION	REFERENCE
Unnamed "reefal unit"	Late Ordovician (Richmondian)	Stromatoporoids, corals	Coral stromatolites	Sanford (1977) Bolton (1977)
Steinvika Lst	Late Ordovician (Caradocian)	Stromatoporoids, corals, stromatoids, pelmatozoans	Stromatoporoid-coral-stromatolitic-pelmatozoan moundrock	Harland (1981)
Mjosa Lst	Late Ordovician (Caradocian)	Stromatoporoids, corals, stromatoids, Solenopora, pelmatozoans	Stromatoporoid-coral-stromatolitic-Solenopora-pelmatozoan moundrock	Harland (1981)
Fossil Hill Lst	Late Ordovician (Gisbornian)	Corals, stromatoids, stromatoporoids, bryozoans	Coral-stromatolitic-stromatoporoid-bryozoan moundrock	Webby and Packham (1982)
Rockdell	Late Ordovician (Mohawkian)	Bryozoans, stromatoids, pelmatozoans, minor sponges, Solenopora, corals, and calcareous algae	Bryozoan-stromatolitic stromatactoid mud mound	Read (1980, 1982) Ruppel and Walker (1982)
Crown Point	Middle Ordovician (Chazyan)	Stromatoids, ?Solenopora	Solenopora stromatolite	Pitcher (1964)
Antelope Valley (Meiklejohn Peak)	Early-Middle Ordovician (Whiterockian)	?Stromatoids	?Stromatolitic stromatactoid mud mound	Ross and others (1975) Pratt (1982a)
Wahwah	Early Ordovician (Cassinian)	Stromatoids, sponges	Sponge stromatolite	Rigby (1966, 1971)

[continued next page]

TABLE 3-1 (cont.)

FORMATION	AGE	DOMINANT FRAMEWORK\BAFFLING COMPONENTS	CLASSIFICATION	REFERENCE
Fillmore	Early Ordovician (Jeffersonian)	Sponges, Calathium, stromatoids.	Sponge-Calathium-stromatolitic moundrock	Rigby (1966) Church (1974)
McKelligon Canyon (1979)	Early Ordovician (Jeffersonian)	Sponges, Calathium, Pulchrilamina, stromatoids.	Sponge-Calathium-Pulchrilamina-stromatolitic moundrock	Toomey (1970) Toomey and Nitecki
Kindblade (lower horizon)	Early Ordovician (Jeffersonian)	Sponges, Calathium, stromatoids.	Sponge-Calathium-stromatolitic moundrock	Toomey and Nitecki (1979)
Kindblade (upper horizon)	Early Ordovician (Jeffersonian)	Calathium, sponge, stromatoids, thromboids (Renalcis, Epiphyton), Pulchrilamina	Calathium-sponge-stromatolitic-thrombolitic moundrock	Toomey and Nitecki (1979)
Kindblade (algal "miniherms")	Early Ordovician (Jeffersonian)	Stromatoids, sponges, Calathium.	Sponge-Calathium stromatolites	Toomey and Nitecki (1979)
Catoche (Hare Bay)	Early Ordovician (Jeffersonian)	Sponges, Calathium (see Toomey & Nitecki, 1979, p.154-5), thromboids & Renalcis (see Pratt, 1979, p.97-8).	Sponge-Calathium-thrombolitic Renalcis moundrock	Stevens and James (1976) Toomey and Nitecki (1979) Pratt (1979)
Catoche (Port au Choix)	Early Ordovician (Jeffersonian)	Thromboids, Pulchrilamina, sponges, stromatoids.	Pulchrilamina-sponge-stromatolitic thrombolite	Pratt and James (1982, Fig. 17)
Watts Bight (formerly Isthmus Bay) (Green Head)	Early Ordovician (Gasconadian)	Thromboids, Lichenaria, Renalcis, stromatoids.	Lichenaria-Renalcis-stromatolitic thrombolite	Pratt and James (1982, Fig. 20)

[Epochs based on Palmer (1983); Series and Stages based on Ross and others (1982)]

CHAPTER 4

THE THROMBOLITES OF WESTERN NEWFOUNDLAND

4.1 INTRODUCTION

Thrombolites and stromatolites abound within the Cambro-Ordovician platformal carbonates of western Newfoundland. These buildups are beautifully exposed in a series of coastal rock platforms on the southern shore of the Port au Port Peninsula in the south, and on the western side of the Great Northern Peninsula in the north (Fig. 4-1). Although a large portion of this sequence has been extensively dolomitized, especially on the Great Northern Peninsula, many buildups are preserved as limestone, and in these cases their original fabric and microstructure have not been significantly altered since their deposition and initial burial. In this chapter eighteen separate horizons of thrombolites and related stromatolitic and microbial-metazoan buildups on the Port au Port Peninsula, which jointly comprise eighty distinct microbial lithologies, are analysed according to the scheme presented in Chapter 2. Each analysis is concluded by an ecological reconstruction of the microbial and metazoan communities that constructed and inhabited the buildups; symbols used in these reconstructions are given in Appendix A. A summary of the structure, volumetric composition, classification and interpreted origin of representative samples from each buildup is given in Appendix B.

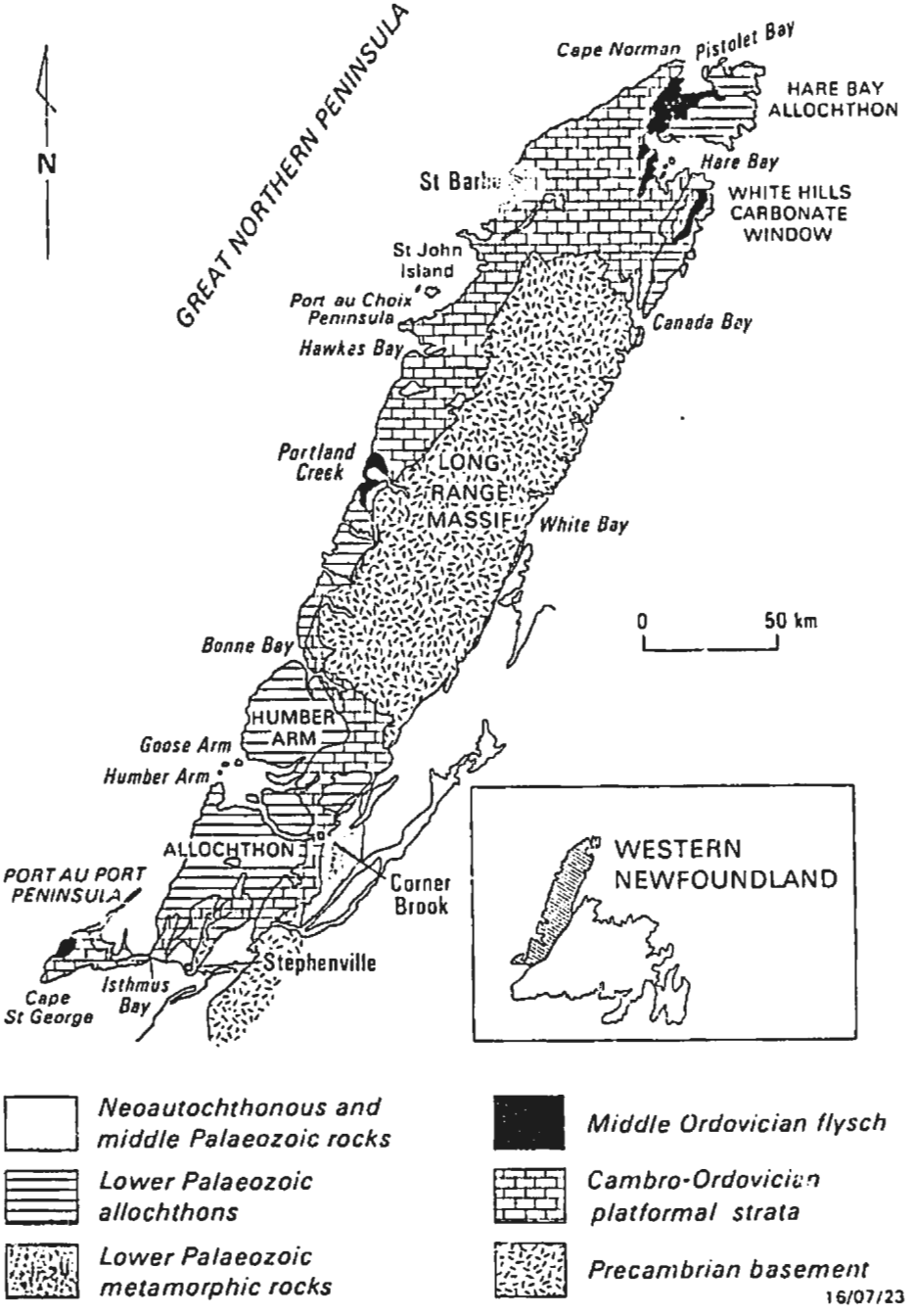

Figure 4-1. Geological map of western Newfoundland showing distribution of Cambro-Ordovician platformal strata (modified after Knight and James, 1987).

4.1.1 REGIONAL SETTING

The Cambro-Ordovician platformal strata in western Newfoundland forms part of the Humber Zone of the Appalachian Orogen, a tectono-stratigraphic subdivision that comprises a partially deformed remnant of the ancient North American continental margin (Williams and Stevens, 1974; Williams, 1979). This margin originally faced the proto-Atlantic Iapetus Ocean to the palaeo-south (Scotese and others, 1979). The platformal strata unconformably overlies crystalline Grenville basement, is overlain by siliciclastic flysch, and both are locally structurally overlain by allochthonous Cambro-Ordovician rocks.

The carbonate-dominated platform strata were deposited on the outer portion of the continental shelf (James and Stevens, 1982; Pratt and James, 1986; Chow and James, 1987), within a tropical, southern equatorial zone (Ross, 1976; Scotese and others, 1979; Deutsch and Prasad, 1987). They form part of an eastward-thickening prism of Lower Cambrian to Middle Ordovician shelf deposits, the central portion (mid shelf or intrashelf basin) of which is buried by middle Palaeozoic strata in the Gulf of St. Lawrence, and the western clastic dominated portion (inner shelf and shoreface) of which is exposed in Quebec and southern Labrador. Platform accretion was terminated by the onset of the Middle Ordovician Taconic Orogeny, an event that records the closing of the Iapetus Ocean and the westward (palaeo-northward) obduction of coeval Cambro-Ordovician slope and deep-water

sediments, volcanics and ophiolitic rocks (the Hare Bay and Humber Arm Allochthons) onto the carbonate platform. Platform margin carbonates were either obliterated by this orogeny or are now obscured by overlying rocks. Autochthonous and allochthonous strata were both subsequently affected by Acadian (Devonian) faulting, and the autochthonous platformal strata are now mostly gently dipping to flat-lying.

Beyond Newfoundland and the Appalachian Orogen, equivalent carbonate-dominated platformal strata form a near-continuous girdle around the North American craton (Holland, 1971; Ross, 1976; Barnes, 1984). These rocks, designated the Sauk Sequence by Sloss (1963), record a major episode of cratonic flooding, platform accretion, and finally a period of extensive cratonic emergence. Similar strata were also deposited coevally in Australia, Siberia, Kazakhstania, China, south Asia, the Middle East, northwest Africa, and South America (Scotese and others, 1979).

4.1.2 CAMBRO-ORDOVICIAN PLATFORM STRATIGRAPHY

The Cambro-Ordovician platformal strata of western Newfoundland has been the focus of much recent stratigraphic, sedimentologic and palaeontologic research, the results of which has been synthesized by Knight (1980), James and Stevens (1982, 1986), James and Hiscott (1982), Pratt and James (1986), Chow and James (1987), Ross and James (1987), Williams and others (1987), Williams and Hiscott (1987), and Knight and James (1987). These rocks have been subdivided

into four groups (Fig. 4-2): the Lower Cambrian Labrador Group, the Middle to Upper Cambrian Port au Port Group, the Lower Ordovician St. George Group, and the Middle Ordovician Table Head Group.

The Labrador Group (Schuchert and Dunbar, 1934) overlies Grenville basement and, locally, latest Proterozoic to Early Cambrian, synrift, terrestial clastics and volcanics (James and Hiscott, 1982; Williams and Hiscott, 1987). It represents the initial phase of platform accretion on the newly formed (ca. 550-570 Ma) northeastern continental margin of the North American craton. It consists of 1) a basal sequence of fluvial to shallow marine sandstones (Bradore Formation) (Hiscott and others, 1984), overlain by 2) open marine shales, siltstones, carbonates and archaeocyathan patch reefs (Forteau Formation) (James and Kobluk, 1978), and 3) an upper regressive sequence of nearshore marine sandstones (Hawke Bay Formation). These latter sandstones result from a relative fall in sealevel along the entire eastern margin of the North American craton (Palmer and James, 1980).

The overlying Port au Port Group (Chow, 1986; Chow and James, 1987) records the first widespread marine transgression onto the lower Palaeozoic North American craton in this region; these sediments were deposited on the outer portion of the continental shelf, whereas earlier sedimentation was restricted to the margin of the craton. This group, comprising the March Point, Petit Jardin and Berry Head Formations (Fig. 4-2), locally records three large-scale sedimentary cycles or "Grand Cycles" (Chow and James, 1987).

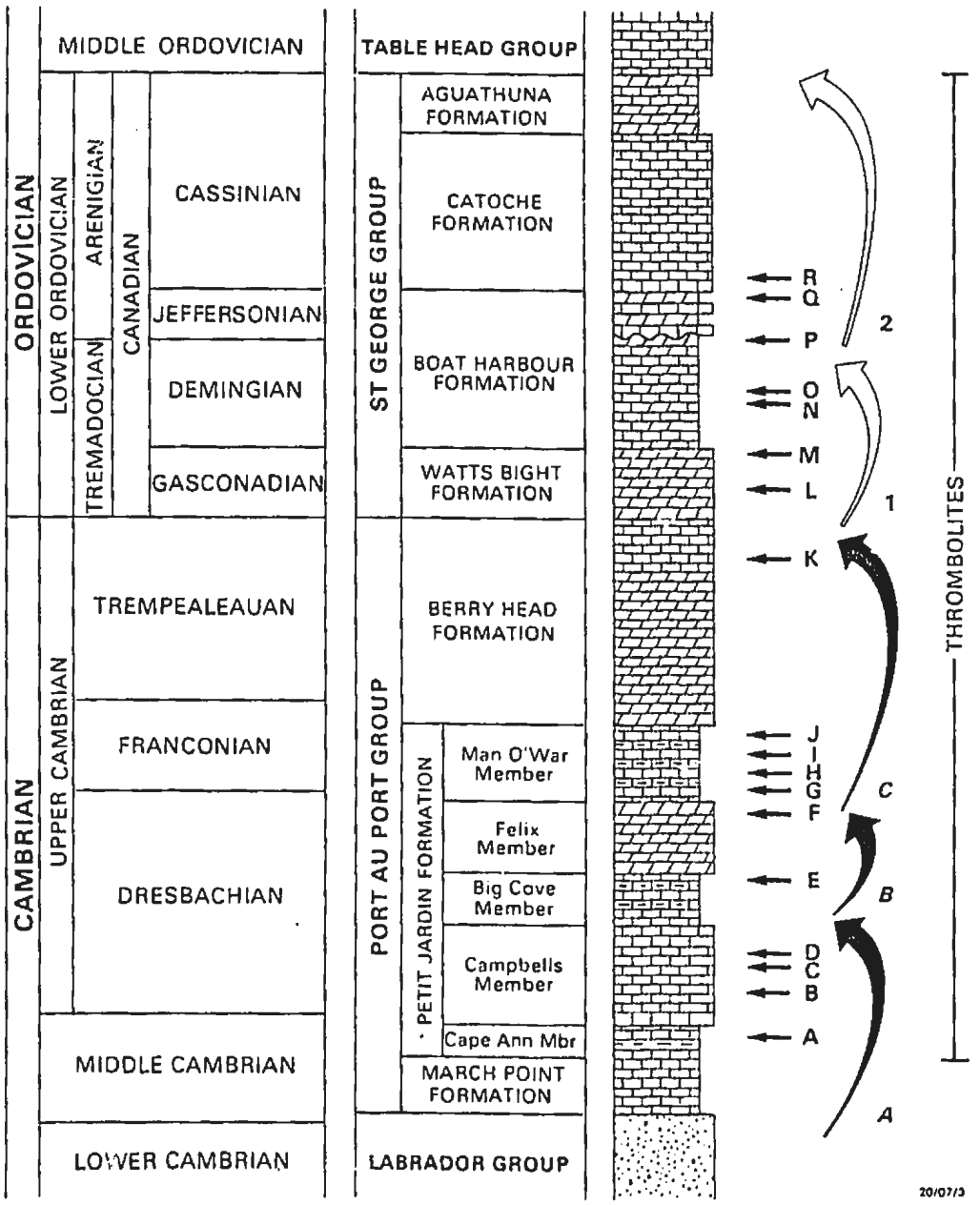

Figure 4-2. Composite stratigraphic section of the Cambro-Ordovician platformal strata of western Newfoundland (after Chow and James, 1987; Knight and James, 1987). Arrows A to R indicate the thrombolite horizons analysed in this study. Cycles *A, B, C* denote Cambrian Grand Cycles, and Cycles 1 and 2 denote Ordovician megacycles as discussed in text.

Each cycle consists of: 1) a lower, recessive-weathering, shaly-half cycle primarily composed of parted limestone and shale, and 2) an upper, resistant-weathering, carbonate half-cycle primarily composed of ooid grainstone and laminated carbonate mudstone. These cycles are interpreted to result from: 1) a rapid marine transgression, which inundated the platform with shoreward-derived siliciclastic muds and resulted in the development of muddy tidal flats seaward of a shallow and narrow intrashelf basin, and 2) the gradual development of ooid shoal complexes which encroached shelfward onto the tidal flats and intrashelf basin in response to slowed transgression and waning of siliciclastic sediments (Chow and James, 1987). Thrombolites first appear in the Middle Cambrian Cape Ann Member of the Petit Jardin Formation, and thereafter occur apparently equally in both shaly and carbonate half-cycles (Chow, 1986).

The St. George Group (Schuchert and Dunbar, 1934; Knight and James, 1987) is a succession of limestones, dolostones and minor calcareous and dolomitic shales which accumulated near the outer edge of the shelf. It comprises four rock units (the Watts Bight, Boat Harbour, Catoche and Aguathuna Formations; Fig. 4-2) which form two unconformity-bound megacycles (Knight and James, 1987). Each megacycle is characterized by: 1) a basal peritidal facies, 2) a middle subtidal facies, and 3) an upper peritidal facies. The lower megacycle comprises the Watts Bight and most of the Boat Harbour Formation, and terminates at a subaerial exposure unconformity near the top of the Boat Harbour Formation. The

upper megacycle comprises the upper part of the Boat Harbour Formation, and the Catoche and Aguathuna Formations. These megacycles probably reflect eustatic sea level fluctuations (Knight and James, 1987) across a shallow shelf studded with small, laterally accreting, tidal flat islands and banks (Pratt and James, 1986). Thrombolites occur in all rock units of the St. George Group, but are larger and more abundant in the middle subtidal facies of each megacycle; that is, the upper portion of the Watts Bight Formation, and the entire Catoche Formation. The St. George buildups are frequently of mixed microbial and metazoan origin (Pratt, 1979; Pratt and James, 1982); lithistid corals (*Lichenaria*) are common in several mound horizons in the lower megacycle, whereas numerous archaeoscyphiid sponges, rare receptaculids (*Calathium*) and rare problematic spicular organisms (*Pulchrilamina*) occur in mounds in the upper megacycle.

The Table Head Group (Schuchert and Dunbar, 1934; Klappa and others, 1980) records the final phase of accretion and subsequent collapse of the platform at the onset of the Middle Ordovician Taconic Orogeny. It comprises a deepening shelf through slope to basinal sequence of 1) local, peritidal limestones and dolostones, 2) subtidal, thinly bedded, bioturbated limestones and sponge bioherms (Klappa and James, 1980), 3) slump-folded bioclastic limestones, ribboned limestones and shales, 4) euxinic black shales, and 5) black shales and carbonate breccia-conglomerates (Klappa and others, 1980; Ross and James, 1987). Thrombolites are unknown in this sequence.

The thrombolites and related microbial buildups analysed in this study occur within the Petit Jardin and Berry Head Formations of the Port au Port Group, and the Watts Bight, Boat Harbour and basal Catoche Formations of the St. George Group (Horizons A to R, Figs. 4-2, 4-3). Analysis of sponge-rich mounds within the Catoche Formation is beyond the scope of this study. Thrombolites in the overlying Aguathuna Formation were considered unsuitable for detailed analysis since they are relatively uncommon, generally thin and poorly differentiated, and are almost entirely pervasively dolomitized (Pratt, 1979). The thrombolite horizons selected for analysis are representative of the total spectrum of thrombolites within the Cambro-Ordovician platformal strata, and although most are composed of limestone, several dolomitized examples have also been included.

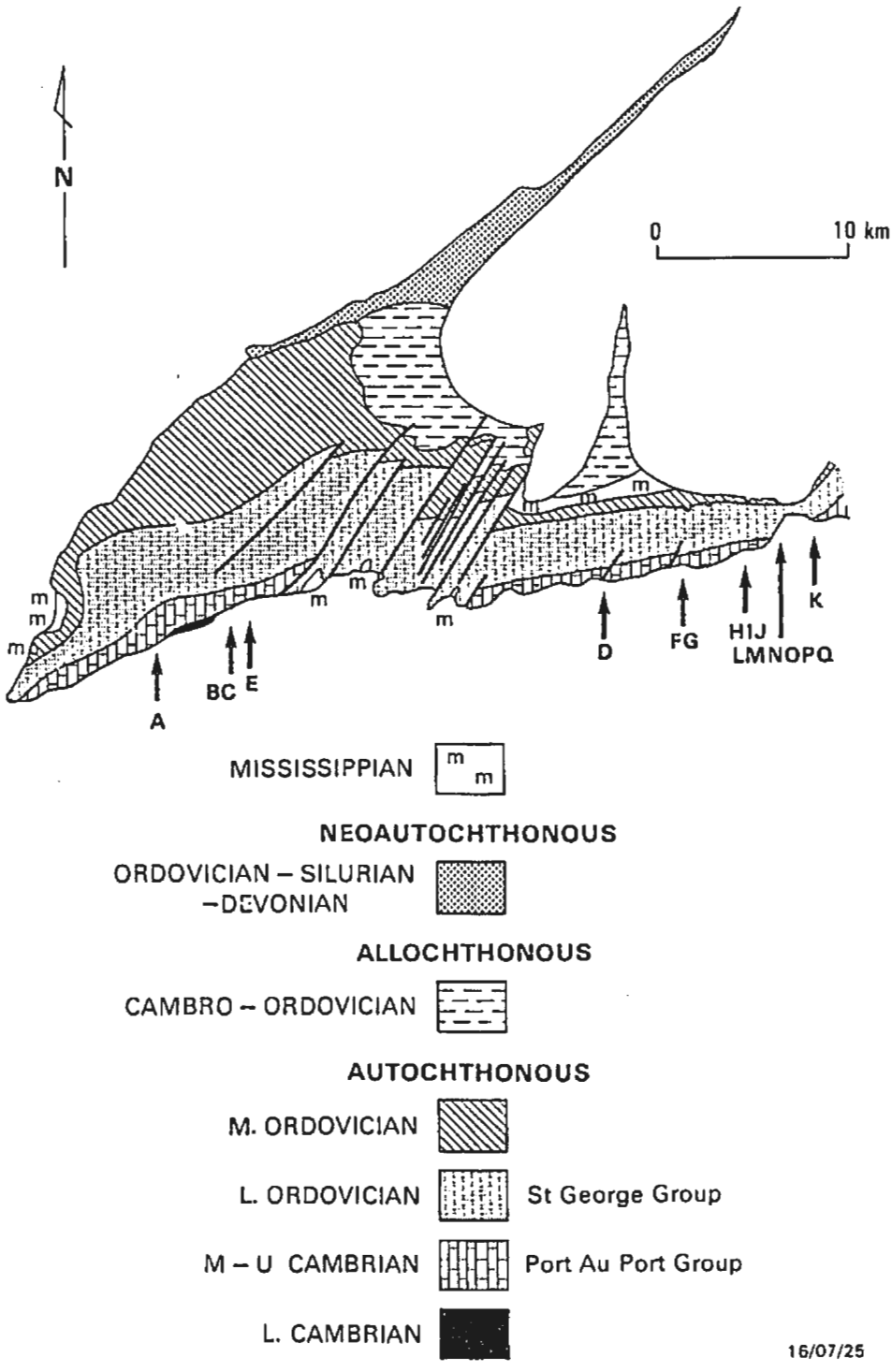

Figure 4-3. Geologic map of the Port au Port Peninsula, western Newfoundland, showing location of thrombolite horizons analysed in this study (modified from James and Stevens, 1982; Chow, 1986).

4.2 HORIZON A

CAPE ANN THROMBOLITE-STROMATOLITE COMPLEX

A thick thrombolite-stromatolite complex (Fig. 4-4) is spectacularly exposed in the coastal cliff-face 0.5 km southwest of the settlement of Cape St. George on the Port au Port Peninsula. The complex occurs within the Cape Ann Member of the Petit Jardin Formation, and corresponds to Interval 13 of Chow's (1986) Degras Section. The complex is underlain and overlain by thinly interbedded grey, green and red shales, ripple cross-laminated nodular to parted limestone, and pebble conglomerate. Three prominent microbial boundstone beds occur in the shaly sequence immediately beneath the complex, and a fourth occurs in the shaly sequence above (Beds A, B, C and D respectively, Fig. 4-4). The structure of these underlying and overlying boundstones is described separately from that of the main complex.

The thrombolite-stromatolite complex does not occur at the next adjacent exposure of the Cape Ann Member at Marches Point (8.5 km to the east), nor elsewhere on the Port au Port Peninsula (Chow, personal communication 1985). The prominent thrombolite biostrome just below the base of the complex (Bed C, Fig. 4-4), however, has greater lateral continuity and crops out as a series of fault repeated tabular and ellipsoidal bioherms at Marches Point.

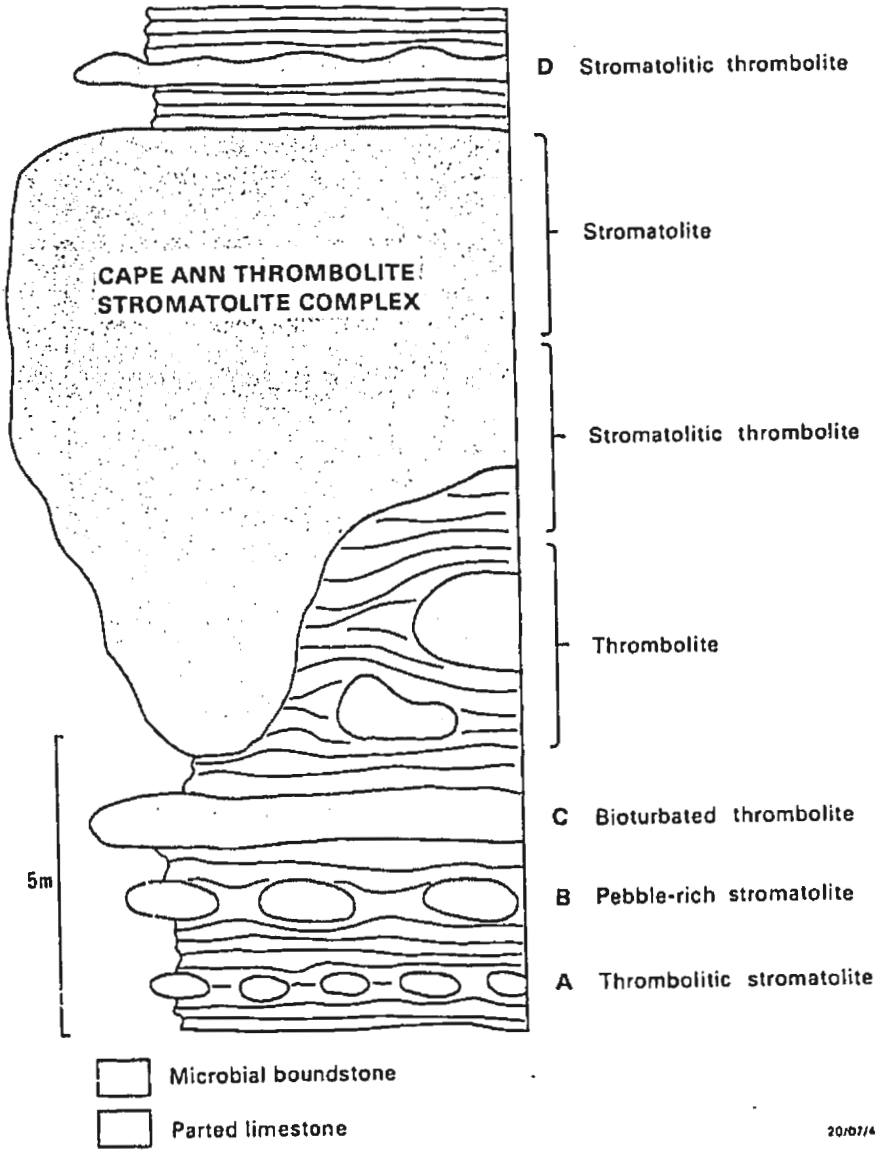

Figure 4-4. Lithological section of the Cape Ann Complex, Horizon A, Cape Ann Member of the Petit Jardin Formation (modified from Chow, 1986).

MEGASTRUCTURE

The complex is approximately 10 m thick and is continuous across the exposed width of the Cape Ann Member, a distance of about 80 m. It comprises a series of large, upwardly expanding, bulbous thrombolite pedestals which progressively coalesce upward to form a laterally continuous stromatolitic thrombolite zone (Plate 1). This zone in turn grades up into a stromatolite zone, the crest of which is truncated by a planar erosion surface (Plate 2-A,B). Lateral variations are not evident within the complex.

Several isolated and closely packed sub-spherical, ellipsoidal and irregularly domed thrombolite bioherms are present between the basal thrombolite pedestals. These bioherms are randomly scattered throughout the enclosing inter-biohermal sediments, are 25-100 cm thick, have either gently convex or hummocky surfaces, and an apparent maximum synoptic relief of 15-35 cm. These basal bioherms, together with the "roots" of the upwardly expanding thrombolite pedestals, are encased and buried in thinly interbedded, ripple cross-laminated, peloid limestone and shale (parted limestone), and minor lenses of pebble conglomerate. These inter-biohermal sediments have locally slumped off the crests and flanks of the bioherms (Plate 2-F). Thin tongues, lenses and irregular pockets of similar sediments also occur within the basal bioherms.

A large thrombolite bioherm is well exposed at the basal eastern edge of the complex (Plate 2-D). It has a smoothly

rounded ellipsoidal shape, is 3.5 m long, 2.7 m wide and 1.6 m high, and is aligned east-west parallel to the cliff-face, tapering to the east. It has a distinct dark-coloured outer rind which is 25 cm thick on the flanks, thins to about 10 cm at the crest, and progressively wedges out around the undersides of the bioherm. This rind consists predominantly of botryoidal marine cement (see Micro-structure) which grew "naked" on the surface of the bioherm whilst exposed on the sea floor. A synoptic relief of 1.6 m is thus evident for the final growth stage of this bioherm. Thin dark crusts of marine cement also occur sporadically on the crest of some of the smaller basal bioherms, and at the margins of the pedestals.

The synoptic relief of the thrombolite pedestals is difficult to determine due to their massive non-bedded nature, the lack of lamination-defined growth surfaces, and subsequent compaction of the inter-biohermal sediments. Local onlapping relationships between the inter-biohermal sediments and the pedestals (Plate 2-E), however, indicate that portions of the pedestals stood at least 30 cm above the adjacent sediment substrate. Elsewhere, however, inter-biohermal sediments abut abruptly against the steep margins of the pedestals and provide no indication of their synoptic relief. The tops of the pedestals, however, expand laterally such that they directly overlie the inter-biohermal sediments or form "bridges" several metres long across the inter-biohermal sediments. These oblique and sub-horizontal thrombolite-on-sediment contacts formed by lateral

accretionary growth of the thrombolite pedestals across the adjacent sediment substrate, thus indicating that during the later stages of their upward growth these pedestals had relatively little topographic relief, perhaps 10-30 cm.

The thrombolite pedestals and bridges coalesce upwards to form a laterally continuous, non-bedded to weakly stylo-bedded, stromatolitic thrombolite zone approximately 3 m thick. Irregular decimetre-sized pockets of thin-bedded peloid limestone and shale occur encased within this zone (Plate 2-C), thus suggesting that the growth surface of this zone was characterized by irregular protuberances and depressions several decimetres in relief.

The upper stromatolitic zone, approximately 4 m thick, comprises thin wavy and linked hemispheroidal stromatolites, several centimetres to several decimetres thick, interspersed with thin lenses and beds of intraclastic peloid grainstone (Plate 2-A). The contact between these stromatolites and the underlying stromatolitic thrombolite lies within inaccessible sea-cliffs, but the contact appears to be gradational over an interval of about one metre. Individual stromatolite heads are 5-30 cm in diameter and have a maximum synoptic relief of 10-15 cm. At the crest of the complex these stromatolites are truncated by a planar palaeo-erosion surface which is riddled with pyritic macroborings cf. *Trypanites* (Plate 2-B). By extrapolating the curvature of the truncated stromatolite layers, it is estimated that at least 10 cm of lithified stromatolite has been eroded from the biostrome. This surface is interpreted to be a subaerial corrosion (karst) or

corrasion surface which was subsequently re-inundated by the sea and bored by marine organisms. It is overlain by a thin veneer of intraclast-peloid-ooid-skeletal grainstone and a thin (5-15 mm) stromatolite layer. The upper surface of the stromatolite forms tiny irregular ridges and pimples which are aligned approximately east-west.

MESOSTRUCTURE

The mesostructural composition of the complex is summarized in Figure 4-5.

Basal Thrombolites: These thrombolites have a finely clotted fabric composed of dark, millimetre-sized, lobate and pendant grape-like thromboids and interstitial lime-mudstone (Plate 3-A,B). They lack bedding and are cut by oblique, highly sutured stylolites. The thromboids are encrusted by equally dark to lighter coloured botryoidal marine cement and hemispheroidal stromatoids (Plate 3-B). These crusts are several millimetres thick and are non geotropic; they only occur on the flanks and undersides of the thromboids. The crests of the thromboids are directly overlain by interstitial lime-mudstone, the accumulation of which evidently pre-dated and limited the growth of the cement and stromatoid crusts. These two types of crusts tend to be mutually exclusive such that within a particular bioherm one type of crust predominates. Composite cement-stromatoid and

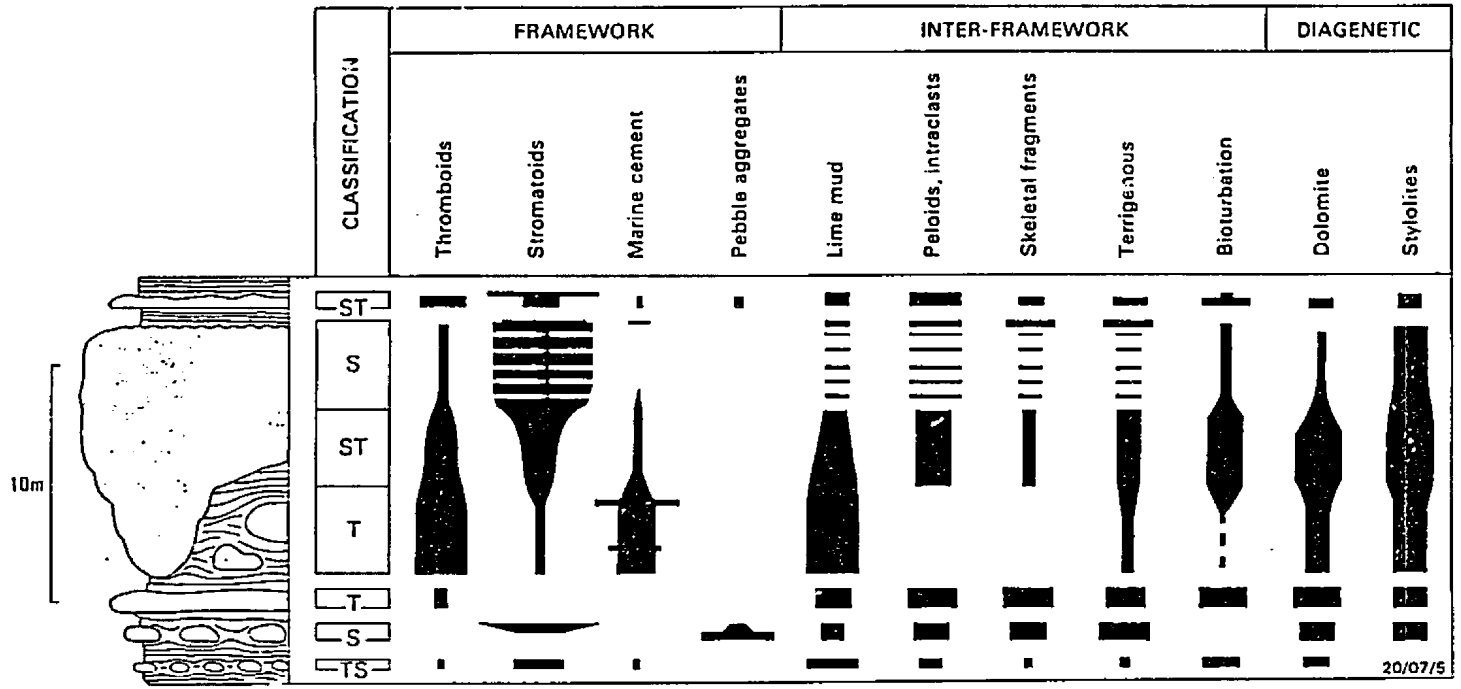

Figure 4-5. Composition and relative abundance of framework, inter-framework and diagenetic components within the Cape Ann Complex, Horizon A.

(?)stromatoid-cement crusts do occur, however, but they can only be definitively identified in thin section (see Microstructure). Furthermore, it is frequently difficult to distinguish between thromboids and encrusting cement or stromatoid layers in slabbed samples. Minor patches of brown dolomite occur throughout the thrombolites, and are particularly prevalent at the margins of the thromboid-cement-stromatoid framework.

Central Stromatolitic Thrombolites: These stromatolitic thrombolites have a more variable and complex fabric composed of: 1) dark thromboids, 2) stromatoids, 3) marine cement (not differentiated in hand samples), 4) detrital sediment, 5) dolomite patches, 6) stylolitic seams, and 7) void and vein filling sparry cement (Plate 4-A,B). A crude horizontal layering is generated by the stylolitic seams and discontinuous stromatoid sheets. The thromboids vary greatly in shape and size from isolated subrounded, lobate and saccate forms 0.5-2 mm in diameter, to grape-like aggregates several centimetres across. They also commonly occur intergrown with stromatoids, and as reworked fragments (microbial corpuscles) within inter-framework sediment. In contrast to the pendant stromatoids within the basal thrombolites, the stromatoids are geotropic and construct three intergradational forms: 1) moderately convex to rarely rectangular columns which are 1-3 cm high and 0.5-1 cm in diameter, 2) isolated and laterally linked hemispheroids 1-3 cm in diameter, and 3) undulose sheets several

millimetres thick and several centimetres long. Stromatoid columns and hemispheroids typically encrust single clusters of thromboids, whereas stromatoid sheets extend across several adjacent clusters of thromboids as well as the intervening patches of detrital sediment. Small interstices within and immediately adjacent to the thromboids are filled by homogenous lime-mudstone, whereas the irregular centimetre-sized pockets between the thromboids and stromatoids comprise weakly laminated or mottled, silty peloid-skeletal wackestone. Numerous burrows are evident within this sediment. Irregular patches and seams of brown microcrystalline dolomite are abundant and appear to have selectively replaced detrital sediment rather than thromboids or stromatoids. Some dolomite is clearly related to late stage solution compaction, either as a stylo-cumulate or stylo-reactant. In many instances thin, dolomite-rich, stylolitic seams form a rim around the margins of the thromboids and stromatoids.

Upper Stromatolites: These stromatolites have a coarse wavy-laminated fabric composed of 1) light coloured, 1-10 mm thick, and 2) episodic dark coloured, less than 1 mm thick, stromatoids (Plate 3-C,D). The stromatoids have a low degree of inheritance, a micro-relief of up to 3 cm, are laterally discontinuous, and are extensively disrupted by dolomite-rich stylolitic seams. Thick light coloured stromatoids locally pinch and swell in thickness to form a series of indistinctly laminated pustular protuberances or columns 2-3 cm high and

0.5-1 cm wide (Plate 3-D). Lenses and layers of intraclastic grainstone within these stromatolites contain abundant crescent-shaped stromatolitic clasts and poorly defined, crudely laminated, stromatoid columns.

MICROSTRUCTURE

Primary microstructures are poorly to moderately well preserved. Most thromboids have been substantially modified by neomorphism, and it is difficult to distinguish between thromboids and encrusting marine cement in both hand specimen and thin-section.

1. Thromboids

The thromboids are subrounded to lobate, 0.5-2 mm in diameter, and commonly coalesce to form cauliflower-like aggregates several millimetres across (Plate 5). Locally they have a saccate or cellular lobate microstructure (Plate 5B), but otherwise they comprise an irregular mosaic of turbid microspar or cryptocrystalline carbonate (massive lobate microstructure) (Plate 5-A,C). They are commonly encrusted by various types of turbid marine cement (Plate 5-A,C,D), but due to extensive neomorphism it is generally difficult to clearly distinguish these two components. This is especially difficult when optical continuity has developed between the neomorphic microspar of the thromboids and the encrusting cement. This type of neomorphic process has been designated **coalescive syntaxial neomorphism** by Mazzullo and Cys (1977).

Detrital silt rarely occurs within the thromboids, but commonly forms pockets between adjacent thromboids, and is a minor constituent of the encasing inter-framework sediment.

2. Stromatoids

Columnar, linked hemispheroidal, and undulose stromatoid layers within the central portion of the complex have a diffuse streaky microstructure (Plate 6-A). The laminae are 100-500 μm thick, laterally discontinuous, and contain numerous tubular borings about 450 μm in diameter. They are delineated by a weak, frequently gradational, textural differentiation and comprise: 1) massive cryptocrystalline calcite, and 2) fine microcrystalline calcite, with or without terrigenous silt and rare silt-sized peloids. Cryptocrystalline laminae are particularly discontinuous and locally grade into a series of disconnected lenses and microclots (striated and grumous microstructures, respectively).

The irregular wavy stromatoids in the upper portion of the complex have a streaky, variously mottled, grumous, silty peloidal or rarely filamentous microstructure (Plate 6-B,C,D). They are several hundred to several thousand microns thick, and are locally disrupted by metazoan burrows 0.5-2 mm in diameter. Peloidal laminae represent (?)filament-trapped detrital layers, and commonly contain 10-25 volume percent terrigenous silt. Grumous laminae, however, are probably predominantly *in situ* precipitates since they:

1) lack recognizable detrital grains and silt, and 2) locally intergrade with erect filamentous microstructures (Plate 6-C,D) and thromboids with massive or saccate lobate microstructure. These stromatoids thus appear to have been constructed by a complex and somewhat poorly differentiated community of sediment-trapping filaments, calcified filaments, and calcified coccoid microbes.

The tiny ridge-like and pimpled stromatoids that encrust the planar erosion surface at the crest of the complex, have an indistinct, streaky, silty and peloidal microstructure (Plate 6-E). The laminae are several hundred microns thick and are episodically interlayered with mamillate crusts of fibrous marine cement, 60-200 μm thick. The ridges and pimples are buried by silty and intraclastic peloid-skeletal-ooid packstone.

3. Marine Cement

Turbid marine cement is a minor constituent of the central and lower portions of the complex, and is particularly prevalent within the ellipsoidal and pedestal thrombolite bioherms at the base of the complex. Cement types present are: 1) divergent-radial botryoids, 2) fascicular-optic botryoids, 3) pendant fibrous-concentric botryoids, 4) fibrous botryoids, and 5) isopachous prismatic rims.

Divergent-radial botryoids are predominant and form non-geotropic mamillate encrustations 0.5-2 mm thick around thromboids (Plates 5-D, 8-A,B) and, less commonly,

interlayered with stromatoids and detrital sediment (Plate 7-A,B). Individual and coalesced fascicular-optic botryoids (Plate 7-C,D), 0.3-2 mm thick, and pendant fibrous-concentric botryoids (Plate 8-A,B), up to 700 μm thick, similarly locally encrust thromboids and stromatoids. The fibrous-concentric crusts are themselves commonly encrusted by divergent-radial mamelons. Coalesced fibrous botryoids form mamillate crusts interlayered with the ridge and pimple-like stromatoids (Plate 6-E) that encrust the grainstone veneer overlying the planar erosion surface at the crest of the complex. Individual crusts are 60-200 μm thick and are locally superimposed one on top of the other. Isopachous rims of prismatic calcite form semi-continuous 50-100 μm thick layers around thromboids (Plate 5-A,C) and columnar stromatoids. In contrast to the more extensive frame-building botryoidal cements, isopachous rims represent the first phase of inter-framework void filling. Marine cement has not been detected in the upper stromatolitic portion of the complex.

Marine cement is the dominant and locally the sole constructional component of the 10-25 cm thick dark crust which partially envelops the large ellipsoidal bioherm at the basal eastern edge of the exposed complex (Plate 2-D). This crust is composed of superimposed botryoids of either divergent-radial or fascicular-optic fabric, together with minor amounts of interlayered lime-mud and stromatoids (Plate 8-C,D). The lime-mud occurs as irregular patches between and overlying the botryoids, and fills tubular borings 500 μm in

diameter that have been excavated into the cement (Plate 8-C). Thin bands of cryptocrystalline carbonate also occur within the botryoids and probably represent detrital lime-mud inclusions. Some cryptocrystalline layers, however, thicken across the crests of the botryoids, and thus almost certainly represent microbial layers; that is, stromatoids. This enveloping crust of marine cement is strikingly similar in both overall morphology and microfabric to the dark encrustations of "radial fibrous marine cement" on foreslope talus blocks in the Permian Capitan Reef Complex, southern New Mexico (Toomey and Babcock, 1983, Figs. 9-1A and B).

5. Detrital Sediment

Detrital sediment within the basal thrombolites comprises homogenous lime mudstone and minor amounts of terrigenous silt and silt-size peloids (Plate 5-C). Inter-framework sediment within the overlying stromatolitic thrombolite comprises bioturbated, silty peloid-skeletal-intraclast wackestone and minor lime or dolomitic mudstone (Plate 4-A,B). This sediment is largely autochthonous; fragments of calcified thromboids (peloids, intraclasts and microbial corpuscles), phosphatic brachiopods, and rare trilobites and *Girvanella* fragments.

UNDERLYING AND OVERLYING BOUNDSTONE BEDS

Bed A: Thrombolitic Stromatolite

This boundstone forms scattered domal bioherms 20-35 cm thick. The upper surface of the bioherms are remarkably smooth and they have a prominent cerebroid fabric in plan view (Plate 9-B). They comprise a framework of relatively dark, indistinctly laminated, irregular stromatoid columns and, particularly near their base, scattered clusters of black, millimetric, lobate and saccate thromboids (Plate 9-A). The columns are 2-10 mm thick, branch and coalesce in vertical and horizontal directions, are partially laterally linked, and commonly coalesce at the surface of the bioherms. They are disrupted by numerous burrows and (?)borings, have ragged and embayed margins, are commonly rimmed by a semi-continuous dark selvage, and are locally encrusted by lobate and saccate thromboids. The columns are encased within burrow-mottled peloidal and intraclastic wackestone. Most peloids and intraclasts within this sediment clearly represent reworked fragments of the columns.

The columns have a variable massive to streaky, mottled and grumous microstructure, and contain scattered terrigenous silt and rare peloids (Plate 9-C,D). Streaky laminae are differentiated by slight variations in colour and crystal size, and have an irregular mamillate form. Mottled microstructures (Plate 9-E) comprise irregular bands, lenses and spherical to tubular patches, approximately 300-450 μm in size, of microcrystalline calcite, and probably result from

extensive bioturbation. The margins of the columns may be either constructional or erosional. Constructional margins are relatively smooth and are rimmed by a semi-continuous 30-100 μm thick cryptocrystalline selvage (Plate 9-D). This selvage indicates that the columns had significant micro-relief (up to a few centimetres) during their growth, and that their flanks were colonized by carbonate-precipitating, perhaps endolithic, microbes. Erosional margins on the other hand, lack selvages and are characterized by numerous ragged embayments, probably the result of rasping and bioturbating organisms or physical erosion. The columns were evidently constructed by weakly laminated, mamillate microbial communities. Although there is no microstructural evidence as to the composition of this community (coccoid or filamentous microbes), poorly laminated mamillate fabrics with low detrital grain content typically result from coccoid-dominated communities (Hofmann, 1973; Gebelein, 1974; Golubic, 1983; Awramik, 1984; Pentecost and Riding, 1986). These columns were encrusted by endolithic microbes and locally lobate colonies of calcified coccoid microbes.

Bed B: Pebble-Rich Stromatolite

This boundstone forms elongate tabular bioherms several metres long and 50-60 cm thick. The bioherms are established on a 15 cm thick layer of edgewise pebble conglomerate in which mesoscopic microbial constructions are absent. These pebbles are locally arranged in a series of fan-like arrays and are encased within silty peloid-skeletal wackestone and

grainstone. This pebble foundation is gradationally overlain by pebble-rich stromatolite in which individual pebbles or groups of pebbles and infiltrated sediment are encrusted by convex columnar stromatoids or linked pseudo-columnar stromatoids (Plate 10-A). Pebbles progressively decrease in abundance in the upper portion of the bioherms which comprises laterally continuous pseudo-columnar stromatoids and scattered, predominantly flat-lying, pebbles. A series of small stromatolite domes with 10-20 cm synoptic relief occur at the crest of the bioherms.

The pebbles comprise laminated, silty lime-mudstone and cross-laminated, very fine sandy peloid grainstone. They are clearly allochthonous with respect to the bioherms and represent clasts of subtidal shelf sediments eroded and deposited by storm waves. The encrusting stromatoid layers have a streaky silty microstructure (Plate 10-B), are laterally discontinuous and 100-500 μm thick. They selectively encrust and cap edgewise pebbles with significant micro-relief (Plate 10-A), and progressively bridge inter-pebble voids and infiltered sediment, thereby binding the pebble framework. The stromatoids are themselves overlain by more edgewise pebbles and successive stromatoid crusts, and thus pebbles and stromatoids jointly construct the framework of the bioherms. Infiltered sediment between the clasts and stromatoids comprises subrounded fine to medium peloids, phosphatic brachiopod shells, abundant terrigenous silt and sand, and minor lime-mud.

Bed C: Bioturbated Thrombolite

This boundstone forms a one metre thick tabular biostrome which breaks up into a series of close-packed subspheroidal bioherms at the extreme western limit of the exposed section. It has a distinctive clotted and mottled fabric composed of very irregular, anastomosing dark thromboids and lighter coloured, extensively burrow-mottled, interstitial sediment (Plate 11-A). The thromboids display a diverse range of shapes and sizes: irregular amoeboid, stubby digitate, prostrate, pendant, cerebroid and lobate forms a few millimetres to several centimetres in size. They have ragged margins and are extensively bioturbated.

The thromboids have poorly defined grumous grading to diffuse streaky, mottled and lobate microstructures (Plate 11-B,C). Terrigenous silt is scarce within the thromboids, but is common in the surrounding inter-framework sediment. This sediment has a variable wackestone-packstone texture and contains a variety of irregular, very fine to coarse sand-sized, lobate and saccate microbial corpuscles, trilobite and phosphatic brachiopod fragments, silty intraclasts, and *Girvanella* fragments. On the basis of its distinctive mesostructure and microstructure, this thrombolite is correlated with tabular and ellipsoidal bioherms at Marches Point, 8.5 km to the east of the Cape Ann Complex.

Bed D: Stromatolite Capped Stromatolitic Thrombolite

This boundstone forms a tabular biostrome within the parted limestone sequence that overlies the complex (Fig 4-4).

It comprises a lower stromatolitic thrombolite, 25-35 cm thick, capped by a stromatolite 5-10 cm thick.

The lower stromatolitic thrombolite comprises poorly defined 0.5-2 cm thick layers of fine digitate and arborescent thromboids, episodically encrusted and draped by partially linked, convex and undulose stromatoid sheets a few millimetres thick (Plate 12-A). The thromboids are 3-15 mm high, and each digit or branch is approximately 200-600 μm thick. They are thus an order of magnitude larger than similarly shaped digitate *Epiphyton* thalli (Riding and Toomey, 1972; Wray, 1977). They have a diffuse grumous microstructure which is partially or locally extensively replaced by turbid microspar. Some thromboids, however, comprise discrete clots of cryptocrystalline calcite, and resemble clotted or rarely saccate *Renalcis* forms (Plate 12-C). Thin arcuate and mamillate layers of fibrous marine cement occur within the thromboids, and also commonly encrust the overlying stromatoids (Plate 12-B). These cement crusts are 20-100 μm thick. The stromatoids have a streaky, diffuse grumous to mottled microstructure and contain scattered grains, lenses and layers of terrigenous silt, peloids and ooids. They are commonly extensively disrupted by metazoan burrows. The thromboids and stromatoids are encased within burrow-mottled, silty peloid packstone and wackestone which contains scattered pelmatozoan fragments and intraclasts. Most of the smaller crescent and lath-shaped intraclasts clearly represent autochthonous stromatoid fragments, whereas the larger rounded pebbles comprise silty peloid grainstone

and are allochthonous with respect to the biostrome. These larger clasts are frequently encrusted by fibrous marine cement and thromboids or stromatoids.

The mesoscopic fabric of this stromatolitic thrombolite is similar to the fabric of the Upper Triassic "Cotham Landscape Marble" described by Hamilton (1961), and Wright and Mayall (1981). The arborescent structures within these Triassic structures, however, are composed of "micrite laminations 10-50 μm thick, which coat tubes of *Microtubus communis* Flügel 1964" (Wright and Mayall, 1981, p.81). Although the organism that formed these microfossils is unknown, Flügel (1964) thought it could be a small serpulid worm. In contrast, the arborescent structures (thromboids) within the present Bed D lack tubular forms and are interpreted as calcified colonies of coccoid microbes (?cyanobacteria), analogous to the clotted and saccate *Renalcis*-like forms described by Pratt (1984).

The upper stromatolite cap of Bed D comprises convex columnar and linked hemispheroidal stromatoids which are 2-6 cm in diameter and have 2-3 cm synoptic relief. They have a micro-fenestrate, streaky microstructure comprised of relatively thick (0.5-5 mm) grumous, diffuse grumous grading to massive, or micro-streaky laminae (Plate 12-D,E). The laminae are commonly disrupted by sediment-filled burrows, and micro-fenestrae probably represent cement-filled borings.

ORIGIN AND PALAEOECOLOGY

The Cape Ann Complex was constructed by a succession of distinct microbial communities, each characterized by a specific composition and sediment-forming activity (Fig. 4-6). The interaction of these communities with processes of physical sedimentation, marine cementation and metazoan activity generated a diverse spectrum of microstructures, mesostructures and megastructures. Subsequent diagenesis has generally accentuated, rather than obscured, the complexity of these structures.

The complex formed on a tranquil subtidal shelf otherwise characterized by the deposition of very fine peloid grainstone, lime-mudstone, shale and episodic storm conglomerates. This environment was subsequently significantly modified, however, by the progressive buildup of the complex. The interpreted changes in energy level and water depth are shown in Figure 4-6 (columns 8 and 9).

The columnar bioherms of Bed A were constructed by an indistinctly laminated, mamillate, probably coccoid-dominated microbial community. The columns had a few centimetres relief and their flanks were probably encrusted by endolithic microbes and scattered calcified coccoid colonies. They were disrupted by burrowing and (?)boring organisms, and incipiently lithified fragments were eroded from the columns and incorporated into mud-rich sediments between the columns. These sediments contain little allochthonous material. The bioherms probably stood well above the level of the

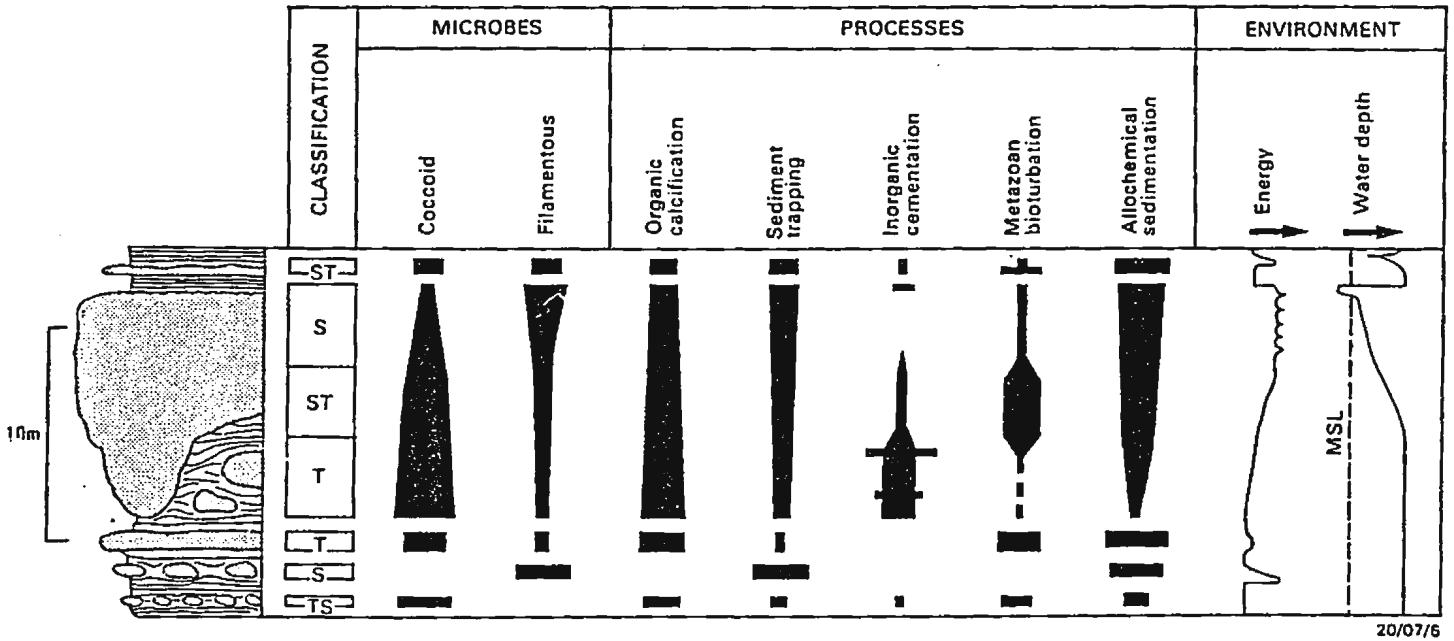

Figure 4-6. Interpreted microbial composition, sediment-forming processes and environment of deposition of the Cape Ann Complex, Horizon A.

surrounding sediment substrate, and were subsequently buried and draped by fine grained subtidal shelf sediments. A reconstruction of the bioherms is shown in Figure 4-7.

Bed B was constructed by laminated, sediment-trapping (?)filamentous mats on a foundation of storm-deposited pebble conglomerate. Storms continued to wash pebbles onto the bioherms where they were rapidly encrusted and bound by these mats. The sediment substrate surrounding the bioherms, however, was evidently swept clear since pebbles do not occur in the adjacent inter-biohermal strata. The bioherms comprise predominantly allochthonous material trapped and bound by the mats (pebbles, peloids, lime-mud, terrigenous silt and sand, and phosphatic brachiopod fragments), and they show no evidence of bioturbating metazoans. Perhaps an infauna was precluded from the bioherms and adjacent shelf sediments by frequent storm disturbance. A reconstruction of the bioherms is shown in Figure 4-7.

Biostrome Bed C was constructed by an extensively bioturbated microbial community. Its variegated grumous, mottled, and lobate microstructure suggests that this community was dominated by poorly calcified coccoid microbes. However, the presence of filamentous microbes is confirmed by the occurrence of *Girvanella* fragments within the inter-framework sediment. In addition to soft-bodied burrowing metazoans, the biostrome was probably inhabited by trilobites and perhaps brachiopods. It grew in a slightly turbulent subtidal environment in which the microbial framework was episodically abraded and eroded, and into which

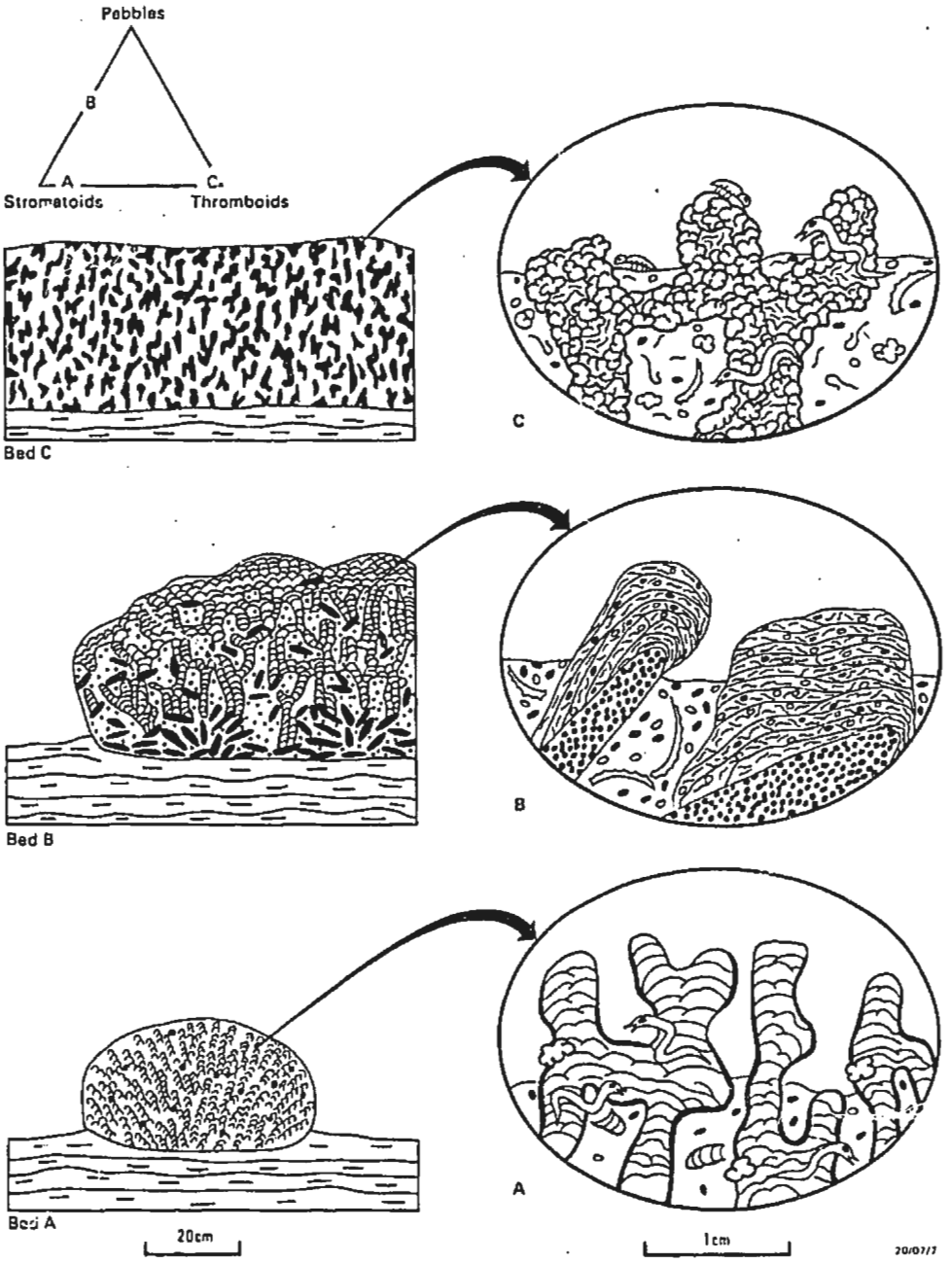

Figure 4-7. Schematic reconstructions and triangular plot of main framework components of Beds A, B and C beneath the Cape Ann Complex, Horizon A.

terrigenous silt and carbonate intraclasts were washed. A reconstruction of the biostrome is shown in Figure 4-7.

Following a relatively brief period of renewed fine terrigenous and carbonate shelf sedimentation, a prolonged period of microbial buildup ensued. Distinct growth stages within this buildup reflect an ecologic zonation of microbial and, to a lesser extent, metazoan communities that developed in response to the progressive buildup and shoaling of the complex. Reconstructions of these growth stages are shown in Figure 4-8.

Stage 1. The basal thrombolite bioherms were constructed by lobate, cauliflower-like colonies of calcified coccoid microbes. These colonies were encrusted by botryoidal marine cement and, less frequently, pendant layers of sediment-trapping, probably filamentous, microbes. This cement-encrusted, microbial framework was infilled by carbonate mud. The bioherms grew in a tranquil, probably relatively deep, subtidal environment and were apparently devoid of metazoans. Since the bioherms are not confined to specific time horizons, they clearly grew in different places at different times. Similarly, many bioherms ceased to grow and were buried by fine current and suspension-laid sediments at different times. Locally these sediments slumped off the crest of the buried bioherms. Some bioherms, however, continued to grow and constructed massive bulbous pedestals, the crests of which remained permanently above the sediment substrate. The bioherms had varible relief during their growth; some stood as high as 1.6 m, but most were probably

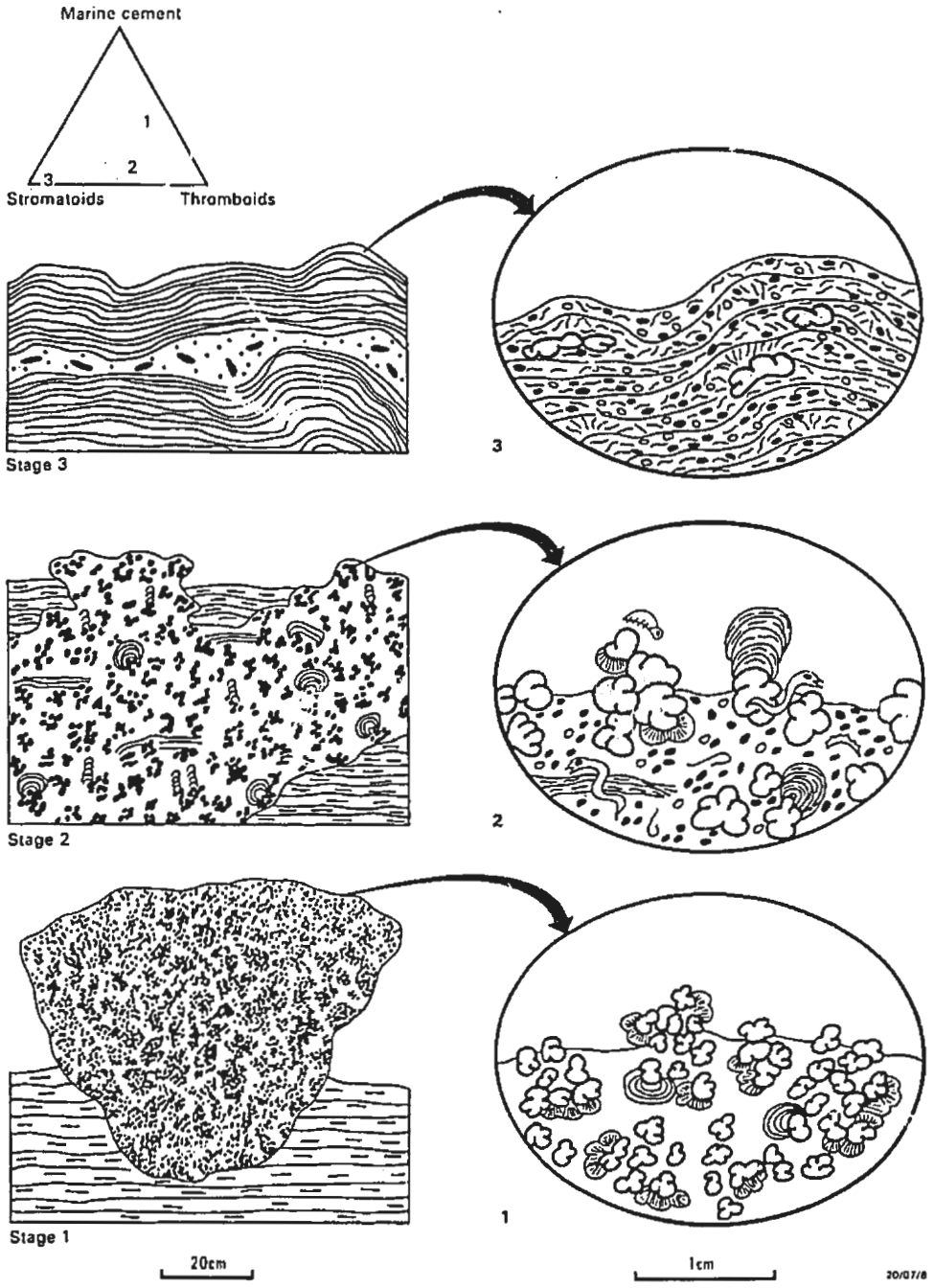

Figure 4-8. Schematic reconstructions and triangular plot of main framework components of growth Stages 1 to 3 of the Cape Ann Complex, Horizon A.

20-50 cm high. During periods of reduced microbial activity and little or no sediment influx, some bioherms were encrusted by relatively thick layers of botryoidal marine cement. Thus the initial growth of the complex was characterized by sporadic fluctuations in 1) the growth of coccoid microbial communities, 2) the precipitation of marine cement, and 3) the accumulation of fine-grained current and suspension-laid sediments.

Stage 2. The stromatolitic thrombolites in the central portion of the complex were constructed by two co-occurring, either mutually isolated or encrusting, microbial communities: 1) lobate colonies of calcified coccoid microbes, and 2) hemispheroidal, convex columnar and undulose mats of unknown composition. Irregular pockets and lenses of muddy carbonate sand accumulated between, and episodically buried, these communities. This detritus was predominantly generated by physical and biological erosion of the microbial framework, and was extensively bioturbated by soft-bodied metazoans. Skeletal metazoans (brachiopods and trilobites) were relatively scarce. The stromatolitic thrombolites formed laterally and vertically expanding bridges between the thrombolite pedestals of Stage 1, and culminated in the construction of a laterally continuous biostrome. There was a progressive decrease in the accumulation of fine-grained current and suspension laid sediments during this stage, such that thin-bedded inter-biohermal sediments progressively gave way to small lenses and pockets of intra-biostromal sediments which accumulated in irregular depressions at the surface of

the biostrome. The central portion of the complex was thus characterized by: 1) vigorous growth of co-occurring coccoid and unknown microbial communities, 2) increased generation and accumulation of autochthonous carbonate sand and mud, 3) increased abundance of bioturbating soft-bodied and, to a lesser extent, skeletal metazoans, 4) reduced precipitation of marine cement, and 5) decreased accumulation of fine grained current and suspension-laid sediments. These changes reflect the progressive buildup and shoaling of the complex to form a shallow subtidal shoal or reef within moderately turbulent waters.

Stage 3. The stromatolites in the upper portion of the complex were constructed by a poorly differentiated mat-like community of 1) sediment-trapping filaments, 2) calcified filaments, and 3) calcified coccoid microbes. They were inhabitated by a small population of soft-bodied burrowing metazoans, and perhaps rare trilobites. They built thin, gently domed biostromes of low relief, and were episodically eroded and buried by sheets of intraclastic peloidal sand and gravel. This portion of the complex was thus characterized by 1) vigorous growth of laterally extensive, filamentous-coccoid mats, 2) a reduced metazoan population, and 3) episodic erosion and reworking of the lithified mats. It probably represents a shallow subtidal to partially emergent reef flat which was episodically swept by storm waves.

Stage 4. Growth of the complex was terminated by a relative fall in sea-level and subaerial exposure, at which

time the crest of the complex was truncated by a planar (?)karst erosion surface.

Stage 5. The eroded complex was bored by marine organisms and buried by a veneer of intraclast-peloid-ooid-skeletal sand. This sand was stabilized by (?)filamentous microbial mats and thin mamillate crusts of fibrous marine cement, prior to the renewed deposition of fine-grained carbonate and terrigenous shelf sediments.

The Cape Ann Complex thus records an ecologic zonation of microbial communities which progressively constructed an upward shoaling thrombolite - stromatolitic thrombolite - stromatolite reef. This reef grew on an open marine shelf which was rimmed by an ooid shoal complex (Chow, 1986; Chow and James, 1987).

Boundstone Bed D was constructed by arborescent colonies of calcified coccoid microbes which were episodically encrusted by sediment-trapping filamentous mats and, less commonly, thin crusts of fibrous marine cement. Muddy carbonate sand and edgewise pebbles accumulated between these colonies, and similar material was also trapped and bound by the encrusting filamentous mats. Most of this detritus was probably generated by physical and\or biological erosion of the partially lithified microbial communities (lime-mud, irregular peloids and stromatolitic clasts). Terrigenous silt and carbonate pebbles, however, were washed onto the biostrome from the surrounding subtidal shelf. The biostrome was extensively burrowed by soft-bodied metazoans, and its surface was possibly colonized by a small number of attached

pelmatozoans. Following a brief hiatus, or possibly a rapid fall in sea-level, the biostrome was encrusted by relatively thick stromatolitic mats of unknown composition. The biostrome was subsequently buried by fine-grained shelf sediments. A reconstruction of the biostrome is shown in Figure 4-9.

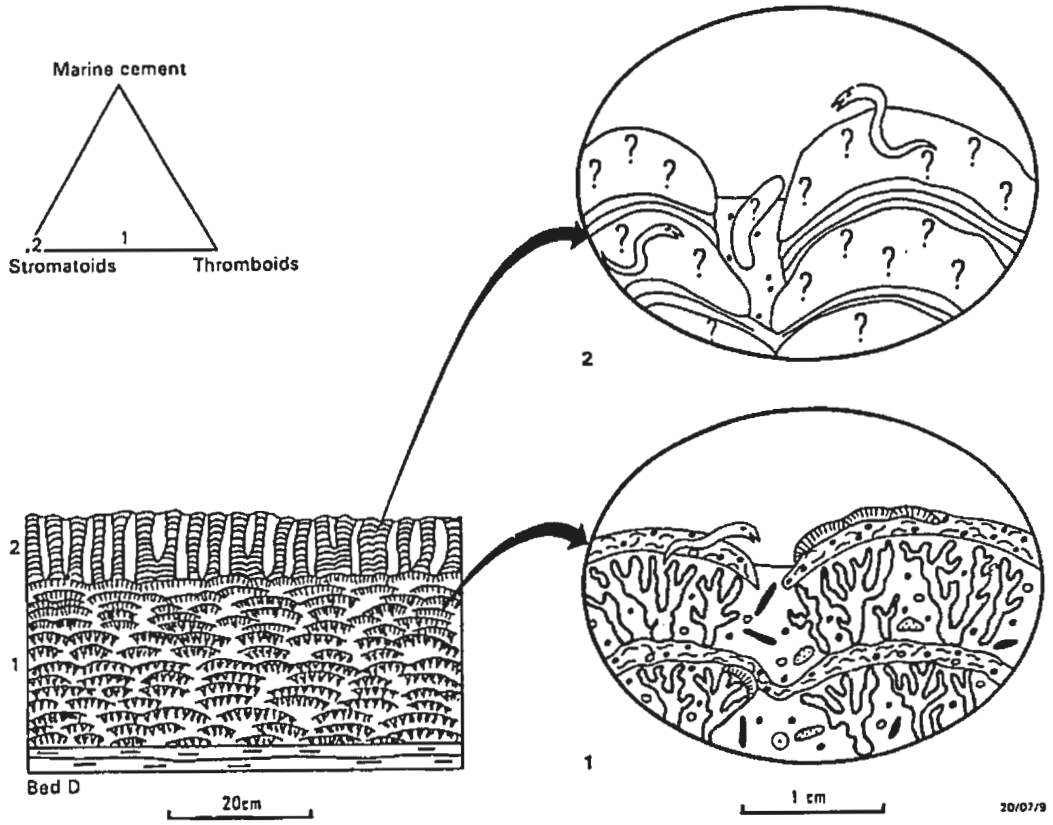

Figure 4-9. Schematic reconstruction and triangular plot of main framework components of Bed D above the Cape Ann Complex, Horizon A.

4.3 HORIZON B

NODULAR AND DIGITATE THROMBOLITE

This thrombolite occurs within a predominantly oolitic limestone sequence in the lower part of the Campbells Member of the Petit Jardin Formation, to the east of Marches Point (Fig. 4-10; interval 6 of Chow's 1986 March Point Section).

MEGASTRUCTURE

The thrombolite forms a gently to strongly mounded biostrome 70-100 cm thick (Plate 13-A). Irregular bulbous he. ds at the top of the biostrome have 30-40 cm apparent synoptic relief (Plate 13-B). At the eastern (present seaward) edge of the exposed sequence, the upper portion of the biostrome breaks up into a series of spheroidal bioherms. Depressions between the mounded forms, bulbous heads, and isolated bioherms are filled by thinly interbedded and nodular skeletal lime-wackestone and red argillaceous dolomitic limestone. The crests of the mounds and bulbous heads commonly protrude above these sediments, and are flanked by lenses of flat-pebble conglomerate. The biostrome is underlain by thin-bedded, fine ooid grainstone, and wavy to columnar laminated stromatolite biostromes, and is overlain by laminated and desiccation-cracked lime-mudstone.

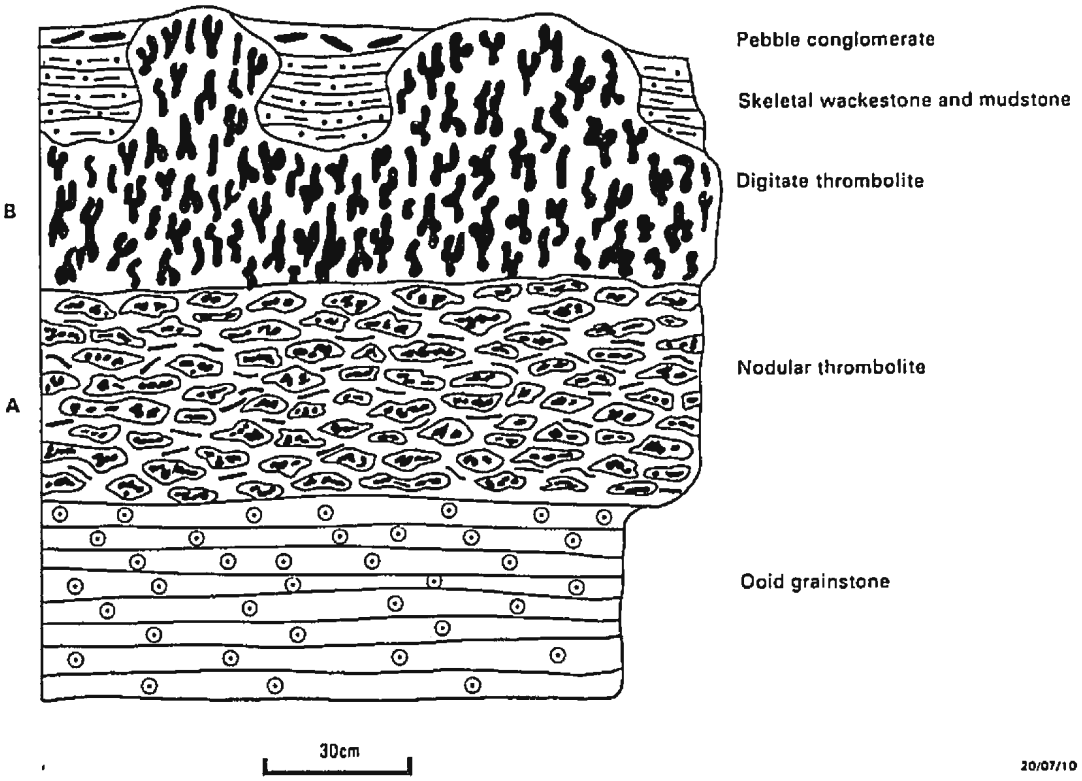

Figure 4-10. Lithological section of Horizon B, Campbells Member of the Petit Jardin Formation.

MESOSTRUCTURE

The biostrome comprises two distinct zones (Plate 13-A): 1) a lower nodular thrombolite, approximately 40 cm thick, and 2) an upper digitate thrombolite which pinches and swells in thickness from 30 to 60 cm. The lower nodular thrombolite comprises irregularly rounded thrombolite nodules, 2-5 cm thick and up to 20 cm long, separated by thin seams of argillaceous and silty dolomitic limestone. The thrombolite nodules are composed of ragged amoeboid and lobate thromboids, 1-10 mm in size, separated by burrow-mottled lime-mudstone and wackestone (Plate 13-D). The ragged nature of the thromboids is largely the result of bioturbation. The argillaceous and silty seams between the nodules pinch out into a series of irregular stylolites, and they commonly enclose tiny "eyes" of thrombolitic material. These seams are clearly solution-compaction features which have cannibalized a previously laterally continuous thrombolite.

The upper digitate thrombolite has an indistinct mottled and clotted fabric and contains abundant stylolites and wispy seams of red argillaceous and silty dolomitic limestone (Plate 13-C). Although individual mesoscopic components generally cannot be identified on outcrop surfaces, irregular digitate and amoeboid thromboids, and interstitial patches of bioturbated skeletal wackestone are poorly differentiated on polished and etched slabbed surfaces (Plates 13-E). Digitate thromboids are sub-circular in cross section, 3-10 mm wide, and range from relatively straight vertical forms to

irregular stubby sub-vertical and amoeboid forms. They have an anastomosed and rarely furcate style of branching (see Hofmann, 1969), a mottled to indistinctly laminated internal fabric in which dark lobate and saccate bodies are scattered (Plate 13-E), and in places a weakly defined selvage. They are commonly replaced by patches of clear and light brown spar.

MICROSTRUCTURE

Primary microstructures are generally moderately well preserved, with the exception of the digitate thromboids in the upper portion of the biostrome.

1. Thromboids

The ragged amoeboid thromboids within the lower nodular thrombolite have a complex variegated microstructure consisting of: 1) patches of massive, mottled, grumous and spongeous silty lime-mud, 2) filamentous to grumous bush-like structures, and 3) indistinctly spherulitic lobate micro-structures (Plate 14-A,B). The bush-like structures are 1-3 mm high and commonly display a radiating, arborescent or lace-like network of cryptocrystalline rods or hollow tubules (Plate 14-D,E). These rods and tubules are 10-30 μm in diameter and up to 300 μm long, and most likely represent entire calcified filaments or impregnated and encrusted filamentous sheaths comparable to *Hedstroemia* (H. Hofmann,

personal communication, 1989). The filamentous bushes have either upright, prostrate or pendant growth forms. In transverse section, they appear as close-spaced circular and hollow microclots (Plate 14-D), a structure resembling grumous microstructure. This apparent grumous microstructure is commonly enhanced by the partial replacement of the bushes by turbid microspar. Minor amounts of terrigenous silt occur between the individual filaments within the bushes, and pockets of silty peloidal lime-mud occur between the bushes.

The dark lobate and saccate bodies identified in slabbed samples (see Plate 13-E) have an indistinct spherulitic lobate microstructure, and are accordingly interpreted as (?)bacterial precipitates within degraded coccoid colonies. In view of the fact that some of these spherulitic structures are encrusted by non-degraded calcified filamentous bushes, this interpretation implies that the coccoid colonies were more susceptible to degradation than the encrusting filamentous bushes.

Silty sediment between the filamentous and spherulitic structures has a massive to diffuse grumous, mottled, or rarely diffuse streaky microstructure. These sediments are riddled with tubular cement-filled borings 250-450 μm in diameter, and are cut by irregular wedge-shaped cracks (Plate 14-A). These cracks are filled by microcrystalline cement, and only rarely extend beyond the thromboids into the surrounding inter-framework sediment; they possibly result from the dehydration and shrinkage of gelatinous organic mucilage which surrounded the filamentous and coccoid

colonies. Terrigenous silt, peloids and rare pelmatozoan and brachiopod fragments were trapped within this sticky mucilage. This mucilage was probably also the site of extensive *in situ* carbonate precipitation.

The digitate and amoeboid thromboids in the upper portion of the biostrome have a silty crypto- to micro-crystalline, massive or diffuse streaky microstructure, together with minor poorly preserved saccate lobate and grumous microstructures (Plate 15-A,B,C). The thromboids have been extensively replaced by very fine to coarse sparry calcite and dolomite. They commonly have poorly defined margins and appear to have suffered extensive bioerosion. Some of the thromboids are cut by thin wedge-shaped shrinkage cracks similar to those within the thromboids in the underlying nodular thrombolite.

Small isolated pyritic thromboids commonly occur within the detrital metazoan-rich sediments in the upper digitate thrombolite. Their microstructure is comparable to saccate lobate microstructures, except that their saccate form is defined by pyrite-enriched walls. This pyrite was probably precipitated as a result of the degradation of lobate coccoid colonies by sulphate-reducing bacteria (Thomsen and Vorren, 1984). Although some of these pyritic structures appear to be *in situ* constructions, many are clearly reworked fragments of the digitate framework. Pyritic structures also encrust pelmatozoan fragments within the inter-framework sediment, and rarely form pendant grape-like growths within voids sheltered by these fragments (Plate 15-D).

2. Stromatoids

Rare stromatoid layers occur within the (?)mucilage-bound silty sediments between the filamentous and spherulitic microstructures in the lower nodular thrombolite. They comprise indistinct 100-500 μm thick layers of massive to diffuse grumous cryptocrystalline calcite and silt-rich laminae, and are cut by borings, sediment-filled burrows and shrinkage cracks.

3. Detrital Sediment

Detrital sediment in the lower nodular thrombolite consists of burrow-mottled lime-mud and minor amounts of terrigenous silt, tubular and rod-like fragments of calcified filaments, and rare pelmatozoan and brachiopod fragments (Plate 14-A,B). In contrast, detrital sediment within the upper digitate thrombolite contains abundant pelmatozoan plates, fragments of pyritic thromboids, minor phosphatic brachiopod fragments, terrigenous silt, and rare ooids and trilobite fragments (Plate 15-C,D). This sediment is extensively bioturbated, and has a wackestone-packstone texture. The pelmatozoan plates (?eocrinoids) have an elongate straight to curved shape, are 60-250 μm wide and up to 3.5 mm long. They are commonly aligned in an edgewise manner between the digitate thromboids, and are invariably surrounded by syntaxial calcite cement. Many of the burrows and shelter voids

within this sediment are filled by radiaxial calcite cement (Plate 15-C).

ORIGIN AND PALAEOECOLOGY

This biostrome displays an abrupt change from a basal, low relief, nodular thrombolite constructed by abundant bushes of calcified filaments and lobate coccoid colonies, to a mounded biostrome constructed by digitate structures of unknown microbial composition. This digitate framework was evidently chiefly constructed by *in situ* carbonate precipitation, rather than the trapping and binding of detrital particles. The basal nodular thrombolite grew in a tranquil, probably relatively deep, subtidal environment in which thin discontinuous layers of terrigenous silt and clay episodically accumulated. The thrombolite was extensively bored and burrowed by small soft-bodied metazoans, and the disintegration of calcified filaments probably generated significant amounts of carbonate mud.

The upper digitate portion of the biostrome was probably colonized by numerous attached, high-level suspension feeding pelmatozoans, soft-bodied burrowing metazoans and possible minor numbers of low-level suspension feeding inarticulate brachiopods. This portion of the biostrome grew in a moderately high energy, probably shallower, subtidal environment in which the digitate microbial framework was frequently abraded and eroded. Minor amounts of allochthonous ooids, terrigenous silt, and skeletal debris were washed onto

the biostrome at this time. Schematic reconstructions of the biostrome are shown in Figure 4-11.

The abrupt transition of microbial and metazoan communities recorded within this biostrome probably reflects a relative sea-level fall and increase in water turbulence.

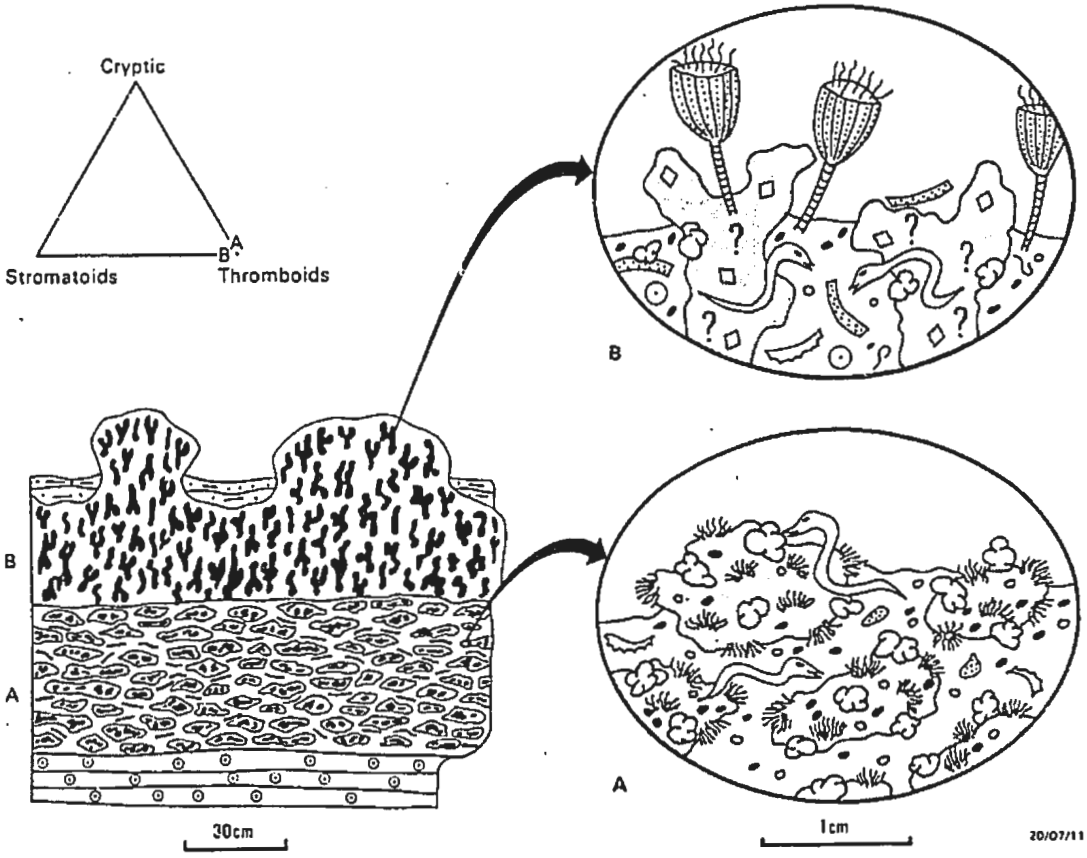

Figure 4-11. Schematic reconstructions and triangular plot of main framework components of Horizon B.

4.4 HORIZON C

ZONED THROMBOLITE-STROMATOLITE

Two zoned thrombolite-to-stromatolite beds occur within a thick sequence of ooid dolostone in the middle portion of the Campbells Member of the Petit Jardin Formation, to the east of Marches Point (Fig. 4-12; interval 9 of Chow's 1986 March Point Section).

MEGASTRUCTURE

Each bed consists of closely spaced domed bioherms established on a foundation of ooid-intraclast grainstone, and buried by fine ooid dolostone. Bioherms in the lower bed (Bed A, Fig. 4-12) are 30-40 cm thick, 50-200 cm wide, and appear to have a synoptic relief equivalent to their thickness. Bioherms in the upper bed (Bed B, Fig. 4-12) range from 30 to 110 cm thick. The crests of the largest bioherms extend well above the level of the inter-biohermal ooid dolostone, and are capped by gently to steeply domed stromatolites (Zones B2 to B7). The crests of the stromatolite domes are truncated by a planar karst erosion surface. The truncated stromatolites have a preserved thickness of 10-25 cm, and a preserved synoptic relief of 40 cm. By extrapolating the curvature of the truncated stromatolite domes, it is evident that at least 15 cm has been eroded from their crest. Thus their original synoptic

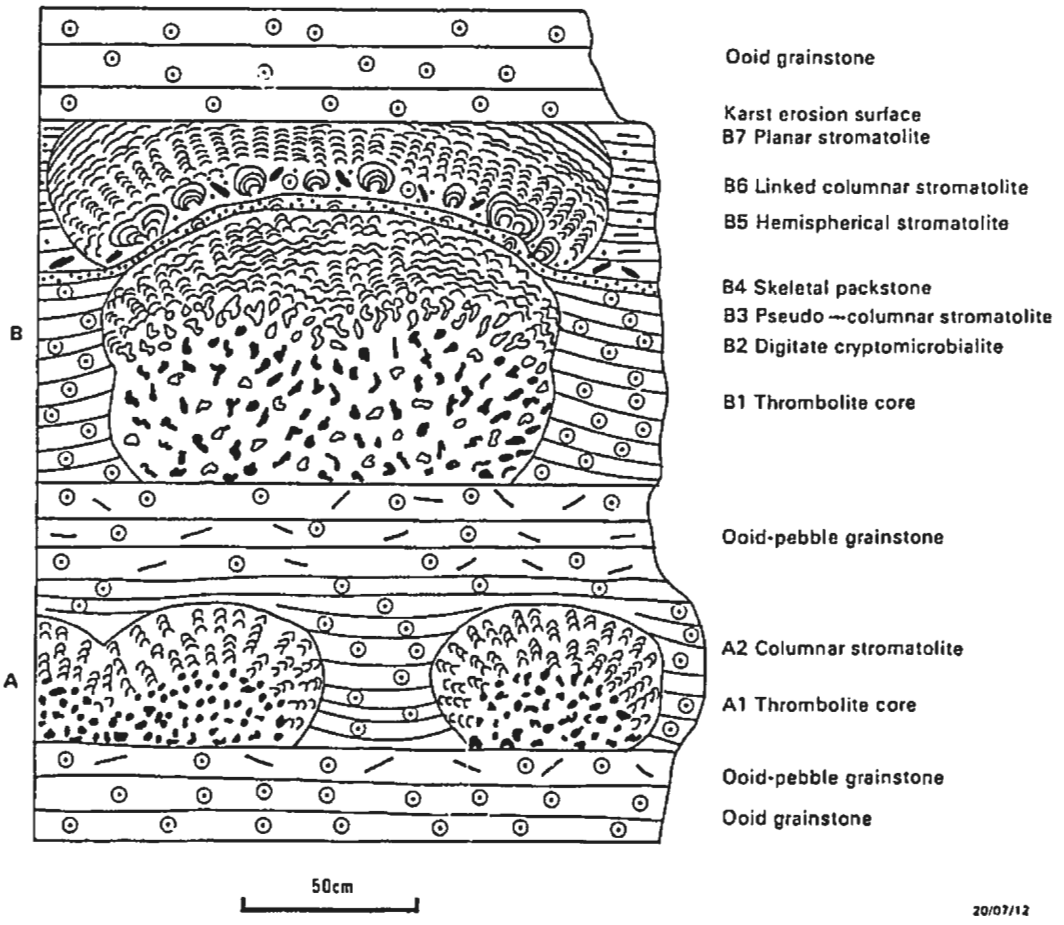

Figure 4-12. Lithological section of Horizon C, Campbells Member of the Petit Jardin Formation.

relief was approximately 55 cm. Pebble conglomerates occur between the encrusting stromatolite domes and are similarly truncated by the karst erosion surface. This surface is directly overlain by ooid dolostone.

MESOSTRUCTURE

The core of the lower bioherms (Zone A1) consists of a dense framework of interconnected lobate and grape-like thromboids 1-6 mm in size, and minor interstitial packstone and orange dolomite (Plate 16). This thrombolite core is abruptly overgrown by crudely laminated columnar stromatoids and a subequant volume of inter-columnar skeletal packstone (Zone A2; Plate 16). Stromatoid columns on the flanks of the thrombolite core have sub-horizontal to gently inclined orientations, whereas those at the crest are vertical. The columns are 3-8 mm in diameter and up to several centimetres long, but their continuity is disrupted by a network of irregular stylolites. Laminae within the columns have an irregular convex shape and 2-5 mm synoptic relief.

The core of the upper bioherms (Zone B1) consists of a framework of dark lobate to stubby arborescent thromboids, and amoeboid cryptomicrobial fabrics which have been selectively replaced by fine pink dolomite (Plate 17-C). The arborescent thromboids are 5-10 mm high, the individual branches of which are 1-2 mm thick and have a tuberous, slightly divergent shape. In transverse section these branches have a hollow saccate morphology. Burrow-mottled

skeletal wackestone occurs between the thromboid-cryptomicrobial framework.

This thrombolite core grades upward into a zone of erect to outward radiating, pink dolomitic, cryptomicrobial digits which are encrusted by scattered small dark lobate thromboids (Zone B2, Plate 17-B). The cryptomicrobial digits are tuberous, rarely branched, 5-10 mm wide, and vertically impersistent due to a network of irregular stylolites. At the crests of the smaller bioherms, these digits have an apparent micro-relief of up to 5 mm and are directly overlain by ooid dolostone. The digits are infilled by a subequant volume of burrowed skeletal packstone.

The crests of the larger bioherms, in contrast, are overgrown by several stromatolitic zones (Fig. 4-12, Plates 17-A, 18):

Zone B3 Pseudo-columnar and columnar-layered stromatoids; 20 cm thick.

Zone B4 Dark brown sandy and silty skeletal packstone which contains scattered small tuberous stromatoid columns and digitate thromboids; up to 4 cm thick.

Zone B5 Isolated and linked hemispheroidal stromatoids and ooid-intraclast conglomerate; 1-8 cm thick.

Zone B6 Linked columnar and pustular stromatoids; 2-4 cm thick.

Zone B7 Planar and corrugate stromatoids; 3-7 cm thick.

Columns and pseudo-columns within Zone B3 are 1-4 cm wide and comprise irregularly alternating 1) thin light coloured

dolomitic, and 2) thick dark coloured calcitic, laminae (Plate 17-A). The laminae are gently to moderately convex, laterally impersistent, and have 5-15 mm micro-relief.

Tuberous columns within the dark skeletal-rich layer (Zone B4) are indistinctly laminated, 3-6 mm wide and up to 10 mm high. This layer extends across the surface of the inter-biohermal ooid dolostone and defines a synoptic surface with 20-30 cm relief. The contact between this layer and the overlying stromatolite zone is abrupt.

The upper stromatolite zones (B5 to B7) are inter-gradational (Plate 18). They form steep to overhanging encrustations on the flanks of the bioherms, and, prior to karst erosion, presumably formed continuous domes across the crest of the bioherms. The micro-relief of the individual stromatoids within these zones progressively decreases from about 20 mm within Zone B5, to 1-5 mm within Zone B6, and 1-2 mm or less within Zone B6. The stromatoids contain numerous fine laminoid fenestrae occluded by sparry dolomite, and are disrupted by sediment-filled shrinkage cracks. They comprise: 1) grey calcitic laminae, episodically interlayered with, 2) pink oolitic, intraclastic, and skeletal-rich dolomitic laminae and lenses, and less commonly, 3) dark 1-4 mm thick crusts of botryoidal marine cement (Plate 18).

Small pockets of what appear to be intraclastic and oolitic calcrete fill small depressions within the karst surface that truncates the upper stromatolite zones.

MICROSTRUCTURE

The bioherms exhibit a range of microstructural preservation; stromatoids are generally well preserved, botryoidal marine cement is moderately preserved, thromboids are poorly preserved, and cryptomicrobial structures are pervasively dolomitized.

1. Thromboids

The lobate and grape-like thromboids within the core of the lower bioherms (Zone A1) have a saccate to diffuse cellular lobate microstructure (Plate 19-A,B). The individual lobes and "cells" consist of an irregular mosaic of turbid, amber coloured microspar. They range from about 100 to 1000 μm in diameter, and occur in clusters up to 6 mm across.

Stubby arborescent and lobate thromboids within Zones B1 and B2 comprise a mosaic of turbid xenotopic microspar, have irregular poorly defined margins, and range from 400 to 1000 mm in diameter (Plate 20-A,B). They locally support small framework cavities occluded by sediment and cement.

Thromboids within both bioherm beds are interpreted as selectively calcified coccoid colonies.

2. Stromatoids

Stromatoid columns within Zone A2 have a diffuse streaky microstructure consisting of irregularly alternating

1) silt-rich laminae, 250-600 μm thick, and 2) massive to diffuse grumous, microcystalline laminae up to 300 μm thick (Plate 19-C). The laminae are laterally discontinuous and contain minor trilobite debris. They were most likely constructed by alternating sediment-trapping and calcified microbial layers; however there is no microstructural indication of the morphology of these microbes. Although the inter-column sediments contain abundant metazoan burrows, the burrows do not penetrate the stromatoid columns.

Pseudo-columnar and columnar-layered stromatoids within Zone B3 have a banded microstructure consisting of; 1) massive cryptocrystalline laminae, 2) silt and peloid-rich laminae (PLate 21-A,B), and less commonly, 3) grumous laminae, and 4) thin crusts of botryoidal marine cement. The massive and silty peloidal laminae generally have smooth planar to convex shapes, and are laterally continuous. Locally, however, these laminae are partially detached from each other and are separated by lensoidal fenestrae occluded by blocky dolomite. The alternating massive and silty peloidal laminae were probably constructed by sediment-trapping filamentous mats. In contrast, the episodic grumous laminae have an irregular hummocky to knobbly shape, are laterally discontinuous, and probably represent calcified coccoid layers.

Small tuberous columns within the dark skeletal layer of Zone B4 have a streaky, diffuse to distinct, grumous or massive lobate microstructure (Plate 21-C). They contain rare botryoidal marine cement, and scattered terrigenous silt and

euhedral authigenic quartz. They were probably constructed by poorly laminated coccoid mats.

Hemispheroidal, columnar, pustular and planar stromatoids within the encrusting stromatolites (Zones B5, B6 and B7) have a banded microstructure comprised of: 1) thick hummocky and knobbly laminae which have a diffuse to distinct, grumous, or less commonly streaky, microstructure (Plate 21-D,E), and 2) episodic grain-rich dolomitic laminae. The grumous laminae are 500-2500 μm thick, and contain numerous fine subrounded and lensoidal, dolomite-filled, fenestrae which impart a weak, 300-600 μm thick, second-order lamination (Plate 21-E). Within the columnar and pustular stromatolites (Zone B6), the grumous laminae are partially detached from one another and buckle upwards to form irregular 2-3 mm high pustules above dolomite-filled fenestrae or grumous lenses (Plate 21-D). Grumous laminae are commonly discontinuous within the hemispheroidal and columnar to pustular laminated zones (Zones B5 and B6), but are very continuous in the outer planar and corrugate Zone B7. Based on their shape, thickness and microstructure, the grumous laminae were probably constructed by coccoid mats which had little or no sediment trapping capability.

The episodic interlayers of pink dolomite contain abundant poorly preserved intraclasts, ooids, peloids, microbial corpuscles, trilobite and pelmatozoan fragments, and terrigenous silt. These predominantly allochthonous particles were washed onto the bioherms where they were mixed with autochthonous fragments eroded from the stromatolites

(microbial corpuscles and stromatolite clasts). Since these layers accumulated on the steep and overhanging margins of the bioherms, they were clearly trapped and bound by micro-organisms, probably filamentous forms. Any vestige of these microbes, however, has been destroyed by selective dolomitization of the grain-rich laminae.

3. Cryptomicrobial Fabrics

Amoeboid and digitate cryptomicrobial components within Zones B1 and B2 comprise hypidiotopic microcrystalline dolomite (Plate 20-D). Scattered grains of terrigenous silt and rare relic patches of massive, diffuse grumous, or diffuse streaky microspar provide the only clue to their original composition and structure. It is speculated that these selectively dolomitized fabrics may have originally comprised weakly laminated stromatoids similar to those within Zone A2 of the lower bioherms, or Zone B4 of the upper bioherms.

4. Marine Cement

Cement crusts within Zones B3 to B7 comprise mamillate layers of fibrous botryoids (Plate 22-A,B). Individual fibrous subcrystals are 100-500 μm long, and contain numerous inclusion-defined outlines of precursor acicular crystals 5-8 μm wide (Plate 22-D,E), as well as scattered rhombic dolomite inclusions 1-10 μm in size (Plate 22-C).

The habit and microfabric of these botryoids differ from the divergent-radial botryoids within the Cape Ann Complex (Horizon A) in that 1) the subcrystals are thinner and more elongate, 2) inclusion-defined relics of precursor acicular crystals are more abundant, and 3) curved, convex outward, twin lamellae are less common.

5. Detrital Sediment

Detrital sediment within the lower bioherms comprises burrow-mottled silty skeletal packstone. Whereas trilobite debris and elongate pelmatozoan plates are equally abundant within thrombolite Zone A1 (Plate 19-A), trilobites are predominant in the outer stromatolite Zone A2 (Plate 19-C). Lobate pyritic corpuscles 150-1000 μm in size are common within both zones, and are interpreted as reworked fragments of calcified coccoid colonies (Plate 19-D). These corpuscles are locally cut by borings 60 μm in diameter.

Detrital sediments within thrombolitic Zones B1 and B2 also comprise burrow-mottled skeletal packstone or wackestone (Plate 20-A,C,D). They are dominated by trilobite debris, together with minor amounts of pelmatozoans, phosphatic brachiopods, microbial corpuscles and terrigenous silt. Most of the silt grains have euhedral authigenic quartz overgrowths.

The dark brown skeletal-rich sediments of Zone B4 comprise silty to very fine sandy, skeletal and corpuscular packstone (Plate 21-C). In contrast to the trilobite-dominated

sediments within the underlying thrombolitic zones, this layer is dominated by pelmatozoan debris, and trilobite fragments are less common. Light to dark brown coloured microbial corpuscles, 200-1000 μm in diameter, are also abundant within this layer. They have an irregular lobate or reniform shape, and comprise crypto- to microcrystalline calcite and numerous tiny pyrite spheroids, 5-12 μm in diameter. Some corpuscles are cut by irregular shrinkage cracks which clearly post-date the deposition of the corpuscles. The corpuscles are interpreted as reworked fragments of gelatinous coccoid colonies, and the pyrite spheroids were probably precipitated as a result of degrading, sulfate-reducing bacteria (see Thomsen and Vorren, 1984). Some of the pelmatozoan fragments within this layer appear to be encrusted by small lobate colonies of calcified coccoid microbes. The dark brown skeletal-rich layer is interpreted as a veneer of poorly bound sediment produced by a community of coccoid microbes, attached pelmatozoans and scavenging trilobites.

Shelter cavities are common beneath the larger trilobite and pelmatozoan fragments within the detrital sediments of Zones A1, A2, B1 and B2. They are occluded by a mosaic of radiaxial-fibrous cement (Bathurst 1959, 1975), although curved (concave outward) twin lamellae are rarely evident. Where this cement is in direct contact with a sheltering trilobite fragment, it has a pronounced fibrous habit due to syntaxial overgrowth of the prismatic trilobite microfabric (Plate 20-C). In contrast, cement immediately adjacent to

sheltering pelmatozoan fragments, forms a monocrystalline syntaxial overgrowth (Plate 19-D).

ORIGIN AND PALAEOECOLOGY

The lower bioherms were initially constructed by a dense framework of lobate calcified coccoid colonies. This framework was infilled by abundant skeletal metazoan debris, lime-mud, eroded and bored fragments of the calcified coccoid colonies, and minor terrigenous silt. These sediments were extensively burrowed by metazoans. Skeletal debris was probably generated largely within the bioherms by a community of attached pelmatozoans and vagile scavenging trilobites. This coccoid community was abruptly succeeded by a microbial community of unknown composition which trapped and bound fine detrital particles to form small stromatolitic columns. Attached pelmatozoans were probably absent from the bioherms at this time, but scavenging trilobites continued to be abundant. The bioherms evidently grew with moderate relief in a shallow subtidal environment between ooid shoals, and their growth was terminated by the migration of these shoals. Schematic reconstructions of the lower bioherms are shown in Figure 4-13.

The upper bioherms were initially constructed by lobate to sub-arborescent colonies of calcified coccoid microbes and discontinuous mats (now dolomitized) of unknown composition and structure (Zone B1). The coccoid colonies subsequently declined greatly in abundance, and unknown microbial

communities constructed small digits of low relief (Zone B2). During these early growth stages, the bioherms were inhabited by abundant burrowing metazoans, scavenging trilobites and perhaps minor attached pelmatozoans and inarticulate brachiopods. They grew in an environment very simlar to that of the underlying bioherms. Reconstructions of these early growth stages are shown in Figure 4-14.

The crests of the tallest bioherms were gradually colonized by well laminated, column-forming, fenestral (?)filamentous mats, as well as episodic hummocky to knobbly layers of coccoid microbes, and thin crusts of botryoidal marine cement (Zone B3). Burrowing and scavenging metazoans evidently did not inhabit these crestal mats. The zonation of microbial and metazoan communities was probably controlled by the upward shallowing of the larger bioherms, and perhaps an increased frequency of their exposure. Whereas the smaller bioherms remained permanently submerged, the crests of the larger bioherms probably extended into the intertidal zone where sediment-trapping (?)filamentous mats proliferated and metazoans were absent. The larger stromatolite-capped bioherms probably stood 60-80 cm above their substrate.

The smaller bioherms were subsequently buried by ooid sands, but the crests of the larger stromatolite-capped bioherms either remained permanently above the level of these sands, or were subsequently re-exhumed. Their lithified crests, and the surrounding ooid sands, were covered by a veneer of poorly bound, skeletal sediment derived from a community of gelatinous coccoid microbes, attached

pelmatozoans and scavenging trilobites (Zone B4). Thin crusts of botryoidal marine cement helped to stabilize small tuberous columns constructed by poorly laminated (?)coccoid mats.

The crests of the largest bioherms were then colonized by isolated and linked, hemispheroidal grading to columnar, pustular, corrugate and planar mats comprised of irregularly interlayered calcified coccoid and sediment-trapping filamentous microbes (Zones B5 to B7). These mats constructed large domes with steep to overhanging margins and high synoptic relief. At times of reduced microbial activity, the domes were encrusted by layers of botryoidal marine cement. The domes grew in a shallow subtidal or periodically emergent intertidal environment, into which intraclasts, ooids, peloids, skeletal debris and terrigenous silt were episodically washed. Burrowing, scavenging and suspension-feeding metazoans were excluded from this environment, perhaps due to poor water circulation and\or elevated salinities. Reconstructions of the upper stromatolitic growth stages are shown in Figure 4-15.

The domes were subsequently buried by fine carbonate sediments, and following an abrupt fall in sea-level they were subaerially eroded.

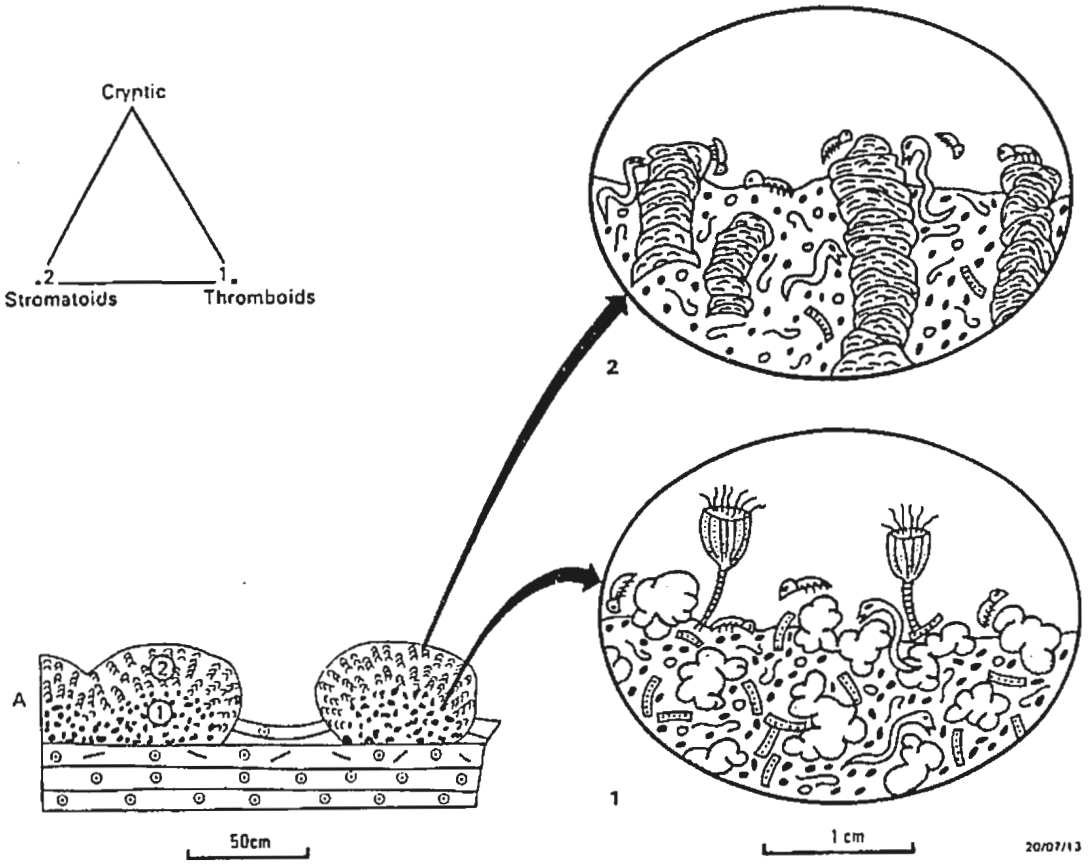

Figure 4-13. Schematic reconstructions and triangular plot of main framework components of Bed A (Zones A1 and A2), Horizon C.

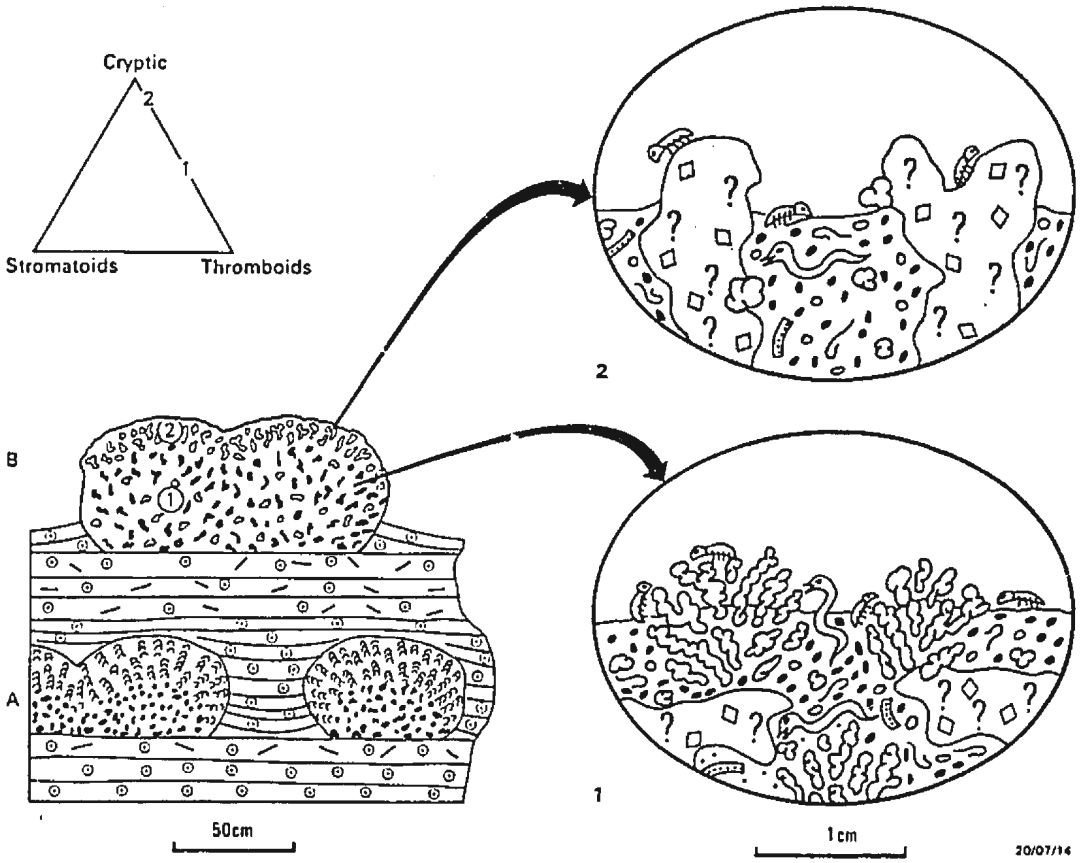

Figure 4-14. Schematic reconstructions and triangular plot of main framework components of the early growth stages (Zones B1 and B2) of Bed B, Horizon C.

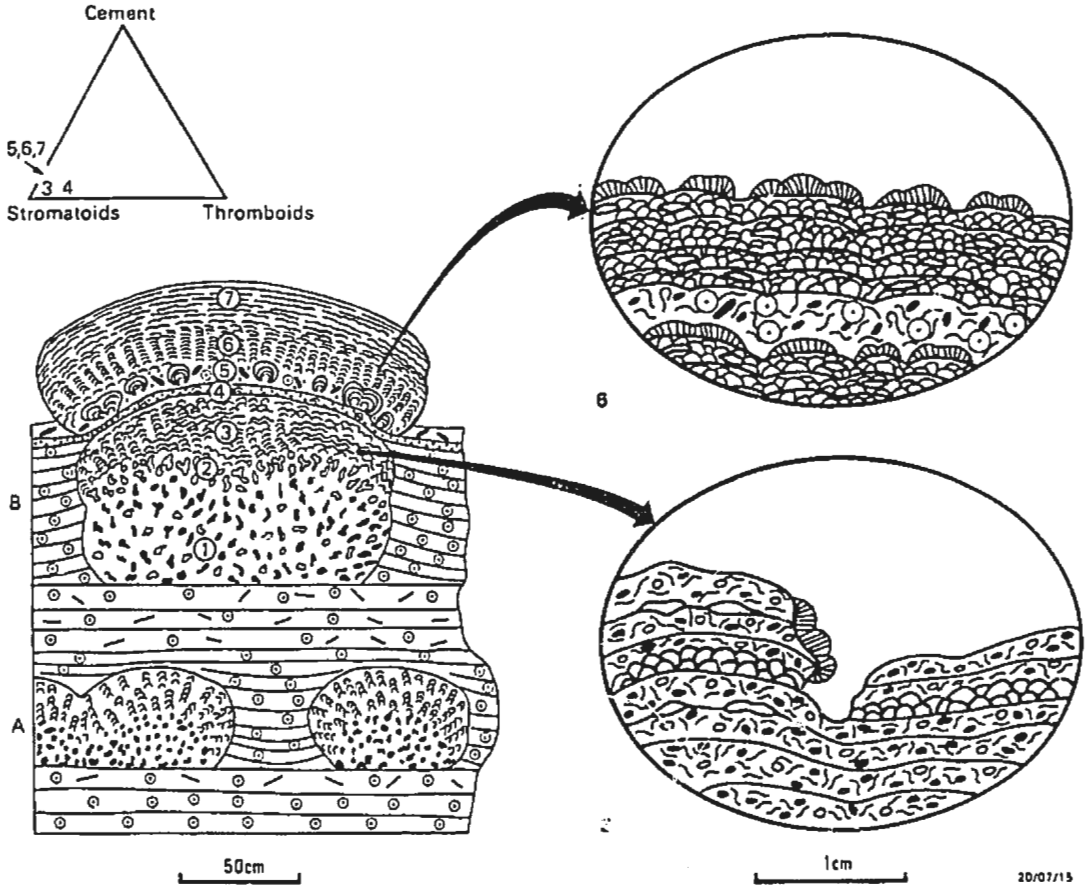

Figure 4-15. Schematic reconstructions and triangular plot of main framework components of the upper stromatolitic growth stages (Zones B5 to B7) of Bed B, Horizon C.

4.5 HORIZON D

RENALCIS AND OOID-RICH THROMBOLITES

Three thrombolitic beds occur within a sequence of ooid grainstone exposed at the eastern end of Campbells Cove, 1 km east of the settlement of Campbells Creek. This sequence represents the central portion of the Campbells Member of the Petit Jardin Formation, and probably correlates with Interval 9 of that member at the March Point Section (Chow, personal communication 1985). Thus, these thrombolitic beds are approximate lateral equivalents of the zoned thrombolite-stromatolite bioherms of Horizon C. A stratigraphic section of the sequence at Campbells Cove is shown in Figure 4-16.

MEGASTRUCTURE

The microbialites are interbedded with thin beds of ripple cross-laminated ooid grainstone and lenses of pebble conglomerate. The lower microbialite (Bed A, Fig. 4-16) forms close packed ellipsoidal bioherms, 65 cm thick and 80-200 cm long, which are flanked by thin-bedded lime-mudstone and argillaceous limestone. These bioherms have a synoptic relief of at least 30 cm (Plate 23-A). The overlying thin tabular and domed biostromes and bioherms (Bed B) have low synoptic relief, and are commonly capped by thin stromatolites. The upper domed bioherms (Bed C) are 10-25 cm thick, 20-45 cm in diameter, and are flanked and draped by thinly interbedded

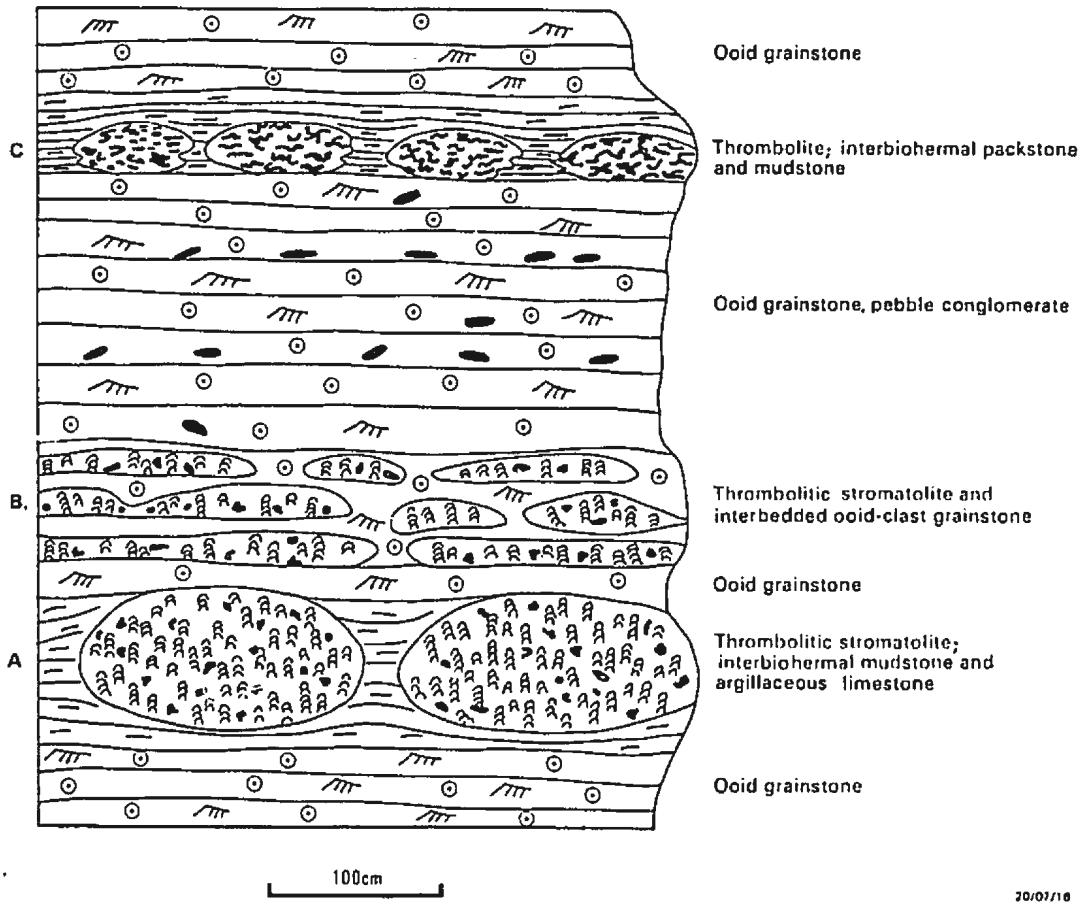

Figure 4-16. Lithological section of Horizon D, Campbells Member of the Petit Jardin Formation.

skeletal-peloid packstone and dolomitic argillaceous limestone (Plate 23-B). The basal portion of these bioherms intertongues with inter-biohermal strata, and they probably only attained minor topographic relief, about 10 cm, during the final stages of their growth. Some of these bioherms are truncated by a planar erosion surface (Plate 23-C) which may correlate with the karst surface at the top of Horizon C.

MESOSTRUCTURE

Beds A and B comprise a framework of indistinctly and irregularly laminated stromatoid columns, lobate and arborescent thromboids, and minor planar stromatoid sheets (Plate 24-A,B). The stromatoid columns have a stubby, sub-vertical, tuberous shape (terminology of Preiss, 1976), and locally branch in an umbellate style (terminology of Hofmann, 1969). They are 3-15 mm in diameter, 1-2 cm tall, and have 2-10 mm synoptic relief. The columns locally encrust thromboids or planar stromatoids, and within Bed A, they are partially linked by bridging stromatoids (columnar-layered fabric). They have an irregular convex laminated and mottled fabric, and are commonly disrupted by burrows and minor laminoid fenestrae. The flanks and crests of the columns are encrusted by thromboids (Plate 24-B) and thin isopachous rims of dark marine cement. Numerous isolated and semi-continuous layers of thromboids also occur within the stromatoid columns. Thromboids have a lobate or squat, non-geotropic,

bush-like form, and are 1-5 mm in size. Those occurring at the crest of the stromatoids columns, however, are typically erect, elongate arborescent forms up to 10 mm high and 1-2 mm wide (Plate 24-A). Inter-framework sediment contains abundant ooids and skeletal debris, and is extensively bioturbated. Crescent-shaped intraclasts up to 1 cm long are abundant within Bed B, and represent fragments eroded from the stromatoid columns. In some cases these clasts are encrusted by *in situ* stromatoids.

Bed C comprises prostrate, centimetre-sized, anastomosing thromboids and interstitial patches of mottled micritic sediment (Plate 24-C). It has numerous sub-horizontal stylolitic seams and locally has a stylo-breccoid fabric. The thromboids are extensively bioturbated, and contain scattered cauliflower-like clusters of smaller, millimetre-sized, dark lobate and saccate bodies. Pendant grape-like clusters of these bodies are particularly conspicuous on the undersides of prostrate thromboids. The thromboids grade into indistinctly laminated, prostrate to inclined, stubby digits at the margins of the bioherms.

MICROSTRUCTURE

Microstructures are generally moderately well preserved, but it is frequently difficult to differentiate between thromboids and inter-framework sediment within Bed C. This difficulty results from: 1) thromboids and inter-framework

sediment have a similar micritic composition, 2) mild neomorphism, and 3) intense bioturbation.

1. Thromboids

Thromboids within Beds A and B comprise well preserved calcified coccoid and, less commonly, filamentous "microfossils" (*Girvanella*). Grape-like clusters and arborescent bushes of clotted and saccate *Renalcis* are the dominant coccoid morphotypes (Plates 25-A,E), but chambered *Renalcis* and rare branching tubular *Izhella*-like forms (Plate 25-D) are also present. The various morphotypes occur adjacent to and intergrown with each other, and exhibit a spectrum of intermediate forms. Individual clots within clotted morphotypes range from 30 to 300 μm in diameter, whereas individual saccate and chambered forms are larger (250-500 μm diameter) and have a relatively thick (30-120 μm) cryptocrystalline rim. *Renalcis* occurs scattered within and interlayered with columnar stromatoids, and forms erect arborescent bushes and pendent encrustations at the crest and flanks, respectively, of stromatoid columns.

Girvanella has three forms: 1) "caps" of sub-parallel prostrate filaments at the crest of *Renalcis* bushes (Plate 25-C), 2) crusts up to 2mm thick of substrate-parallel, substrate-perpendicular or randomly oriented filaments on the flanks of stromatoid-*Renalcis* columns (Plate 25-B), and 3) detrital aggregates or balls, 0.5-1 mm in size, of twisted filaments within the inter-column sediments. Individual

tubules have an external diameter of 10-15 μm and are up to 200 μm long. They are either closely packed with minor inter-tubule micrite and microspar, or form a relatively open network infilled by turbid microcrystalline marine cement.

Thromboids within Bed C have a highly variable and mottled, in part indistinctly laminated, diffuse grumous to silty bioclastic-peloidal microstructure (Plate 26-A). Some microclots have vague filamentous forms. Terrigenous silt, silt-sized peloids, trilobite debris, and reworked pyritic microbial corpuscles commonly occur bound within the thromboids, particularly in the upper portion of prostrate forms (Plate 26-B). Thromboids generally have irregular poorly defined margins, but are locally lined by sub-isopachous rims of turbid fibrous marine cement, or bordered by bound trilobite carapaces (Plate 26-A,B). They are extensively disrupted by burrows and (?)borings, and are cut by numerous stylolitic seams.

The dark lobate and saccate, millimetre-sized bodies within these thromboids have an indistinct spherulitic lobate microstucture (Plate 26-B,C). The lobes are 400-1500 μm in diameter, and comprise a mosaic of turbid, very fine calcite (50-100 μm in size), each crystal of which has undulatory or radial sweeping extinction. Some lobes have a saccate form comprised of a thin cryptocrystalline rim and a large microcrystalline core. Quartz spherulites also rarely occur at the centre of some lobes (Plate 26-C). They consist of length-slow chalcedony (quartzine), are 350-500 μm in diameter, and contain numerous 1-10 μm rhombic and

rectangular inclusions of clear carbonate or possibly sulfate minerals. The spherulitic bodies are interpreted as bacterial precipitates within degraded coccoid colonies. The quartzine spherulites may have replaced evaporites, either gypsum or anhydrite (Folk and Pittman, 1971; Siedlecka, 1972; Milliken, 1979), which precipitated within open voids following the decay of the central portion of coccoid colonies.

2. Stromatoids

Tuberous stromatoid columns and planar stromatoid sheets within Beds A and B have a streaky to striated, variegated grumous, silty peloidal, and mottled microstructure (Plate 26-D). The individual laminae, lenses and patches are 100-1000 μm thick. The columns and sheets also contain minor amounts of skeletal debris (trilobites and pelmatozoans), ooids, scattered tubular and laminoid fenestrae, and *Renalcis*, and are extensively burrowed and bored. They have irregular erosional margins and are commonly encrusted by *Renalcis* and, less commonly, *Girvanella*.

3. Detrital Sediment

Detrital sediment within Beds A and B comprises fine to very coarse, peloid-ooid-skeletal packstone and wackestone (Plates 25-A,D, 26-D). Trilobite and pelmatazoan debris is abundant, as well as microbial corpuscles eroded from the stromatoid-*Renalcis* columns. Minor phosphatic brachiopod

fragments and variable amounts of terrigenous silt and very fine sand are also present. The sediment has been extensively bioturbated, and whereas the larger burrows (0.5-2 mm diameter) are generally filled with peloidal and silty lime-mud, small burrows and borings (200-500 μm diameter) are occluded by turbid or clear cement.

The irregular sediment patches between the prostrate thromboids in Bed C comprise skeletal mudstone and very fine peloid-skeletal wackestone (Plate 26-A,B). They contain abundant trilobite debris and numerous tubular to rod-like *Girvanella* fragments. These fragments indicate that partially calcified filaments were probably prolific within the microbial community that generated the prostrate thromboids. Terrigenous silt is relatively rare, but is locally abundant at the margins of the bioherms.

4. Marine cement

Turbid microcrystalline cement is commonly present in close association with the calcified "microfossils". It occludes fine interstices within *Renalcis* bushes and between individual *Girvanella* tubules (Plate 25-B). Microcrystalline marine cement also locally forms sub-isopachous rims, 20-60 μm thick, around thromboids and stromatoid-*Renalcis* columns (Plates 26-A). This cement also forms an initial fibrous fringe within voids occluded by mosaics of clear blocky calcite.

ORIGIN AND PALAEOECOLOGY

The bioherms were constructed by calcified, and to a lesser extent sediment-trapping, mixed coccoid and filamentous microbial communities. Pervasive and selective calcification of coccoid colonies gave rise to a variety of clotted, saccate and minor chambered *Renalcis* morphotypes within Beds A and B, whereas coccoid colonies were degraded and replaced by spherulitic (?)bacterial precipitates within Bed C. Calcified filamentous microbes (*Girvanella*) are commonly preserved *in situ* within Beds A and B, whereas their former presence within Bed C is recorded only by occasional diffuse filamentous microstructures, and numerous *Girvanella* fragments within the inter-framework sediment.

The lower thrombolitic stromatolites (Beds A and B), grew in a relatively high energy environment between migrating ooid shoals. Laterally discontinuous microbial mats (discontinuity probably being a function of high sediment influx, erosion and bioturbation) constructed relatively large columnar bioherms which stood at least 30 cm above the substrate. Individual columns within these bioherms projected several millimetres or centimetres above the sandy sediment that accumulated between them, and laterally linking microbial mats were probably only established during periods of relative quiescence. In contrast, the thrombolites of Bed C grew in a tranquil environment, possibly in the lee of an ooid shoal, in which more laterally continuous mats were

established. In this environment, disruption of the mats was probably controlled not so much by erosion or high sediment influx, but by bioturbation. These mats constructed a prostate framework which was infilled by bioturbated lime-mud. Cauliflower-like coccoid colonies within this mat were extensively degraded, and former weakly calcified filaments disintegrated to form *Girvanella* fragments and lime-mud. In the higher energy bioherms (Beds A and B), however, grape-like and arborescent coccoid colonies and encrusting networks of filamentous microbes were extensively calcified and encrusted by microcrystalline marine cement, thereby ensuring their preservation as well defined "microfossils".

The bioherms were inhabited by an active bioturbating infauna (soft-bodied ?worms), scavenging trilobites, and minor suspension feeding inarticulate brachiopods. High level suspension feeding pelmatozoans may have grown attached to the surface of the higher energy thrombolitic stromatolites (Beds A and B), but their remains are rare or absent in the lower energy thrombolites (Bed C). Schematic reconstructions of the bioherms are shown in Figure 4-17.

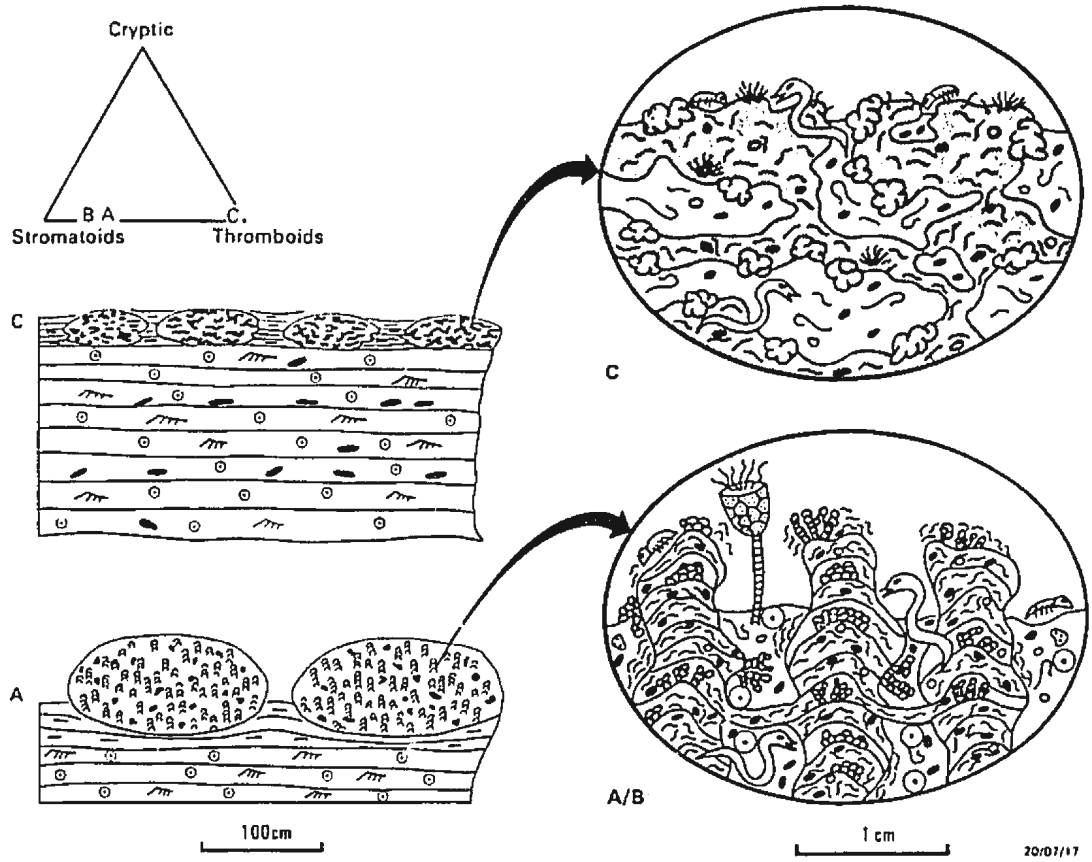

Figure 4-17. Schematic reconstructions and triangular plot of main framework components of Horizon D.

4.6 HORIZON E

PEBBLE AND *GIRVANELLA*-RICH THROMBOLITE

This thrombolite occurs within a peritidal sequence of mud-cracked parted limestone, pebble conglomerate and minor ooid grainstone near the top of the Big Cove Member of the Petit Jardin Formation, 2 km east of Marches Point (Fig. 4-18; interval 5 of Chow's 1986 March Point Section). The conglomerates typically comprise edgewise fan-like arrays of silty peloid grainstone and lime-mudstone pebbles. This sequence is abruptly overlain by a thick succession of ooid grainstone (Felix Member of the Petit Jardin Formation).

MEGASTRUCTURE

The thrombolite forms a gently domed to tabular biostrome, 60 cm thick and at least 50 m long, which pinches out westward into enclosing parted limestone. It is locally interrupted by narrow wedges of thin-bedded, intra-biostromal sediments (grainstone and parted limestone) which are either restricted to the upper portion of the biostrome, or disrupt its entire thickness (Plate 27-A). Abutting and intertonguing relationships with inter-biostromal parted limestone indicate up to 20 cm synoptic relief for the basal position of the biostrome, and less than 10 cm synoptic relief for the upper portion of the biostrome.

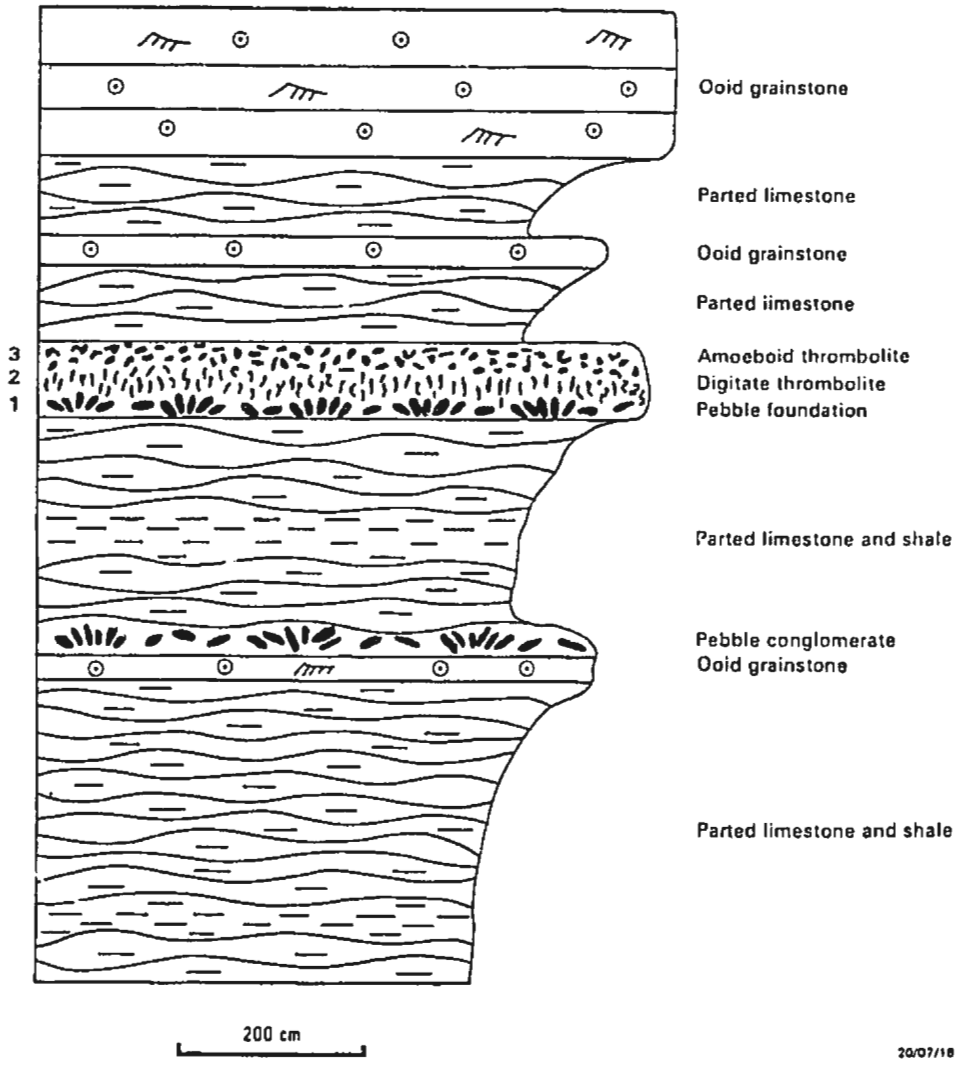

Figure 4-18. Lithological section of Horizon E, Big Cove Brook Member of the Petit Jardin Formation.

MESOSTRUCTURE

The biostrome is composed of three relatively sharply defined zones (Fig. 4-18; Plate 27-B,C), in ascending order: 1) a foundation layer of pebble conglomerate, 2) digitate thrombolite, and 3) amoeboid thrombolite.

The basal pebble conglomerate is about 10 cm thick and contains sub-evenly spaced fans of discoidal pebbles separated by areas of predominantly flat-lying pebbles (Plate 27-B). Lateral discontinuities of this conglomerate are reflected in either a thinned encrusting digitate zone, or lateral discontinuity of the biostrome.

The encrusting digitate zone is approximately 20 cm thick and consists of a relatively open framework of dark digitate thromboids and weakly laminated to mottled inter-framework sediment rich in ooids, skeletal fragments and pebbly intraclasts (Plate 28-A). Thromboids average 1 cm in diameter, are rarely branched, and commonly encrust the crests of edgewise pebbles. They have a mottled, in part crudely laminated, internal fabric and are rimmed by a thin dark selvage. Numerous burrows, about 1 mm in diameter, are evident within them. Vertical continuity of the selvage and the occurrence of large edgewise pebbles between the thromboids, indicate that they had a synoptic relief of at least several centimetres. The thromboids and inter-framework sediment are disrupted by numerous sub-horizontal stylolites.

The upper amoeboid zone, about 30 cm thick, comprises very irregular, interconnected amoeboid thromboids separated by

patches of mottled skeletal and peloidal wackestone (Plate 28-B). The thromboids contain abundant brown, millimetre-sized, sub-rounded bodies. Irregular stylolites disrupt and partially border the thromboids, and impart a prominent stylo-breccoid fabric to outcrop surfaces (Plate 27-C).

MICROSTRUCTURE

Microstructures are relatively well preserved. Digitate thromboids are locally partially replaced by coarse sparry calcite and scattered dolomite rhombs.

1. Thromboids

The digitate thromboids have a mottled microstructure comprised of irregular, horizontally elongate, millimetre-sized patches of dark cryptocrystalline calcite separated by lighter coloured patches and lenses of fine-microcrystalline calcite (Plate 29-A). The dark cryptocrystalline patches have either a massive or diffuse grumous microstructure, and contain disseminated pyrite. Detrital grains rarely occur within the dark cryptocrystalline patches whereas minor terrigenous silt, skeletal fragments and rare ooids are present within the fine-microcrystalline patches. The thromboids are encrusted by *Girvanella* selvages, 0.2-1.5 mm thick, in which the filament tubules are aligned parallel to the margins of the thromboids (Plate 29-B). Individual tubules are 10-15 μm in diameter and up to 200 μm long. There

is no microstructural indication of the morphology of the microbes that constructed the digitate thromboids.

Amoeboid thromboids in the upper zone have a diffuse grumous grading to *Girvanella* microstructure. The microclots have a variety of subequant, elongate, arcuate and cuspate shapes (Plate 29-C), are 20-100 μm wide, and commonly define a series of subrounded knobs 2-3 mm in diameter. They intergrade with diffuse to distinct *Girvanella* tubules, or discrete clusters of twisted sub-parallel *Girvanella* tubules (Plate 29-D,E); these *Girvanella* clusters form the sub-rounded darker bodies visible within thromboids in slabbed samples (Plate 28-B). These amoeboid thromboids thus represent masses or colonies of variously calcified filaments; selective calcification of their sheaths resulted in tubular *Girvanella* microfossils, whereas pervasive calcification and micritic encrustation of the filaments generated a network of variously shaped microclots (grumous microstructure). Minor terrigenous silt occurs between the tubules and microclots.

2. Detrital Sediment

Inter-framework sediment within the central digitate zone comprises weakly laminated and bioturbated peloid-ooid-skeletal-intraclast packstone and wackestone (Plate 29-A). Several texturally distinct grain populations are recognised: 1) well sorted and rounded, medium to coarse pelmatozoan debris and ooids, 2) well rounded pebbles of ooid-pelmatozoan

grainstone, 3) discoidal pebbles of silty peloid grainstone and mudstone, 4) irregular microbial corpuscles, 5) poorly sorted trilobite and minor gastropod debris, and 6) lime-mud. The ooid-pelmatozoan sand and pebbles clearly represent allochthonous, high energy sediment washed into the biostrome, whereas the microbial corpuscles, trilobites, gastropods and lime-mud were probably generated within the biostrome.

Detrital sediment within the upper amoeboid zone comprises bioturbated wackestone with abundant irregular microbial corpuscles, common trilobite and gastropod debris, and numerous *Girvanella* fragments. Minor terrigenous silt occurs throughout the biostrome.

ORIGIN AND PALAEOECOLOGY

The biostrome was established on a pebble storm lag deposit on a shallow shelf otherwise dominated by very fine peloidal and muddy carbonate sediment. Ooid-pelmatozoan shoals (the overlying Felix Member of the Petit Jardin Formation) occupied the seaward margin of this shelf (Chow, 1986). Minor topographic relief provided by the pebble conglomerate favoured the establishment of microbial communities. However, microbial communities did not colonize numerous other pebble conglomerates within the underlying parted limestones. Thus a combination of 1) substrate topography, and 2) proximity to a high energy carbonate shoal, controlled the development of the biostrome.

The digitate thrombolite was constructed by (?)calcified microbial colonies of unknown composition which had little ability to trap detrital particles. A high influx of sandy sediment from the adjacent ooid-pelmatozoan shoal may have limited the lateral continuity of these colonies, and they accreted vertically to construct slender digits of several centimetres relief. The flanks of the digits were encrusted by layers of calcified filaments. The digitate thrombolite was inhabited by abundant deposit feeding and scavenging trilobites and minor grazing gastropods.

More laterally continuous microbial colonies or mats constructed the upper amoeboid thrombolite zone, and coincide with an abrupt decrease in sediment influx. This community was extensively reworked by soft-bodied (?)worms, scavenging trilobites and grazing gastropods. It comprised a network of variously selectively and pervasively calcified filaments. Growth of the biostrome was terminated by a blanket of lime-mudstone and the shoreward progradation of the overlying ooid shoal. Reconstructions of the biostrome are shown in Figure 4-19.

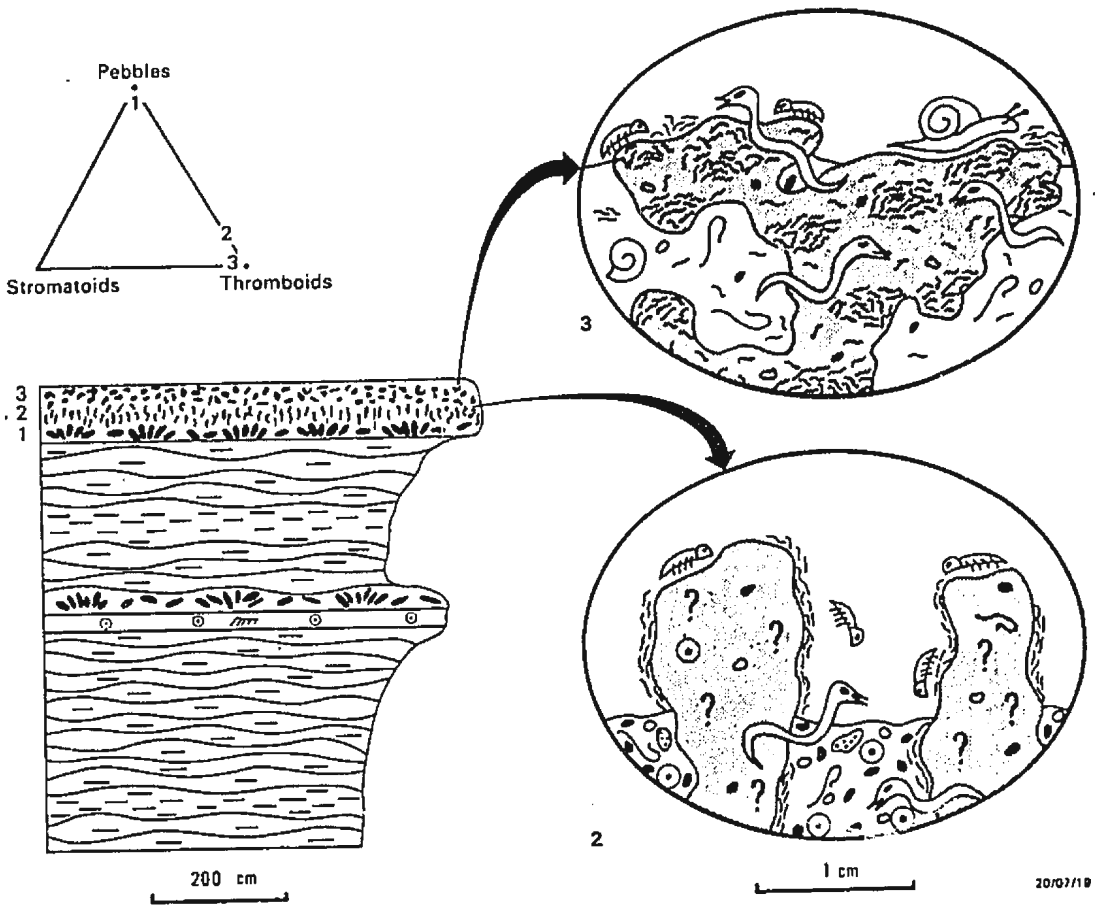

Figure 4-19. Schematic reconstructions and triangular plot of main framework components of Horizon E.

4.7 HORIZON F

ARBORESCENT STROMATOLITE

This stromatolite occurs within ooid grainstone near the top of the Felix Member of the Petit Jardin Formation at Felix Cove (Fig. 4-20; interval 11 of Chow's 1986 Felix to Man O' War Coves Section).

MEGASTRUCTURE

The stromatolite forms small isolated, close-packed, and coalesced domed bioherms embedded within poorly sorted peloid-ooid grainstone. The bioherms are circular in plan view, 15-70 cm in diameter, and 10-40 cm thick.

MESOSTRUCTURE

The bioherms comprise thin arborescent stromatoid columns and inter-column silty dolomitic mudstone (Plate 30-A). The columns have a slightly divergent style of branching (Preiss, 1976) and are 2-10 mm in diameter. Individual laminae are gently convex, and have 1-2 mm synoptic relief.

Some of the larger bioherms comprise several sub-concentric zones: 1) two or more basal layers, each about 3-5 cm thick, of thin, divergently branched columns, 2) a central zone of thicker, slightly divergent to sub-parallel, columns, 3) a crestal zone of markedly divergent to prostrate, poorly

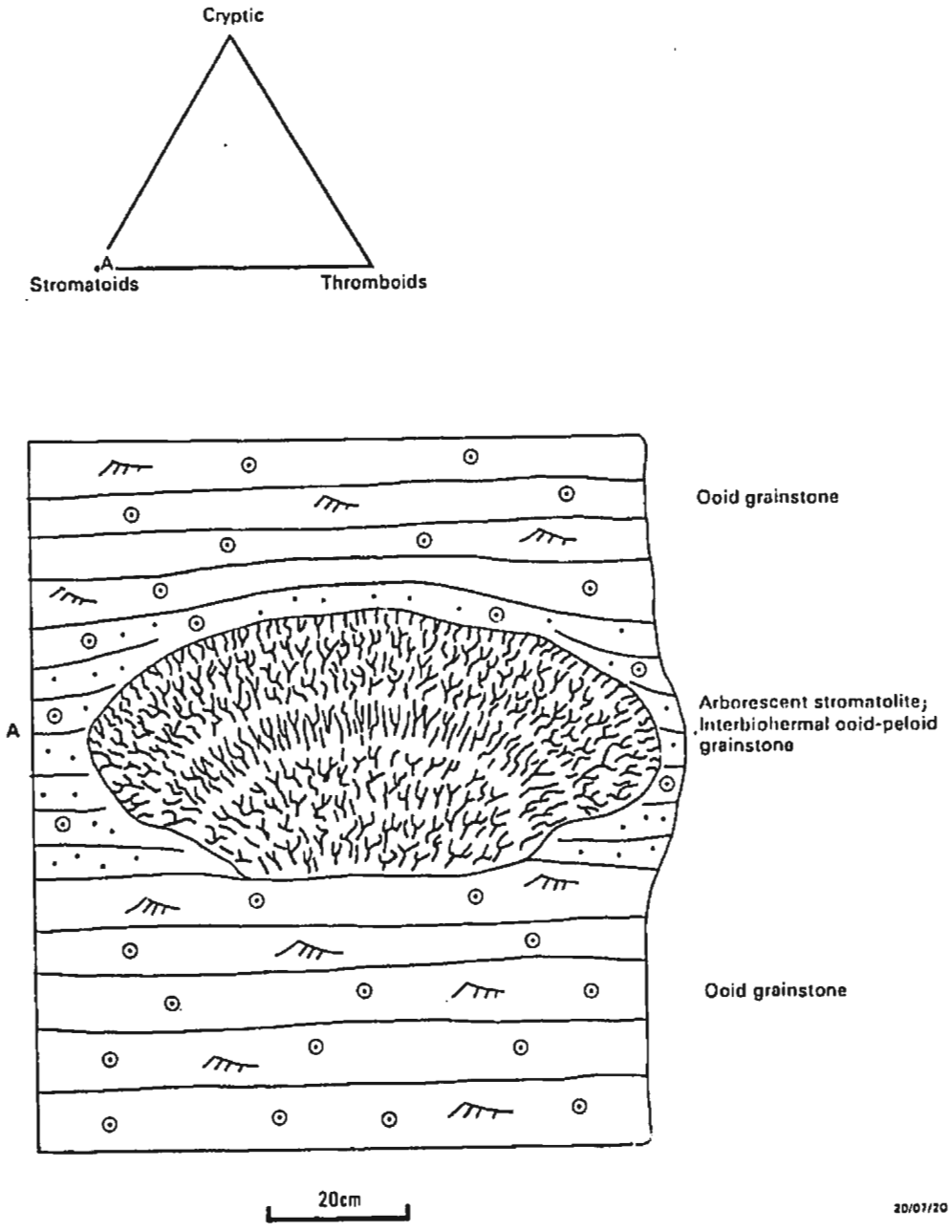

Figure 4-20. Lithological section and trianglar plot of main framework components of Horizon F, Felix Member of the Petit Jardin Formation.

laminated columns, and 4) a marginal zone of thin outwardly radiating, slightly divergent columns which are sub-perpendicular to the margin of the bioherm. The sub-concentric arrangement of zones indicates a synoptic relief of about 10-15 cm for the bioherms.

MICROSTRUCTURE

1. Stromatoids

The stromatoid columns are replaced by a mosaic of micro- to very finely crystalline turbid calcite and retain no vestige of their primary microstructure (Plate 30-B,C). Laminae, which are clearly evident in hand samples, are poorly defined in thin-section by subtle changes in crystal size and\or the relative abundance of sub-micron sized inclusions. The columns have smoothly rounded to lobate margins, and contain rare pockets of terrigenous silt which probably fill burrows.

2. Detrital Sediment

Inter-column sediment consists of silty and very fine sandy dolomitic lime-mudstone, scattered peloids and rare ooids and phosphatic skeletal fragments. There is little or no evidence of bioturbation.

ORIGIN AND PALAEOECOLOGY

The delicate arborescent columns were constructed by low relief button-like microbial colonies of unknown composition and microstructure. The columns evidently grew within a relatively tranquil environment in the absence of skeletal infauna and epifauna. Reconstruction of the microbial community is not possible.

Although the microstructure of the columns has been destroyed by neomorphism, their primary laminated fabric is clearly evident in field exposures and hand samples, and they are thus readily distinguished from similar sized, non-laminated, digitate thromboids within thrombolites. This observation is significant since Howe (1966), and other subsequent workers, assumed that non-laminated digits simply represent previously laminated columns (stromatoids) in which the laminae were destroyed by neomorphism, dolomitization or dissolution. Undoubtedly diagenesis can partially or completely obscure laminated stromatolitic fabrics, but the present example demonstrates that lamination can persist despite extensive diagenetic alteration, whilst numerous apparently pristine and less altered microbial fabrics in the underlying and overlying thrombolitic horizons are definitively non-laminated. Similarly Aitken (1967) observed a close spatial association between non-laminated thrombolites and well-laminated stromatolites, and consequently abandoned Howe's assumption that non-laminated thrombolitic fabrics are diagenetic artifacts of precursor laminated stromatolites.

4.8 HORIZON G

DOLOMITIC CRYPTOMICROBIALITES

Two beds of pervasively dolomitized microbialites occur within fine to medium crystalline (?)ooid dolostones at the top of the Felix Member of the Petit Jardin Formation at Felix Cove. These beds probably correlate with Interval 14 of Chow's 1986 Felix to Man C' War Coves Section (Chow, personal communication, 1985).

MEGASTRUCTURE

The lower bed (Bed A, Fig. 4-21) forms large, closely packed domed bioherms, about 90 cm thick and 1-3 m in diameter, which protrude 30-40 cm above weakly stratified inter-biohermal (?)ooid dolostone (Plate 31-A). This exhumed surface of the bioherms probably reflects their original synoptic relief, the draping sediments having been selectively removed by present erosion. The upper boundstone (Bed B) forms a domed biostrome, 60-70 cm thick, which appears to comprise laterally coalesced bioherms of similar proportion to the lower bioherms.

MESOSTRUCTURE

The lower bioherms have an irregularly variegated, in part breccoid-like, cryptomicrobial fabric comprised of

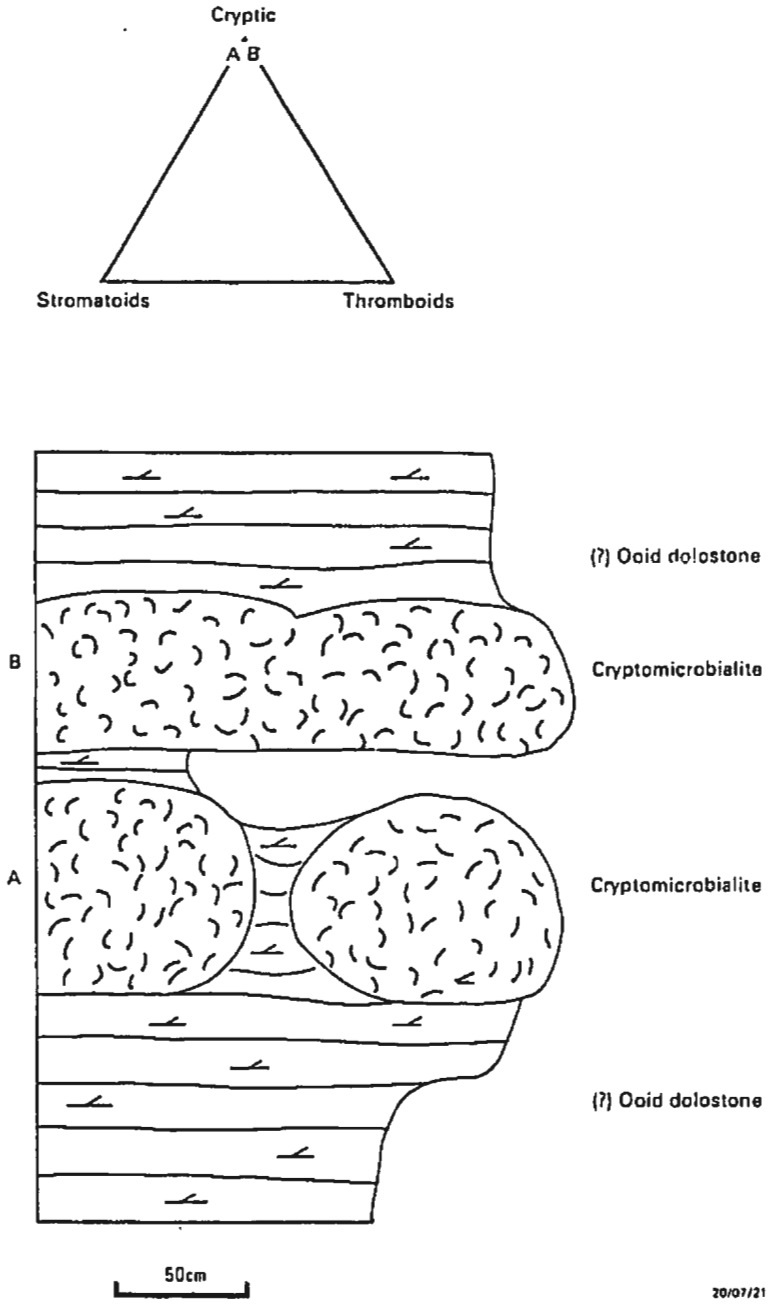

Figure 4-21. Lithological section and triangular plot of main framework components of Horizon G, Felix Member of the Petit Jardin Formation.

millimetre to centimetre-sized patches of micro-, very finely and finely crystalline dolomite. Although this diagenetic fabric cannot be systematically related to the original microbial fabric, the scale and erratic distribution of the patches suggest a clotted thrombolitic, rather than laminated stromatolitic, precursor.

The upper biostrome (Bed B) has a mottled cryptomicrobial fabric comprised of irregular, partially interconnected, centimetre-sized patches of 1) relatively dark, coarser crystalline, pink-grey dolomite, and 2) light coloured, finer crystalline, cream dolomite. These patches have a uniform three-dimensional arrangement such that horizontal and vertical sections exhibit a similar distribution of dark and light patches (Plates 31-B,C). The light patches are commonly rimmed by stylolitic seams and have an indistinctly laminated fenestral-like fabric in vertical section. The gross geometry of the patches resembles amoeboid thromboids, but based on mesoscopic features, it is ambiguous as to whether the dark (coarser) or light (finer) patches represent framework or inter-framework components.

MICROSTRUCTURE

Not surprisingly, primary microstructures have been destroyed by dolomitization. The darker coloured patches (lighter coloured in thin section) within the upper biostrome comprise irregular inequigranular intergrowths of cloudy, xenotopic, microcrystalline dolomite (10-40 μm crystal size)

and relatively clear, hypidiotopic, very fine to fine dolomite (60-200 μm crystal size). These intergrowths locally define diffuse, relatively coarse grumous microstructures in which microcrystalline microclots, 60-300 μm in size, are separated by clear very fine to fine crystalline dolomite (Plate 30-D). The darker coloured patches also contain fine to medium euhedral dolomite, and are locally rimmed by a thin cryptocrystalline selvage. By analogy to non-dolomitized thrombolite horizons, these dark patches most probably represent amoeboid thromboids which, at least locally, had a grumous microstructure and a micritic selvage.

The lighter coloured patches (darker coloured in thin section) comprise equigranular microcrystalline dolomite (10-40 μm crystal size), together with scattered domains of of fine to medium euhedral dolomite (?cement). They most likely represent inter-framework micritic sediment, and the euhedral dolomite domains could be cement-filled primary or secondary voids within inter-framework sediment, such as burrows, shelter cavities or solution vugs.

ORIGIN AND PALAEOECOLOGY

These microbialites appear to have been constructed by an amoeboid microbial framework between which lime-mud rich sediments accumulated. They contain no recognizable detritus, and the former presence or absence of metazoans cannot be determined. Despite pervasive dolomitization, a thrombolitic rather than stromatolitic affinity is apparent.

4.9 HORIZON H

PEBBLE RICH STYLO-NODULAR THROMBOLITE

This thrombolite occurs within a sequence of parted limestone, pebble conglomerate and prism-cracked dolostone in the lower portion of the Man O' War Member of the Petit Jardin Formation, east of Man O' War Cove (Fig. 4-22; interval 17 of Chow's 1986 Felix to Man O' War Coves Section). The pebble conglomerates characteristically comprise sub-evenly spaced fan-like arrays of elongate discoidal pebbles (Plate 32-A).

MEGASTRUCTURE

The thrombolite forms elongate tabular bioherms, up to 16 m long and 1-2 m thick, spaced several to tens of metres apart and separated by parted limestone (Plate 32-C,D). Smaller ellipsoidal bioherms, about 75 cm across and 50 cm thick, locally occur between the tabular bioherms. The lower portions of the bioherms have poorly defined intertonguing contacts with inter-biohermal strata, whereas their upper margins are sharply defined and are onlapped and draped by these strata (Plate 32-C,D). During much of their growth the bioherms probably had only minor synoptic relief (about 10 cm or less), but they appear to have attained at least 10-30 cm relief during their final stage of accretion.

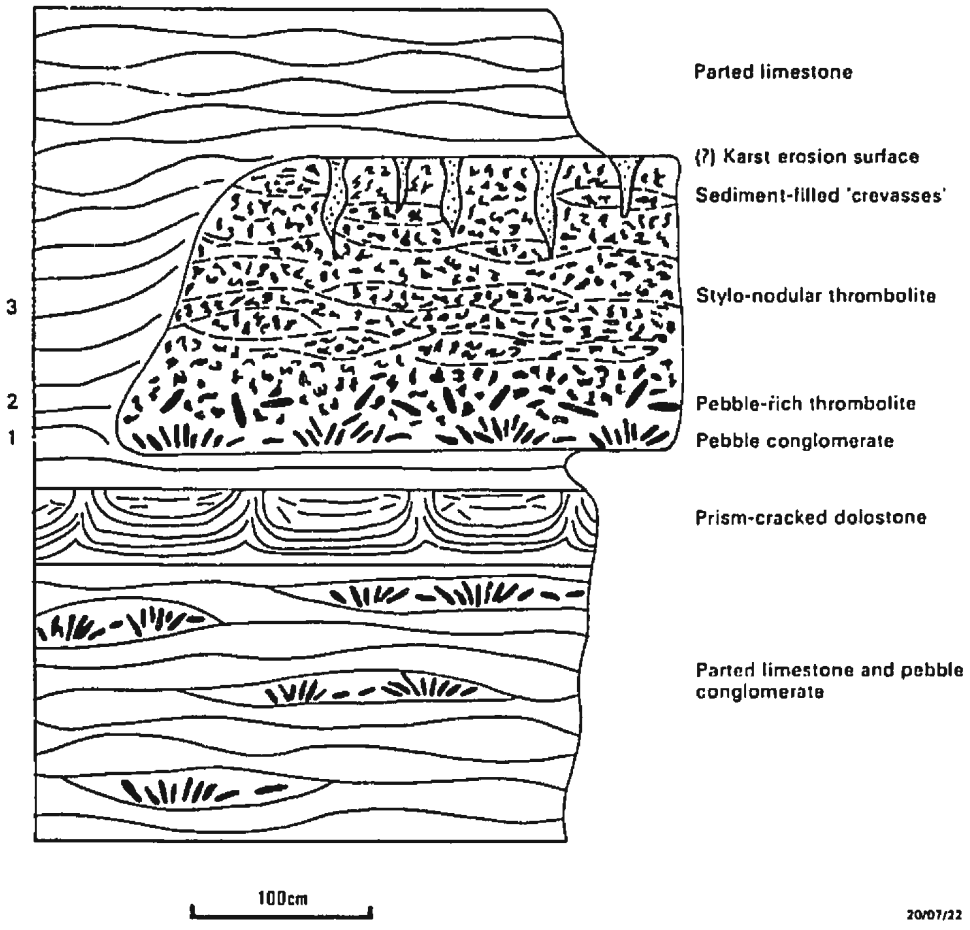

Figure 4-22. Lithological section of Horizon H, Man 'O War Member of the Petit Jardin Formation.

The upper surface of the bioherms commonly has an irregular micro-relief, in which discrete club-like heads are separated by thin wedges of pebbly grainstone which extend 10-40 cm into the body of the bioherm (Plate 32-C). These sediments apparently filled narrow gaps or "crevasses" between club-like growth protrusions at the surface of the bioherms. The protruding heads are locally truncated by a planar (?karst) erosion surface which, in plan view, displays a cerebroid pattern of thrombolite heads and intervening sediment wedges (Plate 32-B).

MESOSTRUCTURE

The bioherms comprise three relatively distinct zones (Plate 32-C): 1) a basal layer of pebble conglomerate; 10-15 cm thick, 2) a lower zone of pebble-rich thrombolite; 15-20 cm thick, and 3) a thick upper zone of stylo-nodular thrombolite, 70-160 cm thick.

The basal pebble conglomerate comprises sub-evenly spaced rosettes of discoidal pebbles and shows no evidence of microbial binding. The lateral continuity of this layer determines the lateral continuity of the bioherms.

The overlying pebble-rich thrombolite comprises dark, isolated and partially interconnected, amoeboid and sub-digitate thromboids encased in pebbly skeletal-ooid packstone (Plate 33-B). Thromboids range from 0.5 to 2 cm in size, and are truncated by numerous sub-horizontal stylolites. They have a mottled internal fabric, or rarely an indistinct,

irregular coarse hemispheroidal lamination. Discoidal pebbles comprise about 20 percent or more of the volume of this zone (an equivalent volume to the thromboids), and have erratic edgewise orientations. They occur between and are encrusted by thromboids.

The upper stylo-nodular zone forms the bulk of the bioherms and comprises poorly interconnected amoeboid and sub-digitate thromboids and interstitial skeletal wackestone (Plate 33-A). The thromboids are 3-10 mm wide and their vertical continuity is limited by abundant sub-horizontal stylolites which impart a prominent stylo-nodular fabric to this zone (Plate 32-C). They have a massive or in part crudely laminated internal fabric, and in contrast to the thromboids within the underlying pebble-rich zone, and indeed most other thrombolites, they are lighter coloured than the interstitial detrital sediment. Numerous centimetre-thick lenses of skeletal-peloid-intraclast packstone and grainstone occur throughout the upper zone.

MICROSTRUCTURE

Microstructures are generally poorly preserved due to widespread neomorphic microspar and patchy dolomitization.

1. Thromboids

The amoeboid and sub-digitate thromboids generally comprise neomorphic microspar with relict cryptocrystalline

grumous and massive microstructures (Plate 34-A). Locally these cryptocrystalline relicts define indistinct, millimetre-sized, lobate and knobbly bodies, or rarely form distinct clotted and saccate *Renalcis*-like "microfossils" (Plate 34-B). They probably represent relicts of calcified coccoid colonies. Minor terrigenous silt and rare peloids, pelmatozoan fragments, mollusc fragments and *Nuia* are present between these relict coccoid microstructures, and were probably trapped between and overgrown by these colonies. Clear authigenic euhedral feldspar and quartz crystals are also present. The thromboids are disrupted by numerous cement- and sediment-filled burrows, and have irregularly embayed margins, presumably the result of bio-erosion.

Some of the thromboids have a distinct spongeous-grumous microstructure of anastomosing, ragged to sub-tubular, patches of clear microspar (30-200 μm wide), separated by irregular patches and microclots of cryptocrystalline calcite (Plate 34-C). The microspar patches comprise up to 40 percent of the volume of these thromboids and appear to represent a network of former cement-filled fenestrae, since replaced by neomorphic microspar. These spongeous thromboids have a distinct 60-150 μm thick cryptocrystalline selvage, and intergrade with grumous microstructures in which the microspar network is rare or absent (Plate 34-C).

2. Detrital Sediment

Detrital sediment within all zones comprises skeletal-peloid packstone and wackestone with abundant gastropod shells and numerous reworked microbial corpuscles, abraded pelmatozoan debris and ooids (Plate 34-A,B). Pebbles of silty peloid grainstone and lime-mudstone are abundant within the lower zones, and terrigenous silt is generally present in minor amounts in all zones. Detrital grains decrease in abundance in the uppermost portion of the upper zone where lime-mudstone predominates. In contrast to many other thrombolite horizons, trilobite debris is absent.

Thin wedges of pebbly grainstone between thrombolite heads at the top of the bioherms comprise very fine to fine peloids, coarse pelmatozoan debris, terrigenous silt, and abundant discoidal pebbles of silty peloid grainstone and lime-mudstone.

ORIGIN AND PALAEOECOLOGY

The bioherms have a similar setting and broadly similar mesoscopic fabric to the pebble and *Girvanella*-rich biostrome of Horizon E. They were established on a storm-lag pebble conglomerate on a peritidal flat dominated by very fine peloidal and lime-mud sediments. Although similar pebble conglomerates are abundant throughout the enclosing sequence, only a few were colonized by microbial (thrombolite-forming) communities. Since all of these thrombolites contain well

sorted ooid and pelmatozoan sand, it appears that microbial communities were only established on conglomerate layers deposited near high energy carbonate shoals.

The bioherms were constructed by calcified coccoid colonies. These colonies probably originally constructed digits of moderate micro-relief which were subsequently foreshortened by extensive stylolitic solution to form the present amoeboid to sub-digitate, stylo-nodular, fabric. The bioherms were inhabited by a large population of grazing gastropods and an active burrowing/boring infauna. Ooid and pelmatazoan sand was washed into the bioherms from nearby shoals, together with pebbles ripped-up by storms from the surrounding tidal flat. During much of their growth the bioherms were probably low relief structures and they only attained significant topographic relief during their final stage of accretion, at which time discrete 10-40 cm high heads developed at the surface of the bioherms. At this stage their synoptic relief was probably sufficient to preclude further accumulation of allochthonous sand and pebbles within the bioherms, and only carbonate mud (either deposited from suspension or generated within the bioherms) accumulated between the digitate coccoid colonies. Growth of the bioherms was terminated by erosion (probably associated with emergence), and gaps between the thrombolite heads were filled by pebbly peloid-pelmatozoan grainstone. The bioherms were then buried by peritidal sediments (parted limestone). Schematic reconstructions of the bioherms are shown in Figure 4-23.

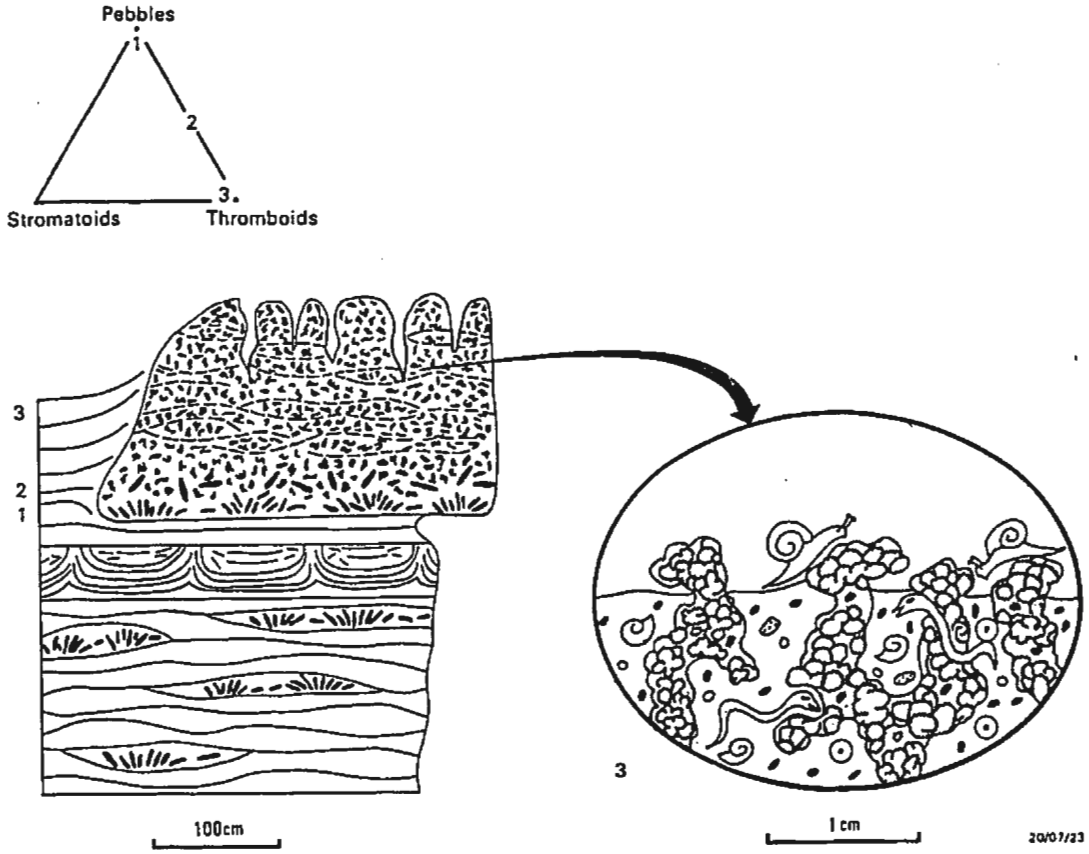

Fig. 4-23. Schematic reconstruction and triangular plot of main framework components of Horizon H.

4.10 HORIZON I

CRUDELY LAMINATED STROMATOLITES

Two superimposed stromatolite beds occur within peritidal parted limestone, pebble conglomerate, prism-cracked dolostone and hemispherical stromatolites in the central portion of the Man O' War Member of the Petit Jardin Formation (Fig. 4-24; base of interval 18 of Chow's 1986 Felix to Man O' War Coves Section, approximately 15 m above the pebble-rich stylo-nodular thrombolites of Horizon H). In contrast to most stromatolites and thrombolites within the shaly half-cycles of the Petit Jardin Formation (Big Cove and Man O' War Members) these stromatolites do not have a pebble conglomerate foundation; they directly overlie weakly laminated microcrystalline dolostone (?mudstone).

MEGASTRUCTURE

The lower stromatolite (Bed A in Fig. 4-24) forms closely spaced tabular bioherms 1.2 - 1.4 m thick and up to 30 m wide. The bioherms are separated by parted dolostone, and the upper portions of adjacent bioherms locally coalesce to form bridges across these inter-biohermal sediments. The bioherms are commonly cut by narrow, 5-20 cm thick, crevasse-like structures filled with coarse peloid-intraclast grainstone (Plate 35-A). These "crevasses" may represent sediment-filled

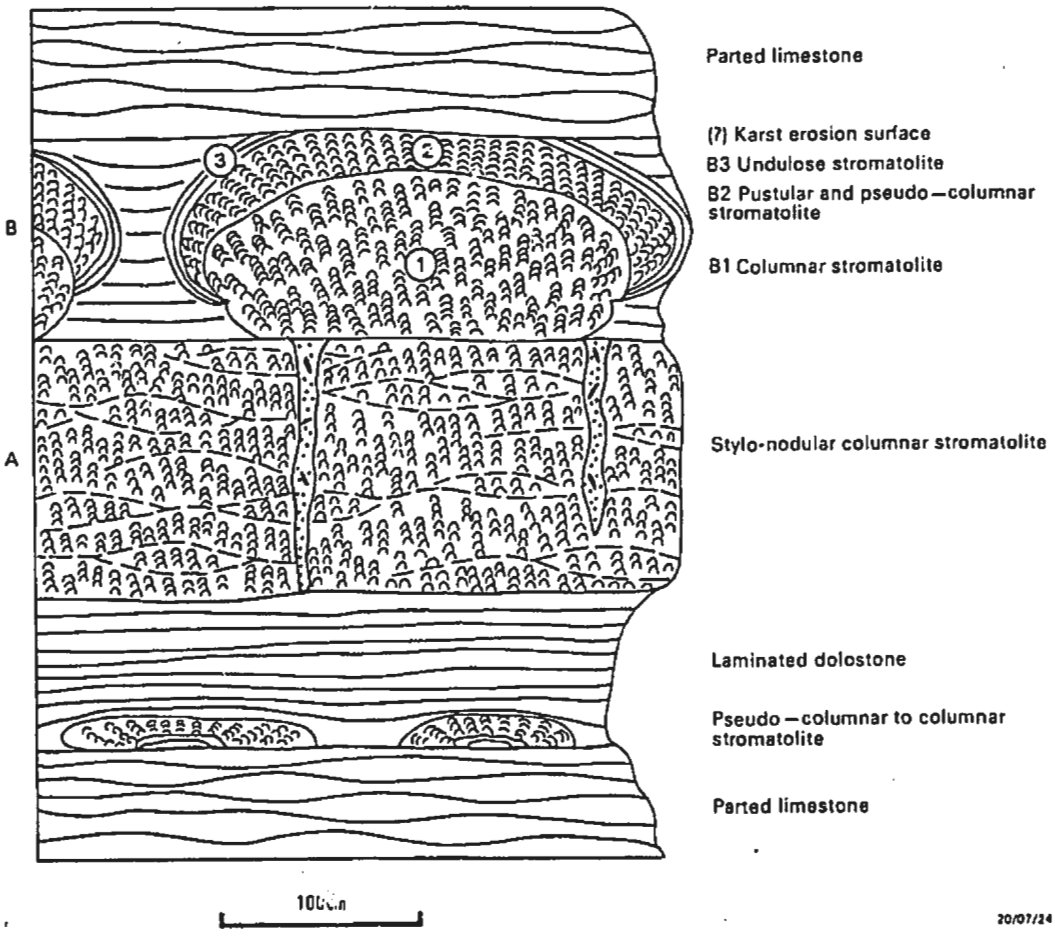

Figure 4-24. Lithological section of Horizon I, Man 'O War Member of the Petit Jardin Formation.

fractures (neptunian dykes) that post-date the lithification of the biostrome. The bioherms are commonly truncated by a planar (?)karst erosion surface.

The upper stromatolite (Bed B) forms concentrically zoned, ellipsoidal and coalesced oblate spheroidal bioherms 1.2 - 1.6 m thick and 2-4 m in diameter. The base of these bioherms appears to lie directly on the erosion surface of the underlying bioherms, and they are flanked and onlapped by parted dolostone. The thickest bioherms are themselves truncated by a planar (?)karst erosion surface on which their concentrically zoned internal structure is beautifully displayed (Plate 35-B).

The lower tabular bioherms appear to have had little or no significant relief above their substrate, whereas inter-biohermal sediment relationships and the concentric zonation within the upper bioherms indicate a synoptic relief of 60 cm to at least 85 cm (see below).

MESOSTRUCTURE

The lower bioherms (Bed A) and the central core of the upper bioherms (Zone B1) comprise crudely laminated, light coloured, stromatoid columns separated by darker coloured skeletal and peloidal wackestone and scattered intraclasts (Plate 35-C). In the lower bioherms, the columnar framework is extensively disrupted and foreshortened by abundant sub-horizontal stylolites, and these bioherms consequently have an irregular stylo-nodular, sub-columnar fabric. The columns

are 5-15 mm in diameter, partially linked, have bumpy margins, and form sub-parallel coalescing branches. In horizontal section the framework has an irregular cerebroid pattern which is highlighted by selective dolomitization of the columns. Dolomitization has also selectively enhanced crudely laminated columnar fabrics within the upper bioherms, whereas laminae are indistinct in non-dolomitized columns within both upper and lower bioherms. The laminae have an irregular gently convex shape, 2-5 mm of micro-relief, and are disrupted by numerous burrows and borings.

The columnar core of the upper bioherms is abruptly overgrown by pustular and pseudo-columnar stromatolite (Zone B2), ranging from 10 to 55 cm thick, which in turn is gradationally overgrown by a thin layer of undulose stromatolite on the flanks of the bioherms (Zone B3; Plate 35-B). The laminae within Zone B2 have a bumpy irregular convex shape, 3-15 mm of micro-relief, and are commonly disrupted by mud- and spar-filled burrows and borings (Plate 35-C). Individual laminae or groups of laminae within Zones B2 and B3 can be continuously traced from the crest of the bioherms to their steep and overhanging margins, thus indicating that: 1) the columnar core of Zone B1 stood approximately 60 cm above the sediment substrate prior to the growth of Zone B2, and 2) the bioherms attained a relief of at least 85 cm during the growth of Zones B2 and B3. Prior to the erosion of their crests, the largest bioherms probably had 1 - 1.2 m growth relief.

MICROSTRUCTURE

Microstructures are locally well preserved, but stromatoid columns are commonly replaced by patches of microcrystalline dolomite and are cut by irregular vein-like networks of neomorphic microspar and coarse spar.

1. Stromatoids

Columnar stromatoids within Bed A and Zone B1 have a crudely laminated to irregularly clotted fabric. Alternating dark cryptocrystalline and light microcrystalline laminae are locally well defined, 100-500 μm thick, and either continuous or discontinuous across the width of the columns. They have a bumpy mamillate shape and a streaky, grumous or massive microstructure (Plate 36-A). Poorly laminated columns have a variegated mottled to diffuse grumous microstructure, with patches of saccate lobate, vermiform, and rarely peloidal microstructure (Plate 36-B,C,D).

The columns are rimmed by a massive cryptocrystalline or diffuse grumous selvage, 60-500 μm thick, which commonly pinches and swells to form small bumpy protrusions (Plate 36-E). This selvage results from the downward continuation of cryptocrystalline laminae at the margin of the columns; such selvages are designated "walls" (see Walter, 1972).

The columns contain numerous spar-filled (?)borings, about 250 μm in diameter. Skeletal fragments, peloids and

terrigenous silt are relatively rare within the columns, and they contain scattered euhedral authigenic quartz.

Pseudo-columnar, pustular and undulose stromatoids within Zones B2 and B3 have an irregular pustular, mamillate or undulose shape, and pinch and swell in thickness from 200 to 2500 μm (Plate 35-D). They have a variegated grumous, massive and lobate microstructure generally similar to that within the stromatoid columns of Bed A and Zone B1, but contain scattered laminae and lenses of fine peloids and minor ooids (peloidal microstructure). Skeletal debris and terrigenous silt are notably absent. Laminae are commonly disrupted by millimetre-sized, spar- and sediment-filled burrows.

2. Detrital Sediment

Inter-columnar detrital sediment within Bed A and Zone B1 comprises burrow-mottled skeletal-peloid wackstone. Trilobite debris is abundant, together with minor pelmatozoan and (?)gastropod fragments. Subrounded to irregular, very fine to coarse peloids are also abundant, and are typically rimmed by an isopachous layer, 15-30 μm thick, of turbid marine cement (Plate 36-A,C). The smaller cement-rimmed peloids have a structure similar to the problematic (?)alga *Nuia*; however their gradation to larger and more irregular (similarly rimmed) peloids and intraclasts, as well as the co-occurrence of isopachous cement rims around skeletal fragments, clearly indicates that they are cement-rimmed detrital grains. Minor

terrigenous silt, irregular microbial corpuscles, and rounded lime-mud intraclasts are also present.

ORIGIN AND PALAEOECOLOGY

The columnar framework of the lower bioherms (Bed A) and the core of the upper bioherms (Zone B1) were constructed by a poorly laminated coccoid and minor filamentous (vermiform patches) community which had limited sediment trapping ability. The columns probably had a relief of at least a few centimetres, and were progressively infilled by lime-mud, (?)faecal pellets, corpuscles eroded from the columns, and the remains of deposit-feeding and scavenging trilobites, rare grazing gastropods, and possibly minor attached pelmatozoans. Minor allochthonous material, including ooids, intraclasts, terrigenous silt and perhaps pelmatozoan fragments, was also washed onto the bioherms. Columns and inter-column sediments were bored and burrowed by (?)soft-bodied metazoans.

The growth of the lower tabular bioherms was terminated, or at least areally restricted, by a cover of peloidal and shaly carbonate. Small exposed or re-exposed protuberances were subsequently re-colonized by similar column-building coccoid colonies. The areal extent of these colonies remained restricted however, possibly due to shallower more turbulent water conditions and higher sediment influx, and they constructed isolated domes about 60 cm high (Zone B1). The

upward growth of these domes, or alternatively a relative fall in sea-level, probably restricted water circulation between them and resulted in a relatively stressed (more saline and\or intermittently exposed) environment in which metazoans, particularly trilobites, could no longer flourish. Microbes, however, continued to thrive and the crests and flanks of the domes were encrusted by pseudo-columnar and pustular (Zone B2), and then undulose (Zone B3) microbial mats. Upward and outward accretion of these mats constructed concentric zones around the domes and locally resulted in their lateral coalescence. These mats were also dominated by coccoid microbes, together with episodic (?)filamentous layers capable of trapping and binding detrital peloids and ooids on the steep and overhanging margins of the bioherms. Their growth was subsequently terminated by subaerial erosion. Schematic recontructions of the bioherms are shown in Figure 4-25.

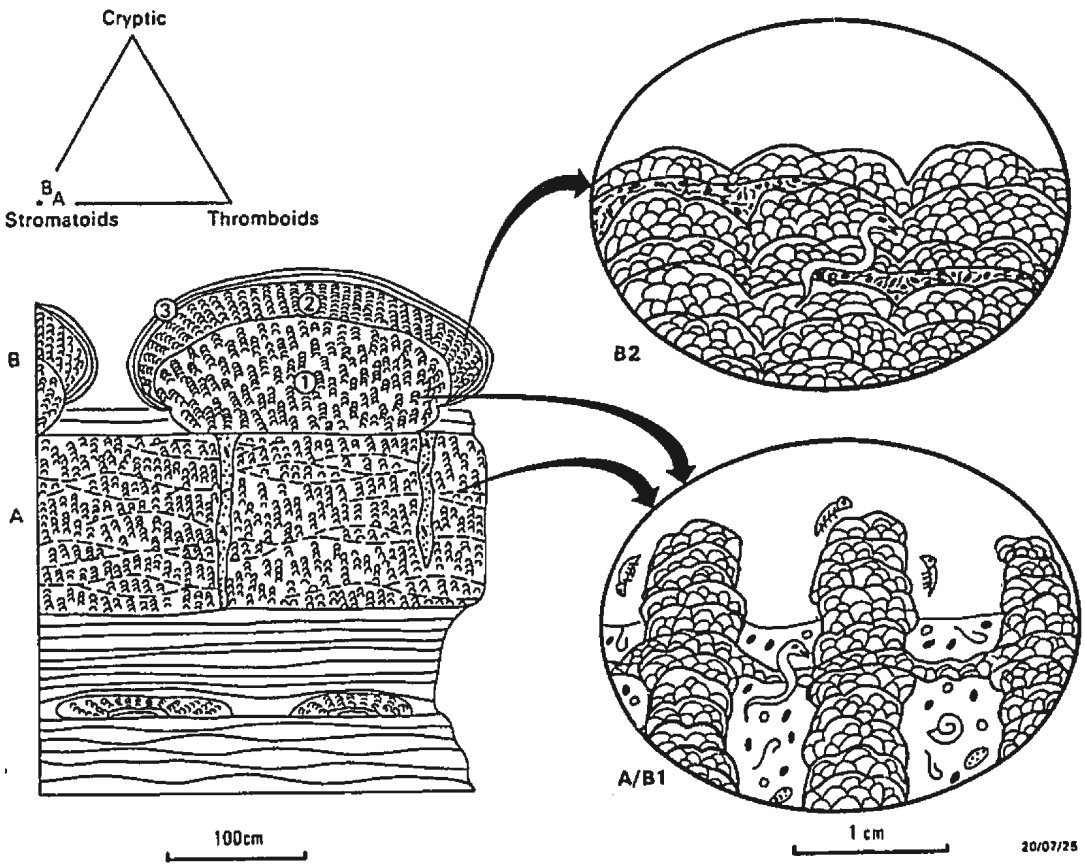

Figure 4-25. Schematic reconstructions and triangular plot of main framework components of Horizon I.

4.11 HORIZON J

ZONED THROMBOLITE-STROMATOLITE

Two zoned thrombolite-stromatolite biostromes are present near the top of the Man O' War Member of the Petit Jardin Formation at Man O' War Cove (Fig. 4-26; interval 20 of Chow's 1986 Felix to Man O' War Coves Section). The biostromes are separated by recessive shale, and are underlain and overlain by laminated and mud-cracked dolo-mudstone and variegated red and green shale.

MEGASTRUCTURE

The lower biostrome (Bed A, Fig. 4-26) is 30 cm thick and comprises a lower tabular thrombolite (Zone A1), approximately 20 cm thick, overlain by thin, closely spaced stromatolite mounds (Zone A2). The stromatolite mounds are 15-30 cm in diameter, have 5-10 cm synoptic relief, and are flanked by buff dolostone.

The upper biostrome (Bed B) is about 1.9 m thick and comprises four distinct units (Fig. 4-26): B1) spaced and locally coalesced thrombolite mounds, B2) tightly clustered stromatolite heads, B3) thin dark thrombolite crust, and B4) small isolated bulbous stromatolites.

The basal thrombolite mounds (B1) are about 120 cm thick, and are separated by poorly bedded, medium to very coarse peloid-(?)ooid dolostone. They, together with the inter-mound

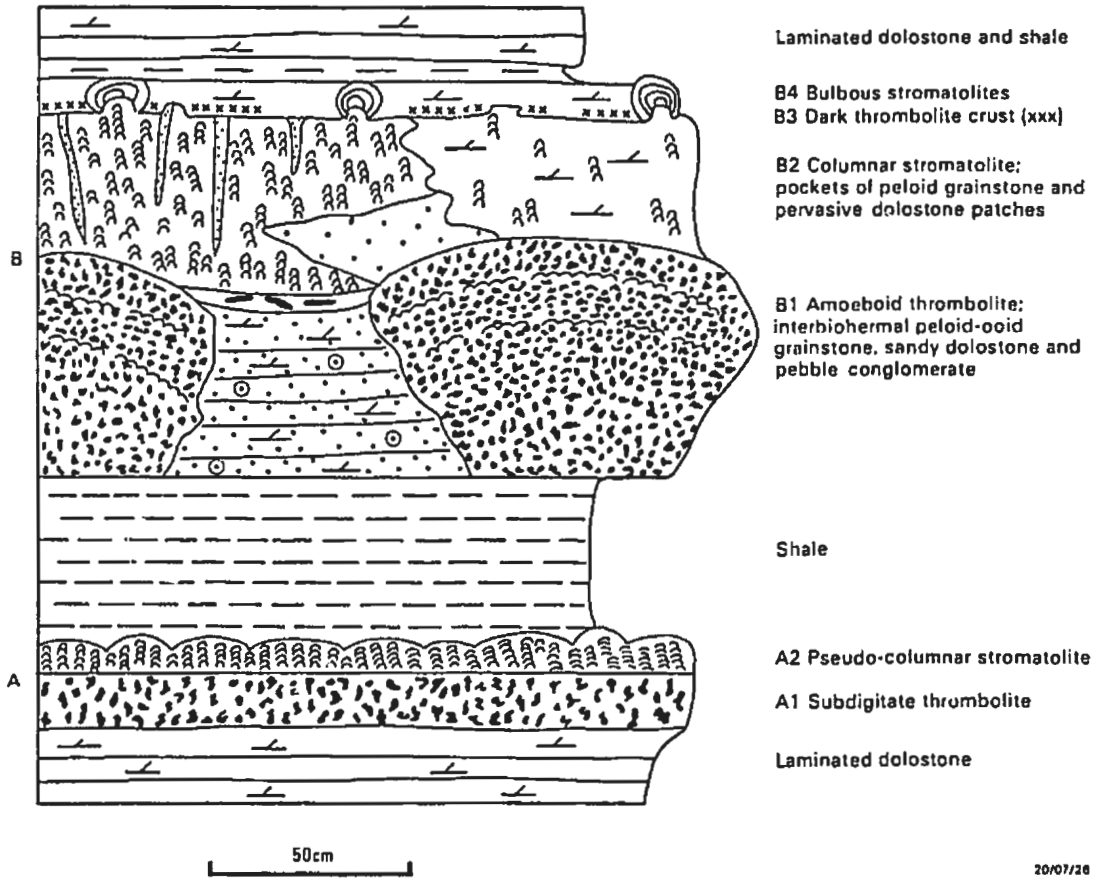

Figure 4-26. Lithological section of Horizon J, Man O' War Member of the Petit Jardin Formation.

sediments, are onlapped by thin-bedded peloid ooid grainstone, sandy dolostone and lenses of flat-pebble conglomerate. These latter lithologies were deposited after the mounds had ceased to accrete, and indicate about 45 cm synoptic relief for the mounds.

The overlying unit (B2) consists of tightly clustered, club-shaped stromatolite heads, 30-80 cm in diameter, and irregular pockets and lenses of very coarse peloid grainstone. The stromatolite heads have vertically laminated walls, 1-3 cm thick, and are separated by narrow wedges of very coarse peloid grainstone (Plate 37-A,B). These wedges have a remarkably uniform thickness (1.5 - 2 cm), and extend 10-50 cm down between adjacent heads. Portions of this unit are pervasively dolomitized, which not only destroys its meso- and microstructures, but also obscures the definition of stromatolite heads and intervening sediment wedges.

The stromatolite heads and intervening sediment wedges are truncated by a smooth undulating erosion surface with scattered, small mesa-like protuberances (Plate 37-B). These protuberances have 1-5 cm relief and are erosional remnants of the underlying stromatolite heads and\or sediment wedges. Their three dimensional shape is not known. This erosion surface probably represents an exposed, non soil-covered, karst surface. However, it lacks the scalloped ridge and basin-like morphology typical of many modern and ancient exposed tidal rock platforms (see Revelle and Emery, 1957, and Kaye, 1959; and for ancient examples Read and Grover, 1977, and Cherns 1982). Its morphology, however, readily

distinguishes it from furrowed karren developed on exposed sloping carbonate rock platforms (Allen, 1982, p. 222-251) and smooth hummocky and pot-holed karst surfaces developed under soil-vegetation covers (Sweeting, 1972; Walkden, 1974; Wright, 1982).

A thin discontinuous layer of dark thrombolite (Unit B3, 1-5 cm thick) selectively encrusts areas immediately adjacent to protrusions of this karst surface. This layer has a smooth rippled or irregular pimpled upper surface with 1-2 cm relief.

Bulbous to spheroidal stromatolites (Unit B4) selectively encrust topographic highs of the underlying dark thrombolite layer, as well as protruding erosional remnants of Unit B2 (Plate 37-B). They are 3-15 cm in diameter, and have 2-8 cm synoptic relief. These stromatolites are flanked and overlain by weakly laminated dolostone which contains scattered, cauliflower chert nodules after evaporites.

MESOSTRUCTURE

Thrombolite Unit A1 comprises dark sub-digitate to amoeboid thromboids up to several centimetres in size, separated by volumetrically dominant, burrow-mottled, dolomitic wackestone (Plate 37-C). The thromboids have ragged and smoothly embayed margins, and are partially rimmed by a thin dark selvage. They have a variegated internal fabric in which numerous dark, millimetre-sized lobate bodies, poorly defined

mamillate forms, and irregular patches of micrite are evident.

The overlying mounded stromatolite (Unit A2) has a pseudo-columnar grading upwards to discrete radially divergent columnar fabric. The columns are 1-2 cm in diameter and comprise superimposed thin dark and thick light coloured, irregular convex stromatoids. Depression between adjacent columns have a thin dark selvage which indicates at least 2-3 cm synoptic relief for the columns. The columns are locally capped by a thin weakly laminated crust which tapers from about 10 to 1 mm thick down their flanks. Peloid grainstone and lime-mudstone occur between the columns.

Thrombolite mounds at the base of the upper biostrome (Unit B1) comprise small amoeboid to sub-digitate thromboids, 3-10 mm in size, and interstitial lime-mudstone (Plate 37-D). The thromboids and interstitial sediment are difficult to differentiate in hand samples (both have a micritic texture), except for the fact that the thromboids contain abundant sub-millimetre to millimetre sized, dark lobate bodies. The mounds are cut by a network of stylolitic seams which produce a prominent thin stylo-bedded fabric on outcrop surfaces.

The overlying stromatolite heads of Unit B2 consist of crudely laminated stromatoid columns and inter-columnar, burrow-mottled, peloid-skeletal wackestone. Numerous patches of very fine dolomite obscure their internal fabric. The columns are 1-2 cm in diameter, have a bumpy tuberous shape, a poorly defined selvage, and commonly contain fine to medium laminoid fenestrae.

The thin thrombolite layer (Unit B3) that encrusts portions of the karst surface, comprises poorly differentiated:
1) sub-millimetre to millimetre-sized, lobate thromboids,
2) inter-framework peloid-ooid-skeletal grainstone, and
3) laminoid fenestral-like patches of white very fine dolomite.

The bulbous stromatolites of Unit B4 comprise alternating thin dark and thick light coloured, finely corrugated, concentric laminae (Plate 37-E).

MICROSTRUCTURE

1. Thromboids

Sub-digitate thromboids: Unit A1

These thromboids have a variegated, spherulitic lobate, grumous grading to filamentous, vermiform, massive, peloidal and film microstructure (Plate 38-A,B). Lobate spherulitic aggregates are volumetrically predominant, and are interpreted as (?)bacterial precipitates within degraded coccoid colonies. They typically comprise several to tens of individual spherulites, range up to 1.5 mm in diameter, and are commonly partially enclosed within a dark 20-60 μm thick cryptocrystalline rim (Plate 39-A,B,C,D). Individual spherulites are 180-300 μm in diameter, commonly exhibit curved convex outward twin lamellae, and contain numerous submicron-sized inclusions which locally delineate radial fibrous crystallites less than 2 μm wide and 90-150 μm long.

Spherulitic microstructures commonly intergrade with turbid microspar and grumous microstructures in which spherulites are either indistinct or absent. They are surrounded and\or encrusted by grumous, vermiform, massive and peloidal microstructures.

Grumous microstructures are slightly less abundant, and intergrade with filamentous, vermiform, massive and peloidal microstructures. Individual microclots form a relatively open interconnected network, have circular to elliptical and thread-like shapes, and are typically 20-60 μm in diameter (Plate 38-A,B). They are surrounded by slightly turbid, microcrystalline cement fringes 40-50 μm thick. This grumous microstructure is thought to result from the micritic impregnation and encrustation of an open network of randomly oriented microbial filaments or filament bundles.

Vermiform microstructures are poorly and patchily developed, and intergrade with grumous and massive microstructures. Filament moulds are 25-50 μm wide, commonly have T or Y-shaped junctions, and are separated by volumetrically dominant cryptocrystalline carbonate.

Diffuse to moderately distinct rounded and subrounded peloids, 50-500 μm in diameter, are common throughout the sub-digitate thromboids. They occur either singularly within massive cryptocrystalline calcite, or in clusters (peloidal microstructure; Plate 38-A,B) in which case they are commonly individually rimmed by turbid sub-isopachous cement. The majority of these peloids probably represent detrital grains

that were either trapped by filaments or accumulated in depressions between lobate coccoid colonies. Poorly defined and irregularly shaped peloids, however, could well be *in situ* precipitates since they intergrade with grumous microstructures. The only unequivocal detrital particles within the thromboids are rare terrigenous silt grains.

Multiple films of cryptocrystalline carbonate locally encrust lobate spherulitic aggregates and discrete knob-like patches of grumous and peloidal microstructure, and form a discontinuous selvage around the margins of the thromboids (Plate 38-A,B). They are 10-30 μm thick and are separated by a similar thickness of clear microspar. They are interpreted as successive layers of calcified organic matter which enveloped coccoid colonies or encrusted semi-lithified thromboids.

The sub-digitate thromboids are disrupted by numerous burrows (0.5 - 1.5 mm in diameter) which are filled by geopetal lime-mud, peloids or cement.

Amoeboid thromboids: Unit B1

These thromboids comprise abundant lobate bodies (dark coloured in hand specimen) of slightly turbid, undulose microspar (massive lobate microstructure), surrounded by diffuse grumous to indistinctly streaky fine-microcrystalline calcite. Lobate bodies range from 200 to 1000 μm in diameter, and locally display well defined cellular lobate microstructures (Plate 39-E); they are thought to represent neomorphosed spherulitic (?)bacterial precipitates within

degraded coccoid colonies similar to those within Units A1 and B3. Numerous terrigenous silt grains occur within the enclosing grumous material which probably represents trapped lime-mud and\or micritic precipitates within enveloping mucilaginous matter.

Lobate thromboids: Unit B3

These thromboids have a spherulitic microstructure similar to that within the sub-digitate thromboids of Unit A1, and are also interpreted as degraded coccoid colonies. They are encased within fenestral peloid-ooid-skeletal grainstone.

2. Stromatoids

Pseudo-columnar to columnar stromatoids: Unit A2

These stromatoids have a diffuse, streaky to striated microstructure composed of superimposed thin, dark coloured, silty peloidal laminae, laminoid micro-fenestrae, and episodic thick, light coloured, pustular laminae (Plate 40-A). Silty peloidal laminae range from 200 to 1000 μm thick and commonly lens-out laterally. They comprise subrounded silt-sized peloids, terrigenous silt, rare fine to medium cement-rimmed peloids, ooids and intraclasts, and micrite. Pustular laminae are also laterally discontinuous, have an irregular bumpy shape, and are 1000-4000 μm thick. They are composed of massive cryptocrystalline calcite with abundant rounded to tubular patches (60-500 μm in diameter) of fine-microcrystalline calcite. These patches probably

represent burrows. Similar sized burrows at the upper surface of these laminae are filled by silty and peloidal micrite from the overlying silty peloidal laminae. The thick pustular laminae are interpreted as calcified coccoid layers which grew during periods of relative quiescence and decreased silt and peloid influx. This interpretation is consistent with the observation that modern pimpled, pustular, and mamillate mats are dominated by coccoid rather than filamentous microbes (Hofmann, 1973; Gebelein 1974; Golubic, 1983; Awramik, 1984). The thin silty peloidal laminae were probably trapped and bound by filamentous microbes.

Crudely laminated stromatoid columns: Unit B2

These columns have a diffuse streaky to striated, grumous and silty peloidal microstructure which is partially obscured by scattered dolomite rhombs (Plate 40-B). Individual microclots within grumous laminae are probably predominantly *in situ* precipitates, but some are obviously detrital grains (peloids) similar to those occurring in burrows, fenestrae, and trapped within silty peloidal (?filamentous) laminae. There is no microstructural indication of the morphology of the microbes that formed these grumous laminae. The columns locally have a weakly defined selvage, about 200-500 μm thick, which contains scattered lobate microstructures. Numerous mud and\or cement-filled burrows (0.5 - 1.5 mm in diameter) and minor laminoid fenestrae are present within the columns.

Bulbous concentric stromatoids: Unit B4

These stromatoids are composed of concentrically banded thick (250-2500 μm) light coloured, and thin (10-200 μm) dark coloured laminae. These laminae generally rhythmically alternate, but locally several laminae of the same type are superimposed directly one on top of the other. The thick laminae have a spongeous, grumous to filamentous microstructure composed of subrounded to sinuous and linear thread-like microclots, about 20-60 μm in diameter and 150-500 μm long, separated by irregular patches of clear microcrystalline spar (Plate 40-C,D,E). The microclots locally have an erect linear arrangement and terminate against the overlying lamina. Thin dark coloured laminae consist of massive cryptocrystalline calcite or locally superimposed micritic films each about 5-10 μm thick. Thick and thin laminae are locally interrupted by laminoid fenestrae and veins of fibrous gypsum.

The microstructure of these bulbous stromatolites is strikingly similar to the lacustrine oncolites described by Monty and Mas (1981) from the Lower Cretaceous of eastern Spain (compare Plates 37-E and 40-C,D,E with their Figs. 13 and 16). Monty and Mas point out that this microstructure is analogous to the modern calcified *Scytonema-Schizothrix* associations in freshwater supratidal marshes in the Bahamas (Monty 1967, 1976), and *Phormidium-Schizothrix* associations in hardwater creeks in Belgium (Monty 1976). By analogy, the thick spongeous grumous-filamentous laminae within Unit B4 are interpreted as layers of erect, relatively coarse,

calcified filaments or filament bundles, and thin crypto-crystalline laminae probably represent dense layers of pervasively calcified prostrate filaments. Alternating thick and thin laminae may have been constructed by different (large and small) filamentous species (as suggested by Monty and Mas, 1981), or else they could represent alternating erect and prostrate growth forms of the same species, such as the laminated *Scytonema* mats on Andros Island (see Monty 1967, Fig. 5; and Monty 1976, Fig. 3).

3. Detrital Sediment

Detrital sediment within both the upper and lower biostromes typically comprises burrow-mottled, very fine to coarse, peloidal wackestone and packstone. In the case of Unit B1, however, detrital sediment consists of lime-mudstone. Inter-framework sediments were probably largely derived by the erosion, bioerosion and disintegration of the microbial communities and their partially lithified constructions. Allochthonous material is rarely present, except in Unit B3 which contains abundant terrigenous silt, ooids, and peloid-ooid intraclasts. These grains are commonly rimmed by isopachous marine cement.

Metazoan debris is rare; scattered trilobite fragments are present within the stromatolite heads of Unit B2, and micrite-rimmed (?endolith-bored) mollusc fragments are common in Unit B3. Unidentified skeletal fragments are present in minor amounts in the lower biostrome (Units A1 and A2). These

fragments have a blade-like shape, are 60-100 μm thick, and at least 1.2 mm long (Plate 38-D,E). Internally they contain regularly spaced micritic rods, 50-80 μm in diameter, surrounded by a mosaic of clear spar, and generally have a diffuse micritic wall 10-15 μm thick. These fragments are reminiscent of modern *Halimeda* (codiacean green alga) plates in which the cortical utricules have been micritized and the enclosing aragonitic skeleton replaced (via solution) by cement. These blade-like fragments are unlike any of the Lower Palaeozoic codiacean algae decribed by Wray (1977), all of which have cylindrical thalli 1-2 mm in diameter. They are quite similar, however, to the monostromatic (one-cell thick) blades of the Middle Carboniferous codiacean genus *Calcifolium* (see Wray 1977, Fig. 84). Alternatively, they may be fragments of dasycladacean algae (H. Hofmann, personal communication, 1989). The micritic rods within these skeletal fragments (possibly micritized filaments) are similar in size to the majority of the rounded peloids and microclots within the sub-digitate thromboids and detrital sediment of Unit A1. It is thus postulated that some of these peloids and microclots may represent the fragmented micritized filaments of bladed algae.

ORIGIN AND PALAEOECOLOGY

The lower biostrome was initially constructed by a discontinuous community of coccoid and filamentous microbes (thrombolite unit A1). This community built a sub-digitate

framework in which lobate coccoid colonies were selectively degraded and replaced by spherulitic (?)bacterial precipitates, and filaments were either variously calcified and encrusted by micitic precipitates, or oxidized to form micro-tubular moulds. Pockets of detrital grains were locally trapped and bound into this framework by non-calcified filaments, or overgrown by coccoid colonies. This portion of the biostrome accreted in a (?)moderately turbulent environment in which incipiently lithified microbial colonies and peloids were eroded from, and accumulated between, the sub-digitate framework. It was extensively burrowed by a soft-bodied infauna, but skeletal metazoans were either scarce or absent. Bladed algae may have grown attached to the biostrome, and their fragmentation may have contributed silt-sized peloids to the inter-framework sediment.

This coccoid-filamentous community was succeeded, possibly in response to shoaling, by laterally continuous, filament-dominated mats which constructed pseudo-columnar stromatolites of low relief (Unit A2). Laminae and lenses of silt and peloids were trapped and bound by the filaments, and episodic, thick mamillate layers of pervasively calcified coccoid microbes probably developed at times of reduced turbulence and low sediment influx. These coccoid layers were extensively burrowed, and their growth was terminated by the re-establishment of silt and peloid trapping filament layers. Accretion of the biostrome was terminated by a thick blanket of terrigenous mud. Schematic reconstructions of this lower biostrome are shown in Figure 4-27.

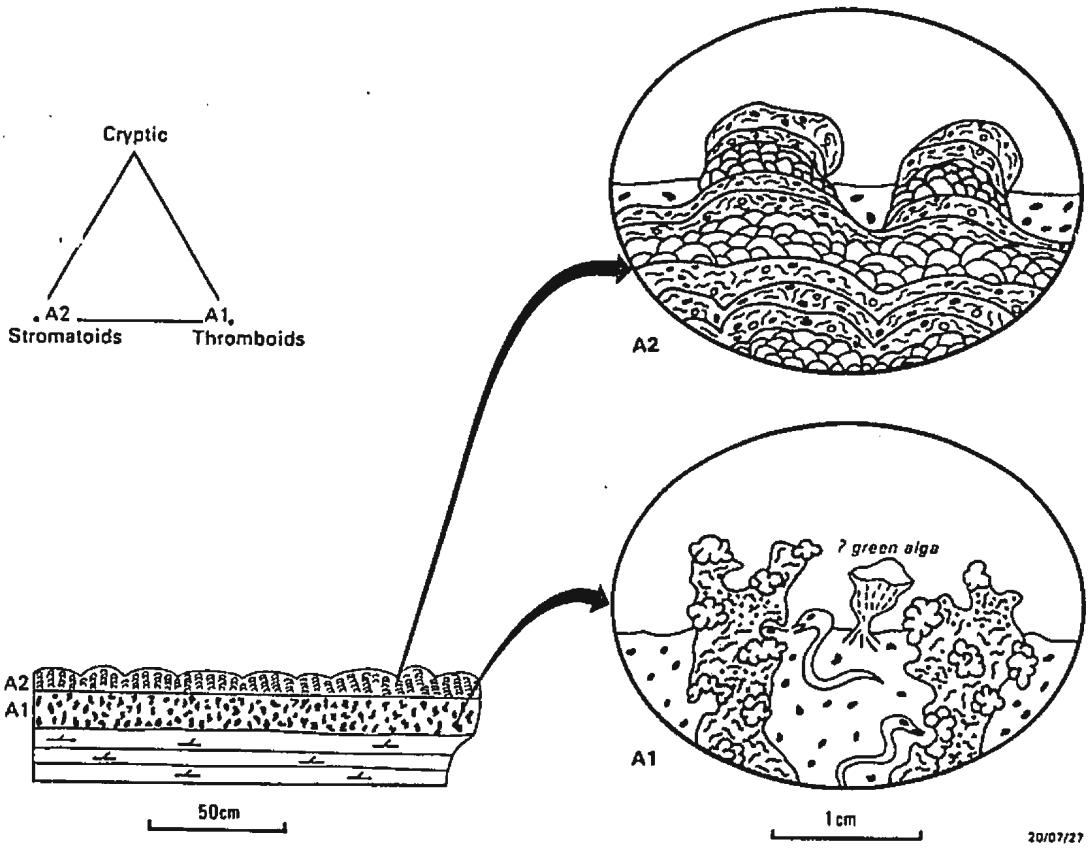

Figure 4-27. Schematic reconstructions and triangular plot of main framework components of the lower biostrome (Bed A) of Horizon J.

A discontinuous coccoid community was subsequently re-established within a tranquil, probably relatively deep, environment, and constructed large mounds of several decimetres relief (Unit B1). Poorly calcified coccoid colonies within this community were largely degraded and replaced by spherulitic (?)bacterial precipitates or microcrystalline cement. Terrigenous silt and lime-mud were probably trapped and precipitated, respectively, within enveloping mucilaginous matter. Homogenous lime-mud also accumulated in pockets between coccoid colonies. These mounds were locally burrowed by soft-bodied metazoans, and were subsequently partially buried by peloid-ooid sands, sandy dolostone and flat pebble conglomerate.

More laterally continuous, poorly laminated microbial mats were once more re-established and constructed columnar stromatolite heads several decimetres high (Unit B2). (?)Filamentous layers trapped terrigenous silt and peloids, and alternated with layers of calcified or lime-mud trapping microbes of unknown composition. Inter-column depressions were infilled by debris eroded from the columns, and these sediments were extensively burrowed by soft bodied metazoans and minor scavenging trilobites. The stromatolite heads were rimmed by vertically laminated walls of precipitated or trapped micrite, and narrow crevices between these heads were infilled by coarse debris eroded from the heads.

Accretion of the stromatolite heads was terminated by their subaerial exposure, and they and the intervening grainstone

crevices were truncated along an exposed karst surface. This smooth undulating surface contained scattered angular erosional protuberances of several centimetres relief. Following the re-submergence of the eroded biostrome, a discontinuous veneer of rippled carbonate sand was deposited on the karst surface, and this sediment was invaded, stabilized and partially bound by coccoid colonies, spherulitic (?)bacterial precipitates and inter-particle marine cement (thrombolite layer B3). Topographic highs of this stabilized sediment veneer, as well as erosional remnants that protruded above this layer, were subsequently encrusted by filamentous mats comprised of alternating layers of erect and (?)prostrate calcified filaments. These mats constructed small concentrically laminated, bulbous stromatolites (Unit B4), and show no evidence of trapped detrital grains or burrowing and scavenging metazoans. These stromatolites most likely accreted on a shallow, hypersaline, tidal flat. They are overlain and infilled by weakly laminated dolostone with evaporite nodules, the deposition of which terminated the accretion of the upper biostrome. Schematic reconstructions of this upper biostrome are shown in Figure 4-28.

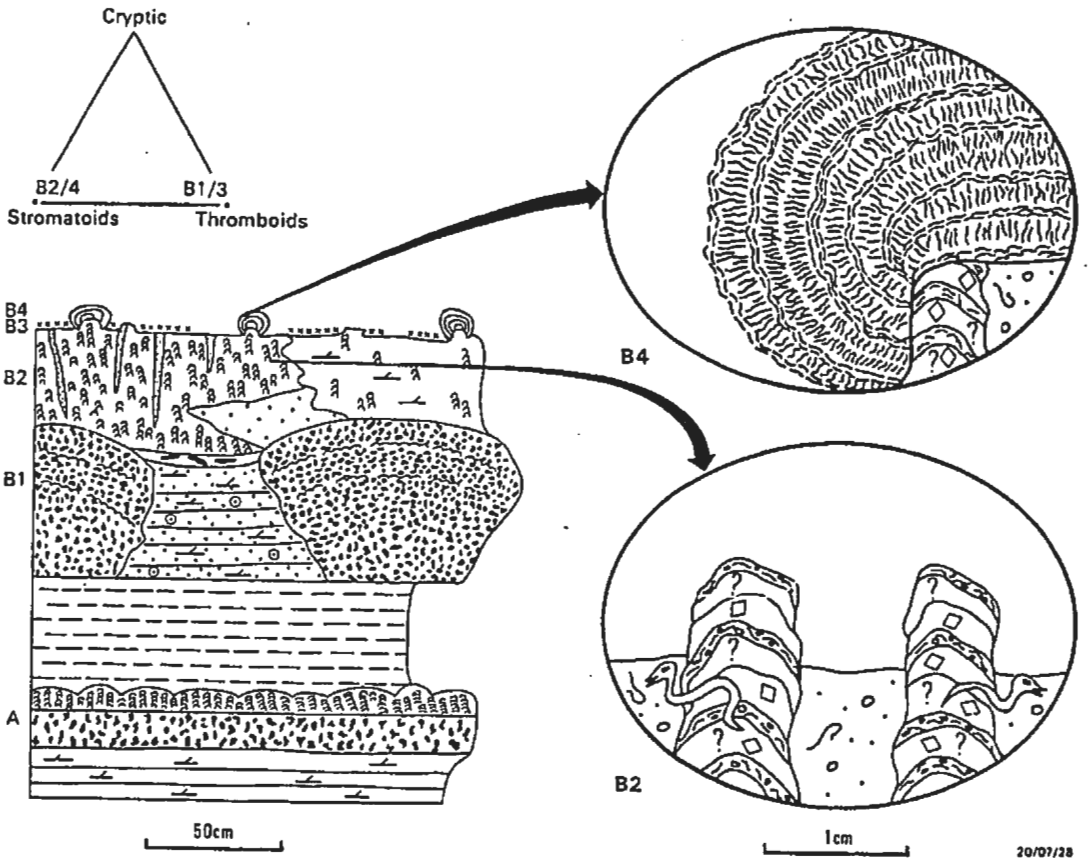

Figure 4-28. Schematic reconstructions and triangular plot of main framework components of the upper biostrome (Bed B) of Horizon J.

4.12 HORIZON K

COLUMNAR STROMATOLITE

This stromatolite occurs within a sequence of ooid grainstone and laminated dolostone in the upper portion of the Berry Head Formation on the eastern side of Isthmus Bay (Fig. 4-29; interval 24 of Chow's 1986 Isthmus Bay East Section). Although stromatolites and (?)thrombolites are common throughout the Berry Head Formation, the lower and central portions of the formation are pervasively dolomitized, and the mesostructure and microstructure of the boundstones have been largely destroyed.

MEGASTRUCTURE

The stromatolite forms a tabular biostrome, 30-40 cm thick, with a sharp planar base and an undulating upper surface which has a few centimetres synoptic relief.

MESOSTRUCTURE

The biostrome comprises two distinct zones (Plate 41-A): 1) closely spaced and coalesced columnar mounds, 15-20 cm thick and 20-30 cm wide, overlain by 2) a thin planar to undulose laminated cap.

The basal columnar mounds comprise arborescent stromatoid columns infilled by ooid-peloid-skeletal sediment. The

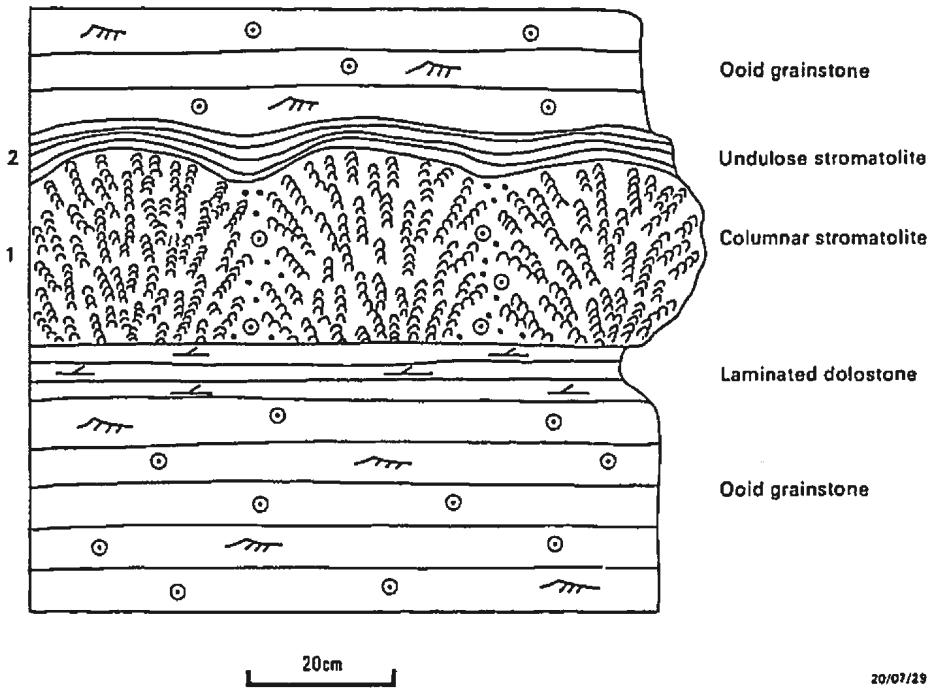

Figure 4-29. Lithological section of Horizon K, Berry Head Formation.

columns have a sub-vertical to radial arrangement, a slightly divergent style of branching, and sharply defined bumpy margins (Plate 41-B). They are 5-15 mm in diameter and vertically impersistent. In transverse section they are roughly equidimensional and vary from subcircular to irregular with numerous indentations. They have an indistinct to moderately distinct laminated fabric, which is disrupted by numerous millimetre-sized burrows and scattered fine laminoid fenestrae. The laminae have an asymmetrical, wavy convex to sub-rectangular shape, and 1-5 mm synoptic relief. They commonly bend down and coat the margins of the columns for a short distance to form a poorly defined wall.

The columnar mounds are cut by numerous dark, phosphatic, sub-horizontal stylolites which have locally telescoped the arborescent columns to form a sub-digitate and amoeboid framework. These mounds have a prominent stylo-nodular fabric in field exposures.

The overlying stratiform cap comprises thin planar to undulose micritic stromatoids with episodic 5-10 mm thick layers of mottled micrite (Plate 41-C).

MICROSTRUCTURE

1. Stromatoids

The columnar stromatoids have a streaky microstructure comprised of superimposed vermiform and episodic massive laminae (Plate 42-A,C). Successive laminae are poorly

differentiated from one another, laterally discontinuous, and range from about 200 to 2000 μm in thickness. Filament moulds are 20-60 μm thick (average about 30 μm), range up to several hundred microns long, and are aligned parallel to the laminae or, less commonly, form a randomly oriented reticulate network (Cf. *Spongiostroma maeandrinum* Gürich 1906; Plate 42-B). They may be either abundant and closely spaced or scarce and widely spaced, and are absent altogether within some laminae. Within any one lamina, however, they tend to have a uniform size, shape, orientation and density, and it is chiefly the variation of these parameters from lamina to lamina that defines the laminae. Cryptocrystalline carbonate between the filament moulds may be micritic precipitates or lime-mud trapped by the filaments. Allochthonous grains are rarely present within the columns, whereas peloids, ooids and skeletal fragments are abundant between the columns. The columns are disrupted by numerous mud and peloid-filled burrows, 250-1000 μm in diameter, and cement-filled (?)borings 250 μm in diameter.

Planar and undulose stromatoids at the crest of the bioherm have a banded microstructure comprised of rhythmically alternating 1) thin dark massive cryptocrystalline laminae, 20-100 μm thick, and 2) thicker light coloured laminae, 80-2000 μm thick, which have a massive grading to grumous (*structure grumeleuse*) and peloidal microstructure (Plate 42-D). These grumous laminae comprise moderately distinct, rounded and subrounded microclots 60-120 μm in size, and probably represent layers of trapped, partially merged,

poorly indurated detrital peloids. The alternation of thin massive and thicker grumous laminae probably represents sediment-poor and sediment-rich, probably filamentous, layers. Scattered tiny irregular nodules of spherulitic length-slow quartz, 60-180 μm in diameter, occur throughout the laminae and are locally concentrated in the upper portions of the clotted laminae. They may be pseudomorphs after gypsum or anhydrite.

Thick episodic layers of mottled micrite, 5-10 mm thick, interrupt the rhythmic alternation of massive and grumous laminae. They comprise swirling and contorted micritic laminae separated by patches of mottled micrite. These layers appear to result from the disruption (?bioturbation) of several interlaminated massive and grumous laminae.

2. Detrital Sediment

Inter-column sediment comprises poorly sorted peloid-ooid grainstone and packstone (Plate 42-A). Small gastropod fragments and vermiform intraclasts are also common, and gastropods are locally concentrated in pockets between adjacent arrays of arborescent columns.

ORIGIN AND PALAEOECOLOGY

The lower columnar mounds were constructed by discontinuous mats of prostrate filaments. The filaments evidently had only a limited ability to trap or agglutinate detrital particles

other than lime-mud, and were probably encrusted by micritic precipitates. The mats grew in a moderately turbulent subtidal environment in which ooid and peloid sands were continuously washed into inter-column interstices from adjacent carbonate shoals. The mounds were grazed by numerous gastropods and were extensively burrowed and (?)bored by soft-bodied metazoans.

The mounds were subsequently colonized, possibly in response to shoaling and reduced influx of carbonate sand, by laterally continuous mats comprised of alternating sediment-poor and sediment-rich ?filamentous layers. This layering probably resulted from the periodic trapping and binding of storm or tidal sediment (as is the case for similar laminae on the Andros Island tidal flat; Hardie and Ginsburg, 1977). The mats grew in a shallow, perhaps hypersaline, intertidal to supratidal environment devoid of gastropods and burrowing metazoans. Schematic reconstructions of the biostrome are shown in Figure 4-30.

The columnar stromatolites are very similar to the stromatolite form *Madiganites mawsoni* described by Walter (1972) from Middle-Upper Cambrian strata within the Amadeus Basin, central Australia. Examples of these Australian forms are described in detail in Chapter 5, Section 5.5.

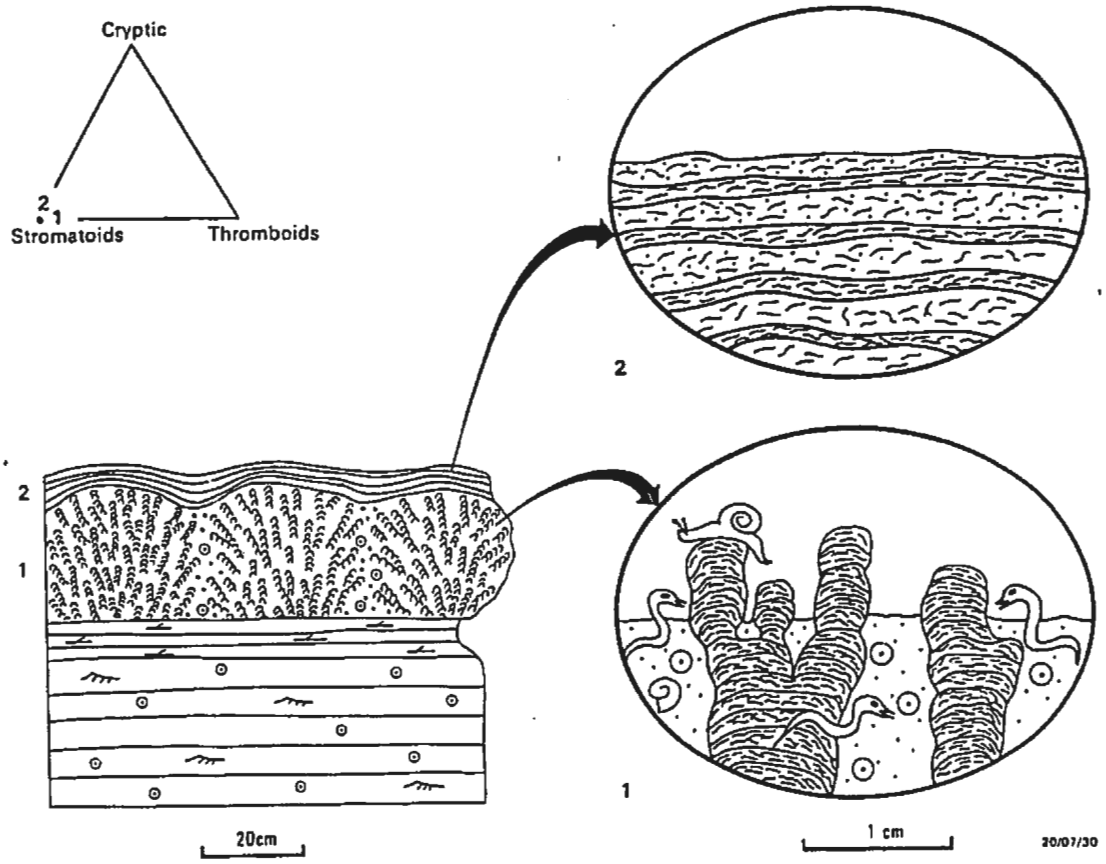

Figure 4-30. Schematic reconstructions and triangular plot of main framework components of Horizon K.

4.13 HORIZON L

GREEN HEAD MICROBIAL-METAZOAN COMPLEX

This complex was described in considerable detail by Pratt (1979) and Pratt and James (1982), and corresponds to the *Diphragmoceras* beds of Schuchert and Dunbar (1934) and Flower (1978). It records the first appearance of composite microbial and metazoan framework-building communities within the Cambro-Ordovician sequence of western Newfoundland, and as such heralds the transition from Cambrian microbial buildups (thrombolites and stromatolites) to Middle Ordovician metazoan buildups constructed by sponges, corals, stromatoporoids, bryozoans or calcareous algae. The Green Head Complex was thus re-examined in order to document the interaction between microbial and metazoan frame-building communities, and to assess the impact that this interaction has on the mesostructural and microstructural fabric of the buildup.

The complex is exposed at Green Head at the southwestern end of Isthmus Bay, in the middle portion of the Watts Bight Formation (Beds 57-61 of Pratt's 1979 Isthmus Bay Section). It is underlain by massive dolostone with chert nodules and relict pods of burrowed wackestone and mudstone, and is overlain by thinly interbedded, burrowed and cross-laminated, lime-grainstone and mudstone. These underlying and overlying beds represent open subtidal facies (Pratt, 1979; Pratt and James, 1982, 1986).

The following megastructural and mesostructural analysis of the complex is largely based on Pratt's (1979) and Pratt and James's (1982) study. The microstructure of the complex, however, particularly that of the microbial components, has not been specifically analysed before.

MEGASTRUCTURE

The complex is 12 m thick and has an exposed width of 70 m. It is flanked to the west by interfingering dolomitic grainstone, and its eastern (present seaward) extent is unknown. Pratt (1979) distinguished eight boundstone units within the complex, referred to here as Units 1 to 8, each partially separated by beds or channels of bioclastic grainstone (Fig. 4-31). The bedforms of these boundstones are generally poorly defined; Units 1, 5, 6 and 7 form tabular biostromes 1.5 - 4 m thick; Units 3, 4 and 8 form lenticular and tonguing bioherms about 2 m thick; and Unit 2 comprises a series of gently domed tabular bioherms 30-40 cm thick. Based on the relationship of the boundstones to the flanking grainstones, Pratt (1979) estimated that their maximum synoptic relief was about one metre.

MESOSTRUCTURE

With the exception of Units 2 and 7, the boundstones are characterized by complex, poorly differentiated internal fabrics which are partially obscured by widespread

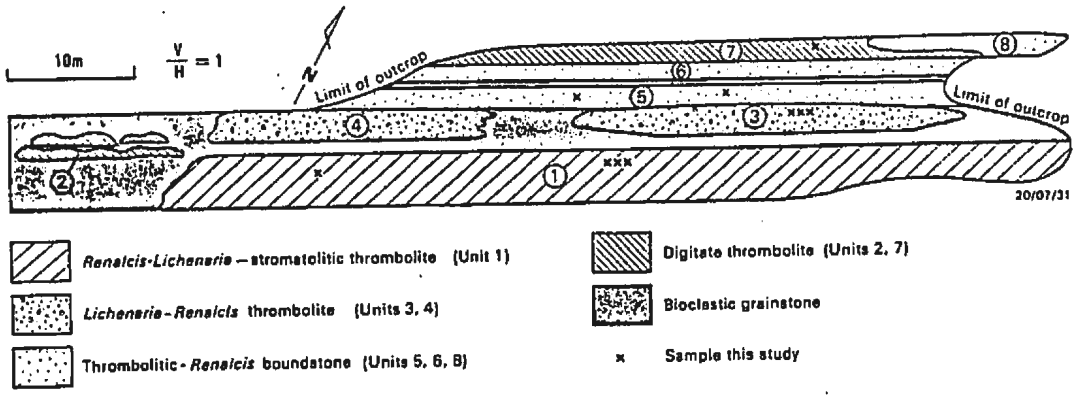

Figure 4-31. Outcrop sketch of the Green Head Complex, Watts Bight Formation (Horizon L). Modified after Pratt and James (1982).

dolomitization and, less frequently, silicification. Four types of framework components occur within the complex: 1) thromboids (synonymous with "thrombolite" as used by Pratt, 1979, and Pratt and James, 1982), 2) *Lichenaria* corals, 3) *Renalcis*, and rarely 4) stromatoids (synonymous with "cryptalgal laminite" as used by Pratt, 1979, and Pratt and James, 1982). Sponges have long been suspected within these rocks (N.P. James, personal communication 1985), but none have been recognized despite numerous searches of outcrops, slabs and thin sections. Based on the distribution and relative abundance of these framework components, Pratt (1979) and Pratt and James (1982) recognized the following boundstone lithologies:

1. Thrombolite-*Lichenaria*-*Renalcis* boundstone (Units 1,4)
2. Thrombolite mounds (Units 2,7)
3. Thrombolite-*Renalcis* boundstone (Unit 3)
4. *Renalcis*-thrombolite boundstone (Unit 5, 6, 8)

During the present study, serial slabs and several large thin sections were prepared of at least two representative samples of each moundrock lithology. *Lichenaria* corals do not occur within any of the samples of Unit 1, but are conspicuous within all samples of Unit 3; exactly the reverse of Pratt and James's (1982) observations. Thus, assuming that Pratt and James did not mis-label their samples (the present samples were re-checked during subsequent field work), it appears that Units 1, 3 and 4 all contain *Lichenaria* corals. Apparent discrepancies in the observed composition probably result from marked variations in the abundance and

distribution of corals within a unit, or perhaps equally significant, simply reflect the fact that the internal fabrics of the boundstones are poorly differentiated and obscured by bioturbation, dolomitization and silicification.

1. Thrombolite-*Lichenaria-Renalcis* Boundstone (Units 1,4)

This lithotype comprises irregular closely spaced, thrombolitic heads approximately 5-15 cm wide, separated by thin wedges, channels and tunnels of skeletal wackestone and grainstone. The individual thrombolitic heads are generally poorly differentiated, but are locally delineated by partial dolomitization and silicification, or selective silicification of their margins (Plate 43-A). They have a complex variegated internal fabric comprised of: 1) clusters of dark lobate, sub-arborescent or amoeboid thromboids, 2) light coloured masses of *Renalcis*, 3) *Lichenaria* corals*, 4) irregularly laminated (?)stromatoids, 5) patches of burrowed grainstone, packstone and wackestone, 6) light coloured cavity-filling lime-mudstone, 7) cavity-filling radiaxial fibrous calcite, and 8) lodged nautiloids, gastropods, brachiopods and trilobites (Plates 43-B, 44-A). These components vary in abundance within the units and within individual thrombolitic heads, and are generally poorly differentiated. For the samples collected during this

* *Lichenaria* was described and illustrated in these units by Pratt (1979) and Pratt and James (1982), but was not observed during the present study.

study, it is difficult to reliably trace out the distribution of the components on polished or etched slabs in the manner illustrated by Pratt and James (1982, Figs. 20, 22). Microbial components (thromboids, *Renalcis*, and ?stromatoids) are particularly poorly differentiated and exhibit a spectrum of intergradational fabrics; for example, masses of *Renalcis* intergrade with clusters of thromboids, and thromboids are variously mixed with patches of bioturbated inter-framework sediment, and merge with crudely laminated (?)stromatoids and cavity-filling sediment.

Thromboids range from tiny sub-millimetric lobes, to millimetre-sized sub-arborescent, and ragged amoeboid forms several centimetres in size (Plate 43-B, 44-A). They are encased within light coloured micro-clotted lime-mudstone and are commonly disrupted by metazoan burrows. *Renalcis* predominantly occurs as an encrusting wall 1-3 cm thick around the margins of the thrombolitic heads. It has an outward growth direction, and on overhanging margins it forms pendant downward directed bushes. *Renalcis* walls are commonly selectively silicified.

In terms of the classification scheme proposed for mixed microbial-metazoan buildups (Chapter 3), these boundstone units are classified *Renalcis-Lichenaria*-?stromatolitic thrombolites.

2. Digitate Thrombolite (Units 2,7)

This lithotype comprises a framework of dolomitic and siliceous digitate thromboids infilled by burrow-mottled packstone and wackestone. The digits are 1-2 cm in diameter and have either slightly divergent (Unit 2) or parallel (Unit 7) anastomosed style of branching (Plate 43-C). In plan view they form a discontinuous fine cerebroid pattern. Internally the digits have a diffuse clotted, mottled, massive or crudely laminated fabric.

3. Thrombolite-*Lichenaria-Renalcis* Boundstone (Unit 3)

This boundstone has a similar fabric and composition to Units 1 and 4. It has a prominent cerebroid outcrop pattern comprised of: 1) dark coloured, roughly pitted thrombolite heads 20-80 cm in diameter, encrusted by, 2) light coloured, smooth textured *Renalcis*-rich walls 3-10 cm thick, and separated by 3) thin dark coloured wedges or channels of packstone and wackestone with lodged gastropods and nautiloids (Plate 43-D,E). The thrombolitic heads comprise an anastomosing, semi-prostrate framework (approximately 60% by volume) of intergrown clusters of thromboids and *Lichenaria* corals, and light coloured inter-framework lime-mudstone (Plate 44-B). The proportion of corals appears to increase at the top of the thrombolite heads; they are rare or absent within the core of the heads, but comprise up to 30-50% of the crest of the heads where they form a self-supporting

framework encrusted by thromboids or *Renalcis* (Plate 45-A,B). The coral colonies are 1-3 cm in size, and the corallites have a divergent, upward and outward growth direction. The corals thus occur in a similar manner to that described by Pratt (1979) and Pratt and James (1982) at the crest of the thrombolitic heads in Unit 1, but were not recorded in Unit 3 by those authors. The corals, and to a lesser extent thromboids and *Renalcis*, are frequently replaced by dolomite and\or silica. Thromboids, *Renalcis* and inter-framework lime-mudstone are commonly disrupted by metazoan burrows.

This lithotype is classified a *Lichenaria-Renalcis* thrombolite, and exhibits an internal zonation from 1) *Lichenaria* and *Renalcis*-poor thrombolite, to 2) thromboid-*Lichenaria-Renalcis* framestone at the crests of the heads, and 3) encrusting walls of *Renalcis* boundstone. Stromatoids have not been observed within this unit.

4 *Renalcis*-Thrombolite Boundstone (Units 5, 6, 8)

This lithotype comprises small, free-standing or coalesced, light coloured masses of *Renalcis,* intergrown with clusters of thromboids, and separated by darker coloured wedges and channels of nautiloid, brachiopod, gastropod and trilobite wackestone and packstone. The *Renalcis*-thromboid masses have variable rounded, club or wall-like shapes, range from a few to several centimetres in size, and are commonly selectively dolomitized or silicified. *Renalcis* generally has an upward and outward growth direction and encrusts, or is in turn

encrusted by, clusters of dark millimetre-sized thromboids. *Renalcis* is volumetrically dominant, but intergrades with thromboids. Metazoan burrows are common throughout this boundstone. Framework cavities are relatively scarce and corals are absent.

This lithotype is classified a thrombolitic *Renalcis* boundstone.

MICROSTRUCTURE

1. Thromboids

The thromboids have a variegated lobate, grumous, spongeous and massive microstructure, and commonly intergrade with clotted, saccate and chambered *Renalcis* (Plates 46-49). Lobate structures comprise crypto- or micro-crystalline lobes 100-500 μm in diameter, separated by irregular patches of massive micrite (composite lobate-massive microstructure), clotted micrite (composite lobate-grumous microstructure), or amoeboid micro-fenestrae (composite lobate-spongeous microstructure) (Plates 46-C,D, 47-C,D, 48-A, 49-C). Diffuse and distinct grumous microstructures also commonly occur in conjunction with amoeboid micro-fenestrae (composite grumous-spongeous microstructure; Plate 48-B), and intergrade with clotted *Renalcis* (Plate 46-A,B,E). Individual microclots are 30-80 μm in size and commonly form pendant clusters beneath

coral colonies (Plate 48-D) or lobate thromboids (Plate 49-C). Within spongeous microstructures, micro-fenestrae range from about 100 to 600 μm wide, show no preferred orientation, and frequently increase in abundance away from the margins of individual heads. They contain variable amounts of infiltered pellets (Plates 46, 49), and are occluded by microcrystalline cement.

Gradations between lobate, grumous and *Renalcis* microstructures suggest that they have a related origin and were probably generated by various degrees of preservation, decay and calcification of different coccoid growth forms.

Thromboids are commonly disrupted by small metazoan burrows. Apart from infiltrated pellets within burrows and micro-fenestrae, detrital grains such as peloids or skeletal debris do not occur within thromboids. Detrital pellets within burrows and micro-fenestrae are possibly disintegrated and reworked microbial precipitates or faecal pellets.

The grumous-spongeous-*Renalcis* crusts around the coral framework at the crest of the thrombolitic heads in Unit 3 (Plate 47-A,B) are a micro-fenestrate framework of calcified coccoid colonies [*Renalcis*] and *in situ* microbial precipitates [microclots] which had little or no ability to trap and bind detrital grains.

2. *Renalcis*

Renalcis generally has an upward and outward growth direction, but also forms 1) pendant downward directed growth

forms that roof shelter cavities (Plate 49-C), 2) randomly oriented to prostrate growth forms (Plate 49-A,B), and 3) constructs overhanging encrusting walls at the margins of individual thrombolitic heads (Plate 47-A,B). Chambered, saccate and clotted morphotypes (Pratt, 1984) are approximately equally abundant, and range in shape from botryoidal aggregates to branching arborescent forms. The individual chambers, sacs and clots range from about 20 to 250 μm in diameter. Interstices between *Renalcis* thalli variously consist of massive or clotted lime-mud, microspar or amoeboid fenestrae with infiltered pellets. With progressive infilling and coalescence of the individual chambers, sacs and clots, *Renalcis* intergrades with grumous and lobate microstructures (Plates 46-B,C,D,E, 49-B). Within all units, *Renalcis* has commonly been selectively replaced by coarse epigenetic dolomite or microcrystalline quartz.

3. Corals

Corals form irregular sub-rounded to fan shaped colonies 1-3 cm in size. The individual corallites are sub-circular in cross-section, about 500-600 μm in diameter, and have divergent upward and outward growth directions (Plate 48-C,D). They comprise a thin cryptocrystalline calcite wall and a hollow centre variously infilled by geopetal pellets and calcite cement. Very commonly however, the corals have been extensively replaced by microcrystalline quartz or coarse epigenetic dolomite, and their microstructure has

accordingly been largely destroyed. The corals belong to the tabulate genus *Lichenaria* (Pratt and James, 1982; identification confirmed by J.E. Sorauf, State University of New York at Binghamton).

4. Detrital Sediment

Several types of detrital sediment occur within the boundstones: 1) geopetal pellets within burrows and micro-fenestrae, 2) massive or weakly laminated lime-mudstone within framework cavities, 3) bioturbated peloid-skeletal wackestone, packstone and grainstone between framework components, and 4) thin wedges or channels of skeletal wackestone or grainstone between individual thrombolitic heads. The inter-framework and inter-head sediment contains abundant peloids, silt-size ?faecal pellets, reworked microbial fragments, nautiloids, gastropods, brachiopods, trilobites, minor pelmatozoan fragments and, only in one sample each, rare *Girvanella* clasts and *Nuia*. Metazoan debris is relatively scarce, however, within the digitate thrombolites of Units 2 and 8. Inter-framework sediments within Unit 3 are mud-dominated, and small stromatactis-like cavity fillings, 1-3 mm high and up to 15 mm long, are common within this unit (Plates 47-C,48-A). Brachiopods are particularly abundant within the inter-framework sediments of Units 5 and 6 (Plate 49-D).

ORIGIN AND PALAEOECOLOGY

The boundstones were predominantly constructed by variously degraded and calcified coccoid microbes (thromboids and *Renalcis*) and *Lichenaria* corals, and were inhabited by a rich endobiontic, epibiontic and nektobiontic fauna of soft bodied ?worms, gastropods, trilobites, brachiopods and nautiloids. Variable proportions of thromboids, *Renalcis* and *Lichenaria* formed a rigid framework with numerous irregular nooks and cavities in which whole gastropod and nautiloid shells, various other skeletal debris, microbial fragments, ?faecal pellets and lime-mud accumulated. Open shelter cavities were inhabited by small burrowing metazoans, *Renalcis* and rarely laminated sediment-trapping microbial mats (stromatoids). Framework and inter-framework sediments were extensively bioturbated. The boundstones accreted in an open subtidal environment, and were flanked and episodically inundated by sheets of bioclastic sand. A typical macroscopic reconstruction of the thrombolite-*Lichenaria*-*Renalcis* boundstones is shown by Pratt and James (1982, Fig.29). Since pelmatozoan debris is scarce throughout the boundstones, it is doubtful that they grew attached to the mound surface as depicted in their figure. Certainly they make up a significant proportion of the flanking sand sheets. A microscopic reconstruction of these boundstones is shown in Fig. 4-32.

The initial boundstone-forming community was dominated by coccoid microbes and corals were generally relatively scarce

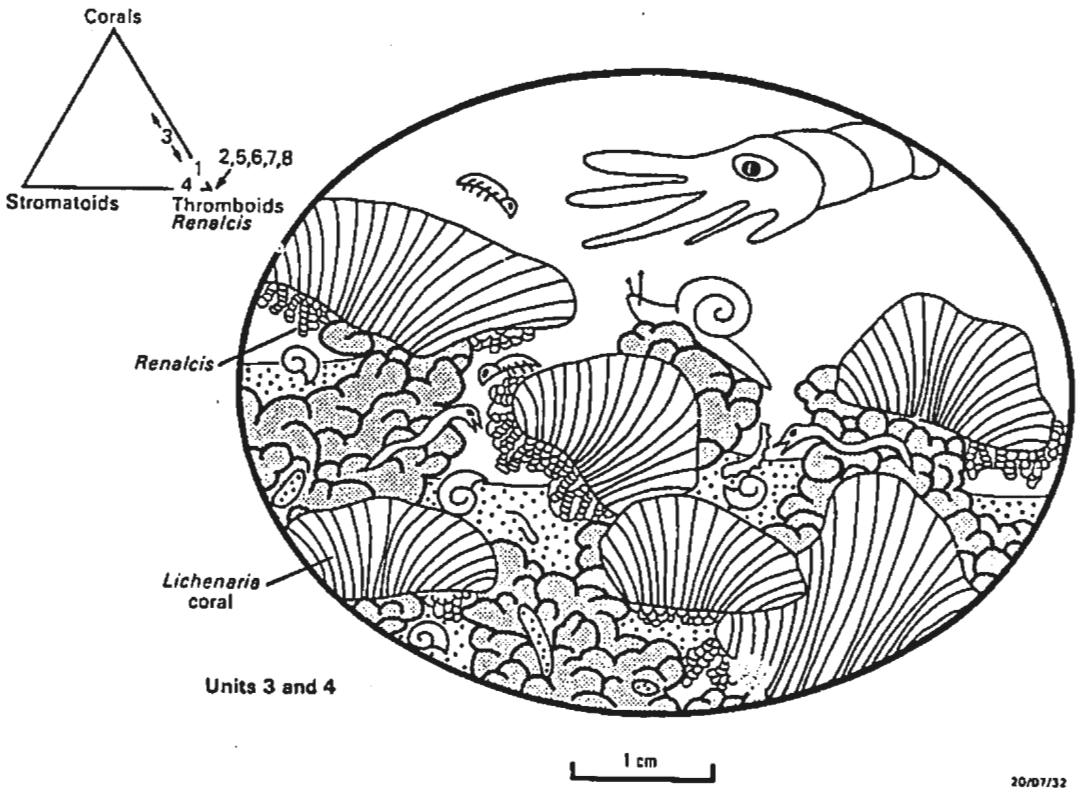

Figure 4-32. Schematic reconstruction of *Lichenaria-Renalcis* thrombolite (Units 3 and 4) and triangular plots of main framework components of the Green Head Complex (Horizon L).

or only locally abundant. The tabular biostrome constructed by this community (Unit 1) was subsequently buried by bioclastic sands. Microbial communities of unknown structure and composition constructed low relief digitate bioherms on the flanks of the complex at this time (Unit 2), and metazoans were scarce. Microbial and metazoan communities were soon re-established across much of the aggrading complex (Units 3 and 4); variously degraded and calcified coccoid colonies constructed a series of small thrombolite heads, the crests of which comprised intergrown corals and coccoid colonies (thrombolitic *Lichenaria-Renalcis* framestone), and the flanks of which were encrusted by walls of arborescent *Renalcis* (*Renalcis* boundstone). Allochthonous and autochthonous grains were greatly reduced in abundance at this time, and framework interstices were filled with lime-mud and cement to form small *Stromatactis*-like structures. These coral-coccoid mounds probably grew within a more tranquil environment than the underlying unit. Relatively tranquil conditions probably persisted during the subsequent widespread establishment of *Renalcis* communities (Units 5, 6 and 8), at which time corals disappeared and brachiopods increased in abundance. These faunal changes possibly resulted from subtle environmental changes in either water turbulence, clarity, salinity or temperature. Microbial communitites then constructed a digitate biostrome at the top of the complex (Unit 7), at which time metazoans were essentially excluded from the complex. Although there is no evidence of the cause of their demise, progressive upbuilding

and shallowing of the complex may have restricted water circulation and resulted in elevated salinities, conditions traditionally regarded as hostile to metazoans.

The palaeoecological controls of the microbial-metazoan communities are poorly understood, but the sequence of boundstones appears to represent an ecological succession loosely comparable to that described by Walker and Alberstadt (1975) for younger metazoan reefs. Microbial communitities clearly had a pioneering role in the establishment of the complex (Unit 1), and were subsequently accompanied and locally displaced by corals in what can be regarded as a diversification stage (Unit 3 and 4, and perhaps the uppermost part of Unit 1). Endobiontic, epibiontic, nektobiontic and coelobiontic organisms were most abundant at this stage. The succeeding *Renalcis*-dominated and digitate microbial communitites of Units 5, 6, and 7 may represent a domination stage, but typical encrusting or laminated organic growth forms are not present. In the absence of encrusting skeletal metazoans or calcareous algae (Chlorophytes or Rhodophytes), this stage might reasonably be expected to be represented by stromatolites, but stromatolites are conspicuous by their virtual absence throughout the complex. In view of the fact that there is no evidence of increased turbulence or wave action at the crest of the complex, it is perhaps not surprising that a true climax community did not develop since, as noted by Walker and Alberstadt (1975), such a stage may represent an allogenic response to turbulence.

4.14 HORIZON M

ABERRANT STROMATOLITIC AND CRYPTIC MICROBIALITES

Three stromatolitic beds with unusual internal fabrics occur at the top of the Watts Bight Formation on the eastern side of Isthmus Bay (Beds 78-83 of Pratt's 1979 Isthmus Bay Section). They are underlain and overlain by cross-bedded, peloid-intraclast grainstone. A lithological section of this horizon is shown in Figure 4-33.

MEGASTRUCTURE

The beds form a series of closely spaced domed to discoidal bioherms up to 140 cm thick and 6 m long (Plates 50-A, 51-A). They are flanked by cross-bedded, poorly sorted, peloid-intraclast grainstone, and appear to have moderate synoptic relief, probably 30 cm or more. Narrow channels between the mounds are commonly filled with flat-lying or edgewise pebble conglomerate.

MESOSTRUCTURE

The lower bioherms (Bed A, Fig. 4-33) comprise irregularly mottled, amoeboid cryptomicrobial boundstone (Zone A1; Plate 50-B), capped by a 10-20 cm thick zone of aberrant digitate and cup-like structures (Zone A2; Plate 50-A). They contain numerous gastropods and nautiloids, particularly towards

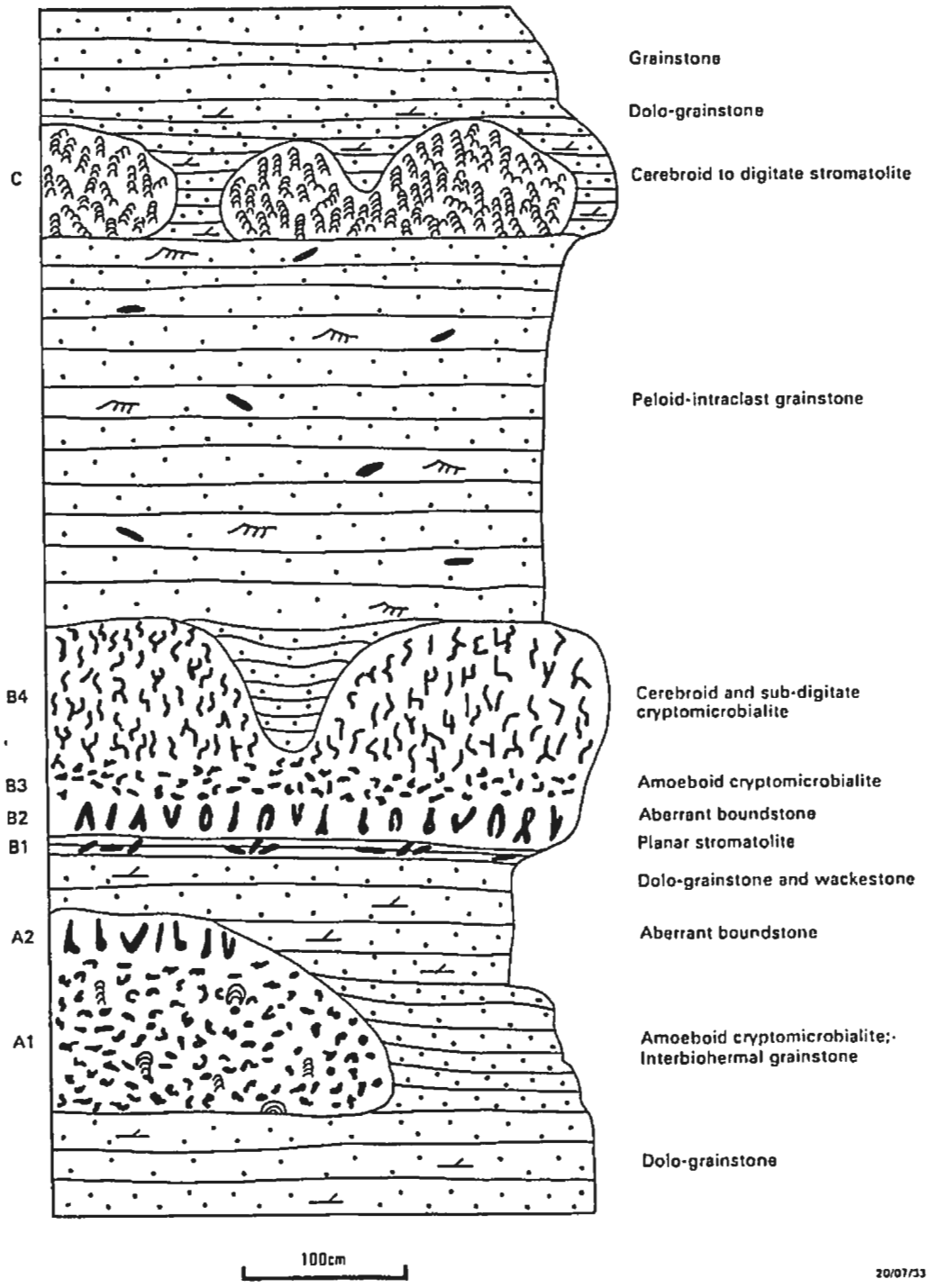

Figure 4-33. Lithological section of Horizon M, Watts Bight Formation.

their crest, and are extensively bioturbated. Crudely laminated stromatoid columns and hemispheroids, 1-3 cm wide and several centimetres high, separated by patches of burrowed peloid-skeletal wackestone, are locally discernible on slabbed and polished samples of Zone A1. Generally however, the original fabric has been obscured by dolomitization, stylolitization and bioturbation. The aberrant digitate and cup-like structures in the upper zone are vaguely suggestive of stromatoid encrusted sponges*, but diagnostic morphological evidence is lacking, and micro-structurally they are indistinguishable from the other dolomitized cryptomicrobial structures.

Bioherms of Bed B have a complex zoned fabric. A thin basal layer of flat-pebble conglomerate and planar stromatoid sheets (Zone B1) is overlain by a zone of aberrant conical and cup-like stromatoids with edgewise pebbles lodged between them (Zone B2; Plate 50-C,D). These aberrant structures consist of steep to overhanging, either downward opening (convex) or upward opening (concave), stromatoid laminae around an axial core of coarse calcite cement, dolomite and locally geopetal sediment. The origin of these structures is highly enigmatic, but clearly their axial portion was dissolved after the growth and lithification of the enveloping stromatoid laminae. This zone passes abruptly, possibly with erosional contact, into zones of amoeboid

* Definitive sponges first appear in the upper portion of the overlying Boat Harbour Formation, approximately 25 m above the base of the upper, unconformity-bound, megacycle of the St. George Group.

(Zone B3, approximately 10-20 cm thick) grading to cerebroid and sub-digitate (Zone B4, approximately 100 cm thick) cryptomicrobial structures (Plate 50-E). The amoeboid, cerebroid and sub-digitate structures are pervasively dolomitized and generally retain no vestige of their original fabric and microstructure.

The bioherms of Bed C comprise an anastomosing, cerebroid to digitate framework of weakly laminated stromatoid columns and inter-column dolomitic sediment (Plate 51). The columns are approximately 1-3 cm wide and range from irregular stubby forms to elongate arborescent forms at the crests of the bioherms. They have ragged margins and an indistinct dark selvage (Plate 51-C). Small cement-filled shelter cavities are common between the stromatoids.

MICROSTRUCTURE

1. Stromatoids

Crudely laminated stromatoid columns; Beds A and C.

These stromatoids have a spongeous, *structure grumeleuse* microstructure. Laminae are 300-1500 μm thick and comprise diffuse subrounded cryptocrystalline microclots 20-60 μm in size, and irregular amoeboid to laminoid fenestrae 100-350 μm wide (Plate 52-A,C,D). The origin of the microclots is uncertain; they could be *in situ* microbial precipitates, or partially merged, trapped detrital peloids. Although definitive detrital peloids are rarely present within the

columns, detrital silt-sized peloids indistinguishable from the microclots commonly occur as geopetal accumulations within the fenestrae. It thus seems likely that this *structure grumeleuse* results from the selective trapping and binding of similar silt-sized peloids by microbial (?filamentous) communities, whereas coarser sand-sized peloids accumulated between the columns. Selective trapping and binding of the finer grained fraction of sediments is a common feature of stromatolites (Black, 1933; Gebelein, 1969; Frost, 1974; Hardie and Ginsburg, 1977).

Local patches of spherical cellular bodies, approximately 200 μm in diameter, occur within the columns, encased within *structure grumeleuse* material (Plate 52-B). These spherical bodies may represent former coccoid colonies (cf. cellular lobate microstructure) or, perhaps more likely, calcispheres (calcareous reproduction cysts of dasycladacean algae; Marszalek, 1975, and Wray, 1977) that were trapped and bound within the columns.

The dark selvage around the columns within Bed C have a massive to diffuse vermiform microstructure (Plate 52-A). Filament moulds are 30-40 μm wide, and are predominantly oriented parallel to the margins of the columns. This selvage locally intergrades with the spongeous *structure grumeleuse* microstructure of the columns.

Planar stromatoid sheets; Bed B, Zone B1

These stromatoids have a weakly striated microstructure

comprised of relatively thick peloidal layers and lenses, 350-2000 μm thick, episodically alternating with thinner micritic laminae, 20-100 μm thick (Plate 53-A). Scattered skeletal debris (pelmatozoans, trilobites and gastropods) occurs within the peloidal layers and lenses. These sheets were most likely constructed by alternating sediment-rich and sediment-poor filamentous layers.

Aberrant conical and cup-like stromatoids; Bed B, Zone B2

These forms have a finely banded to striated microstructure comprised of rhythmically alternating 1) peloidal laminae and lenses, 100-1000 μm thick, and 2) thin micritic laminae, 10-30 μm thick (Plate 53-B). Their microstructure is essentially similar to that of the underlying stromatoid sheets (Zone B1) except that: 1) the laminae are thinner and more sharply defined, 2) peloidal and micritic laminae occur in rhythmic rather than episodic alterations, and 3) peloids are finer grained and better sorted (20-80 μm in size). The axial portion of these structures comprises coarse calcite cement and locally geopetal sediment. These enigmatic structures may possibly represent stromatolite-encrusted sponge moulds.

2. Cryptomicrobial Structures

The amoeboid, cerebroid and digitate cryptomicrobial structures of Zones A1, B3 and B4 are largely replaced by medium grained dolomite, or have a poorly preserved diffuse

grumous, mottled and massive microstructure (Plate 53-C,D). They locally show evidence of bioturbation, and rarely have a relict weakly laminated fabric. It seems likely that their original microstructure was similar to that of the stromatoid columns of Beds A and C.

3. Detrital Sediment

Detrital sediment ranges from burrowed peloid-skeletal wackestone and packstone within the irregularly mottled and amoeboid cryptomicrobial Zones A1 and B3, to poorly sorted peloid-intraclast packstone and grainstone within zones which have vertically elongate, cup-like, conical, cerebroid and digitate frameworks (Zones A2, B2, B4, and C). Reworked framework fragments are common within all three beds. Gastropods, nautiloids and trilobite fragments are common within Bed A, but skeletal debris is generally scarce within Beds B and C.

ORIGIN AND PALAEOECOLOGY

The bioherms grew in a moderately turbulent subtidal environment between migrating peloid shoals. Although it is not possible to determine the detailed composition, structure and palaeoecology of the microbial communities within each boundstone bed, they were probably all constructed by broadly similar communities. Their framework was evidently constructed by the selective trapping and binding of silt-

sized peloids by poorly laminated ?filamentous communities, the specific architecture of the framework probably being a function of the rate of sediment influx and degree of bioturbation. Thus the irregularly mottled and amoeboid frameworks of Zones A1 and B3 probably reflect low sediment influx and intense bioturbation; the vertically elongate cup-like, conical, cerebroid, digitate and columnar frameworks of zones A2, B2, B4 and C reflect high sediment influx and moderate bioturbation; and the stratiform fabric of Zone B1 reflects episodic sediment influx and minor bioturbation. The aberrant cup-like and conical structures of Zones A2 and B2 possibly owe their origin to former sponges which, in Zone B2, were encrusted by finely laminated filamentous communities. Skeletal metazoans were otherwise generally scarce, except for the bioherms of Bed A which were inhabited by numerous gastropods and nautiloids. A tentative reconstruction of the bioherms of Bed C is shown in Figure 4-34, and is probably equally applicable to the non-aberrant zones of Beds A and B.

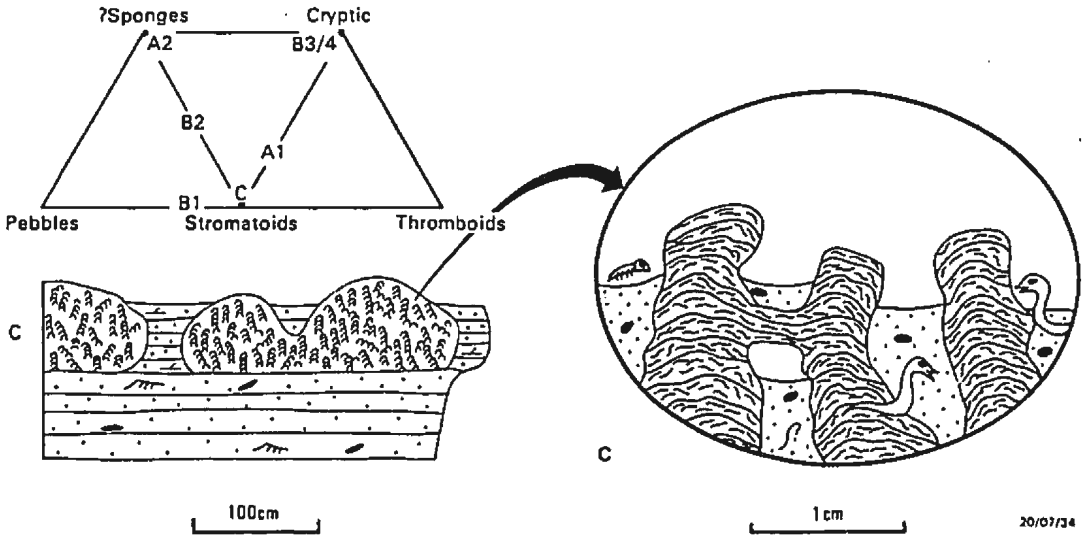

Figure 4-34. Schematic reconstruction of Bed C and triangular plot of main framework components of Horizon M.

4.15 HORIZON N

ZONED STROMATOLITE-THROMBOLITE

This zoned stromatolite-thrombolite bed directly overlies a series of stromatolite mounds in the lower portion of the Boat Harbour Formation on the western side of Isthmus Bay (Fig. 4-35; Beds 123-125 of Pratt's 1979 Isthmus Bay Section). These microbial beds are underlain by alternating thin-bedded grainstone and mudstone, interspersed with undulose stratiform stromatolites and small isolated and linked hemispheroidal stromatolites (Pratt and James's, 1986, intertidal lithotypes D and E), and are overlain by thinly interbedded grainstone and mudstone, and cryptalgal laminated dolostone (Pratt and James's intertidal and supratidal lithotypes D and A).

MEGASTRUCTURE

The underlying stromatolite (Bed A in Fig. 4-35) forms isolated and coalesced, domed and discoidal bioherms, 20-75 cm thick and 40-400 cm in diameter. These bioherms locally coalesce to form elongate composite bioherms up to 5 m long (Plate 54-A). They are flanked and draped by thin-bedded grainstone and dolo-mudstone, and probably had minor topographic relief during their growth (10-15 cm).

The overlying zoned microbialite (Bed B) comprises 1) a lower stratiform stromatolite (Zone B1; Plate 54-B),

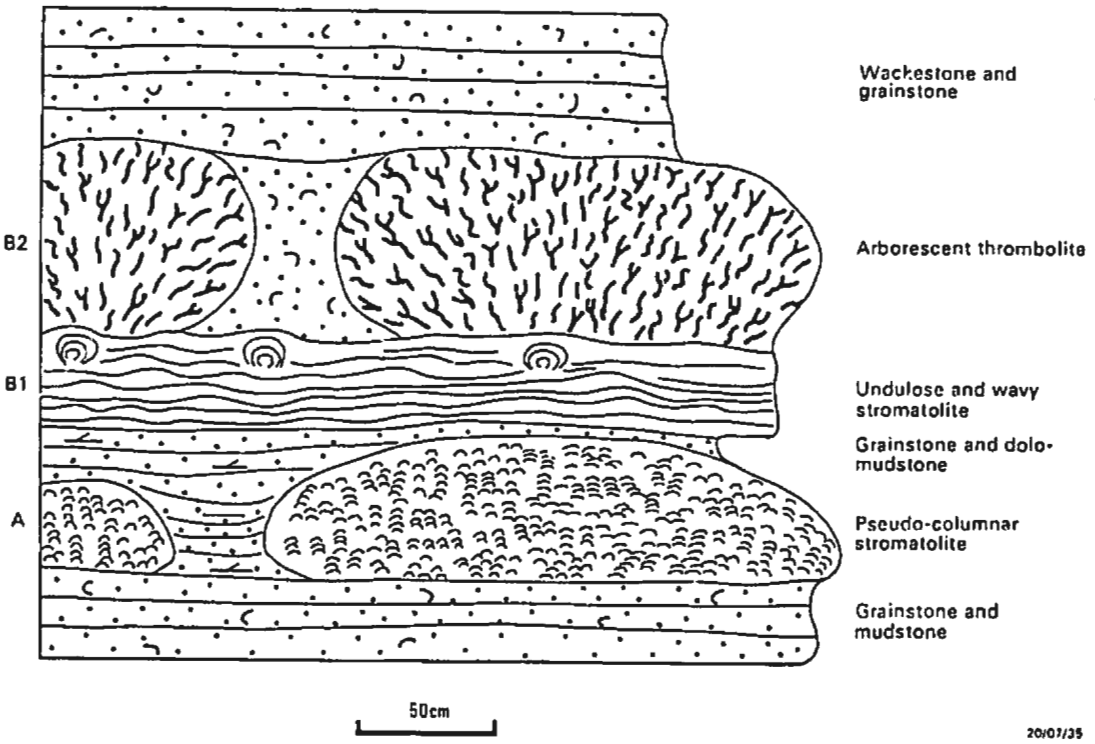

Figure 4-35. Lithological section of Horizon N, Boat Harbour Formation.

30-40 cm thick, which abruptly passes upwards to,
2) arborescent thrombolite bioherms (Zone B2, Plate 54-C). These thrombolites are 40-60 cm thick and 50-400 cm in diameter, have an oblate spheroidal to ellipsoidal shape, and are encased within cross-laminated, medium to granule peloid-intraclast grainstone. They have 15-30 cm synoptic relief as indicated by abutting and onlapping relationships of the inter-biohermal grainstones.

MESOSTRUCTURE

The lower stromatolites (Bed A) are composed of superimposed, thick light coloured and thin dark coloured, pseudo-columnar to linked columnar and hemispheroidal stromatoids. Laminae are laterally discontinuous and vary greatly in shape; at any particular horizon they range from smooth steeply convex slender columns, to broad corrugated linked columns, and small hemispheroidal heads up to 8 cm wide. Vertically successive laminae similarly vary in shape and have a low degree of inheritance. The columns and small hemispheroidal heads are infilled by lime-mudstone and scattered, edgewise, lime-mudstone pebbles. These pebbles are encrusted by convex stromatoids, and in this way successive series of columns or hemispheroids are generated.

The larger bioherms within Bed A, as well as the basal portion of some smaller bioherms, are non-laminated and have an indistinctly clotted fabric. They comprise diffuse, partially interconnected, subrounded and lobate thromboids,

2-8 mm in diameter, encased within light coloured cryptomicrobial micrite.

The stromatolite at the base of Bed B (Zone B1) has an undulose to wavy laminated fabric (Plate 54-B), and scattered laterally linked hemispheroids, about 5 cm high, occur at the top of this zone. Stromatoid layers are cut by numerous sub-horizontal stylolites, and are commonly interlayered with laminae and lenses of fine to medium ooids.

The overlying thrombolite (Zone B2) comprises 1) dark sub-digitate to arborescent thromboids, 2) burrowed inter-framework peloidal and skeletal sediment, and 3) irregular, millimetre to centimetre-sized patches of light coloured lime-mudstone (Plates 54-D,E, 55-A). The thromboids are several millimetres wide and up to 4 cm long, and although individual thromboids appear to be vertically discontinuous, they are aligned one above the other and are probably interconnected. They have up to 2 cm synoptic relief at the surface of the bioherms, and in transverse section are subrounded to amoeboid. They have a variegated internal fabric dominated by clusters of black, millimetre-sized, lobate and saccate bodies. Light coloured lime-mudstone patches (Plate 54-E, 55-A) represent former shelter cavities between arborescent thromboids which were filled by lime-mud, scattered gastropods and peloids. These former cavities are locally roofed by pendant, grape-like thromboids.

Irregular wedges and pockets of medium to very coarse grainstone occur in the crestal portion of the thrombolite bioherms (Plate 54-D,E). These sediments fill former crevices

between adjacent arborescent heads, and comprise debris eroded from the bioherms.

MICROSTRUCTURE

Framework and inter-framework components of the thrombolite bioherms are poorly differentiated in thin section. This difficulty results from extensive bioturbation and mixing of these components, and perhaps incipient microbial binding of the inter-framework sediments. In contrast, microstructures are clearly differentiated within the underlying stromatolite zones.

1. Thromboids

The arborescent thromboids have a complex variegated microstructure comprised of spherulitic lobate micro-structures, surrounded by irregular patches of grumous (*structure grumeleuse*), peloidal, vermiform and tubiform microstuctures (Plate 55-B,C). Spherulitic aggregates are several to tens of millimetres in size, and individual lobes range from 30 to 700 μm in diameter. Individual spherulites are 30-200 μm in diameter, and have a distinctive turbid appearance due to abundant submicron-sized inclusions. They exhibit curved, convex outward, twin lamellae (cf. fascicular-optic fabric). In rare instances, several spherulites at the centre of lobes are replaced by length slow fibrous quartz in which linear trains of elongate

inclusions define the outlines of precursor radial-fibrous crystals. The spherulites are interpreted as bacterial precipitates within degraded coccoid colonies, and are locally enclosed within a 10-20 μm thick cryptocrystalline wall which probably represents the selectively permineralized outer sheath of these colonies. The spherulites locally intergrade with clotted, saccate, and rarely chambered *Renalcis*-like microstructures which are 50-300 μm in diameter.

The remaining portions of the thromboids, that is the frame-building material between spherulitic lobes, comprises irregular patches of diffuse grumous (*structure grumeleuse*) grading to peloidal, vermiform and tubiform microstructures, and scattered bound gastropod shells. These patches were evidently formed by the partial calcification and sediment-trapping activities of a separate, filament-dominated, microbial community that surrounded isolated coccoid colonies. In these patches, vermiform microstructures commonly occur in conjunction with grumous and peloidal microstructures, such that individual micro-clots and peloids are separated by micro-tubular filament moulds (Plate 55-A,B); these microstructures clearly represent trapped and bound detritus, possibly faecal pellets. In rare instances filamentous microbes are preserved as delicate thread-like "microfossils" (Plate 55-D). These filaments are about 20 μm in diameter and 500-700 μm long. Grumous microstructures are locally cut by numerous larger sub-linear to meandering tubes, 60-150 μm in diameter and up to 2 mm long, that are

rimmed by a dark brown organic-rich wall, and filled with clear cement (tubiform microstructure, Plate 56-A). These tubes are probably metazoan burrows.

The thromboids are disrupted by numerous burrows 0.5 - 3 mm in diameter, which are variously occluded by lime-mud, silt-size (?)faecal pellets, peloids or cement.

2. Stromatoids

Pseudo-columnar to columnar stromatoids; Bed A

These stromatoids comprise 1) thick vermiform or composite vermiform-peloidal laminae, 500-4000 μm thick, and 2) episodic dark, weakly banded, cryptocrystalline laminae 50-500 μm thick (Plate 56-B). At the crests of the columns and hemispheroids, however, these laminae rhythmically alternate with each other, and vermiform-peloidal laminae are significantly thinner, about 200-600 μm. The vermiform-peloidal laminae are characterized by the co-occurrence of tubular filament moulds, 20-50 μm in diameter and up to several hundred microns long, and subrounded peloids 40-120 μm in size (Plate 56-C). They exhibit a spectrum of microstructures ranging from 1) sparse discontinuous tubules within massive or diffuse peloidal micrite, to 2) a reticulate network of prostrate, erratic or erect tubules within massive micrite, diffuse peloidal micrite or peloidal aggregates, to 3) a dense network of tubules interwoven between individual sharply defined peloids. It is this latter variant that provides the clearest evidence for the origin of

these vermiform-peloidal microstructures. Relatively soft peloids were trapped and bound by microbial filaments, the subsequent oxidation or upward gliding of which generated tubular moulds. In those instances where several peloids occur between adjacent filament moulds, individual peloids are less distinct and have partially merged with one another. Similarly, in those laminae where filament moulds are widely spaced or poorly preserved, most of the trapped peloids are in direct contact with one another, and have partially merged to produce a diffuse peloidal or *structure grumeleuse* microstructure. That is, peloids are well defined when enmeshed in a dense network of filament moulds, but are diffuse when trapped within a sparse or poorly preserved network of filaments. In addition to peloids, various amounts of lime-mud were probably also trapped between the filaments.

An important feature of the composite vermiform-peloidal laminae is that they typically commence with a layer of prostrate filament moulds (Plate 56-B). Thus it appears that peloids and mud were initially deposited on a thin (?)sticky layer of prostrate filaments, and were subsequently bound, and more sediment trapped, by the upward growth or motile gliding of these filaments. If sediment influx was relatively low a prostrate growth form was maintained, but if sediment influx was high, filaments developed an erect growth form.

The thin dark banded laminae within this stromatolite probably represent organic-rich layers that developed at times of minimal or no sediment influx. Their regular lamination suggests that they were also comprised of

filamentous microbes. These filaments could be the same species that constructed the vermiform-peloidal laminae or a separate, perhaps non-motile, species.

Vermiform-peloidal and banded stromatoids are disrupted by numerous peloid and spar-filled burrows 250-600 μm in diameter, and non-compacted spar-filled borings 80-180 μm in diameter (Plates 56-B).

Composite vermiform-peloidal microstructures are also locally present within what are obviously geopetal sediment accumulations in depressions between stromatoid columns and hemispheroids. It appears that these detrital accumulations were invaded and bound by filamentous microbes after their deposition.

The larger, non-laminated and diffusely clotted bioherms within Bed A are similarly dominated by composite vermiform-peloidal microstuctures. However, in this case they do not form superimposed laminae but form a pervasive cryptic matrix between diffuse, partially interconnected patches of massive, diffuse grumous or saccate lobate microstructure (Plate 56-D). These lobate patches locally have an indistinct concentric layering formed by successively stacked lobes. The lobes are 1-3 mm in diameter, and are commonly cut by irregular wedge-shaped shrinkage cracks that generally do not extend into the encasing vermiform-peloidal microstructures. The lobate patches appear to represent incipiently calcified gelatinous coccoid colonies encased within a network of sediment-trapping filaments. Perhaps the vigorous growth of these coccoid colonies prevented the formation of laminated

fabrics such as those developed in the non-coccoid bearing, filament-dominated stromatolitic bioherms.

Undulose, wavy and hemispheroidal stromatoids; Zone A1

These stromatoids are similarly composed of superimposed vermiform-peloidal and banded laminae, together with episodic layers and lenses of fine to medium ooids. Their micro-structure is poorly preserved, however, due to incipient neomorphism and abundant stylolites.

3. Detrital Sediment

The arborescent thromboids of Zone B2 are encased within burrow-mottled, peloid-skeletal grainstone, packstone and wackestone. This sediment commonly merges and intergrades with thromboids, and locally has a vague lobate micro-structure. It appears that it was invaded and partially bound by micro-organisms subsequent to its accumulation between the thromboids. It is dominated by autochthonous particles: 1) subrounded very fine to coarse peloids and microbial corpuscles eroded from the arborescent framework, 2) reworked spherulitic fragments, 3) abundant gastropod shells and minor trilobite fragments, 4) diffuse silt-sized peloids, possibly faecal pellets, 5) irregular grains with dark micritic rims, probably bored mollusc fragments, and 6) lime-mud (see Plate 55-A,B). Gastropod shells and many burrows are partially filled by diffuse silt-sized peloids (cf. *structure grumeleuse*)

and blocky cement.

In contrast to this grainy burrow-mottled sediment, light coloured cavity-filling sediment comprises massive to weakly laminated mudstone or sparse peloid-skeletal wackestone. This muddy sediment contains relatively few cement or mud-filled burrows and borings (Plate 55-D).

ORIGIN AND PALAEOECOLOGY

The pseudo-columnar and columnar stromatolitic bioherms of Bed A were constructed by thick layers of filamentous microbes in which peloids and ?faecal pellets were trapped and bound, and episodic thin organic-rich layers, probably also dominated by filaments. This community constructed small and large domed to discoidal bioherms of low topographic relief which were buried and draped by thin-bedded grainstone and mudstone. Within some mounds, however, numerous coccoid colonies grew in conjunction with filamentous communities, and the vigorous growth of these colonies generated a finely clotted rather than laminated fabric. The bioherms probably grew in a shallow subtidal to lower intertidal environment, and were inhabited by a few soft-bodied burrowing and boring metazoans. Skeletal metazoa were evidently absent.

The basal stromatolitic zone of the overlying bed (Zone B1) was similarly constructed by a community of alternating thick, sediment-trapping filamentous layers, and thin, organic-rich layers. In this case, however, the community formed a laterally continuous mat (although individual

filamentous layers within this mat were somewhat discontinuous), and it constructed a thin biostrome capped by small hemispheroidal heads. Ooid sands were episodically washed onto this biostrome, and metazoans were apparently precluded from this (?)stressed, probably intertidal, environment.

In response to rapid deepening, this stromatolite was overgrown by thrombolite bioherms constructed by arborescent coccoid colonies and encrusting filamentous masses. Coccoid colonies were selectively degraded and largely replaced by spherulitic (?)bacterial precipitates. Their tough outer sheaths, however, were calcified. The encrusting filamentous microbes appear to have had a dual sediment-trapping and carbonate precipitating role, although individual filamentous forms were rarely preserved, either as tubular moulds or calcified filaments. The arborescent framework was infilled by debris eroded from it, together with large quantities of (?)faecal pellets and gastropod shells. This sediment was invaded and partially bound by micro-organisms, and was extensively burrowed and mixed with framework constituents by a metazoan infauna. These bioherms had moderate topographic relief and grew in a relatively high energy subtidal environment. They were inhabited by a large population of grazing gastropods, minor trilobites, and a small number of burrowing and boring coelobiontic (cavity dwelling) metazoans. The bioherms were subsequently buried by cross-laminated peloidal and intraclastic sand. Schematic reconstructions of the bioherms are shown in Figure 4-36.

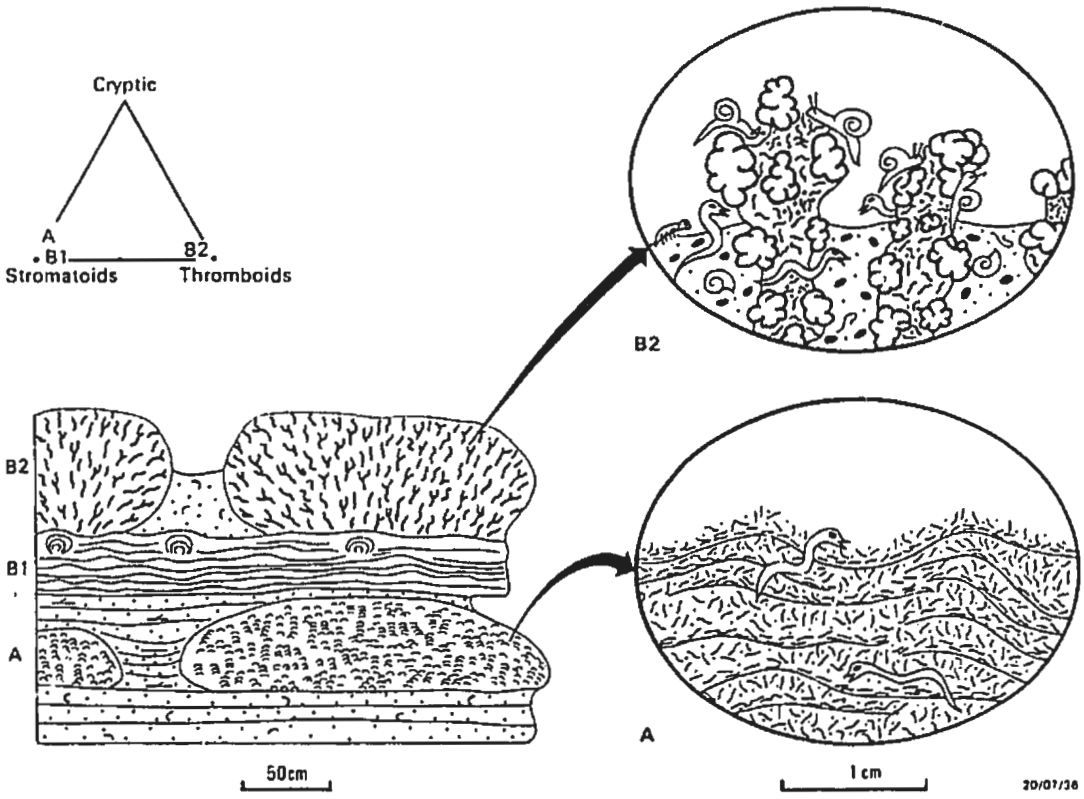

Figure 4-36. Schematic reconstructions and triangular plot of main framework components of Horizon N.

4.16 HORIZON O

KARST ERODED THROMBOLITE

This thrombolite occurs within peritidal carbonates in the lower portion of the Boat Harbour Formation on the eastern side of Isthmus Bay (Fig. 4-37; Bed 134 of Pratt's 1979 Isthmus Bay Section). This portion of the formation comprises 1) thinly interbedded grainstone and mudstone, characterized by lenticular, wavy and flazer bedding, ripple cross-lamination and minor bioturbation (intertidal lithotype D of Pratt and James, 1986), 2) cryptalgal laminated dolostone with desiccation cracks (supratidal lithotype A), 3) small thrombolite bioherms flanked by peloid and skeletal grainstone (subtidal lithotype F), and in the overlying sequence, 4) thinly interbedded and burrowed grainstone, wackestone and mudstone (intertidal lithotype E).

MEGASTRUCTURE

The thrombolite has an irregularly scalloped, pillar or ridge-like form* which represents the multiply eroded remnants of former closely-spaced, club or dome-shaped bioherms (Fig. 4-37, Plate 57-A). The bioherms are

* Although the thrombolites have a pillar-like form in cross-section, in three dimensions they may form a series of partially interconnected ridges and pillars.

preferentially established on small positive topographic features of an eroded lime-mudstone substrate (surface S1 in Fig. 4-37).

The bioherms are truncated by two subsequent erosion surfaces: a lower irregularly scalloped surface S2, and an upper planar surface S3. The lower, non-eroded, portions of the bioherms are flanked by relatively dark coloured, medium to very coarse peloid-intraclast-ooid grainstone (G1, Fig. 4-37). The eroded upper portions have an irregular pillar-like form with overhanging scalloped margins. These pillars project 20 cm above adjacent smooth-floored "basins" that have selectively developed within the flanking grainstone G1. The scalloped pillar and basin morphology of erosion surface S2 is characteristic of exposed karst surfaces on modern coastal carbonate rock platforms (Revelle and Emery, 1957; Kaye, 1959; Sweeting, 1972), and of palaeokarst surfaces within other peritidal sequences (Walkden, 1974; Read and Grover, 1977; Cherns, 1982). The basins between the scalloped thrombolite pillars are filled by light coloured, fine to very coarse skeletal-peloid-ooid grainstone (G2, Fig. 4-37). This grainstone and the crests of the scalloped thrombolite pillars are in turn truncated by the upper planar erosion surface S3. This surface is interrupted by low relief erosional remnants of the thrombolite pillars, and is overlain by flat-pebble conglomerate.

The thrombolite bioherms were originally 50 cm or more thick, and probably had moderate synoptic relief prior to their burial by carbonate sand (grainstone G1).

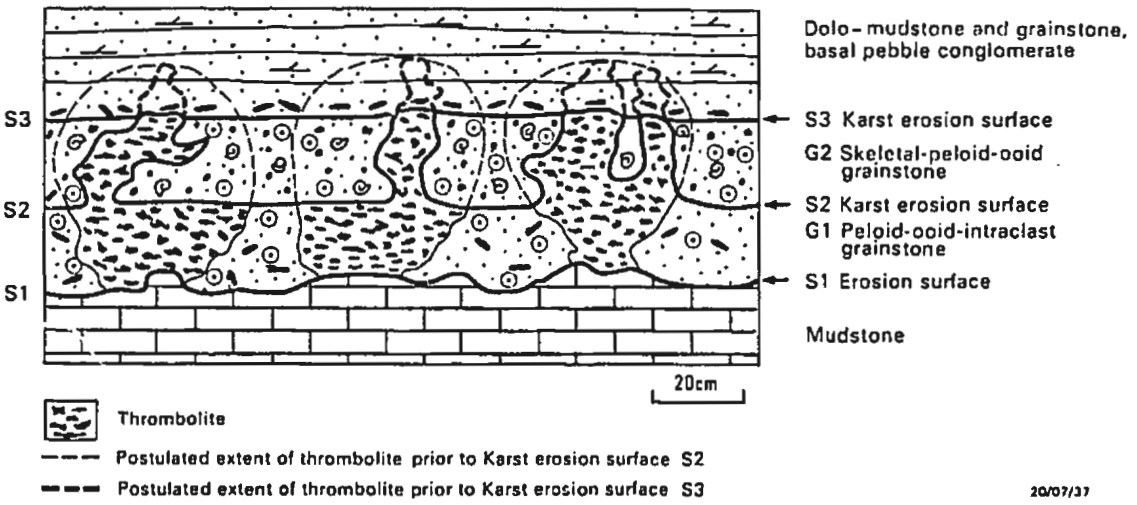

Figure 4-37. Lithological section of Horizon O, Boat Harbour Formation.

MESOSTRUCTURE

The thrombolite consists of interconnected, centimetre-sized, irregular prostrate thromboids and a subequant volume of inter-framework peloidal sediment. Former framework cavities are roofed by pendant thromboids and filled with peloidal lime-mudstone and cement (Plate 57-B).

The thromboids contain numerous clusters of very dark lobate and saccate bodies, a few millimetres in diameter, encased within lighter coloured microcrystalline carbonate. Their margins are generally poorly defined, and it is commonly difficult to distinguish framework and inter-framework components in outcrop and, to a lesser extent, on polished slabbed surfaces. Inter-framework sediments are extensively bioturbated and contain numerous burrows and scattered gastropod shells.

MICROSTRUCTURE

1. Thromboids

The thromboids have a variegated spongeous, lobate and grumous grading to peloidal microstructure (Plate 58-A,B,C). Lobate microstructures are slightly predominant, and comprise partially coalesced lobes of turbid microspar, with or without a cryptocrystalline wall (saccate lobate micro-structure; Plate 58-B). The lobes are partially encased within grumous grading to peloidal microstructures in which

diffuse cryptocrystalline, silt-sized, microclots intergrade with aggregates of poorly defined, micro-clotted or massive peloids (Plate 58-D). The origin of these grumous-peloidal patches is uncertain. They may represent *in situ* precipitates within an organic mucilage that enveloped the adjacent lobate coccoid colonies, or detrital peloids and mud trapped by a separate (?filamentous) sub-community, or a combination of trapped and precipitated sediments. In view of the fact that grumous-peloidal microstructures commonly merge with peloids within burrows, fenestrae, cavities and inter-framework sediment, they most probably represent trapped peloids that were subsequently obscured by *in situ* precipitates.

The thromboids are commonly disrupted by burrows which are occluded by peloids, lime-mud or cement.

2. Detrital Sediment

Detrital sediment comprises poorly sorted peloid grainstone, wackestone and mudstone. The peloids are predominantly silt-sized but range up to 500 μm in size. Many of these larger peloids comprise micro-clotted carbonate, and clearly represent reworked fragments of the thromboid framework. The smaller peloids may be faecal pellets. Reworked spherulitic corpuscles and minor gastropod and trilobite fragments also occur within this sediment.

ORIGIN AND PALAEOECOLOGY

The bioherms were constructed by lobate calcified coccoid colonies which were either encased within partially calcified mucilage, or were surrounded by a separate, sediment-trapping (?filamentous) sub-community. These colonies were buried by peloidal lime-mud, and supported small shelter cavities roofed by pendant coccoid colonies. Silt-size peloids within the inter-framework sediment may well be faecal pellets, but larger peloids clearly represent reworked fragments of calcified coccoid colonies. The bioherms grew within a high energy subtidal peloid shoal, and were extensively burrowed by small metazoans and grazed by gastropods. They were established on an irregular erosion surface, and were subsequently buried by peloid-intraclast-ooid sands. A reconstruction of the thrombolite is shown in Fig. 4-38.

The bioherms and inter-biohermal sediments were subsequently eroded by two phases of karst solution. During the first phase, a scalloped karst surface (S2) developed; the bioherms were clearly more resistant to erosion than the flanking grainstone (G1), since pillar-like thrombolite remnants project 20 cm or more above smooth-floored basins eroded into this grainstone. This scalloped surface was subsequently re-inundated and buried by coarse carbonate sand (grainstone G2). During a second phase of subaerial exposure, the crests of the thrombolite pillars and lithified grainstone G2 were eroded by a planar karst surface (S3).

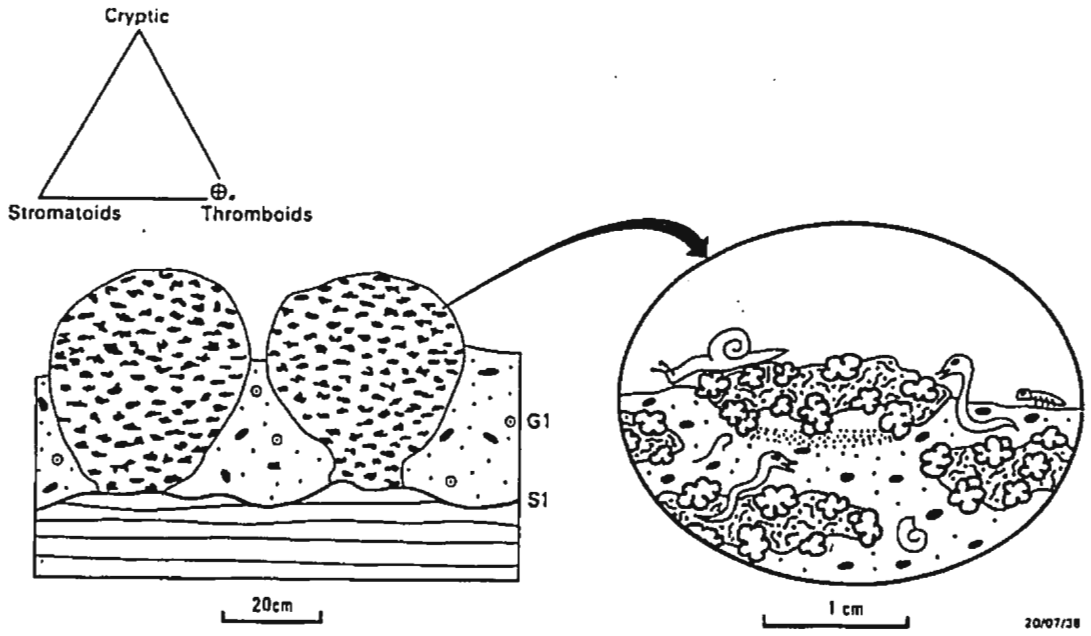

Figure 4-38. Schematic reconstruction and triangular plot of main framework components of Horizon O.

4.17 HORIZON P

CRYPTOMICROBIAL-CORAL-?SPONGE BOUNDSTONE

This boundstone occurs in the upper portion of the Boat Harbour Formation on the eastern side of Isthmus Bay (Fig. 4-39; Bed 190 of Pratt's 1979 Isthmus Bay Section). It lies within a sequence of irregularly alternating supratidal, intertidal and subtidal carbonate facies (Lithotypes A to F of Pratt and James, 1986).

MEGASTRUCTURE

The boundstone has a poorly defined bedform. It is approximately 60 cm thick and has a mounded, in part erosional, upper surface. Depressions within this surface are filled by peloid-intraclast grainstone, but it is not clear whether the moundrock forms a series of separate, close-spaced bioherms as depicted by Pratt (1979, Fig.7) and Pratt and James (1986, Fig. 13B) (see Fig. 4-39), or a laterally continuous mounded biostrome.

The boundstone is underlain by cryptomicrobial laminated dolostone and, at the eastern edge of the outcrop, is flanked by burrow mottled dolo-wackestone. It is erosionally overlain by cryptomicrobial laminated dolostone which is extensively brecciated above the flanking burrow mottled dolo-wackestone. This breccia is interpreted as a solution collapse feature

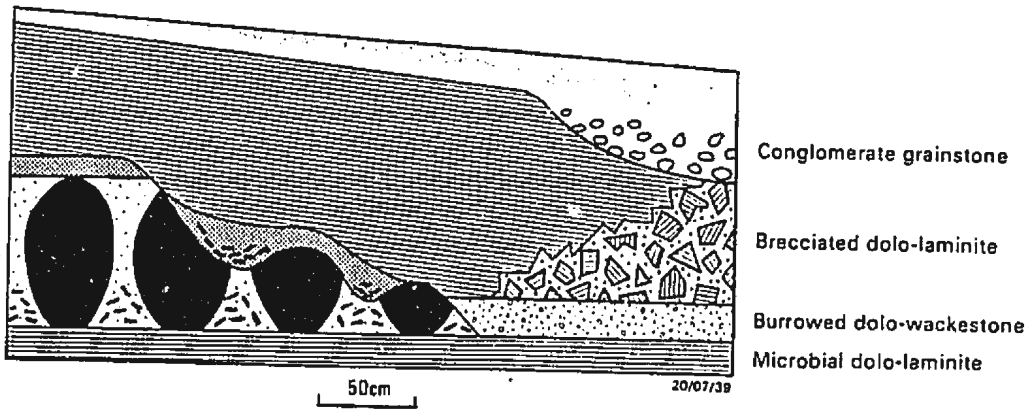

Figure 4-39. Lithological section of Horizon P, Boat Harbour Formation. After Pratt and James (1986).

associated with subaerial exposure and palaeokarst (Pratt and James, 1986).

MESOSTRUCTURE

The boundstone has a complex mottled and patchy fabric in which microbial, metazoan and detrital components are poorly differentiated. It contains numerous dark coloured colonial corals, vague thromboids and cryptomicrobial structures, gastropods, nautiloids, trilobites, intraclasts, peloids, and irregular dolomite patches; these features are difficult to recognize in hand samples, and photographs of slabs are not instructive. Some of the dolomite patches have geometric circular, crescentic or annulated shapes, and are possibly replaced sponges. Others are probably dolomitized burrows, but numerous non-dolomitic, spar and peloid-filled burrows are also evident. Thromboids and cryptomicrobial fabrics appear to encrust various metazoan components, especially corals, and they merge with patches of detrital sediment.

In many respects the boundstone has a similar fabric to the sponge-algal mounds described by Toomey and Nitecki (1979) and Klappa and James (1980), although neither sponges nor calcareous algae have been definitively identified. As noted by Klappa and James (1980), Bourque and Gignac (1983) and James and Macintyre (1985), however, optimal conditions of exposure and a well trained eye are often required to recognize sponges within seemingly massive mud mounds.

MICROSTRUCTURE

1. Thromboids and Cryptomicrobial Fabrics

Although microbial components are generally poorly defined, merge with detrital sediment, and are partially obscured by dolomite, they are locally well defined. They have a variable spongeous, diffuse grumous (*structure grumeleuse*) and massive microstructure (Plate 59-A,B). Sparse to dense networks of irregular amoeboid micro-fenestrae are encased within massive or micro-clotted cryptocrystalline carbonate. The fenestrae are occluded by clear microcrystalline cement and locally contain infiltered silt-sized peloids, probably faecal pellets. They have relatively sharply defined smooth margins, are 60-250 μm wide, and show no prefered orientation. Their origin is unclear; they may have formed by gas accumulation or partial oxidation of a microbial community otherwise preserved by *in situ* precipitation. Thromboids and cryptomicrobial fabrics are cut by numerous burrows 0.5-2 mm in diameter.

2. Corals

Coral colonies are sub-rounded and range from 1 to 3 mm in size. They are commonly encrusted by, and intergrown with, cryptomicrobial fabrics (Plate 59-A,C), and are preserved in growth position. The corallites are 300-500 μm in diameter, and diverge upward and outward. The corals are identical to

those within the Green Head Complex (Horizon L) and are thus similarly assigned to the genus *Lichenaria*.

3. Detrital Sediment

Detrital sediment between the microbial and metazoan framework has a variable grainstone-packstone-wackestone fabric due to extensive bioturbation. It contains abundant silt-sized peloids (?faecal pellets), reworked crypto-microbial and coral fragments, gastropod, trilobite and nautiloid debris, and subspherical micrite-rimmed grains (Plate 59-C). Micrite-rimmed grains probably represent eroded corallite fragments that have been micritized by endolithic microbes. Although they are somewhat similar in appearance to calcispheres, they are significantly larger (average size 400 μm), and their outer cryptocrystalline wall is thicker and more irregular.

Calcareous sponge spicules are commonly visible within mud-rich sediment patches. They are 15-20 μm in diameter, up to 500 μm long, and comprise microcrystalline calcite or rarely silica partially replaced by calcite. They show no preferred orientation or arrangement.

4. ?Sponges

A possible alternative interpretation of the crypto-microbial fabrics is that they represent former sponges.

Based on a study of Silurian stromatactis mud mounds, Bourque and Gignac (1983, p.523) concluded that early diagenesis and\or bacterial decay of sponges can generate a microfacies that consists of:

> "agglomerates of pelletlike bodies or pelletoids forming an irregular pelletoidal networklike pattern surrounded by rather uniform lime mudstone containing a small proportion of silt-sized quartz grains. Contacts between the pelletoidal network and the uniform mudstone, although discernable, are usually diffuse. Pelletoids of the network range from 20 to 70 μm in size and may be closely packed or 'cement-supported'. Sponge spicules are ubiquitous and their number is variable, from abundant to very few; mostly they occur in the pelletoidal network, but they also are found in the uniform mud. No sponges identifiable by gross morphology have been found in the mound facies".

Could the spongeous, grumous (*structure grumeleuse*; pelletoidal *sensu* Bourque and Gignac) microstructures of the present boundstone be similarly attributed to former sponges? To evaluate this hypothesis, the following factors need to be considered:

1. Sponge spicule moulds indicate that sponges were present either within, or in the vicinity of, the mounds. However, the spicules apparently only occur within lime-mud patches <u>between</u> cryptomicrobial fabrics, and have not been observed <u>within</u> cryptomicrobial fabrics.

2. Sponges have not been definitively identified by gross morphology within the boundstone, but numerous dolomite patches have circular, crescentic or annulated shapes suggestive of sponges (Plate 59-D).

3. *Stromatactis*, ubiquitous within many sponge mounds, does not occur within the boundstone. However, irregular networks of cement filled micro-voids or fenestrae are locally prominent, and could have a similar origin to *Stromatactis* cavities.

4. Cryptomicrobial fabric lacks definitive evidence of microbial origin. Although clotted microstructures are commonly generated by microbial activity, they are by no means diagnostic of such activity and may form in many other ways; for example compaction and cementation of detrital pellets (Bathurst, 1975), inorganic cementation (Deelman, 1975; Macintyre, 1977, 1978; Alexandersson 1972; Marshall, 1983), and neomorphism of micrite (Beales, 1965).

5. The cryptomicrobial structures are poorly defined and merge with patches of detrital peloids and lime-mud which contain scattered quartz silt. Quartz silt does not occur, however, within the cryptomicrobial structures.

Thus it appears likely that sponges were an element of the mound-forming community, and although the cryptomicrobial structures have certain similarities to sponge-derived pelletoidal microfabrics observed elsewhere in the St. George Group and overlying Table Head Group (see Klappa and James, 1980), and as described by Bourque and Gignac (1983), the

available evidence is inconclusive as to whether they were generated by former sponges or microbial communities. Conceivably they could represent either or both.

ORIGIN AND PALAEOECOLOGY

This boundstone was constructed by a composite microbial-metazoan community. The major frame-building components were 1) microbial communities of unknown composition and structure, 2) small colonial corals, and possibly 3) poorly preserved sponges. Extensive biological and, to a lesser extent, (?)physical reworking of the mound sediments obscures framework and inter-framework relationships. Large quantities of detrital sediment, including ?faecal pellets, reworked cryptomicrobial and coral fragments, metazoan skeletal debris and lime-mud, accumulated between the framework. The mounds were inhabited by a large population of burrowing soft-bodied metazoans, grazing gastropods, scavenging trilobites, and carnivorous nautiloids, and grew in a moderately low energy subtidal environment. A tentative mesoscopic reconstruction of the boundstone community is shown in Fig. 4-40; a microscopic reconstruction is not possible.

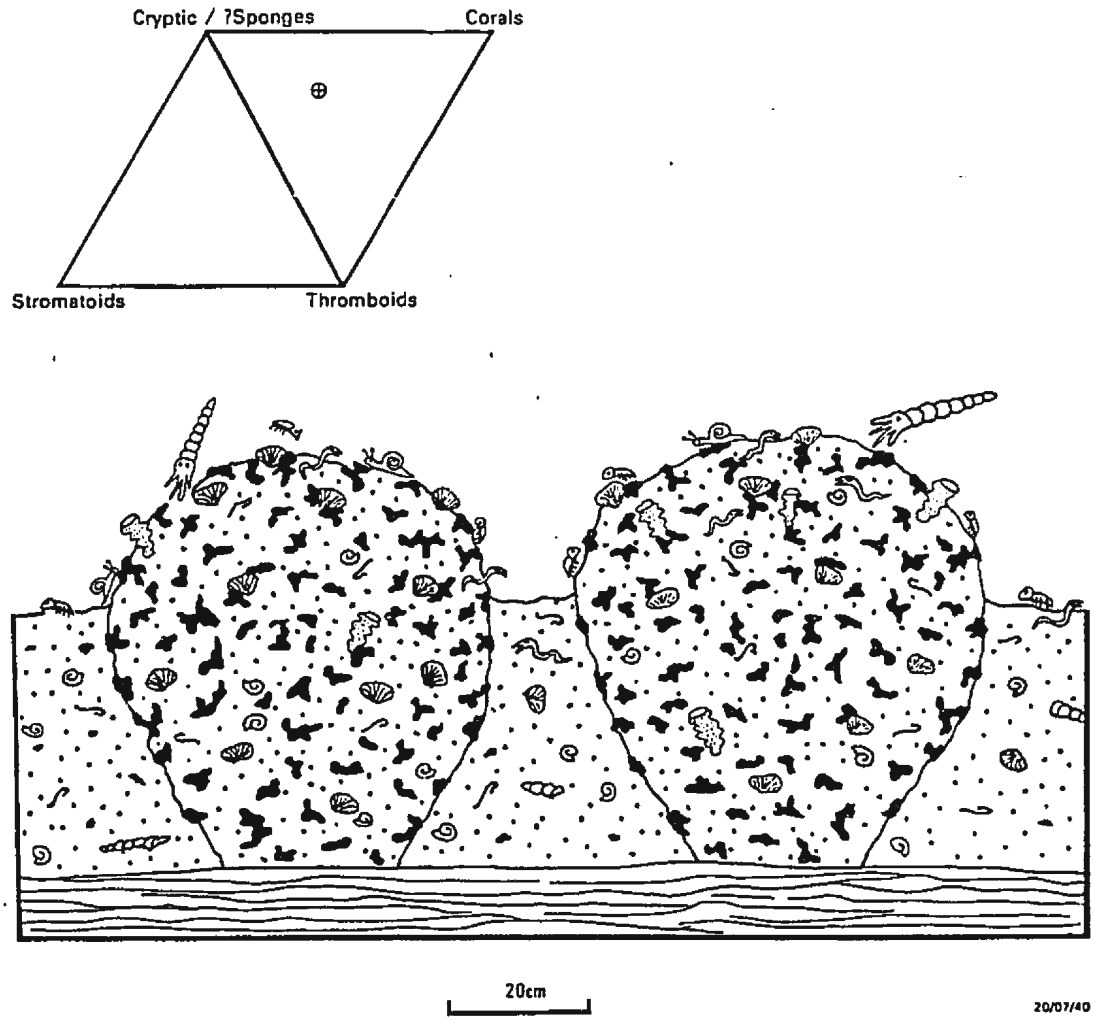

Figure 4-40. Schematic mesoscopic reconstruction and triangular plot of main framework components of Horizon P.

4.18 HORIZON Q

BURROW MOTTLED THROMBOLITES

Several beds of small, poorly defined thrombolites occur near the top of the Boat Harbour Formation on the eastern side of Isthmus Bay (Fig. 4-41; Beds 232, 234 and 242 of Pratt's 1979 Isthmus Bay Section). This portion of the formation comprises alternating skeletal-peloid-ooid grainstone, burrowed grainstone and wackestone, and less commonly, cryptomicrobial laminated dolostone with desiccation cracks (subtidal, intertidal and suptratidal lithotypes F, E and A, respectively, of Pratt and James, 1986).

MEGASTRUCTURE

The thrombolites form small, closely spaced, subspherical to discoidal bioherms encased within coarse grained, skeletal-peloid-ooid grainstone. The bioherms are 10-30 cm thick, have low synoptic relief, and poorly defined, irregularly eroded margins.

MESOSTRUCTURE

The bioherms have a diffuse clotted and mottled fabric in which framework and inter-framework components are very poorly differentiated (Plate 60-A,B). They comprise partially

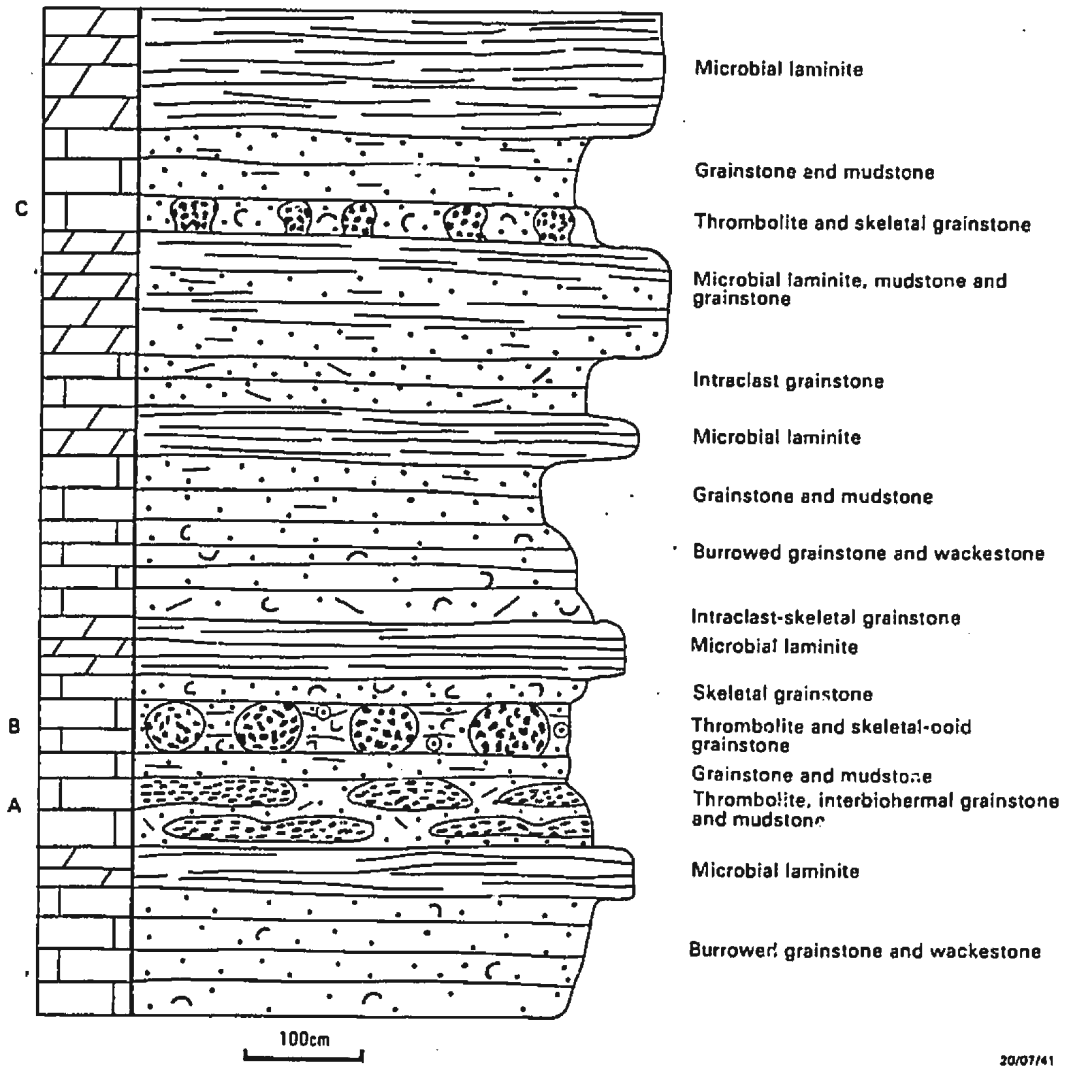

Figure 4-41. Lithological section of Horizon Q, Boat Harbour Formation.

interconnected, ragged amoeboid and sub-digitate thromboids, variously intermixed with pellets, peloids and skeletal debris. Thromboids range from a few millimetres to several centimetres in size. They are disrupted by numerous burrows, and intense bioturbation has commonly generated a pervasively mottled, cryptomicrobial fabric. Abundant gastropods, trilobites, nautiloids and pelmatozoan debris occur between thromboids and intermixed with cryptomicrobial fabrics.

MICROSTRUCTURE

1. Thromboids and Cryptomicrobial Fabrics

The thromboids have a variegated lobate, grumous, peloidal, spongeous, and rarely massive, vermiform, and filamentous microstructure (Plate 61-A,B,D). Lobate microstructures tend to be dominant within relatively clearly defined thromboids, whereas poorly differentiated cryptomicrobial fabrics are dominated by grumous and peloidal microstructures. Lobate bodies range from 300 to 1500 μm in diameter and comprise turbid, undulatory or spherulitic microspar. Saccate lobes are relatively scarce. These lobate microstructures, interpreted as colonies of variously degraded calcified coccoid microbes, are encased within poorly defined masses of grumous grading to peloidal microstructures (cf. *structure grumeleuse*, Plate 61-C,E), with rare massive, vermiform and filamentous patches. These microstructures were probably generated by partially calcified filaments (diffuse

microclots and filament-like forms) which trapped (?)faecal pellets and peloids. Rare calcispheres 180-350 μm in diameter occur scattered within these structures, and presumably represent trapped reproduction cysts of dasycladacean algae (Marszalek, 1975; Wray, 1977).

2. Detrital Sediment

Detrital sediment comprises burrow-mottled grainstone, packstone and wackestone. It contains abundant ?faecal pellets, peloids, gastropods, trilobites, nautiloids and pelmatozoan fragments, and minor ooids and terrigenous silt. Fragments of grumous and spherulitic lobate microstructures, and calcified filaments are also present.

ORIGIN AND PALAEOECOLOGY

The thrombolites were constructed by composite communities of 1) variously degraded and calcified, lobate coccoid colonies, and 2) sediment-trapping and calcified filamentous microbes. These communities constructed irregular frameworks of low micro-relief, between which ?faecal pellets, detrital peloids, eroded microbial fragments, metazoan skeletal debris and minor amount of ooids and terrigenous silt accumulated. Both the framework and inter-framework sediments were extensively mixed by burrowing metazoans, thereby resulting in a diffuse thrombolitic or pervasively mottled cryptomicrobial fabric. The bioherms were inhabited by a

large population of grazing gastropods, scavenging and detritus feeding trilobites, carnivorous nautiloids, and possibly attached suspension feeding pelmatozoans. They grew within a high energy peloid-skeletal grainstone shoal. A reconstruction of the bioherms is shown in Fig. 4-42, and is similar to that envisaged for the karst eroded thrombolites of Horizon O which are less bioturbated.

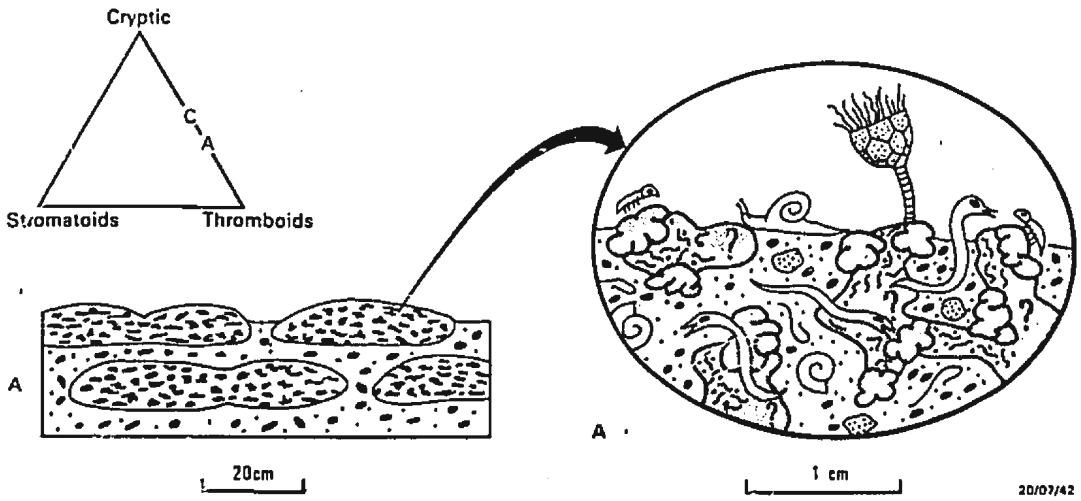

Figure 4-42. Schematic reconstruction and triangular plot of main framework components of Horizon Q.

4.19 HORIZON R

GIRVANELLA-RICH THROMBOLITE

This thrombolite occurs near the base of the Catoche Formation on the eastern side of Isthmus Bay (Fig. 4-43; Bed 254 of Pratt's 1979 Isthmus Bay Section). It is underlain and overlain by thinly interbedded, burrowed peloid-skeletal-intraclast grainstone, wackestone and mudstone, with scattered beds of desiccated cryptomicrobial laminated limestone (intertidal and supratidal Lithotypes E and A, respectively, of Pratt and James, 1986).

MEGASTRUCTURE

The thrombolite forms a tabular to gently domed biostrome, 25-30 cm thick, the upper surface of which has a maximum synoptic relief of 5 cm. The biostrome overlies a foundation layer of intraclast-peloid grainstone, and passes laterally into thinly bedded peloid-skeletal-intraclast packstone. It is buried by thinly interbedded grainstone, wackestone and mudstone.

MESOSTRUCTURE

The thrombolite has a speckled light and dark coloured micritic texture comprised of small subrounded to amoeboid thromboids, and a subequant volume of skeletal wackestone

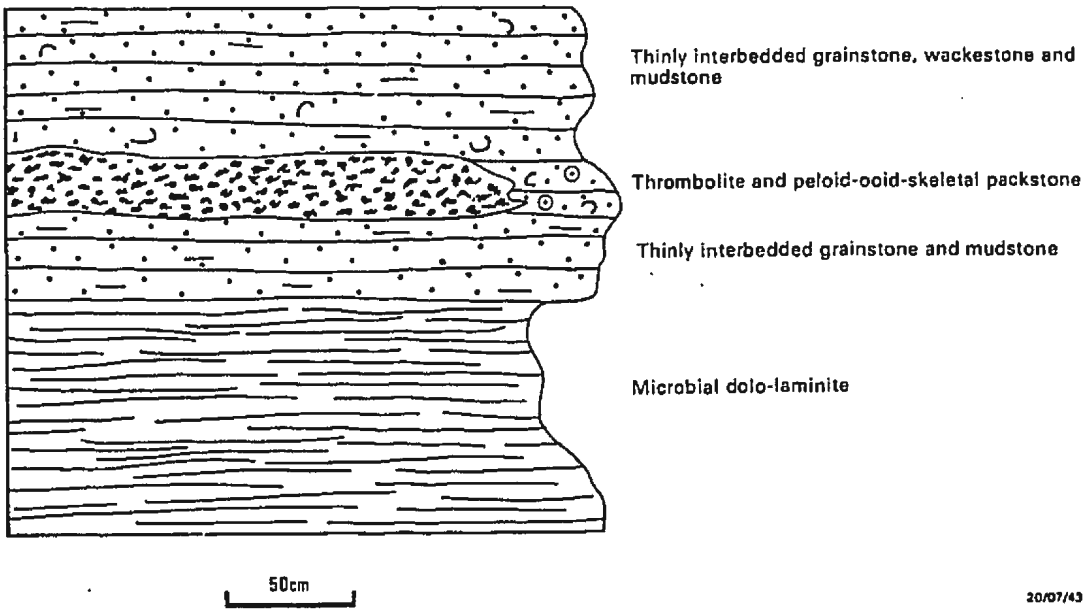

Figure 4-43. Lithological section of Horizon R, Catoche Formation.

(Plate 62-A). Thromboids are variously sharply defined or diffuse, and range from a few millimetres to about 1 cm in size. The inter-framework sediment contains abundant trilobites and brachiopods, and is moderately bioturbated.

MICROSTRUCTURE

Thromboids and inter-framework sediment are generally poorly differentiated in thin section due to partial replacement by microspar.

1. Thromboids

The thromboids have a variable microstructure ranging from a dense network of *Girvanella* tubules to diffuse grumous microstructure comprised of irregular microclots, scattered *Girvanella* relicts and interstitial microspar (Plate 62-B,C,E). *Girvanella* tubules are 15-20 μm in diameter, up to 200 μm long, and occur in sub-parallel bundles. They are generally tightly packed one against the other, but locally form a more open network separated by interstitial microspar. They are frequently partially or pervasively replaced by equigranular microspar. Elsewhere, however, discrete tubules intergrade with irregular micro-clots and diffuse grumous microstructure. This latter microstructure evidently resulted from partial, non-selective calcification of filamentous microbes, whereas the typical *Girvanella* forms resulted from selective impregnation and encrustation of their sheaths.

Rare calcispheres 200 μm in diameter also occur within grumous microstructures. The thromboids are frequently disrupted by small metazoan burrows about 0.5 mm in diameter.

2. Detrital Sediment

Detrital sediment comprises burrowed skeletal wackestone partially replaced by neomorphic microspar (Plate 62-A,B). It contains abundant trilobites, calcareous brachiopods, gastropods, peloids, reworked fragments of diffuse grumous and *Girvanella* thromboids, and minor terrigenous silt. Some brachiopod shells are encrusted by *Girvanella*, the individual tubules of which are oriented parallel to the shell substrate. The thin-bedded packstone into which the biostrome laterally grades, has a similar composition to the detrital sediment within the biostrome, and also contains numerous *Girvanella* clasts (Plate 62-D).

ORIGIN AND PALAEOECOLOGY

The biostrome was constructed by calcified filamentous microbes. The filamentous network was disrupted by numerous burrowing, scavenging, grazing and sessile filter feeding metazoans (?worms, trilobites, gastropods and brachiopods), and minor current or wave erosion. Lime-mud, metazoan skeletons, peloids, filamentous clasts and minor terrigenous silt accumulated within disrupted portions of this network. The biostrome grew within a shallow subtidal, mildly

turbulent environment, and its lateral extent was probably limited by the abundant and diverse benthic metazoan community. A reconstruction of the biostrome is shown in Figure 4-44.

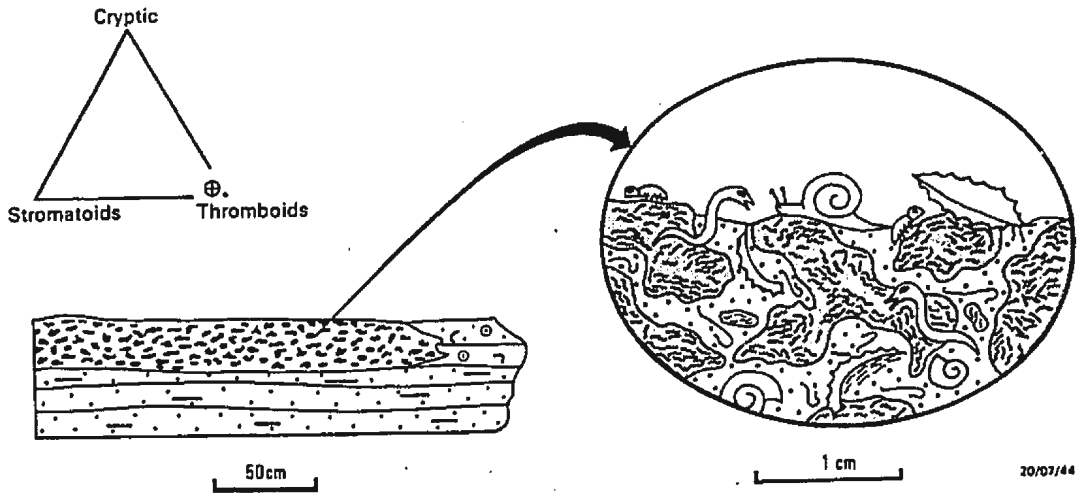

Figure 4-44. Schematic reconstruction and triangular plot of main framework components of Horizon R.

CHAPTER 5

THROMBOLITES FROM OTHER LOCALITIES

In this chapter, a selection of Cambro-Ordovician thrombolites and related microbial buildups from other localities are briefly examined in order to 1) test the wider applicability of the analytical scheme presented in Chapter 2, and more specifically, 2) determine if the spectrum of microbial microstructures exhibited by thrombolites on the Port au Port Peninsula, western Newfoundland, is representative of Cambro-Ordovician microbial buildups in general. A summary analysis of each sample from these localities is given in Appendix B, Part 2.

5.1 GREAT NORTHERN PENINSULA, WESTERN NEWFOUNDLAND

Thrombolites are also plentiful within the Cambro-Ordovician strata of the Great Northern Peninsula, western Newfoundland, but are more commonly replaced by diagenetic and epigenetic dolomite than those on the Port au Port Peninsula (Levesque, 1977; Knight, 1977a, 1977b, 1978, 1980; Edwards, 1978; Pratt, 1979; Haywick and James, 1984; Chow, 1986; Knight and James, 1987). They also tend to form larger structures than those exposed on the Port au Port Peninsula, and locally coalesce to form thick, laterally extensive,

banks. Within the Catoche Formation, many buildups are dominated by sponges (Stevens and James, 1976; Pratt, 1979; Knight and James, 1987) and are beyond the scope of this study. Differences between the Great Northern Peninsula and Port au Port buildups probably reflect their relative position on the shelf: 1) slightly deeper subtidal environments predominate in inboard, northwestern localities such as the St. Barbe coast, 2) shallow peritidal environments predominate in more outboard southern localities such as the Port au Port Peninsula, and 3) thick high energy banks are present in the most outboard, near shelf-margin, para-autochthonous sequences at Pistolet Bay, Hare Bay, Canada Bay and White Bay on the easterm side of the Great Northern Peninsula (Chow, 1986; Knight and James, 1987; Knight, 1986, 1987). Large blocks of *Epiphyton* and *Girvanella* boundstone within coeval allochthonous continental slope deposits (Cow Head Group) testify that platform-margin microbial buildups occurred immediately to the east of the autochthonous platform strata (James, 1981; James and Stevens, 1986). These para-autochthonous and allochthonous buildups were not examined in this study.

Thrombolites examined on the western side of the Great Northern Peninsula fall within the general spectrum of mega-, meso- and micro-structures observed on the Port au Port Peninsula. Three horizons (see locality map, Fig. 5-1), however, have an unusual mesostructure or mesostructural zonation, and were thus analysed in detail.

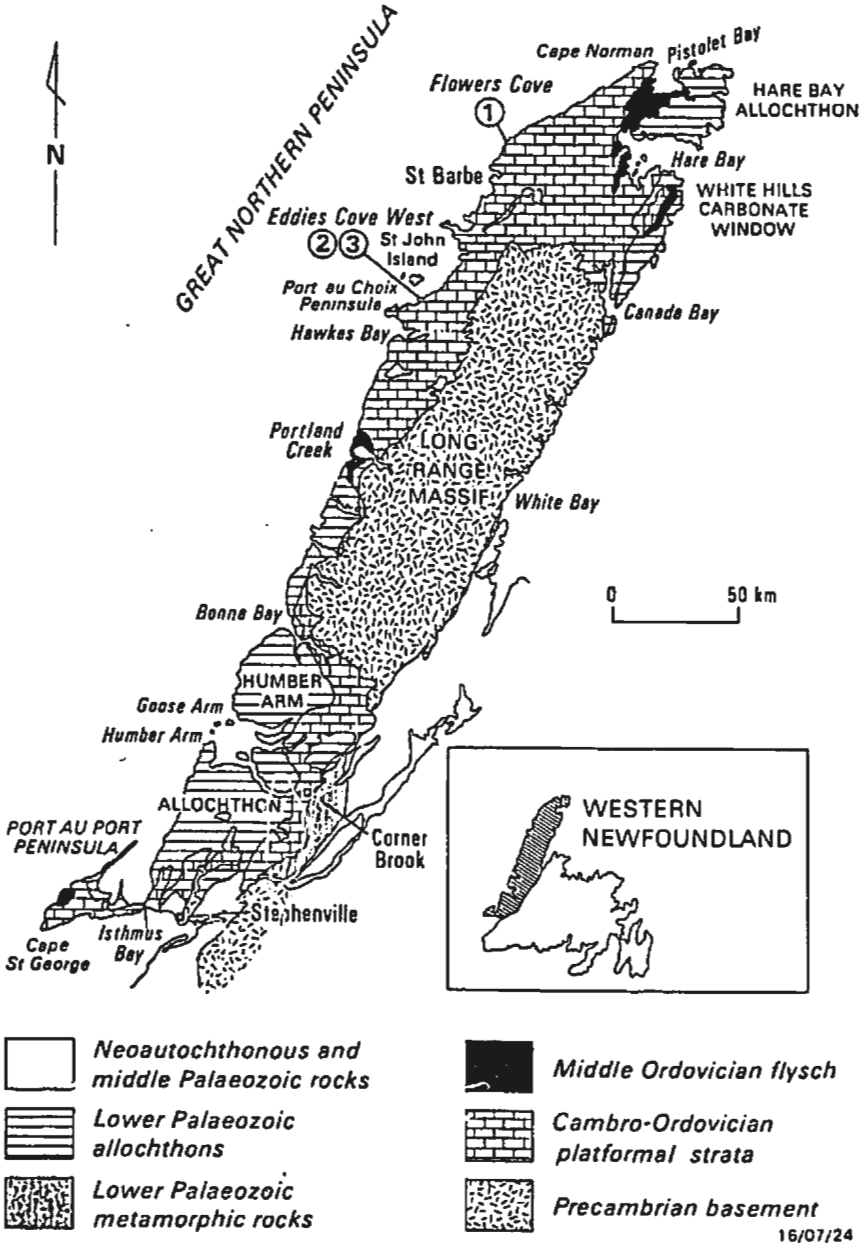

Figure 5-1. Geological map of western Newfoundland showing location of thrombolite horizons analysed on the Great Northern Peninsula (modified after Knight and James, 1987).

5.1.1 PETIT JARDIN FORMATION, FLOWERS COVE

Large cryptomicrobial bioherms are beautifully exposed on the coastal rock platform on the southeastern shore of Flowers Cove, 15 km north of St. Barbe. They occur within a sequence of thin-bedded dolostones and dolarenite, near the base of the "stromatolite member" of the Upper Cambrian Petit Jardin Formation (Knight, 1980; "dolomite formation" of Knight, 1978). Regional mapping by Knight (1977a, 1977b, 1978, 1980) indicates that the bioherms lie on the northwestern (palaeo-shoreward) edge of a large southwest-northeast trending microbial bank which extends at least 35 km to the northeast. These bioherms were briefly described by Edwards (1978).

The bioherms are discoidal, remarkably circular in plan view, range from 3 to 20 m in diameter, and are 65-95 cm thick (Plate 63-A). They comprise few to several tens of individual dome-shaped mounds, and progressively coalesce to the southeast to form a laterally continuous biostrome. Towards the southeast, the crests of the individual mounds, composite bioherms and laterally continuous biostrome are progressively truncated by a planar erosion surface (Plate 63-B). This surface is commonly riddled with tiny 5-10 mm (?)solution pits (Plate 63-B), and is possibly a palaeo-karst surface.

The bioherms and inter-biohermal substrate are draped by thin beds of desiccation-cracked shale, dolo-mudstone and lenses of pebble conglomerate. These draping sediments have

locally slumped off the flanks of the bioherms to form contorted and brecciated slump lobes (Plate 63-D), and indicate that the bioherms have a synoptic relief equivalent to their thickness.

The bioherms have an irregular mottled to anastomosing cerebroid fabric composed of 2-tone, or locally 3-tone, dark and light coloured microcrystalline dolomite (Plate 63-C). The nature and origin of this fabric is not obvious; the dark coloured mottles appear to represent a primary cerebroid microbial framework, and the light coloured mottles are probably inter-framework sediment.

The dark coloured (?framework) mottles comprise structureless, diffuse grumous, or rarely faintly laminated, xenotopic dolomite and disseminated pyrite (Plate 63-E,F). Light coloured (?inter-framework) mottles comprise slightly coarser xenotopic dolomite and commonly contain patches and subrounded peloids of pyritic dolomite, minor skeletal debris (predominantly trilobites) and rare quartz silt (Plate 63-E). Medium tone halos around the dark coloured mottles comprise non-pyritic dolomite. Thus the mottled colouration results from both variations in crystal size and the presence or absence of disseminated pyrite.

Origin: Although primary microstructures have been extensively destroyed by dolomitization, comparison with buildups on the Port au Port Peninsula suggests that the dark coloured mottles represent frame-building microbial components, and the surrounding light coloured mottles are

inter-framework sediment. The primary thrombolitic or stromatolitic affinity of the framework, however, cannot be determined. The bioherms are accordingly classified cryptomicrobial boundstones.

5.1.2 BOAT HARBOUR FORMATION, EDDIES COVE WEST - A

Zoned stromatolite-thrombolite bioherms occur on the coastal rock platform 1.4 km northeast of the settlement of Eddies Cove West (Bed ?48 of Pratt's 1979 Eddies Cove West section). The bioherms occur within a sequence of thinly interbedded lime-mudstone, wackestone, grainstone and dolostone, in the central portion of the Boat Harbour Formation.

The bioherms have a symmetrical dome shape (Plate 64-A), are 0.7-1 m thick and 1-4 m in diameter, and locally coalesce to form elongate banks several metres long. They have 30-60 cm synoptic relief, and are buried and draped by thin-bedded grainstone and lime-mudstone.

The bioherms comprise a basal stromatolitic core concentrically overgrown by thrombolite (Fig. 5-2). The stromatolitic core comprises a basal zone of poorly bound, pebble-peloid-skeletal-ooid grainstone (Zone 1), which grades upward and outward into irregularly mottled and weakly laminated stromatolite (Zone 2), and branched columnar stromatolite (Zone 3). Stromatoid columns are separated by bioturbated wackestone and grainstone, and whole gastropod shells are commonly lodged between them. The outer surface

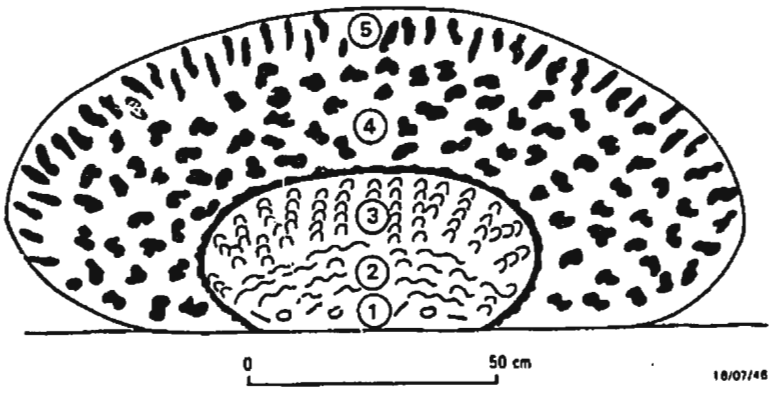

Figure 5-2. Schematic diagram of zoned stromatolite-thrombolite bioherms, Eddies Cove West - A, Great Northern Peninsula, western Newfoundland. 1 Poorly bound pebbly grainstone; 2 Mottled, weakly laminated stromatolite; 3 Columnar stromatolite; 4 Amoeboid thrombolite; 5 Digitate thrombolite.

of the stromatolitic core is generally marked by a band of dark chert. This surface has about 30 cm synoptic relief and probably represents a significant hiatus in the growth of the bioherms.

The encrusting thrombolite comprises anastomosing amoeboid thromboids and interstitial peloid-skeletal wackestone (Zone 4), grading outward to poorly defined radiating digitate thromboids which are encrusted by masses of smaller lobate and saccate thromboids (Zone 5). The thrombolite is extensively bioturbated and contains numerous stylolites.

Stromatoids within Zones 2 and 3 have a diffuse to distinctly striated, spongeous grading to vermiform, peloidal microstructure (Plate 64-B,C,D). They comprise prostrate, or alternating prostrate and erect, micro-fenestrae and vermiform tubules, diffuse silt-sized peloids, and minor fine metazoan fragments and calcispheres. Amoeboid and digitate thromboids within Zones 4 and 5 also have a spongeous grading to vermiform peloidal microstructure, but differ from the underlying stromatoids in that: 1) trapped and bound peloids are poorly sorted, coarser grained, and commonly merge to form massive micrite, 2) vermiform tubules and micro-fenestrae are randomly oriented, 3) metazoan burrows are more prevalent, and 4) lamination is absent (Plate 64-E,F). The small encrusting lobate and saccate thromboids within Zone 5 have a spherulitic lobate microstructure.

Origin: The stromatolite core (Zones 2 and 3) and encrusting amoeboid thrombolite (Zone 4) were constructed by sediment-

trapping filamentous communities. Initially, layers of prostrate or alternating prostrate and erect filaments selectively trapped silt-sized peloids to form discrete stromatoid columns between which coarser grained peloids and skeletal debris accumulated. Subsequently, a network of randomly oriented filaments trapped both silt and sand-sized peloids to form amoeboid thromboids which were extensively bioturbated (Zone 4). This filamentous community was progressively replaced by coccoid colonies (Zone 5).

5.1.3 BOAT HARBOUR FORMATION, EDDIES COVE WEST - B

A zoned thrombolitic and aberrant stromatolitic biostrome occurs on the coastal rock platform 1.6 km west of the settlement of Eddies Cove West (Bed 86 of Pratt's 1979 Eddies Cove West section). The biostrome, described briefly by Pratt (1979, p.61, Figs. 20c,d), occurs within a sequence of thinly interbedded and burrowed lime-mudstone, wackestone, grainstone and dolostone near the top of the Boat Harbour Formation.

The biostrome ranges from about 40 to 100 cm thick and culminates in a series of closely spaced mounds or heads (Fig. 5-3). These mounds have an apparent synoptic relief of 60-70 cm, are 1-3 m in diameter, and are flanked and draped by thin-bedded micritic limestone and dolostone. The biostrome directly overlies gently domed, pseudo-columnar grading to undulose-laminated, stromatolite.

Three distinct zones are evident within the biostrome (Fig. 5-3, Plate 65-A): 1) a basal 40 cm thick thrombolite, 2) a central 20-40 cm thick aberrant thrombolitic and stromatolitic zone, and 3) an upper 20-30 cm thick thrombolite. The basal and upper thrombolite zones are characterised by rubbly outcrops and poorly differentiated mottled fabrics. They comprise anastomosing prostrate, pendant and subdigitate thromboids, in part crudely laminated, and light coloured inter-framework wackestone (Plate 66-A). Dark millimetre-sized lobate and saccate bodies are locally prominent within the thromboids.

The central aberrant zone comprises: 1) a dark coloured, cerebroid coral-thromboid framework, which is encrusted by, 2) vertical to steeply convex and conical, stromatoid walls 1-3 cm thick, and 3) light coloured inter-framework dolomitic sediment (Plate 65-A,B,C,D). Small patches of micro-breccia occur within the cerebroid coral-thromboid framework, and have clearly resulted from the partial dissolution of the framework (probably selective dissolution of aragonite corals), and the subsequent fragmentation and collapse of the encrusting lithified stromatoids. Numerous veins of white sparry calcite are associated with these micro-breccias.

Thromboids within the basal and upper zones have a highly variegated, mottled to weakly laminated, vermiform-peloidal, spherulitic lobate, spongeous, *structure grumeleuse*, and massive microstructure, and are extensively disrupted by metazoan burrows (Plate 66-B,C,D). Minor skeletal debris

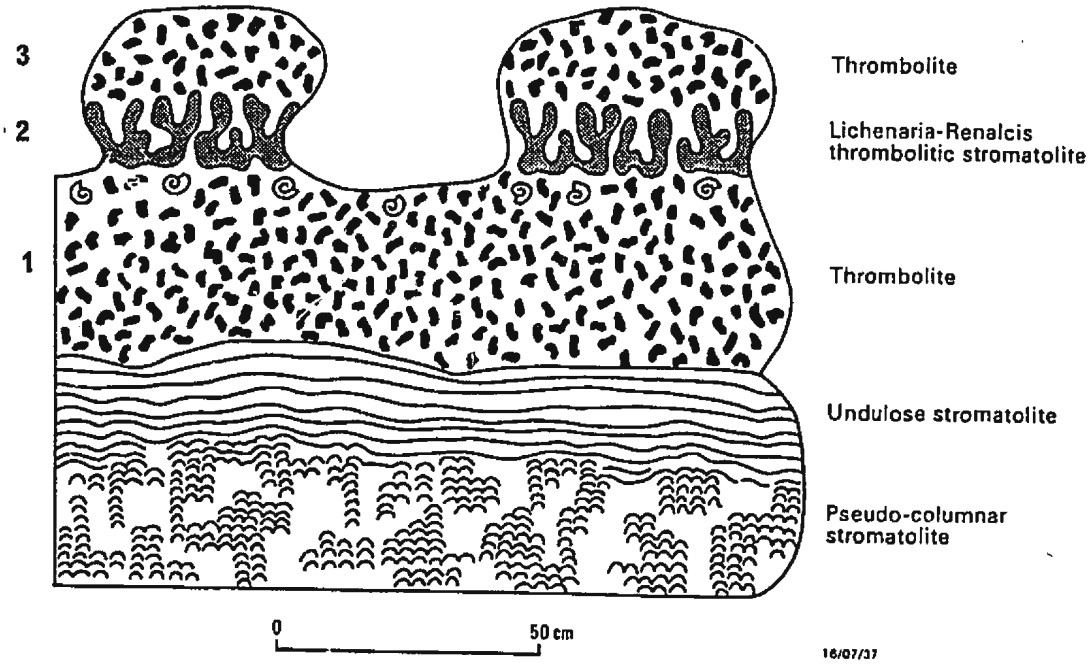

Figure 5-3. Schematic diagram of zoned thrombolitic and aberrant stromatolitic biostrome, Eddies Cove West - B, Great Northern Peninsula, western Newfoundland.

occurs within the thromboids, and within burrows that disrupt them.

The stromotoid-encrusted cerebroid framework within the central zone consists of intergrown 1) upward and outward directed *Lichenaria* corals, 2) pendant and outward directed *Renalcis*, 3) spongeous *structure grumeleuse* microstructures, 4) diffuse spherulitic lobate microstructures, 5) massive to diffuse grumous microstructures, and 6) interstitial patches of spiculitic lime-mudstone (Plates 67-A,B). Corals are commonly partially dissolved or silicified, and individual corallites are occluded by silt-sized peloids. These micro-peloids have an identical texture to the diffuse microclots within the surrounding *structure grumeleuse* microstructures, thus suggesting that this later microstructure represents trapped and bound silt-sized peloids. The encrusting stromatoids have a diffuse streaky, spongeous grading to vermiform, *structure grumeleuse* microstructure (Plate 67-C,D). Vermiform tubules are prostrate or alternate from prostrate to erect. Metazoan burrows are relatively scarce within the stromatoids. This central zone is classified a stromatolitic *Lichenaria-Renalcis* thrombolite.

Origin: The basal and upper thrombolite zones were apparently constructed by prostrate filmentous microbes and scattered calcified coccoid colonies. Carbonate mud, peloids and minor skeletal particles were trapped and bound by the filaments, and the thrombolites were extensively burrowed. The central

zone was constructed by a complex community of corals (*Lichenaria*), calcified coccoid colonies (*Renalcis*), indeterminate microbial matter which trapped and bound silt-sized peloids (*structure grumeleuse*), and encrusting layers of sediment-trapping filaments (stromatoids).

The aberrant stromatoid-encrusted framework within the crestal zone of this biostrome resembles the aberrant conical and cup-like stromatoid framework of Horizon M on the Port au Port Peninsula. In both cases the axial portions of the framework were partially or completely dissolved after the lithification of the encrusting stromatoids. In Horizon M this framework may have consisted of soft sponges, whereas aragonitic corals were probably selectively dissolved from the framework of this present biostrome.

5.2 SOUTHERN CANADIAN ROCKY MOUNTAINS

The Cambro-Ordovician strata of the southern Canadian Rocky Mountains can be regarded as the type area of thrombolites, since it was here that Aitken (1967) first documented the widespread occurrence of non-laminated, clotted microbial buildups, and, to emphasize their distinction from laminated stromatolites, coined the term "thrombolite". Apart from Aitken's original study, these thrombolites have not been studied in any detail, and their microstructure is poorly known. Thus in order to assess the wider applicability of the analytical, interpretive and classification schemes presented in Chapters 2 and 3, representative examples of these "type area thrombolites" were examined* and sampled for microstructural analysis.

The depositional history, palaeogeography and cyclicity of Cambro-Ordovician strata in the Canadian Rocky Mountains is best summarized by the concept of three persistent, but temporally shifting, facies belts (Palmer, 1960; Robison, 1960; Aitken, 1981a): 1) an **inner detrital facies** deposited adjacent to the stable craton and characterized by subtidal shales and siltstones with subordinate carbonates, 2) a **middle carbonate facies** characterized by shallow subtidal and peritidal carbonates, and 3) an **outer detrital facies** deposited "outboard" of the middle carbonate belt and

* Field studies were undertaken with the invaluable field guidance of J.D. Aitken (Institute of Sedimentology and Petroleum Geology, Geological Survey of Canada, Calgary), together with N. Clow (Memorial University of Newfoundland).

characterized by deeper water shales and argillaceous carbonates. Large scale **Grand Cycles** (Aitken, 1966, 1978) are conspicuous throughout this sequence, and record cyclical shifts of the boundary between inner detrital and middle carbonate facies belts. In contrast, the outer edge of the middle carbonate facies belt, that is the platform-margin, remained relatively fixed and is represented by a persistent narrow belt of peritidal carbonates, referred to by Aitken (1971) as the "Kicking Horse Belt". Small-scale shallowing upward cycles are common in the middle carbonate and inner detrital belt facies. They are generally similar to the sequences observed in the Grand Cycles; namely shales and\or siltstones passing upwards to subtidal and intertidal carbonates.

Thrombolites are abundant within both inner detrital and middle carbonate belt facies ranging from Early Cambrian to Lower Ordovician in age (Fig. 5-4). They are unknown in outer detrital facies west of the Kicking Horse Rim (Aitken, personnal communication 1984). Allochthonous blocks of platform-margin buildups locally occur within Middle Cambrian outer detrital facies (McIlreath, 1977; Aitken and McIlreath, 1981), but they comprise *Epiphyton* boundstone rather than thrombolite. Thrombolites are also unknown in the subsurface east of the Mountain Front, but this may simply be due to the scarcity of Cambro-Ordovician core samples, and the fact that cuttings are insufficient to recognize thrombolites.

Several thrombolite and stromatolite horizons were briefly examined within the Middle-Late Cambrian succession

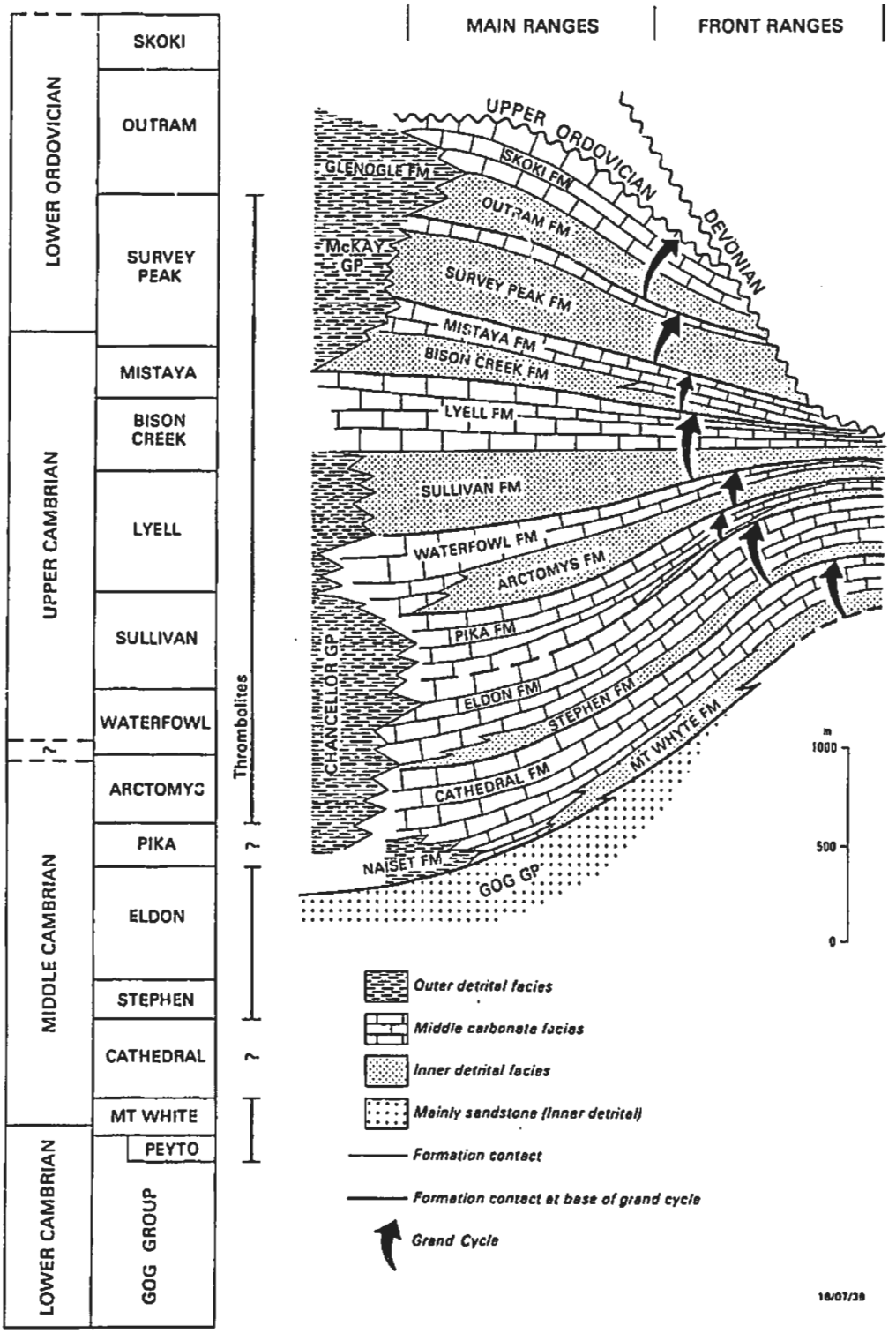

Figure 5-4. Stratigraphic column and diagrammatic restored cross-section of Lower Palaeozoic strata, southern Canadian Rocky Mountains, showing distribution of inner, middle and outer facies belts, Grand Cycles and thrombolites (after Aitken and others, 1972; Aitken, 1981a).

(Arctomys, Waterfowl, Sullivan, Lyell and Bison Creek Formations) at three localities: Windy Point north of the Saskatchewan River, Totem Creek on the western side of Mount Murchison, and Sunwapta Pass east of the Columbia Icefields. Five thrombolite horizons were sampled for microstructural analysis: two from the Waterfowl Formation (a carbonate half-Grand Cycle), and three from the Sullivan Formation (a shaly half-Grand Cycle).

With two exceptions, the observed thrombolites are megastructurally and mesostructurally directly comparable to those in western Newfoundland. Firstly, thrombolites within the Sullivan Formation were probably deposited in deeper water than the thrombolites in western Newfoundland. They form small to medium subspherical to domed bioherms rooted in ooid-skeletal grainstone and packstone, and draped by greenish-grey shales (Plate 68-A). Although the origin of these oolitic sands is somewhat uncertain, judicious evaluation of regional data led Aitken (1978, p.526-528) to conclude that they are allochthonous sediments which were probably transported by storm surge currents from the shallow water carbonate belt 100 km or more to the west, and which accumulated in a relatively deep (greater than 12 m), terrigenous mud-dominated, intra-shelf basin (the inner detrital belt). With the possible exception of the thrombolites at the base of the Cape Ann Complex (Horizon A, Chapter 4), the thrombolites in western Newfoundland occur within shallow peritidal carbonate shoals or adjacent

(shoreward) peritidal carbonate-terrigenous environments (Pratt and James, 1986; Chow and James, 1987; Knight and James, 1987). That is, an equivalent intra-shelf shale basin is not well represented within the Cambro-Ordovician strata of western Newfoundland.

Secondly, two of the observed thrombolite horizons comprise a framework of delicate arborescent and dendritic black thromboids, one millimetre or less thick, which superficially resemble *Epiphyton*[*] (Plate 68-B). *Epiphyton senso stricto*, however, does not occur within the thrombolites of western Newfoundland, and is generally thought to be restricted to platform-margin, rather than platform-interior, microbial buildups (Pfeil and Read, 1980; James, 1981, 1983; Read and Pfeil, 1983; Demicco, 1985; see further discussion in Section 5.4.3).

Microstructures are generally poorly preserved within the five sampled horizons. Amoeboid and sub-digitate thromboids within the "deep water" thrombolites in the Sullivan Formation have ragged bioturbated margins and are encased within silty peloid-skeletal or ooid-skeletal packstone and wackestone. They have a massive microcrystalline or slightly silty, diffuse grumous microstructure (Plate 68-C), and masses of *Girvanella* tubules are vaguely discernible (Plate 68-D; these vague tubular microstructures are best seen as the microscope is slowly racked in and out of focus under moderate magnification (X 300) and are difficult to

[*] During field studies, these structures were informally referred to as *Epiphyton* by J.D. Aitken.

illustrate in photomicrographs). Thromboids and cryptomicrobial fabrics within the Waterfowl Formation bioherms have a spongeous, silty peloidal grading to massive or diffuse grumous microstructure in which isolated *Girvanella* tubules occur (Plate 68-E). *Girvanella*-dominated microstructures were also noted within some thrombolites by Aitken (1967, p.1172).

Tiny arborescent and dendritic thromboids within the Waterfowl Formation thrombolites have a microcrystalline lobate, locally grading to diffuse cellular lobate, microstructure (Plate 68-F). Thus although they superficially resemble *Epiphyton* in hand sample, they are readily distinguished on the basis of their microstructure (lobes of clear to turbid microspar, versus cryptocrystalline dentritic thalli), larger size (500-1000 μm versus 10-50 μm wide), and colour (black versus light coloured in hand speciman). The only known occurrence of *Epiphyton* within the Cambro-Ordovician strata of the Canadian Rocky Mountains is within talus blocks derived from the Middle Cambrian, shelf-margin, Cathedral escarpment (McIlreath, 1977; Aitken and McIlreath, 1981). This occurrence is analogous to the blocks of *Epiphyton* boundstone within platform-margin derived megabreccias in the Cow Head Group of western Newfoundland (James, 1981; James and Stevens, 1986).

Thus, although based on a very limited number of samples, these "type area" Rocky Mountains thrombolites are also microstructurally directly comparable to the thrombolites in western Newfoundland.

5.3 EASTERN UNITED STATES OF AMERICA

Thrombolites are also widespread within Cambro-Ordovician platformal strata in the central and southern Appalachians (Bova and other, 1982; Bova and Read, 1987; Demicco, 1983, 1985; Demicco and others, 1982; Markello and Read, 1981, 1982; Moshier, 1986; Owen and Friedman, 1984; Pfeil and Read, 1980; Read, 1983; Read and Pfeil, 1983). They generally occur in shallow platform-interior settings analogous to those in western Newfoundland and the Southern Canadian Rocky Mountains, but locally also form allochthonous blocks derived from the platform margin (Reid and Pfeil, 1983). These platform-margin thrombolites have similar fabrics and microstructures to *in situ* platform-margin thrombolites in the Great Basin, western United States of America (see Section 5.4).

Although relatively few details on the fabric and microstructure of the platform-interior thrombolites in the central and southern Appalachians have been published, scrutiny of several unpublished theses and thesis thin-section collections housed at the Virginia Polytechnic Institute* (Markello, 1979; Bova, 1982; Koerschner, 1983) revealed a similar spectrum of mesostructures and microstructures to that displayed by the thrombolites in western Newfoundland. Three thrombolite horizons were also sampled for microstructural analysis, one in the Middle

* Thin-sections were kindly made available by J.F. Read, Virginia Polytechnic Institute.

Cambrian Elbrook Formation (sampled in a roadcut on Interstate Highway 81 near the Clayfor Lake turnoff, Virginia), and two in the Late Cambrian Conococheague Formation (sampled in a road cut on Interstate Highway 77, 0.5 km north of Interstate Highway 81).

Horizon 1: Elbrook Formation

These bioherms have a complex clotted and mottled fabric in which thromboids and inter-framework sediments are poorly differentiated (Plate 69-A). They have a variegated spherulitic lobate and spongeous, diffuse grumous (*structure grumeleuse*) microstructure (Plate 69-B,C,D,E). The spherulitic lobes either form free-standing structures surrounded by silty inter-framework mudstone and wackestone, or are enmeshed in spongeous grumous microstructures. Numerous silt-sized peloids partially occlude the micro-fenestrae, some of which are obviously burrows.

Horizons 2 and 3: Conococheague Formation

Bioherms within both of these horizons comprise anastomosing sub-digitate thromboids, sediment- and cement-filled shelter cavities, and extensively burrowed inter-framework peloid-skeletal packstone. The thromboids generally comprise variegated diffuse grumous, massive lobate, and mottled microstructures (Plate 69-F), but locally have a crudely laminated silty peloidal microstructure. Their

microstructure is commonly obscured by abundant stylolites and microcrystalline dolomite.

Discussion

Bova (1982) and Koerschner (1983) recognized two broad types of microfabrics within the Cambro-Ordovician thrombolites in the Virginian Appalachians: 1) grain-dominated, the dominant type, and 2) mud-dominated. All horizons sampled in this study belong to their grain-dominated type. Their mud-dominated microfabrics are characterized by vermiform microstructures comparable to that occurring within Horizons J, K, M, N and Q on the Port au Port Peninsula, and at Eddies Cove West A and B on the Great Northern Peninsula, western Newfoundland.

Bova (1982, p.72) recognized two types of grain-dominated microfabrics: crudely layered "pelletal" microfabrics, and cement-dominated "grainy" microfabrics. His "pelletal" microfabrics are identical to streaky peloidal micro-structures as defined in this study, and warrant no further comment. As described by Bova (1982, p.72), cement-dominated "grainy" microfabrics consist of:

> "irregular layers and patches of `pelsparite' and `pelmicrite', abundant millimetre to centimetre sized botryoids and spherulites of amber fibrous neospar or microspar cement, abundant irregular fenestrae, and multiple borings and cavities.... Botryoids and spherulites of amber coloured, fibrous neospar and

microspar are scattered through fingers [thromboids], concentrated in layers, or concentrated along finger margins. They make up 80 pecent of the fabric, occurring as botryoidal aggregates (that are not an obvious void fill) separated by floating clumps of pellets and micrite".

As elaborated by Koerschner (1983, p.61), individual pellets surrounding the spherulitic aggregates are 20-100 μm in size and range from "circular grains with sharp boundaries" to "filamentous bodies with blurred boundaries". These "cement-dominated" microfabrics are identical to variegated, lobate spherulitic and spongeous grumous microstructures as defined in this study; "spherulitic cements" being equivalent to spherulitic lobes, and "pellets" being equivalent to microclots. The spherulites are interpreted to be marine bacterial precipitates (see Chapter 2, Section 2.3.2), not inorganic cavity-filling precipitates as implied by Bova (1982), Koerschner (1983), and most recently, Bova and Read (1987, Fig. 9C). This microstructure occurs within the Elbrook Formation thrombolite horizon described above, and is widespread in thrombolites in western Newfoundland (for example, Horizons N, O, Q on the Port au Port Peninsula, and at Eddies Cove West on the Great Northern Peninsula).

In summary, the mesostructures and microstructures displayed by thrombolites in the Virginian Appalachians fall within the spectrum observed for thrombolites in western Newfoundland.

5.4 WESTERN UNITED STATES OF AMERICA

Thrombolites are also common in the Cambro-Ordovician strata of the Great Basin, western United States of America (Kepper, 1976; Lohmann, 1976; Palmer and Halley, 1979; Cooper and others, 1981; Robison and Rees, 1981; Taylor and Repetski, 1985; Rees, 1986). Five thrombolite horizons were examined in this study: one in the Middle Cambrian Wheeler Formation in the Drum Mountains, Utah (Robison and Rees, 1981; Rees, unpublished), and four in the Late Cambrian Orr Formation in the House Range, Utah (Lohmann, 1975, 1977; Robison and others, 1981). These buildups are of special interest since 1) they occur on the ocean-facing margin of the Cambrian platform margin, at or near the eastern perimeter of the House Range Embayment, an embayment of outer detrital belt facies that extends eastward into the carbonate platform (Kepper, 1972, 1976, 1981; Lohmann, 1976, 1977; Rowell and Rees, 1981; Rees, 1986), and 2) they are dominated by calcified "microfossils" (*Renalcis*, *Epiphyton* and\or *Girvanella*). Such *Renalcis-Epiphyton-Girvanella* assemblages characterize many Cambro-Ordovician platform margins (McIlreath, 1977; James, 1981; Pfeil and Read, 1980; Read and Pfeil, 1983; Demicco, 1985), but whereas they are preserved *in situ* in the Wheeler and Orr Formations, elsewhere they are only known to occur as allochthonous blocks derived from the platform margin. The Wheeler and Orr Formation thrombolites thus provide an ideal opportunity to study *in situ* platform-margin thrombolites, and to compare them with more typical

platform interior thrombolites. They are the most "outboard" occurrence of Cambro-Ordovician thrombolites examined in this study. Figure 5-5 shows the palaeogeographic setting of these thrombolites in relation to the shifting configuration of the carbonate and outer detrital facies belts in Middle-Late Cambrian time.

5.4.1 MIDDLE CAMBRIAN WHEELER FORMATION

In the Drum Mountains, western Utah, the Wheeler Formation represents a shallowing-upward sequence from 1) basinal agnostid-bearing shale and limestone, to 2) thin-bedded lime-mudstone, wackestone, packstone and shale deposited below wave base, 3) thin to medium bedded lime-mudstone, wacke-stone, packstone, and minor intraclastic and skeletal grainstone, periodically reworked by wave and current action, and 4) shallow subtidal, burrow-mottled, peloid-intraclast-ooid-skeletal packstone and wackestone, and skeletal-ooid-intraclast grainstone (Robison and Rees, 1981; Rees, 1986). This shallowing-upward basin-to-ramp sequence culminates in platformal dolostones of the Pierson Cove Formation.

A *Renalcis* and *Epiphyton*-rich buildup occurs within thin to medium bedded and burrow-mottled shallow subtidal facies in the upper part of the Wheeler Formation (Robison and Rees, 1981; Rees, unpublished). This buildup was examined and sampled near its southeastern limit of outcrop where it is approximately 3 m thick (Sections A and B, Fig. 5-6), and

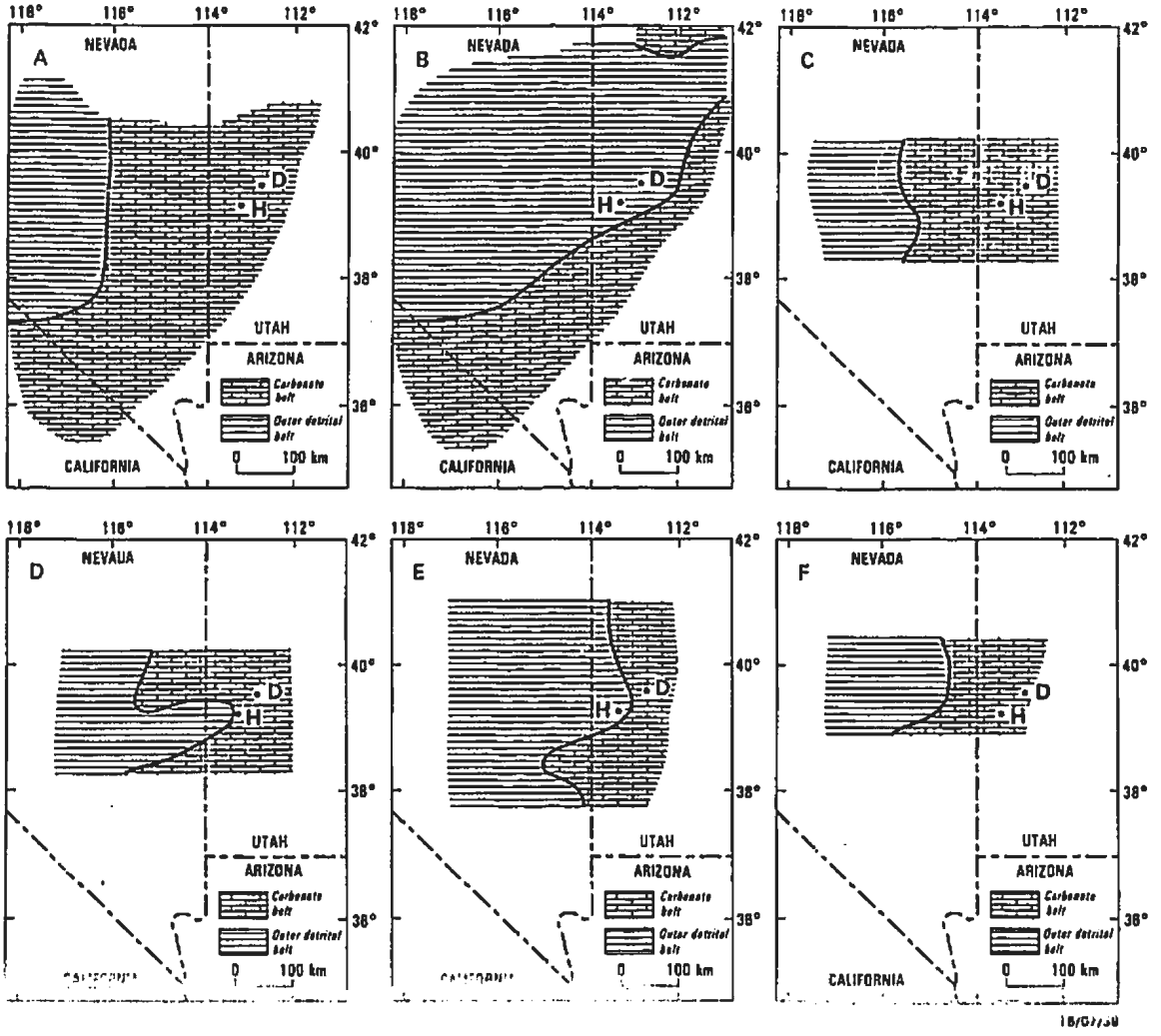

Figure 5-5. Palaeogeographic maps showing changes in the configuration of the western margin of the carbonate facies belt in the western United States during Middle and Late Cambrian time. A) Early Middle Cambrian time prior to deposition of the Wheeler Formation. B) During deposition of the Wheeler Formation, immediately prior to southward progradation of the ramp and deposition of microbial buildups in the upper Wheeler Formation. C) During late Middle Cambrian time prior to deposition of the Orr Formation. D) During deposition of microbial buildups in the Big Horse Limestone Member of the Orr Formation. E) During deposition of microbial buildups in the Candland Shale Member of the Orr Formation. F) During deposition of the Johns Wash Limestone Member of the Orr Formation. After Palmer (1971), Rowell and Rees (1981), and Lohmann (1977). The location of the Drum Mountains and House Ranges are shown by letters D and H.

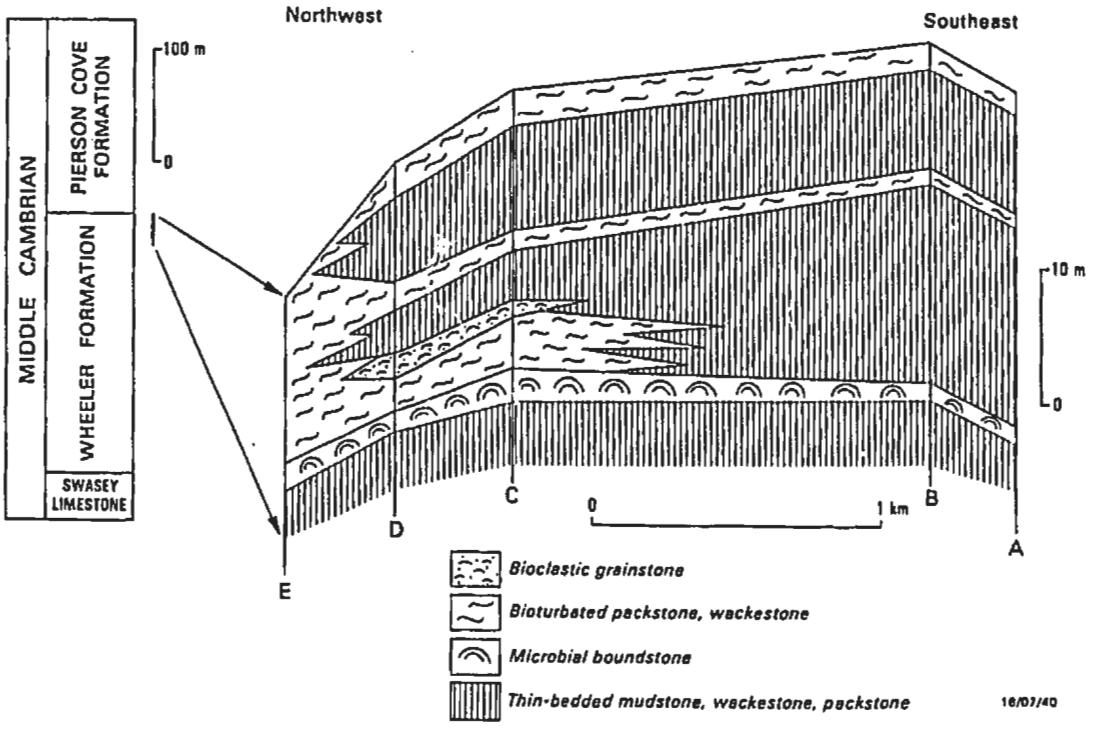

Figure 5-6. Upper Middle Cambrian stratigraphic section in the Drum Mountains, western Utah (after Robison and Rees, 1981; Rees, 1986).

traced to the northwest where it comprises smaller isolated bioherms encased in grainstone.

Rees (unpublished) recognised seven distinct units within this buildup (Fig. 5-7):

1. Foundation layer of intraclastic grainstone.
2. Irregularly stacked *Renalcis* thrombolite and stromatolite domes, several centimetres to 80 cm in diameter, and intraclastic grainstone channels.
3. Thin layer of black *Epiphyton* thrombolite.
4. Compound columnar stromatolites, with at least 50 cm synoptic relief, separated by channels of intraclast-oncolite grainstone.
5. Broad, gently domed, laterally-linked stromatolites.
6. Closely spaced *Renalcis* thrombolite domes, 20-50 cm in diameter.

Rees considered that the buildup was initiated in a shallow subtidal environment (Units 1, 2 and 3), built into the inter-tidal zone (Units 4 and 5), and was subsequently re-submerged (Unit 6) and buried by fine grained sediment.

Representative samples were collected from each unit of the buildup during the present study and, together with samples previously collected by N.P. James, form the basis of the following analysis.

Renalcis thrombolite and stromotolite (Unit 2)

This unit comprises two framework components: 1) masses of tiny black thromboids, less than one to a few millimetres in

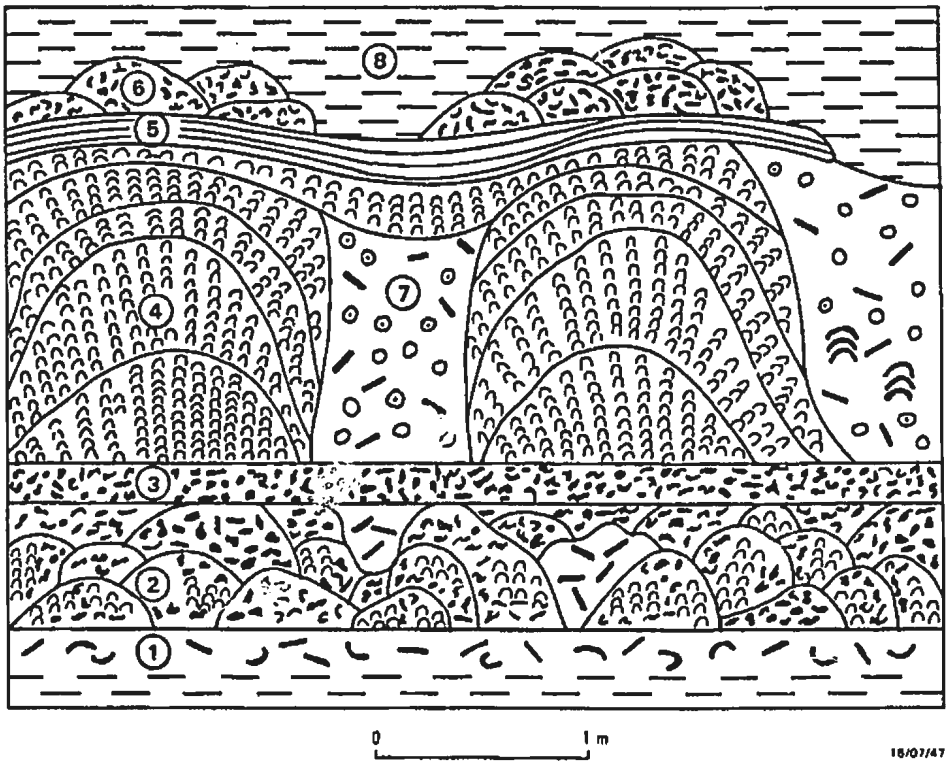

Figure 5-7. Schematic cross-section of microbial buildup in the Wheeler Formation, Drum Mountains, Utah. 1 Intraclast grainstone; 2 *Renalcis* thrombolite and stromatolite, and intraclast channels; 3 *Epiphyton* boundstone; 4 Columnar stromatolite; 5 Laterally linked stromatolite; 6 *Renalcis* thrombolite; 7 Intraclast-oncolite channels; 8 Platy limestone. Modified after Rees (unpublished).

diameter, commonly forming lobate and arborescent clusters up to one centimetre or more in size, and 2) laterally linked columnar, pseudo-columnar and crenulate stromatoids (Plate 70-A). The proportion of thromboids and stromatoids varies widely from dome to dome and within a single dome, there being a complete gradation from thrombolite to stromatolitic thrombolite, thrombolitic stromatolite and stromatolite. Where co-occurring, thromboids and stromatoids are mutually encrusting. Inter-framework components are lime-mudstone (neomorphosed to microspar), scattered pockets of peloids and trilobite debris, and rare sediment- and cement-filled shelter cavities. Although bioturbation is not evident within the samples examined, Rees (unpublished) reported that thrombolites and stromatolites within this unit are locally disrupted by small burrows and possible borings.

Thromboids exhibit three intergradational microstructures: chambered *Renalcis*, clotted *Renalcis* and diffuse micro-crystalline lobes. Chambered *Renalcis* is predominant, and forms squat to erect, upward and outward directed colonies a few millimetres in size (Plate 70-B). Individual chambers are 60-200 μm in diameter. Clotted *Renalcis* consists of irregular subequant to sub-arborescent clusters of cryptocrystalline microclots which are distinctly darker and smaller (20-100 μm, generally less than 60 μm) than individual chambers. Chambered and clotted morphotypes form discrete colonies, mutually encrusting colonies, or complex intergrowths (Plate 70-C), and are encased in turbid microcrystalline marine cement. With increasing neomorphism,

they intergrade with microcrystalline lobate microstructure (Plate 71-A). All three morphotypes are interpreted as calcified coccoid colonies.

Stromatoids generally have a massive streaky microstructure comprised of alternating cryptocrystalline and microcrystalline layers, respectively 20-30 μm and 300-1000 μm thick (Plate 71-A,B). Locally they have a distinct grumous microstructure, in which case the layers and lenses of microclots closely resemble prostrate forms of clotted *Renalcis* (Plate 71-C). These grumous laminae commonly encrust and bridge individual chambered *Renalcis* colonies, or alternate with layers of *Renalcis*. They are interpreted to be layers of calcified coccoid microbes.

Rare colonies of *Epiphyton* also occur in this unit (Plate 72-A). The "thalli" are uniformly thick (about 30 μm) and have an outward or upward directed dentritic form. Rees (unpublished) also reported rare *Girvanella* within stromatolitic laminae, but none were observed in the present study.

This unit was thus constructed by four forms of calcified coccoid microbes: 1) arborescent chambered colonies (chambered *Renalcis*), 2) squat clotted colonies (clotted *Renalcis*), 3) thin layered mats (massive and grumous stromatoids), and 4) rare dendritic colonies (*Epiphyton*). Intergradations of these growth forms (except *Epiphyton*) suggest that they are not species specific, but rather may simply reflect subtle changes in the rates of growth,

calcification and degradation of a single coccoid community (see Chapter 2, section 2.3.1).

On the basis of mesoscopic field examination, this unit is classified a stromatolitic thrombolite. Since the thromboids are wholly comprised of *Renalcis* and *Renalcis*-like "microfossils", however, the preferred classification (see Chapter 3) is a stromatolitic *Renalcis* boundstone.

Epiphyton **thrombolite (Unit 3)**

This unit has a dense black clotted and locally white speckled fabric with fine, discontinuous hummocky laminae. Two framework components are recognized in thin section (Plate 72-B): 1) diffuse hummocky layers, and 2) squat *Epiphyton* colonies. The hummocky layers comprise turbid microcrystalline calcite with scattered terrigenous silt, equidimensional silt-sized peloids and rare ooids. The peloids in these layers are strikingly similar in size and texture to *Epiphyton* "thalli", and undoubtedly represent fragments of *Epiphyton*. Although neomorphism has obscured their fabric, these layers are reminiscent of the cement-stromatoid crusts that occur in the basal portion of the Cape Ann thrombolite-stromatolite complex in western Newfoundland (Horizon A, Chapter 4). A similar origin is accordingly tentatively proposed for these layers, but cannot be verified on the basis of the available samples.

Epiphyton predominantly occurs in association with ooid and skeletal wackestone in what appears to be crevasse-like cavities between steep sided "cement-stromatoid" growths

(Plate 72-B). These colonies are directed outward from the "cement-stromatoid" substrate into the cavity. Isolated *Epiphyton* colonies also occur enclosed within the "cement-stromatoid" layers, in which case they have a more variable outward, downward or upward orientation.

Walled tubular structures also occur in this unit (Plate 72-C). The tubes are slightly sinuous and are filled with sparry cement. They have an internal diameter of approximately 70 μm, are up to 700 μm long, and their micritic walls are 10-20 μm thick. These tubes are strikingly similar to *Microtubus communis* Flügel 1964, and were probably constructed by small serpulid worms.

Rees (unpublished) considered that this unit was constructed by a framework of rigid arched laminae (of unspecified origin) which enclosed shelter cavities subsequently filled with *Epiphyton*. However the lack of preferred downward directed *Epiphyton* colonies (the archetypal growth form displayed by this "microfossil"), an observation also made by Rees, instead suggests that they grew on indurated "cement-stromatoid" substrates (the arched laminae of Rees), and were in turn encrusted by subsequent stromatoid layers. The colonies are commonly encased within turbid, poorly fibrous calcite cement, and it thus appears likely that they were calcified and cemented whilst exposed on the sea-floor.

Microstructural analysis thus suggests that this unit represents a lithified submarine crust comprised of 1) sediment-trapping microbial layers, 2) marine cement,

3) calcified dentritic coccoid colonies (*Epiphyton*), and

4) ?serpulid worm tubes.

This unit is difficult to classify in terms of the classification scheme proposed in Chapter 3 since distinct framework and interframework components are not discernable in outcrop, hand samples or polished slabs. On the basis of the above microstructural interpretation, it is classified a stromatoid-cement-*Epiphyton* boundstone.

Compound stromatolite (Unit 4)

This unit has a columnar-layered fabric in which inter-column spaces and laterally linked laminae are accentuated by selective dolomitization. Individual columns are 1-2 cm wide and comprise gently convex stromatoids.

The stromatoids are 1-3 mm thick, laterally discontinuous, and contain numerous elongate to laminoid fenestrae several millimetres long. They have a streaky microstructure comprised of alternating massive cryptocrystalline and microcrystalline laminae (Plate 73-A). They are commonly disrupted by mottled and tubiform microstructures (Plate 73-B), apparently the result of bioturbation. Pockets of peloidal, oolitic and rarely skeletal sediment (extensively dolomitized) occur between, and less commonly within, columns.

These stromatolites are microstructurally similar to the stromatolitic layers within Unit 2, except that they do not intergrade with distinct microclots (grumous microstructure) of probable coccoid origin. It is not known whether these

columnar-layered stromatolites were also constructed by coccoid microbial communities.

Laterally-linked stromatolite (Unit 5)

This unit has a fine undulose to crenulate laminated fabric. The stromatoids generally have a diffuse streaky, massive to grumous microstructure (Plate 73-C), and less commonly comprise rhythmic alternations of thin crypto-crystalline (70-200 μm thick) and thicker grumous (500-2000 μm thick) laminae (Plate 73-D). They are locally disrupted by pockets of oolitic and rarely skeletal wackestone. The composition of the formative microbial mats cannot be determined, but they evidently had little ability to trap and bind ooids and skeletal debris.

Renalcis **thrombolite (Unit 6)**

This unit has a dense, black, finely clotted fabric. It comprises arborescent colonies of chambered and clotted *Renalcis* enclosed within micrite and turbid marine cement. Clotted *Renalcis* is generally slightly predominant, and forms darker, squatter colonies than chambered *Renalcis*. These two morphotypes are either intimately intergrown, in which case clotted morphotypes consistently cap chambered morphotypes (Plate 74-B), or else they form separate adjacent colonies or alternate layers (Plate 74-A). With the progressive increase in size of individual clots, and a decrease in size of lunate chambers, clotted morphotypes intergrade with chambered

morphotypes (plate 74-C,D). Euhedral authigenic quartz crystals preferentially occur within clotted morphotypes.

This unit is similar to the stromatolitic *Renalcis* boundstone of Unit 2, except that here *Renalcis* colonies are not encrusted by stromatoid layers. In accordance with the classification scheme presented in Chapter 2, this unit is most appropriately classified a *Renalcis* boundstone.

5.4.2 LATE CAMBRIAN ORR FORMATION

In the central House Range, western Utah, the Orr Formation consists of five members (Fig. 5-8): in ascending order, the Big Horse Limestone, Candland Shale, Johns Wash Limestone, Corset Spring Shale, and Sneakover Limestone Members (Hintze and Palmer, 1976). Four thrombolitic horizons were examined and sampled for microstructural analysis at the type section of the formation; two within each of the Big Horse Limestone and Candland Shale Members. Regional stratigraphic analysis indicates that the Big Horse Limestone Member represents the ocean-facing margin of the carbonate platform, and that the Candland Shale-Johns Wash Limestone-Corset Spring Shale triad is a continuous regressive sequence representing outer detrital, carbonate platform, and inner detrital belts, respectively (Palmer, 1971; Robison, 1975; Rees and others, 1976, Robison and others, 1981).

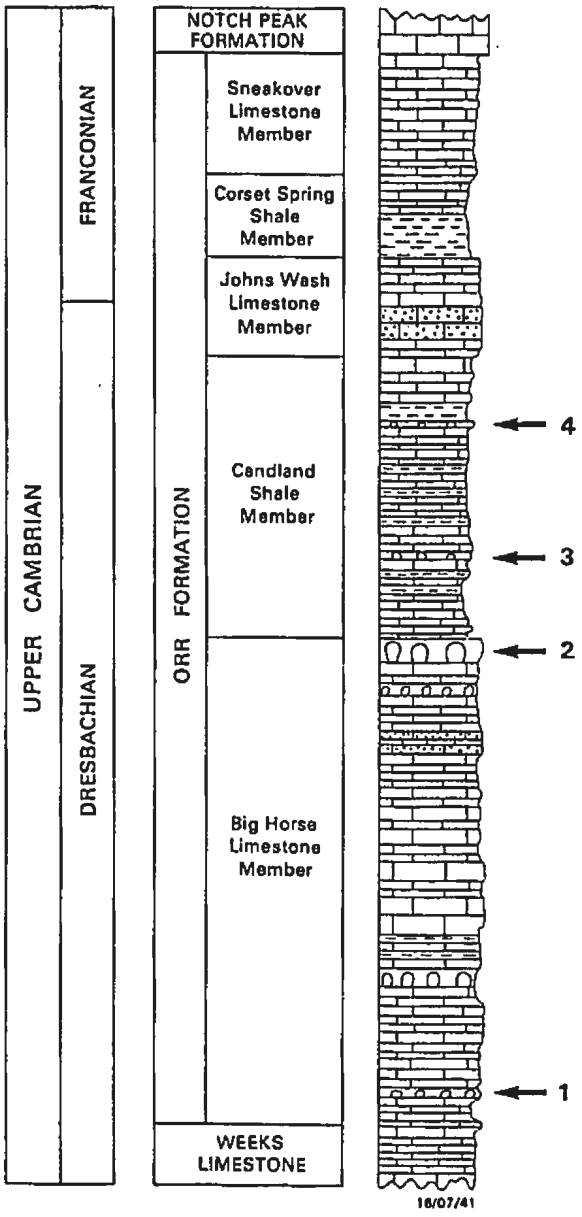

Figure 5-8. Stratigraphic section of the Orr Formation, House Range, western Utah, showing location of thrombolitic horizons analyzed in this study. Modified after Hintze, 1973; Hintze and Palmer, 1976.

Big Horse Limestone Member

The Big Horse Limestone Member of the Orr Formation consists of a series of upward-shallowing cycles, an ideal cycle comprising (in ascending order): 1) burrowed wackestone deposited below wave base, 2) cross-stratified skeletal and oncolitic packstone and grainstone, and 3) microbial boundstone or cross-stratified ooid grainstone (Lohmann, 1976, 1977). These cycles resulted from repeated progradation and subsidence of a gently inclined platform-margin rimmed by ooid shoals and microbial buildups. Lohmann (1976, 1977) reported that microbial boundstones at the top of the cycles typically show an upward transition from subtidal thrombolites to intertidal stromatolites, and are locally capped by a thin layer of subtidal thrombolite deposited during the initial flooding and transgression of the platform-margin at the commencement of the next cycle. Two representative thrombolite horizons are analysed below.

Horizon 1: lower Big Horse Limestone

This horizon, at the base of the *Crepicephalus* zone (base of Lohmann's 1977 Section 1), consists of domed bioherms 50-150 cm in diameter and up to one metre thick. The bioherms are separated by wackestone and packstone channels, and are underlain and overlain by skeletal and oolitic grainstone.

The bioherms comprise prostrate to pendant thromboids, micrite and spar-filled shelter cavities, and weakly stratified, partially dolomitized patches of silty peloid-

skeletal packstone. Narrow stromatoid columns, the margins of which are encrusted by scattered lobate thromboids, are locally present near the crest of the bioherms.

The thromboids have a massive to diffuse grumous, turbid microcrystalline microstructure, with numerous diffuse *Epiphyton* colonies (Plate 75-A,B). Where well preserved, transverse sections of *Epiphyton* appear as clusters of circular microclots (20-30 μm in diameter), each microclot locally surrounded by an isopachous rim or mosaic of turbid microcrystalline cement. Dendritic longitudinal sections (Plate 75-E) are surprisingly rare in the samples examined, thus suggesting that the "thalli" may be shorter than archetypal *Epiphyton*, and\or they have suffered *in situ* fragmentation and collapse. With increasing neomorphism, dendritic and "microclotted" *Epiphyton* intergrade with grumous and finally massive microcrystalline microstructures (Plate 75-C,D,E). These massive microstructures are in turn locally replaced by coarse poikilitic spar. In rare instances, faint *Girvanella*-like tubules* are also barely discernable within grumous microstructures. Thromboids and inter-framework sediment are extensively bioturbated. Skeletal debris consists of trilobites, pelmatozoans and sponge spicules.

---

* In his more extensive study of the Big Horse Limestone Member, Lohmann (1977, p.125) noted that although *Girvanella* is a common minor constituent of the thrombolites and stromatolites, it is very poorly preserved and "frequently destroyed by even mild recrystallization ... as little as ten percent of the primary skeletal microfabric may be preserved."

The narrow stromatoid columns at the crest of the bioherms have a streaky, massive to mottled silty microstructure, and are separated by burrowed silty peloid-skeletal packstone.

Although neomorphism has obscured its primary fabric, this thrombolite was evidently predominantly constructed by 1) non-specific calcified microbes, 2) dendritic calcified coccoid colonies (*Epiphyton*), and 3) minor calcified filamentous colonies (*Girvanella*). Since the dominance of *Epiphyton* is inferred, rather than directly observed, the designation *Epiphyton* thrombolite is considered more appropriate than *Epiphyton* boundstone.

Horizon 2: upper Big Horse Limestone

A 6 m thick thrombolite-stromatolite complex is well exposed at the top of the Big Horse Limestone on the crest of Orr Ridge. This complex was described in considerable detail by Lohmann (1977), who mapped the spatial distribution of four distinct lithological units (Fig. 5-9): 1) *Epiphyton-Girvanella* thrombolite which overlies mega-rippled oncolite-skeletal packstone and grainstone at the base of the complex, and encrusts the margins of, 2) *Girvanella* stromatolite columns and composite columnar pedestals, 3) *Epiphyton-Renalcis* thrombolite which encrusts the crests of *Girvanella* stromatolite columns, and 4) skeletal-intraclast grainstone which fills channels between thrombolites and thrombolite-encrusted stromatolite columns and pedestals. Representative samples of each lithology were sampled for microstructural analysis.

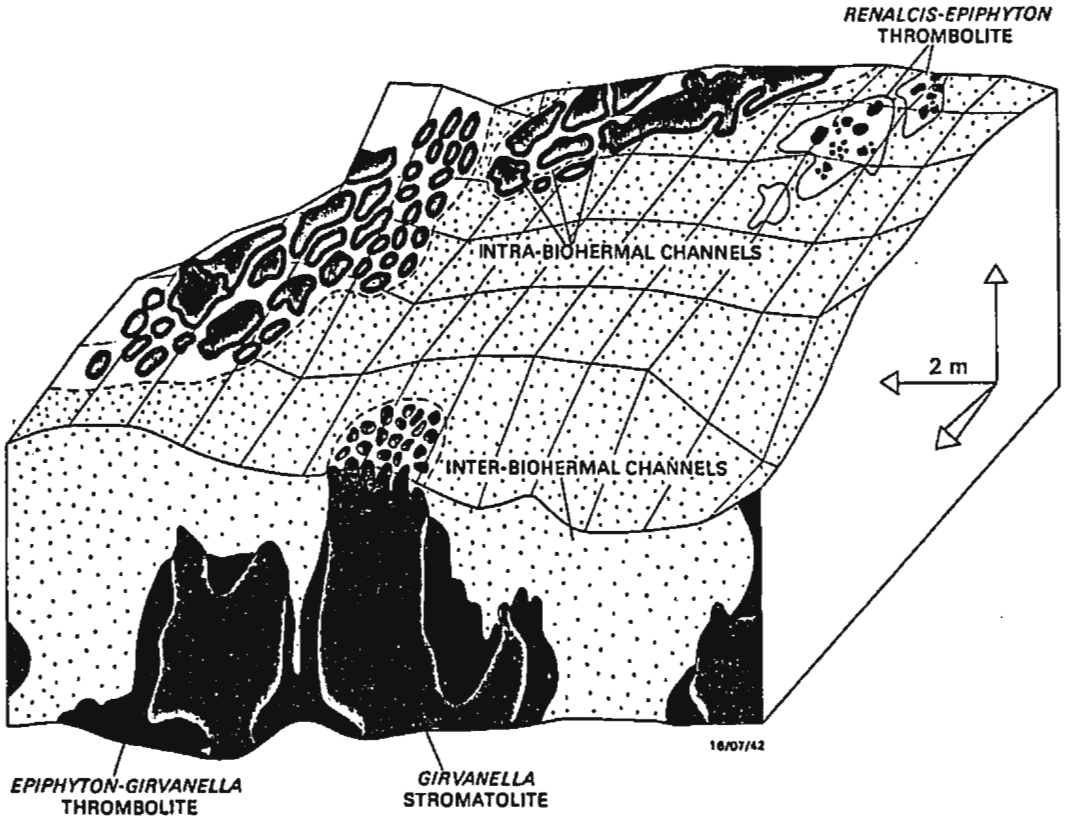

Figure 5-9. Distribution of units within thrombolite-stromatolite buildup at the top of the Big Horse Limestone Member of the Orr Formation, Orr Ridge, House Range, western Utah (from Lohmann, 1977).

Unit 1: *Epiphyton-Girvanella* thrombolite. This unit has a chaotic, clotted to weakly stratified fabric comprised of variably prostrate, amoeboid and lobate thromboids, lime-mudstone, and pockets of peloid-skeletal packstone. It is extensively bioturbated and disrupted by numerous stylolites and patches of dolomite. The thromboids have a variegated mottled, tubular, grumous and massive microstructure (Plate 76-A,B). Infrequently they have a poorly developed filamentous microstructures in which networks of wispy micritic threads and films, about 10 μm wide and less than 100 μm long, are enmeshed in turbid microspar (Plate 76-C). These filamentous microstructures superficially resemble *Girvanella*, except that solid thread-like forms are far more abundant than diagnostic tubular forms which are poorly defined within the available sample of this unit. This sample may not be fully representative of this lithotype, since Lohmann (1977, p.116) notes that "*Girvanella* develops thin encrusting draping structures 0.1 to 1.0 millimetres thick, subvertical blades, or subhorizontal masses rich in microcavities". Many of the examples illustrated by Lohmann, however, are poorly defined. *Epiphyton*, also recorded by Lohmann (1977), similarly does not occur within the sample of this unit. In the absence of definitive calcified "microfossils", the sample of this unit is simply classified a thrombolite.

Unit 2: *Girvanella* stromatolite. This unit comprises closely packed, in part laterally linked, club-shaped columns

(10-25 cm wide and up to 70 cm or more high) separated by narrow channels or crevasses filled with skeletal-intraclast grainstone (Plate 77-A). The columns comprise thick gently convex stromatoids, partially replaced and accentuated by irregular dolomite layers, and are encrusted by thrombolitic rims 2-6 cm thick (Plate 77-B). The stromatoids have a diffuse streaky, spongeous grumous microstructure (Plate 77-C), are commonly replaced by massive microspar or coarse poikilotopic spar, and are disrupted by numerous sediment and spar-filled burrows. In rare instances, micritic microclots within grumous microstructures form an irregular linear network which resembles filamentous microstructures (Plate 77-D). These latter structures are probably equivalent to the *Girvanella* forms recorded by Lohmann* (1977), but definitive tubular forms do not occur within the samples collected from this unit. The dark thrombolitic crusts at the margins of the columns consist of *Epiphyton* boundstone (Plate 77-E,F). *Epiphyton* predominantly forms outward to pendant growths which locally roof cavities filled with burrowed lime-mudstone and cement (Plate 78-A,B). Individual dendritic "thalli" are surrounded by turbid microcrystalline cement, and with progressive neomorphism, they intergrade with diffuse grumous microstructures. On the basis of the samples

---

* Although Lohmann (1977, p. 125) states that the stromatolitic laminae [stromatoids] "consist of poorly preserved *Girvanella* boundstones interleaved with mildly burrowed spiculitic mudstones", he notes (p. 128) that "skeletal evidence of the algae that formed the stromatolite is lacking except for the scattered occurrence of [poorly preserved] *Girvanella* tubules".

collected for analysis, this unit is classified an *Epiphyton*-encrusted stromatolite.

Unit 3: *Epiphyton-Renalcis* thrombolite. This unit forms a black knobbly crust, 5-15 cm thick, on individual stromatolite columns at the top of the complex (Plate 78-C). It appears to be an upward continuation of the *Epiphyton* rims on the lateral margins of the columns. It consists of outward to pendant *Epiphyton* colonies and turbid microcrystalline cement, encased within poor to moderately sorted peloid grainstone and packstone (Plate 78-D). With increasing neomorphism, *Epiphyton* intergrades with diffuse grumous and massive microcrystalline microstructures. An unusual feature of this lithotype is the association of *Epiphyton* and sand-sized detritus, including peloids and intraclasts that are not obviously derived from the breakdown of the *Epiphyton* colonies, and minor trilobite debris. *Renalcis* was also recorded in this unit by Lohmann (1977), but does not occur in the sample analysed in this study which is classified an *Epiphyton* boundstone.

Candland Shale Member

The Candland Shale Member of the Orr Formation is composed of fissile shale, thin platy limestone rich in phosphatic brachiopods and trilobite debris, and minor microbial boundstone, flat-pebble conglomerate and oolitic limestone (Hintze and Palmer, 1976; Koepnick and Brady, 1974; Koepnick,

1976). These sediments accumulated below wave base on an open shelf that lay seaward of the carbonate platform (represented by the overlying Johns Wash Limestone Member). Allodapic sediments (flat-pebbles and ooids) were periodically transported from the carbonate platform to the deeper water shelf. On the crest of Orr Ridge, several thrombolitic horizons are well exposed; two were sampled for micro-structural analysis (Horizons 3 and 4 in Fig. 5-8).

Horizon 3: lower Candland Shale

This horizon forms a laterally continuous 25 cm thick biostrome. It consists of dark lobate to arborescent thromboids which have a lobate grading to grumous micro-structure, and inter-framework packstone and grainstone exceptionally rich in trilobite, pelmatozoan and brachiopod debris, and scattered sponge spicules (Plate 79-A). Lobate microstructures are either saccate or massive cryptocrystalline, and range from 150 to 600 μm in diameter (Plate 79-B,C).

Horizon 4: upper Candland Shale

This horizon consists of domed 60 cm thick bioherms which have irregular intertonguing margins with parted argillaceous lime-mudstone, and a knobbly surface overlain by skeletal packstone and wackestone. The bioherms comprise an open framework of arcuate, concave downward, micritic sheets and pendant *Epiphyton*, and subequant volumes of inter-framework lime-mudstone (micrite or microspar) and turbid marine cement

(Plate 80-A). The arcuate micritic sheets are 20-80 μm thick, locally bifurcate, range from prone to steeply inclined, and are spaced one to several millimetres apart. Their concave surfaces are encrusted by botryoidal masses of turbid, locally fibrous, marine cement, and poorly defined pendant *Epiphyton* colonies (Plate 80-B,D). Their upper surfaces are either encrusted by sub-isopachous, fibrous marine cement, or are directly overlain by lime-mudstone. Although the micritic sheets appear to consist of homogeneous micrite when viewed in cross-section, horizontal sections clearly indicate that they comprise a network of tiny prostrate filaments variously encrusted by micrite (Plate 80-C). The filaments are about 10 μm wide, and micrite-encrusted filaments locally have a poorly defined tubular form that resembles *Girvanella*. Similar arcuate *Girvanella*-like sheets were briefly described within a Candland Shale bioherm by James (1981, p.809). Skeletal metazoan debris is absent.

This horizon is classified a filamentous (*Girvanella*) *Epiphyton* boundstone. It has a very similar composition and fabric to the blocks of *Girvanella-Epiphyton* boundstone derived from the Cambrian platform-margins in western Newfoundland (James, 1981) and southwest Virginia (Pfeil and Read, 1980; Read and Pfeil, 1983).

5.4.3 PLATFORM-MARGIN VERSUS PLATFORM-INTERIOR BUILDUPS

The platform-margin buildups examined within the Wheeler and Orr Formations differ from the platform-interior buildups of western Newfoundland, southern Canadian Rocky Mountains and southern Appalachians in that 1) they are dominated by *Renalcis**Epiphyton**Girvanella* boundstones, and 2) thrombolites and stromatolites *senso stricto* are subordinate. Although *Renalcis* and *Girvanella* are locally common in platform-interior thrombolite\stromatolite buildups, they are generally subordinate to more cryptic microstructures that do not lend themselves to Linnaean classification. *Epiphyton*, apart from one exception discussed below, does not occur in platform-interior thrombolite\ stromatolite buildups.

The localization of calcified "microfossil" boundstones to platform-margin settings is now well established from many areas (Lohmann, 1976; McIlreath, 1977; James, 1981; Pfeil and Read, 1980; Kepper, 1981; Read and Pfeil, 1983; Demicco, 1985; Coniglio and James, 1985), whereas the co-occurrence of thrombolites or stromatolites *senso stricto* and "microfossil" boundstones at platform margins appears to be less common. Based on a study of the fabric and microstructure of allochthonous microbial blocks within the Lower-Middle Cambrian Shady Dolomite, Virginian Appalachians, Read and Pfeil (1983) demonstrated that the platform margin from which these blocks were derived consisted of a variety of microbial lithologies, namely (in decreasing order of abundance):

1) "microfossil" boundstone, including *Girvanella, Epiphyton, Epiphyton-Girvanella*, and *Renalcis* boundstones, 2) thrombolites, and 3) stromatolites. This variety of microbial lithologies is similar to that preserved *in situ* at the platform margin in western Utah (Wheeler and Orr Formations), but is in sharp contrast with other North American Cambro-Ordovician platform-margin buildups which are solely comprised of "microfossil" boundstone.

The unique co-occurrence of *in situ* platform-margin "microfossil" boundstones, thrombolites and stromatolites in the Great Basin (Wheeler and Orr Formations), provides an ideal opportunity to assess differences between "microfossil" boundstones and thrombolites\stromatolites. The most obvious difference of course, is that they comprise a framework of *Epiphyton, Girvanella* and\or *Renalcis*, rather than thromboids or stromatoids whose origin is frequently more obscure. Several other distinguishing features, which are common to all Cambro-Ordovician calcified "microfossil" boundstones, are evident:

1. Marine cement is ubiquitous, and is commonly the most volumetrically dominant component.
2. Inter-framework sediment consists of lime-mudstone or silt-sized peloids, both of which are probably of autochthonous origin, either *in situ* precipitates or disintegrated calcified "microfossils".
3. Allochthonous inter-framework detritus (terrigenous silt, ooids, intraclasts and abraded metazoan debris) is absent or scarce.

4. Frame-building metazoans are absent.

5. The framework shows little or no evidence of bioturbation or breakage, although inter-framework and cavity-filling sediments are commonly bioturbated.

6. *Epiphyton* is restricted to "microfossil" boundstones. The only known exception to this rule is the "algal sheets and laminated heads" (stromatolites of this study) in the Point Peak and San Sabla Members of the Wilburns Formation in central Texas described by Ahr (1971, Fig. 4d, Table 1). Ahr does not specifically discuss this occurrence apart from noting (p. 210) that "*Epiphyton* (Fig. 4d) was not found in stromatolites, and was not common in other structures", his other structures being "algal bioherms" and "algal reefs" (thrombolites and stromatolites of this study). Microbial buildups in the underlying Morgan Creek Limestone Member of the Wilberns Formation are more usual in that they contain *Renalcis, Girvanella* and *Nuia*, whereas *Epiphyton* is not present (Chafetz, 1973).

7. Distinct tubular *Girvanella* forms are rarely evident, and are subordinate to indistinct micritic threads which form arcuate sheets. Although these structures can frequently be confidently interpreted as calcified filaments and show certain affinity to *Girvanella*, their calcification was evidently more variable and less selective than that which gave rise to the well defined twisted tubular *Girvanella* forms typical of platform-interior settings. Whereas selective micritic impregnation

and\or encrustation of filamentous sheaths generates tubular forms (Riding, 1975, 1977b; Danielli, 1981), non-selective impregnation and encrustation of trichomes and\or sheaths would probably generate more irregular thread and sheet-like forms such as those observed in the Wheeler and Orr Formation buildups, and as described from other platform-margin boundstones by Pfeil and Read (1980) and James (1981). This different style of calcification could reflect either micro-chemical or biological differences between platform-margin and platform-interior filamentous communities.

These observations suggest that calcified "microfossil" boundstones formed in submerged, probably relatively high energy, environments characterized by rapid marine cementation and little or no external sediment influx. Such conditions typify platform-margin settings where rapid marine cementation strengthens the otherwise seemingly delicate framework of calcified "microfossils", and rapid local upbuilding and\or sediment bypassing precludes an influx of carbonate and terrigenous detritus from the adjacent platform.

In contrast, thrombolites *senso stricto* generally formed in subtidal (either high or low energy) platform interior environments, and stromatolites predominated in shallow peritidal environments. If the platform forms an homoclinal "ramp" (Ahr, 1973) and lacks a distinct, high relief rim

("rimmed shelf"; Read, 1985), then stromatolites and thrombolites may persist to the margin of the carbonate platform, and co-occur with calcified "microfossil" boundstones. This latter situation appears to have been the case for the mixed stromatolite - thrombolite - "microfossil" boundstone assemblage within the House Embayment in Utah.

5.5 AMADEUS BASIN, CENTRAL AUSTRALIA

Thrombolites and stromatolites are widespread within the Middle to Late Cambrian Shannon Formation in the Amadeus Basin, central Australia (Kennard and others, 1986). In contrast to the thrombolites and stromatolites within the Cambro-Ordovician platformal carbonates of North America, microbial buildups within the Shannon Formation (and throughout the late Proterozoic and early Palaeozoic strata of the Amadeus Basin) were deposited in an extensive intracratonic epeiric sea well removed from the ancient Australian continental margin.

5.5.1 REGIONAL AND SEDIMENTOLOGICAL SETTING

The Amadeus Basin, the remnant of a broad intracratonic depression now 800 km long and 500 km wide, contains a thick succession, up to 14 km, of shallow marine and terrestrial deposits of Late Proterozoic and early Palaeozoic age (Wells and others, 1970; Kennard and others, 1986). During Middle-Late Cambrian time, sedimentation was characterized by a west to east transition from 1) coarse fluvial and deltaic siliciclastic facies, to 2) mixed fluvial and shallow marine siliciclastic facies, 3) shallow marine fine siliciclastic and minor carbonate facies, and 4) mixed shallow marine carbonate and fine siliciclastic facies (Fig. 5-10). This eastern carbonate-siliciclastic sequence, represented in part by the late Middle to Late Cambrian Shannon Formation and

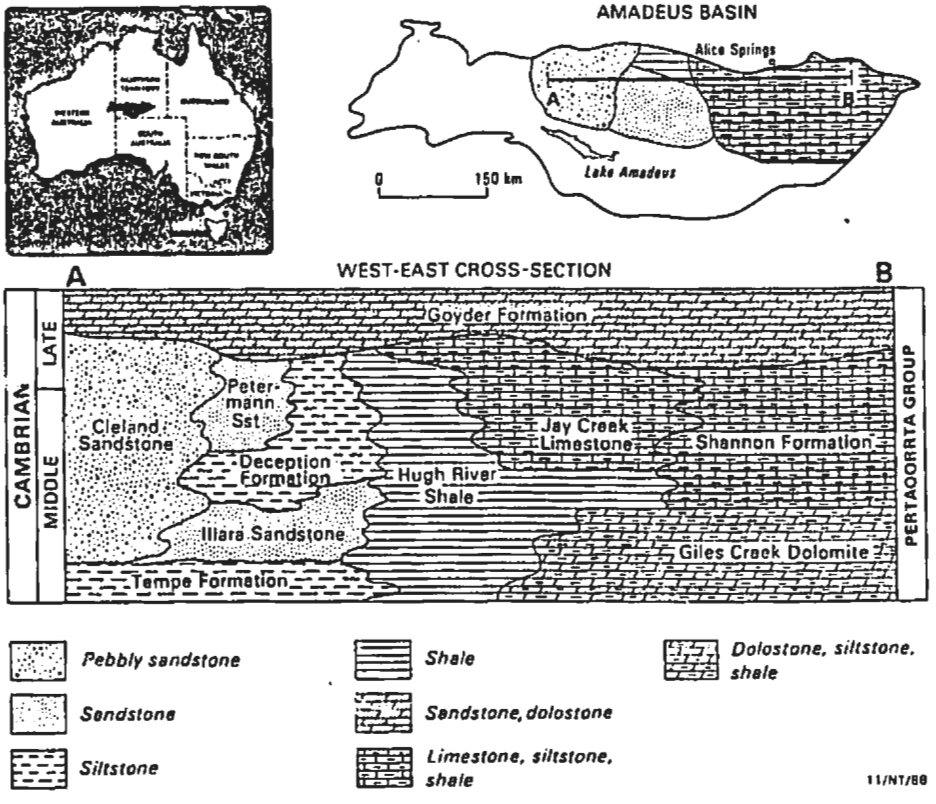

Figure 5-10. Location, distribution and relationship of late Middle to Late Cambrian facies in the Amadeus Basin, central Australia. Modified after Kennard and others (1986), and Wells and others (1970).

equivalent Jay Creek Limestone, contains the thrombolites and stromatolites analysed in this section.

The Shannon Formation is characterized by the alternation of recessive siliciclastic mudrocks and thin carbonate cycles of great lateral continuity. Individual carbonate cycles can be traced in outcrop for tens of kilometres, and some can be correlated over distances of up to 120 km. The formation is subdivided into two units: a lower mudrock-rich unit, and an upper carbonate-rich unit (Fig. 5-11). Within both units, carbonate cycles are abruptly overlain by siliciclastic mudrocks, whereas their basal contact may be either sharp and erosional or gradational over several decimetres.

Carbonate cycles in the lower unit invariably comprise dolostone, are typically 0.2 - 2 m thick, and are dominated by stromatolites of low synoptic relief. They commonly exhibit the following shallowing-upward sequence (Fig. 5-12A, Plate 81-A):

1. Fine-coarse peloid or ooid grainstone, commonly wave-rippled with lenticular and wavy dolo-mudstone drapes.
2. Linked hemispherical and wavy-laminated stromatolite biostromes.
3. Undulose or planar-laminated stromatolite biostromes, and less frequently,
4. Thinly interbedded dolo-mudstone, peloid grainstone and flake conglomerate.

Silicified evaporite pseudomorphs, including cubic, pagoda and reticulate ridge halite (terminology of Southgate, 1982), ?halite ooids and cauliflower chert nodules after gypsum

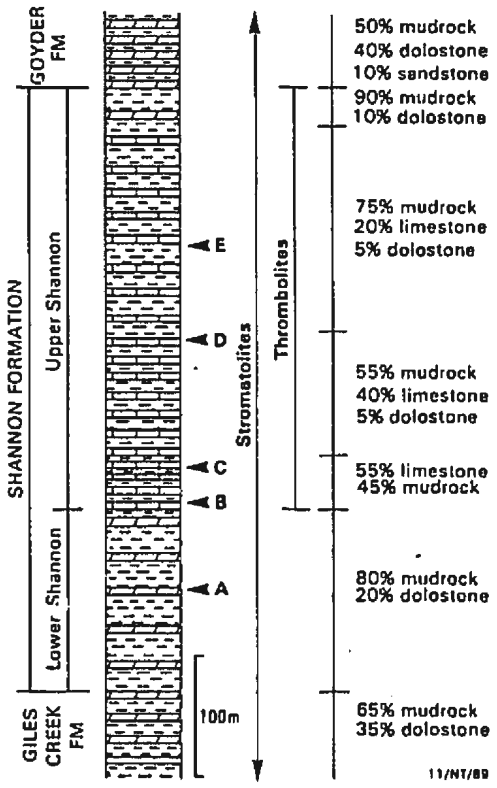

Figure 5-11. Generalized lithological section of the Shannon Formation in the northeast Amadeus Basin (locality B in Fig. 5-10). Carbonate cycles A to E are shown in Fig. 5-12.

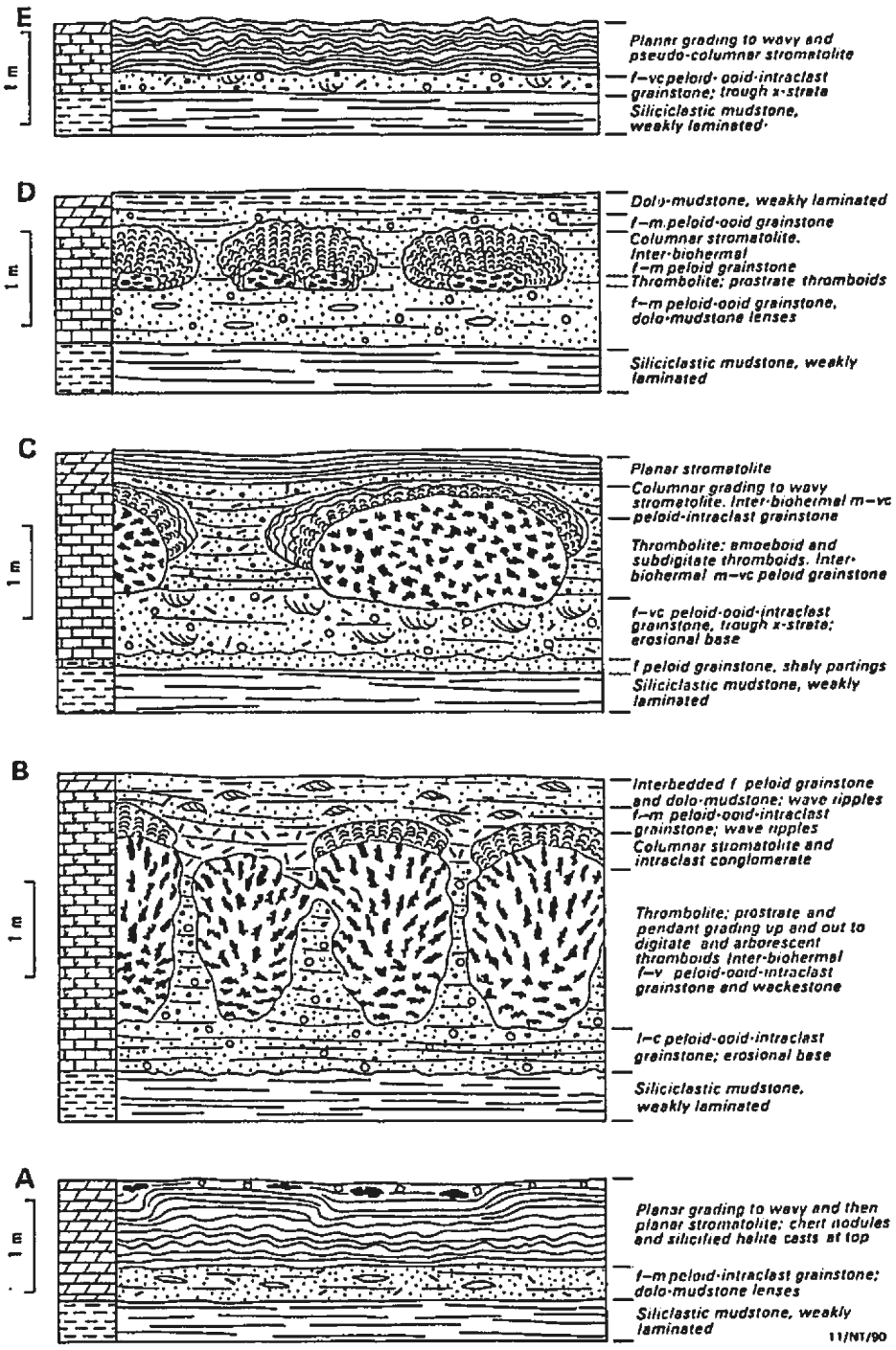

Figure 5-12. Lithological sections of representative stromatolitic and thrombolitic carbonate cycles in the Shannon Formation. **A** Lower unit. **B-E** Upper unit.

commonly occur at the top of these cycles (Plate 81-B). Thrombolites are not present in this lower mudrock-rich unit.

Carbonate cycles in the upper unit consist of limestone and subordinate dolostone, are typically 1-3 m thick, and are characterized by thrombolites of high synoptic relief and stromatolites of moderate to low synoptic relief. They commonly exhibit the following shallowing-upward sequence (Fig. 5-12B,C,D,E, Plate 82-A,B,C):

1. Fine to very coarse grained, locally trough cross-stratified, peloid-ooid-intraclast grainstone, which forms a foundation for;
2. Large thrombolite bioherms, or alternatively;
2A. Small thrombolite bioherms and poorly defined thrombolitic masses enclosed within ribboned and nodular bedded, peloid-bioclast packstone and wackestone.
3. Inter-biohermal fine to very coarse grained, peloid-intraclast grainstone with abundant thrombolite fragments.
4. Columnar grading upward to wavy-laminated stromatolites which cap the thrombolite bioherms, and which are flanked by;
5. Intraclast conglomerate.
6. Fine to medium grained peloid-ooid grainstone with symmetrical wave ripples.
7. Undulose or planar-laminated stromatolite biostromes and dolo-mudstone with desiccation cracks.

These cycles are frequently incomplete, however, such that any of the above lithotypes may be abruptly overlain by siliciclastic mudrock or, less frequently, truncated by a karst erosion surface. Composite deepening-shallowing cycles

are also rarely present. They overlie karst eroded dolomudstone or grainstone, the erosional protuberances of which are encrusted by a thin stromatolite layer which rapidly passes upward into thrombolite (Plate 81-D). This initial, deepening, karst-stromatolite-thrombolite sequence is then succeeded by a shallowing thrombolite-stromatolite sequence as described above.

There is a progressive upward trend within the upper carbonate-rich unit to thinner carbonate cycles, a decrease in the relative proportion of thrombolites to stromatolites, a decrease in the synoptic relief of both thrombolites and stromatolites, and an increase in the proportion of dolostone, ooid grainstone and quartz sand.

Each carbonate cycle corresponds to a period of reduced or nil siliciclastic influx, and is abruptly terminated either by the renewed influx of siliciclastic mud, or less commonly, subaerial exposure and karst erosion.

5.5.2 DESCRIPTION OF THROMBOLITES AND STROMATOLITES

Throughout the Shannon Formation and equivalent Jay Creek Limestone, several distinct types of thrombolites and stromatolites re-occur at different horizons, each type characterized by a specific mesostructure and microstructure, and displaying relatively minor megastructural variation. This uniformity from horizon to horizon contrasts with the marked mesostructural and microstructural variation observed between successive thrombolite and stromatolite horizons

within the Cambro-Ordovician platformal strata of North America. For this reason, microbial buildups in the Shannon Formation are not described on an horizon-by-horizon basis, but rather each re-occurring type is described separately. Two types of thrombolites (designated Type 1 and 2) and five types of stromatolites (columnar, hemispherical, wavy, planar and undulose) are recognized, together with undifferentiated cryptomicrobial boundstones. A summary analysis of each type is given in Table 5-1.

Type 1 Thrombolites

This is the predominant type of thrombolite and forms relatively large club, spherical or ellipsoidal bioherms (Plate 82-A,B) up to 2 m thick, 4 m long, and with 50-100 cm synoptic relief. They comprise a framework of prostrate, amoeboid, digitate or arborescent thromboids, inter-framework bioturbated peloid-ooid-intraclast grainstone and packstone, and in many instances, small spar-filled shelter cavities. Thromboids range from several millimetres to 2 cm in size, and commonly exhibit an upward transition from prostrate and pendant forms at the base of the bioherms (Plate 83-B), to digitate and arborescent forms at the crest and margins of the bioherms (Plate 83-C). They have a variegated massive microcrystalline to weakly spherulitic lobate, saccate lobate, and massive cryptocrystalline microstructure (Plates 84, 85). Massive microstructures occur between individual lobate bodies, are volumetrically minor, and locally contain terrigenous silt. The margins of the thromboids are

	MEGASTRUCTURE	MESOSTRUCTURE	MICROSTRUCTURE
THROMBOLITES			
TYPE 1	club, spherical & ellipsoidal bioherms	prostrate, amoeboid, digitate & arborescent thromboids; spar-filled shelter cavities; inter-framework peloid ooid-skeletal grainstone & packstone	variegated lobate & massive; saccate & diffuse spherulitic lobes
TYPE 2	irregular masses & small bioherms	larger lobate, saccate & amoeboid thromboids; spar-filled burrows; inter-framework silty peloid-skeletal wackestone	as for Type 1
STROMATOLITES			
COLUMNAR	discoidal & domed bioherms	bumpy tuberous columns; inter-colum intraclast-peloid grainstone	vermiform or alter-alternating vermiform & massive; locally grumous
HEMISPHERICAL	domed bioherms & biostromes	hemispherical stromatoids	banded micro- & crypto-crystalline
WAVY	domed & tabular biostromes	wavy sinusoidal stromatoids	banded micro- & crypto-crystalline
PLANAR	tabular biostromes	planar stromatoids	banded micro- & crypto-crystalline
UNDULOSE	tabular biostromes	undulose stromatoids; evaporite pseudomorphs	irregular streaky microcrystalline
CRYPTOMICROBIAL BOUNDSTONES			
	discoidal & domed bioherms, domed biostromes	irregularly mottled, vaguely clotted & crudely laminated fabrics	massive & mottled local diffuse vermiform, grumous & lobate

TABLE 5-1. Summary of the Mega-, Meso- and Micro-structure of thrombolites, stromatolites and cryptomicrobial boundstones in the Shannon Formation, Amadeus Basin, central Australia.

locally ragged and embayed, probably a consequence of bio-erosion. Minor trilobite, mollusc and pelmatozoan fragments occur within the inter-framework sediment.

These thrombolites were constructed by colonies of coccoid microbes. Depending on the relative extents of calcification, degradation and bacterial precipitation, the colonies were variously preserved as microcrystalline lobate, saccate lobate or spherulitic lobate bodies. Massive cryptocrystalline microstructures between these lobate bodies probably represent detritus that accumulated between, and was then subsequently overgrown by, successive coccoid colonies. The only indication of former filamentous microbes within the thrombolites is a single observation of tufted, *Girvanella*-like tubules and filaments within a thrombolite fragment incorporated in inter-biohermal grainstone (Plate 85-D). Detrital peloids were clearly trapped and bound between the individual filaments of this tuft, whereas the ubiquitous calcified coccoid colonies within the thrombolites evidently had little or no ability to trap and bind detrital particles other than minor amounts of lime-mud and terrigenous silt.

Type 2 Thrombolites

These thrombolites form irregular centimetre-sized masses and poorly defined bioherms of low synoptic relief that are enclosed within ribboned and nodular bedded packstone and wackestone. They comprise relatively large lobate, saccate and amoeboid thromboids (typically 4-10 cm in size), and inter-framework, bioturbated, silty skeletal-peloid

wackestone (Plate 83-E). They have a similar microstructure to Type 1 thrombolites except that, 1) lobate microstructures are less distinct, especially spherulitic microstructures, 2) individual lobes are slightly smaller and more densely clustered, and 3) metazoan fragments and burrows are more abundant (Plate 85-C).

Columnar Stromatolites

These forms were described in detail by Walter (1972) who classified them as *Madiganites mawsoni*. They form domed biostromes and domed and discoidal bioherms 15-40 cm thick, and commonly cap Type 1 thrombolite bioherms. They comprise small tuberous columns 5-30 mm wide and up to several centimetres high (Plate 86-A). The columns are characterized by bumpy margins, sub-parallel to slightly divergent branching, a discontinuous selvage, infrequent lateral linkage, vertical impersistence and coalescence. They are radially disposed within bioherms, and generally erect within biostromes. The stromatoids have an irregular, commonly asymmetrical, gently convex to rectangular shape, a low degree of inheritance, and are 300-3000 μm thick. They have a streaky, random reticulate to prostrate vermiform microstructure (Plate 87); Gürich (1906) refers to comparable microstructures as *Spongiostroma maeandrinum*. Vermiform laminae are either successively stacked or episodically alternate with massive cryptocrystalline and microcrystalline laminae of comparable thickness (Plate 87-B). Minor quartz silt commonly occurs within these massive laminae, and both

types of laminae are locally disrupted by metazoan burrows. With slight neomorphism, this vermiform microstructure intergrades with grumous microstructure (Plate 87-D). Inter-column sediment consists of peloidal and intraclastic grainstone and layers of carbonate mudstone.

The vermiform columns were constructed by filamentous microbial mats in which micritic sediment was trapped and\or precipitated. Alternating massive laminae probably represent layers of carbonate mud that periodically blanketed these filamentous mats.

These columnar stromatolites are megastructurally, mesostructurally and microstructurally indistinguishable from the columnar stromatolites in the Late Cambrian (Trempealeauan) Berry Head Formation at Isthmus Bay, Port au Port Peninsula, western Newfoundland (Horizon K, Chapter 4).

Hemispherical Stromatolites

Hemispherical stromatolites form laterally linked biostromes and isolated domed bioherms, are commonly oblate to flat-topped, and are 10-50 cm thick (Plate 86-C). They commonly alternate with or are linked by wavy stromatolites. The stromatoids have a smooth to irregular shape, and a moderate degree of inheritance. They have a well defined banded microstructure comprised of either alternating micro-crystalline and cryptocrystalline laminae, or less commonly, successively stacked microcrystalline laminae. Micro-crystalline laminae have an equigranular xenotopic texture, are 300-2000 μm thick, show marked crestal thickening

(commonly an order of magnitude), locally pinch out laterally, and frequently contain minor quartz silt and silt-sized peloids. Cryptocrystalline laminae are generally uniformly thin (10-100 μm thick) and continuous.

The precise origin of these banded microstructures is uncertain; microcrystalline laminae probably represent layers of trapped (neomorphosed) carbonate mud, together with minor peloids and quartz silt, and cryptocrystalline laminae may be calcified organic-rich layers. Although the composition of the formative microbial community (filamentous or coccoid) cannot be determined, such uniformly laminated fabrics are typically constructed by filamentous rather than coccoid-dominated communities (Gebelein, 1974; Semikhatov and others, 1979; Awramik, 1984).

Wavy Stromatolites

Wavy stromatolites have a wavy, pseudo-columnar shape reminiscent of an egg-carton (Plate 86-D). They form tabular biostromes, and commonly cap columnar and hemispherical forms, or alternate with undulose forms. The stromatoids have a smooth sinusoidal shape, a wavelength of 5-10 cm and amplitude of 2-3 cm, and high degree of inheritance. They have a banded microstructure indistinguishable from that of hemispherical stromatolites, and were similarly probably constructed by filamentous mats.

Planar Stromatolites

Planar stromatolites comprise smooth stromatoids of

negligible relief, high degree of inheritance, and considerable lateral continuity (Plate 86-E). They form tabular biostromes, and commonly alternate with wavy and undulose forms. They have a banded microstructure (Plate 88-A) indistinguishable from that of hemispherical and wavy forms, and were similarly probably constructed by filamentous mats.

Undulose Stromatolites

These forms comprise irregular undulose stromatoids of low relief (typically less than 1 cm), low degree of inheritance, and limited lateral continuity. They form tabular biostromes, and either cap or alternate with wavy and planar forms (Plate 86-E), or cap Type 1 thrombolites. They are commonly fenestral, and are variously disrupted by chert nodules, silicified evaporite pseudomorphs and desiccation cracks. The laminae have a pustular to mamillate shape, are 200-3000 μm thick, and are generally discontinuous. They have an irregular streaky microstructure comprised of poorly defined inequigranular (10-100 μm crystal size), hypidiotopic, laminae (Plate 88-B).

Although definitive evidence is lacking, these irregular streaky microstructures were probably constructed by calcified coccoid communities. This interpretation is consistent with the observation that modern pustular and mamillate mats are dominated by coccoid rather than filamentous microbes (Hofmann, 1973; Gebelein, 1974; Golubic,

1983; Awramik, 1984; Pentecost and Riding, 1986), and the absence of detrital particles (quartz silt and peloids).

Cryptomicrobial boundstones

Some of the bioherms in the upper carbonate-rich unit have an irregular mottled, vaguely clotted, or crudely laminated fabric in which distinct mesoscopic constituents (thromboids, stromatoids and inter-framework sediment) cannot be differentiated. They generally comprise irregular to digitate patches of mottled or crudely laminated microcrystalline and cryptocrystalline carbonate, locally with poorly preserved vermiform grading to grumous and lobate microstructures, and patches of silty peloid-skeletal grainstone, packstone and wackestone (Plate 88-C). They are commonly extensively bioturbated (Plate 88-D), and contain much metazoan debris (molluscs, pelmatozoans, brachiopods, and trilobites). These boundstones were evidently constructed by a relatively complex filamentous and coccoid microbial community, the precise composition and structure of which has been largely obscured by extensive bioturbation, degradation and neomorphism.

5.5.3 INTERPRETATION

The sequences of stromatolites and thrombolites observed within the carbonate cycles are interpreted as ecologic successions of distinct microbial communities in response to shoaling sedimentation. Each thrombolite and stromatolite

type is constructed by a community of specific composition and\or sediment-forming activity, and this community is restricted to a particular depositional environment. The observed relative frequency of transition between the various thrombolite and stromatolite types is shown in Figure 5-13.

Within the lower mudrock-rich unit, the most common sequence is one of decreasing synoptic relief, from 1) hemispherical, to 2) wavy, and 3) undulose stromatolites. The stromatolites were established on wave-rippled and lenticular bedded, peloid or ooid tidal sands and lime mud, and were commonly disrupted by halite and gypsum crystals in the upper part of the sequence. They are interpreted as intertidal microbial mats, and are directly comparable to the sequence of intertidal stratiform mats observed in Hamelin Pool, Shark Bay, Western Australia (Logan and others, 1974; Golubic, 1976a; Hoffman, 1976a); the banded (?filamentous) hemispherical, wavy and planar forms correspond to smooth filamentous (*Schizothrix*) mats in lower intertidal zones, and the streaky (?coccoid) undulose forms correspond to pustular coccoid (*Entophysalis*) mats in middle to upper intertidal zones.

The most common sequence in the upper carbonate-rich unit is also one of decreasing synoptic relief, from 1) Type 1 thrombolites (or undifferentiated cryptomicrobial bioherms), to 2) columnar stromatolites, and locally, 3) wavy and 4) planar and undulose stromatolites. The thrombolites were established on a foundation of peloid-ooid-intraclast

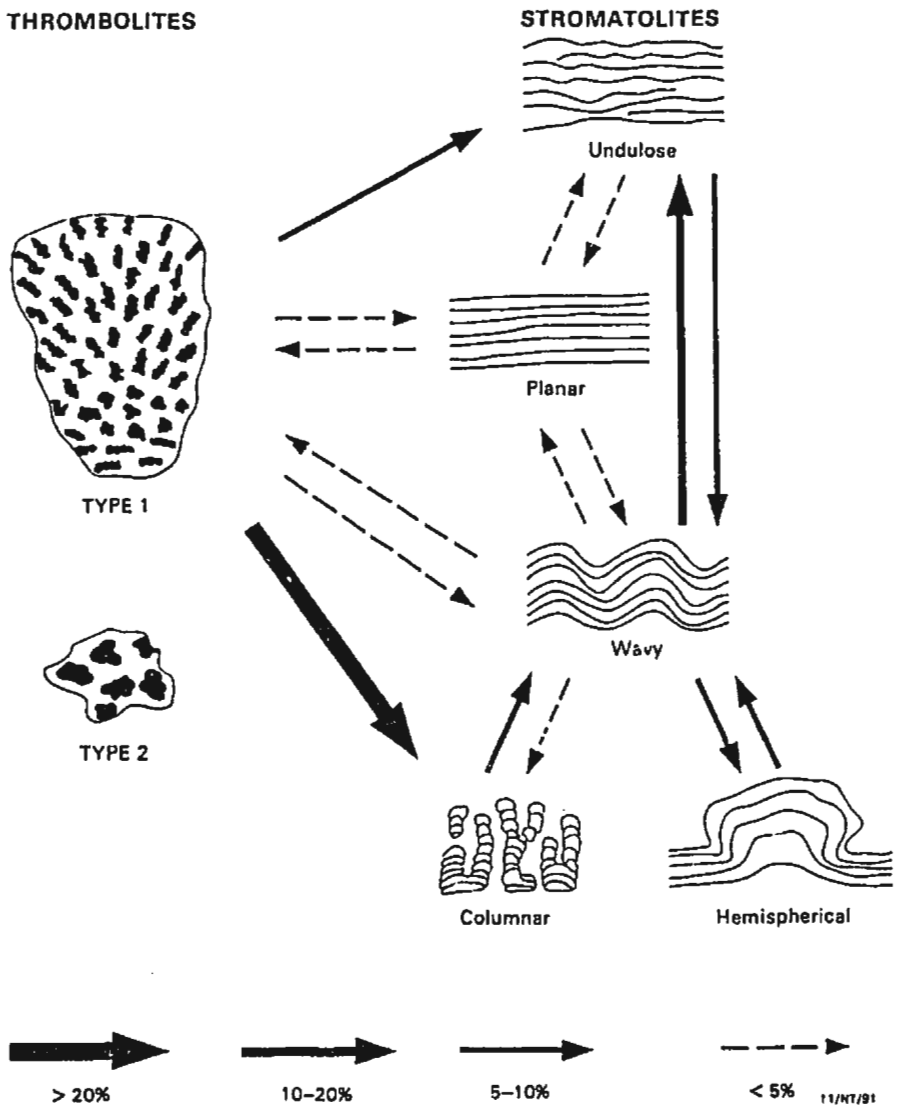

Figure 5-13. Relative frequency of sequence transitions between thrombolite and stromatolite types, Shannon Formation (126 transitions recorded).

subtidal sand, are flanked by peloid-intraclast sand, and pass laterally into ribboned and nodular bedded, peloidal and bioclastic subtidal carbonate mud. The capping columnar stromatolites are flanked by intraclast conglomerate, and are buried by wave-rippled, peloid-ooid intertidal sand and desiccated carbonate mud. The initial coccoid (thrombolite-forming) community grew in a moderately turbulent shallow subtidal environment, probably within a few to several metres of water, and was inhabited by grazing molluscs, scavenging trilobites and other soft-bodied burrowing metazoans. Upward growth and progressive shoaling of the thrombolites culminated in the establishment of column-forming filamentous mats across their crest, probably within very shallow subtidal or lower intertidal environments largely devoid of metazoans. These mats were in turn locally succeeded by banded (?filamentous) wavy and planar intertidal mats.

This succession of microbial communities is broadly comparable to the sequence of subtidal and intertidal communities observed at Flagpole Landing, Carbla Point and Booldah Well in Hamelin Pool, Shark Bay, Western Australia (Playford and Cockbain, 1976; Burne and James, 1986): the thrombolites correspond to subtidal club-shaped stromatolites built by colloform mats (a diverse community dominated by *Microcoleus* filaments, eucaryotic algae, serpulid worms and bivalves), and the capping vermiform (filamentous) columnar forms and banded (?filamentous) wavy and planar forms correspond to smooth filamentous (*Schizothrix*) mats in intertidal environments.

5.5.4 INTRACRATONIC VERSUS CONTINENTAL SHELF BUILDUPS

The thrombolites and stromatolites analysed within the Amadeus Basin clearly fall within the spectrum of structures (mega, meso and micro) observed in western Newfoundland and elsewhere in North America. In contrast to the microbial buildups on the Cambro-Ordovician North American continental shelf, however, they show great mesostructural and microstructural uniformity from horizon to horizon and formation to formation (those in the Shannon Formation are identical to those in the Jay Creek Limestone), and are almost certainly laterally more continuous. This difference implies a greater ecological stability of microbial communities within the extensive Cambro-Ordovician intracratonic sea of the Amadeus Basin. This sea was characterized by uniformly shallow environments across distances of one hundred kilometres or more, elevated or periodically elevated salinities, and a low abundance of metazoans. Microbial communities flourished across vast areas, and following periodic influx of terrigenous muds, essentially identical microbial communities were rapidly re-established. The stability of these communities through space and time is probably due to the high ecologic stress within this intracratonic sea. In contrast the Cambro-Ordovician North American continental shelf comprised a broader spectrum of environments and ecological niches, and was inhabited by a more diverse and abundant metazoan

community. Consequently a myriad of lithofacies developed on the shelf, and slightly different microbial communities constructed a wide spectrum of thrombolites and stromatolites at different times and places on the shelf.

It thus appears that microbial communities have greater ecological stability within intracratonic seas than on continental shelves. As a consequence of this ecologic stability, intracratonic microbial buildups may have a greater potential for biostratigraphic correlation than microbial buildups on continental shelves. Although this potential has yet to be demonstrated for Phanerozoic stromatolites and thrombolites, biostratigraphic correlation of stromatolite forms is now well established for Proterozoic stromatolites (see Walter, 1972; Semikhatov, 1976; Preiss, 1976, 1977; Hofmann, 1987).

5.6 CONCLUSION

This analysis of thrombolites from the Great Northern Peninsula of western Newfoundland, Canadian Rocky Mountains, Appalachian Mountains, Great Basin and central Australia demonstrates that the analytical and classification schemes developed for the thrombolites of the Port au Port Peninsula of western Newfoundland are equally applicable to most, if not all, Cambro-Ordovician thrombolites. Furthermore, with the exception of the platform-margin thrombolites in the Great Basin, the range of microstructures displayed by these examples falls within the spectrum observed on the Port au Port Peninsula.

Whereas platform-interior and intracratonic Cambro-Ordovician microbial buildups are dominated by thrombolites and stromatolites, platform-margin buildups are dominated by *Epiphyton, Renalcis* and\or *Girvanella* "microfossil" boundstones, and thrombolites and stromatolites are either subordinate or absent (Fig. 5-14). Dendritic calcified "microfossils" referable to the genus *Epiphyton* are largely restricted to platform-margin buildups, either as a major framework constituent of calcified "microfossil" boundstones, or a minor cavity-dwelling or encrusting constituent of thrombolites or stromatolites.

Intracratonic microbial buildups apparently display greater mesostructural and microstructural uniformity than

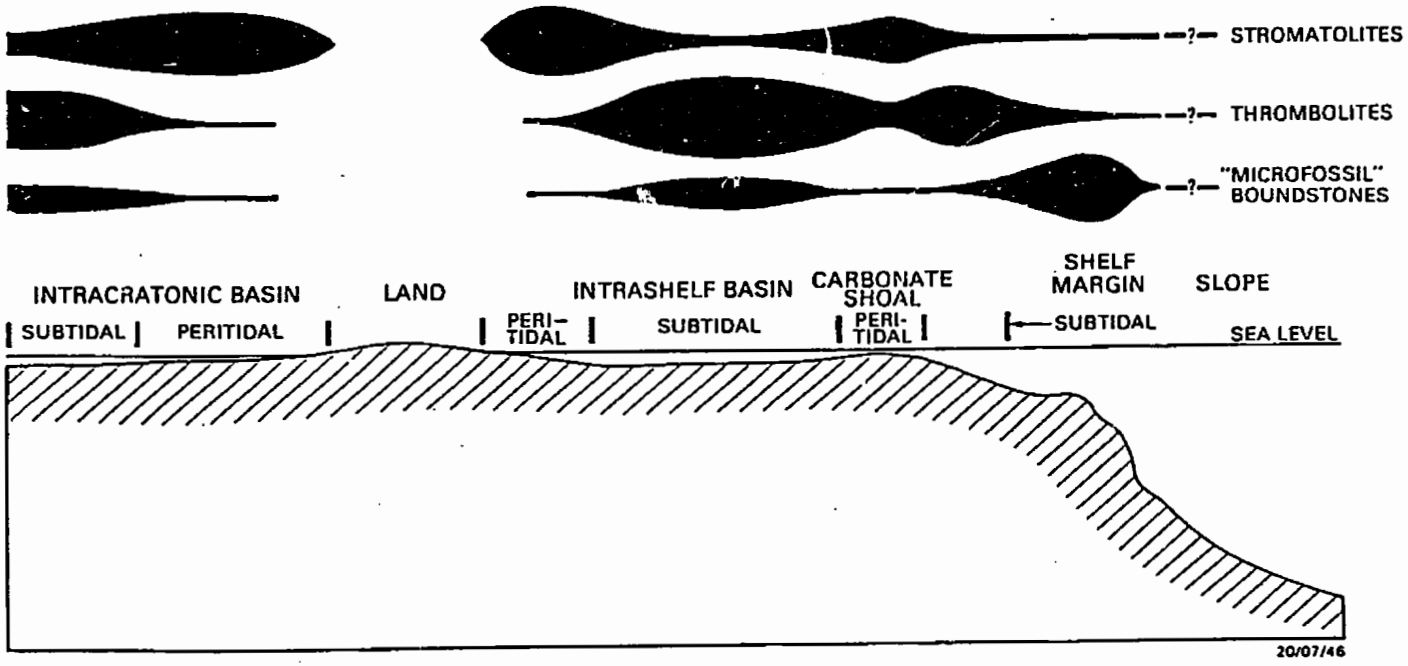

Figure 5-14. Schematic distribution of Cambro-Ordovician microbialites (stromatolites, thrombolites and calcified "microfossil" boundstones) across the continental shelf and an intracratonic basin.

microbial buildups developed on continental shelves. This uniformity is probably a direct response of more uniform environments and higher ecologic stress within intracratonic seas than on continental shelves.

CHAPTER 6

SYNTHESIS AND COMPARATIVE ANALYSIS OF THROMBOLITES AND STROMATOLITES

This chapter presents a synthesis of the thrombolites and stromatolites analysed in Chapters 4 and 5, and summarized in Appendix B. As such, it provides an overview and comparative analysis of the structure and origin of Cambro-Ordovician thrombolites and stromatolites from several geographic areas, and palaeo-geographic and tectono-sedimentary settings. These findings are considered to be equally applicable to most, if not all, Cambro-Ordovician microbial buildups, and not restricted to just those areas from which the samples were analysed. This chapter also examines the relative importance of environmental and biological controls on the megastructure, mesostructure, and microstructure of thrombolites and stromatolites.

This synthesis is based on a total of 152 microbialites; 80 are from the Port au Port Peninsula, western Newfoundland, 8 from the Great Northern Peninsula, western Newfoundland, 7 from the Canadian Rocky Mountains, 3 from the Virginian Appalachians, 19 from the Great Basin, and 35 from central Australia. Thrombolites and stromatolites are equally represented.

6.1 MEGASTRUCTURAL SYNTHESIS

Although thrombolites exhibit a similar spectrum of bed forms to stromatolites, they most commonly have a greater thickness to width ratio than stromatolites (Fig. 6-1). Thus they are predominantly biohermal (75% of analysed thrombolites), and whereas pedestal, club, egg, spherical and ellipsoidal thrombolite bioherms are relatively common (33% of analysed samples), similarly shaped stromatolite bioherms are scarce (13% of analysed samples). Furthermore, since the synoptic relief of bioherms and biostromes is generally closely related to their bed form or megastructure, it follows that thrombolites generally have a greater synoptic relief than stromatolites. A majority of the thrombolites analysed in Chapters 4 and 5 have at least 20-30 cm synoptic relief, several have 60-100 cm relief, and a few exceed 100 cm in relief. In contrast the associated stromatolites predominantly have less than 20 cm synoptic relief, but a few have 50-80 cm relief.

Both thrombolites and stromatolites are commonly established on a foundation layer of pebble conglomerate, or selectively encrust positive topographic features on an eroded substrate. Clearly a firm or stable sediment substrate with minor topographic relief favours the establishment of benthic microbial communities.

Facies associations and ecologic microbial successions indicate that thrombolites are exclusively subtidal, and that co-occurring stromatolites invariably formed in shallower

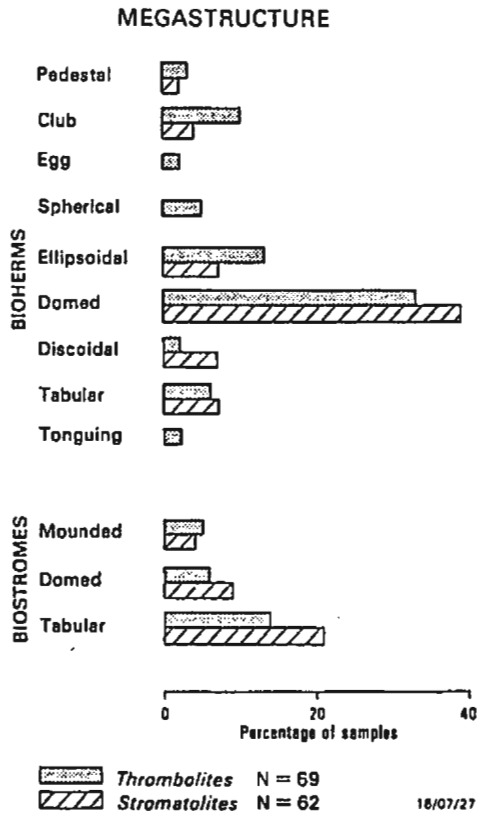

Figure 6-1. Comparative megastructural analysis of thrombolites and stromatolites.

subtidal to intertidal environments. Thus the relative sequential order of thrombolites and stromatolites within a continuous depositional sequence provides diagnostic evidence of shoaling versus deepening sedimentation; a thrombolite capped by or grading up into stromatolite (by far the most commonly observed relationship) indicates shoaling (regressive) conditions, and a stromatolite capped by or grading up into thrombolite indicates deepening (transgressive) conditions.

The precise depth of water in which these thrombolites grew, however, is difficult to quantify. Obviously they grew in water deeper than their synoptic relief; that is, in water at least a few decimetres deep. In some cases they grew below wave base, but more commonly they show evidence of turbulent water conditions and are intimately associated with peritidal facies. Their most likely depth range is probably about 1-10 metres, but deeper water conditions are also possible. For example, Aitken (1978) concluded that thrombolites within the Sullivan Formation in the Southern Canadian Rocky Mountains grew on a foundation of allodapic oolitic sands in at least 12 metres of water (these are the thrombolites described in Section 5.2). Although several occurrences of deep water stromatolites have been reported (Playford and Cockbain, 1969; Playford and others, 1976; Jenkyns, 1970, 1971; Hoffman, 1974; Monty, 1977; Wright and others, 1978; James and Ginsburg, 1979), comparable deep water thrombolites are unknown.

The megastructure of thrombolites and stromatolites is commonly independent of both their mesostructure and microstructure. Thus mesostructurally and microstructurally distinct thrombolites and stromatolites commonly have a similar megastructure (for example, domed bioherms of similar size, shape and synoptic relief), and conversely buildups characterized by a specific mesostructure and microstructure frequently exhibit a range of megastructures either within a single horizon (for example the pedestal, spherical and ellipsoidal thrombolite bioherms in the basal portion of Horizon A, western Newfoundland), or from horizon to horizon (for example the lobate arborescent thrombolites in the Shannon Formation, central Australia, and the vermiform columnar stromatolites in both Horizon K, western Newfoundland, and the Shannon Formation, central Australia).

The megastructure of microbial buildups is probably principally controlled by 1) their depositional environment, and 2) the lateral continuity of the microbial community, which is itself largely controlled by environmental parameters such as the degree of turbulence and erosion, rate of detrital sedimentation, and pre-existing relief of the substrate. However, no simple relationship can been observed between megastructure and any one environmental parameter. For example, similar megastructures occur in shallow and relatively deep environments, high and low energy environments, and within carbonate and shaly facies. It thus appears that thrombolite and stromatolite megastructure reflects the sum of several independent and\or inter-related

environmental parameters, but it is frequently difficult or impossible to assess the relative individual importance of any one parameter from the rock record.

Neither the composition nor the sediment-forming activity of the microbial community appears to exert a direct control on the shape and size of the buildup. For example, calcified coccoid communities may construct large bioherms with considerable synoptic relief, or small bioherms and extensive biostromes with negligible relief.

6.2 MESOSTRUCTURAL SYNTHESIS

The framework composition of all analysed thrombolites and stromatolites is shown in Figure 6-2. The vast majority are composed either solely of thromboids (42% of samples; herein classified "thrombolites") or stromatoids (36% of samples; herein classified "stromatolites"). Only 11% of analysed samples are jointly composed of thromboids and stromatoids (herein classified "stromatolitic thrombolites" or "thrombolitic stromatolites"), and a further 11% are composed of cryptomicrobial fabrics with or without thromboids or stromatoids (herein classified "cryptomicrobial boundstones" or "disrupted thrombolites\stromatolites"). The relative proportion of buildups dominated by cryptomicrobial fabrics, however, is not representative of Cambro-Ordovician microbial buildups in general due to a deliberate sampling bias in this study towards buildups with well preserved and differentiated

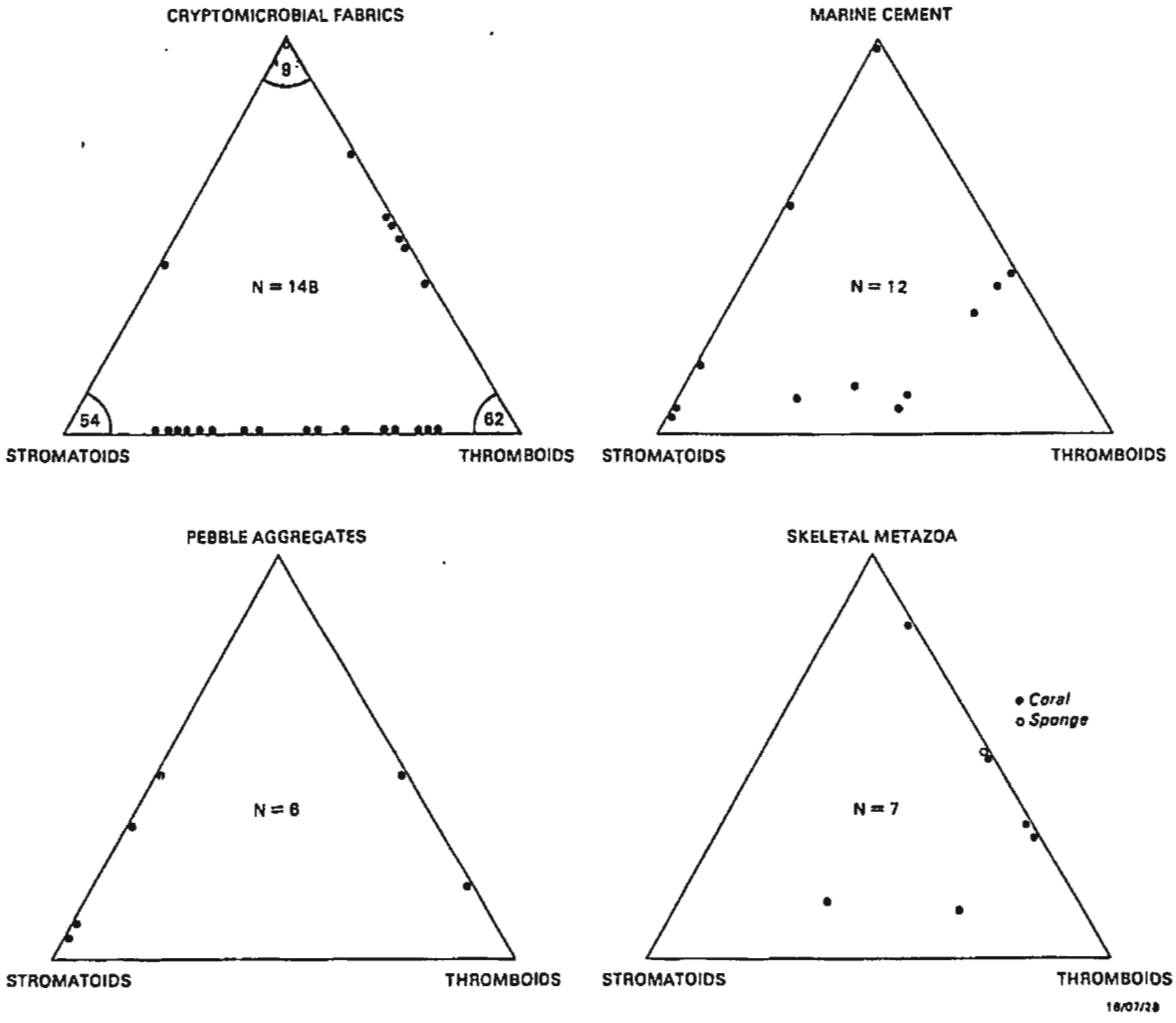

Figure 6-2. Framework composition of analysed thrombolites and stromatolites.

mesostructures. The fact that no analysed sample contains all three types of microbial framework components (thromboids, stromatoids and cryptomicrobial fabrics), supports the earlier interpretation based on microstructural evidence (see Section 2.2.1) that cryptomicrobial fabrics owe their origin to the disruption, modification or replacement of former thromboids or stromatoids, and do not represent a primary, fundamentally distinct, microbial component.

Marine cement, pebble aggregates and skeletal metazoa only locally form significant framework constituents of Cambro-Ordovician microbial buildups (Fig. 6-2).

The mesostructure of thrombolites and stromatolites is apparently controlled by a complex interaction of several biological and environmental factors, the most important being the relative rates and degrees of:

1. Microbial growth, calcification, degradation and sediment-trapping activities.
2. Metazoan bioturbation and bioerosion.
3. Physical turbulence and erosion.
4. Production and accumulation of autochthonous sediment.
5. Influx and accumulation of allochthonous sediment.
6. Subsequent diagenetic modification.

The basic shape and size of thromboids and stromatoids largely reflects the shape and lateral continuity of the formative microbial community. Thus arborescent, lobate and saccate thromboids, for example, reflect the shape of calcified coccoid colonies, which is in turn directly

controlled by the relative rates of growth, degradation and calcification of the colonies. Similarly, planar, wavy and hemispherical stromatoids simply reflect the shape of successively stacked, laterally continuous microbial mats, and columnar stromatoids are constructed by a series of laterally discontinuous, button-like, mats.

To what extent, however, is the shape of the microbial community also influenced by environmental factors? Perhaps the best record of the environmental conditions in which a thrombolite or stromatolite grew is provided by the unbound inter-framework sediment. Thus, in order to evaluate possible biological and environmental interactions in determining the overall shape of thromboid and stromatoid frameworks, relationships between the shape of thromboids and stromatoids, and the amount (volume %) and texture (grainstone, packstone, wackestone, mudstone) of the associated inter-framework sediment were examined (Fig. 6-3). For this purpose, the various categories of thromboids and stromatoids (see Section 2.2.1) were first grouped into three shape classes: 1) vertically elongate forms (digitate and arborescent thromboids; columnar, conical and columnar-layered stromatoids), 2) forms without preferred vertical or horizontal elongation (rounded, lobate, saccate, grape-like and amoeboid thromboids; hemispherical stromatoids), and 3) horizontally elongate forms (prostrate and pendant thromboids; planar, undulose, crenulate, pustular and wavy stromatoids).

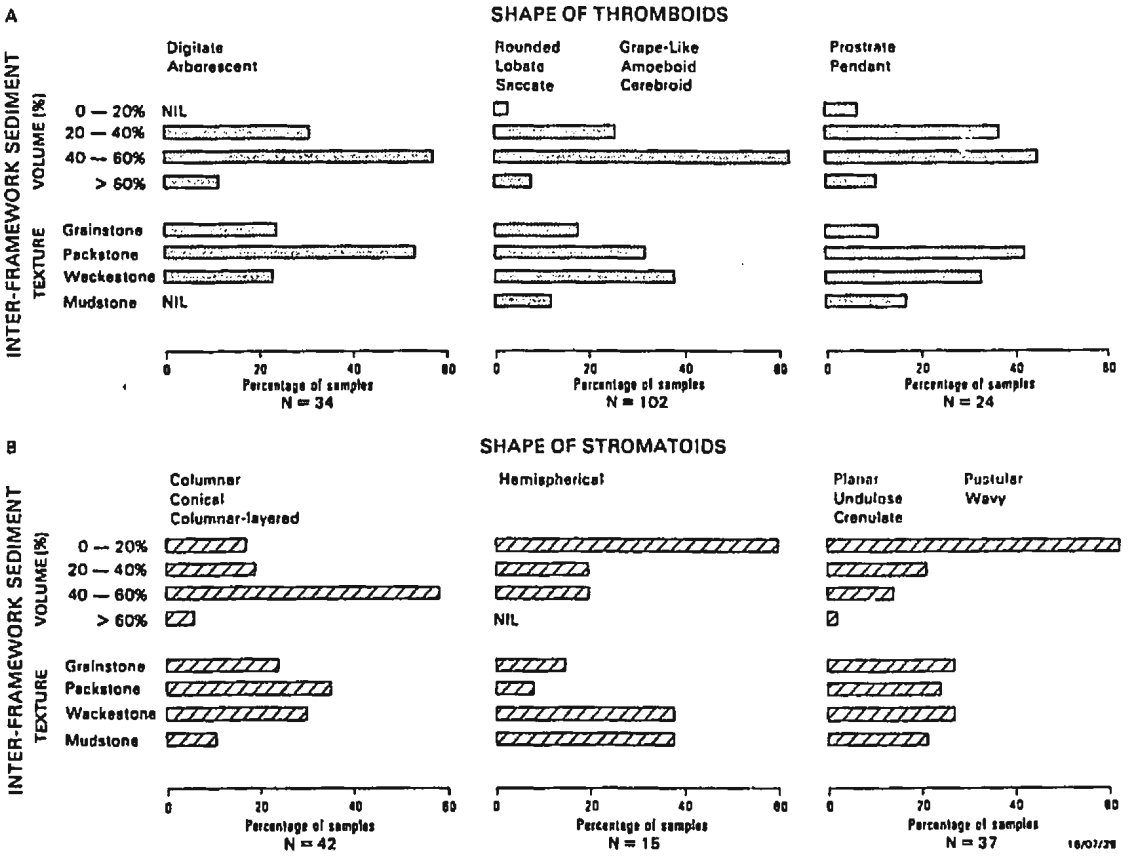

Figure 6-3. Shape of thromboids (A) and stromatoids (B) in relation to the volume percent and texture of the associated inter-framework sediment.

It was intuitively expected that under high rates of detrital sediment influx and accumulation, a microbial framework may develop a preferred vertical elongation in order to keep pace with, and remain above, the level of the accumulating inter-framework sediment, and conversely, that conditions of low or periodic sediment influx and accumulation would favour the development of horizontally elongate frameworks. Such a relationship is evident in Fig. 6-3; vertically elongate thromboids and stromatoids are most commonly associated with a greater volume of unbound inter-framework sediment than frameworks which have a preferred horizontal orientation. Furthermore, the predominance of grain-supported (grainstone and packstone) textures between vertically elongate thromboid frameworks, and the sub-equal occurrence of grain-supported and mud-supported (wackestone and mudstone) textures between horizontally elongate thromboid frameworks, suggests that vertically elongate thromboids commonly form in higher energy environments than horizontally elongate thromboids. A similar textural relationship is less evident, however, for stromatoid frameworks.

Differences are also evident between the inter-framework sediment of thrombolites and stromatolites (Fig. 6-4);

1. Thrombolites generally contain a greater volume of unbound detrital sediment than stromatolites, but there appears to be no significant difference in the texture of this sediment.

2. Metazoan fragments are more abundant in thrombolites.

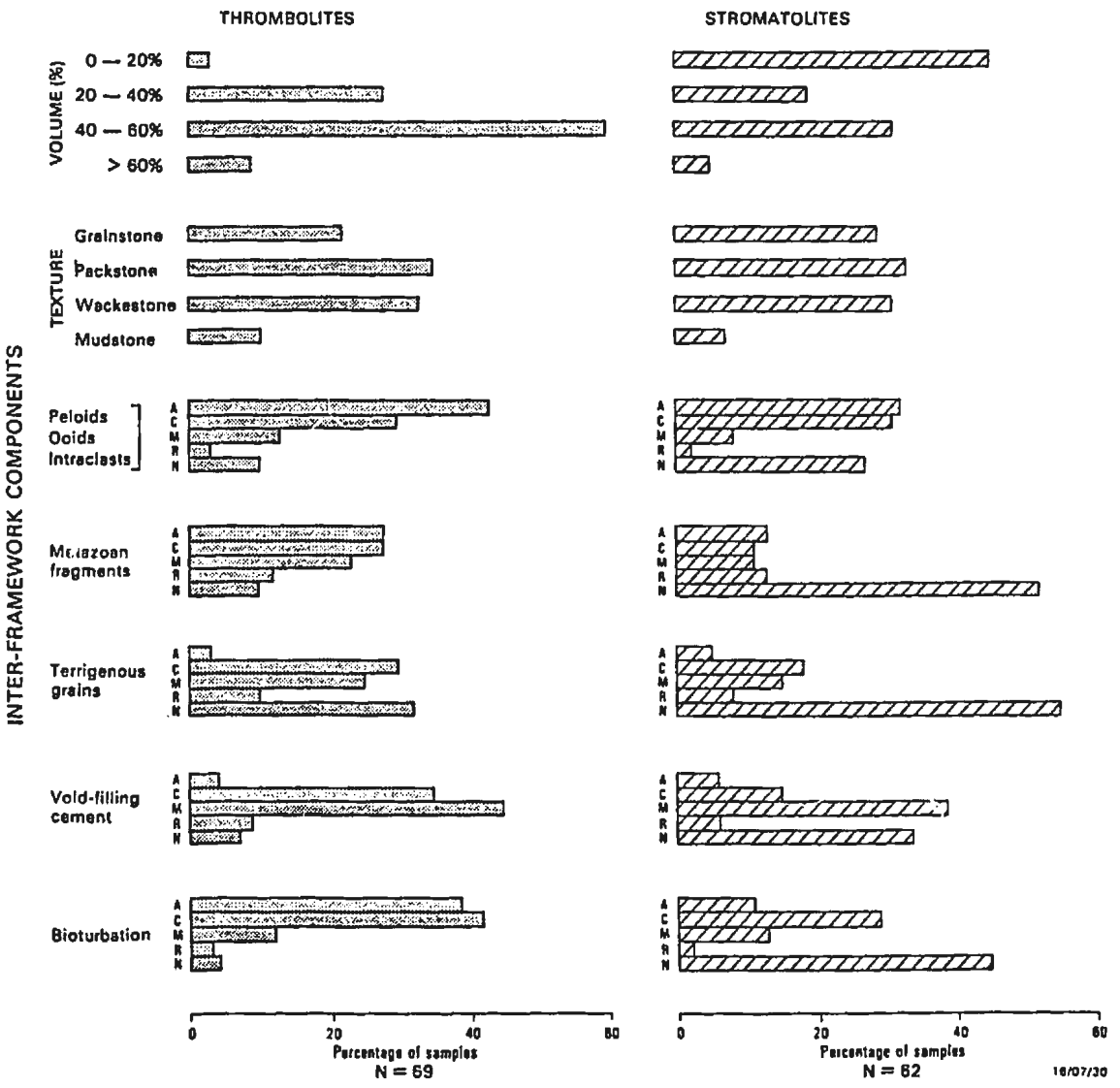

Figure 6-4. Comparative analysis of the volume percent, texture, composition and degree of bioturbation of inter-framework components within thrombolites and stromatolites. A-Abundant, C-Common, M-Minor, R-Rare, N-Nil.

3. Bioturbation (affecting both framework and inter-framework components) is more prevalent in thrombolites.

The greater volume of unbound inter-framework detrital sediment within thrombolites is thought to reflect a fundamental difference in the microbial processes that form thromboids and stromatoids; thromboids are predominantly formed by *in situ* calcification and typically exhibit little or no evidence of sediment-trapping processes, whereas stromatoids are predominantly formed by sediment-trapping and binding, and *in situ* calcification is less prevalent (see Microstructural Synthesis below). Thus detrital sediment preferentially accumulates between the calcified microbial framework of thrombolites, but is commonly actively trapped, bound and incorporated within the stromatoid framework of stromatolites.

The greater abundance of metazoan fragments and bioturbation within thrombolites is undoubtedly due to the different environmental setting of thrombolites and co-occurring stromatolites; thrombolites are exclusively subtidal and typically show no evidence of conditions adverse to metazoans, whereas co-occurring stromatolites invariably occur in shallower subtidal and intertidal environments which, due to poor water circulation, elevated salinity or frequency of exposure and desiccation, are commonly relatively depleted or devoid of metazoans (see Kepper, 1978). In fact, metazoan remains commonly progressively increase in abundance towards thrombolite mounds (an

observation previously noted by Pratt and James, 1982), thus indicating that these buildups provided a favoured habitat for metazoans.

In conclusion, thrombolite and stromatolite mesostructure reflects a balance between biological and environmental factors.

6.3 MICROSTRUCTURAL SYNTHESIS

The microstructure of microbial buildups is widely acknowledged to be the feature most closely controlled by biological factors* (see Semikhatov and others, 1979). It provides a direct record of the sediment-forming activities of the microbial community, and commonly provides clear evidence of the composition of that community. A synthesis of the relative abundance of observed microstructural types within thromboids and stromatoids (Fig. 6-5A) reveals significant differences between thrombolites and stromatolites in general. Thromboids (thrombolites) are dominated by lobate, grumous and, to a lesser extent, *Renalcis* and massive microstructures, whereas stromatoids (stromatolites) are dominated by streaky, massive, grumous and peloidal microstructures.

---

* Diagenesis also significantly contributes to, and commonly masks the biological imprint on, observed microstructures.

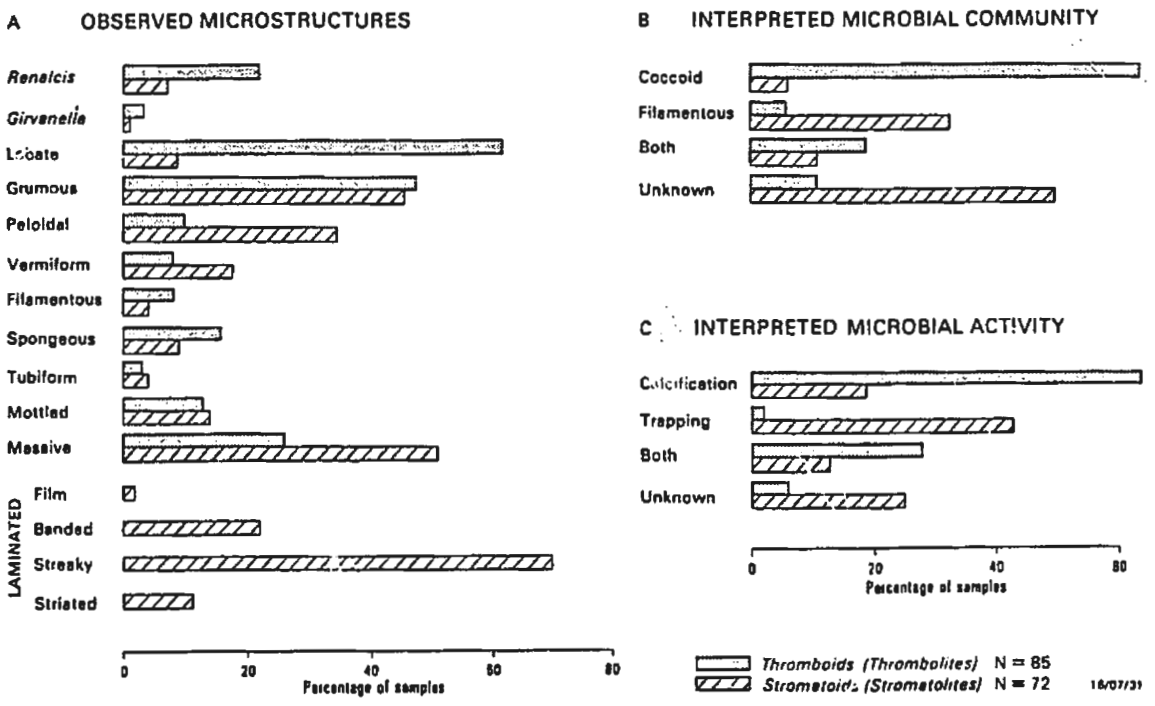

Figure 6-5. Comparative analysis of (A) observed microstructures, (B) interpreted microbial community, and (C) interpreted microbial activity of thromboids (thrombolites) and stromatoids (stromatolites).

Although the origin of some of the observed microstructures are intrinsically difficult or impossible to interpret (for example grumous, spongeous, mottled and massive microstructures), others are diagnostic of coccoid or filamentous microbes, and *in situ* calcification or sediment-trapping processes (see earlier discussion of each type of microstructure in Section 2.3). Commonly, however, the predominant sediment-forming process and original microbial composition of an otherwise non-diagnostic microstructural type, can be assessed on the basis of the context of a particular case (that is, by circumstantial evidence). For example, the intergradation of a non-diagnostic micro-structural type with a diagnostic type, or the contrasting distribution and abundance of definitive detrital grains within framework and inter-framework components. Such circumstantial evidence, together with direct diagnostic evidence, was used to interpret the composition and dominant sediment-forming microbial process(es) of the samples analysed in this study.

This data (Fig. 6-5B,C) indicates that the great majority of thromboids (65% of analysed samples), and hence thrombolites in general, are constructed by coccoid or coccoid-dominated microbial communities, and that a smaller proportion (19% of samples) are constructed by mixed (although still coccoid-dominated) coccoid-filamentous communities. Only rarely are thrombolites constructed by filamentous or filament-dominated communities (6% of samples). Most thrombolites are formed by the *in situ*

calcification of microbial colonies (65% of samples), whereas sediment-trapping and sediment-binding processes are rarely dominant (2% of samples). In several cases, *in situ* calcification and sediment-trapping\binding processes are of sub-equal importance (18% of samples).

In contrast, stromatoids, and hence stromatolites in general, are predominantly constructed by the sediment-trapping and sediment-binding activities (43% of samples) or *in situ* calcification (19% of samples) of predominantly filamentous communities. Although the composition of many stromatolite-forming communities could not be determined, the data suggests that stromatolites are infrequently constructed by either coccoid or mixed coccoid-filamentous communities (each less than 10% of samples).

Final Note

A brief summary of the above microstructural synthesis was presented by Kennard and James (1986a), and was subsequently discussed by Burne and Moore (1987). Based on their examination of some present-day Australian microbialites*, Burne and Moore cautioned against the over generalization in attributing a particular type of microbial community (coccoid versus filamentous) and process of formation (calcification versus sediment-trapping processes) to all thrombolites and stromatolites, respectively. I fully concur with Burne and Moore's comments; the type of microbial community and process

* These modern microbialites are discussed in Chapter 7, Section 7.1.

of formation of a particular microbialite can only be determined by careful analysis of its microstructure, and cannot be inferred from its mesostructural fabric. Nevertheless, the above microstructural analysis indicates significant microstructural differences (Fig. 6-5A) and interpreted modes of origin (Fig. 6-5B,C) for most Cambro-Ordovician thrombolites and co-occurring stromatolites.

CHAPTER 7

THROMBOLITES IN TIME AND SPACE

This chapter examines the temporal and spatial distribution of thrombolites in the rock record. It is based on a compilation of thrombolite bearing formations from published literature, available unpublished data, and personal observations during the course of this study. Wherever possible each author's usage of the term "thrombolite" has been carefully evaluated on the basis of their description of the fabric or available photographic figures. Although the term "thrombolite" has gained little or no usage in Soviet literature, equivalent structures are nonetheless widespread in Cambro-Ordovician strata in Siberia (H. Hofmann, personal communication, 1989; for example Maslov, 1960, Plates XXIV-1,2, XXXII-1,2,3, XXXIV-3,4,5). Re-interpretation of Soviet literature, however, was not attempted in this study.

Sixty one formations of Cambro-Ordovician age are known to contain thrombolites (Appendix C), and fourteen post Early Ordovician formations are known to contain thrombolitic metazoan-calcareous algal buildups (Appendix D).

7.1 TEMPORAL DISTRIBUTION

Thrombolites are not uniformly distributed in time; they are essentially a lower Palaeozoic phenomenon (Fig. 7-1).

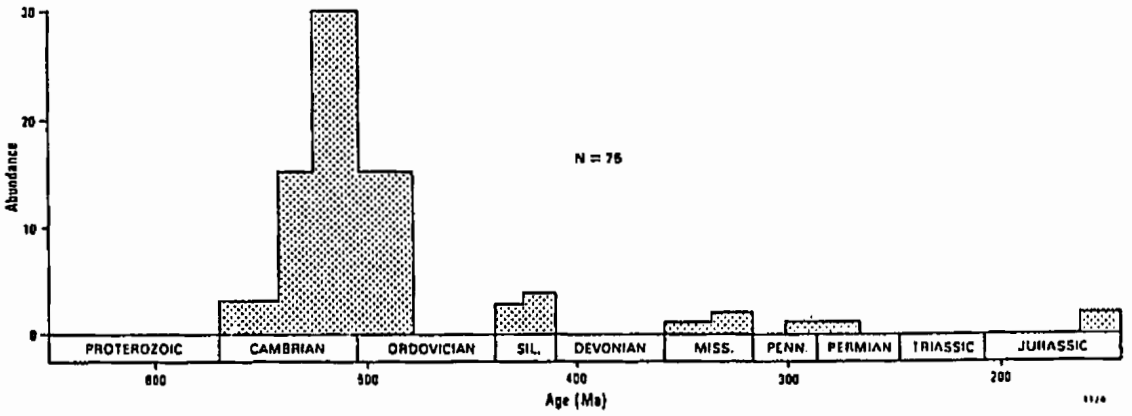

Figure 7-1. Abundance of thrombolites through time (exluding Recent). Abundance values are the number of known thrombolite-bearing formations within each epoch. Age of periods and epochs are from Palmer (1983).

They first appeared in Early Cambrian time, were most abundant in Late Cambrian time, and rapidly declined in Early Ordovician time. Thereafter thrombolites are rare.

Despite intensive studies of Precambrian microbialites (stromatolites) for several decades, definitive thrombolites of that age have not been reported (Walter and Heys, 1985). There are four possible exceptions to this statement:

1. Schmitt (1978, 1979) and Schmitt and Monninger (1977) reported latest Proterozoic thrombolites and stromatolites within the Series Lie de Vin, Adoudounian Group, Morocco. However, the age of this sequence has been disputed by Bertrand-Sarfati (1981) who regards it as Early Cambrian on the basis of associated a) stromatolite forms, b) *Renalcis*-like, *Epiphyton*-like and *Girvanella* micro-structures, and c) Archaeocyaths (see Debrenne and Debrenne, 1978).

2. Chen and Zhung (1983) reported thrombolites in the 1.0-1.4 Ga Wumishan Formation in China. Samples and thin-sections of these "thrombolites" were examined by M.R. Walter (see Walter and Heys, 1985, p.163) who concluded that they are coarsely crystalline pseudo-columnar stromatolites.

3. Hoffman (1975), Grotzinger and Hoffman (1983) and Grotzinger (1986a) reported thrombolites in the 1.9 Ga Rocknest Formation in the Northwest Territories, Canada. Slabbed samples and thin sections of these "thrombolites" were examined, courtesy of J.P. Grotzinger, at the Virginia Polytechnic Institute, Blacksburg, Virginia. They comprise

partially silicified microcrystalline dolomite and have an irregular "splotchy fabric" (Grotzinger and Hoffman, 1983) in which neither thromboids nor stromatoids can be differentiated. Grotzinger (1986a, p.1217) states that "the microfabric consists of isolated or connected clots, defining a very crude internal lamination. Clots have irregular to wavy concentric internal lamination that contrasts with the massive internal structure of clots in Cambrian and Ordovician thrombolites". All of the "clots" within the samples examined comprise microcrystalline quartz and dolomite, and show no evidence of direct microbial origin. These "thrombolites" are accordingly classified cryptomicrobial boundstones, and their unusual "splotchy" fabric is considered to result from the early diagenetic overprint of a precursor laminated stromatolite.

4. In a brief abstract, Ricketts and Donaldson (1987) mention the presence of thrombolites in the Middle Precambrian Mavor Formation, Belcher Group, Hudson Bay, Canada. In the absence of supporting data this report cannot be evaluated, and for the purpose of this study these "thrombolites" are regarded as undifferentiated (?crypto-) microbial boundstones.

Thrombolites (including structures designated "leopard rock") are only known to occur in a few formations of post Early Ordovician age, namely in Silurian, Carboniferous, Permian and Jurassic formations (Table 7-1). These younger

TABLE 7-1
POST-EARLY ORDOVICIAN THROMBOLITIC METAZOAN-ALGAL BUILDUPS

FORMATION	AGE	MICROBIAL CONSTITUENTS	METAZOA, ALGAE	REFERENCE
Mullersfelsen	Late Jurassic	?Thromboids, Stromatoids	Sponges, Foraminifera	Flügel & Steiger (1981)
Abenaki	Late Jurassic	Thromboids, Stromatoids	Tubiphytes, Sponges, Foraminifera	Jansa & others (1983) Ellis & others (1985)
Laborcita ("leopard rock")	Early Permian	Thromboids	Foraminifera, Bryozoans, Red Algae	Toomey & Cys (1979) Toomey & Babcock (1983)
Holder ("leopard rock")	Pennyslvanian	Thromboids	Foraminifera	Toomey & others (1977) Toomey & Babcock (1983)
Codroy Group	Mississippian	Thromboids	Bryozoans	Dix (1982) Dix & James (1987)
Pitkin	Mississippian	Thromboids, Stromatoids	Bryozoans, Foraminifera, Red Algae, Phylloid Algae, Girvanella, Crinoids, Corals, Sponges	Webb (1987)
Red Hill Oolite	Early Carboniferous	Thromboids	Corals, ?Foraminifera, Red Algae	Adams (1984)
Kolitna Group	Late Silurian - Early Devonian	?Thromboids\Cryptomicrobial, Stromatoids	Sphaerocodium, Solenopora, Renalcis, Dasycladaceans, Sponges, Corals	Clough & Blodgett (1985)
Petit Rocher	Late Silurian	Stromatoids, ?Thromboids	Stromatoporoids, Corals	Noble (1985)
Glenbower	Late Silurian	Thromboids, Stromatoids	Stromatoporoids, Corals	Feary (1986)
West Point	Late Silurian	?Thromboids\Cryptomicrobial	Sponges	Bourque (1987)
La Vieille	Early Silurian	?Stromatoids\Cryptomicrobial	Bryozoans, Corals, Red Algae, Green Algae, Stromatoporoids	Bourque & others (1987)
Sayabec Fm	Early Silurian	?Stromatoids\Cryptomicrobial	Bryozoans, Corals, Red Algae, Green Algae, Stromatoporoids	Bourque & others (1987)
Red Head Rapids	?Early Silurian - Late Ordovician	?Thromboids, Stromatoids	?Nil	Haywood & Sandford (1976) Dewing & Copper (1987)

TABLE 7-2
MODERN THROMBOLITIC STRUCTURES

LOCATION	ENVIRONMENT	FABRIC, INTERNAL STRUCTURE & FORMATIVE COMMUNITY	MINERALOGY	REFERENCE
Great Salt Lake, Utah.	Hypersaline inland lake (190-275 g\litre), nearshore 0-4 m water depth.	Variably clotted and laminated; framework of microbial precipitates (Girvanella & microcrystalline lobate microstructures), internal sediment (ooids, ostracods, gastropods, clasts, pellets, silt, clay), cavity cement: Coccoid & filamentous microbes, ostracods, gastropods.	Aragonite	Eardly (1938) Carozzi (1962) Halley (1976)
Green Lake, New York.	Fresh inland lake, 0-12 m water depth.	Knobbly partially laminated; framework of botryoidal concentrically layered or radial ?microbial precipitates, bound detritus (Chara), cavity cement: Filamentous & coccoid cyanobacteria, green algae, mosses, diatoms, gastropods, sponges.	Calcite	Bradley (1929) Dean & Eggleston (1975) Eggleston & Dean (1976)
Lake Clifton, W. Australia	Hyposaline coastal lake (15-30 g\litre), bioherms seasonally emergent & submerged, distribution controlled by groundwater influx.	Clotted, weakly layered; framework of calcified filaments (Scytonema), inter-framework unconsolidated sediment (including ostracods & gastropods): Filamentous cyanobacteria (Scytonema), gastropods, ostracods, crustaceans, polychaetes, bivalves.	Not known	Moore & others (1984) Moore (1986, 1987) Moore (in press)
L. Fellmongery (formerly Karatta), S. Australia	Hyposaline coastal lake (24 g\litre), emergent to submerged shore platform.	Clotted; knobbly framework of cryptocrystalline pellets (0.5-2 mm) with nucleus of organic matter, inter-framework and embedded gastropods, sand grains and weed fagments: Filamentous cyanobacteria, green algae, gastropods.	Monohydro-calcite	Mawson (1929) Taylor (1975)
Sleaford Mere S Australia	Schizohaline coastal lake, overgrow semi-emergent tepees in zone of groundwater resurgence.	Clotted; framework of knobbly grumous precipitates, bound detritus (skeletal fragments, faecal pellets, grapestone aggregates), cement, interstitial cavities: Unknown microbial community.	Aragonite	Warren (1982)
L. Tanganyika, Central Africa.	Large freshwater rift lake, 15-50 m water depth	Non-laminated, porous: Unknown microbial community, gastropods, fish.	High-Mg calcite	Cohen & Thouin (1987)
Gulf of Salwah, Persian Gulf.	Hypersaline marine, intertidal-subtidal.	Poorly laminated\non-laminated, porous; palisade radial & concentric elements: Filamentous cyanobacteria.	Aragonite	Golubic (1973) Park (1977)

thrombolites invariably contain a significant proportion of frame-building and\or encrusting metazoans and calcareous algae, such as bryozoans, corals, stromatoporoids, sponges, red and green algae, foraminifera, dasycladaceans, phylloid algae and various Problematica. They also commonly contain stromatoids. They are classified metazoan and\or calcareous algal-bearing thrombolites or stromatolitic thrombolites.

Some modern microbial structures resemble Cambro-Ordovician thrombolites (Table 7-2), but these modern thrombolitic structures only occur within lacustrine or restricted hypersaline marine environments. The only known examples of lithified subtidal microbial structures within modern open marine environments comparable to those in which Cambro-Ordovician thrombolites proliferated are those on the Eleuthera Bank (Dravis, 1982) and between the Exuma Islands (Dill and others, 1986) in the Bahamas. These open marine forms are characterized by a laminated (albeit sometimes crudely laminated) fenestral fabric and oolitic micro-structure. They are clearly stromatolites rather than thrombolites. These Bahaman examples are megastructurally, mesostructurally and microstructurally similar to the classic club-shaped subtidal stromatolites in Hamelin Pool, a hyper-saline barred marine basin in Shark Bay, Western Australia (Logan, 1961; Logan and others, 1974; Playford and Cockbain, 1976; Burne and James, 1986). These club-shaped forms have been cited as modern analogues of Lower Palaeozoic thrombolites (eg. Golubic, 1973; Playford and Cockbain, 1976; Kennard, 1981), but this analogy is limited to their

megastructure, subtidal setting, and occurrence of associated metazoans, and does not extend to their internal mesoscopic and microscopic structure. The only other possible example of modern marine thrombolites are the lithified domes in the Gulf of Salwah on the Saudi Arabian coast of the Persian Gulf (Golubic, 1973; Park, 1977). However these domes have not been described in detail, and photographs of them have not been published. Golubic (1973, p.456) states that "Their internal structure is porous, poorly laminated and thrombolitic", and Park (1977, p.496-497) states that "Internally they lack any well defined laminar structure comprising instead, a conglomerate of small pellets, each formed of an irregular mass of aragonite needles; reminiscent in part, of the structure described by Aitken (1967) as 'thrombolites'".

Perhaps the best known modern examples of thrombolites are the "algal bioherms" in the Great Salt Lake, Utah (Eardley, 1938; Carozzi, 1962; Halley, 1976). These bioherms occur in shallow (0-4 m) nearshore areas of the hypersaline lake, and are surrounded by rippled ooid sands. They form isolated to coalesced discoidal, ring-like and ridge-like mounds ranging from a few decimetres to several metres in lateral extent, and have 15-100 cm synoptic relief. Their internal structure is highly variable, ranging from weakly laminated to mixed laminated\non-laminated and non-laminated. Laminated portions comprise convex homogenous micritic laminae [cf. stromatoids] defined by millimetre-scale variations in grainsize and colour. Non-laminated structures have a porous clotted

appearance produced by three distinct elements (Halley, 1976): 1) a framework of microbially induced aragonite precipitates, 2) internal sediments, and 3) aragonite cement. The frame-building aragonite precipitates have two forms: clusters of tubules rimmed by micritic walls, and clusters of light coloured aragonite "grains" composed of aragonite microspar and measuring 100-300 μm in diameter. These two forms are directly comparable to thromboids composed of *Girvanella*, and microcrystalline lobate microstructures, respectively, within Cambro-Ordovician thrombolites. These framework elements are infilled by various types of internal sediment, including ooids, ostracod and gastropod shells, faecal pellets, framework fragments, micrite, siliciclastic silt and clay. Micritic and radiating needle-like aragonite cements encrust internal sediment and framework elements. The Great Salt Lake mounds are thus direct megastructural, meso-structural and microstructural analogues of Lower Palaeozoic thrombolites.

Halley (1976) concludes that since the internal structure of the Great Salt Lake mounds bears little or no resemblance to the living crudely layered film of coccoid cyanobacteria (*Aphanothece packardii*) and diatoms at their surface, the interior of the mounds are probably relict and were formed by a different, now extinct, microbial community. On the basis of the microstructures described by Halley, this former community comprised both filamentous microbes (*Girvanella* clusters) and coccoid microbes (lobate clusters of microspar "grains"), together with gastropods and ostracods which

probably grazed on the microbial community. Halley considered that the extinction of this community (including the gastropods and ostracods) was controlled by a relatively recent increase in the salinity of the lake, and suggested that laminated and non-laminated textural variations within the mounds may similarly reflect changes in the biota in response to former salinity fluctuations.

Microbial mounds reminiscent of thrombolites also occur in modern fresh or hyposaline lakes, the best studied examples of which are those in Green Lake, New York State (Bradley, 1929; Dean and Eggleston, 1975; Eggleston and Dean, 1976). These bioherms comprise concentrically layered or radial botryoidal calcite precipitates, trapped and bound detrital fragments, and calcite cement within cavities between botryoidal precipitates. A community of filamentous and coccoid cyanobacteria, green algae, mosses, diatoms, gastropods and locally small sponges live on the surface of the bioherms. Although the precise origin of the botryoidal precipitates is not known, Eggleston and Dean (1976) considered that they are triggered by seasonal temperature increase and\or photosynthetic microbial activity. These precipitates bind calcareous grains trapped by the microbial community, the most common particle being fragments of the green alga *Chara* derived from the lake banks. The botryoidal precipitates within these bioherms are structurally analogous to thromboids within Cambro-Ordovician thrombolites, but comparable concentrically layered or radial microstructures

have not been observed in ancient thrombolites.

Comparable knobbly or botryoidal thrombolite-like structures also occur in Lake Fellmongery (formerly Lake Karatta) (Mawson, 1929; Taylor, 1975; Burne, personal communication, 1987) and Sleaford Mere (Warren, 1982) in South Australia, and Lake Clifton (Moore and others, 1984; Moore, 1987) in Western Australia. The Lake Clifton structures are particularly interesting since, like their Lower Palaeozoic counterparts, they comprise clearly differentiated framework and inter-framework components; in this case an irregular framework of calcified *Scytonema* filaments supports interstices in which unconsolidated sediment, including ostracod and gastropod shells, accumulates (Moore, 1987).

Thrombolitic microbial bioherms have also recently been discovered in relatively deep water (15-50 m) in Lake Tanganyika, central Africa (Cohen and Thouin, 1987), although their detailed structure and origin have yet to be determined. This discovery is especially significant since it suggests that equivalent thrombolitic structures may well exist in other relatively unexplored, deep freshwater lakes.

In all cases where the composition of the microbial community that formed or is forming these modern thrombolites is known, filamentous microbes (either on their own or together with coccoid microbes) played a major role in the construction of these thrombolites and the type(s) of microstructures preserved within them (see Table 7-2). In this respect, these modern thrombolites do **not** provide a good

analog of Cambro-Ordovician thrombolites, the great majority of which are interpreted to be constructed by coccoid or coccoid-dominated microbial communities (see Microstructural Synthesis, Section 6.3, and Fig. 6-5). Nevertheless, analogous filament-dominated thrombolites do occur, albeit not commonly, within the Cambro-Ordovician strata of western Newfoundland (for example, Horizons E and R).

7.1.1 FACTORS CONTROLLING TEMPORAL DISTRIBUTION

If, as concluded in Chapter 6, the diagnostic clotted fabric of thrombolites (that is, thromboids) is most commonly generated by the *in situ* calcification of microbial communities (chiefly coccoid cyanobacteria), then can the first appearance of thrombolites be simply attributed to the first appearance of calcified cyanobacteria? Although silicified and organic-walled cyanobacteria have a long Precambrian record (Schopf and others, 1983), Precambrian calcified forms* are scarce. Heavily calcified cyanobacteria first appear and proliferate near the Proterozoic\Cambrian boundary (Riding, 1982, 1984; Shenfil, 1983; Riding and Voronova, 1984; Chuvashov and Riding, 1984), at approximately

---

* Calcareous moulds of cyanobacteria-like organisms do occur within some Proterozoic stromatolites, for example the *Scytonematacean*-like filament moulds reported from the Rocknest Formation by Hofmann and Schopf (1983), and the erect filament moulds (cf. vermiform microstructure) illustrated by Shapolalova (1974, Plate 10, Fig. 3, and Plate 11, Fig. 1), but because these features are not the actual calcified or encrusted remains of microbes or microbial sheaths, they constitute "trace fossils" rather than calcified "microfossils".

the same time as the appearance of a diversified skeletal fauna.

The data accumulated during this study (Fig. 7-1) confirms the observations of Brasier (1979), Bertrand-Sarfati (1981) and Walter and Heys (1985) that thrombolites first appear at or near the Proterozoic\Cambrian boundary. This event was apparently synchronous with the first appearance of both calcified cyanobacteria and skeletal metazoans. It is unlikely that this synchroneity of events near the Proterozoic\Cambrian boundary was coincidental. Rather, could the appearance of calcified cyanobacteria, and hence thrombolites, represent a major adaptive evolutionary change in the history of micro-organisms?, and could this evolutionary change be a response to the increased grazing and burrowing pressure exerted by the newly evolved metazoans?; see Garrett (1970) and Awramik (1971). Since modern cyanobacterial calcification, however, 1) is not directly dictated by the organism, 2) requires suitable environmental conditions, and 3) is probably, at least for coccoid forms, a post-mortem process (see Monty, 1972; Monty and Hardie, 1976; Golubic, 1973, 1983; Osborne and others, 1982; Pentecost, 1985; Pentecost and Riding, 1986; Burne and Moore, 1987), it is unlikely that the first appearance of calcified cyanobacteria can be solely attributed to biological evolution. Thus, as suggested by Monty (1973) and Riding (1982), calcification of cyanobacteria was probably triggered by environmental rather than evolutionary changes.

The first appearance of shelly metazoans, be they

phosphatic, calcareous or siliceous, has also been related to environmental factors (such as changes in available habitats or the composition of the Earth's atmosphere and oceans) that acted as catalysts for biological evolution (Brasier, 1979, 1982; Runnegar, 1982; Shenfil, 1983; Fischer, 1984; Cook and Shergold, 1984). Perhaps these same environmental changes also triggered the calcification of cyanobacteria. Cook and Shergold (1984) consider that a global phosphogenic episode, probably related to a period of enhanced oceanic overturn, continental plate movement, and the formation of extensive shallow epicontinental seas, provided the driving force for many of the evolutionary changes at the Proterozoic-Cambrian boundary. They suggested that a relative abundance of available phosphorous during latest Proterozoic and initial Cambrian time is indicated by a clustering of phosphorites of this age, and is also reflected in the relatively high proportion of organisms with calcium phosphate rather than calcium carbonate skeletons at this time. By the end of Early Cambrian time, and throughout the remainder of the Phanerozoic, calcium carbonate became the main skeletal component. Cook and Shergold further suggested that since phosphorous inhibits calcification in living coccolithophores (Black, 1968), and perhaps marine invertebrates in general (Simkiss, 1964), increased phosphorous levels in latest Proterozoic\earliest Cambrian time may have favoured phosphatic, and inhibited calcareous, metazoan skeletons. Dissolved phosphate is also known to inhibit inorganic carbonate precipitation in sea-water (Brasier, 1986; Walter,

1986). This being the case, calcareous metazoan skeletons probably only became dominant after the withdrawal of phosphorus from the oceans into 1) widespread phosphorites of latest Proterozoic and Early Cambrian age (Cook and Shergold, 1984), and 2) Early Cambrian phosphatic metazoan skeletons. One might thus expect that high phosphorous concentrations would have also initially inhibited calcification of cyanobacteria in latest Proterozoic and earliest Cambrian time, and that calcification of cyanobacteria would become more widespread in Middle and Late Cambrian time. This is precisely the observed trend in the abundance of thrombolites (Fig. 7-1). It thus appears that although calcification of cyanobacteria was initiated, and consequently thrombolites first appeared, in latest Proterozoic\earliest Cambrian time, widespread calcification of cyanobacteria and thrombolite formation was probably inhibited by high concentrations of phosphorous in Early Cambrian oceans, and thrombolites did not proliferate until the phosphorous concentration of the water column had significantly decreased, apparently by Middle Cambrian time.

Renalcis, Epiphyton and *Girvanella* "microfossils", however, are widespread in Lower Cambrian strata, and commonly form framestone mounds, especially in association with calcareous archaeocyaths (Zamarreno and Debrenne, 1977; James and Debrenne, 1980; James and Gravestock, 1986; Rees and others, 1986; Zhuravlev, 1988). These "microfossils" are widely regarded as calcified cyanobacteria (see Hofmann, 1975a; Pratt, 1984), and one might thus expect thrombolites to be

equally abundant in Lower Cambrian strata. This apparent anomolous situation of 1) abundant Early Cambrian calcified "microfossils", and 2) scarce Early Cambrian thrombolites, might be due to the fact that the taxa represented by *Renalcis, Epiphyton* and *Girvanella* displayed specificity for calcification, as do some extant cyanobacteria taxa (Pentecost and Riding, 1986). The fact that these calcified "microfossil" forms can, albeit with some limitations (Pratt, 1984), be assigned Linnaean-like taxa, is possibly a consequence of such taxa-specific calcification.

The co-appearance of calcified benthic microbial communities and thrombolites can also be viewed as the development of a new suite of microbial communities similar to those that characterize each of the four columnar stromatolite-defined time intervals within the Late Proterozoic (Riphean) of the Soviet Union and elsewhere (see Walter, 1972; Semikhatov, 1976; Preiss, 1976, 1977; Hofmann, 1987). According to the model proposed by Gebelein (1974), the time range of each of these communities (100-300 million years) was determined by periods of major transgression and regression, or tectonic reorganization in the distribution of shallow seas. Commencing with each transgression a new suite of benthic microbial communities, and resultant columnar stromatolite forms, became established and persisted for the duration of the ensuing stable tectonic period. During the next regression or tectonic reorganization, these communities

broke down because the selective advantages for their survival were no longer applicable under the newly established environmental conditions. Because the suite of cyanobacteria that existed at the beginning of the Riphean (1.6 Ga ago) was phenotypically similar to those that exist today, Gebelein (1974) concluded that the changes in community structure and organization need not have been accompanied by biological evolution within the cyanobacteria.

More recent palaeobiological research, however, has shown that morphology alone does not accurately reflect the physiological characteristics of Precambrian organisms. Rather these organisms "appear to have been characterized by a sort of `Volkswagon syndrome', a lack of change in external body form that served to mask the evolution of internal biochemical machinery" (Schopf and others, 1983, p.361). Thus the changes in microbial community structure that were responsible for the assemblage of columnar stromatolites within Upper Proterozoic sequences may, in fact, have been controlled by microbial evolution. Or, perhaps more likely, these changes may have resulted from the interaction between microbial evolution and environmental factors.

In applying the concept of successive suites of persistent benthic microbial communities to the appearance and subsequent rapid decline of Lower Palaeozoic thrombolites, the following points are pertinent:

1. Thrombolites first appeared in earliest Cambrian time, a period marked by a world-wide marine transgression (Brasier, 1979; Matthews and Cowie, 1979) and, as noted

earlier, the first appearance of calcified cyanobacteria. These calcified microbes are the dominant component of a newly established calcified microbiota, the so called "Cambrian flora" of Chuvashov and Riding (1984).

2. In North America, the source of most of my data, the decline of Lower Palaeozoic thrombolites correlates with the onset of a marine regression in early to middle Ordovician (early Whiterockian) time (Ross, 1977; Barnes, 1984). That is, these thrombolites are restricted to the Cambrian-Lower Ordovician "Sauk Sequence", the oldest of a series of unconformity-bound cratonic sequences proposed by Sloss (1963). The decline of thrombolites also apparently correlates with the appearance of a new calcareous "Ordovician flora" (dominated by green and ?red calcareous algae) in Early to Middle Ordovician time (Chuvashov and Riding, 1984).

3. Similarly in Australia, all Lower Palaeozoic thrombolites (see Appendix C) predate, and their development was apparently terminated during, episodes of regression associated with phases of the Late Cambrian-Early Ordovician Delamerian Orogeny (see Webby, 1978). Insufficient data preclude a comparative analysis of the temporal distribution of thrombolites, relative sea level changes, and calcareous microbiotas within other continents.

4. Thrombolites have a scarce post-Early Ordovician record (Table 7-1), which is analogous to the scarce Phanerozoic record of columnar stromatolite forms (see Awramik, 1971, 1984; Walter and Heys, 1985). Similarly, the

main reef-building elements of Chuvashov and Riding's (1984) "Cambrian flora" (*Epiphyton, Renalcis* and related forms) have, except for a somewhat enigmatic resurgence in Devonian reefs (Wray, 1977; Chuvashov and Riding, 1984), a scarce post-Early Ordovician record.

5. The time range of Lower Palaeozoic thrombolites is approximately 100 million years, an interval comparable to the time range of the suites of Upper Proterozoic columnar stromatolite forms.

It thus appears that Lower Palaeozoic thrombolites represent an assemblage of microbialites constructed by a persistent suite of calcified benthic microbial communities analogous to those that formed the distinct assemblage of columnar stromatolites within Upper Proterozoic sequences. The time range of these thrombolite-forming communities was apparently controlled, firstly, by the initial calcification of cyanobacteria at the onset of a world-wide marine transgression in Late Proterozoic-Early Cambrian time, and secondly, by the appearance of a new calcareous algal flora following regional (non-global) regressions in Early-Middle Ordovician time. These changes were most likely controlled by interactions between microbial evolution and environmental changes.

The distribution of thrombolites in the geologic record also provides new insights into our understanding of the evolution and development of Palaeozoic carbonate buildups. Prior to the Palaeozoic, stromatolites were the only type of

organic buildup. These early buildups were constructed by well laminated benthic microbial communities, and locally formed impressive reef complexes comparable to modern coral-algal reefs (Hoffman, 1974; Aitken, 1981b, in press; Horodyski, 1983; Grotzinger, 1986b, in press). The oldest known thrombolites, those in the Lower Cambrian (?Tommotian) Series Lie de Vin in Morocco (Schmitt and Monninger, 1977; Schmitt, 1979, Monninger, 1979; Bertrand-Sarfati, 1981), occur at approximately the same time as that at which *Epiphyton-Renalcis-Girvanella* mounds first appear (James and Macintyre, 1985; James and others, 1987). These small mounds initially contained accessory archaeocyaths, but by mid and late Early Cambrian time relatively complex reefs dominated by archaeocyaths, calcified "microfossils" and a variety of sessile and vagrant calcareous benthos were established (Debrenne and others, 1981). Thrombolites of Early Cambrian age are scarce and are known in only two other areas: southern Spain (Zamarreno, 1977), and western Canada (Peyto Limestone, Aitken, 1981a). Following the abrupt extinction or drastic decline of archaeocyaths at the end of Early Cambrian time (James and Debrenne, 1980; Debrenne and others, 1984), thrombolites rapidly filled this vacant subtidal niche throughout Middle and Late Cambrian time. The only other Middle and Late Cambrian buildups are stromatolites and "microfossil" boundstones. With the appearance of the Ordovician reef-building skeletal biota, including sponges, receptaculids (*Calathium*), corals, bryozoans, stromatoporoids, and calcareous algae, and the rapid

radiation of several other shelly taxa such as articulate brachiopods, ostracods, gastropods, cephalopods, bivalves, and crinoids (Sepkoski, 1981), thrombolites abruptly declined in Early Ordovician time. This decline probably resulted from a combination of 1) niche competition by skeletal metazoans, calcareous algae, and non-calcareous algae (Monty, 1973; Pratt, 1982b), and 2) increased predation by rapidly radiating metazoans, especially molluscs (see Runnegar, 1982, Fig. 3).

The decline of typical Cambrian faunas (trilobites, inarticulate brachiopods, eocrinoids) and radiation of typical Palaeozoic faunas (articulate brachiopods, ostracods, gastropods, cephalopods, bivalves, crinoids, as well as reef-building sponges, receptaculids, corals, bryozoans, stromatoporoids, and calcareous algae) in early-Middle Ordovician time, one of the largest turnovers of marine faunas seen in the history of the oceans (Sepkoski, 1981), also had a marked impact on the internal structure of thrombolites. In comparison to Cambrian thrombolites, Ordovician thrombolites are commonly characterized by: 1) assessory metazoan frame-builders (corals, sponges, receptaculids, *Pulchrilamina*), 2) abundant gastropods and scarce trilobites, 3) more intense bioturbation, 4) abundant silt-sized ?faecal pellets, 5) poorly differentiated mesostructures, 6) more common peloidal and *structure grumeleuse* microstructures, and 7) a greater preponderance of complex variegated microstructures. The first four of the above features can be directly related to the terminal

Cambrian\ Ordovician faunal turnover described by Sepkoski (1981), whereas the remaining features document the impact that these faunal changes had on microbial communities. Thus microbial framework components (thromboids and stromatoids) were commonly extensively disrupted and mixed with inter-framework sediment by grazing and burrowing metazoans; large quantities of faecal pellets were commonly trapped and bound by micro-organisms to form peloidal and *structure grumeleuse* microstructures, and the microbial communities generally became less organized, probably due to predatory stress. These changes culminated in the virtual demise of thrombolites by middle Ordovician time.

Throughout the remainder of Phanerozoic time, thrombolites evidently had a restricted distribution, and microbial buildups are generally subordinate to reefs constructed by organisms that secrete hard calcareous skeletons. The composition and structure of these buildups closely parallels the evolution and history of skeletal invertebrates (Heckel, 1974; Copper, 1974; Wilson, 1975; James, 1983; Sheehan, 1985), but the role of thrombolitic and stromatolitic microbial communities within these buildups, has yet to be fully assessed (see Pratt, 1982b, 1984).

The limited occurrence of Recent marine microbial buildups, including thrombolites, is similarly a consequence of several factors: 1) substrate competition by eukaryotic algae, aquatic plants, and metazoans (Monty, 1972, 1973; Golubic, 1976a; Pratt, 1982b), 2) destruction by grazers (Garrett,

1970; Awramik, 1971), and 3) balances between primary production and bacterial decomposition (Golubic, 1973).

7.2 SPATIAL DISTRIBUTION

Thrombolites occur in Lower Palaeozoic platformal strata in many continents; they are particularly widespread in North America and Australia, and have also been reported in Morocco, Spain, Argentina, India, China and Scotland (see Appendix C). Equivalent structures are also widespread in Cambro-Ordovician strata in Siberia (H. Hofmann, personal communication, 1989), but have not been designated **"thrombolites"** by Soviet workers.

In order to evaluate possible controls on the observed geographic distribution of Cambro-Ordovician thrombolites, known thrombolite occurrences are plotted on recent published palaeogeographic reconstructions (Scotese, 1986) for Early Cambrian (Fig. 7-2), Middle Cambrian (Fig. 7-3), Late Cambrian (Fig. 7-4) and Early Ordovician (Tremadocian) (Fig. 7-5) times. These figures indicate that Cambro-Ordovician thrombolites are restricted to shallow epicontinental seas within the equatorial zone (30 degrees north to 30 degrees south), and, in accordance with the atmospheric and oceanic circulation patterns expected for these reconstructions (see Ziegler and others, 1979, 1981), these thrombolites formed within warm tropical or subtropical climates.

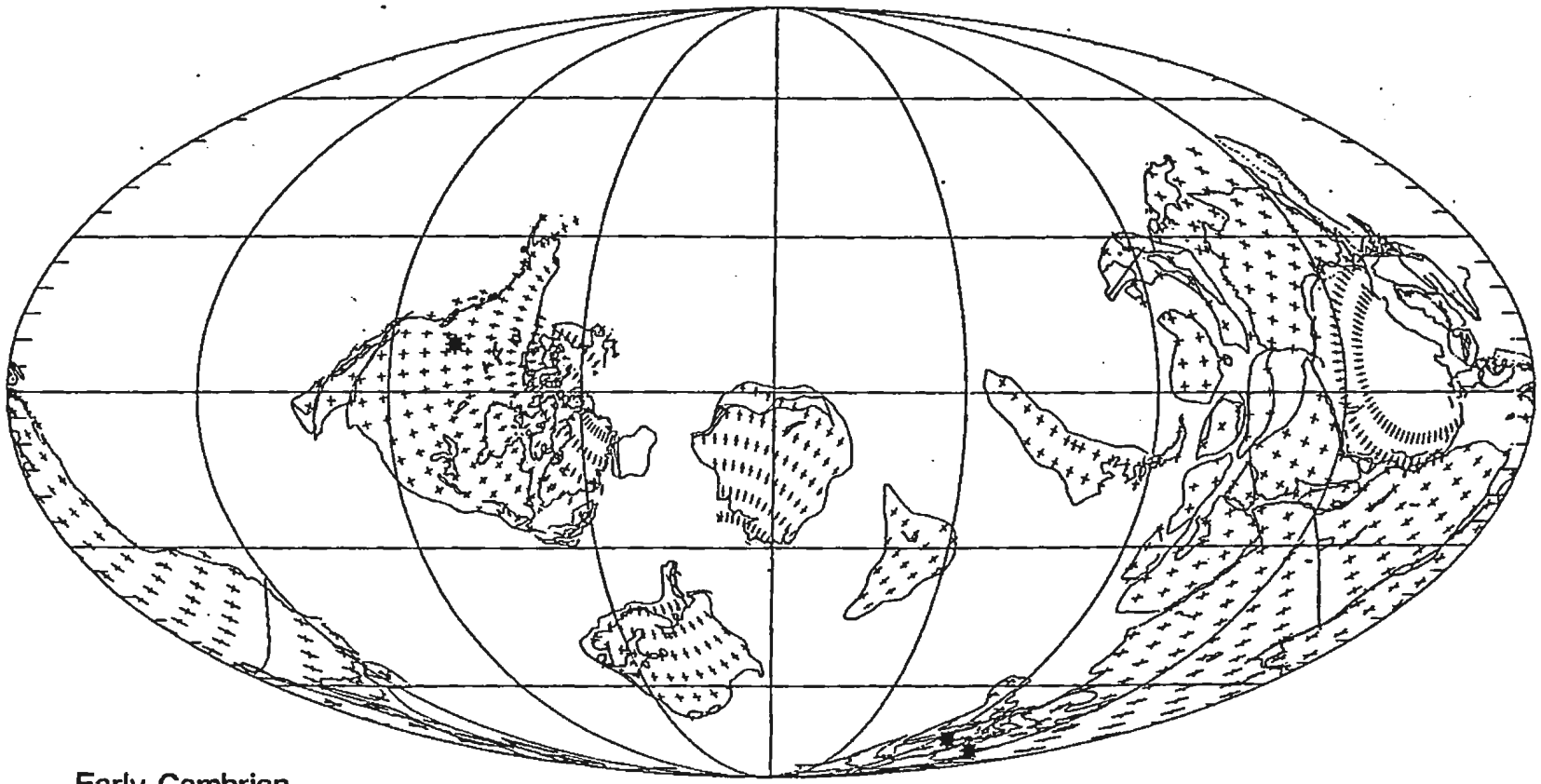

Figure 7-2. Early Cambrian palaeogeographic reconstruction (after Scotese, 1986) showing distribution and number of thrombolite-bearing formations of this age.

✸ = 1 ✸ = 2 to 4 ✸ = 5 or more Total = 3

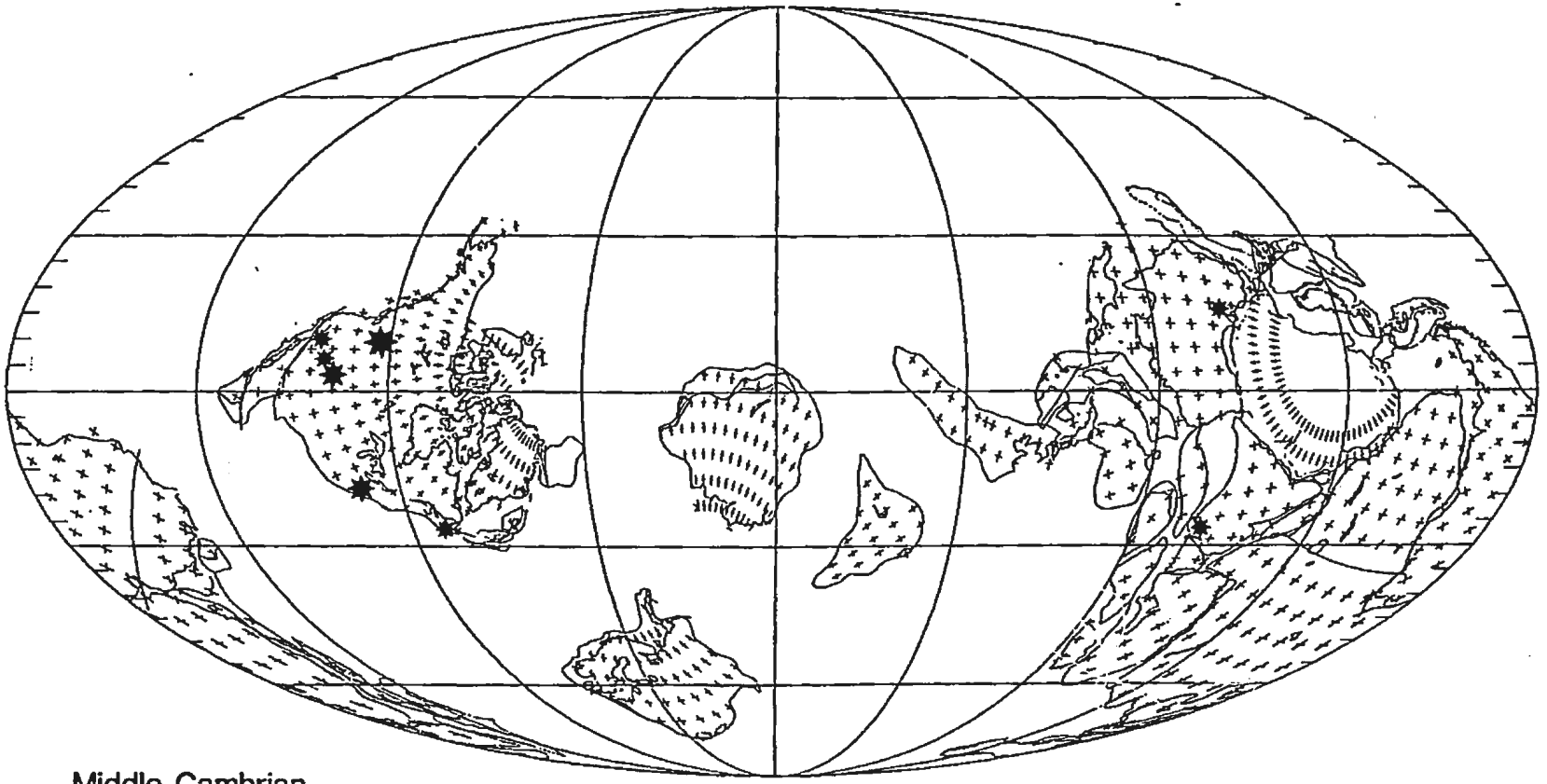

Figure 7-3. Middle Cambrian palaeogeographic reconstruction (after Scotese, 1986) showing distribution and number of thrombolite-bearing formations of this age.

✱ = 1 ✱ = 2 to 4 ✱ = 5 or more Total = 14

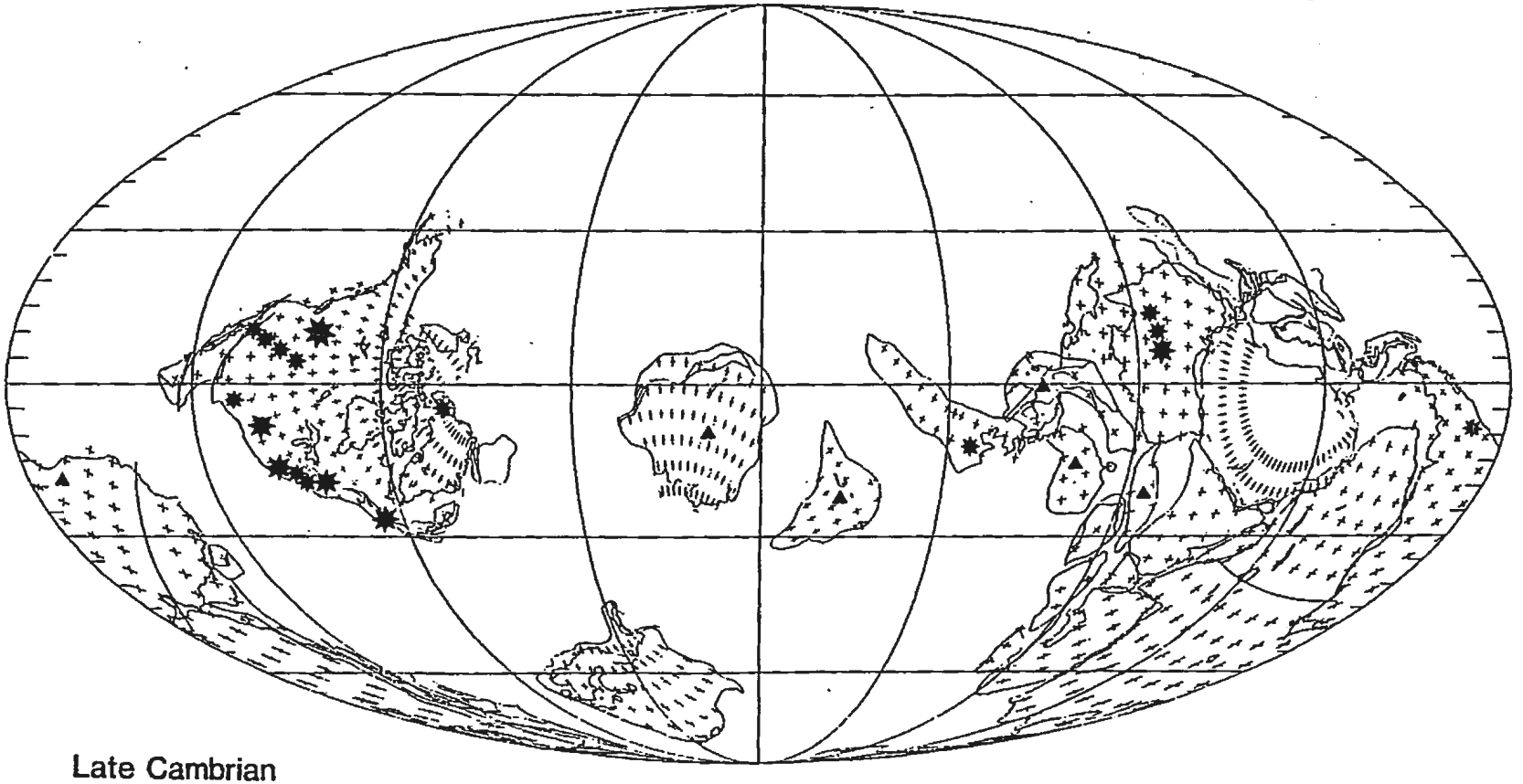

Figure 7-4. Late Cambrian palaeogeographic reconstruction (after Scotese, 1986) showing distribution and number of thrombolite-bearing formations of this age, and areas where thrombolites might also be expected to occur [▲]

✱ = 1 ✱ = 2 to 4 ✱ = 5 or more Total = 30

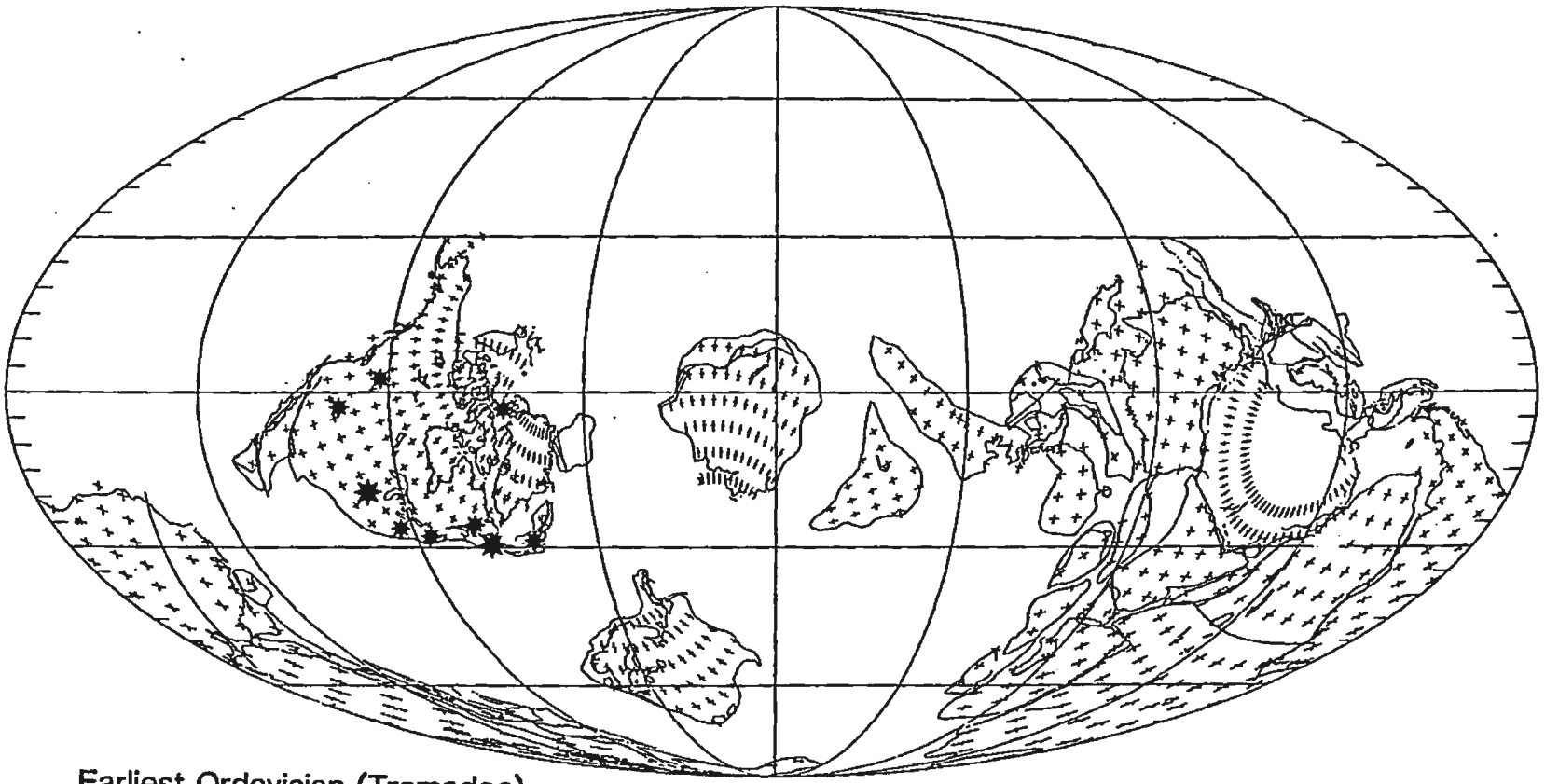

Figure 7-5. Early Ordovician (Tremadocian) palaeogeographic reconstruction (after Scotese, 1986) showing distribution of thrombolite-bearing formations of this age.

✸ = 1 ✸ = 2 to 4 ✸ = 5 or more Total = 14

There are two possible exceptions to this statement: Lower Cambrian thrombolites in Morocco (Schmitt and Monninger, 1977; Schmitt, 1979; Monninger, 1979) and southern Spain (Zamarreno, 1977) plot at very high latitudes (*ca*.75 degrees south) where polar or cold temperate climates would be expected. However, a cold climatic setting is unlikely for the host Moroccan sequence (Serie Lie de Vin) which is interpreted by Monninger (1979) and Schmitt (1979) to be deposited in a warm, schizohaline, shallow marine environment. Certainly the widespread occurrence of stromatolitic carbonates, together with ooids (Monninger, 1979; Tucker, 1984) and archaeocyaths (Debrenne and Debrenne, 1978) in the overlying strata, strongly suggest a warm climate. Oolitic, archaeocyathan and stromatolitic facies are similarly present in Lower Cambrian strata in Spain (Zamarreno, 1977, 1981). In a more recent palaeogeographic reconstruction of the Early Cambrian, Burrett and Stait (1987, Fig. 1) plot Morocco adjacent to Spain on the western (Tethyan) margin of Gondwanaland at a latitude of about 35 degrees south. The inferred subtropical climate for Morocco and Spain in this reconstruction is more consistent with the available sedimentological data, and the sub-equatorial distribution of Cambro-Ordovician thrombolites in general. During Middle Cambrian to Early Ordovician time, North Africa and Spain apparently drifted further south to near polar locations (Scotese, 1986, Maps 45-48; Burrett and Stait, 1987, Figs. 2-7), and thrombolites accordingly ceased to develop in these areas at these times.

Another feature evident from Figures 7-2, 7-3, 7-4 and 7-5 is that most thrombolites (excluding those in Siberia) occur around the margins of the Laurentian continent. The remainder occur around the margins of Gondwanaland (Australia, North China, South America, India, Morocco and Spain). Other areas where Cambro-Ordovician thrombolites might also be expected to occur are central western South America (Peru and Bolivia), south China, Indo-China, Tibet and Kazakhstan (see Fig. 7-4).

CHAPTER 8

CONCLUSIONS

Thrombolites, either on their own or together with stromatolites, are the most prominent carbonate buildups within Cambro-Ordovician platformal strata. They are characterized by a complex myriad of unusual, and commonly vague, fabrics and microstructures which have hitherto precluded systematic description and interpretation. Based on detailed studies of a diverse range of exceptionally well preserved thrombolites on the Port au Port Peninsula in western Newfoundland, an integrated scheme has been developed to systematically analyse the structure and interpret the origin of thrombolites. Co-occurring stromatolites, calcified "microfossil" boundstones and mixed microbial-metazoan buildups have also been analysed by means of this scheme, thereby enabling comparisons between these buildups. This scheme has proved equally applicable to a range of Cambro-Ordovician microbial buildups elsewhere in North America and in central Australia, and is considered to be equally applicable to all thrombolites and microbial buildups regardless of their age.

The proposed scheme utilizes a three-tiered analysis of buildups: 1) Megastructure - overall bed form (tens of metres to decimetre scale), 2) Mesostructure - internal fabric (decimetre to millimetre scale), and 3) Microstructure - microscopic fabric (millimetre to micron scale).

Megastructure provides a record of the growth relationship between a buildup and its enclosing strata. Thrombolites most commonly form a series of dome-shaped, metre-size bioherms which have a growth relief comparable to their thickness, and which rest on a common stratigraphic plane. Laterally continuous, low-relief biostromal thrombolites are less common, and in a few examples biohermal and biostromal thrombolites occur one on top of another to form reef-like complexes up to twelve metres thick and one hundred metres in lateral extent. The megastructure of thrombolites is generally independent of their mesostructure and microstructure, and reflects the sum of several environmental factors, especially the degree of turbulence and erosion, the rate of detrital sedimentation, and pre-existing substrate relief.

Mesostructure delineates the spatial relationship between framework and inter-framework components within a buildup. Thromboids, the diagnostic millimetre to centimetre-sized "clots" within thrombolites, are interpreted as a rigid microbial framework between which detrital sediment accumulated. Although thromboids collectively display a variety of shapes and arrangements, they tend to have a characteristic morphology or morphological gradation within a particular thrombolite. Their morpholgy is governed by the shape and lateral continuity of the formative microbial community, as modified by physical erosion, bioerosion, bioturbation, and subsequent diagenesis. The shape and lateral continuity of the community may in turn commonly be

related to specific biological and\or environmental factors; thus lobate and saccate thromboids were largely constructed by coccoid microbes, ragged amoeboid thromboids can generally be attributed to intensely bioturbated microbial communities, vertically elongate thromboids commonly developed in response to high rates of detrital influx, and conversely, horizontally elongate thromboids usually formed under conditions of low or periodic sediment influx.

Other accessory framework components that are locally important in thrombolites are stromatoids, undifferentiated cryptomicrobial fabrics, botryoidal marine cements, pebble aggregates, sketelal metazoans and rarely calcareous algae.

Microstructure provides a direct record of sediment-building microbial activities within a buildup, and commonly yields clear evidence of 1) specific sediment-forming processes, and 2) the gross morphologic composition (coccoid or filamentous) of a community. This primary biological imprint may be easily obscured or obliterated, however, by subsequent diagenesis. Thrombolites commonly have a complex variegated microstructure consisting of one or more of the following microstructural types: specific calcified "microfossils" (*Renalcis, Girvanella*, and rarely *Epiphyton)*, lobate, peloidal, vermiform, filamentous, spongeous, tubiform, mottled, massive, laminated, and compound microstructures. Lobate and grumous microstructures are most common, followed by *Renalcis* and massive microstructures.

On the basis of direct and circumstantial microstructural evidence, most thrombolites of Cambro-Ordovician age were

constructed by coccoid-dominated microbial communities, a relatively small proportion were constructed by mixed coccoid-filamentous communities, and only a few were constructed by filament-dominated communities. Similarly, the dominant sediment forming process in these thrombolites was *in situ* calcification of microbial communities\colonies, whereas sediment-trapping and sediment-binding processes were rarely dominant. A relatively small proportion of thrombolites show evidence of both *in situ* calcification and sediment-trapping\binding processes.

Comparative mega-, meso- and micro-structural analyses of Cambro-Ordovician thrombolites and co-occurring stromatolites highlights numerous previously unrecognized differences between these laminated and clotted microbial buildups:

1. Thrombolites most commonly have a greater thickness to width ratio, and greater synoptic relief than stromatolites.
2. Thrombolites are exclusively subtidal, whereas co-occurring stromatolites occur in shallower peritidal environments.
3. Thrombolites generally contain a greater volume of unbound detrital sediment than stromatolites.
4. Metazoans are more abundant and bioturbation is more prevalent in thrombolites than in stromatolites.
5. The most common microstructures observed in thrombolites are lobate, grumous, *Renalcis* and massive, whereas most stromatolites comprise laminated-massive, laminated-grumous and laminated-peloidal microstructures.

6. Most thrombolites were constructed by coccoid-dominated microbial communites, whereas most stromatolites were constructed by filament-dominated communities.
7. *In situ* calcification was the dominant sediment-forming process in most thrombolites, whereas sediment-trapping and sediment-binding processes were most prevalent in stromatolites.

These observations suggest that thrombolites and stromatolites are the products of two distinct suites of benthic microbial communities.

Comparative mega-, meso- and micro-structural analyses also highlights some differences between calcified "microfossil" boundstones and thrombolitic\stromatolitic buildups:
1. "Microfossil" boundstones are largely restricted to platform-margin settings, whereas thrombolites and stromatolites occur in platform-interior and intracratonic settings.
2. *Epiphyton, Girvanella*, and *Renalcis* form a rigid framework within "microfossil" boundstones, whereas *Epiphyton* rarely occurs within thrombolites and stromatolites, and *Renalcis* and *Girvanella* are generally subordinate to other microstructural types.
3. Fibrous marine cement is ubiquitous within "microfossil" boundstones, and is only locally significant in thrombolites and stromatolites.
4. Inter-framework sediment within "microfossil" boundstones comprises lime-mud and\or silt-sized peloids, both of which are probably autochthonous, whereas thrombolites and

stromatolites commonly contain a relatively large amount of allochthonous detritus.

5. Frame-building metazoans are absent, and skeletal metazoans are scarce, in "microfossil" boundstones.

6. Bioturbation is less prevalent in "microfossil" boundstones.

These observations suggest that "microfossil" boundstones formed in submerged, probably relatively high energy, environments where rapid upbuilding and\or sediment bypassing precluded an influx and accumulation of platform-derived detritus.

Analysis of thrombolites and stromatolites in central Australia indicates that these buildups have greater mesostructural and microstructural uniformity than comparable continental shelf buildups. This observation suggests that microbial communities had greater ecological stability, and hence have greater biostratigraphic potential, within intracratonic rather than continental shelf settings.

Critical evaluation of the temporal and spatial distribution of thrombolites indicates that they are essentially an Early Cambrian to Early Ordovician "Sauk Sequence" phenomenon, and were restricted to warm subequatorial climates. Their appearance can be attributed to the initial calcification of cyanobacteria at the onset of a world-wide marine transgression in latest Proterozoic-earliest Cambrian time, an event that was probably triggered by environmental rather than evolutionary changes. This calcification event was approximately synchronous with the

evolution and radiation of skeletal metazoans, and both events were probably triggered by related environmental changes at this time (such as major continental plate movements, enhanced overturn of oceanic waters, formation of extensive shallow epicontinental seas, and changes in the composition of the Earth's oceans and atmosphere). Global changes in oceanic phosphorous levels appear to have been particularly important in that 1) high phosphorous levels may have initially inhibited cyanobacterial calcification, and hence thrombolites, in Early Cambrian time, and 2) thrombolites did not proliferate until Middle Cambrian time when excess phosphorous had been withdrawn from the oceans into widespread phosphorites and phosphatic metazoan skeletons of latest Proterozoic and Early Cambrian age.

Thrombolites abruptly declined in Early Ordovician time, an event paralleled by a relative decline of calcified cyanobacteria, the appearance of reef-building skeletal biota (sponges, receptaculids, corals, bryozoans, stromatoporoids, and calcareous algae), the rapid radiation of other shelly taxa (articulate brachiopods, ostracods, gastropods, cephalopods, bivalves and crinoids), and widespread regression. The decline of thrombolite-forming benthic microbial communities, and their continued limited occurrence today, probably resulted from niche competition by skeletal metazoa, calcareous algae and non-calcareous algae, and increased predation by molluscs.

REFERENCES

Adams, A.E., 1984. Development of algal-foraminiferal-coral reefs in the Lower Carboniferous of Furness, northwest England. Lethaia, 17, 233-249.

Aharon, P., Kolodny, Y., and Sass, E., 1977. Recent hot brine dolomitization in the "Solar Lake", Gulf of Elat, isotopic, chemical and mineralogical study. Journal of Geology, 85, 27-48.

Ahr, W.M., 1971. Paleoenvironments, algal structures and fossil algae in the Upper Cambrian of Central Texas. Journal of Sedimentary Petrology, 41, 205-216.

Ahr, W.M., 1973. The carbonate ramp - an alternative to the shelf model. Transactions of the Gulf Coast Association of the Geological Society, 23, 221-225.

Aitken, J.D., 1966. Middle Cambrian to Middle Ordovician cyclic sedimentation, southern Canadian Rocky Mountains of Alberta. Bulletin of Canadian Petroleum Geology, 14, 404-441.

Aitken, J.D., 1967. Classification and environmental significance of cryptalgal limestones and dolomites, with illustrations from the Cambrian and Ordovician of southwest Alberta. Journal of Sedimentary Petrology, 37, 1163-1178.

Aitken, J.D., 1971. Control of Lower Paleozoic sedimentary facies by the Kicking Horse Rim, southern Rocky Mountains, Canada. Bulletin of Canadian Petroleum Geology, 19, 557-569.

Aitken, J.D., 1978. Revised models for depositional grand cycles, Cambrian of the southern Rocky Mountains, Canada. Bulletin of Canadian Petroleum Geology, 26, 515-542.

Aitken, J.D., 1981a. The Cambrian System in the southern Canadian Rocky Mountains, Alberta and British Columbia. Second International Symposium on the Cambrian System, Guidebook for Field Trip 2, 61p.

Aitken, J.D., 1981b. Stratigraphy and sedimentology of the Upper Proterozoic Little Dal Group, Mackenzie Mountains, Northwest Territories. Geological Survey of Canada, Paper 81-10, 47-71.

Aitken, J.D., in press. Giant algal reefs, middle\upper Proterozoic Little Dal Group (>770, <1200 Ma), Mackenzie Mountains, N.W.T., Canada. In Geldsetzer, H., James, N.P., and Tebbutt, G., (Eds.), Canadian Reef Research Symposium, Canadian Society of Petroleum Geology, Memoir 13.

Aitken, J.D., Fritz, W.M., and Norford, B.S., 1972. Cambrian and Ordovician biostratigraphy of the southern Rocky Mountains. 24th International Geclogical Congress, Montreal, Excursion Guidebook A-19, 57p.

Aitken, J.D., and McIlreath, I.A., 1981. Depositional environment of the Cathedral Escarpment near Field, British Columbia. In Aitken, J.D., (Compiler), The Cambrian System in the southern Canadian Rocky Mountains, Alberta and British Columbia. Second International Symposium on the Cambrian System, Guidebook for Field Trip 2, 35-44.

Alexandersson, E.T., 1972. Intergranular growth of marine aragonite and Mg-calcite: evidence of precipitation from supersaturated seawater. Journal of Sedimentary Petrology, 42, 441-460.

Allen, J.R.L., 1982. Sedimentary Structures: Their Character and Physical Basis. Amsterdam, Elsevier.

Armella, C., 1988a (in press). Morfologia y fabrica de trombolitos del límite Cámbrico-Ordovícico de la Precordillera Oriental, Argentina. 1 Reunión del Grupo de Trabajo Internacional del Proyecto 270 (PICG-NESCO), Correlación Geológica No. 3, Universidad Nacional de Tueman (Argentina).

Armella, C., 1988b (in press). Microfacies trombolíticas de un biocíclo ideal de la Formatión La Flecha, Precordillera Oriental, Argentina. 1 Reunión del Grupo de Trabajo Internacional del Proyecto 270 (PICG-NESCO), Correlación Geológica No. 3, Universidad Nacional de Tueman (Argentina).

Awramik, S.M., 1971. Precambrian stromatolite diversity: reflection of metazoan appearance. Science, 1[illegible]., 825-827.

Awramik, S.M., 1984. Ancient stromatolites and microbial mats. In Cohen, Y., Castenholz, R.W., and Halvorson, H.O., (Eds.), Microbial Mats: Stromatolites. New York, Alan R. Liss, 1-22.

Babcock, J.A., 1977. Calcareous algae, organic boundstones, and the genesis of the Upper Capitan Limestone (Permian, Guadalupian), Guadalupian Mts., West Texas and New Mexico. In Hileman, M.E., and Mazzullo, S.J., (Eds.), Society of Economic Paleontologists and Mineralogists, Permian Basin Section, Field Conference Guidebook, Publication 77-16, 3-44.

Baldis, B.A., Beresi, M.S., Bordonaro, O.L., and Uliarte, E., 1981. Estromatolitos, trombolitos y formas afines en el limite Cámbrico-Ordovícico del oeste Argentino. Anain do 2nd Congresso Latino-Americano de Paleontologia, Porto Alegre, 1, 19-30.

Baldis, B., Beresi, M., Bordonaro, O., and Vaca, A., 1984. The Argentine Precordillera as a key to Andean structure. Episodes, 7, 14-19.

Barnes, C.R., 1984. Early Ordovician eustatic events in Canada. In Bruton, D.L., (Ed.), Aspects of the Ordovician System. Palaeontological Contributions from the University of Oslo, 295, 51-63.

Bathurst, R.G.C., 1959. The cavernous structure of some Mississippian *Stromatactis* reefs in Lancashire, England. Journal of Geology, 67, 506-521.

Bathurst, R.G.C., 1975. Carbonate Sediments and Their Diagenesis. Developments in Sedimentolgy, 12. Amsterdam, Elsevier, 658p.

Bauld, J., 1981a. Geobiological role of cyanobacterial mats in sedimentary environments: production and preservation of organic matter. BMR Journal of Australian Geology and Geophysics, 6, 307-317.

Bauld, J., 1981b. Occurrence of benthic microbial mats in saline lakes. Hydrobiologia, 81, 87-111.

Bauld, J., 1984. Microbial mats in marginal marine environments: Shark Bay, Western Australia, and Spencers Gulf, South Australia. In Cohen, Y., Castenholz, R.W., and Halvorson, H.O., (Eds.), Microbial Mats: Stromatolites, New York, Alan R. Liss, 39-58.

Beales, F.W., 1956. Conditions of deposition of Palliser (Devonian) limestone of southwestern Alberta. American Association of Petroleum Geologists Bulletin, 40, 848-870.

Beales, F.W., 1958. Ancient sediments of Bahaman type. American Association of Petroleum Geologists Bulletin, 42, 1845-1880.

Beales, F.W., 1965. Diagenesis in pelletted limestones. In Pray, L.C., and Murray, R.C., (Eds.), Dolomitization and Limestone Diagenesis. Society of Economic Paleontologists and Mineralogists, Special Publication 13, 49-70.

Bertrand-Sarfati, J., 1972. Stromatolite columnaires du Précambrien supérieur, Sahara Nord-Occidental. Centre National de la Recherche Scientifique, Paris, Série Géologie, 14, 245p.

Bertrand-Sarfati, J., 1976. An attempt to classify Late Precambrian stromatolite microstructures. In Walter, M.R., (Ed.), Stromatolites, Developments in Sedimentology, 20, Amsterdam, Elsevier, 251-259.

Bertrand-Sarfati, J., 1981. Problème de la limite Précambrien-Cambrien: la section de Tiout (Maroc); les stromatolites et leur biostratigraphie (Schmitt 1979); critiques et observations. Newsletters on Stratigraphy, 10, 20-26.

Black, M., 1933. The algal sediments of Andros Island, Bahamas. Philosophical Transactions of the Royal Society of London, Series B, 222, 165-192.

Black, M., 1968. Taxonomic problems in the study of coccoliths. Palaeontology, 11, 793-813.

Blatt, H., Middleton, G.V., and Murray, R.C., 1972. Origin of Sedimentary Rocks. New Jersey, Prentice-Hall, 634p.

Bluck, B.J., 1967. Sedimentation of beach gravels. Journal of Sedimentary Petrology, 37, 128-156.

Bolton, T.E., 1977. Ordovician megafauna, Melville Peninsula, southeastern district of Franklin. Geological Survey of Canada Bulletin, 269, 23-39.

Bourque, P-A., 1987. The West Point Formation of Gaspe Basin, Quebec Appalachians: Late Silurian bank and reef complexes controlled by regime of siliciclastic sedimentation on a major paleo-delta system. Canadian Society of Petroleum Geology, Reef Research Symposium, Banff, Abstracts, p 19.

Bourque, P-A., Desrochers, A., and Lavoie, D., 1987. Early Silurian bioherms and biostromes of Gaspe, Quebec Appalachians: bryozoan-coral-stromatoporoid knob reefs at margin of peritidal flat. Canadian Society of Petroleum Geology, Reef Research Symposium, Banff, Abstracts, p 74.

Bourque, P-A., and Gignac, H., 1983. Sponge-constructed *Stromatactis* mud mounds, Silurian of Gaspe, Quebec. Journal of Sedimentary Petrology, 53, 521-532.

Bova, J.A., 1982. Peritidal cyclic and incipiently drowned platform sequence: Lower Ordovician Chepultepec Formation, Virginia. M.Sc. Thesis, Virginia Polytechnic Institute, Blacksburg.

Bova, J.A., Koerschner, W.F., and Mussman, W.J., 1982. Cambro-Ordovician aggraded shelf, drowned shelf and emergent shelf facies, Virginia Appalachians. Geological Society of America, Abstracts and Programs, 14, p 7.

Bova, J.A., and Read, J.F., 1987. Incipiently drowned facies within a cyclic peritidal ramp sequence, Early Ordovician Chepultepec interval, Virginia Appalachians. Geological Society of America Bulletin, 98, 714-727.

Bradley, W., 1929. Algal reefs and oolites of the Green River Formation. United States Geological Survey, Professional Paper 154-G, 203-223.

Brasier, M.D., 1979. The Cambrian Radiation event. In House, M.R., (Ed.), The Origin of Major Invertebrate Groups. London, Academic Press, 103-159.

Brasier, M.D., 1982. Sea-level changes, facies changes and the Late Precambrian-Early Cambrian evolutionary explosion. Precambrian Research, 17, 105-123.

Brasier, M.D., 1986. Precambrian-Cambrian boundary beds and events. In Walliser, O.H., (Ed.), Global Bio-Events. Lecture Notes in Earth Science, 8, 109-117. Berlin, Springer-Verlag.

Buchbinder, B., 1981. Morphology, microfabric and origin of stromatolites of the Pleistocene precursor of the Dead Sea, Isreal. In Monty, C.L.V., (Ed.), Phanerozoic Stromatolites. Berlin, Springer-Verlag, 181-196.

Burne, R.V., and James, N.P., 1986. Subtidal Origin of club-shaped stromatolites, Shark Bay. 12th International Sedimentological Congress, Canberra, Abstracts, p 49.

Burne, R.V., and Moore, L., 1987. Microbialites: organo-sedimentary deposits of benthic microbial communities. Palaios, 2, 241-254.

Burrett, C., and Stait, B., 1987. China and southeast Asia as part of the Tethyan margin of Cambro-Ordovician Gondwanaland. Proceedings of the International Symposium of Shallow Tethys 2, Wagga Wagga, 65-77.

Cameron, B., Cameron, D., and Jones, J.R., 1985. Modern algal mats in intertidal and supratidal quartz sands, north-eastern Massachusetts, U.S.A. In Curran, H.A., (Ed.), Biogenic Structures: their use in interpreting depositional environments. Society of Economic Paleontologists and Mineralogists, Special Publication 35, 211-223.

Carozzi, A.V., 1962. Observations on algal biostromes in the Great Salt Lake. Journal of Geology, 70, 246-252.

Cayeux, L., 1935. Les Roches Sédimentaires de France: Roches Carbonatées. Paris, Masson et Cie, 463p.

Chafetz, H.S., 1973. Morphological evolution of Cambrian algal mounds in response to a change in depositional environment. Journal of Sedimentary Petrology, 43, 435-446.

Chafetz, H.S., 1986. Marine peloids: a product of bacterially induced precipitation of calcite. Journal of Sedimentary Petrology, 56, 812-817.

Chafetz, H.S., and Folk, R.L., 1984. Travertines: depositional morphology and the bacterially constructed constituents. Journal of Sedimentary Petrology, 54, 289-316.

Chen, J., and Zhung, H., 1983. The Middle and Upper Proterozoic in Jixian, Tianjin. International Symposium on Late Proterozoic Geology, Excursion Guide, Chinese Academy of Geological Sciences, 24p.

Cherns, L., 1982. Palaeokarst, tidal erosion surfaces and stromatolites in the Silurian Eke Formation of Gotland, Sweden. Sedimentology, 29, 819-833.

Choquette, P.W., and James, N.P., 1987. Diagenesis in limestones - 3; the deep burial environment. Geoscience Canada, 14, 3-35.

Chow, N., 1986. Sedimentology and diagenesis of Middle and Upper Cambrian platform carbonates and siliciclastics, Port au Port Peninsula, western Newfoundland. Ph.D. Thesis, Memorial University of Newfoundland, St. John's, 458p.

Chow, N., and James, N.P., 1987. Cambrian grand cycles: a northern Appalachian perspective. Geological Society of America Bulletin, 98, 418-429.

Church, S.B., 1974. Lower Ordovician patch reefs in western Utah. Brigham Young University Geological Studies, 21, 41-62.

Chuvashov, B., and Riding, R., 1984. Principal floras of Paleozoic marine calcareous algae. Paleontology, 37, 487-500.

Clough, J.G., and Blodgett, R.B., 1985. Comparative study of the sedimentology and paleoecology of middle Paleozoic algal and coral-stromatoporoid reefs in Alaska. Proceedings of the 5th International Coral Reef Congress, Tahiti, 6, 593-598.

Cohen, A.S., and Thouin, C., 1987. Nearshore carbonate deposits in Lake Tanganyika. Geology, 15, 414-418.

Cohen, Y., Krumbein, W.E., Goldberg, M., and Shilo, M., 1977a. Solar Lake (Sinai) 1. Physical and chemical limnology. Limnology and Oceanography, 22, 597-608.

Cohen, Y., Krumbein, W.E., and Shilo, M., 1977b. Solar Lake (Sinai) 2. Distribution of photosynthetic microorganisms and primary production. Limnology and Oceanography, 22, 609-620.

Cohen, Y., Krumbein, W.E., and Shilo, M., 1977c. Solar Lake (Sinai) 3. Bacterial distribution and production. Limnology and Oceanography, 22, 621-634.

Coniglio, M., and James, N.P., 1985. Calcified algae as sediment contributors to early Paleozoic limestones: evidence from deep-water sediments of the Cow Head Group, western Newfoundland. Journal of Sedimentary Petrology, 55, 746-754.

Cook, P.J., and Shergold, J.H., 1984. Phosphorus, phosphorites and skeletal evolution at the Precambrian-Cambrian boundary. Nature, 308, 5956, 231-236.

Cooper, J.D., Miller, R.H., and Sundberg, F.A., 1981. Upper Cambrian depositional environments, southeastern California and southern Nevada. In Taylor, M.E., (Ed.), Short Papers for the Second International Symposium on the Cambrian System. United States Geological Survey, Open File Report 81-743, 57-62.

Copper, P.C., 1974. Structure and development of early Paleozoic reefs. Proceedings of the Second International Coral Reef Symposium, Brisbane, 1, 365-386.

Cross, S.L., and Lightly, R.G., 1986. Peloidal submarine cementation in ancient reefs: Lower Cretaceous Mural Limestone, southeastern Arizona. Geological Society of America, Abstracts and Programs, 18, p 576.

Cross, T.A., and Klosterman, M.J., 1981a. Autoecology and development of a stromatolitic-bound phylloid algal bioherm, Laborcita Formation (Lower Permian), Sacramento Mountains, New Mexico, U.S.A. In Monty, C.L.V., (Ed.), Phanerozoic Stromatolites. Berlin, Sringer-Verlag, 45-59.

Cross, T.A., and Klosterman, M.J., 1981b. Primary submarine cements and neomorphic spar in a stromatolitic-bound phylloid algal bioherm, Laborcita Formation (Wolfcampian), Sacramento Mountains, New Mexico, U.S.A. In Monty, C.L.V., (Ed.), Phanerozoic Stromatolites. Berlin, Sringer-Verlag, 60-73.

Cuffey, R.J., 1985. Expanded reef-rock textural classification and the geologic history of bryozoan reefs. Geology, 13, 307-310.

Cummings, E.R., 1932. Reefs or bioherms?. Geological Society of America Bulletin, 43, 331-352.

Danielli, H.M.C., 1981. The fossil algae *Girvanella*, Nicholson and Etheridge. Bulletin of the Britsh Museum (Natural History), Geology Series, 35, 79-107.

Davies, G.R., 1970. Algal-laminated sediments, Gladstone Embayment, Shark Bay, Western Australia. In Logan, B.W., Davies, G.R., Read, J.F., and Cebulski, D.E., (Eds.), Carbonate Sedimentation and Environments, Shark Bay, Western Australia. American Association of Petroleum Geology, Memoir 13, 169-205.

Davies, G.R., 1977. Former magnesium calcite and aragonite submarine cements in Upper Paleozoic reefs of the Canadian Arctic: a summary. Geology, 5, 11-15.

Dean, W.E., and Eggleston, J.R., 1975. Comparative anatomy of marine and freshwater algal reefs, Bermuda and central New York. Geological Society of America Bulletin, 86, 665-676.

Debrenne, F., and Debrenne, M., 1978. Archaeocyathid fauna of the lowest fossiliferous levels of Tiout (Lower Cambrian), Southern Morocco. Geological Magazine, 115, 101-119.

Debrenne F., Gangloff, R.A., and James, N.P., 1981. Archaeocyathan buildups - pioneer reefs of the Paleozoic. In Taylor, M.E., (Ed.), Short Papers for the Second International Symposium on the Cambrian System. United States Geological Survey, Open File Report 81-743, p 63.

Debrenne, F., Rozanov, A. Yu., and Webers, G.F., 1984. Upper Cambrian Archaeocyatha from Antartica. Geological Magazine, 121, 291-299.

Deelman, J.C., 1975. Two mechanisms of microbial carbonate precipitation. Naturwissenschaften, 62, 484-485.

Demicco, R.V., 1981. Comparative sedimentology of an ancient carbonate platform: the Conococheague Limestone of the central Appalachians. Ph.D. Thesis. The John Hopkins University, Baltimore, 333p.

Demicco, R.V., 1983. Wavy and lenticular-bedded carbonate ribbon rocks of the Upper Cambrian Conococheague Limestone, central Appalachians. Journal of Sedimentary Petrology, 53, 1121-1132.

Demicco, R.V., 1985. Platform and off-platform carbonates of the Upper Cambrian of western Maryland, USA. Sedimentology, 32, 1-22.

Demicco, R.V., and Hardie, L.A., 1981. Paterns of platform and off-platform carbonate sedimentation in the Upper Cambrian of the central Appalachians and their implications for sea-level history. In Taylor, M.E., (Ed.), Short Papers for the Second International Symposium on the Cambrian System. United States Geological Survey, Open File Report 81-743, 67-70.

Demicco, R.V., Hardie, R.L., and Haley, J.S., 1982. Algal mounds of Upper Cambrian carbonates of Appalachians, western Maryland; examples of early patch and marginal reefs (Abs.). American Association of Petroleum Geologists Bulletin, 66, p 563.

Desrochers, A., 1984. Lower to Middle Ordovician platform carbonates, Mingan Islands, Quebec. Geological Association of Canada, Abstracts and Programs, 9, p 57.

Desrochers, A., 1986. The Lower and Middle Ordovician platform carbonates of the Mingan Islands, Quebec: stratigraphy, sedimentology, paleokarst and limestone diagenesis. Ph.D. Thesis, Memorial University of Newfoundland, St. John's.

Deutsch, E.R., and Prasad, J.N., 1987. Ordovician paleomagnetic results from the St. George and Table Head carbonates of western Newfoundland. Canadian Journal of Earth Sciences, 24, 1785-1796.

Dewing, K., and Copper, P., 1987. Preliminary report on Silurian bioherms of the Red Head Rapids Formation, Southhampton Island, Northwest Territories. Canadian Society of Petroleum Geologists, Reef Research Symposium, Banff, Abstracts, p 81.

Dill, R.f., Shinn, E.A., Jones, A.T., Kelly, K., and Steinen, R.P., 1986. Giant subtidal stromatolites forming in normal salinity waters. Nature, 324, 55-58.

Dionne, J.C., 1971. Vertical packing of flat stones. Canadian Journal of Earth Sciences, 8, 1585-1591.

Dix, G.R., 1982. Stratigraphy, paleontology, sedimentology and diagenesis of the Codroy Group (Upper Mississippian), Port au Port Peninsula, Newfoundland. M.Sc. Thesis, Memorial University of Newfoundland, St. John's, 210p.

Dix, G.R., and James, N.P., 1987. Late Mississippian bryozoan\microbial build-ups on a drowned karst terrane: Port au Port Peninsula, western Newfoundland. Sedimentology, 34, 779-794.

Doemel, W.N., and Brock, T.D., 1974. Bacterial stromatolites: origin of lamination. Science, 184, 1083-1085.

Donaldson, J.A., 1963. Stromatolites in the Denault Formation, Marion Lake, coast of Labrador, Newfoundland. Geological Survey of Canada Bulletin, 102, 33p.

Donaldson, J.A., and Ricketts, B.D., 1979. Beachrock in Proterozoic dolostone of the Belcher Islands, Northwest Territories, Canada. Journal of Sedimentary Petrology, 49, 1287-1294.

Dravis, J., 1979. Rapid and widespread generation of Recent oolitic hardgrounds on a high energy Bahamian platform, Eleuthera Bank, Bahamas. Journal of Sedimentary Petrology, 49, 195-208.

Dravis, J., 1982. Hardened subtidal stromatolites, Bahamas. Science, 219, 385-386.

Dunham, H.J., 1962. Classification of carbonate rocks according to depositional textures. In Ham, W.E., (Ed.), Classification of Carbonate Rocks. American Association of Petroleum Geologists, Memoir 1, 108-122.

Eardly, A.J., 1938. Sediments of the Great Salt Lake. American Association of Petroleum Geologists Bulletin, 22, 1305-1411.

Edwards, J.M., 1978. A paleoenvironmental interpretation of Upper Cambrian stromatolites and associated lithofacies, northern west Newfoundland. B.Sc Thesis, Memorial University of Newfoundland, St. John's.

Eggleston, J.R., and Dean, W.E., 1976. Freshwater stromatolitic bioherms in Green Lake, New York. In Walter, M.R., (Ed.), Stromatolites, Developments in Sedimentology 20. Amsterdam, Elsevier, 479-488.

Ellis, P.M., Crevello, P.D., and Eliuk, L.S., 1985. Upper Jurassic and Lower Cretaceous deep-water buildups, Abenaki Formation, Nova Scotia Shelf. In Crevello, P.D., and Harris, P.M., (Eds.), Deep-water Carbonates: Society of Economic Paleontologists and Mineralogists, Core Workshop 6, New Orleans, 212-248.

Embry, A.F., and Klovan, J.E., 1971. A Late Devonian reef tract on northeastern Banks Island, Northwest Territories. Bulletin of Canadian Petroleum Geology, 19, 730-781.

Feary, D., 1986. Silurian carbonate and siliciclastic facies of the Ravenswood Subgroup, New South Wales, Australia. 12th International Sedimentological Congress, Field Excursion 2C, 34p.

Fischer, A.G., 1984. Biological innovations and the sedimentary record. In Holland, H.D., and Trendall, A.F., (Eds.), Patterns of Change in Earth Evolution. Dahlem Konferenzen, Berlin, Springer-Verlag, 145-157.

Fisher, D.W., and Mazzullo, S.J., 1976. Lower Ordovician (Gasconadian) Great Meadows Formation in eastern New York. Geological Society of America Bulletin. 87, 1443-1448.

Flower, R.H., 1978. St. George and Table Head cephalopod zonation in western Newfoundland. Geological Survey of Canada Paper 78-1A, 217-224.

Flügel, E., 1964. Mikroproblematika aus rhätischen Riffkalken der Nordalpen. Palaontologische Zeitschrift, 38, 74-87.

Flügel, E., and Steiger, T., 1981. An Upper Jurassic sponge-algal buildup from the Northern Frankenalb, West Germany. In Toomey, D.F., (Ed.), European Fossil Reef Models. Society of Economic Paleontologists and Mineralogists, Special Publication 30, 371-397.

Folk, R.L., 1959. Practical petrographic classification of limestones. American Association of Petroleum Geologists Bulletin, 43, 1-38.

Folk, R.L., 1974. The natural history of crystalline calcium carbonate: effect of magnesium content and salinity. Journal of Sedimentary Petrology, 44, 40-53.

Folk, R.L., and Pittman, J.S., 1971. Length-slow chalcedony: a new testament for vanished evaporites. Journal of Sedimentary Petrology, 41, 1045-1058.

Friedman, G.W., Amiel, A.J., Braun, M., and Miller, D.S., 1973. Generation of carbonate particles and laminites in algal mats - examples from sea-marginal hypersaline pool, Gulf of Aqaba, Red Sea. American Association of Petroleum Geologists Bulletin, 57, 541-557.

Frost, J.G., 1974. Subtidal algal stromatolites from the Florida backreef environment. Journal of Sedimentary Petrology, 44, 532-537.

Garrett, P., 1970. Phanerozoic stromatolites: noncompetitive ecological restriction by grazing and burrowing animals. Science, 169, 171-173.

Garzanti, E., Casnedi, R., and Jadoul, F., 1986. Sedimentary evidence of a Cambro-Ordovician orogenic event in the northwestern Himalaya. Sedimentary Geology, 48, 237-265.

Gebelein, C.D., 1969. Distribution, morphology and accretion rate of Recent subtidal algal stromatolites, Bermuda. Journal of Sedimentary Petrology, 39, 49-69.

Gebelein, C.D., 1974. Biologic control of stromatolites microstructure: implications for Precambrian time stratigraphy. American Journal of Science, 274, 575-598.

Geldsetzer, H.H.J., 1986. Glossary of reef related terms. Guideline to authers contributing to the Canadian Reef Inventory Project.

Ginsburg, R.N., and James, N.P., 1976. Submarine botyroidal aragonite in Holocene reef limestones, Belize. Geology, 4, 431-436.

Ginsburg, R.N., and Schroeder, J.H., 1973. Growth and submarine fossilizatiuon of algal cup reefs, Bermuda. Sedimentology, 20, 575-614.

Golubic, S., 1973. The relationship between blue-green algae and carbonate deposits. In Carr, N.G. and Whitten, B.A., (Eds.), The Biology of Blue Green Algae. Oxford, Blackwell, 434-472.

Golubic, S., 1976a. Organisms that build stromatolites. In Walter, M.R., (Ed.), Stromatolites, Developments in Sedimentology 20. Amsterdam, Elsevier, 113-126.

Golubic, S., 1976b. Taxonomy of extant stromatolite-building cyanophytes. In Walter, M.R., (Ed.), Stromatolites, Developments in Sedimentology 20. Amsterdam, Elsevier, 127-140.

Golubic, S., 1983. Stromatolites, fossil and Recent: a case history. In Westbroek, P., and de Jong, E.W., (Eds.), Biomineralization and Biological Metal Accumulation. D. Reidal, 313-326.

Golubic, S., and Focke, J.W., 1978. *Phormidium hendersoni* Howe: identity and significance of a modern stromatolite building micro-organism. Journal of Sedimentary Petrology, 48, 751-764.

Golubic, S., Perkins, R.D., and Lukus, K.J., 1975. Microorganisms and microborings in carbonate substrates. In Frey, R.W., (Ed.), The Study of Trace Fossils. New York, Springer-Verlag, 229-259.

Greenfield, L.J., 1963. Metabolism and concentration of calcium and magnesium and precipitation of calcium carbonate by a marine bacterium. Annals New York Academy of Science, 109, 25-45.

Grey, K., 1984. Biostratigraphic studies from the Proterozoic Earaheedy Group, Nabberu Basin, Western Australia. Geological Survey of Western Australia Bulletin, 130, 123p.

Grotzinger, J.P., 1986a. Cyclicity and paleoenvironmental dynamics, Rocknest Platform, northwest Canada. Geological Society of America Bulletin, 97, 1208-1231.

Grotzinger, J.P., 1986b. Evolution of Early Proterozoic passive-margin carbonate platform, Rocknest Formation, Wopmay Orogen, Northwest Territories, Canada. Journal of Sedimentary Petrology, 56, 831-847.

Grotzinger, J.P., in press. Facies and evolution of Precambrian carbonate depositional systems: emergence of the modern platform archetype. In Crevello, P., (Ed.), Society of Economic Paleontologists and Mineralogists, Special Publication.

Grotzinger, J.P., and Hoffman, P.F., 1983. Aspects of the Rocknest Formation, Asiak thrust-fold belt, Wopmay Orogen, district of Mackenzie. In Current Research, Part B, Geological Survey of Canada, Paper 83-1B, 83-92.

Grotzinger, J.P., and Read, J.F., 1983. Evidence for primary aragonite precipitation, Lower Proterozoic (1.9 Ga) Rocknest dolomite, Wopmay Orogen, northwest Canada. Geology, 11, 710-713.

Grover, G., and Read, J.F., 1978. Fenestral and associated vadose diagenetic fabrics of tidal flat carbonates, Middle Ordovician New Market Limestone, southwest Virginia. Journal of Sedimentary Petrology, 48, 453-473.

Grover, G., and Read, J.F., 1983. Paleoaquifer and deep burial related cements defined by regional cathodoluminescent patterns. American Association of Petroleum Geologists Bulletin, 67, 1275-1303,

Guilbault, J.P., Hubert, C., and Mamet, B., 1976. *Nuia* et *Halysis*, deux algues Ordoviciennes énigmatiques des basses-terres du Saint-Laurent. Naturaliste Canadien, 103, 119-132.

Gürich, G., 1906. Les Spongiostromes du Viséen de la Province de Namur. Extrait des Mémoires du Musée Royal D'Histoire Naturelle de Belgigue, T. II, 55P.

Halley, R.B., 1976. Textural variation within Great Salt Lake algal mounds. In Walter, M.R., (Ed.), Stromatolites, Developments in Sedimentology 20. Amsterdam, Elsevier, 435-445.

Hamilton, D., 1961. Algal growths in the Rhaetic Cotham Marble of southern England. Palaeontology, 4, 324-333.

Hardie, L.A., and Ginsburg, R.N., 1977. Layering: the origin and environmental significance of lamination and thin bedding. In Hardie, L.A., (Ed.), Sedimentation on the Modern Carbonate Tidal Flats of Northwest Andros Island, Bahamas. Baltimore, John Hopkins University Press, 50-123.

Harland, T.L., 1981. Middle Ordovician Reefs of Norway. Lethaia, 14, 169-188.

Harris, P.M., Kendall, C.G.St.C., and Lerche, I., 1985. Carbonate cementation - a brief review. In Schneidermann, N., and Harris, P.M., (Eds.), Carbonate Cements. Society of Economic Paleontologists and Mineralogists, Special Publication 36, 79-95.

Haywick, D.W., and James, N.P., 1984. Dolomites and dolomitization of the Lower Ordovician St. George Group of western Newfoundland. In Current Research, Part A, Geological Survey of Canada, Paper 84-1A, 531-536.

Heckel, P.H., 1974. Carbonate buildups in the geologic record: a review. In Laporte, L.F., (Ed.), Reefs in Time and Space. Society of Economic Paleontologists and Mineralogists, Special Publication 18, 90-154.

Heywood, W.W., and Sandford, B.V., 1976. Geology of Southampton, Coats and Mansel Islands, district of Keewatin, Northwest Territories. Geological Survey of Canada, Memoir 382, 35p.

Hintze, L.F., 1973. Geological history of Utah. Brigham Young University Geology Studies, 20, 181p.

Hintze, L.F., and Palmer, A.R., 1976. Upper Cambrian Orr Formation - its subdivisions and correlations in western Utah. United States Geological Survey Bulletin, 1405-G, 25p.

Hiscott, R.N., James, N.P., and Pemberton, S.G., 1984. Sedimentology and ichnology of the Lower Cambrian Bradore Formation, coastal Labrador: fluvial to shallow-marine transgressive sequence. Bulletin of Canadian Petroleum Geology, 32, 11-26.

Hoffman, E.J., 1985. Distribution patterns of Recent microbial endoliths in the intertidal and supratidal zones, Bermuda. Society of Economic Paleontologists and Mineralogists, Special Publication 35, 179-194.

Hoffman, P., 1974. Shallow and deep water stromatolites in Lower Proterozoic platform-basin facies change, Great Slave Lake, Canada. American Association of Petroleum Geologists Bulletin, 58, 856-867.

Hoffman, P., 1975. Shallowing-upward shale-to-dolomite cycles in the Rocknest Formation (Lower Proterozoic), Northwest Territories, Canada. In Ginsburg, R.N., (Ed.), Tidal Deposits. Berlin, Springer-Verlag, 257-265.

Hoffman, P., 1976a. Stromatolite morphogenesis in Shark Bay, Western Australia. In Walter, M.R., (Ed.), Stromatolites, Developments in Sedimentology 20. Amsterdam, Elsevier, 261-271.

Hoffman, P., 1976b. Environmental diversity of Middle Precambrian stromatolites. In Walter, M.R., (Ed.), Stromatolites, Developments in Sedimentology 20. Amsterdam, Elsevier, 599-611.

Hofmann, H.J., 1969. Attributes of stromatolites. Geological Survey of Canada, Paper 69-39. 58p.

Hofmann, H.J., 1973. Stromatolite characteristics and utility. Earth Science Reviews, 9, 339-373.

Hofmann, H.J., 1975a. Stratiform Precambrian stromatolites, Belcher Islands, Canada: relations between silicified microfossils and microstructures. American Journal of Science, 275, 1121-1132.

Hofmann, H.J., 1975b. Australian stromatolites - essay review. Geological Magazine, 112, 97-100.

Hofmann, H.J., 1977. On Aphebian stromatolites and Riphean stromatolite stratigraphy. Precambrian Research, 5, 175-205.

Hofmann, H.J., 1987. Precambrian biostratigraphy. Geoscience Canada, 14, 135-154.

Hofmann, H.J., and Jackson, G.D., 1987. Proterozoic ministromatolites with radial-fibrous fabric. Sedimentology, 34, 963-971.

Hofmann, H.J., and Schopf, J.W., 1983. Early Proterozoic microfossils. In Schopf, J.W., (Ed.), Earth's Earliest Biosphere. Princeton, Princton University Press, 321-360.

Holland, C.H., (Ed.), 1971. Lower Palaeozoic Rocks of the World, Volume 1: Cambrian of the New World. London, John Wiley and Sons, 456p.

Horodyski, R.J., 1983. Sedimentary geology and stromatolites of the Middle Proterozoic Belt Supergroup, Glacier National Park, Montana. Precambrian Research, 20, 391-425.

Horodyski, R.J., and Vonder Haar, S.P., 1975. Recent calcareous stromatolites from Laguna Mormona (Baja California), Mexico. Journal of Sedimentary Petrology, 45, 894-906.

Howe, W.B., 1966. Digitate algal stromatolites from the Cambrian and Ordovician of Missouri. Journal of Sedimentary Petrology, 40, 64-77.

James, N.P., 1981. Megablocks of calcified algae in the Cow Head Breccia, western Newfoundland: vestiges of a Cambro-Ordovician platform margin. Geological Society of America Bulletin, 92, 799-811.

James, N.P., 1983. Reef Environment. In Scholle, P.A., Bebout, D.G., and Moore, C.H., (Eds.), Carbonate Depositional Environments. American Association of Petroleum Geologists, Memoir 33, 346-440.

James, N.P., and Choquette, P.W., 1983. Diagenesis 6. Limestones - the sea floor environment. Geoscience Canada, 10, 162-179.

James, N.P., and Choquette, P.W., 1984. Diagenesis 9. Limestones - the meteoric diagenetic environment. Geoscience Canada, 11, 161-194.

James, N.P., and Debrenne, F., 1980. Lower Cambrian bioherms: pioneer reefs of the Phanerozoic. Acta Palaeontologica Polonica, 25, 655-668.

James, N.P., and Ginsburg, R.N., 1979. The seaward margin of Belize Barrier and Atoll Reefs. International Association of Sedimentologists, Special Publication 3. Oxford, Blackwell, 191p.

James, N.P., Ginsburg, R.N., Marszalek, D.S., and Choquette, P.W., 1976. Facies and fabric specifity of early subsea cements in shallow Belize (British Honduras) Reefs. Journal of Sedimentary Petrology, 46, 523-544.

James, N.P., Gravestock, D.I., 1986. Lower Cambrian carbonate shelf and shelf margin buildups, South Australia. 12th International Sedimentological Congress, Canberra, Abstracts p 154.

James, N.P., Gravestock, D.I., and Kennard, J.M., 1987. Structure and evolution of Early Paleozoic reefs. Canadian Society of Petroleum Geologists, Reef Research Symposium, Banff, Abstracts, p 36.

James, N.P., and Hiscott, R.N., 1982. Lower Cambrian bioherms and sandstones, southern Labrador. 11th International Congress on Sedimentology, Hamilton, Field Excursion Guidebook 1A, 58p.

James, N.P., and Klappa, C.F., 1983. Petrogenesis of Early Cambrian reef limestones, Labrador, Canada. Journal of Sedimentary Petrology, 53, 1051-1096.

James, N.P., and Kobluk, D.R., 1978. Lower Cambrian patch reefs and associated sediments: southern Labrador, Canada. Sedimentology, 25, 1-35.

James, N.P., and Macintyre, I.G., 1985. Carbonate depositional environments, modern and ancient. Part 1: Reefs. Colorado School of Mines Quarterly, 80, 70p.

James, N.P., and Stevens, R.K., 1982. Anatomy and evolution of a Lower Paleozoic continental margin, western Newfoundland. 11th International Congress on Sedimentology, Hamilton, Field Excursion Guidebook 2B, 75p.

James, N.P., and Stevens, R.K., 1986. Stratigraphy and correlation of the Cambro-Ordovician Cow Head Group, western Newfoundland. Geological Survey of Canada Bulletin, 366, 143p.

Jansa, L.F., Termier, G., and Termier, H., 1983. Les biohermes à algues, spongiaires et coreax des series carbonatées de la flexure bordiere du "paleoshelf" au large du Canada oriental. Revue de Micropaléontologue, 25, 181-219.

Jenkyns, H.C., 1970. Fossil manganese nodules from the West Sicilian Jurassic. Eclogue Geologicae Helvetiae, 63, 741-744.

Jenkyns, H.C., 1971. The genesis of condensed sequences in the Tethyan Jurassic. Lethaia, 5, 327-352.

Jorgensen, B.B., and Cohen, Y., 1977. Solar Lake (Sinai) 5. The sulfur cycle of the benthic cyanobacterial mats. Limnology and Oceanography, 22, 657-666.

Kalkowsky, E., 1908. Oolith und stromatolith im norddeutschen Bundsandstein. Zeitschrift der Deutschen Geologischen Gesellschlat, 60, 68-125.

Kaye, C.A., 1959. Shoreline features and Quaternary shoreline changes, Puerto Rico. United States Geological Survey, Professional Paper 317-B, 1-140.

Kendall, A.C., 1977. Fascicular-optic calcite: a replacement of bundled acicular carbonate cements. Journal of Sedimentary Petrology, 47, 1056-1062.

Kendall, A.C., 1985. Radiaxial fibrous calcite: a reappraisal. In Schneidermann, N., and Harris, P.M., (Eds.), Carbonate Cements. Society of Economic Paleontologists and Mineralogists, Special Publication 36, 59-77.

Kendall, A.C., and Tucker, M.E., 1973. Radiaxial fibrous calcite: a replacement after acicular carbonate. Sedimentology, 20, 365-389.

Kendall, C.G.St.C., and Skipwith, P.A.D'E., 1968. Recent algal mats of a Persian Gulf lagoon. Journal of Sedimentary Petrology, 38, 1040-1058.

Kennard, J.M., 1981. The Arrinthrunga Formation: Upper Cambrian epeiric carbonates in the Georgina Basin, central Australia. Bureau of Mineral Resources, Australia, Bulletin 211, 61p.

Kennard, J.M., and James, N.P., 1986a. Thrombolites and stromatolites: two distinct types of microbial structures. Palaios, 1, 492-503.

Kennard, J.M., and James, N.P., 1986b. Early Palaeozoic thrombolites: an integrated approach to their structure, origin and palaeoecology. 12th International Sedimentological Congress, Canberra, Abstracts, p 160.

Kennard, J.M., Nicoll, R.S., and Owen, M., 1986. Late Proterozoic and Early Palaeozoic depositional facies of the northern Amadeus Basin, central Australia. 12th International Sedimentological Congress, Canberra, Field Excursion 25B, 125p.

Kepper, J.C., 1972. Paleoenvironmental patterns in middle to lower Upper Cambrian interval in eastern Great Basin. American Association of Petroleum Geologists Bulletin, 56, 503-527.

Kepper, J.C., 1976. Stratigraphic relationships and depositional facies in a portion of the Middle Cambrian of the Basin and Range Province. Brigham Young University Geology Studies, 23, 75-91.

Kepper, J.C., 1978. Antipathetic relationship between Cambrian trilobites and stromatolites. American Association of Petroleum Geologists, Bulletin 58, 141-143.

Kepper, J.C., 1981. Sedimentology of a Middle Cambrian outer shelf margin with evidence of syndepositional faulting, eastern California and western Nevada. Journal of Sedimentary Petrology, 51, 807-821.

Kinsman, D.J.J., and Park, R.K., 1976. Algal belt and coastal sabkha evolution, Trucial coast, Persian Gulf. In Walter, M.R., (Ed.), Stromatolites, Developments in Sedimentology, 20. Amsterdam, Elsevier, 421-433.

Klappa, C.F., and James, N.P., 1980. Small lithid sponge bioherms, early Middle Ordovician Table Head Group, western Newfoundland. Bulletin of Canadian Petroleum Geology, 28, 425-451.

Klappa, C.F., Opalinski, R.R., and James, N.P., 1980. Middle Ordovician Table Head Group of western Newfoundland: a revised stratigraphy. Canadian Journal of Earth Sciences, 17, 1007-1019.

Klement, K.W., and Toomey, D.F., 1967. Role of the blue-green alga *Girvanella* in skeletal grain destruction and lime mud production in the Lower Ordovician of West Texas. Journal of Sedimentary Petrology, 37, 1045-1051.

Knight, I., 1977a. The Cambro-Ordovician platformal rocks of the Northern Peninsula. Newfoundland Department of Mines and Energy, Mineral Development Division, Report 77-1, 27-34.

Knight, I., 1977b. The Cambro-Ordovician platformal rocks of the Northern Peninsula, Newfoundland. Newfoundland Department of Mines and Energy, Mineral Development Division, Report 77-6, 27p.

Knight, I., 1978. Platformal sediments of the Great Northern Peninsula: stratigraphic studies and geological mapping of the north St. Barbe district. In Gibbons, R.V., (Ed.), Report of Activities for 1977, Newfoundland Department of Mines and Energy, Mineral Development Division, Report 78-1, 140-150.

Knight, I., 1980. Cambro-Ordovician carbonate stratigraphy of western Newfoundland; sedimentation, diagenesis and zinc-lead mineralization. Newfoundland Department of Mines and Energy, Mineral Development Division, Open File NFLD, 1154, 43p.

Knight, I., 1986. Ordovician sedimentary strata of the Pistolet Bay and Hare Bay area, Great Northern Peninsula, Newfoundland. Current Research (1986) Newfoundland Department of Mines and Energy, Mineral Development Division, Report 86-1, 147-160.

Knight, I., 1987. Geology of the Roddickton (12I/16) Map Area. Current Research (1987) Newfoundland Department of Mines and Energy, Mineral Development Division, Report 87-1, 343-357.

Knight, I. and James, N.P., 1987. Stratigraphy of the St. George Group (lower-middle Ordovician), western Newfoundland. Canadian Journal of Earth Sciences, 24, 1927-1951.

Kobluk, D.R., and Risk, M.J., 1977a. Micritization and carbonate-grain binding by endolithic algae. American Association of Petroleum Geologists Bulletin, 61, 1069-1082.

Kobluk, D.R., and Risk, M.J., 1977b. *Girvanella*: a reinterpretation. Geological Society of America, Abstracts with Program 9, p 615.

Kobluk, D.R., and Risk, M.J., 1977c. Calcification of exposed filaments of endolithic algae, micrite envelope formation and sediment production. Journal of Sedimentary Petrology, 47, 517-528.

Koepnick, R.B., 1976. Depositional history of the upper Dresbachian - lower Franconian (Upper Cambrian) *Pterocephaliid* Biomere from west central Utah. Brigham Young University Geology Studies, 23, 123-138.

Koepnick, R.B., and Brady, M.J., 1974. Allochthonous carbonates of the Upper Cambrian Candland Shale Member of the Orr Formation, Fish Springs Range, Utah. American Association of Petroleum Geologists, Annual Meeting 1974, Abstracts, 1, p 54.

Koerschner, W.F., 1983. Cyclic peritidal facies of a Cambrian aggraded shelf: Elbrook and Conococheague Formations, Virginia Appalachians. M.Sc. Thesis, Virginia Polytechnic Institute.

Krumbein, W.E., 1974. On the precipitation of aragonite on the surface of marine bacteria. Naturwissenschaften, 61, p.167.

Krumbein, W.E., 1978. Algal mats and their lithification. In Krumbein, W.E., (Ed.), Environmental Biogeochemistry and Geomicrobiology, Volume 1. Michigan, Ann Arbor Science, 209-225.

Krumbein, W.E., 1979. Photolithotropic and chemoorganotrophic activity of bacteria and algae as related to beachrock formation and degradation (Gulf of Aqaba, Sinai). Geomicrobiology Journal, 1, 139-203.

Krumbein, W.E., 1983. Stromatolites - the challenge of a term in space and time. Precambrian Research, 20, 493-531.

Krumbein, W.E., and Cohen, Y., 1977. Primary production, mat formation and lithification: contributions of oxygenic and facultative anoxygenic cyanophytes (cyanobacteria). In Flügel, E., (Ed.), Fossil Algae. Berlin, Springer-Verlag, 37-56.

Krumbein, W.E., Cohen, Y., and Shilo, M., 1977. Solar Lake (Sinai) 4. Stromatolitic cyanobacterial mats. Limnology and Oceanography, 22, 635-656.

Krumbein, W.E., and Potts, M., 1978. *Girvanella*-like structures formed by *Plectonema gloephilum* (*Cyanophyta*) from the Borrego Desert in southern California. Geomicrobiology Journal, 1, 211-217.

Lalou, C., 1957. Studies on bacterial precipitation of carbonates in seawater. Journal of Sedimentary Petrology, 27, 190-195.

Land, L.S., 1971. Submarine lithification of Jamaican reefs. In Bricker, O.P., (Ed.), Carbonate Cements. The John Hopkins University Studies in Geology, 19, 59-62.

Land, L.S., and Goreau, T.F., 1970. Submarine lithification of Jamaican Reefs. Jounal of Sedimentary Petrology, 40, 457-462.

Levesque, R.J., 1977. Stratigraphy and sedimentology of Middle Cambrian to Lower Ordovician shallow water carbonate rocks, western Newfoundland. M.Sc. Thesis, Memorial University of Newfoundland, St. John's.

Logan, B.W., 1961. *Cryptozoon* and associated stromatolites from the Recent, Shark Bay, Western Australia. Jounal of Geology, 69, 517-533.

Logan, B.W., 1974. Inventory of diagenesis in Holocene-Recent carbonate sediments, Shark Bay, Western Australia. American Association of Petroleum Geologists, Memoir 22, 195-247.

Logan, B.W., Hoffman, P., and Gebelein, C.D., 1974. Algal mats, cryptalgal fabrics and structures, Hamelin Pool, Western Australia. American Association of Petroleum Geologists, Memoir 22, 140-194.

Lohmann, K.C., 1975. Stromatolite-thrombolite associations in Upper Cambrian shallow water carbonates of western Utah. American Association of Petroleum Geologists, Annual Meeting 1975, Abstracts, 2, 44-45.

Lohmann, K.C., 1976. Lower Dresbachian (Upper Cambrian) platform to deep-shelf transition in eastern Nevada and western Utah: an evaluation through lithologic cycle correlation. Brigham Young University Geology Studies, 23, 111-122.

Lohmann, K.C., 1977. Causative factors of the outer detrital belt House Embayment: a sedimentological examination of a terrigenous-carbonate depositional system, early Upper Cambrian (Dresbachian), east-central Utah and west-central Nevada. Ph.D. Thesis, State University of New York at Stony Brook.

Lohmann, K.C., and Meyers, W.J., 1977. Microdolomite inclusions in cloudy prismatic calcites: a proposed criterion of former High-magnesium calcites. Journal of Sedimentary Petrology, 47, 1078-1088.

Longman, M.W., 1980. Carbonate diagenetic textures from nearsurface diagenetic environments. American Association of Petroleum Geologists Bulletin, 64, 461-487.

Lundegard, P.D., and Samuels, N.D., 1980. Field classification of fine-grained sedimentary rocks. Journal of Sedimentary Petrology, 50, 781-786.

Lyons, W.B., Long, D.T., Hines, M.E., Gaudette, H.E., and Armstrong, P.B., 1984. Calcification of cyanobacterial mats in Solar Lake, Sinai. Geology, 12, 623-626.

Macintyre, I.G., 1977. Distribution of submarine cements in a modern Carribean fringing reef, Galeta Point, Panama. Journal of Sedimentary Petrology, 47, 503-516.

Macintyre, I.G., 1978. Reply: Distribution of submarine cements in a modern Carribean fringing reef, Galeta Point, Panama. Journal of Sedimentary Petrology, 48, 669-670.

Macintyre, I.G., 1984. Extensive submarine lithification in a cave in the Belize Barrier Reef platform. Journal of Sedimentary Petrology, 54, 221-235.

Macintyre, I.G., 1985. Submarine cements - the peloidal problem. In Schneidermann, N., and Harris, P.M., (Eds.), Carbonate Cements. Society of Economic Paleontologists and Mineralogists, Special Publication 36, 109-116.

Mamet, B., and Roux, A., 1982. Sur le mode de croissance de *Nuia*, algaue *incertae sedis*. Geobios, 15, 959-965.

Markello, J.R., 1979. Carbonate to deeper shale-shelf transition of an Upper Cambrian (Dresbachian) shelf embayment, Nolichucky Formation, southeast Virginia. M.Sc. Thesis, Virginia Polytechnic Institute, Blacksburg.

Markello, J.R., and Read, J.F., 1981. Carbonate ramp-to-deeper shale shelf transitions of an Upper Cambrian intrashelf basin, Nolichucky Formation, southwest Virginia Appalachians. Sedimentology, 28, 573-597.

Markello, J.R., and Read, J.F., 1982. Upper Cambrian intrashelf basin, Nolichucky Formation, southwest Virginia Appalachians. American Association of Petroleum Geologists Bulletin, 66, 860-878.

Marshall, J.F., 1983. Sumbarine cementation in a high-energy platform reef: One Tree Island, southern Great Barrier Reef. Journal of Sedimentary Petrology, 53, 1133-1149.

Marszalek, D.S., 1975. Calcisphere ultrastructure and skeletal aragonite from the alga *Acetabularia antillana*. Journal of Sedimentary Petrology, 45, 266-271.

Maslov, V.P., 1960. Les Stromatolithes. Genèse, méthode d'étude, lien avec ies faciès et leur valeur géologique d'après l'example de l'Ordovicien de la platforme Sibérienne. Trudy Geol. Inst. Akademy Nauk S.S.S.R., 41, 188p., Trad. M.Pietresson De St Aubin, Traduction No. 4518.

Matthews, S.C., and Cowie, J., 1979. Early Cambrian transgressions. Journal Geological Society of London, 136, 133-135.

Mawson, D., 1929. Some South Australian algal limestones in process of formation. Quarterly Journal of the Geological Society of London, 85, 613-630.

Mawson, D., and Madigan, C.T., 1930. Pre-Ordovician rocks of the McDonnell Ranges (central Australia). Quarterly Journal of the Geological Society of London, 86, 415-429.

Mazzullo, S.J., 1974. Sedimentology and depositional environments of the Cutting and Fort Ann Formations (Lower Ordovician) in New York and adjacent southwestern Vermont. Ph.D. Thesis, Rensselaer Polytechnic Institute, Troy, N.Y.

Mazzullo, S.J., 1980. Calcite pseudospar replacive of marine acicular aragonite, and implications for aragonite cement diagenesis. Journal of Sedimentary Petrology, 50, 409-422.

Mazzullo, S.J., and Cys, J.M., 1977. Submarine cements in Permian boundstones and reef-associated rocks, Guadalupe Mountains, west Texas and southeastern New Mexico. Society of Economic Paleontologists and Mineralogists, Permian Basins Section, Field Conference Guidebook, Publication 77-16, 151-200.

Mazzullo, S.J., and Cys, J.M., 1979. Marine aragonite sea-floor growths and cements in Permian phylloid algal mounds, Sacramento Mountains, New Mexico. Journal of Sedimentary Petrology, 49, 917-936.

McCallum, M.F., and Guhathakurta, K., 1970. The precipitation of calcium carbonate from the Bahama bank sediments. Journal of Applied Bacteriology, 33, 649-655.

McIlreath, I.A., 1977. Accumulation of a Middle Cambrian deep-water limestone debris apron adjacent to a vertical submarine carbonate escarpment, southern Rocky Mountains, Canada. Society of Economic Paleontologists and Mineralogists, Special Publication 25, 113-124.

McKee, E.D., and Gutschick, R.C., 1969. History of Redwall Limestone of northern Arizona. Geological Society of America, Memoir 114, 1-726.

Meng, X., Qiao, X., and Ge, M., 1986. A study of the ancient shallow sea carbonate storm deposits (tempestite) in North China with a model of facies sequences. Unpublished.

Meyers, W.J., and Lohmann, K.C., 1978. Microdolomite-rich syntaxial cements; proposed meteoric-marine mixing zone phreatic cements from Mississippian limestones, New Mexico. Journal of Sedimentary Petrology, 48, 475-488.

Milliken, K.L., 1979. The silicified evaporite syndrome - two aspects of silicification history of former evaporite nodules from southern Kentucky and northern Tennessee. Journal of Sedimentary Petrology, 49, 245-256.

Monninger, W., 1979. The section of Tiout (Precambrian\ Cambrian boundary beds, Anti-Atlas, Morocco): an environmental model. Arbeiten aus dem Palaontologischen Institut Wurzburg, 1, 289p.

Monty, C.L.V., 1967. Distribution and structure of Recent stromatolitic algal mats, eastern Andros Island, Bahamas. Annuales de la Societé Géologique de Belgique, 90, 55-100.

Monty, C.L.V., 1972. Recent algal stromatolitic deposits, Andros Island, Bahamas. Geologische Rundschau, 61, 742-783.

Monty, C.L.V., 1973. Precambrian background and Phanerozoic histoty of stromatolitic communities; an overview. Annuales de la Societé Géologique de Belgique, 96, 585-624.

Monty, C.L.V., 1976. The origin and development of cryptalgal fabrics. In Walter, M.R., (Ed.), Stromatolites, Developments in Sedimentology 20, 193-249.

Monty, C.L.V., 1977. Evolutionary concepts on the nature and the ecological significance of stromatolites: a review. In Flügel, E., (Ed.), Fossil Algae. Berlin, Springer-Verlag, 15-26.

Monty, C.L.V., 1979. Scientific reports of the Belgium expedition on the Australian Great Barrier Reef, 1967. Sedimentology 2: Monospecific stromatolites from the Great Barrier Reef tract and their palaeontological significance. Annuales de la Societé Géologique de Belgique, 101, 163-171.

Monty, C.L.V., 1981. Spongiostromate vs. Porostromate stromatolites and oncolites. In Monty, C.L.V., (Ed.), Phanerozoic Stromatolites. Berlin, Springer-Verlag, 1-4.

Monty, C.L.V., 1982. Editorial. Stromatolite Newsletter, 9, 1-11.

Monty, C.L.V., and Hardie, L.A., 1976. The geological significance of the freshwater blue-green algal calcareous marsh. In Walter, M.R., (Ed.), Stromatolites, Developments in Sedimentology 20, 447-477.

Monty, C.L.V., and Mas, J.R., 1981. Lower Cretaceous (Wealdian) blue-green algal deposits of the Province Valencia, eastern Spain. In Monty, C.L.V., (Ed.), Phanerozoic Stromatolites. Berlin, Springer-Verlag, 85-120.

Moore, L., 1986. The relationship between stromatolite distribution and groundwater influx in Lake Clifton. 12th International Sedimentological Congress, Canberra, Abstracts, p 217.

Moore, L., 1987. Stromatolites of Lake Clifton formed by the calcification of a benthic microbial community. 4th Fossil Algal Symposium, Cardiff, Abstacts.

Moore, L., in press. Waterchemistry and stromatolite distribution in the coastal saline lakes of the Clifton-Preston Lakeland System. Australian Journal of Marine and Freshwater Research.

Moore, L., Knott, B., and Stanley, N., 1984. The stromatolites of Lake Clifton, Western Australia. Search, 14, 309-314.

Moshier, S.O., 1986. Carbonate platform sedimentology, Upper Cambrian Richland Formation, Lebonon Valley, Pennsylvania. Journal of Sedimentary Petrology, 56, 204-216.

Nelson, H.F., Brown, C.W.M., and Brineman, J.H., 1962. Skeletal limestone classification. In Ham, W.E., (Ed.), Classification of Carbonate Rocks. American Association of Petroleum Gelogists, Memoir 1, 224-252.

Neumann, A.C., Gebelein, C.D., and Scoffin, T.P., 1970. The composition, structure, and erodability of subtidal mats, Abaco, Bahamas. Journal of Sedimentary Petrology, 40, 274-297.

Neumann, A.C., Kofoed, J.C., and Keller, G.H., 1977. Lithoherms in the Straits of Florida. Geology, 5, 4-11.

Noble, J.P.A., 1985. Occurrence and significance of Late Silurian reefs in New Brunswick, Canada. Canadian Journal of Earth Sciences, 22, 1518-1529.

Oppenheimer, C.H., 1961. Note on the formation of spherical aragonitic bodies in the presence of bacteria from the Bahama Bank. Geochemica et Cosmochimica Acta, 23, 295-296.

Osborne, R.H., Licari, G.R., and Link, M.H., 1982. Modern lacustrine stromatolites, Walker Lake, Nevada. Sedimentary Geology, 32, 39-61.

Owen, R.W., and Friedman, G.M., 1984. Late Cambrian algal deposition in the Hoyt Limestone, eastern New York State. Northeastern Geology, 6, 222-237.

Packard, J.J., 1987a. A Lower Ordovician thrombolite ?reef complex, Ellesmere Island, Arctic Canada. Canadian Society of Petroleum Geologists, Reef Research Symposium, Banff, Abstracts, p 97.

Packard, J.J., 1987b. Upper Cambrian stromatolitic-thrombolitic mound complexes of the Fjord Formation, Ellesmere Island, Arctic Canada. Canadian Society of Petroleum Geologists, Reef Research Symposium, Banff, Abstracts, p 47.

Palmer, A.R., 1960. Some aspects of the early Upper Cambrian stratigraphy of White Pine County, Nevada, and vicinity. In Boettcher, J.W., and Sloan, W.W., (Eds.), Guidebook to the Geology of East Central Nevada. Intermountain Association of Petroleum Geologists, 11th Annual Field Conference, 53-58.

Palmer, A.R., 1971. The Cambrian of the Great Basin and adjacent areas, western United States. In Holland, G.H., (Ed.), Lower Palaeozoic Rocks of the World, Volume 1: Cambrian of the New World. London, Wiley Interscience, 1-78.

Palmer, A.R., 1983. The Decade of North American Geology 1983 geologic time scale. Geology, 11, 503-504.

Palmer, A.R., and Halley, R.B., 1979. Physical stratigraphy and trilobite biostratigraphy of the Carrara Formation (Lower and Middle Cambrian) in the southern Great Basin. United States Geological Survey, Professional Paper 1047, 131p.

Palmer, A.R., and James, N.P., 1980. The Hawke Bay event: a circum-Iapetus regression near the Lower - Middle Cambrian boundary. In Wones, D.R., (Ed.), Proceedings of the Caledonides in the USA, IGCP Project 27: Caledonides Orogen, 1979 Blacksburg, Virginia. Department of Geological Sciences, Virginia Polytechnic Institute and State University, Memoir 2, 15-18.

Park, R.K., 1977. The preservation potential of some recent stromatolites. Sedimentology, 24, 485-506.

Pentecost, A., 1978. Blue-green algae and freshwater carbonate deposits. Proceedings of the Royal Society of London, Section B, Biological Sciences, 200, 43-61.

Pentecost, A., 1985. Association of cyanobacteria with tufa deposits: identity, enumeration and nature of the sheath material revealed by histochemistry. Geomicrobiology Journal, 4, 285-298.

Pentecost, A., and Riding, R., 1986. Calcification in cyanobacteria. In Riding, R., and Leadbearer, B.S.C., (Eds.), Biomineralization in Lower Plants and Animals. Systematics Association Special Volume, 73-90.

Pfeil, R.W., and Read, J.F., 1980. Cambrian platform margin facies, Shady Dolomite, southwestern Virginia, USA. Journal of Sedimentary Petrology, 50, 91-116.

Pitcher, M., 1964. Evolution of Chazyan (Ordovician) reefs of eastern United States and Canada. Bulletin of Canadian Petroleum Geology, 12, 632-691.

Playford, P.E., 1980a. Devonian "Great Barrier Reef" of Canning Basin, Western Australia. American Association of Petroleum Geologists Bulletin, 64, 814-840.

Playford, P.E., 1980b. Environmental controls on the morphology of modern stromatolites at Hamelin Pool, Western Australia. Western Australia Geological Survey, Annual Report 1978, 73-77.

Playford, P.E., and Cockbain, A.E., 1969. Algal stromatolites: deepwater forms in the Devonian of Western Australia. Science, 165, 1008-1010.

Playford, P.E., and Cockbain, A.E., 1976. Modern algal stromatolites at Hamelin Pool, a hypersaline barred basin in Shark Bay, Western Australia. In Walter, M.R., (Ed.), Stromatolites, Developments in Sedimentology 20. Amsterdam, Elsevier, 389-411.

Playford, P.E., Cockbain, A.E., and Druce, E.C., 1976. Devonian stromatolites from the Canning Basin, Western Australia. In Walter, M.R., (Ed.), Stromatolites, Developments in Sedimentology 20. Amsterdam, Elsevier, 543-563.

Pratt, B.R., 1979. The St. George Group (Lower Ordovician), Western Newfoundland: sedimentology, diagenesis and cryptalgal structures. M.Sc. Thesis, Memorial University of Newfoundland, St. John's, 231p.

Pratt, B.R., 1982a. Stromatolite framework of carbonate mud-mounds. Journal of Sedimentary Petrology, 52, 1203-1227.

Pratt, B.R., 1982b. Stromatolite decline - a reconsideration. Geology, 10, 512-515.

Pratt, B.R., 1984. *Epiphyton* and *Renalcis* - diagenetic microfossils from calcification of coccoid blue-green algae. Journal of Sedimentary Petrology, 54, 948-971.

Pratt, B.R., 1987. Blue-green algae: reef builders for all time. Canadian Society of Petroleum Geologists, Reef Research Symposium, Banff, Abstracts, p 48.

Pratt, B.R. and James, N.P., 1982. Cryptalgal-metazoan bioherms of Early Ordovician age in the St. George Group, Western Newfoundland. Sedimentology, 29, 543-569.

Pratt, B.R. and James, N.P., 1986. The St. George Group (Lower Ordovician) of Western Newfoundland: tidal flat island model for carbonate sedimentation in shallow epeiric seas. Sedimentology, 33, 313-343.

Preiss, W.V., 1976. Basic field and laboratory methods for the study of stromatolites. In Walter, M.R., (Ed.), Stromatolites, Developments in Sedimentology 20. Amsterdam, Elsevier, 5-13.

Preiss, W.E., 1977. The biostratigraphic potential of Precambrian stromatolites. Precambrian Research, 5, 207-219.

Purser, B.H., and Loreau, J.P., 1973. Aragonite supratidal encrustations on the Trucial Coast, Persian Gulf. In Purser, B.H., (Ed.), The Persian Gulf. Berlin, Springer-Verlag, 343-376.

Radke, B.M., 1980. Epeiric carbonate sedimentation of the Ninmaroo Formation (Upper Cambrian - Lower Ordovician), Georgina Basin. BMR Journal of Geology and Geophysics, Australia, 5, 183-200.

Radke, B.M., 1981. Lithostratigraphy of the Ninmaroo Formation (Upper Cambrian - Lower Ordovician), Georgina Basin, Queensland and Northern Territory. Bureau of Mineral Resources, Australia, Report 181, Microfilm MF 153, 141p.

Read, J.F., 1980. Carbonate ramp-to-basin transitions and foreland basin evolution, Middle Ordovician, Virginia Appalachians. American Association of Petroleum Geologists Bulletin, 64, 1575-1612.

Read, J.F., 1982. Geometry, facies, and development of Middle Ordovician carbonate buildups, Virginia Appalachians. American Association of Petroleum Geologists Bulletin, 66, 189-209.

Read, J.F., 1983. Field trip guide to Lower Paleozoic carbonate rocks, Roanoke region, Virginia. Society of Economic Paleontologists and Mineralogists, Eastern Section, Field Trip 1983. Department of Geological Sciences, Virginia Polytechnic Institute and State University, 31p.

Read, J.F., 1985. Carbonate platform facies models. American Association of Petroleum Geologists Bulletin, 69, 1-21.

Read, J.F., and Grover, G.A., 1977. Scalloped and planar erosion surfaces, Middle Ordovician limestones, Virginia: analogues of Holocene exposed karst or tidal rock platforms. Journal of Sedimentary Petrology, 47, 956-972.

Read, J.F. and Pfeil, R.W., 1983. Fabrics of allochthonous reefal blocks, Shady Dolomite (Lower to Middle Cambrian), Virginia Appalachians. Journal of Sedimentary Petrology, 53, 761-778.

Rees, M.N., 1986. A fault controlled trough through a carbonate platform: the Middle Cambrian House Range embayment. Geological Society of America Bulletin, 97, 1054-1069.

Rees, M.N., unpublished. Cambrian calcified algal bioherms: *Epiphyton* and *Renalcis* in a lagoonal setting.

Rees, M.N., Brady, M.J., and Rowell, A.J., 1976. Depositional environments of the Upper Cambrian Johns Wash Limestone (House Range, Utah). Journal of Sedimentary Petrology, 46, 38-47.

Rees, M.N., Rowell, A.J., and Pratt, B.R., 1986. Lower Cambrian reefs and associated deposits, Central Transantarctic Mountains. 12th International Sedimentological Congress, Canberra, Abstracts, 255-256.

Reid, R.P., 1987. Nonskeletal peloidal precipitates in Upper Triassic reefs, Yukon Territory (Canada). Journal of Sedimentary Petrology, 57, 893-900.

Revelle, R., and Emery, K.O., 1957. Chemical erosion of beach rock and exposed reef rock. United States Geological Survey, Professional Paper 260-T, 699-709.

Ricketts, B.D., and Donaldson, D.A., 1987. Stromatolite reef development on a mud-dominated platform from the Middle Precambrian Belcher Group of Hudson Bay. Canadian Society of Petroleum Geologists, Reef Research Symposium, Banff, Abstracts, p 103.

Riding, R., 1975. *Girvanella* and other algae as depth indicators. Lethaia, 8, 173-179.

Riding, R., 1977a. Skeletal stromatolites. In Flügel, E., (Ed.), Fossil Algae. Berlin, Springer-Verlag, 57-60.

Riding, R., 1977b. Calcified *Plectonema* (blue-green algae), a Recent example of *Girvanella* from Aldabra Atoll. Palaeontology, 20, 33-46.

Riding, R., 1982. Cyanophyte calcification and changes in ocean chemistry. Nature, 299, 814-815.

Riding, R., 1984. Sea-level changes and the evolution of benthic calcareous algae during the Palaeozoic. Journal Geological Society of London, 141, 547-553.

Riding, R., and Toomey, D.F., 1972. The sedimentological role of *Epiphyton* and *Renalcis* in Lower Ordovician mounds, southern Oklahoma. Journal of Paleontology, 46, 509-519.

Riding, R., and Voronova, L., 1984. Assemblages of calcareous algae near the Precambrian\Cambrian boundary in Siberia and Mongolia. Geological Magazine, 121, 205-210.

Riding, R., and Voronova, L., 1985. Morphological groups and series in Cambrian calcareous algae. In Toomey, D.F., and Nitecki, M.H., (Eds.), Paleoalgology: contemporary research and applications. Berlin, Springer-Verlag, 56-78.

Rigby, J.K., 1966. Evolution of Lower and Middle Ordovician sponge reefs in western Utah (Abstract). Geological Society of America, Special Publication 87, p.137.

Rigby, J.K., 1971. Sponges and reef and related facies through time. Proceedings North American Paleontological Convention, Part J, 1374-1388.

Robison, R.A., 1960. Lower and Middle Cambrian stratigraphy of the eastern Great Basin. In Boettcher, J.W., and Sloan, J.J., (Eds.), Guidebook to the Geology of East Central Nevada. Intermountain Association of Petroleum Geologists, 11th Annual Field Conference, 43-52.

Robison, R.A., 1975. Cambrian Paleontology and depositional environments. Information packet, Geological Society of America Field Trip Nine, Central and Western Utah.

Robison, R.A., Palmer, A.R., and Rees, M.N., 1981. Lower and Middle Cambrian stratigraphy and paleontology of the Central House range, Utah. In Taylor, M.E., and Palmer, A.R., (Eds.), Cambrian Stratigraphy and Paleontology of the Great Basin and vicinity, Western United States. Second International Symposium on the Cambrian System, Guidebook for Field Trip 1, 81-92.

Robison, R.A., and Rees, M.N., 1981. Middle Cambrian stratigraphy and paleontology of the Drum Mountains, western Utah. In Taylor, M.E., and Palmer, A.R., (Eds.), Cambrian Stratigraphy and Paleontology of the Great Basin and vicinity, Western United States. Second International Symposium on the Cambrian System, Guidebook for Field Trip 1, 93-101.

Ross, R.J., 1976. Ordovician sedimentation in the western United States. In Bassett, M.G., (Ed.), The Ordovician System. Cardiff, University of Wales Press and National Museum of Wales, 73-105.

Ross, R.J., 1977. Ordovician paleogeography of the western United States. In Stewart, J.H., Stevens, C.H., and Fritsche, A.E., (Eds.), Paleozoic Paleogeography of the Western United States. Pacific Coast Paleogeography Symposium 1, 19-38.

Ross, R.J., Jaanusson, V., and Friedman, I., 1975. Lithology and origin of Middle Ordovician calcareous mud-mounds at Meiklejohn Peak, southern Nevada. United States Geological Survey, Professional Paper 871, 48p.

Ross, R.J., and James, N.P., 1987. Brachiopod biostratigraphy of the middle Ordovician Cow Head and Table Head groups, western Newfoundland. Canadian Journal of Earth Sciences, 24, 70-95.

Ross, R.J., and others, 1982. The Ordovician System in the United States. International Union of Geological Sciences, Publication 12, 73p.

Rowell, A.J., and Rees, M.N., 1981. Basinal deposits and outer shelf basins in the Cambrian of Nevada and Utah. In Taylor, M.E., (Ed.), Short Papers for the Second International Symposium on the Cambrian System. United States Geological Survey, Open File Report 81-743, 188-192.

Rubin, D.M., and Friedman, G.M., 1977. Intermittently emergent shelf carbonates: an example from the Cambro-Ordovician of eastern New York State. Sedimentary Geology, 19, 81-106.

Runnegar, B., 1982. The Cambrian explosion; animals or fossils? Journal Geological Society of Australia, 29, 395-411.

Ruppel, S.C., and Walker, K.R., 1982. Sedimentology and distinction of carbonate buildups: Middle Ordovician, east Tennesse. Journal of Sedimentary Petrology, 52, 1055-1071.

Saller, A.H., 1986. Radiaxial calcite in Lower Miocene strata, subsurface Enewetak Atoll. Journal of Sedimentary Petrology, 56, 743-762.

Sandberg, P.A., 1985. Aragonite cements and their occurrence in ancient limestones. In Schneidermann, N., and Harris, P.M., (Eds.), Carbonate Cements. Society of Economic Paleontologists and Mineralogists, Special Publication 36, 33-57.

Sanderson, D.J., and Donovan, R.N., 1974. The vertical packing of shells on some Recent beaches. Journal of Sedimentary Petrology, 44, 680-688.

Sanford, B.V., 1977. Ordovician rocks of Melville Peninsula, southeastern District of Franklin. Geological Survey of Canada Bulletin, 269, 7-21.

Schmitt, M., 1978. Stromatolites from the Tiout section, Precambrian-Cambrian boundary beds, Anti-Atlas, Morocco. Geological Magazine, 115, 95-100.

Schmitt, M., 1979. The section of Tiout (Precambrian\Cambrian boundary beds, Anti-Atlas, Morocco): stromatolites and their biostratigraphy. Arbeiten aus dem Paläontologischen Institut Wurzburg, 2, 188p.

Schmitt, M., and Monniger, W., 1977. Stromatolites and thrombolites in Precambrian\Cambrian boundary beds of the Anti-Atlas, Morocco: preliminary results. In Flügel, E.,(Ed.), Fossil Algae. Berlin, Springer-Verlag, 80-85.

Schopf, J.W., Hayes, J.M., and Walter, M.R., 1983. Evolution of Earth's earliest ecosystem: recent progress and unsolved problems. In Schopf, J.W., (Ed.), Earth's Earliest Biosphere. Princeton, Princeton University Press, 361-384.

Schroeder, J.H., 1972. Fabrics and sequences of submarine carbonate cements in Holocene Bermuda cup reefs. Geologische Rundschau, 61, 708-730.

Schuchert, C., and Dunbar, C.O., 1934. Stratigraphy of western Newfoundland. Geological Society of America, Memoir 1, 123p.

Schwarz, H.U., Einsele, G., and Herm, D., 1975. Quartz-sandy, grazing-contoured stromatolites from coastal embayments of Mauritanian, West Africa. Sedimentology, 22, 539-561.

Scotese, C.R., 1986. Phanerozoic reconstructions: a new look at the assembly of Asia. University of Texas Institute for Geophysics, Technical Report 56, 54p.

Scotese, C.R., Bambach, R.K., Barton, C., Van der Voo, R, and Ziegler, A.M., 1979. Paleozoic base maps. Journal of Geology, 87, 217-277.

Semikhatov, M.A., 1976. Experience in stromatolite studies in the USSR. In Walter M.R., (Ed.), Stromatolites, Developments in Sedimentology 20. Amsterdam, Elsevier, 337-358.

Semikhatov, M.A., Gebelein, C.D., Cloud, P., Awramik, S.M., and Benmore, W.C., 1979. Stromatolite morphogenesis - progress and problems. Canadian Journal of Earth Sciences, 16, 992-1015.

Sepkoski, J.J., 1981. The uniqueness of the Cambrian fauna. In Taylor M.E., (Ed.), Short Papers for the Second International Symposium on the Cambrian System. United States Geological Survey, Open File Report 81-743, 203-207.

Sepkoski, J.J., 1982. Flat-pebble conglomerates, storm deposits, and the Cambrian bottom fauna. In Einsele, G., and Seilacher, A., (Eds.), Cyclic and Event Stratigraphy. Berlin, Springer-Verlag, 377-385.

Shapolalova, I.G., 1974. Stratigrafiya i stromatolity rifeishkikh otlozhenii severnoi chasti Yudomo-Maiskogo progiba. Akademii Nauk SSSR, Sibirskoe Otdelenie Yakutskii Filial Institut Geologii i Geofiziki, Novosibirsk, 140p.

Sheehan, P.S., 1985. Reefs are not so different - they follow the evolutionary pattern of level-bottom communities. Geology, 13, 46-49.

Shenfil, V.Yu., 1983. The problem of the appearance of the skeleton in the oldest organisms. Akademii Nauk SSSR Earth Science Section, 272, 228-230.

Shinn, E.A., 1968. Practical significance of birdseye structures in carbonate rocks. Journal of Sedimentary Petrology, 38, 215-223.

Shinn, E.A., 1983. Birdseye, fenestrae, shrinkage pores, and loferites: a reconsideration. Journal of Sedimentary Petrology, 53, 619-628.

Shinn, E.A., Robbin, D.M., Lidz, B.H., and Hudson, J.H., 1983. Influence of deposition and early diagenesis on porosity and chemical compaction in two Paleozoic buildups: Mississippian and Permian age rocks in the Sacramento Mountains, New Mexico. Society of Economic Paleontologists and Mineralogists, Core Workshop 4, 182-222.

Siedlecka, A., 1972. Length-slow chalcedony and relics of sulphates - evidences of evaporitic environments in the Upper Carboniferous and Permian beds of Bear Island, Svalbard. Journal of Sedimentary Petrology, 42, 812-816.

Simkiss, K., 1964. Phosphates as crystal poisons of calcification. Biological Review, 39, 487-505.

Sloss, L.L., 1963. Sequences in the cratonic interior of North America. Geological Society of America Bulletin, 74, 94-114.

Soudry, D., 1987. Ultra-fine structure and genesis of the Campanian Negev high-grade phosphorites (southern Isreal). Sedimentology, 34, 641-660.

Soudry, D., and Southgate, P.N., in press. Utrastructure of a Middle Cambrian primary non-pelletal phosphorite and its early transformation into phosphate vadoids: Georgina Basin, Australia. Journal of Sedimentary Petrology.

Southgate, P.N., 1982. Cambrian skeletal halite crystals and experimental analogues. Sedimentology, 29, 391-407.

Stevens, R.K., and James, N.P., 1976. Large sponge-like reef mounds from the Lower Ordovician of west Newfoundland. Geological Society of America, Abstracts and Programs, 8, p 1122.

Stolz, J.F., 1983. Fine structure of the stratified community at Laguna Figueroa, Baja California, Mexico. 1 Methods of *in situ* study of the laminated sediments. Precambrian Research, 20, 479-492.

Sweeting, M.M., 1972. Karst Landforms. New York, Macmillan, 362p.

Taylor, G.F., 1975. The occurrence of monohydrocalcite in two small lakes in the south east of South Australia. American Mineralogist, 60, 690-697.

Taylor, M.E., Landing, E., and Gillett, S.L., 1981. The Cambrian-Ordovician transition in the Bear Range, Utah-Idaho: a preliminary evaluation. In Taylor, M.E., (Ed.), Short Papers for the Second International Symposium on the Cambrian System. United States Geological Survey, Open File Report 81-743, 222-227.

Taylor, M.E., and Repetski, J.E., 1985. Early Ordovician eustatic sea level changes in northern Utah and southeastern Idaho. In Kerns, G.J., and Kerns, R.L., (Eds.), Organic patterns and stratigraphy of north-central Utah and southeastern Idaho. Utah Geological Association, Publication 14, 1985 Field Conference Guidebook, 3-42.

Tebbut, G.E., Conley, C.D., and Boyd, D.W., 1965. Lithogenesis of a distinctive carbonate rock fabric. In Parker, R.B., (Ed.), Contributions to Geology, University of Wyoming, 1-13.

Thomsen, E., and Vorren, T.O., 1984. Pyritization of tubes and burrows from Late Pleistocene continental shelf sediments off North Norway. Sedimentology, 31, 481-492.

Toomey, D.F., 1970. An unhurried look at a Lower Ordovician mound horizon, southern Franklin Mountains, West Texas. Journal of Sedimentary Petrology, 40, 1318-1334.

Toomey, D.F., and Babcock, J.A., 1983. Precambrian and Paleozoic algal carbonates, West Texas - Southern New Mexico. Colorado School of Mines, Professional Publication 11, 345p.

Toomey, D.F., and Cys, J.M., 1979. Community succession in small bioherms of algae and sponges in the Lower Permian of New Mexico. Lethaia, 12, 65-75.

Toomey, D.F., and Klement, K.W., 1966. A problematical microorganism from the El Paso Group (Lower Ordovician) of west Texas. Journal of Paleontology, 40, 1304-1311.

Toomey, D.F., and Nitecki, M.H., 1979. Organic buildups in the Lower Ordovician (Canadian) of Texas and Oklahoma. Field Museum of Natural History, Fieldiana Geology, 2, 181p.

Toomey, D.F., and Nitecki, M.H., (Eds.), 1985. Paleoalgology: Contemporary Research and Applications. Berlin, Springer-Verlag, 376p.

Toomey, D.F., Wilson, J.A., and Rezak, R., 1977. Evolution of Yucca Mound Complex, Late Pennsylvanian phylloid-algal buildups, Sacramento Mountains, New Mexico. American Association of Petroleum Geologists Bulletin, 61, 2115-2133.

Tucker, M., 1984. Untitled. In Monty, C.L.V., (Ed.), Stromatolite Newsletter, 11, p.79.

Tsein, H.H., 1985. Algal-bacterial origin of micrites in mud mounds. In Toomey, D.F., and Nitecki, M.H., (Eds.), Paleoalgology: Contemporary Research and Applications. Berlin, Springer-Verlag, 290-296.

Von der Borch, C.C., Bolton, B., and Warren, J.K., 1977. Environmental setting and microstructure of subfossil lithified stromatolites associated with evaporites, Marion Lake, South Australia. Sedimentology, 24, 693-708.

Walkden, G.M., 1974. Palaeokarstic surfaces in the Upper Visean (Carboniferous) limestones of the Derbyshire Block, England. Journal of Sedimentary Petrology, 44, 1232-1247.

Walker, K.R., and Alberstadt, L.P., 1975. Ecological succession as an aspect of structure in fossil communities. Paleobiology, 1, 238-257.

Walter, L.M., 1986. Relative efficiency of carbonate dissolution and precipitation during diagenesis: a progress report on the role of solution chemistry. In Gautier, D.L., (Ed.), Roles of Organic Matter in Mineral Diagenesis. Society of Economic Paleontologists and Mineralogists Special Publication, 38, 1-12.

Walter, M.R., 1972. Stromatolites and the biostratigraphy of the Australian Precambrian and Cambrian. The Palaeontological Association of London, Special Papers in Palaeontology, 11, 190p.

Walter, M.R., (Ed.), 1976a. Stromatolites. Developments in Sedimentology 20. Amsterdam, Elsevier, 790p.

Walter, M.R., 1976b. Glossary of selected terms. In Walter, M.R., (Ed.), Stromatolites. Developments in Sedimentology 20, Appendix 1. Amsterdam, Elsevier, 687-692.

Walter, M.R. and Heys, G.R., 1985. Links between the rise of the metazoa and the decline of stromatolites. Precambrian Research, 29, 149-174.

Walter, M.R., Bauld, J., and Brock, T.D., 1976. Microbiology and morphogenesis of columnar stromatolites (*Conophyton*, *Vacerrilla*) from hot springs in Yellowstone National Park. In Walter, M.R., (Ed.), Stromatolites. Developments in Sedimentology 20. Amsterdam, Elsevier, 273-310.

Warren, J.K., 1982. The hydrobiological significance of Holocene tepees, stromatolites and boxwork limestones in coastal salinas in South Australia. Journal of Sedimentary Petrology, 52, 1171-1201.

Webb, G.E., 1987. Late Mississippian thrombolite bioherms from the Pitkin Formation of northern Arkansas. Geological Society of America Bulletin, 99, 686-698.

Webby, B.D., 1978. History of the Ordovician continental platform shelf margin of Australia. Journal of the Geological Society of Australia, 25, 41-63.

Webby, B.D., and Packham, G.H., 1982. Stratigraphy and regional setting of the Cliefdon Caves Limestone Group (Late Ordovician), central-western New South Wales. Journal of the Geological Society of Australia, 29, 297-317.

Wells, A.T., Forman, D.J., Ranford, L.C., and Cook, P.J., 1970. Geology of the Amadeus Basin. Bureau of Mineral Resources, Australia, Bulletin, 100, 222p.

Wentworth, C.K., 1922. A scale of grade and class terms for clastic sediments. Journal of Geology, 30, 377-392.

Whisonant, R.C., 1987. Paleocurrent and petrographic analysis of imbricate intraclasts in shallow-marine cabonates, Upper Cambrian, southwestern Virginia. Journal of Sedimentary Petrology, 57, 983-994.

Wilkinson, B.H., Janecke, S.V., and Brett, C.C., 1982. Low-magnesium calcite marine cement in middle Ordovician hardgrounds from Kirkfield, Ontario. Journal of Sedimentary Petrology, 52, 47-57.

Williams, H., 1979. Appalachian Orogen in Canada. Canadian Journal of Earth Sciences, 16, 792-807.

Williams, H. and Stevens, R.K., 1974. The ancient continental margin of eastern North America. In Burk, C.A., and Drake, C.L., (Eds.), The Geology of Continental Margins. New York, Springer-Verlag, 781-796.

Williams, H, and Hiscott, R.N., 1987. Definition of the Iapetus rift-drift transition in western Newfoundland. Geology, 15, 1044-1047.

Williams, S.H., Boyce, W.D., and James, N.P., 1987. Graptolites from the Lower-Middle Ordovician St. George and Table Head Groups, western Newfoundland, and their correlations with trilobites, brachiopods, and conodont zones. Canadian Journal of Earth Sciences, 24, 456-470.

Wilson, J.A., 1975. Carbonate Facies in Geologic History. New York, Springer-Verlag, 471p.

Wolf, K.H., 1965a. Gradational sedimentary products of calcareous algae. Sedimentology, 5, 1-37.

Wolf, K.H., 1965b. Petrogenesis and paleoenvironment of Devonian algal limestones of New South Wales. Sedimentology, 4, 113-178.

Wolf, K.H., 1965c. "Grain-diminution" of algal colonies to micrite. Journal of Sedimentary Petrology, 35, 420-427.

Wray, J.L., 1977. Calareous Algae. Developments in Paleontology and Stratigraphy 4. Amsterdam, Elsevier, 185p.

Wright, L.A., Williams, E.G., and Cloud, P., 1978. Algal and cryptalgal structures and platform envirinments of the late pre-Phanerozoic Noonday Dolomite, eastern California. Geological Society of America Bulletin, 89, 321-333.

Wright, S.C., 1984. Untitled. In Monty, C.L.V., (Ed.), Stromatolite Newsletter, 11, p.82.

Wright, V.P., 1982. The recognition and interpretation of paleokarst: two examples from the Lower Carboniferous of South Wales. Journal of Sedimentary Petrology, 52, 83-94.

Wright, V.P., and Myall, M., 1981. Organic-sediment interactions in stromatolites; an example from the Upper Triassic of south west Britain. In Monty, C.L.V., (Ed.), Phanerozoic Stromatolites. Berlin, Springer-Verlag, 74-84.

Wright, V.P., and Wright, J.M., 1985. A stromatolite built by a *Phormidium*-like alga from the Lower Carboniferous of South Wales. In Toomey, D.F., and Nitecki, M.H., (Eds.), Paleoalgology: Contemporary Research and Applications. Berlin, Springer-Verlag, 40-54.

Young, B.C., 1978. The petrology and depositional environments of the Middle Cambrian Wirrealpa and Aroona Creek Limestones (South Australia). Journal of Sedimentary Petrology, 48, 63-74.

Zamarreno, I., 1977. Early Cambrian algal carbonates in southern Spain. In Flügel, E.(Ed.), Fossil Algae. Berlin, Springer-Verlag, 360-365.

Zamarreno, I., 1981. Lower Cambrian stromatolites from northwest Spain and their palaeoenvironmental significance. In Monty, C.L.V., (Ed.), Phanerozoic Stromatolites. Berlin, Springer-Verlag, 5-18.

Zamarreno, I., and Debrenne, F., 1977. Sédimentologie et biologie des constructions organogènes du Cambrien inférieur du Sud de l'Espagne. B.R.G.M. Memoire, 89, 49-61.

Ziegler, A.M., Scotese, C.R., McKerrow, W.S., Johnson, M.E., and Bambach, R.K., 1979. Paleozoic paleogeography. Annual Review of Earth and Planetary Science, 7, 473-502.

Ziegler, A.M., Bambach, R.K., Parrish, J.T., Barrett, S.F., Gierlowski, E.H., Parker, W.C., Raymond, A., and Sepkoski, J.J., 1981. Paleozoic biogeography and climatology. In Nickolas, K.J.,(Ed.), Paleobotany, Paleoecology, and Evolution, 2, 231-266.

Zhuravlev, A.Y., 1988. Cambrian organogenous build-ups of Siberia. Fifth International Symposium on Fossil Cnidaria, Brisbane, unpublished oral presentation.

THE STRUCTURE AND ORIGIN OF CAMBRO-ORDOVICIAN THROMBOLITES WESTERN NEWFOUNDLAND

VOLUME 2

by

John Michael Kennard

TABLE OF CONTENTS

LIST OF PLATES

PLATE 1

Cape Ann thrombolite-stromatolite complex
Horizon A, Port au Port Peninsula

Megastructure - 1

Overview of the basal thrombolite zone (T), and lower portion of the central stromatolitic thrombolite zone (ST).

PLATE 1

PLATE 2

Cape Ann thrombolite-stromatolite complex
Horizon A, Port au Port Peninsula

Megastructure - 2

A - Upper stromatolite zone truncated by planar erosion surface (P).

B - Plan view of planar erosion surface that truncates hemispheroidal stromatolites at top of stromatolite zone. Note small pyritic ?borings (arrows).

C - Pocket of thin-bedded detrital sediment encased within stromatolitic thrombolite; central stromatolitic thrombolite zone.

D - Large ellipsoidal thrombolite mound enveloped by dark crust of botryoidal marine cement (MC); basal thrombolite zone.

E - Thrombolite pedestal (T) abutted and onlapped (arrows) by inter-biohermal sediments; basal thrombolite zone.

F - Flank of small bioherm overlain by inter-biohermal sediments that have slumped off the crest of the bioherm (direction of slump movement shown by arrow); basal thrombolite zone.

Scales: Hammer 30 cm, lens cap 5 cm.

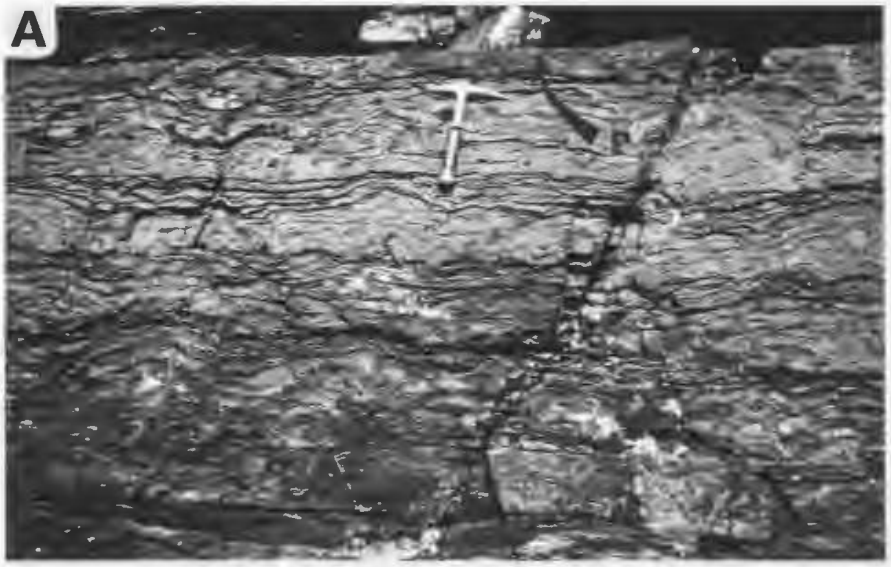
A


B


C


D
MC


E

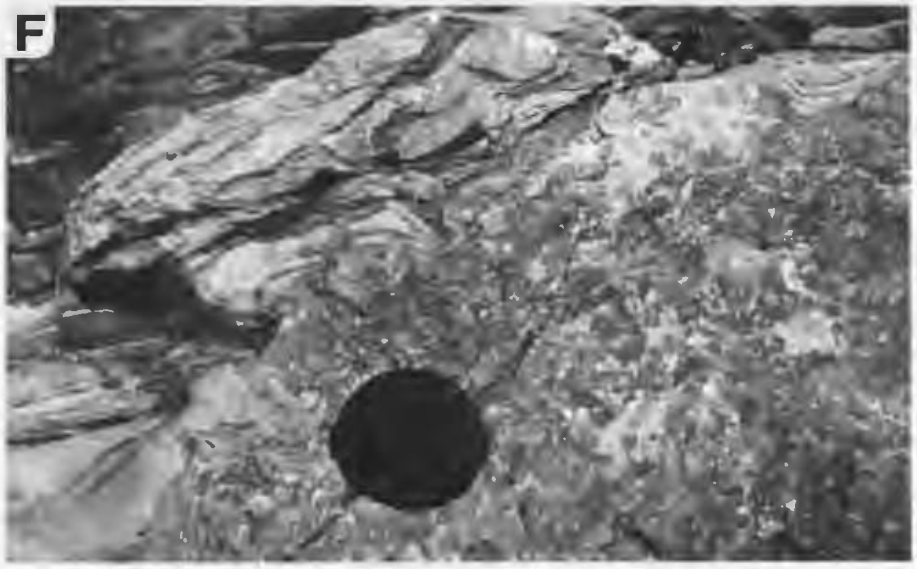
F

PLATE 3

Cape Ann thrombolite-stromatolite complex
Horizon A, Port au Port Peninsula

Mesostructure - 1

A - Finely clotted fabric of basal thrombolite zone, showing pendant grape-like clusters of dark thromboids and light coloured inter-framework lime-mudstone.

B - Vertical slab of basal thrombolite zone. Dark thromboids are encrusted by concentrically banded botryoidal marine cement and hemispheroidal stromatoids (arrows; cement and stromatoid layers can only be differentiated in thin section). Light coloured inter-framework lime-mudstone. Sample CA-6.

C - Wavy and linked hemispheroidal stromatoids, upper stromatolite zone.

D - Vertical slab of upper stromatolite zone. Thick light coloured stromatoids locally swell in thickness to form pustular protuberances and linked or isolated columns. Sample CA-12.

Scales: lens cap 5 cm, scale bars 2 cm.

PLATE 3

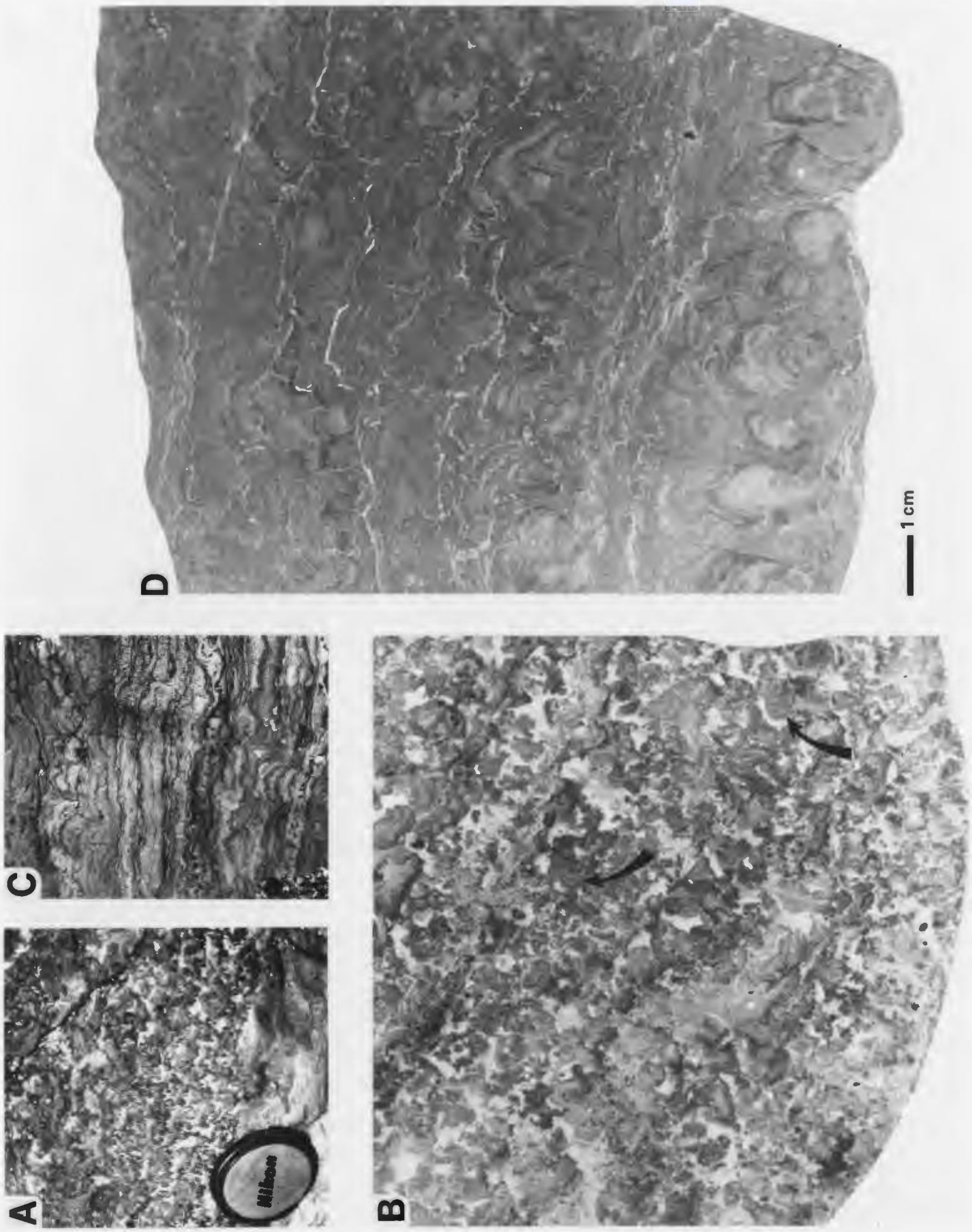

PLATE 4

Cape Ann thrombolite-stromatolite complex
Horizon A, Port au Port Peninsula

Mesostructure - 2

A,B - Vertical serial slabs of central stromatolitic thrombolite zone. Clusters of dark lobate and saccate thromboids are encrusted by hemispheroidal, columnar and undulose stromatoids (s). Thromboid-stromatoid framework is infilled by silty peloid-skeletal wackestone (w), light coloured lime-mudstone (m), and pervasively dolomitized sediment (d). Sample CA-1A.

C - Weakly layered fabric of central stromatolitic thrombolite zone as seen on natural outcrop surface.

Scales: lens cap 5 cm, scale bars 2 cm.

PLATE 4

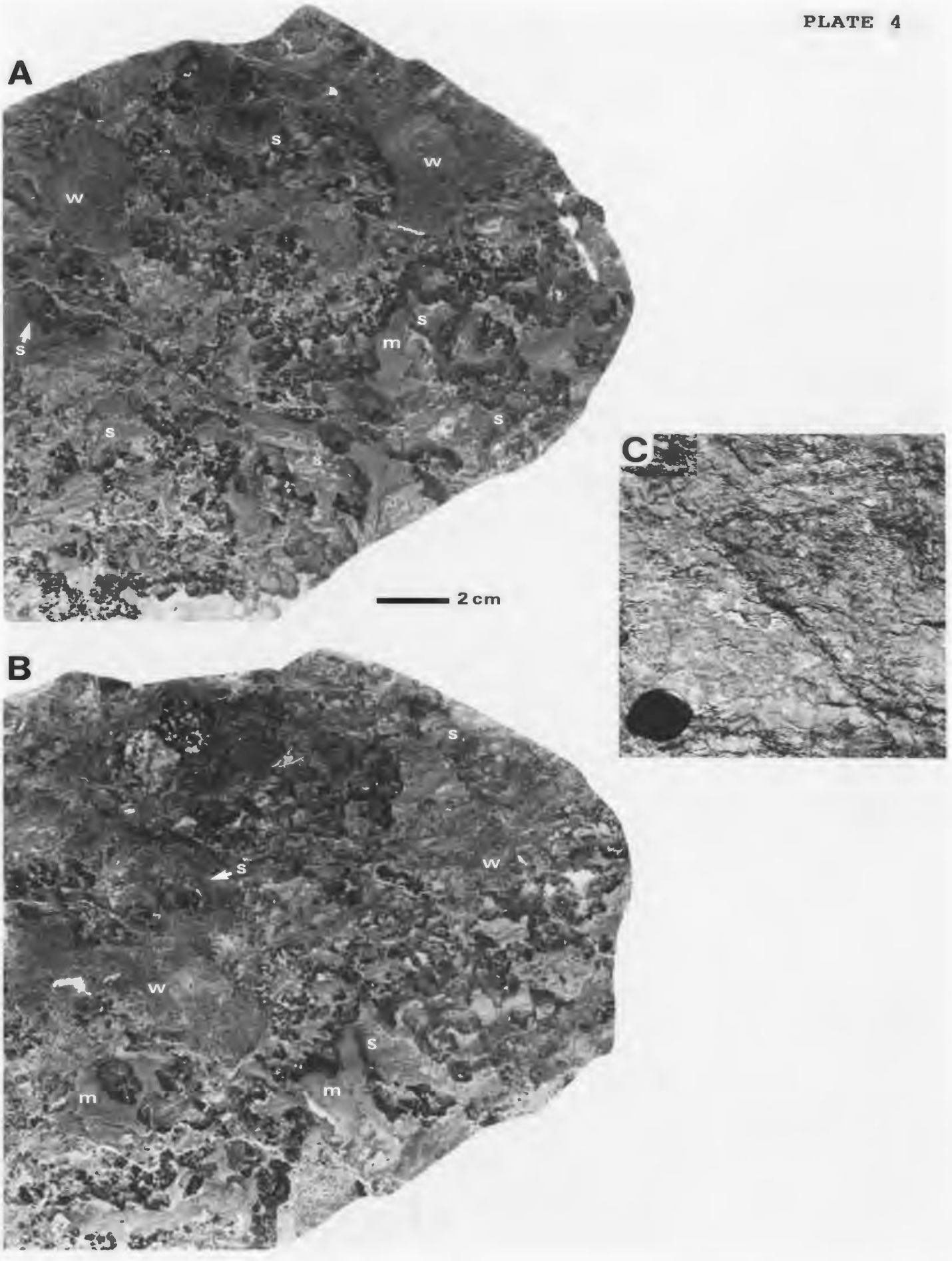

PLATE 5

Cape Ann thrombolite-stromatolite complex
Horizon A, Port au Port Peninsula

Microstructure of thromboids

A - Thromboids with massive to weakly clotted lobate microstructure encased within microspar; central stromatolitic thrombolite zone. Note thin sub-isopachous rims of fibrous marine cement (arrows) around thromboids. Sample CA-1B-H, horizontal section.

B - Thromboids with saccate lobate microstrucure encased within slightly silty microspar; central stromatolitic thrombolite zone. Sample CA-1B-H, horizontal section.

C - Pendant thromboid rimmed by isopachous fibrous marine cement (arrow), and encased within silty micrite; basal thrombolite zone. Cluster of thromboids in upper portion of photo have been replaced by a mosaic of turbid microspar in which individual relict saccate forms are visible. Sample CA-6.

D - Saccate and massive lobate thromboids (left) encrusted by fascicular-optic botryoidal marine cement (arrows); central stromatolitic thrombolite zone. Inter-framework silty micrite visible at right. Sample CA-1A.

Scale bars 1 mm.

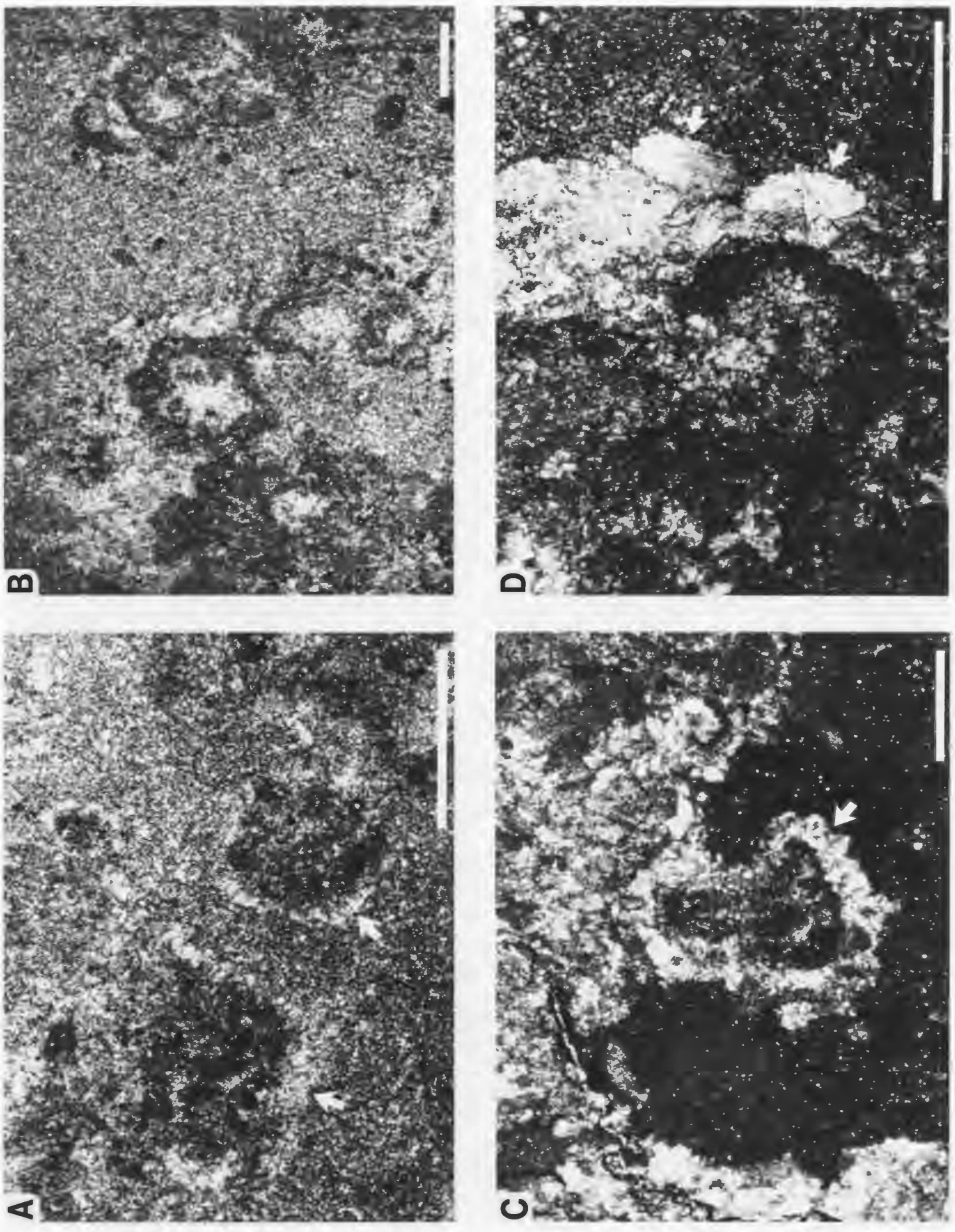
B
D
A
C

PLATE 6

Cape Ann thrombolite-stromatolite complex
Horizon A, Port au Port Peninsula

Microstructure of stromatoids

A - Weak streaky microstructure of columnar stromatoid; central stromatolitic thrombolite zone. Note spar-filled burrow at left. Sample CA-2.

B - Variegated grumous (G), streaky grumous (SG), silty peloidal (P) and mottled (M) microstructure of wavy and columnar stromatoids; upper stromatolite zone. Note sediment-filled burrow (arrow) that disrupts silty peloidal laminae at lower left. Sample CA-12.

C - Grumous (G) grading to streaky grumous (SG) and filamentous (F) microstructure of pustular stromatoid; upper stromatolite zone. Core of pustule has a silty peloidal microstructure. Sample CA-12.

D - Magnified view of filamentous microstructure shown in C. Sample CA-12.

E - Streaky silty peloidal microstructure of pimpled stromatoids that encrust the planar erosion surface at the top of the complex. Note interlayered mamillate crusts of fibrous marine cement (arrows), and silty peloid-skeletal sediment that overlies the pimpled stromatoid crust. Sample CA-15.

Scale bars 1 mm.

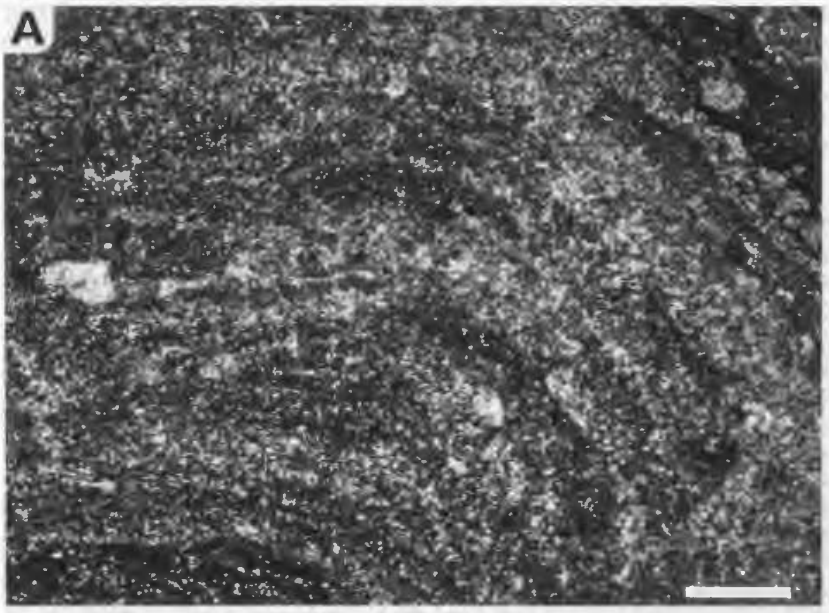
A

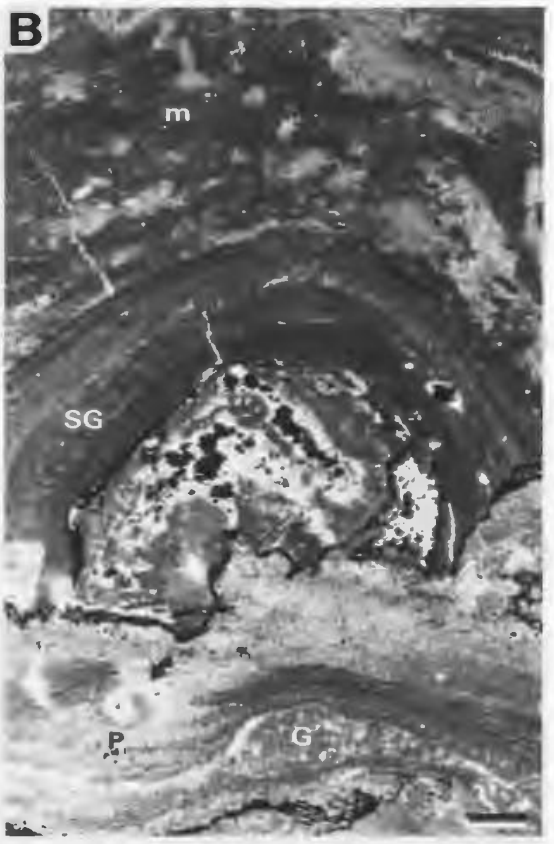
B
m
SG
P
G

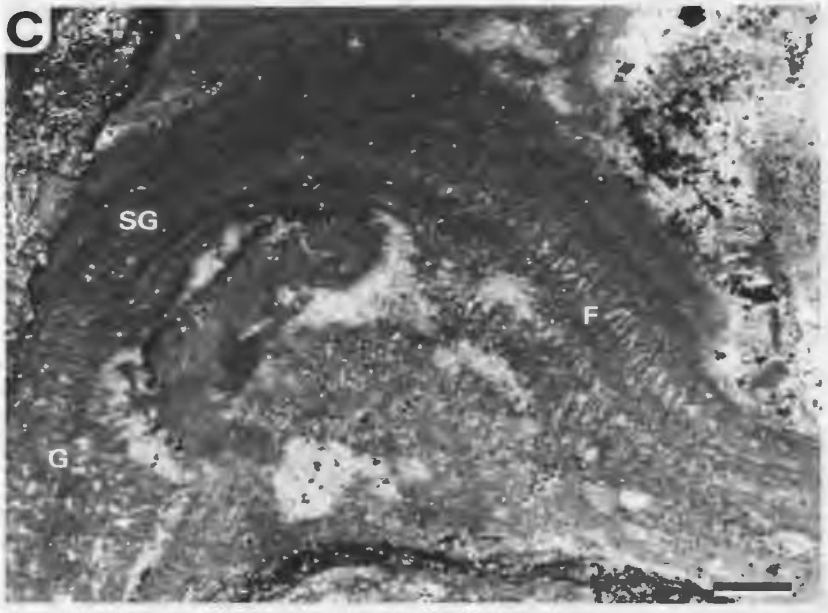
C
SG
F
G


D

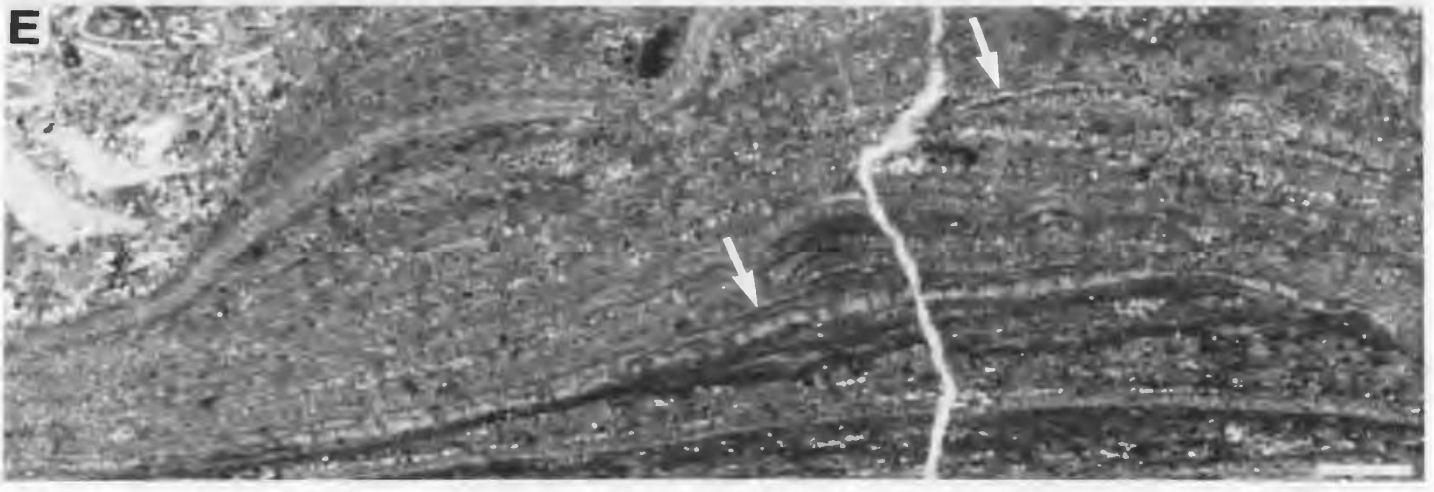
E

PLATE 7

Cape Ann thrombolite-stromatolite complex
Horizon A, Port au Port Peninsula

Microstructure of marine cements - 1

A,B - Divergent-radial botryoids with prominent curved cross-twin lamellae; central stromatolitic thrombolite zone. A) plane polarized light, B) crossed polarized light. Note patchy sweeping extinction pattern in B. Sample CA-10A-2.

C - Nested fascicular-optic botryoids within hemispheroidal stromatoid; central stromatolitic thrombolite zone. Each botryoid comprises a single calcite crystal with smooth sweeping extinction. Plane polarized light. Sample CA-3.

D - Vertical (V) and horizontal (H) sections of nested fascicular-optic botryoids within neomorphic spar; central stromatolitic thrombolite zone. Note turbid appearance due to numerous micro-inclusions and single set of curved cross-twin lamellae within each botryoid. Plane polarized light. Sample CA-3.

E - Micro-dolomite inclusions (arrows) within fascicular-optic botryoid; central stromatolitic thrombolite zone. Note curved cross-twin lamellae. Plane polarized light, scale bar 20 μm. Sample CA-3.

Scale bars 0.5 mm (except E).

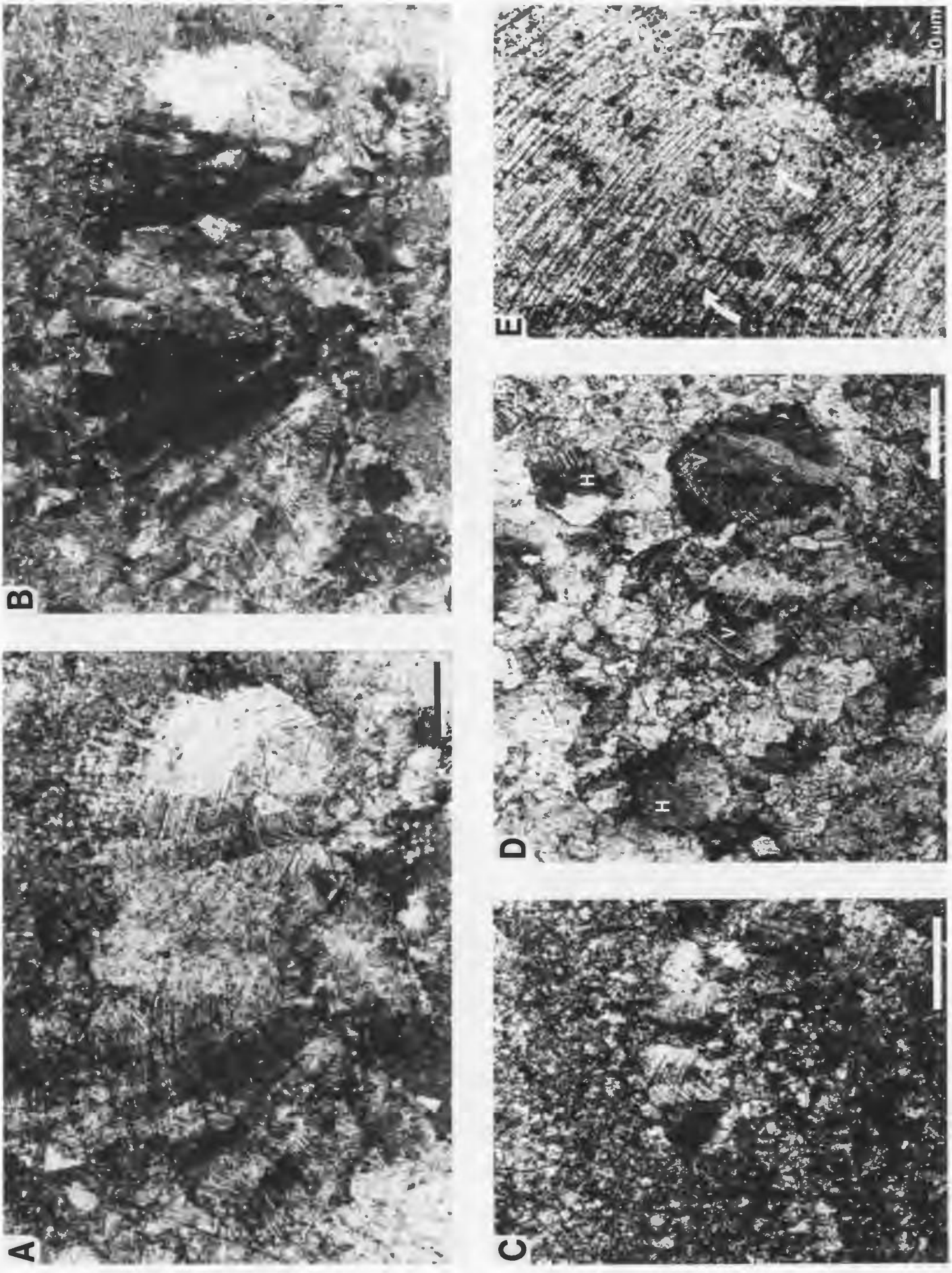
A
B
C
D
H
H
V
E
0.1 μm

PLATE 8

Cape Ann thrombolite-stromatolite complex
Horizon A, Port au Port Peninsula

Microstructure of marine cements - 2

A,B - Cluster of lobate thromboids (T) replaced by turbid microspar, and encrusted by pendant (1) fibrous-concentric, and (2) divergent-radial botryoidal marine cement; lower thrombolite zone. A) plane polarized light, B) crossed polarized light. Note inter-framework mudstone (M). Sample CA-6.

C,D - Mamillate layers of divergent-radial marine cement interlayered with stromatoids and\or detrital sediment layers; central stromatolitic thrombolite zone. A) plane polarized light, B) crossed polarized light. Sample CA-10A-2.

E - Tubular boring filled with microspar after lime-mud; central stromatolitic thrombolite zone. Note truncation of fascicular-optic botryoids (arrows) at margins of the boring. Sample CA-3.

Scale bars 1 mm.

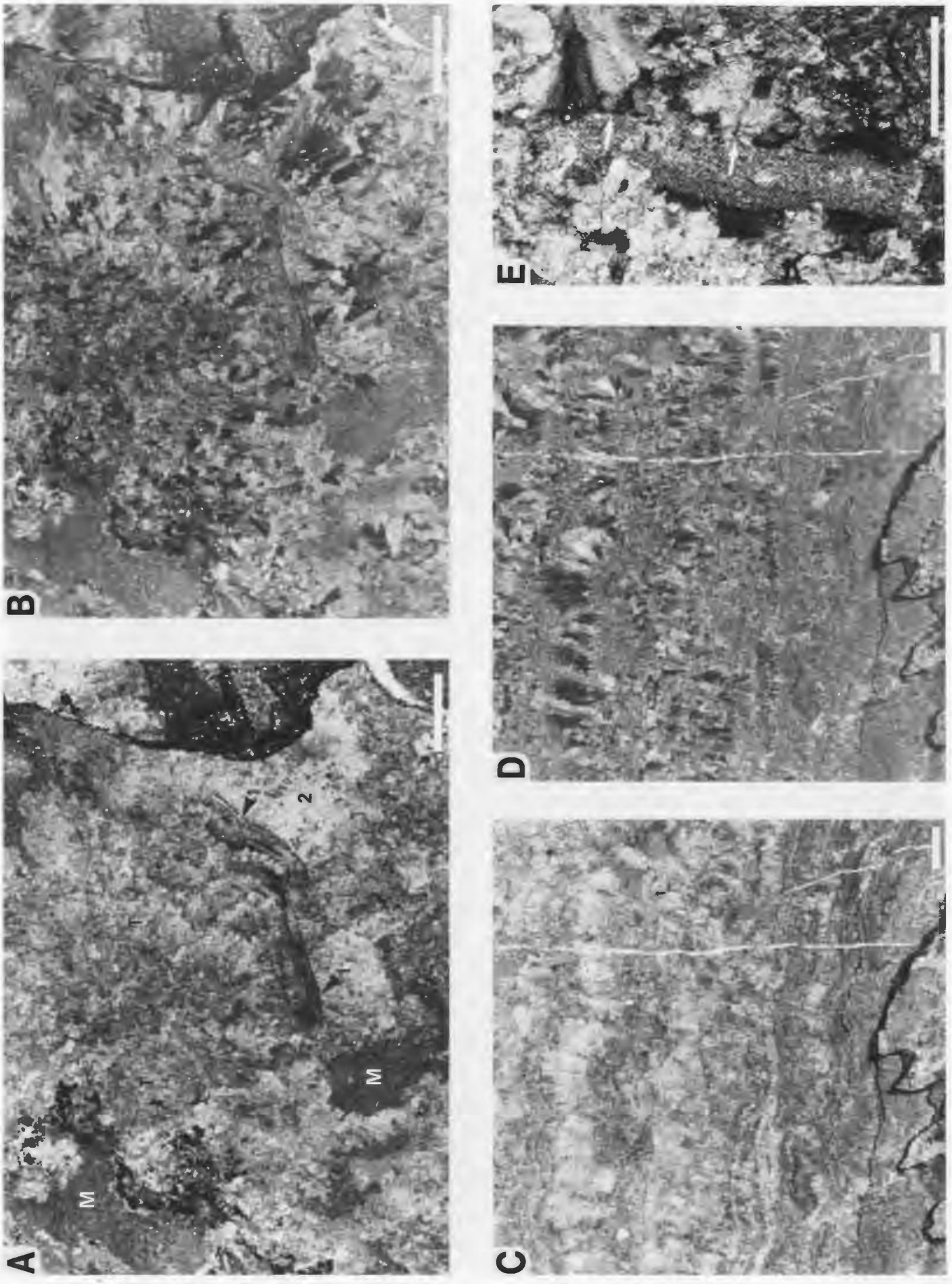
A
M
2
M
B
C
D
E

PLATE 9

Cape Ann thrombolite-stromatolite complex
Horizon A, Port au Port Peninsula

Bed A: Mesostructure and Microstructure

A - Vertical slab showing indistinctly laminated stromatoid columns, clusters of dark lobate and saccate thromboids (base of slab), and burrow-mottled peloidal and intraclastic inter-framework sediment. Note numerous burrows (arrows) within stromatoid columns. Sample CA-7.

B - Cerebroid fabric evident on upper surface of bioherm. Lens cap 5 cm.

C - Massive to diffuse grumous microstructure of columnar stromatoids. Note fragments of columns and abundant quartz silt within inter-framework sediment. Scale bar 1 mm. Sample CA-8.

D - Mottled microstructure of stromatoid columns. Note micritic selvage (arrow) that partially rims the column on the right; the column on the left is bounded by a stylolite. Scale bar 1 mm. Sample CA-7.

E - Mottled microstructure of stromatoid column. Scale bar 1 mm. Sample CA-7.

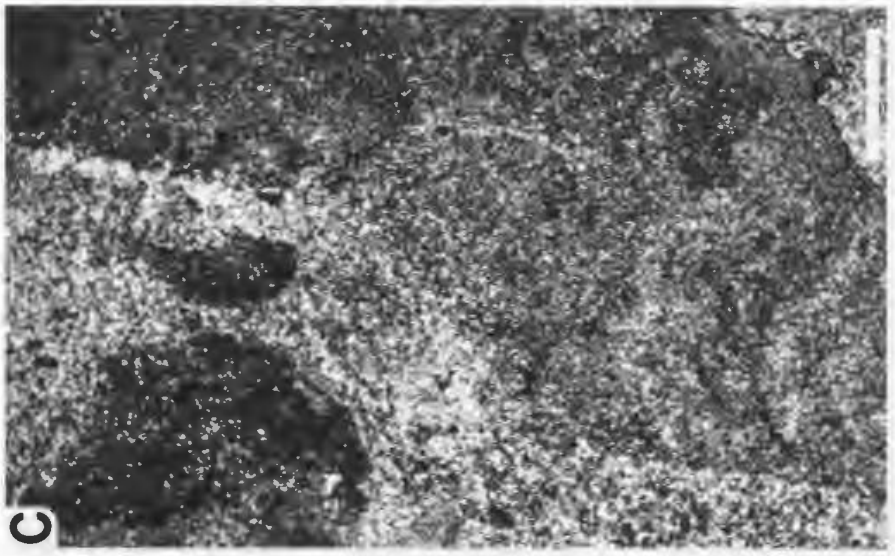
C

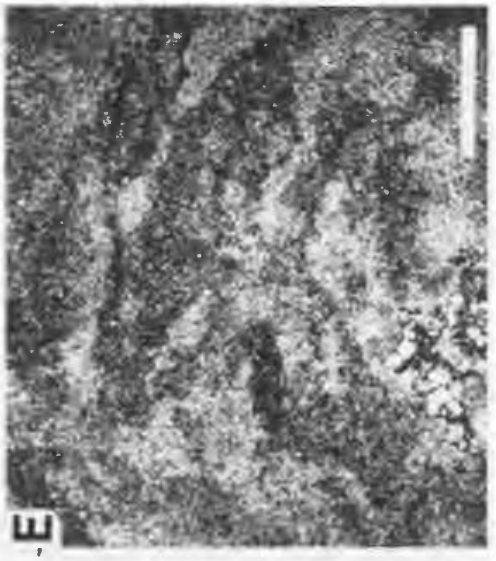
E

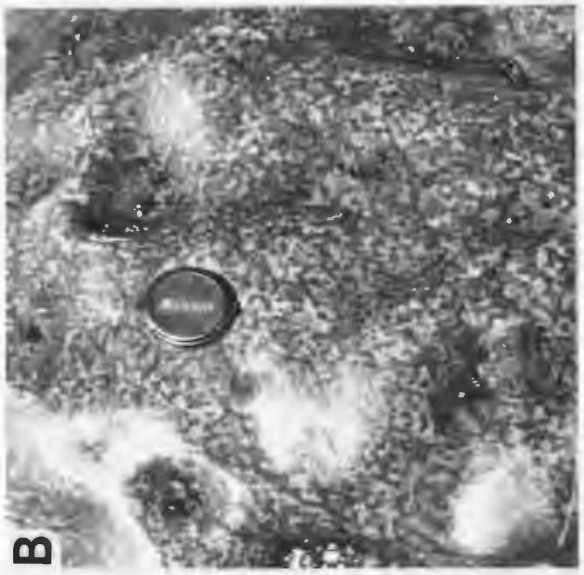
B

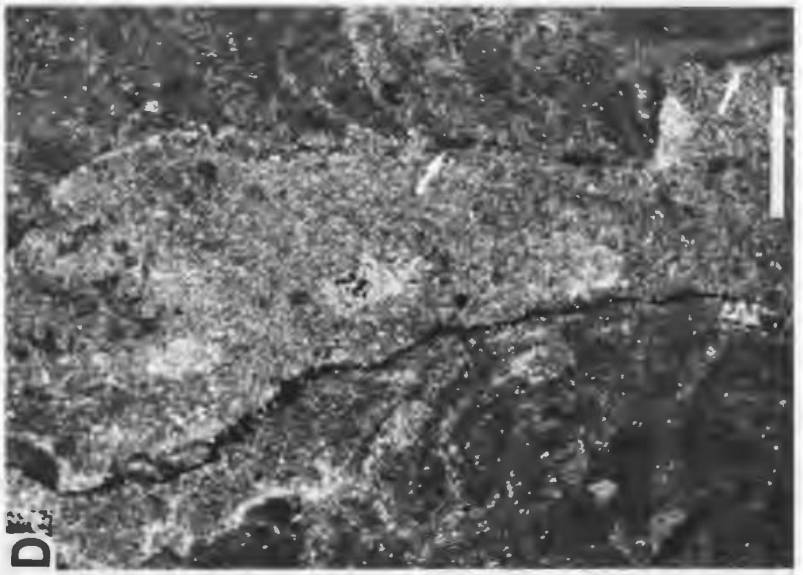
D

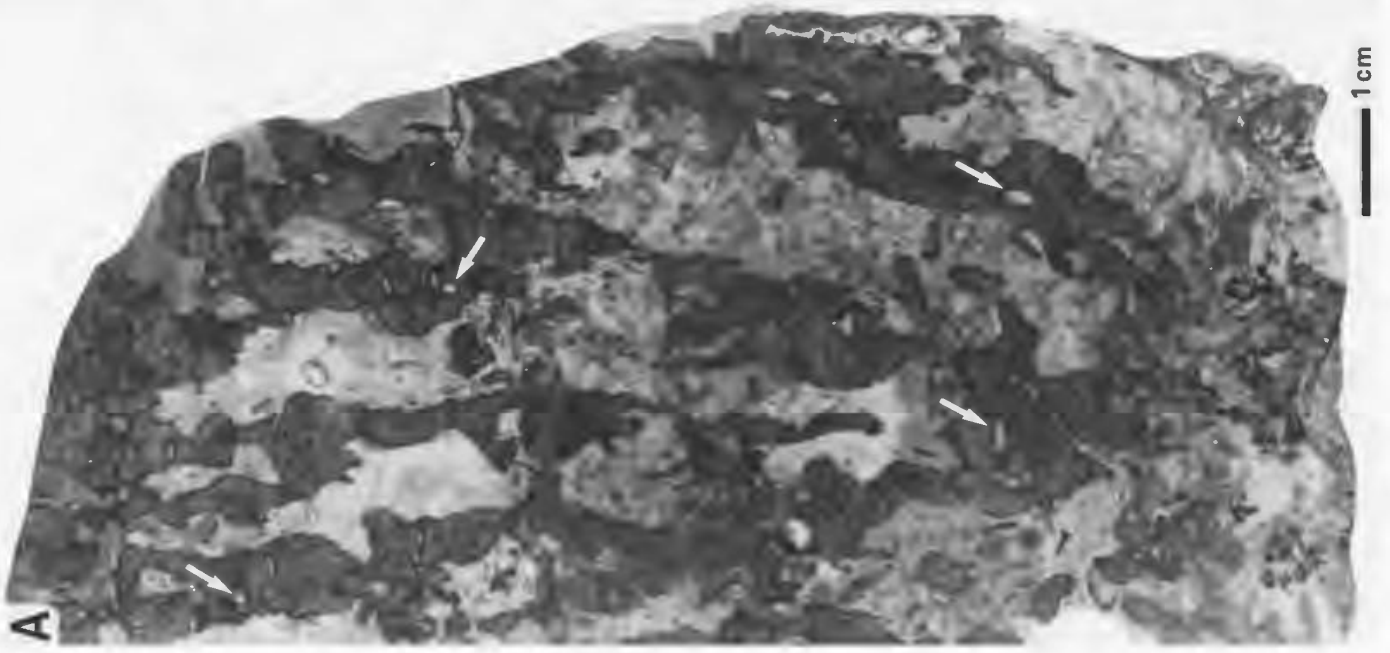
A
1 cm

PLATE 10

Cape Ann thrombolite-stromatolite complex
Horizon A, Port au Port Peninsula

Bed B: Mesostructure and Microstructure

A - Vertical slab of pebble-rich stromatolite. Edgewise pebbles are encrusted and bridged by columnar and linked pseudo-columnar stromatoids (S). The pebble-stromatoid framework is infilled by peloids, terrigenous silt and sand, phosphatic brachiopod fragments (arrows), and white blocky cement. Sample CA-5B.

B - Streaky silty microstructure of stromatoid columns. Dark blebs are pyrite. Scale bar 1 mm. Sample CA-5B.


B

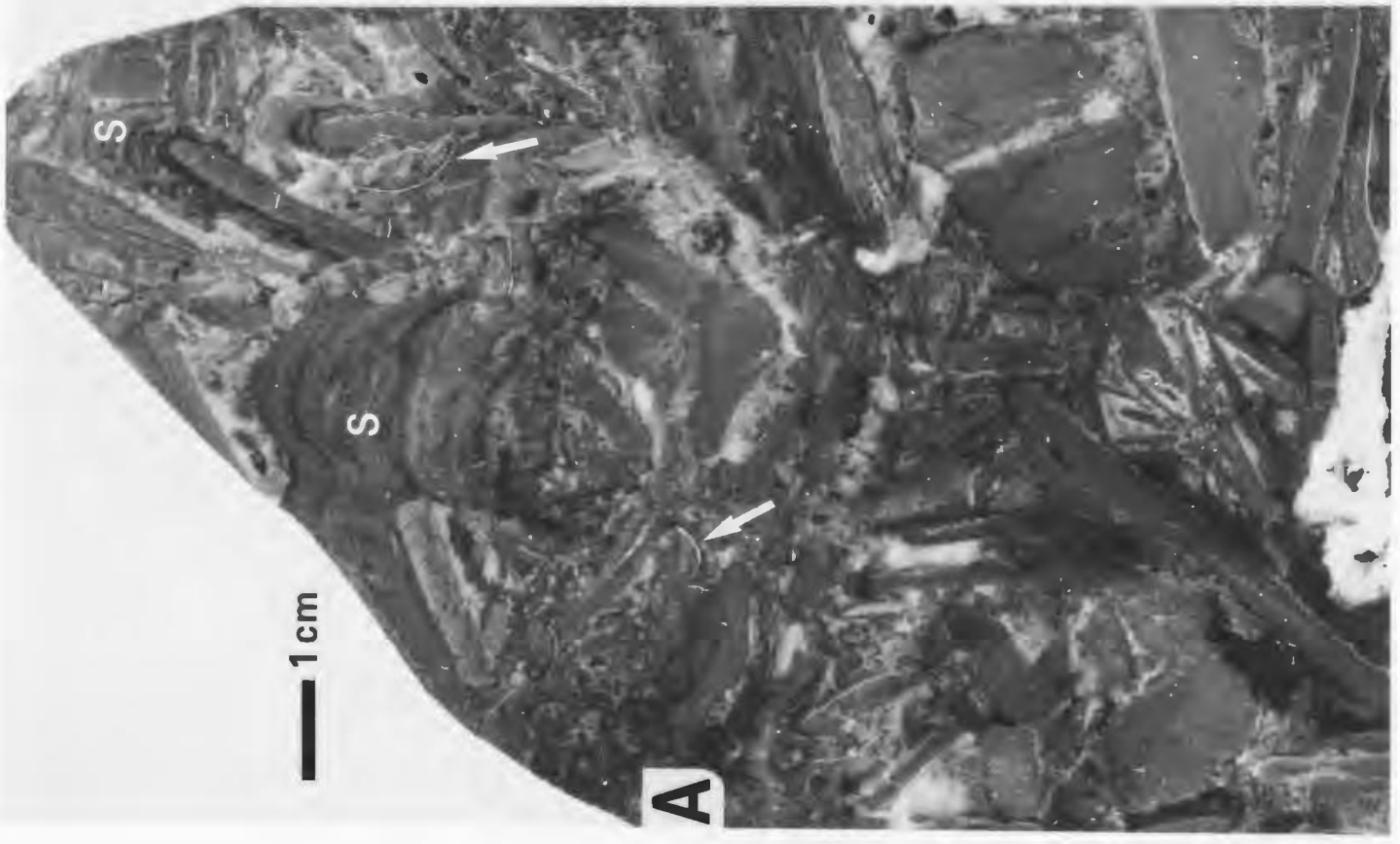
S
S
1 cm
A

PLATE 11

Cape Ann thrombolite-stromatolite complex
Horizon A, Port au Port Peninsula

Bed C: Mesostructure and Microstructure

A - Vertical slab of bioturbated thrombolite. The anastomosing framework of dark and medium coloured thromboids is encased within light coloured, weakly concave laminated, wackestone and packstone. Framework and inter-framework components are extensively bioturbated. Sample CA-4.

B - Digitate thromboid with grumous to streaky microstructure, and ragged bio-eroded margins (arrows). Note silty peloidal-intraclast inter-framework sediment. Scale bar 1 mm. Sample CA-4.

C - Sub-digitate thromboid with diffuse grumous microstructure, and ragged, in part stylolitic, margins (arrows). Inter-framework silty peloid wackestone (W). Scale bar 1 mm. Sample CA-4.

PLATE 11

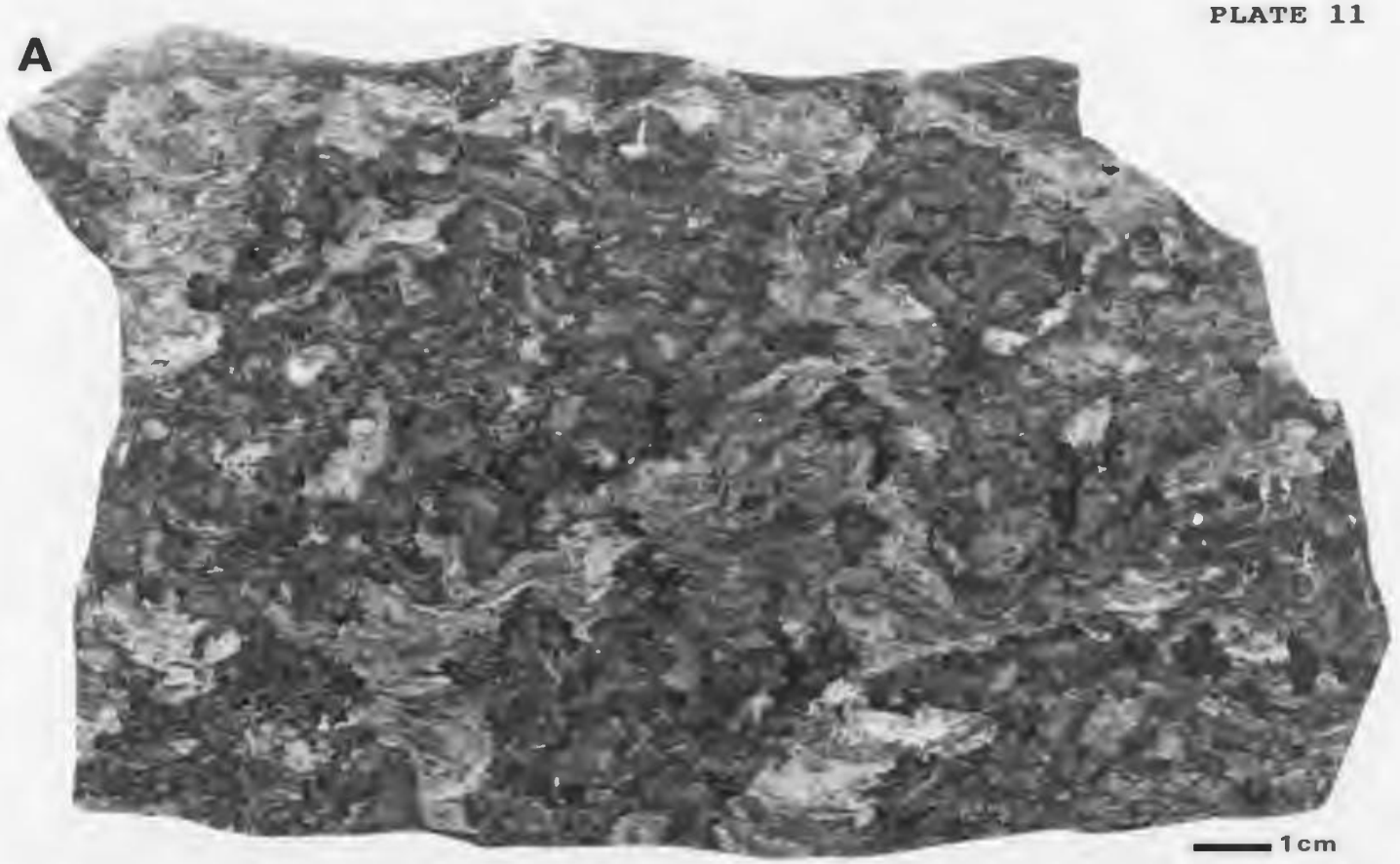

PLATE 12

Cape Ann thrombolite-stromatolite complex
Horizon A, Port au Port Peninsula

Bed D: Microstructure

A - Arborescent thromboids (T) encrusted by convex columnar stromatoids (S); lower zone of biostrome. The thromboid-stromatoid framework is infilled by burrowed silty peloidal-intraclastic wackestone (W) and packstone (P). Note spar-filled burrows (B). Sample CA-16B.

B - Irregular digitate thromboid (T) encrusted by dark micritic stromatoids (S) and thin layers of fibrous marine cement (arrows); lower zone of biostrome. Sample CA-16B.

C - Thromboid with grumous microstructure; lower zone of biostrome. Individual subrounded and saccate microclots (arrows) resemble *Renalcis*. Note edgewise intraclast in inter-framework silty peloidal packstone. Sample CA-16B.

D - Fenestrate stromatoids, upper zone of biostrome. Some of these tubular micro-fenestrae probably represent cement-filled burrows\borings. Sample CA-17.

E - Magnified view of grumous stromatoid laminae shown in upper right portion of D. Sample CA-17.

Scale bars 1 mm.

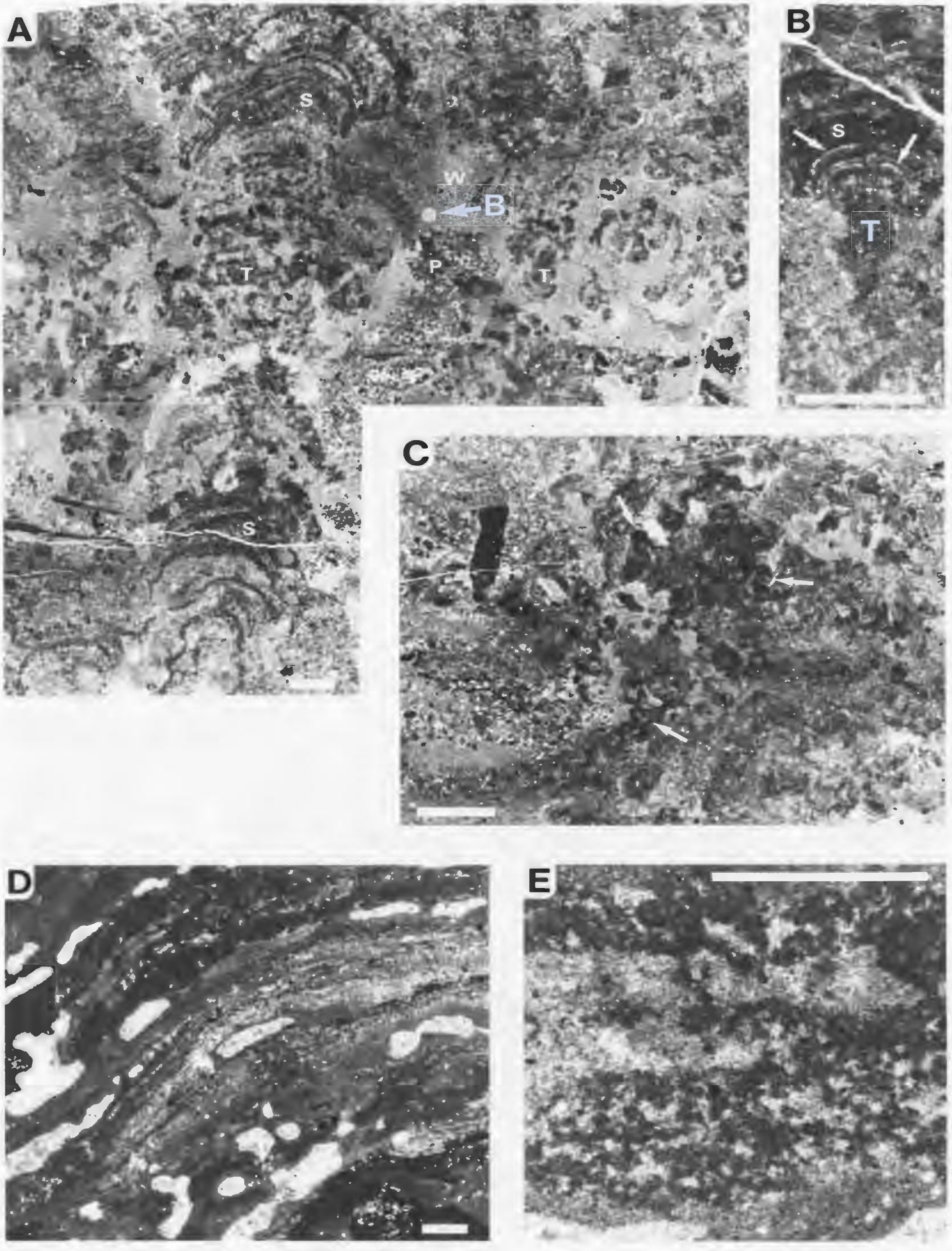
A
S
W
B
T
P
T
S
B
S
T
C
D
E

PLATE 13

Horizon B, Port au Port Peninsula

Megastructure and Mesostructure

A - Tabular to gently mounded biostrome showing lower nodular (1) and upper digitate (2) zones. Hammer 30 cm.

B - Irregular bulbous heads of digitate thrombolite (T). Depressions between the heads (arrows) are filled with wackestone and dolo-mudstone, and these sediments and the protruding heads are overlain by flat-pebble conglomerate (C). Pen 14 cm.

C - Margin of bulbous thrombolite head (T) abutted by thin-bedded wackestone and dolo-mudstone. Digitate fabric of thrombolite is obscured by stylolitic argillaceous seams. Pen 14 cm.

D - Vertical slab of lower nodular thrombolite composed of ragged dark thromboids encased in burrow-mottled wackestone and packstone. Thrombolite nodules are separated by light coloured stylolitic argillaceous seams. Sample CMB-2.

E - Vertical slab of upper digitate thrombolite. Irregular sub-digitate and amoeboid thromboids (T) contain scattered dark lobate bodies (arrows), and are disrupted by numerous stylolites. Light coloured inter-framework wackestone. Sample CMB-1B.

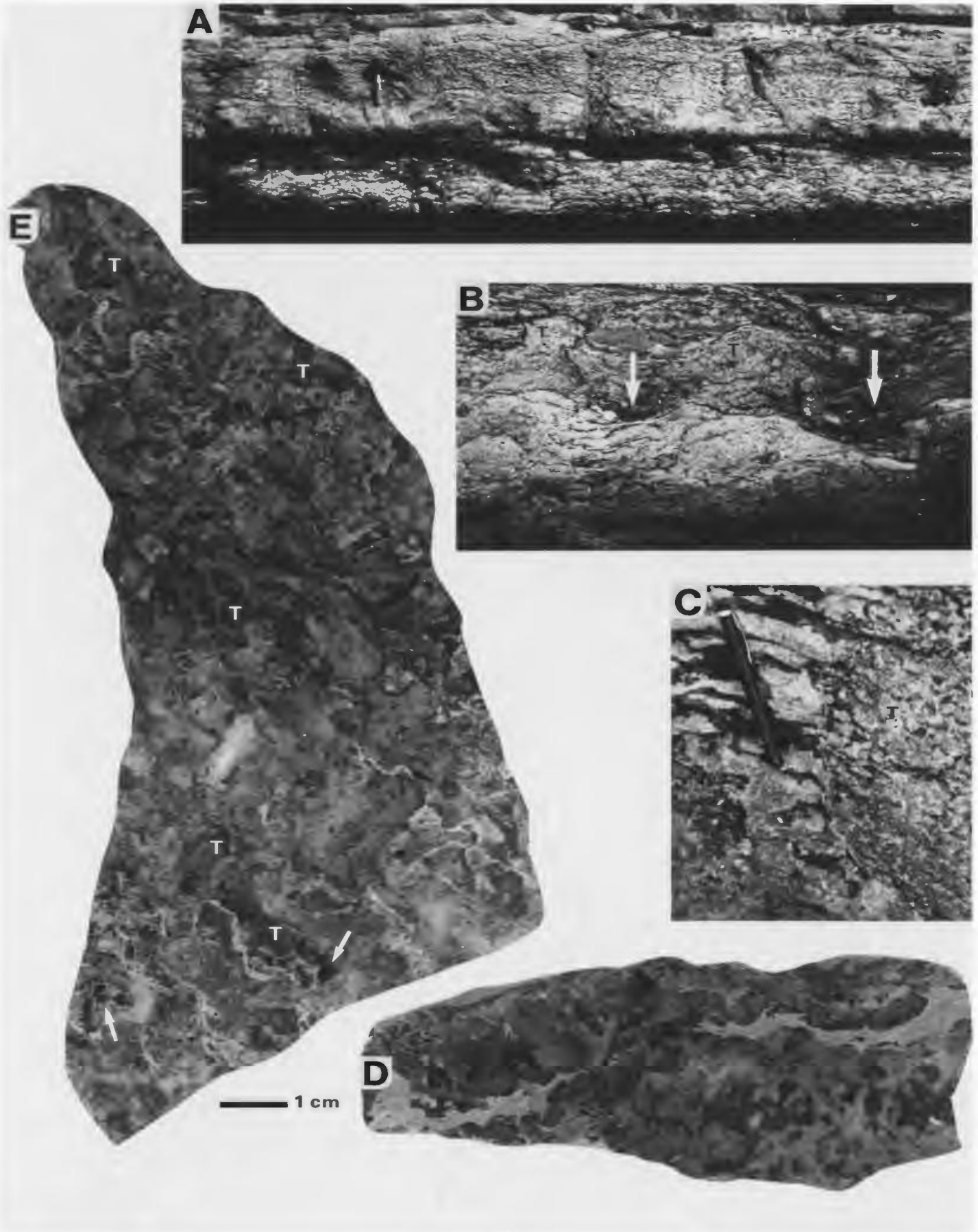
A
B
T
T
C
T
D
E
T
T
T
T
1 cm

PLATE 14

Horizon B, Port au Port Peninsula

Microstructure - lower nodular zone

A - Variegated (1) massive, (2) mottled, and (3) spongeous microstructure of amoeboid thromboids encased in silty mudstone (M) and wackestone (W). Note spar-filled wedge-shaped cracks confined to thromboids, and irregular spar-filled borings within both thromboids and inter-framework sediment. Sample CMB-2.

B - Filamentous (F) and grumous (G) microstructures which represent longitudinal and transverse sections, respectively, of micritic bush-like structures. Spar-filled tubular borings disrupt micritic bushes and inter-framework silty peloidal wackestone. Note spherulitic lobate body (L, lower right). Sample CMB-2.

C - Branching tubular filaments cf. *Hedstroemia* within thromboid. Scale bar 100 μm. Sample CMB-2.

D - Pendant filamentous bush-like structure composed of micritic filaments and tubules cf. *Hedstroemia* (arrow). Dark microclots at crest of bush (lower left) represent transverse sections of filaments\tubules. Sample CMB-2.

E - Lace-like network of micritic threads (interpreted as calcifed filaments), encased in silty peloidal wackestone. Some peloids have a hollow circular or tubular form (arrows), and are probably fragments of filaments\tubules. Sample CMB-2.

Scale bars 1 mm (except C).

A
W
1
2
M
3
2
B
1
F
B
C
100 um
D
E

PLATE 15

Horizon B, Port au Port Peninsula

Microstructure - upper digitate zone

A - Digitate thromboids (T) with variegated massive, mottled and grumous microstructures. Thromboid at far right is cut by sediment-filled burrow (arrow), and spar-filled cracks are largely confined to thromboids. Inter-framework sediment comprises silty peloid-skeletal wackestone (W). Sample CMB-1A.

B - Magnified view of thromboid on the left in A, showing mottled microstructure, poorly defined saccate lobate body (L), and possible burrow (B) occluded by micritic sediment. Peripheral zone of thromboid comprises massive microspar and patchy dolomite. Sample CMB-2.

C - Digitate thromboid with diffuse streaky microstructure (left) encased in silty peloid-pelmatozoan wackestone and packstone. Digitate thromboid at right has been selectively replaced by sparry cement. Note large burrow in inter-framework sediment at center; this burrow is occluded by peloidal sediment and radiaxial fibrous cement. Sample CMB-1B.

D - Inter-framework packstone with abundant elongate pelmatozoan plates and trilobite fragment. Note pendant form of pyritic micrite within shelter cavity beneath pelmatozoan plate (arrow); this structure is interpreted to be a calcified, coelobiontic (cavity-dwelling), microbial community. Remainder of shelter cavity is occluded by cement that syntaxially overgrows the sheltering pelmatozoan plate. Sample CMB-1A.

Scale bars 1 mm.

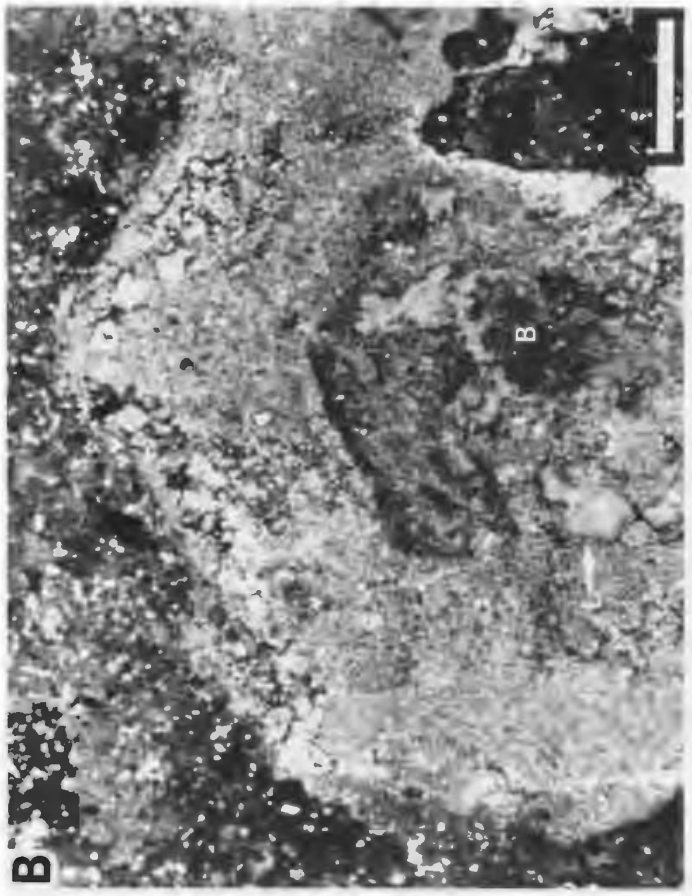
B
B


D

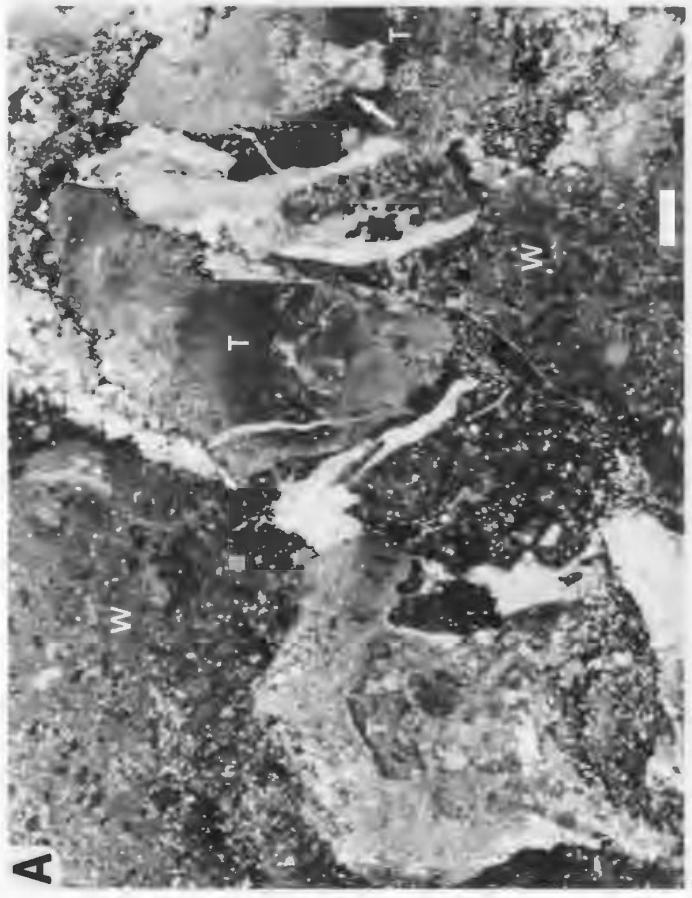
A
T
T
W
W
T

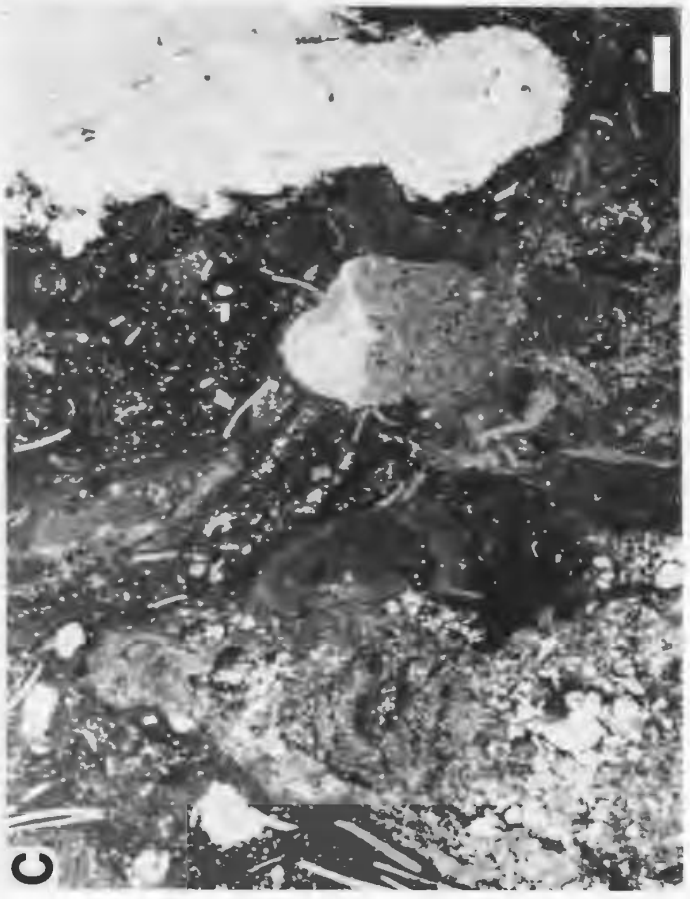
C

PLATE 16

Horizon C, Port au Port Peninsula

Mesostructure - Bed A

Vertical slab showing vertical and lateral transitions from thrombolite core Zone A1 to columnar stromatolite Zone A2. Lobate thromboids (A) and columnar stromatoids (S) are encased in skeletal packstone (P) and wackestone (W). Sample CMB-4.

PLATE 16

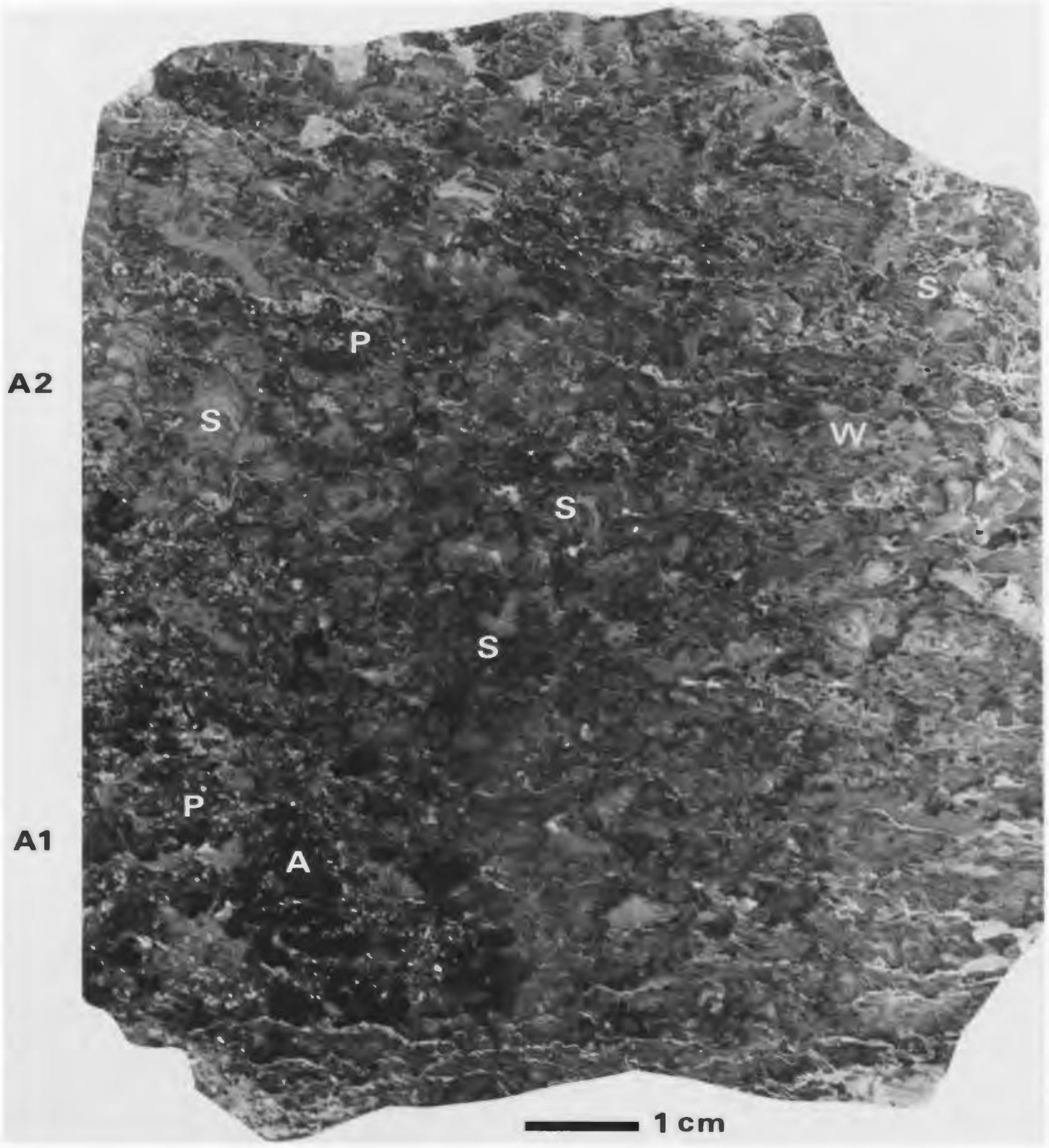

PLATE 17

Horizon C, Port au Port Peninsula

Mesostructure - Bed B: Zones B1-3

A - Vertical slab of columnar-layered stromatolite Zone B3. Sample CMB-5C.

B - Vertical slab of digitate cryptomicrobial Zone B2. Erect to radiating, light coloured, dolomitic cryptomicrobial digits (C) are encased in burrow-mottled skeletal packstone (P). The margins of the digits are locally encrusted by dark lobate thromboids (arrows). Sample CMB-5A.

C - Vertical slab of thrombolite Zone B1, showing dark lobate, saccate (arrows) and arborescent thromboids, light coloured dolomitic cryptomicrobial fabrics, and medium coloured inter-framework wackestone. Sample CMB-5B.

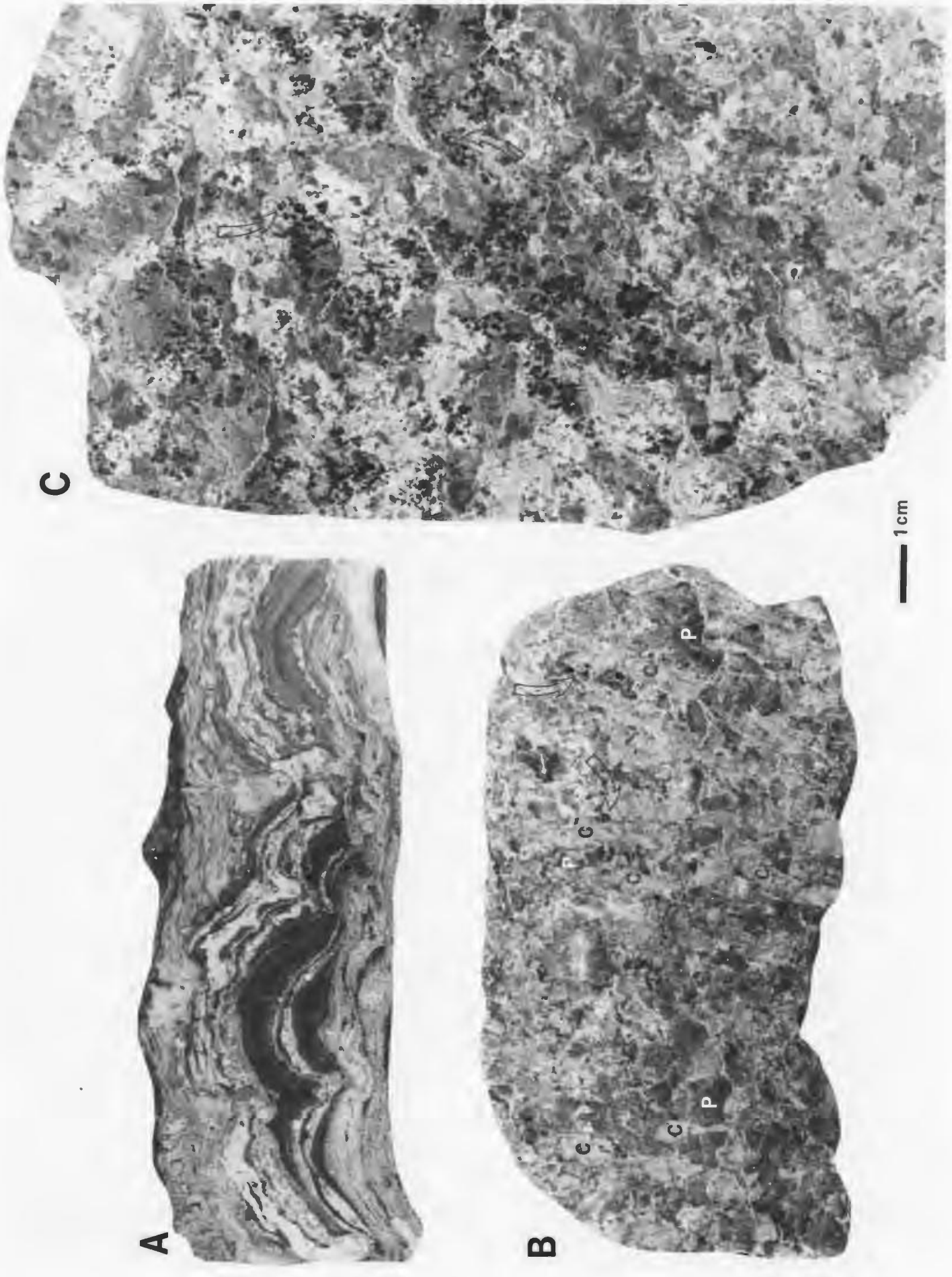
C
1 cm
A
B
P
C
P
C
P
C

PLATE 18

Horizon C, Port au Port Peninsula

Mesostructure - Bed B: Zones B4-B7

Vertical slab showing lateral accretion of successive stromatolite zones:

- B4 - dark skeletal packstone.
- B5 - hemispheroidal stromatoids (S) and ooid intraclast conglomerate (C).
- B6 - linked columnar stromatoids.
- B7 - planar and corrugate stromatoids disrupted by sediment-filled shrinkage cracks (arrows). Light coloured, dolomitic, ooid- intraclast-skeletal grainstone laminae (g) and thin dark crusts of botryoidal marine cement (mc), are interlayered with the stromatoids. Sample CMB-6.

PLATE 18

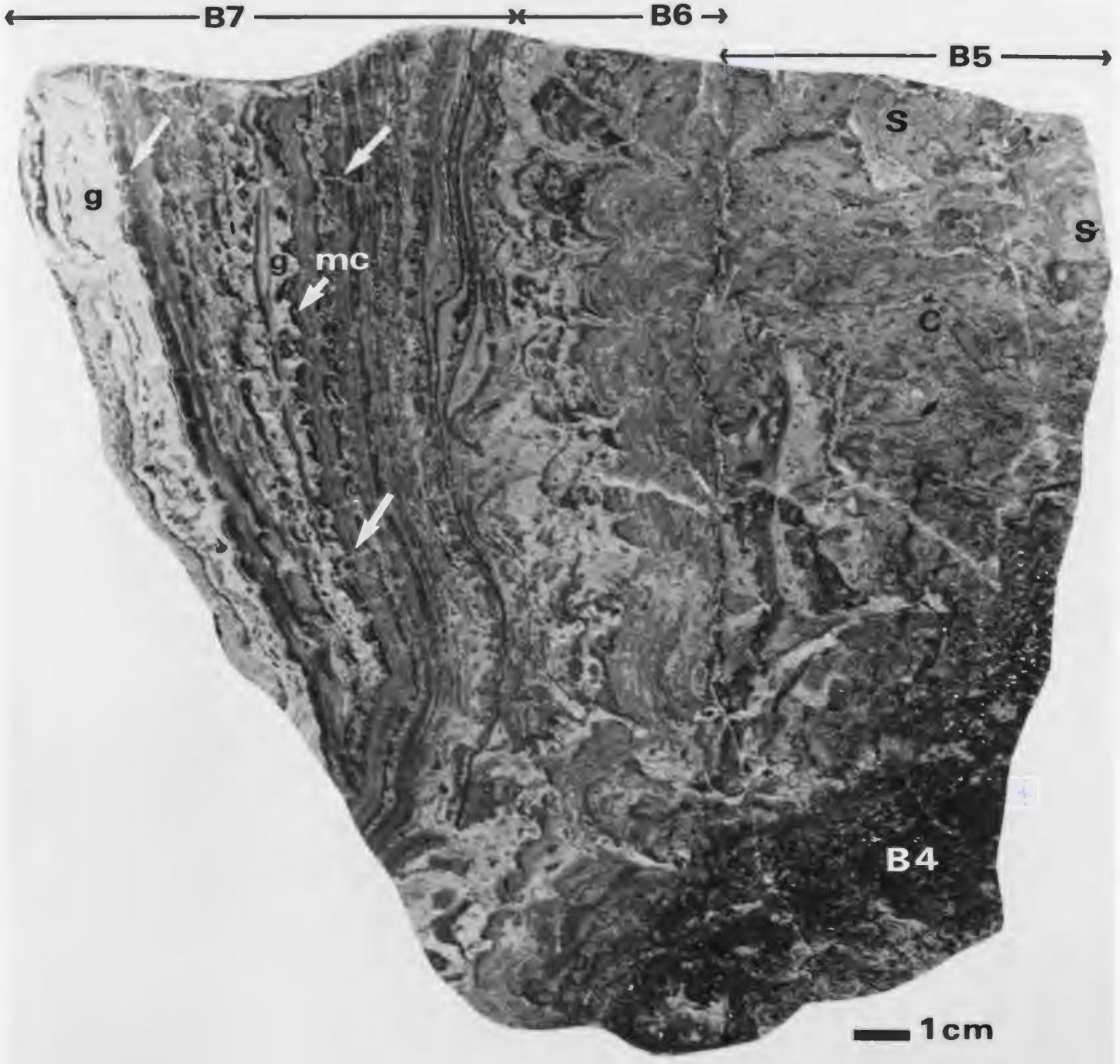

PLATE 19

Horizon C, Port au Port Peninsula

Microstructure - Bed A

A - Saccate to cellular lobate microstructure of thromboids (T) encased in silty pelmatozoan-trilobite-peloid packstone; Zone A1. Sample CMB-4A.

B - Saccate lobate microstructure of thromboid; Zone A1. Note well defined thin cryptocrystalline walls at margins of lobes. Sample CMB-4A.

C - Streaky silty and diffuse grumous microstructure of stromatoid column encased in silty trilobite packstone; Zone A2. Sample CMB-4A.

D - Silty trilobite-pelmatozoan packstone between thromboids (T, top left and centre right) with massive microcrystalline lobate microstructure; Zone A1. Dark pyritic corpuscles are thought to be mineralized microbial colonies. Note syntaxial cement around pelmatozoan plates (arrows). Sample CMB-4A.

Scale bars 1 mm.

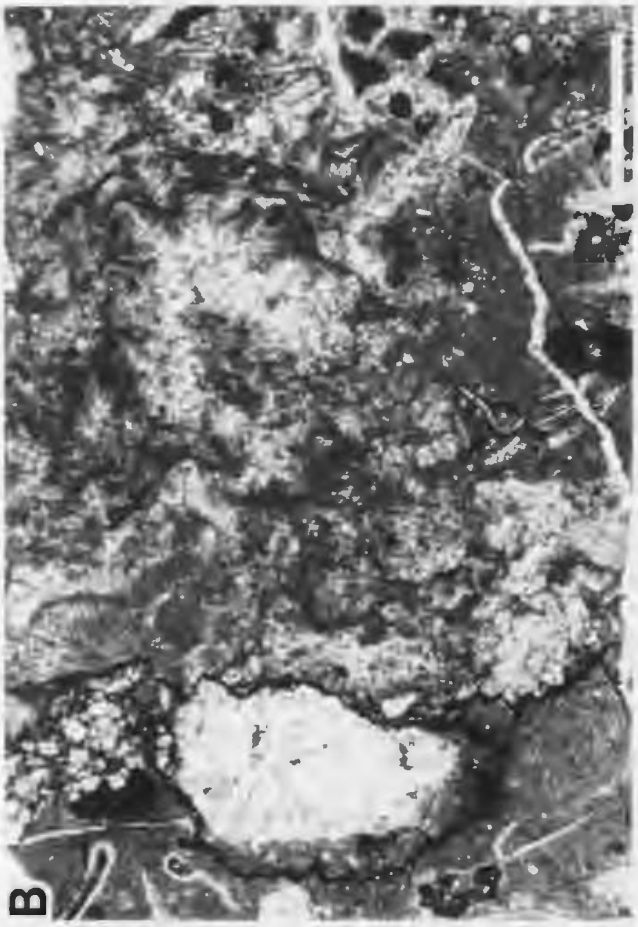
B

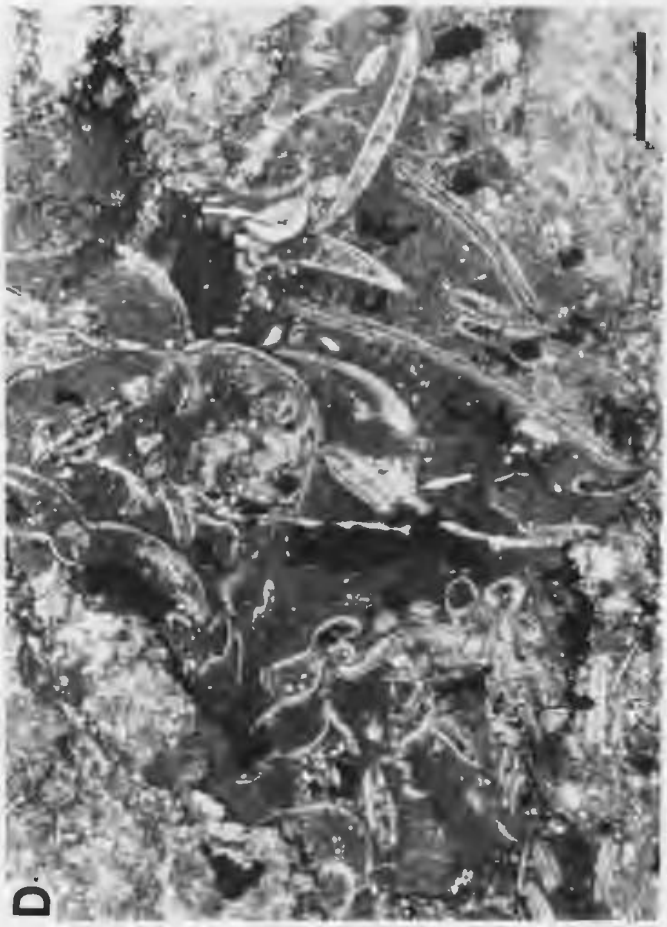
D

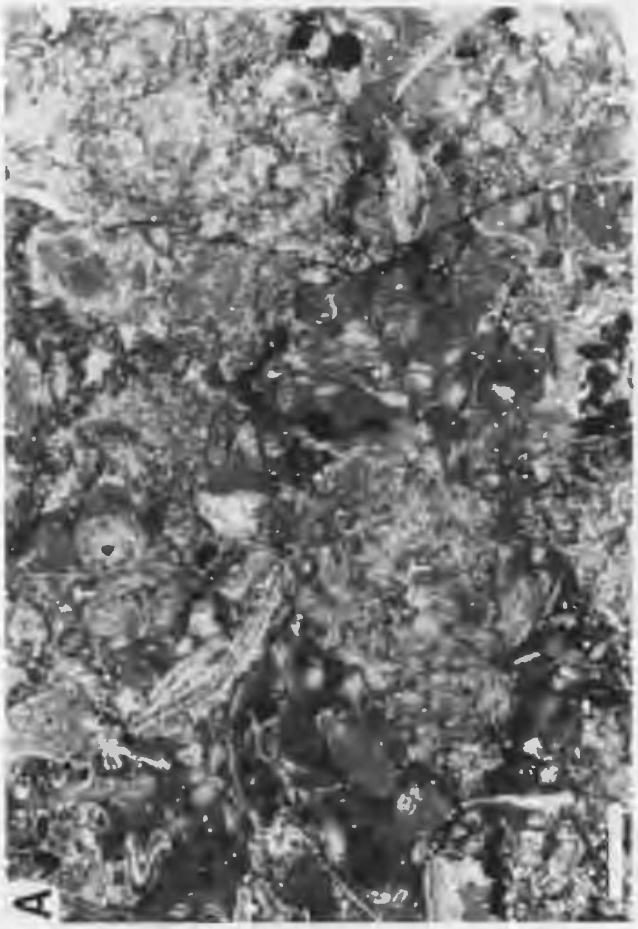
A

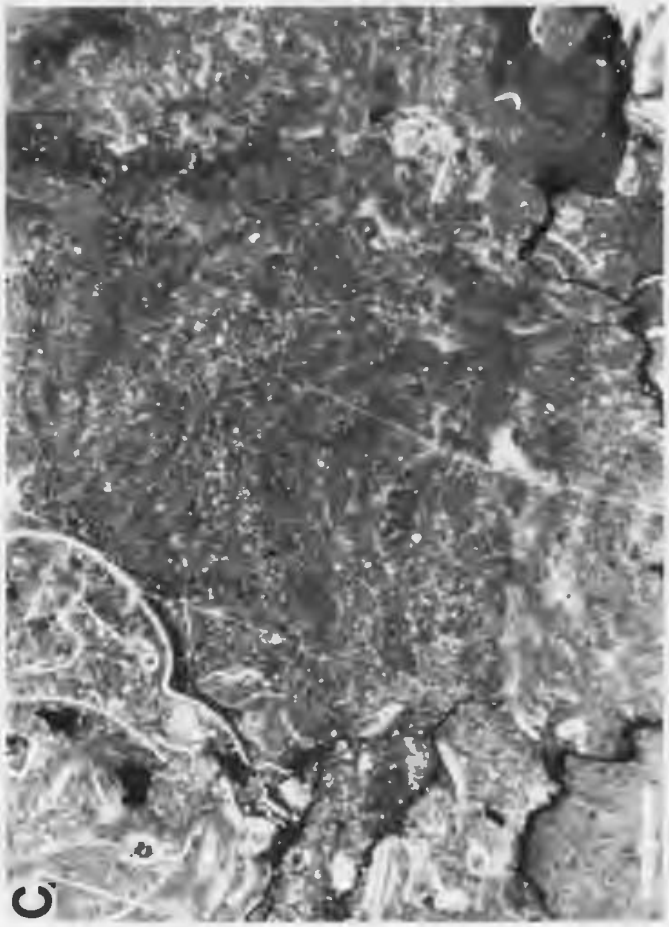
C

PLATE 20

Horizon C, Port au Port Peninsula

Microstructure - Bed B: Zones B1 and B2

A - Poorly defined lobate thromboids (T) comprised of turbid microspar and dolomite (top), and diffuse grumous microstructures (centre left); Zone B1. Inter-framework wackestone contains trilobite carapaces and sediment-filled burrows (arrows). Sample CMB-5B.

B - Oblique section of stubby arborescent thromboids (T) comprised of turbid microspar (massive lobate microstructure); Zone B1. Thromboids at lower right support a small cavity (arrow) filled with peloids, skeletal fragments and cement. Sample CMB-5B.

C - Shelter cavity beneath trilobite carapace occluded by mud (microspar), skeletal fragments (f), and radiaxial-fibrous cement (arrows) which syntaxially overgrows the trilobite shell; Zone B1. Sample CMB-5.

D - Cryptomicrobial digits (C) composed of hypidiotopic microcrystalline dolomite; Zone B2. Digits are encased in burrowed trilobite packstone and wackestone. Sample CMB-5A.

Scale bars 1 mm.

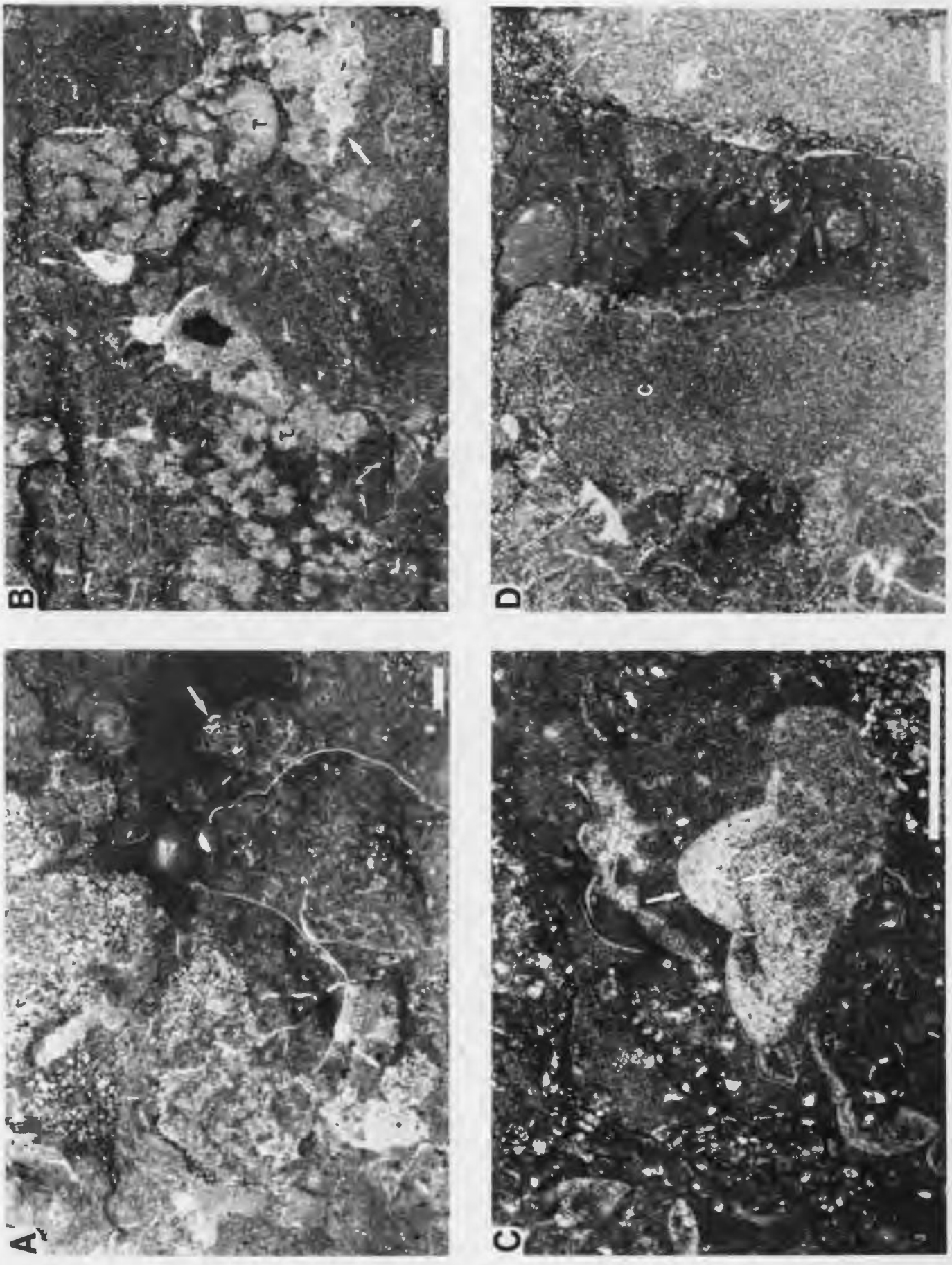
A
B
C
D

PLATE 21

Horizon C, Port au Port Peninsula

Microstructure - Bed B: Zones B3-B7

A - Banded (1) massive cryptocrystalline and (2) silty peloidal microstructure of columnar stromatoids; Zone B3. Note silt and peloid-filled burrow (arrow). Sample CMB-5C.

B - Banded microstructure disrupted by laminoid fenestrae; columnar stromatoids, Zone B3. Fenestrae are commonly floored by quartz silt and peloids, and are occluded by blocky dolomite cement. Sample CMB-5C.

C - Grumous microstructure of poorly differentiated digitate thromboid (margins delineated by arrows) encased within silty trilobite-pelmatozoan packstone; Zone B4. Sample CMB-6A.

D - Banded massive and diffuse grumous microstructure of fenestrate pustular stromatoids; Zone B6. Note partial detachment of successive laminae to form pustules above spar-filled fenestrae (top) or grumous lenses (arrow). Sample CMB-6A.

E - Banded grumous microstructure of planar stromatoids; Zone B7. Fenestrae impart a weak second order lamination to thick grumous laminae. Sample CMB-6B.

Scale bars 1 mm.

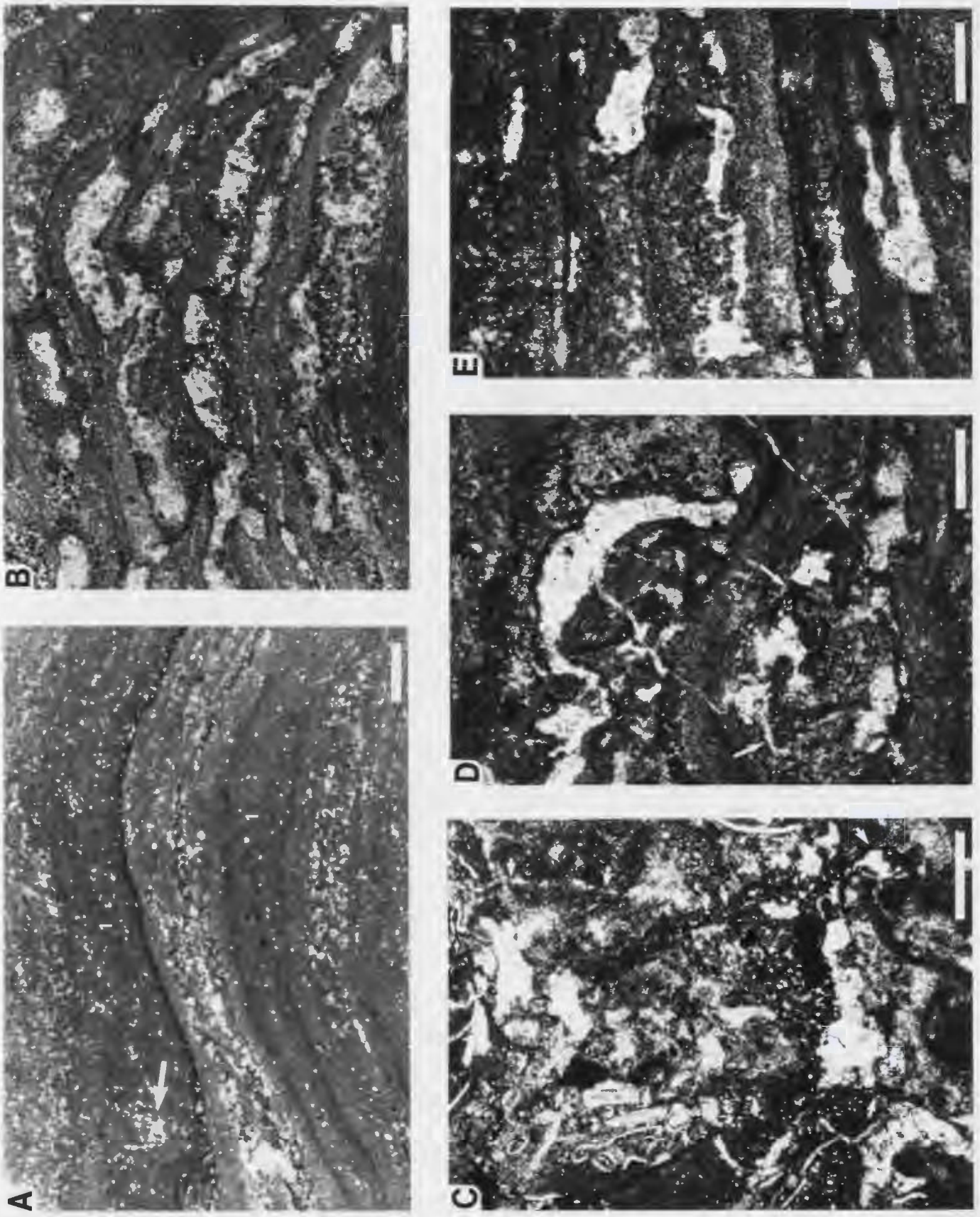
A
B
C
D
E

PLATE 22

Horizon C, Port au Port Peninsula

Microstructure of marine cements - Bed B

A,B - Mamillate crust of fibrous marine cement; Zone B6. A) Plane polarized light, B) crossed polarized light. Sample CMB-6B.

C - Rhombic microdolomite inclusions (arrows) within mamillate marine cement crust; Zone B6. Composition of irregular micron-sized inclusions is not known. Sample CMB-6B.

D,E - Linear arrays of micro-inclusions (arrows) within mamillate marine cement crust; Zone B6. D) Plane polarized light, E) crossed polarized light. These inclusions are thought to define the outlines of precursor acicular cement crystals. Sample CMB-6B.

Scale bars 0.1 mm.

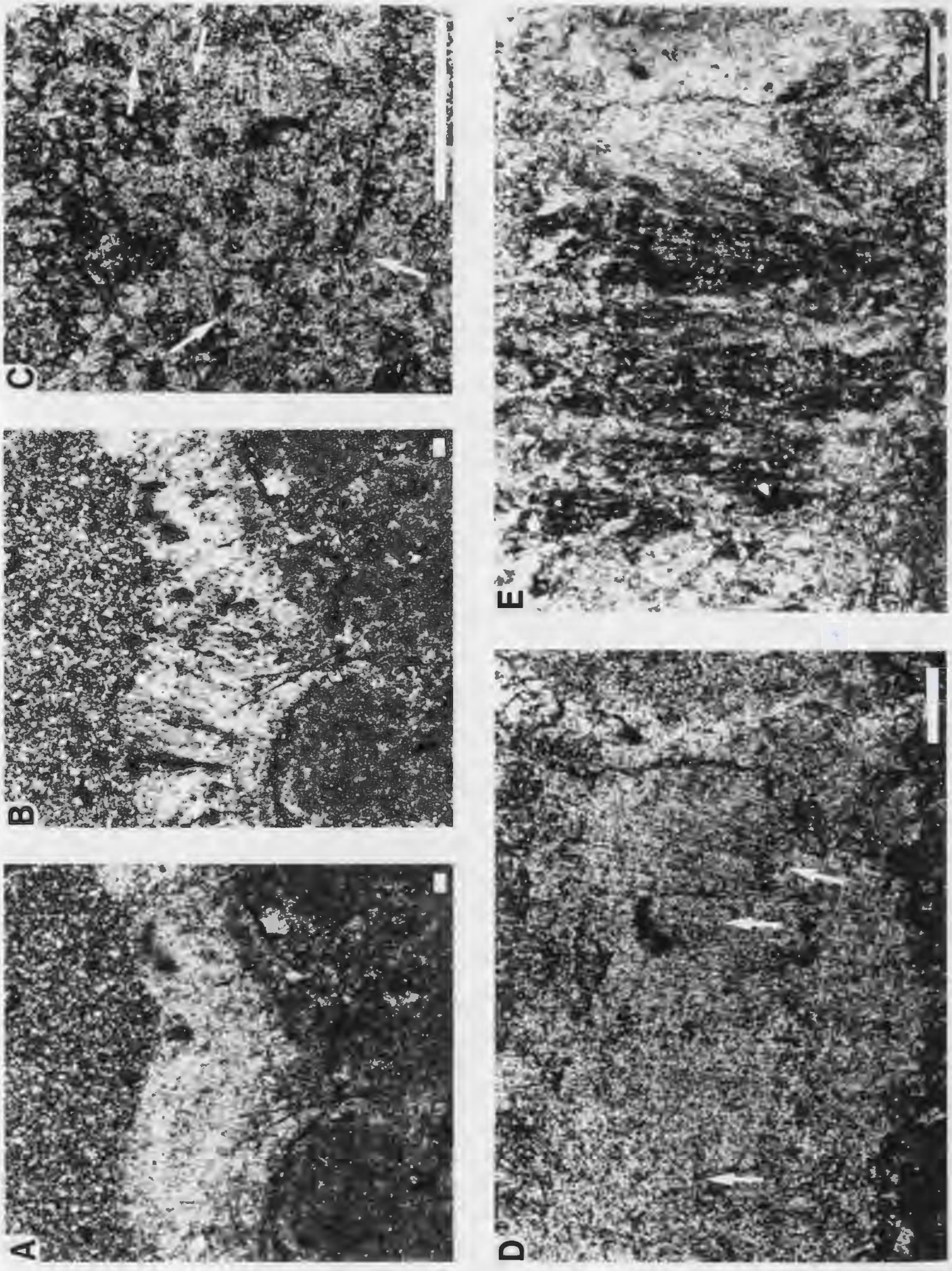
A
B
C
D
E

PLATE 23

Horizon D, Port au Port Peninsula

Megastructure

A - Close-packed ellipsoidal bioherms overlain by ooid grainstone; Bed A. Concentric layering indicates synoptic relief of at least 30 cm for these bioherms.

B - Small domed bioherms flanked and draped by thin-bedded packstone and argillaceous mudstone; Bed C.

C - Domed bioherms truncated by planar erosion surface; Bed C.

Hammer 30 cm, 10 cm scale rule.

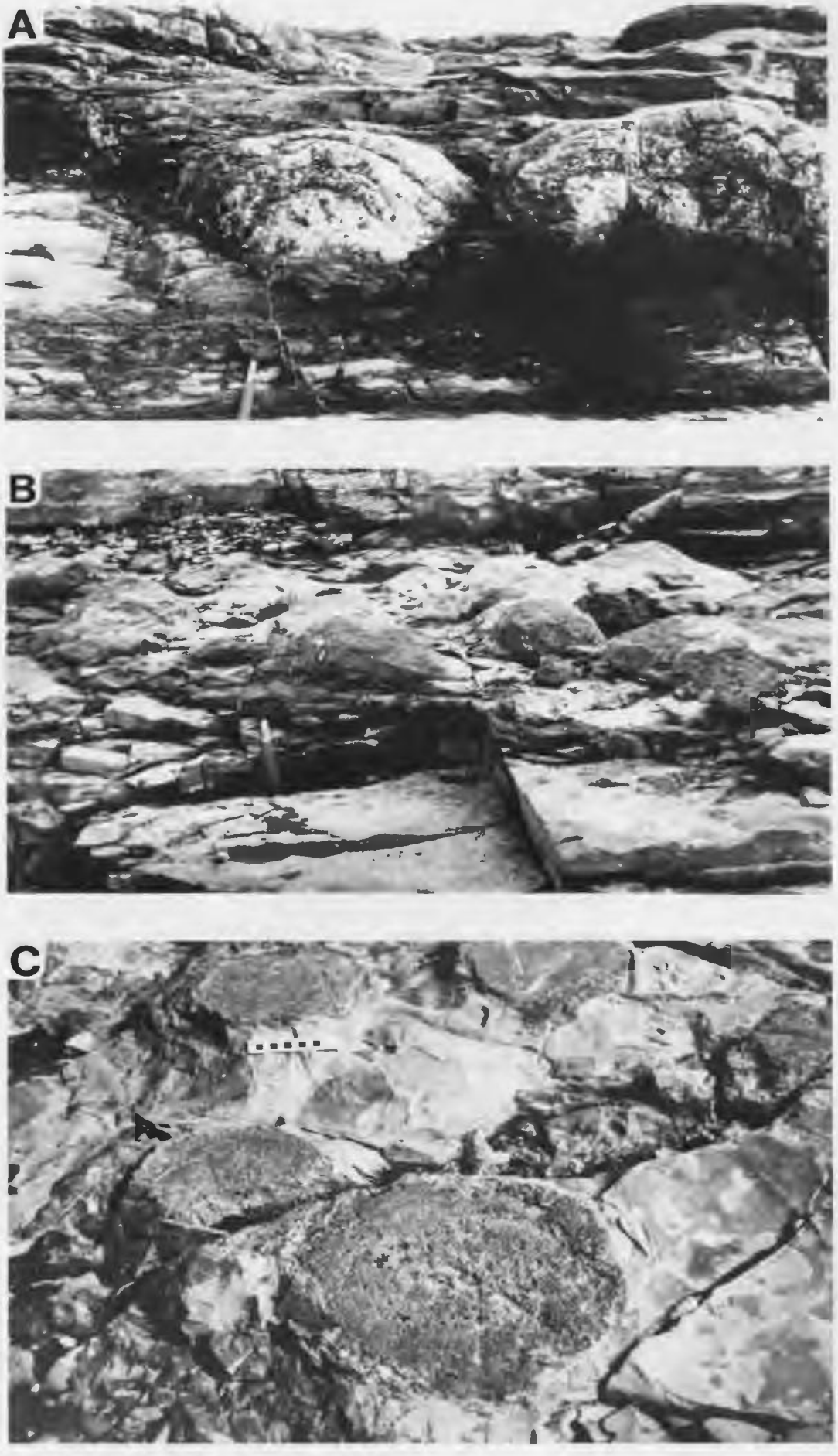
A
B
C

PLATE 24

Horizon D, Port au Port Peninsula

Mesostructure

A - Vertical slab of thrombolitic stromatolite, Bed A. The flanks and crests of the stromatoid columns (S) are encrusted by dark lobate and arborescent thromboids, respectively (arrows). Light coloured inter-framework peloid-ooid-skeletal wackestone. Sample CMB CK-4.

B - Vertical slab of thrombolitic stromatolite, Bed B. Poorly differentiated light coloured, weakly laminated and mottled, stromatoid columns (S) are established on a basal layer of undulose stromatoids, and are encased in darker coloured peloid-ooid-skeletal grainstone. Note lobate and saccate thromboids (arrows) at margin and crests of stromatoid columns. Sample CMB CK-6.

C - Vertical slab of small thrombolite bioherm, Bed C. Patches of light coloured mudstone occur between an anastomosing framework of medium coloured, prostrate and sub-digitate thromboids (T). Thromboids contain numerous small dark coloured lobate and saccate bodies, which locally form pendant growth forms on the undersides of prostrate thromboids. Sample CMB CK-1A.

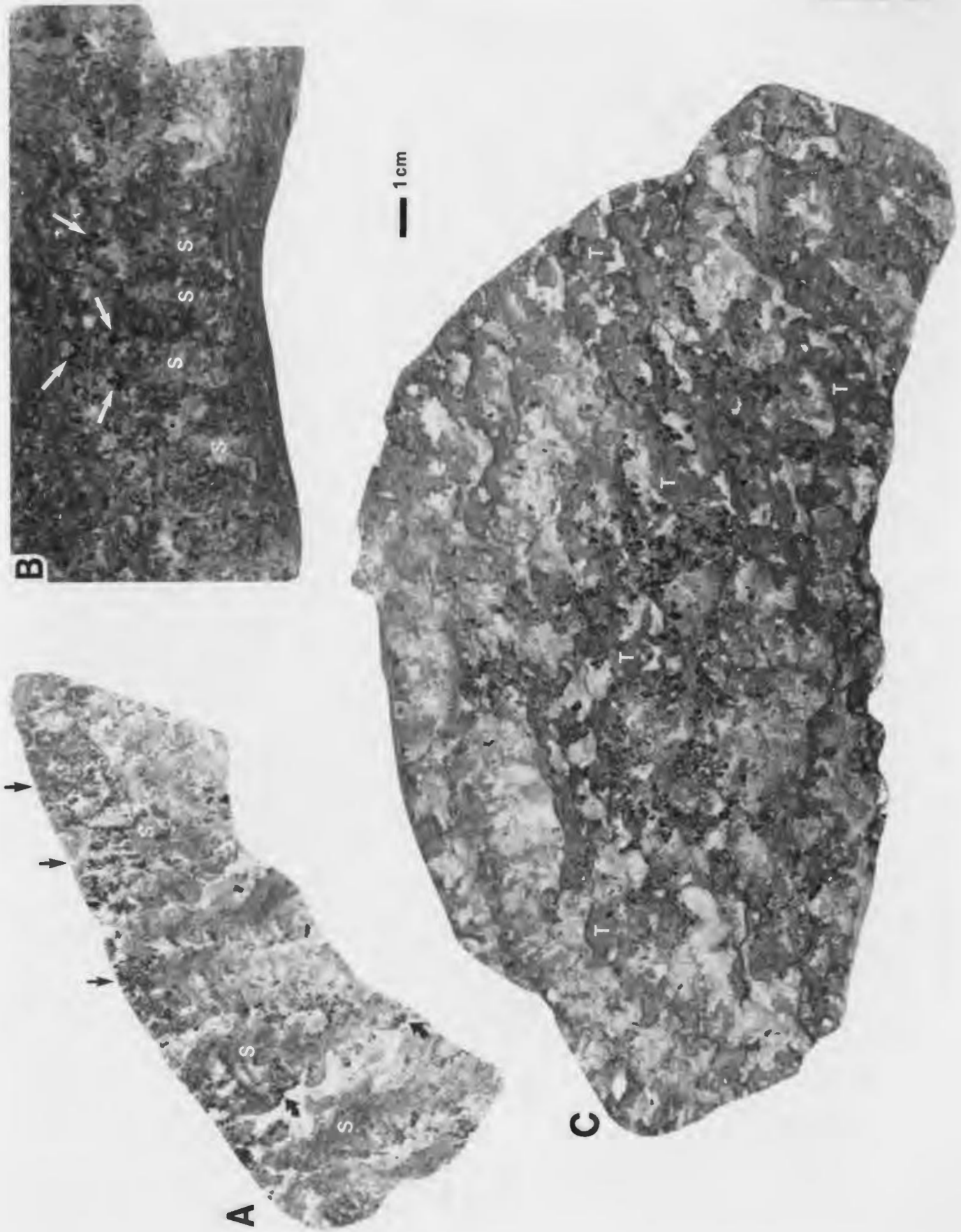
A
B
C
S
T
1 cm

PLATE 25

Horizon D, Port au Port Peninsula

Microstructure - Beds A and B

A - Abundant clotted and saccate *Renalcis* encrusted by stromatoid column (S). Right margin of *Renalcis*-stromatoid column is encrusted by network of *Girvanella* tubules (area between arrows; see enlargement in B. *Renalcis*-stromatoid column is encased in silty peloid-pelmatozoan packstone. Sample CMB CK-4.

B - Magnified view of encrusting *Girvanella* wall shown in A. The tubular filaments are encased in turbid microcrystalline marine cement. Sample CMB CK-4.

C - Poorly defined saccate *Renalcis* (R) "capped" by cluster of *Girvanella* tubules. Sample CMB CK-4.

D - Branching saccate to tubular *Renalcis* or *Izhella*-like form. Individual branches are encased in mudstone (microspar), and branched growth form is overlain and flanked by silty peloid grainstone with numerous pelmatozoan fragments (P). Sample CMB CK-4.

E - Saccate and clotted *Renalcis* encased in microspar. Note pocket (?burrow) of silty sediment (S) that appears to disrupt *Renalcis* at lower centre-right. Sample CMB CK-4.

Scale bars 0.5 mm.

PLATE 25

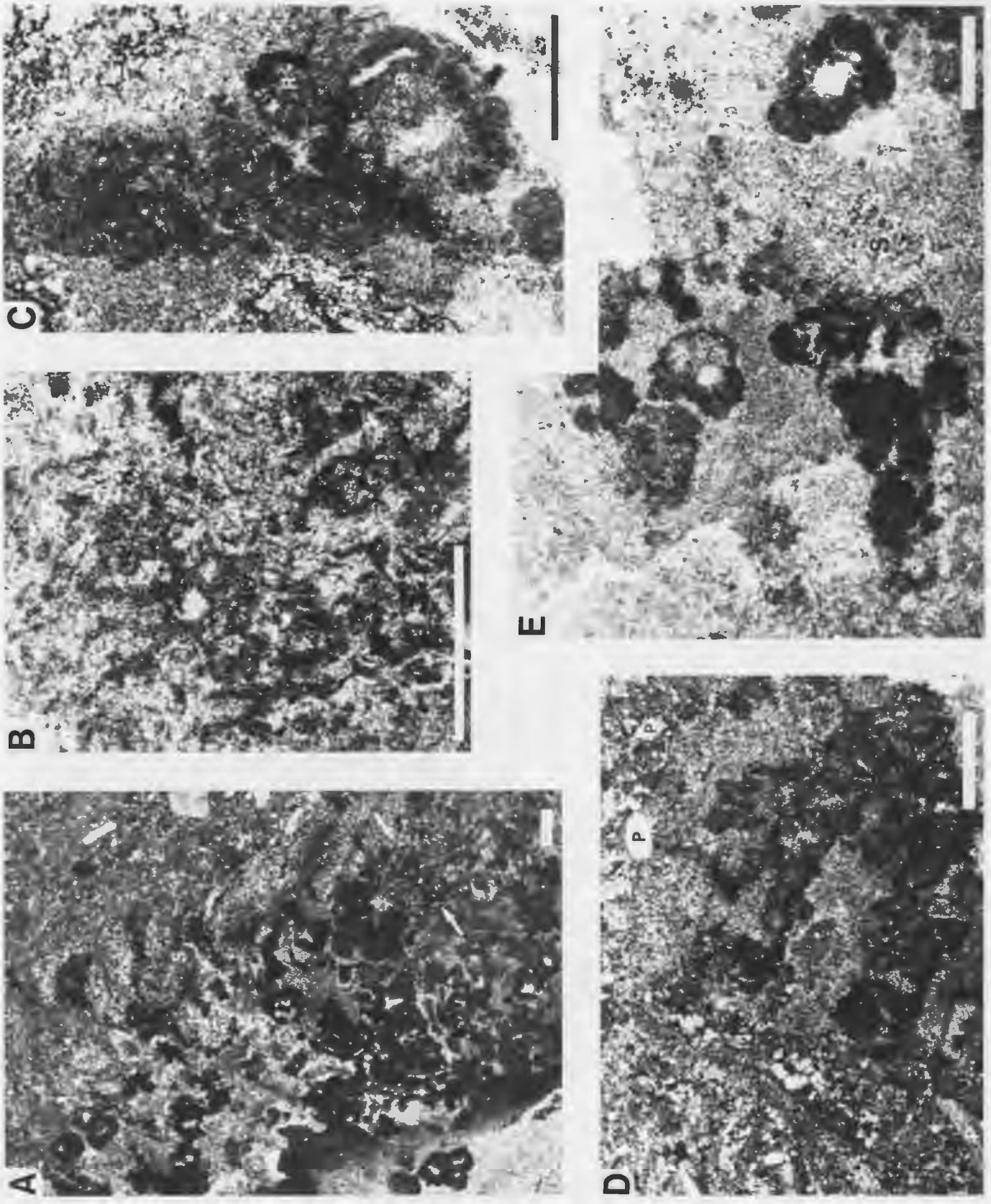

PLATE 26

Horizon D, Port au Port Peninsula

Microstructure - Beds B and C

A - Thromboids (T) with variable silty bioclastic peloidal microstructure (left and right) and grumous microstructure (centre); Bed C. The central thromboid is rimmed by isopachous fibrous cement (arrow), whereas the thromboids on the left and right are partially bordered by bound trilobite carapaces and are difficult to differentiate from unbound inter-framework skeletal wackestone (W). Sample CMB CK-1A.

B - Pendant mass of turbid, massive microcrystalline to weakly spherulitic, lobate microstructure (L) at underside of prostrate thromboid; Bed C (these are the dark lobate and saccate bodies visible in Plate 24-C). Pendant lobes project into a patch of dark inter-framework trilobite wackestone (W) which probably occludes a former framework cavity. Thromboids at base of photo (T) contain abundant bound trilobite debris, and are partially bordered by bound trilobite carapaces. Note siliceous spherulite (S), and mud and cement-filled burrow (B) in inter-framework wackestone. Sample CMB CK-1A.

C - Magnified view of turbid microcrystalline lobes and siliceous spherulite shown in B; crossed polarized light. Note extinction cross within siliceous spherulite. Sample CMB CK-1A.

D - Streaky silty peloidal microstructure of stromatoid column encased in pelmatozoan-trilobite-ooid wackestone; Bed B. Note burrowed margin of column at lower left. Sample CMB CK-6B.

Scale bars 1 mm.

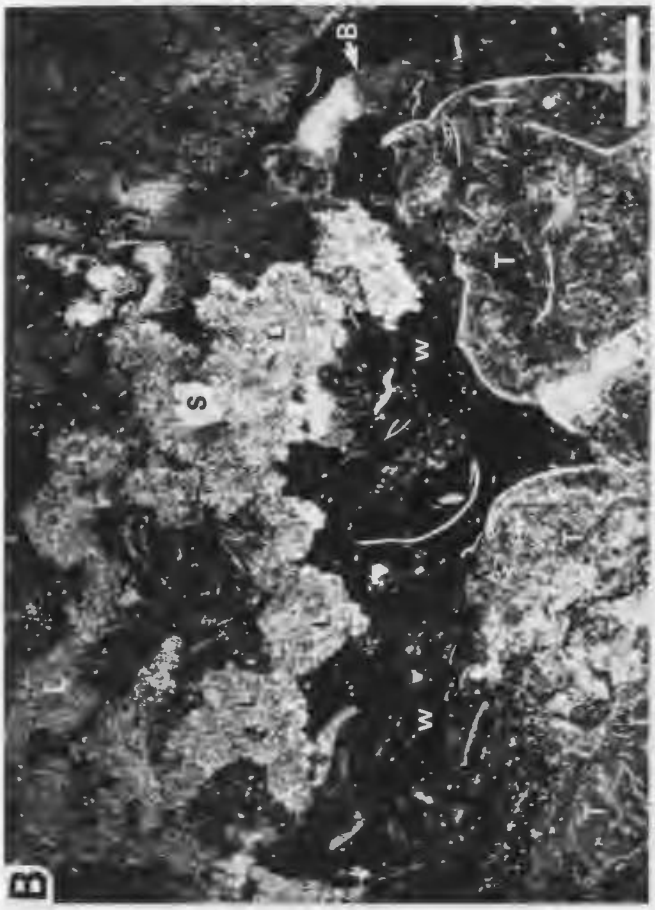
B
S
W
W
W
T
T
T

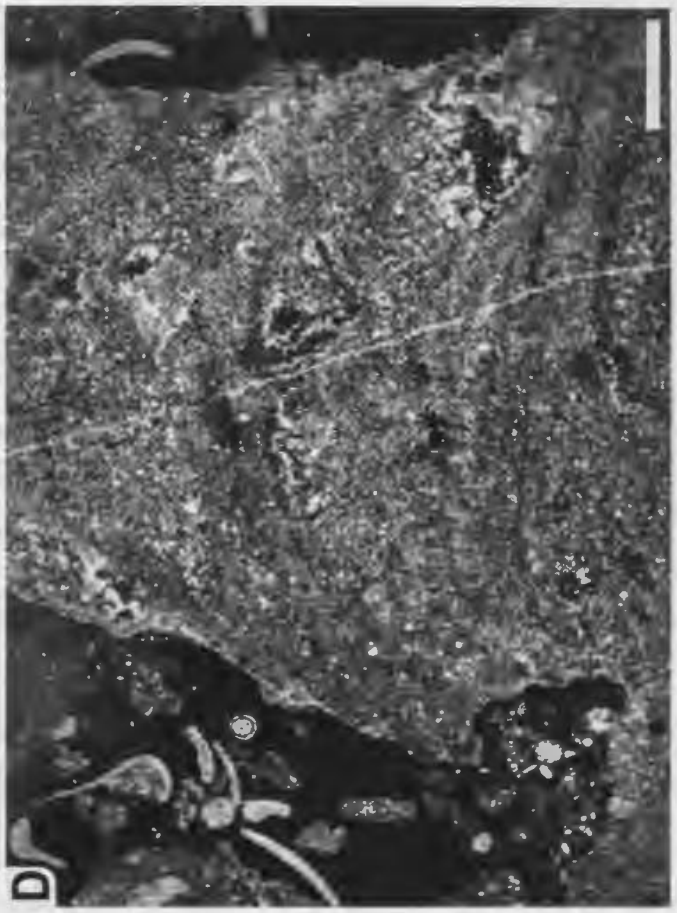
D

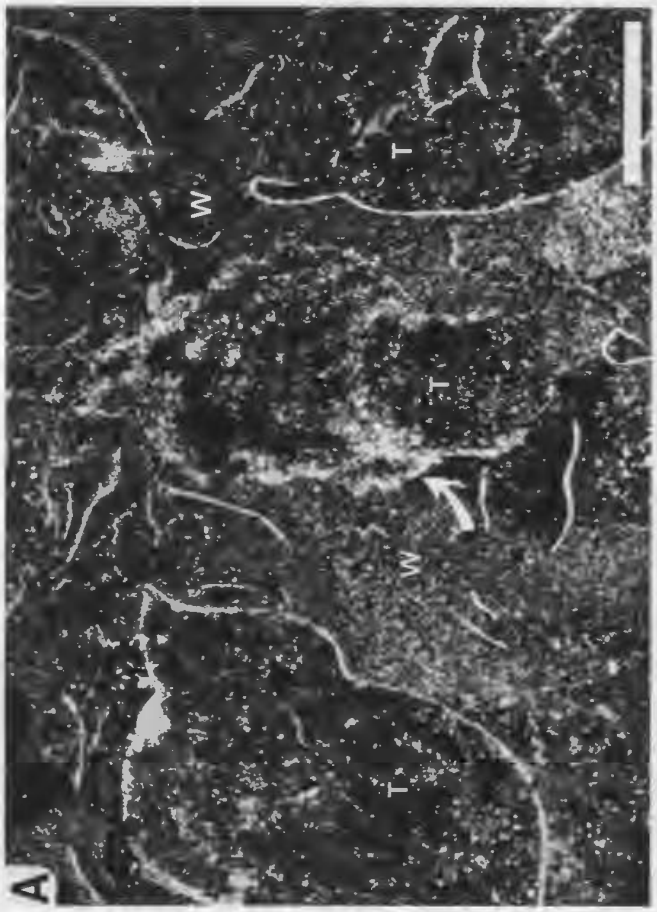
A
W
T
T
W
T


C

PLATE 27

Horizon E, Port au Port Peninsula

Megastructure and Mesostructure

A - Tabular biostrome interrupted by thin bedded intra-biostromal sediments (arrows; top left and far right). 10 cm scale rule.

B - Basal pebble conglomerate (lower third of photo) and central digitate thrombolite zone (upper third) of biostrome. Note fan-shaped array of edgewise pebbles in basal zone.

C - Stylo-breccoid fabric of upper amoeboid thrombolite zone.

Scale bars 10 cm.

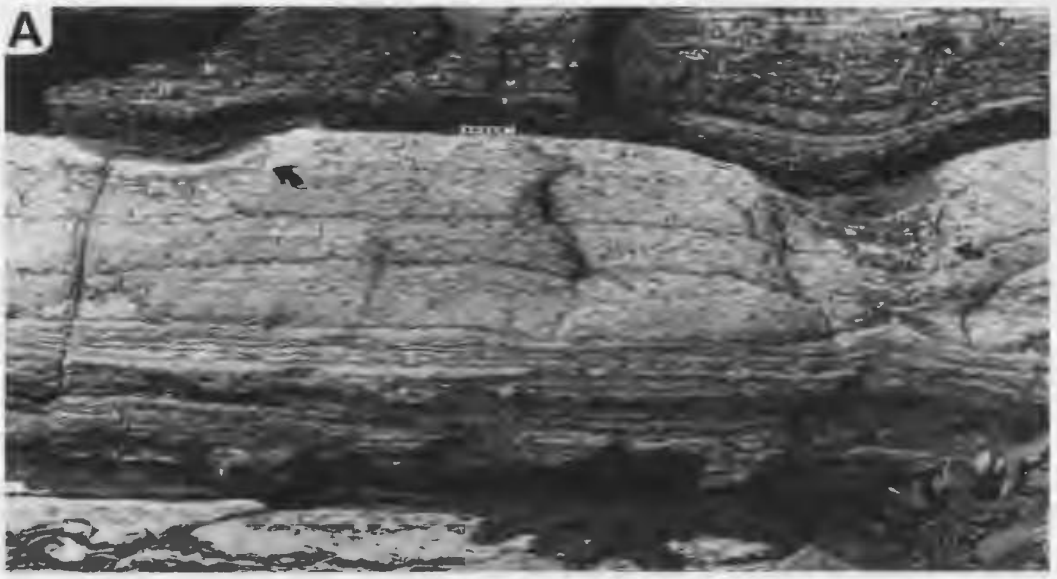
A

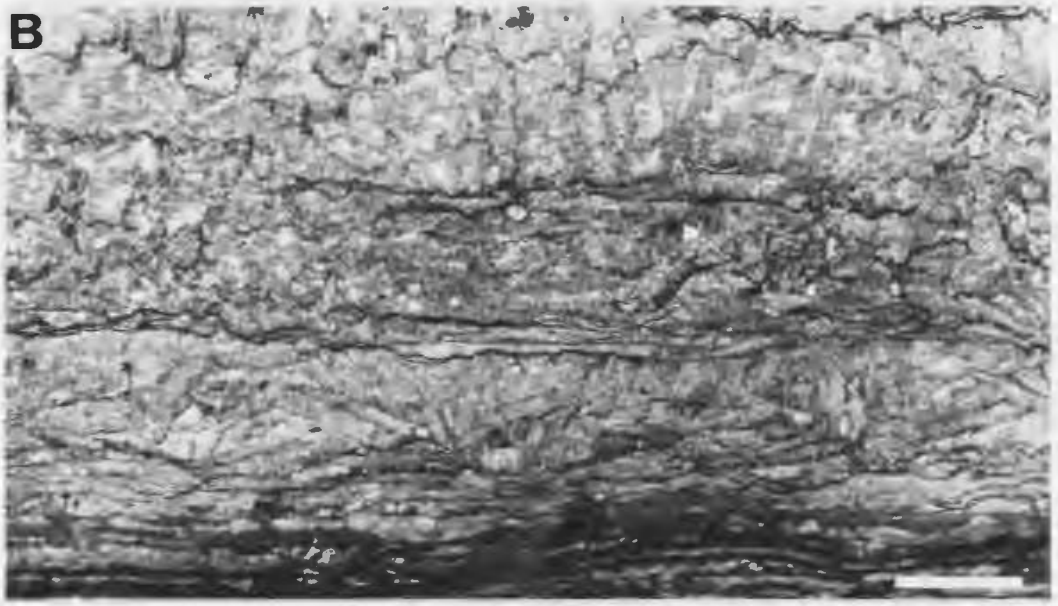
B


C

PLATE 28

Horizon E, Port au Port Peninsula

Mesostructure

A - Vertical slab of central digitate thrombolite zone. Digitate thromboids are rimmed by a dark selvage, and are disrupted by small burrows (arrows). Inter-framework peloid-ooid-skeletal packstone is extensively burrowed, and contains scattered edgewise pebbles. Sample BCB-1A.

B - Vertical slab of upper amoeboid thrombolite zone. Anastomosing amoeboid thromboids are disrupted by numerous small burrows (arrows), and are encased in lighter coloured, burrow-mottled peloid-skeletal wackestone (W) and mudstone (M).

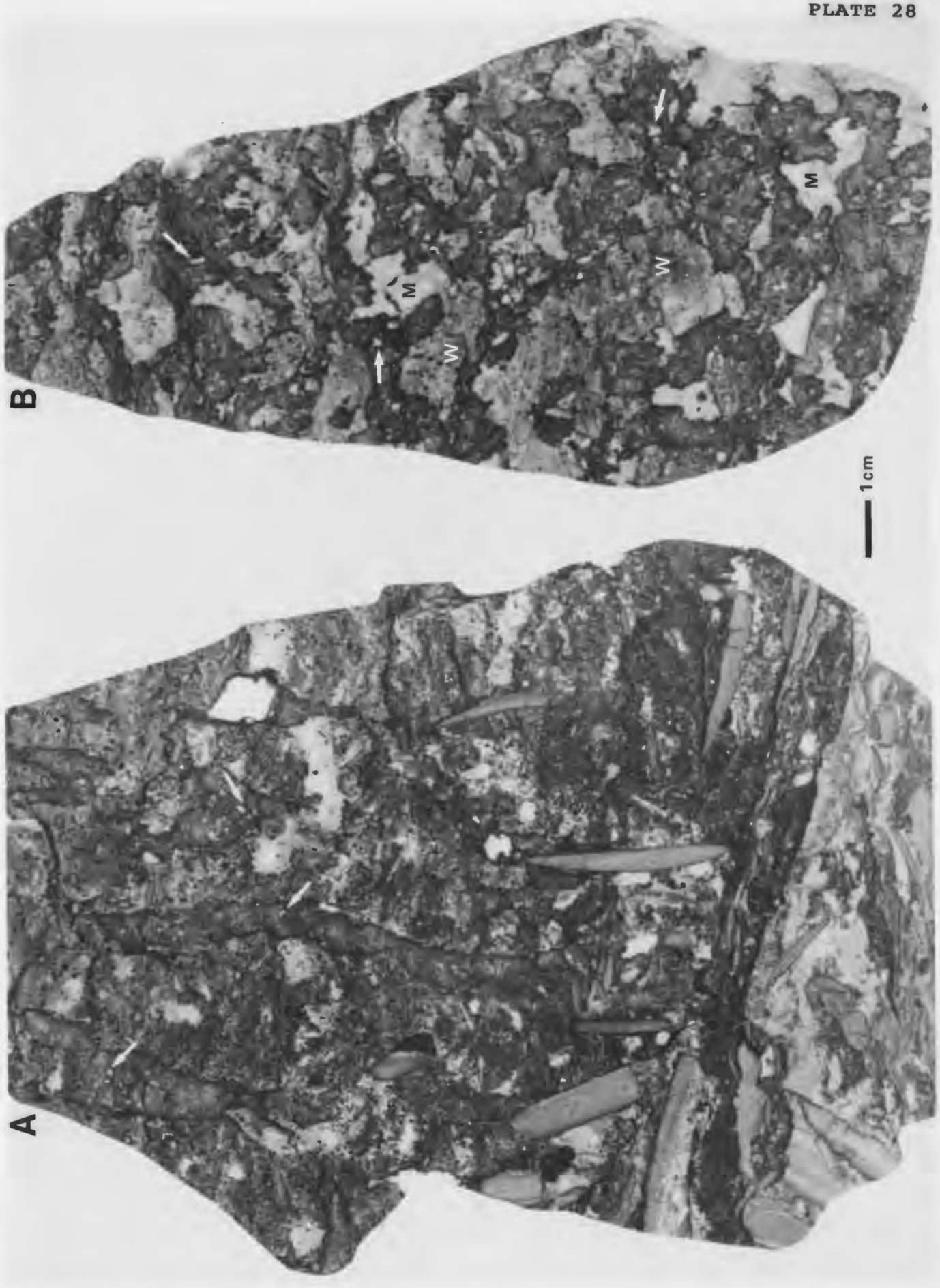
B
M
W
M
W
1cm
A

PLATE 29

Horizon E, Port au Port Peninsula

Microstructure

A - Mottled silty microstructure of digitate thromboid; central digitate thrombolite zone. Left margin of thromboid is encrusted by *Girvanella* selvage (G), whereas selvage on right side has been selectively replaced by sparry calcite and dolomite. Inter-framework sediment (far left) contains pelmatozoan debris, ooids and dark pyritic corpuscles. Note burrow (B) occluded by blocky calcite cement. Sample BCB-1A.

B - Magnified view of *Girvanella* selvage shown in A. Tubular filaments (arrows) are aligned approximately parallel to the margins of the thromboid. Sample BCB-1A.

C - Grumous microstructure of thromboid in upper amoeboid thrombolite zone. Cryptocrystalline microclots range from subequant to elongate thread-like (lower right) forms. Sample BCB-1B.

D - Thromboid with diffuse grumous grading to *Girvanella* microstructure (G); see enlargement of central area in E. Thromboid is disrupted by small mud-filled cavities or burrows (M), and is flanked by inter-framework wackestone (W). Sample BCB-1B.

E - Magnified view of central portion of E showing twisted *Girvanella* tubules (G). Sample BCB-1B.

Scale bars 0.5 mm.

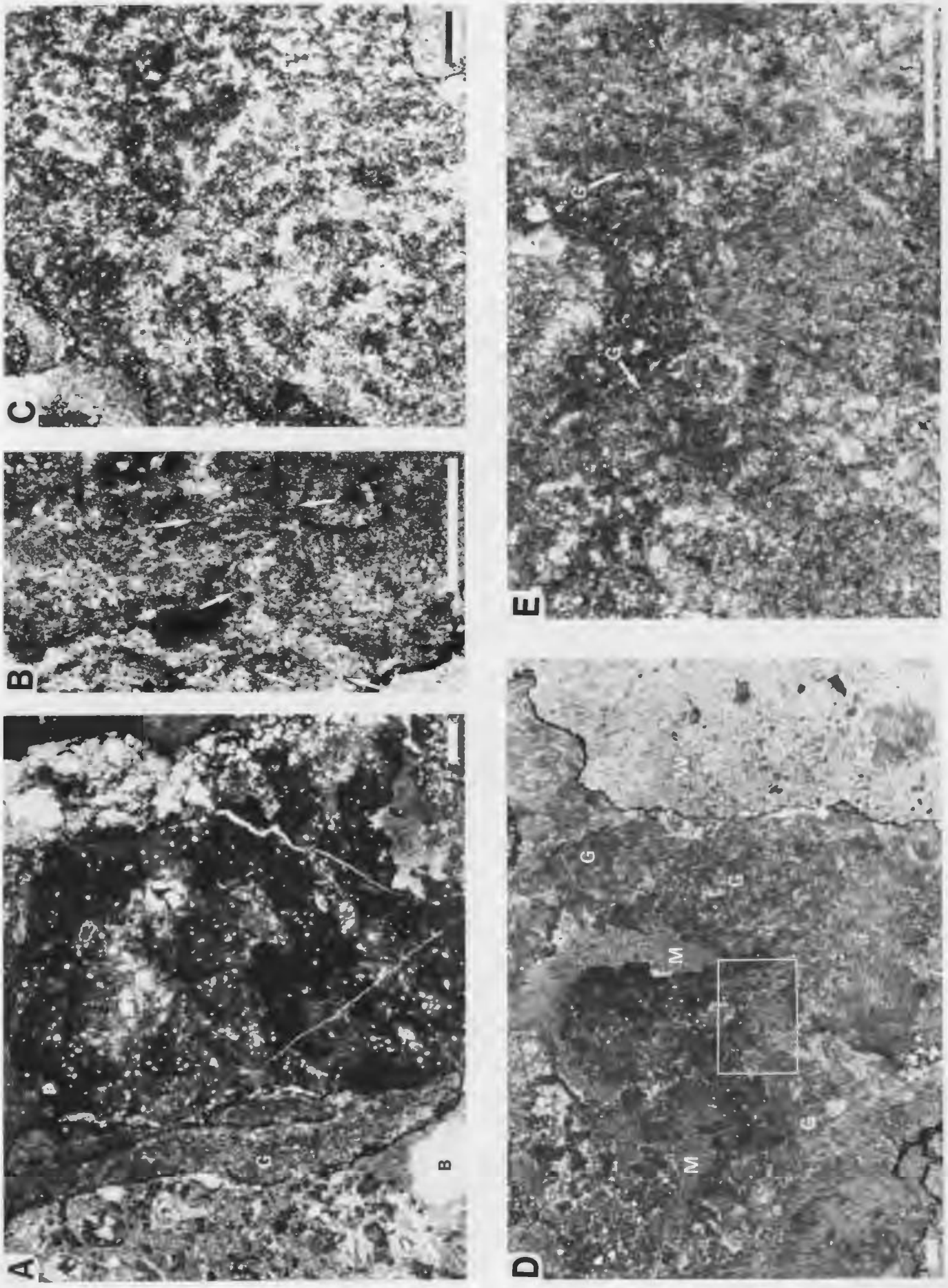
A
G
B
B
C
E
G
G
D
G
M
M

PLATE 30

Horizon F, Port au Port Peninsula

Mesostructure and microstructure

A - Vertical slab showing slightly divergently branched stromatoid columns encased in silty mudstone. Note moderately well defined convex laminae. Sample FLX-1.

B,C - Massive microcrystalline microstructure of stromatoid columns (S) encased in silty inter-framework mudstone (M); B) vertical section, C) horizontal section. Laminae are poorly delineated by subtle changes in crystal size and relative abundance of inclusions (arrow in B). Scale bar 1 mm. Sample FLX-1.

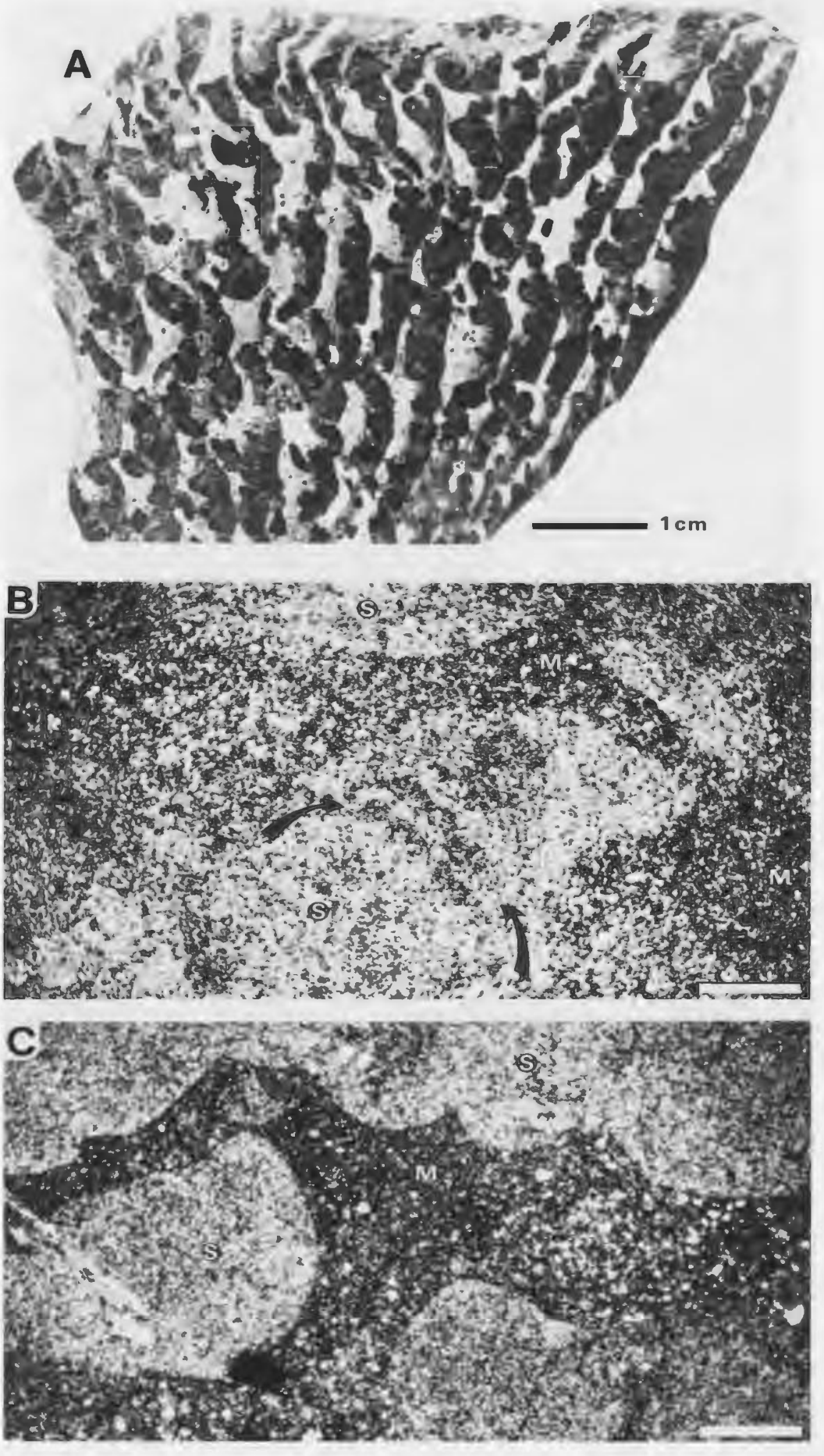
A
1cm
B
S
M
S
M
C
S
M
S

PLATE 31

Horizon G, Port au Port Peninsula

Megastructure, Mesostructure and Microstructure

A - Domed bioherm flanked and underlain by ooid dolostone; Bed A. Hammer 30 cm.

B,C - Horizontal and vertical slabs, respectively, of cryptomicrobial boundstone; Bed B. Dark coarser crystalline patches (D), and light finer crystalline patches probably represent framework and inter-framework components, respectively. Black areas within dark patches are due to iron staining. Sample MOW-2.

D - Inequigranular grumous microstructure (G) of dark ?framework components encased in equigranular microcrystalline dolomite (M)(?inter-framework sediment). Field of view 1 cm wide. Sample MOW-2.

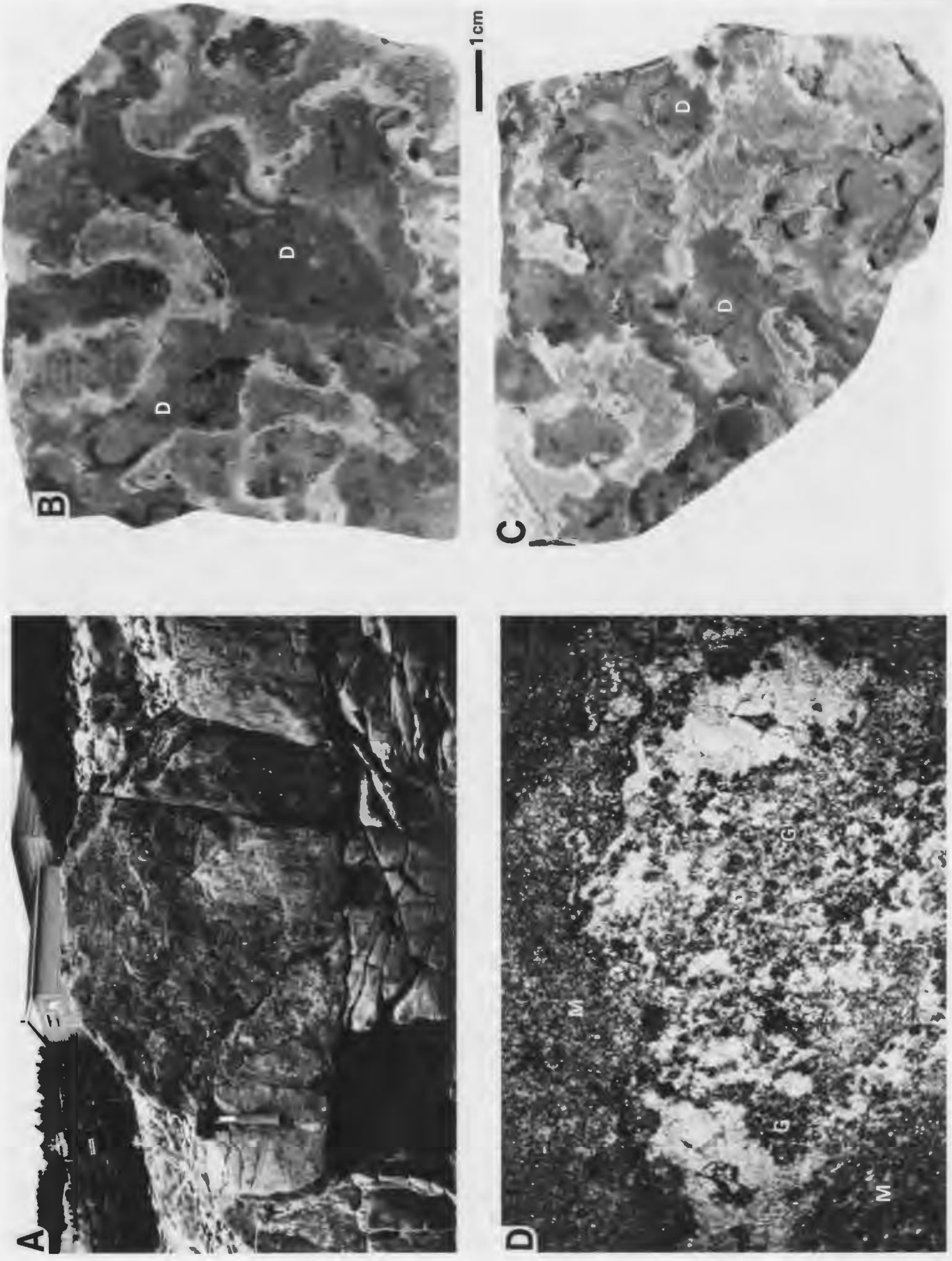
A
B
D
D
C
D
D
1cm
D
M
G
G
M

PLATE 32

Horizon H, Port au Port Peninsula

Megastructure

A - Pebble conglomerate with sub-evenly spaced fan-shaped arrays of edgewise discoidal pebbles. 10 cm scale rule.

B - Plan view of planar erosion surface at top of thrombolite bioherm. Light coloured thrombolite heads are separated by narrow grainstone wedges which represent former crevasses between protruding thrombolite heads.

C - Margin of tabular bioherm flanked by inter-biohermal parted limestone (grainstone and shale with well developed load casts). 1) Basal pebble conglomerate, 2) lower pebble-rich zone, and 3) upper stylo-nodular zone. Note irregular thrombolite heads (arrow) and grainstone fill (G) at top of bioherm.

D - Margin of bioherm 16 m to the east (right) of A. Intertonguing bioherm\inter-biohermal contacts in basal and central zones of bioherm indicate little or no synoptic relief during these growth stages, whereas abutting and onlapping contacts at upper portion of bioherm indicate moderate synoptic relief for final growth stage of bioherm.

Scale bars 10 cm.

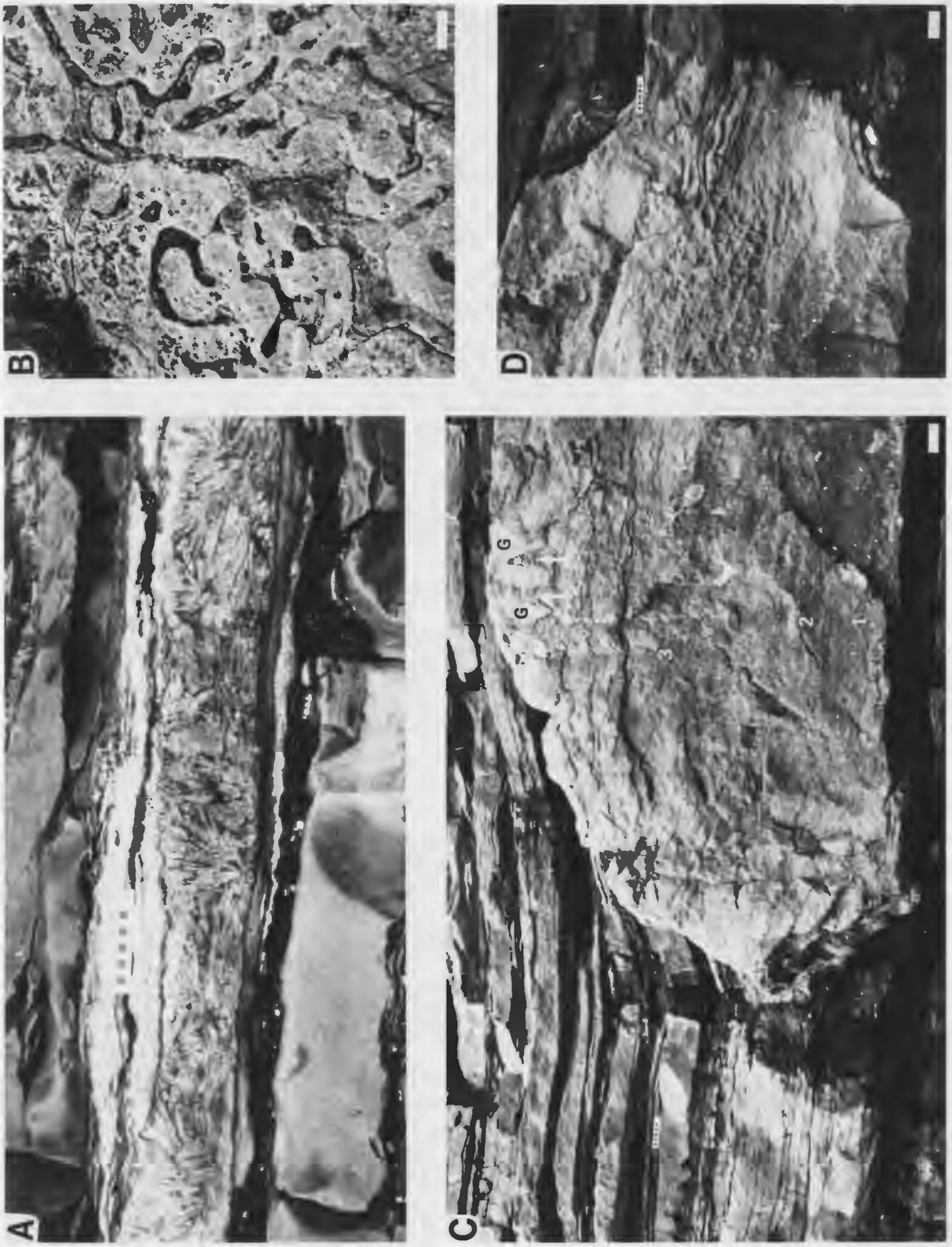
A
B
C
D
G
G
1
2
3

PLATE 33

Horizon H, Port au Port Peninsula

Mesostructure

A - Vertical slab of upper stylo-nodular thrombolite zone of bioherm, showing poorly defined thromboids (T), and light coloured inter-framework wackestone. Sample MOW-23A.

B - Vertical slab of lower pebble-rich thrombolite zone. Irregular, poorly defined digitate and amoeboid thromboids (T) are encased in pebbly skeletal-ooid packstone. Note erratic orientation of pebbles between, and encrusted by, thromboids, and gastropod fragments (arrows). Sample MOW-25.

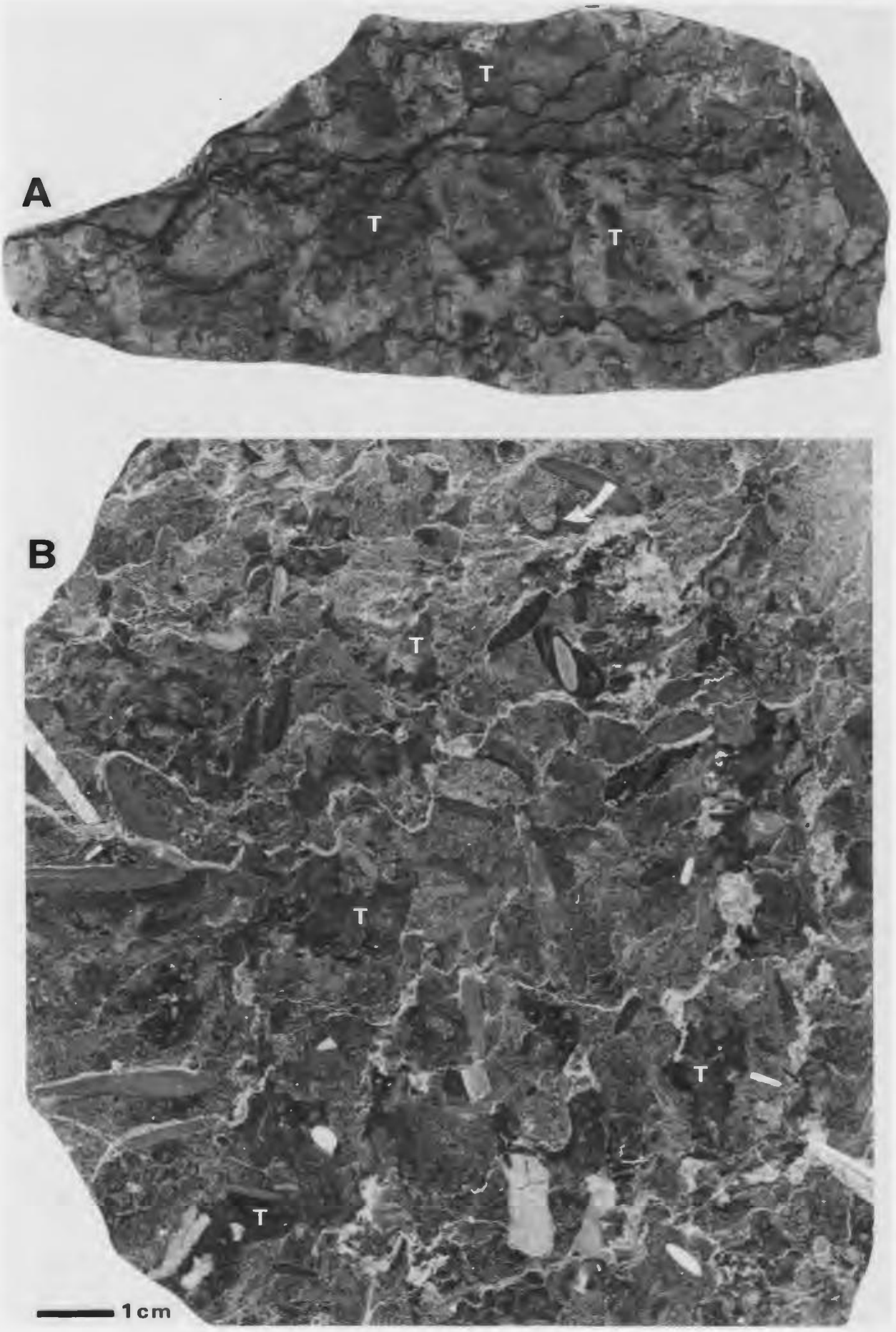
A
T
T
T
B
T
T
T
T
1 cm

PLATE 34

Horizon H, Port au Port Peninsula

Microstructure

A - Thromboid (T) comprised of massive microspar, relict cryptocrystalline patches, and scattered quartz silt. Inter-framework wackestone contains numerous pelmatozoan plates, gastropod fragments, ooids and quartz silt. Sample MOW-25.

B - Massive microcrystalline thromboid (top right) with clotted and saccate *Renalcis* (arrows). Inter-framework silty, ooid (replaced by coarse dolomite) pelmatozoan wackestone, with well rounded microspar pebble (P). Sample MOW-24.

C - Digitate thromboid (T) with silty grumous and spongeous-grumous microstructure, crypto-crystalline selvages (arrows), and spongeous overgrowths on left and right. Inter-framework wackestone (W) with subrounded peloids and clasts. Sample MOW-23.

Scale bars 1 mm.

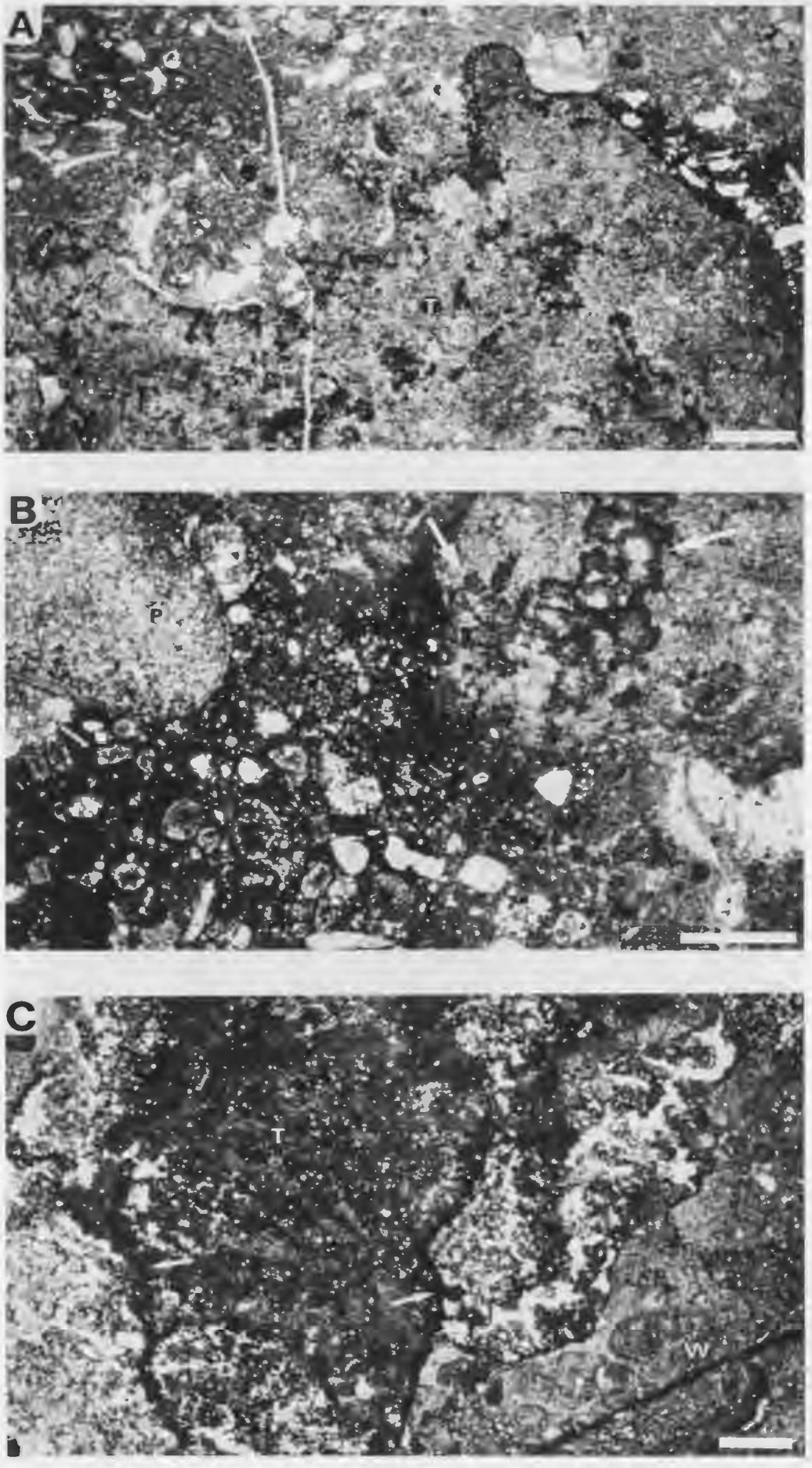
A
B
P
C
T
VV

PLATE 35

Horizon I, Port au Port Peninsula

Megastructure and mesostructure

A - Tabular bioherm cut by sediment-filled crevasse-like structure (arrows) that extends from the upper planar erosion surface (S) to the base of the bioherm; Bed A. Hammer 30 cm.

B - Plan view of close packed, concentrically zoned, bioherms truncated by planar erosion surface; Bed B. Pustular and pseudo-columnar stromatolite (Zone B2) grades outward to undulose stromatolite (Zone B3). 10 cm scale rule.

C - Vertical slab of columnar stromatolite, Zone B1. Light coloured, crudely convex laminated, dolomitic stromatoids (S) are encased in darker coloured wackestone. Note skeletal fragments (arrows). Sample MOW-27.

D - Vertical slab of pseudo-columnar stromatolite, Zone B2. Sample MOW-17.

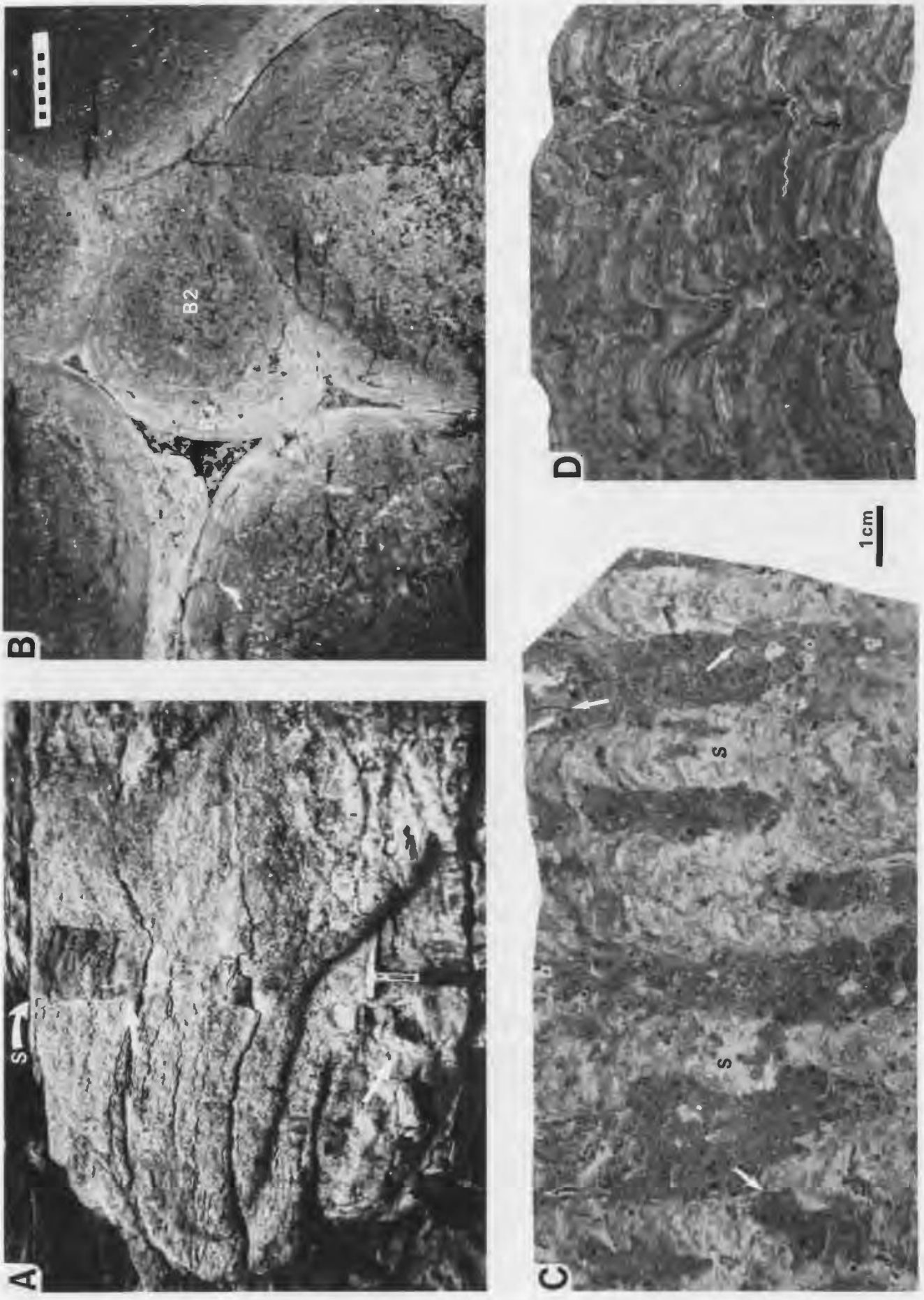
A
S
B
B2
C
S
S
D
1cm

PLATE 36

Horizon I, Port au Port Peninsula

Microstructure

A - Streaky cryptocrystalline and microcrystalline stromatoid column, Bed A. The dark cryptocrystalline laminae have a bumpy mamillate form, and massive to diffuse grumous microstructure. White particles are dolomite. Inter-framework sediment contains ooids, peloids and intraclasts, some of which are rimmed are isopachous fibrous cement. Sample MOW-21.

B - Irregular mottled microstructure of extensively dolomitized stromatoid column, Zone B1. Diffuse vermiform microstructures (V) are evident in non-dolomitic crptocrystalline patches. Note cement-filled boring at top. Sample MOW-16B.

C - Stromatoid column with diffuse grumous microstructure, scattered dolomite, and dark cryptocrystalline selvage; Bed A. Note sediment and microspar-filled cavity (C) within column, and cement-rimmed peloids and dolomitic intraclast (top left) in inter-framework sediment. Sample MOW-21.

D - Saccate lobate microstructures (arrows) at crest of poorly laminated, slightly dolomitic, column; Bed A. Sample MOW-21.

E - Margin of weakly laminated stromatoid column (S) with spongeous-grumous microstructure; Zone B2. Note thin cryptocrystalline selvage (wall *sensu* Walter, 1972) which results from the downward continuation of cryptocrystalline laminae along the margin of the column. Note trilobite fragments (arrows top left) in dolomitic inter-framework wackestone (W). Sample MOW-27.

Scale bars 1 mm

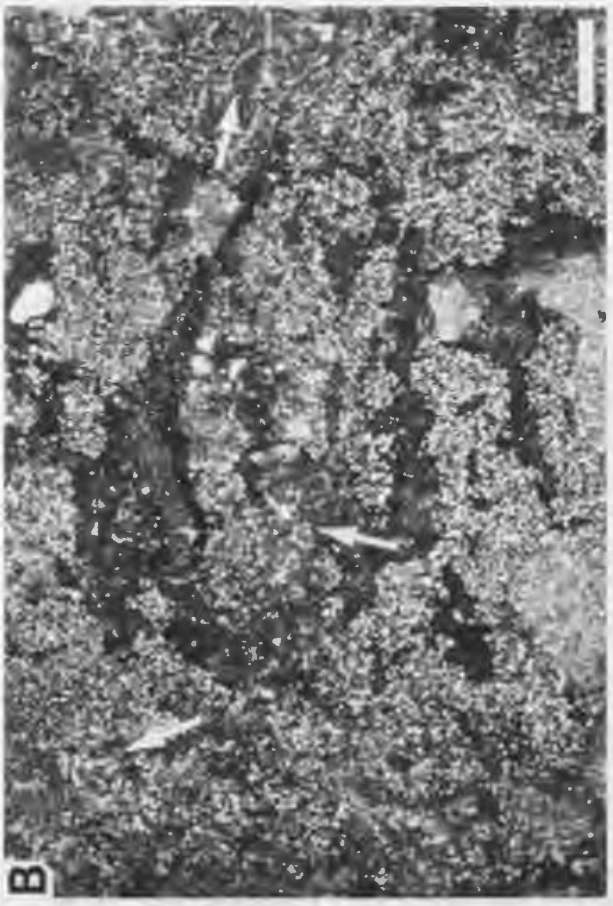
B

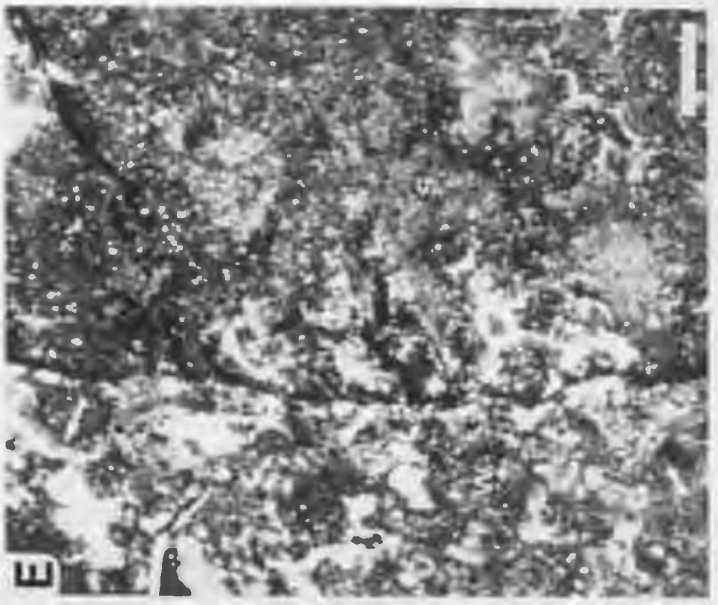
E

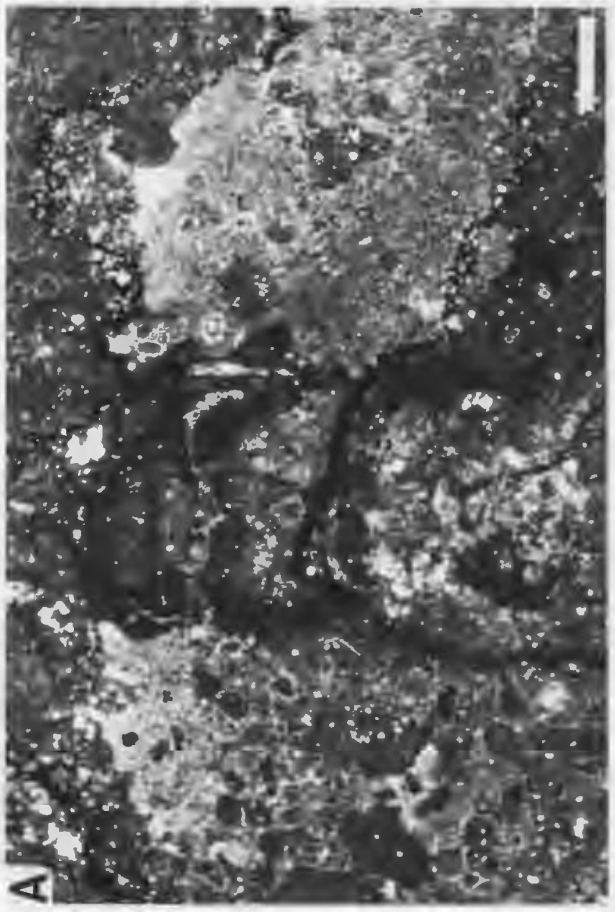
A

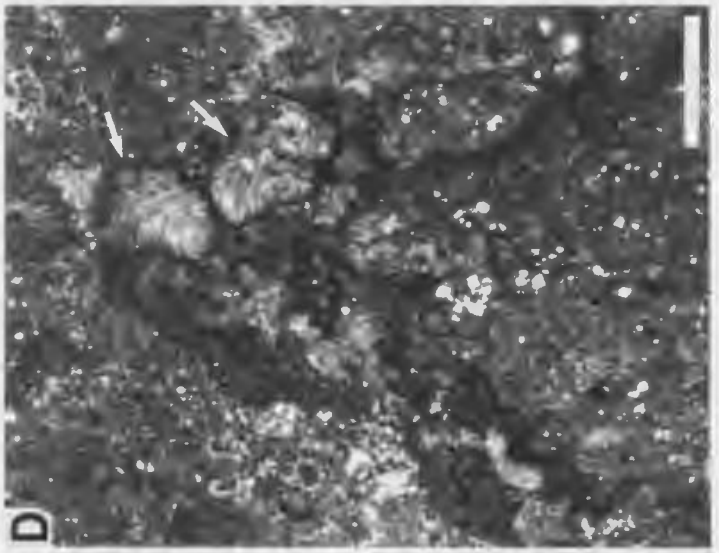
D

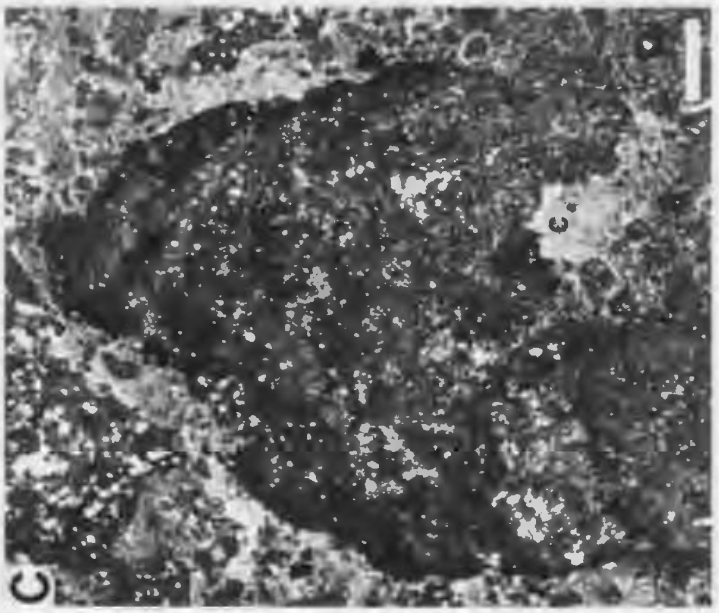
C

PLATE 37

Horizon J, Port au Port Peninsula

Megastructure and mesostructure

A - Plan view of erosion surface that truncates stromatolite heads (S) rimmed by thin vertically laminated walls (arrows) and separated by narrow grainstone wedges (G); Bed B, Zone B2. Pen 14 cm.

B - Vertical section through stromatolite heads (Zone B2) rimmed by vertically laminated walls (W) of unknown origin, and separated by narrow grainstone (G) wedges. Stromatolite heads and grainstone wedges are truncated by karst erosion surface (K) with small, mesa-like, erosional protuberances (E). Erosion surface is overlain by thin dark thrombolite layer (Zone B3), and topographic highs of this layer, or the mesa-like erosional protuberances of Zone B2, are encrusted by small hemispheroidal stromatolites (Zone B4). 10 cm scale rule.

C - Vertical slab of thrombolite Zone A1 showing dark sub-digitate thromboids encased in burrow-mottled, dolomitic wackestone. Note irregular bio-eroded margins of thromboids. Sample MOW-12.

D - Vertical slab of thrombolite Zone B1 showing framework of poorly defined thromboids (T) encased in lighter coloured mudstone. Note clusters of small dark lobate bodies within thromboids. Sample MOW-6.

E - Vertical slab of hemispheroidal stromatolite, Zone B4. Sample MOW-11.

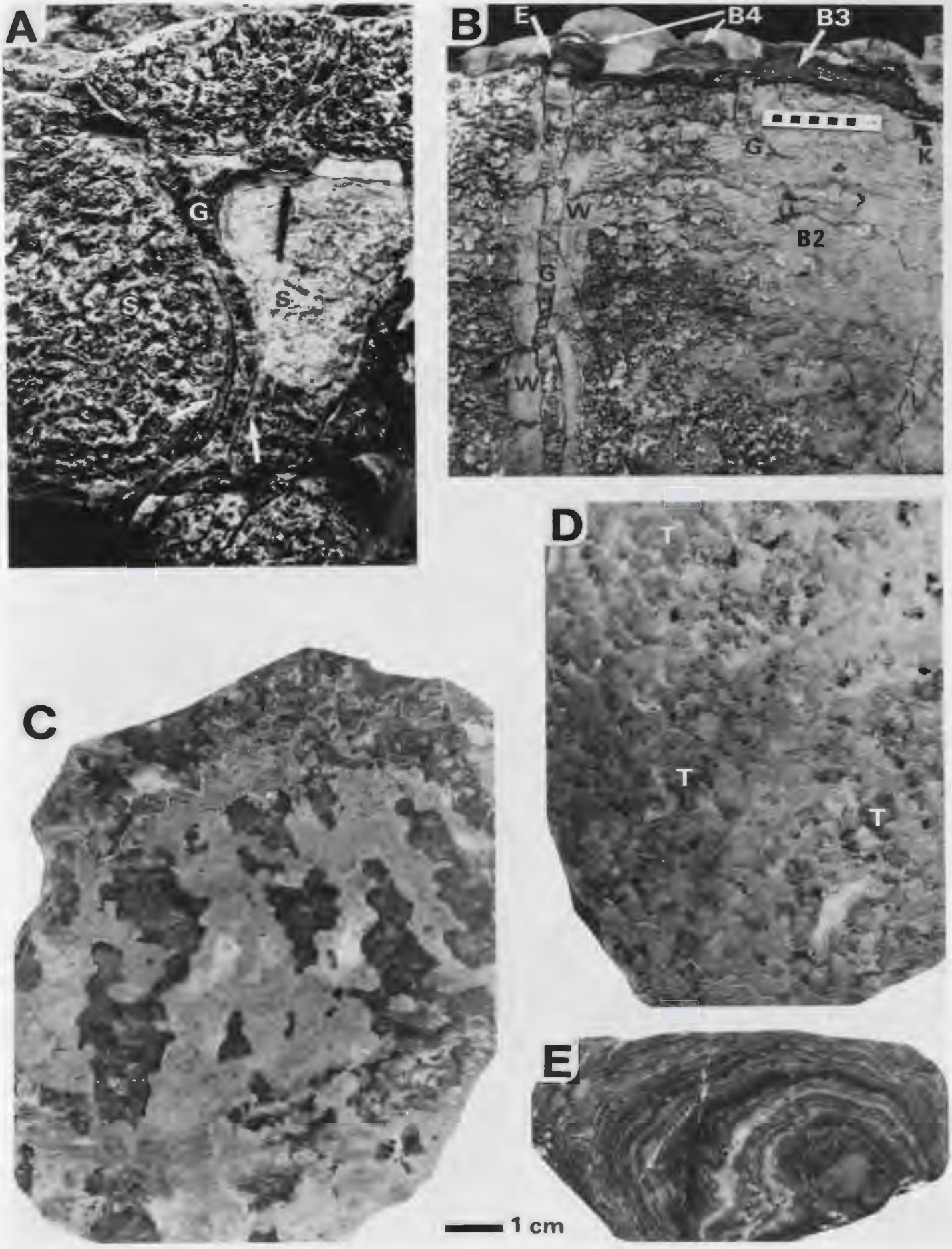
A
G
S
S
B
E
B4
B3
G
K
W
B2
G
W
C
D
T
T
T
E
1 cm

PLATE 38

Horizon J, Port au Port Peninsula

Microstructure - thromboids; Zone A1

A - Variegated spherulitic lobate (L), grumous (G), massive (M), and peloidal (P) microstructure of sub-digitate thromboid flanked to the left and right by dolomitized inter-framework sediment (D). Note thin cryptocrystalline rims (arrows) to spherulitic lobes, and sediment-filled burrow (B). Sample MOW-12.

B - Variegated spherulitic lobate (L), grumous (G), massive (M), and peloidal (P) microstructure of thromboid flanked by inter-framework peloidal wackestone (W). Thromboid is locally bordered by one or more thin layers of cryptocrystalline carbonate (film microstructure; arrow top left), and similar films occur within the thromboid (arrows). Sample MOW-12.

C - Spherulitic lobate microstructure comprised of several well defined spherulites (arrows), and weakly spherulitic to massive, turbid microspar. Note cryptocrystalline nucleii of some spherulites. Spherulitic lobes are encased in massive cryptocrystalline microstructures. Sample MOW-12.

D,E - Blade like form of possible codiacean or dasycladacean alga; D) section parallel to blade showing transverse section of micritic rods; E) section perpendicular to blade showing cylindrical rods. Samples MOW-12, 12B.

Scale bars 1 mm.

A
M
L
G
B
D
P
B
M
L
G
L
P
W
C
D
A
E
A

PLATE 39

Horizon J, Port au Port Peninsula

Microstructure - Thromboids; Zones A1 and B1

A,B - Weakly spherulitic lobate microstructure with discontinuous cryptocrystalline rim; A) plane polarized light; B) crossed polarized light. Spherulites appear as an irregular mosaic of turbid anhedral calcite in plane polarized light, but are characterized by domains of irregular sweeping extinction or maltese-like extinction crosses (arrows) in crossed polarized light. Spherulitic thromboid is encased in dolomitized inter-framework sediment (D). Zone A1, Sample MOW-12.

C,D - Spherulitic lobate microstructure comprised of several relatively distinct spherulites and a discontinuous cryptocrystalline rim. C) Plane polarized light, D) crossed polarized light. Zone A1, Sample MOW-12.

E - Cellular and saccate lobate microstructure of amoeboid thromboid; Zone B1. Lobate bodies are encased in massive to diffuse grumous micro-structures. Sample MOW-6.

Scale bars 0.5 mm

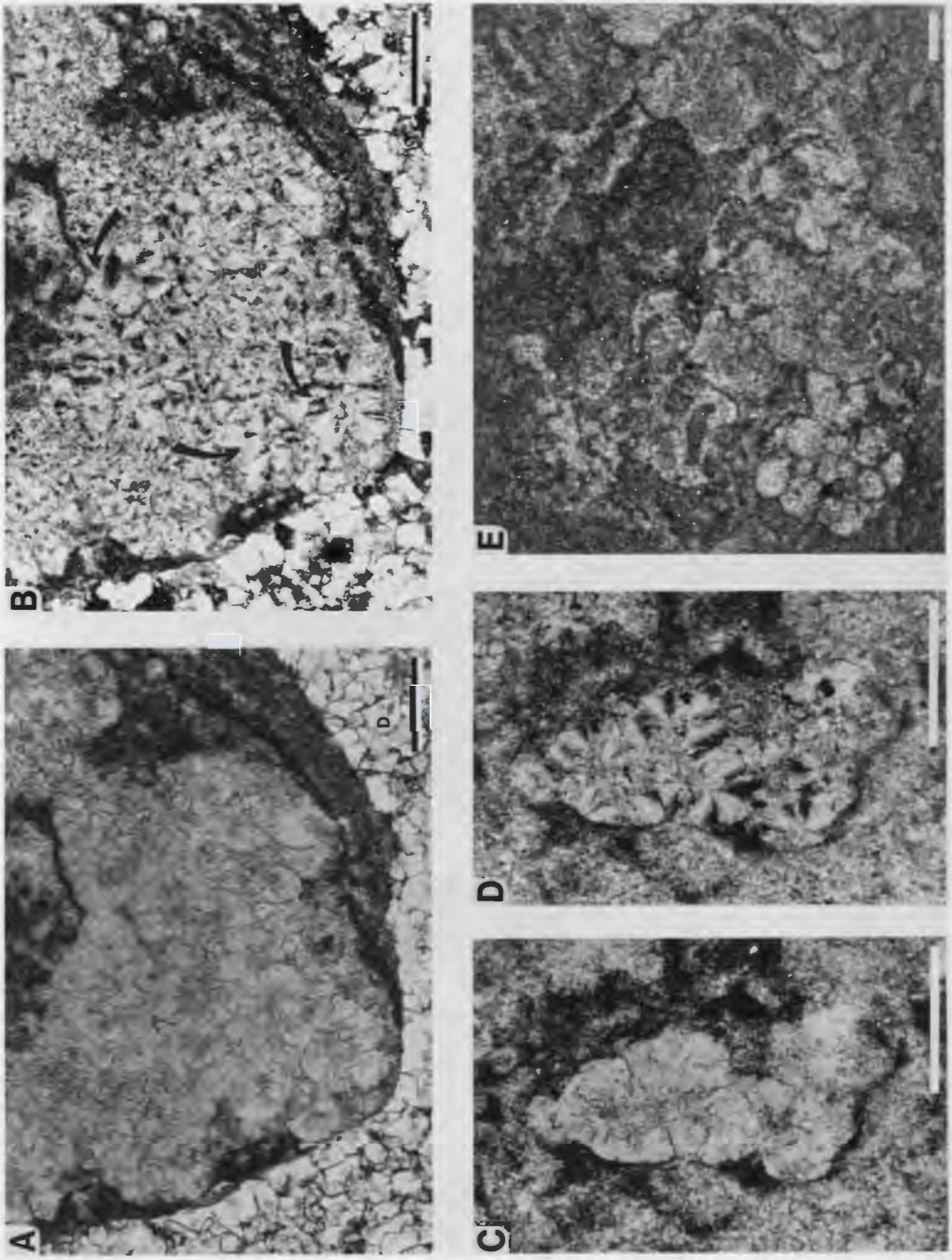
A
B
C
D
E

PLATE 40

Horizon J, Port au Port Peninsula

Microstructure - Stromatoids; Zones A2, B2, B4

A - Streaky, silty peloidal and massive microstructure of stromatoid column, Zone A2. Note diffuse silt-sized peloids (arrows), laminoid micro-fenestrae, and irregular bumpy shape of massive laminae (M). Sample MOW-13.

B - Dolomitized stromatoid column with relict patches of grumous microstructure (G), Zone B2. Cryptocrystalline microclots are difficult to distinguish from silt-size peloids within burrows (arrow).
Sample MOW-8B.

C - Banded microstructure comprised of alternating 1) spongeous grumous grading to filamentous laminae, and 2) thin massive cryptocrystalline laminae; bulbous stromatolite, Zone B4. Note delicate networks of randomly oriented or erect, thread-like microclots.
Sample MOW-11.

D - Streaky microstructure comprised of superimposed spongeous grumous and\or filamentous laminae, without intervening thin crypto-crystalline laminae; bulbous stromatolite, Zone B4. Sample MOW-11.

E - Banded microstructure of relatively thick spongeous grumous grading to filamentous laminae, and thin (?)stylolitic, cryptocrystalline laminae or films; bulbous stromatolite, Zone B4.
Sample MOW-11.

Scale bars 1 mm.

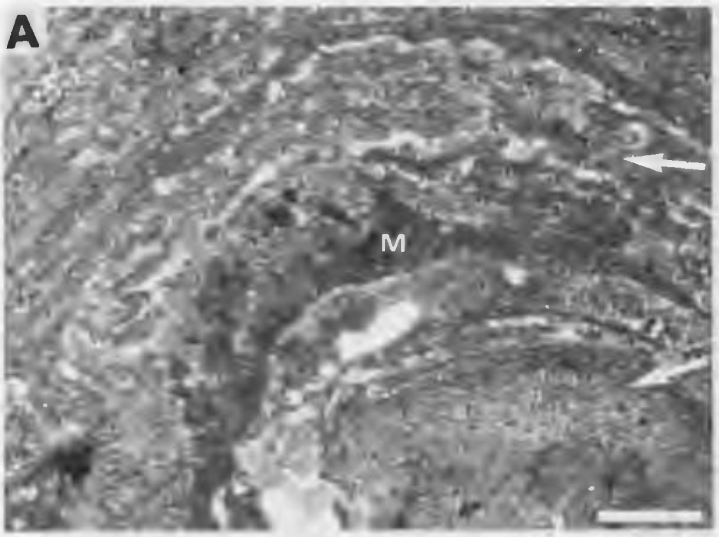
A
M

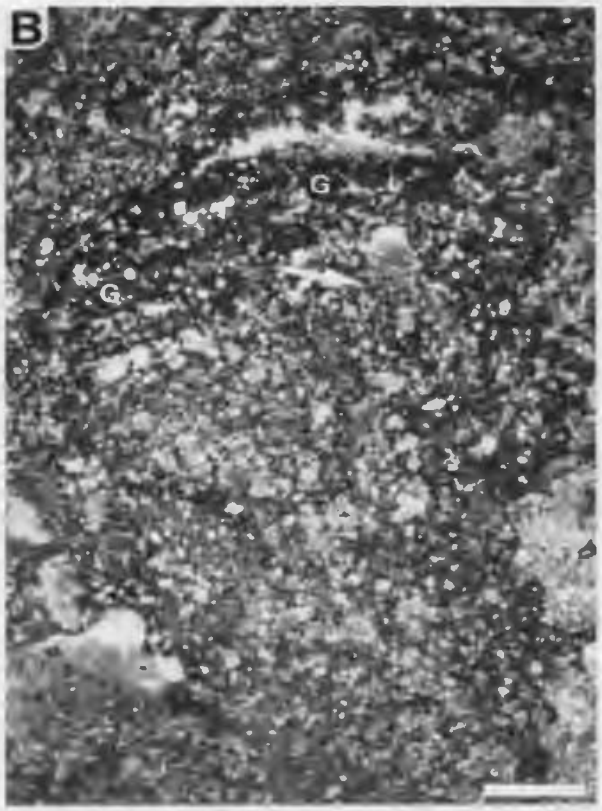
B
G
G

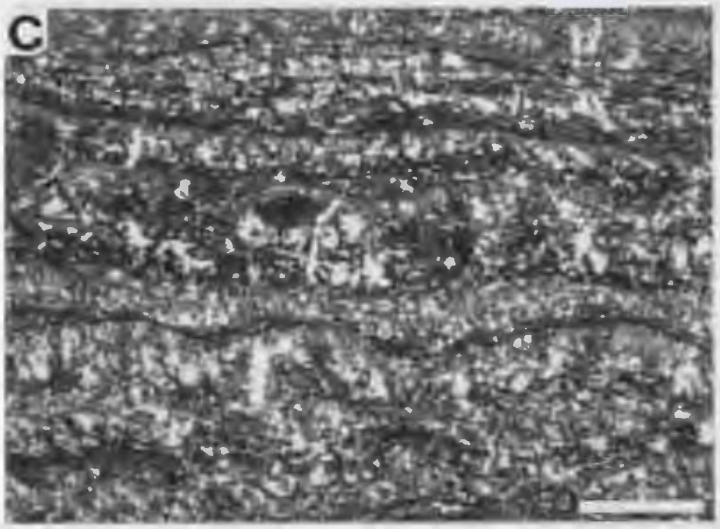
C

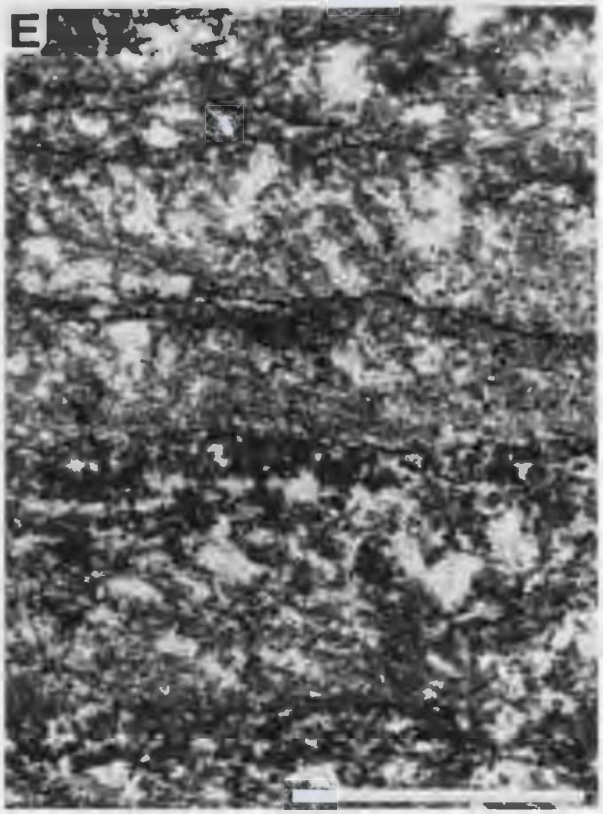
E

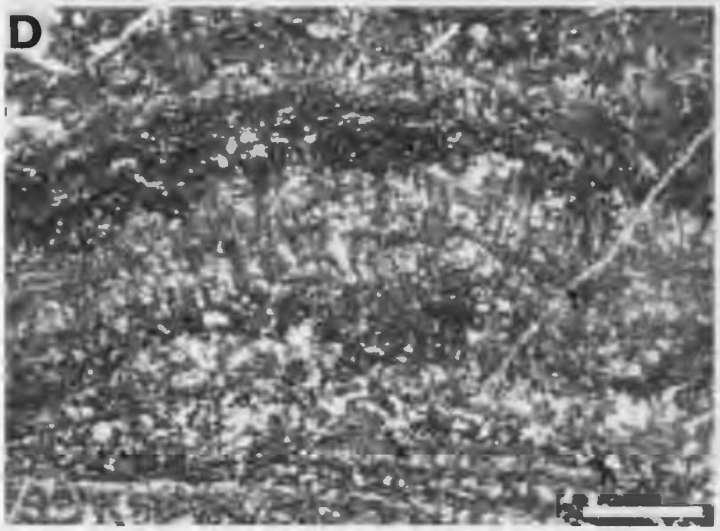
D

PLATE 41

Horizon K, Port au Port Peninsula

Mesostructure

A - Tabular biostrome comprised of columnar stromatolite mounds and planar to undulose stromatolite cap (at scale rule).
Scale rule 10 cm.

B - Vertical slab of columnar stromatolite showing branching stromatoid columns encased in ooid-peloid-skeletal grainstone and packstone.
Sample BEH-1.

C - Vertical slab of undulose stromatolite that caps the columnar stromatolite shown in B.
Sample BEH-3.

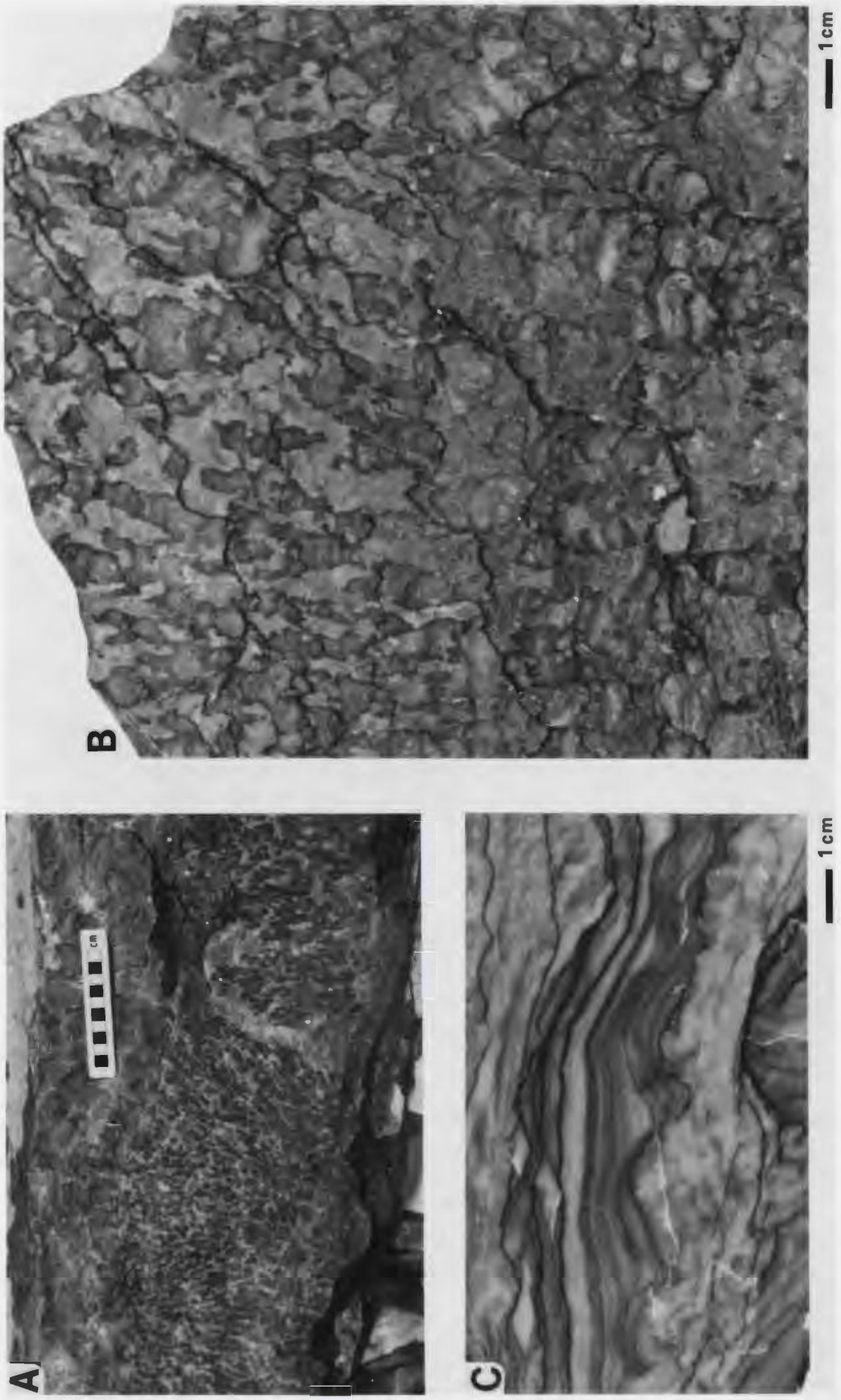
B
1cm
A
cm
C
1cm

PLATE 42

Horizon K, Port au Port Peninsula.

Microstructure

A - Streaky vermiform and massive microstructure of columnar stromatoid encased in peloid-ooid grainstone. Note range in size of filament moulds from lamina to lamina, and scattered ooids bound within the column. Sample BEH-1.

B - Vermiform microstructure with randomly oriented filament moulds. Note sediment-filled burrow lower left. Sample BEH-2.

C - Streaky vermiform and massive microstructure of stromatoid column. Note sediment-filled fenestrae and burrow (arrow). Sample BEH-1.

D - Banded microstructure of planar stromatoids. Thin massive cryptocrystalline laminae alternate with diffuse grumous laminae. Cryptocrystalline microclots are coarser and more distinct in the thick lamina at the top which has an inter-gradational grumous\peloidal microstructure; the uniform, subrounded shape of these microclots\ peloids suggests that they are trapped detrital peloids (possibly faecal pellets). Similarly, diffuse grumous laminae probably represent layers of partially merged, poorly indurated, peloids or pellets. Note small spherulitic quartz nodules (arrows). Sample BEH-3B.

Scale bars 1 mm.

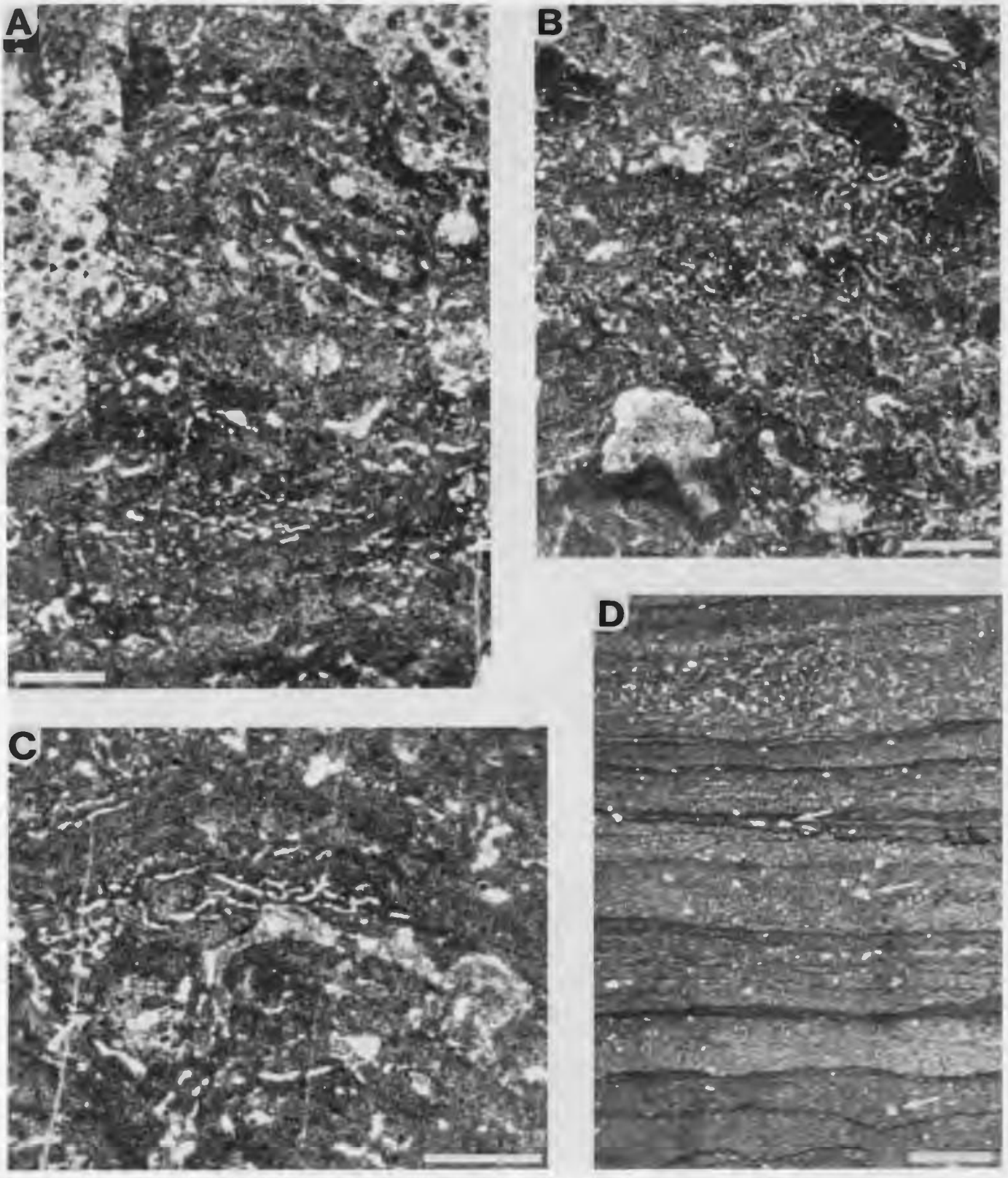
A
B
C
D

PLATE 43

Green Head microbial-metazoan complex
Horizon L, Port au Port Peninsula

Mesostructure

A - Plan view of selectively dolomitized and silicified *Renalcis* thrombolite heads encased in light coloured skeletal wackestone; Unit 1. Scale rule 10 cm.

B - Vertical slab of thrombolite head with dark silicified and dolomitic *Renalcis* (R) mass roofing a small cavity filled with mudstone; Unit 1. Arborescent (top left) and amoeboid (lower right) thromboids (T) are encased in light coloured mudstone. Note grainstone patches (G). Sample GH-A-1A.

C - Digitate thrombolite; Unit 7. Elongate, light coloured, dolomite digits are encased in darker coloured lime-wackestone.

D - Cerebroid outcrop pattern of dark coloured *Lichenaria* thrombolite heads (T) surrounded by light coloured *Renalcis* walls, and separated by dark coloured packstone channels (P); Unit 3. Details of outlined area are shown in E.

E - Field sketch of bedding surface showing distribution of lithologies within area indicated in D; Unit 3.

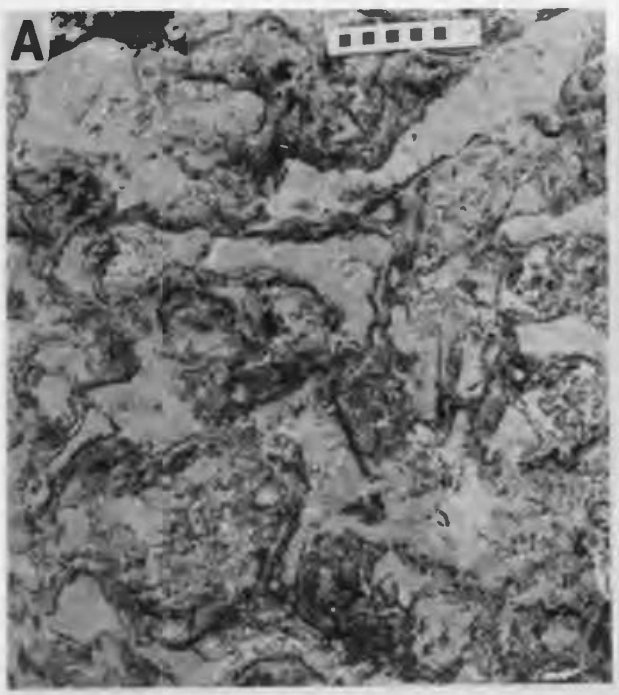
A


B
T
G
T
R
R
1 cm


C
10 cm


D
T
T
P
1 m

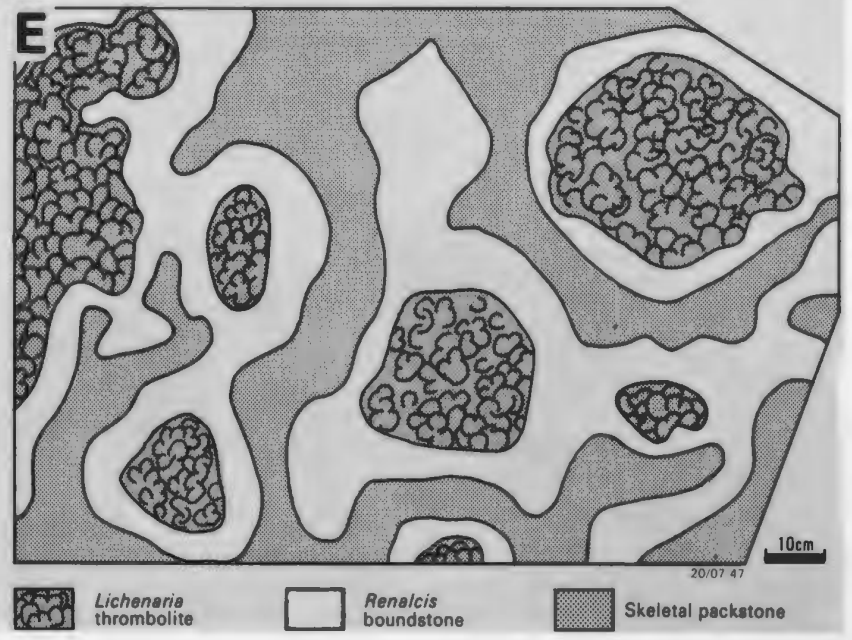
E
10cm
20/07 47
Lichenaria thrombolite
Renalcis boundstone
Skeletal packstone

PLATE 43

PLATE 44

Green Head microbial-metazoan complex
Horizon L, Port au Port Peninsula

Mesostructure - 1

A - Vertical slab of *Renalcis* thrombolite overlain by bioturbated wackestone channel (w); Unit 1. Dark siliceous and dolomitic *Renalcis*-thromboid mass (centre right) roofs a cavity filled with packstone (p) and mudstone (m). Speckled *Renalcis*-thromboid masses (R) are surrounded by patches of grainstone, packstone and wackestone with numerous nautiloid (n) fragments. Sample GH-A-1.

B - Vertical slab of thrombolite-*Lichenaria*-*Renalcis* boundstone heads separated by narrow wedge of peloid-skeletal packstone (p) with lodged nautiloid fragments (n); Unit 3. Intergrown clusters of dark lobate thromboids (t) and partially silicified *Lichenaria* corals (C) form an interconnected framework which is infilled by light coloured lime-mudstone (m). Thrombolite-*Lichenaria* heads are encrusted by light coloured *Renalcis*-rich walls (R). Note upward and outward growth orientation of coral colonies towards margins of thrombolite heads. Sample GH-C-1(2).

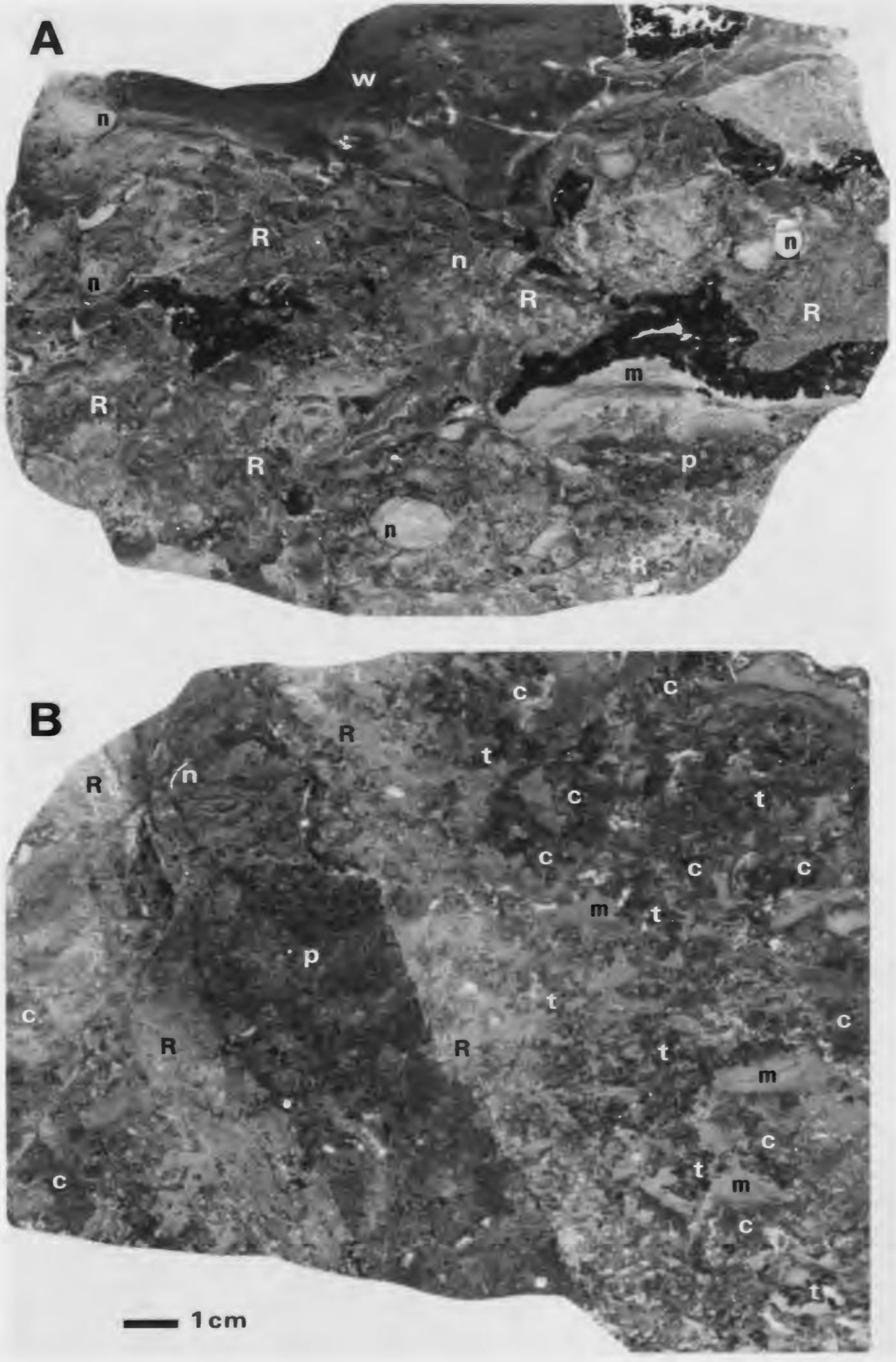
A
w
n
R
n
n
R
n
R
m
R
R
p
n
R
B
c
c
R
t
R
n
c
t
c
c
c
m
t
p
t
c
c
R
R
t
m
c
t
m
c
c
t
1cm

PLATE 45

Green Head microbial-metazoan complex
Horizon L, Port au Port Peninsula

Mesostructure - 2

A - Vertical slab of *Lichenaria*-thromboid-*Renalcis* framestone, Unit 3. Sample GH-C-1.

B - Tracing of slab shown in A, depicting distribution of *Lichenaria*, thromboids*Renalcis* and lime-mudstone.

A
B
1cm
Lichenaria
Thromboids and Renalcis
Lime-mudstone

PLATE 46

Green Head microbial-metazoan complex
Horizon L, Port au Port Peninsula

Microstructure - Unit 1

A - Composite *Renalcis* and spongeous-grumous microstructure of *Renalcis* thrombolite. Dark clotted (lower left within silicified area) and chambered (centre) *Renalcis* occur within diffuse grumous microstructure which is disrupted by numerous irregular, spar-filled, micro-fenestrae. Note diffuse pelletal sediment within fenestrae (?burrow) at centre (arrow).
Sample GH-A-1A.

B - Spongeous diffuse grumous microstructure intergrading with poorly defined clotted (right) and saccate (left) *Renalcis* (R). Irregular fenestra at lower centre is floored by diffuse pelletal (grumous) sediment. Sample GH-A-1B.

C,D - Spongeous, microcrystalline lobate (L) microstructure intergrown and intergrading with diffuse grumous (G) and poorly defined clotted and saccate *Renalcis* (R). Note pellets and ?reworked saccate *Renalcis* within fenestrae (arrows). Sample GH-A-1A.

E - Intergrown chambered and saccate *Renalcis* and spongeous diffuse grumous microstructure. Note abundant lighter coloured pelletal sediment (P) within fenestrae. Sample GH-A-1B.

Scale bars 1 mm.

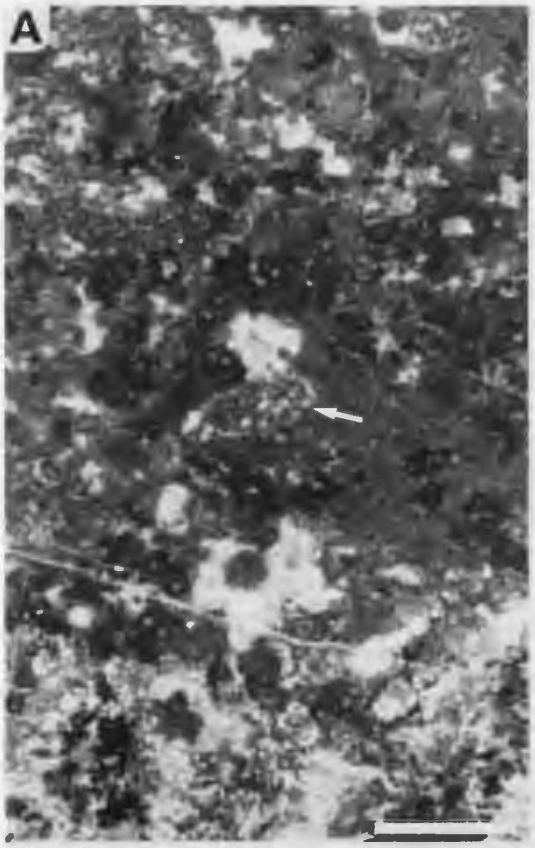
A

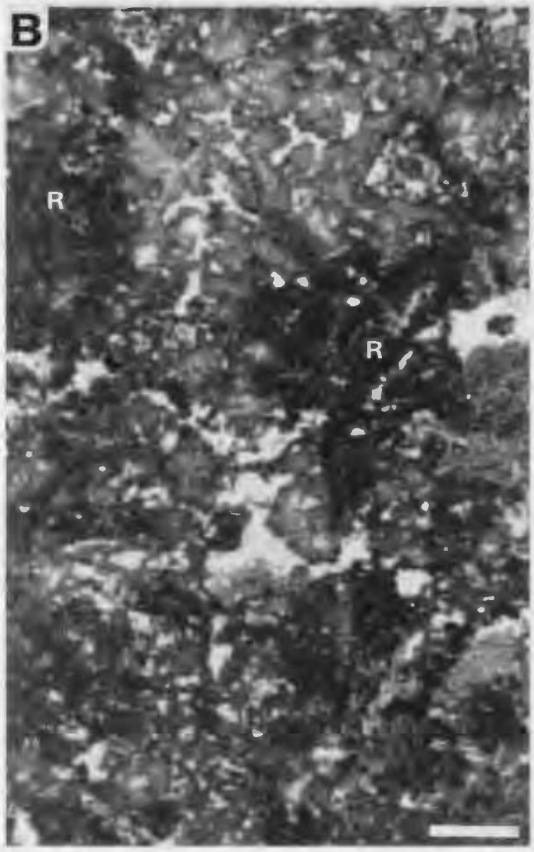
B
R
R

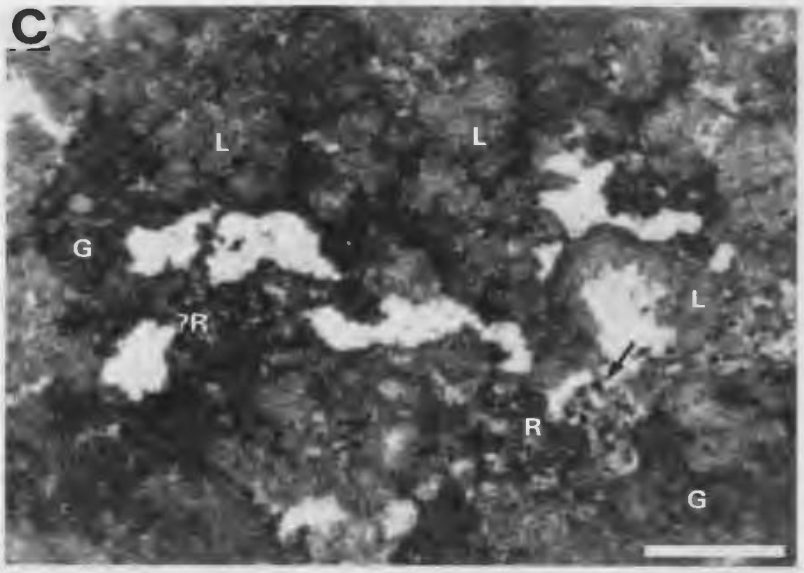
C
L
L
G
R
L
R
G

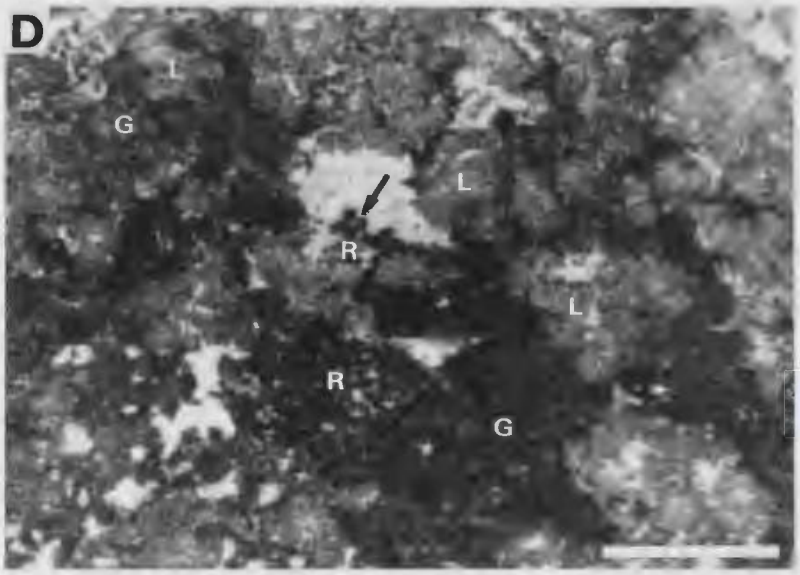
D
L
G
L
R
L
R
G

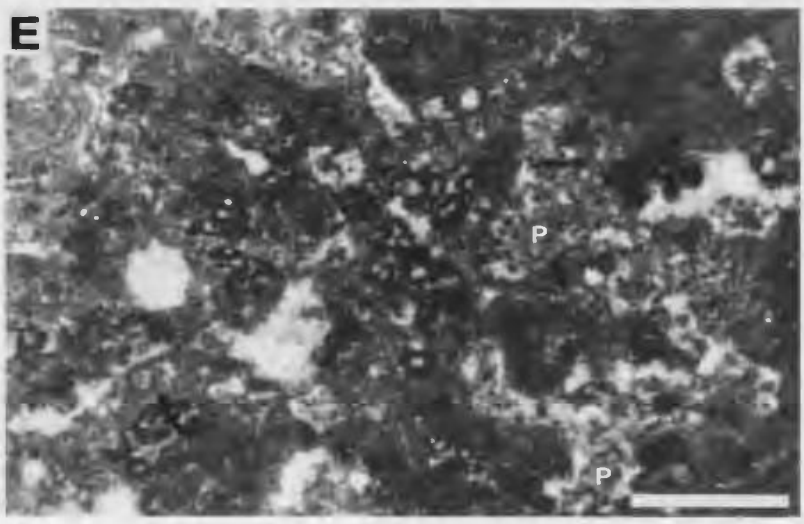
E
P
P

PLATE 47

Green Head microbial-metazoan complex
Horizon L, Port au Port Peninsula

Microstructure - Units 1 and 3

A - *Renalcis* boundstone that forms an encrusting, overhanging wall around thrombolite head (thrombolite out of view to top left); Unit 1. Note pendant, downward directed, growth forms of *Renalcis* (arrows), and irregular spar-filled fenestrae. Channel beneath *Renalcis* wall is filled with gastropod wackestone (W). Pelletal sediment (P) fills gastropod shell and relatively large burrow. Sample GH-A-2.

B - Magnified view of spongeous *Renalcis* boundstone wall shown in A. Note saccate and chambered morphotypes, and pendant growth orientation. Sample GH-A-2.

C - Composite microcrystalline lobate (L) and grumous (g) microstructure of thromboid; Unit 3. The central portion of microcrystalline lobes are commonly replaced by microcrystalline quartz (q). Note sediment and cement-filled burrow within thromboid (arrow), and *Stromatactis*-like structure formed by inter-framework mudstone (M) and blocky spar cement (C). Sample GH-C-1B.

D - Magnified view of central portion of C showing well developed grumous microstructure between microcrystalline lobes (L), the central portions of which are replaced by microcrystalline quartz (q). Sample GH-C-1B.

Scale bar 1 mm.

A
W
P
B
D
L
q
C
M
c
g

PLATE 48

Green Head microbial-metazoan complex
Horizon L, Port au Port Peninsula

Microstructure - Unit 3

A - Variegated spongeous, lobate (L), and grumous (g) microstructure of thromboid. Irregular fenestrae and (?)burrows are partially filled with pelletal sediment (arrows), and centres of microcrystalline lobes are replaced by weakly spherulitic quartz (q). Note *Stromatactis*-like structures formed by laminated mud (M) and blocky cement (C) within former inter-framework cavities. Sample GH-C-1A.

B - Composite spongeous grumous microstructure of thromboid. Sample GH-C-2.

C - Partially silicified *Lichenaria* coral. Corallites are partially occluded by pelletal sediment (arrows). Sample GH-C-1C.

D - Partially silicified *Lichenaria* corals (Cr) encrusted by grumous thromboids (T), and pendant clotted *Renalcis* (R) which projects into mud-filled inter-framework cavity (M); crossed polarized light. Note pelletal sediment within corallites at top centre. Sample GH-C-1D.

Scale bars 1 mm.

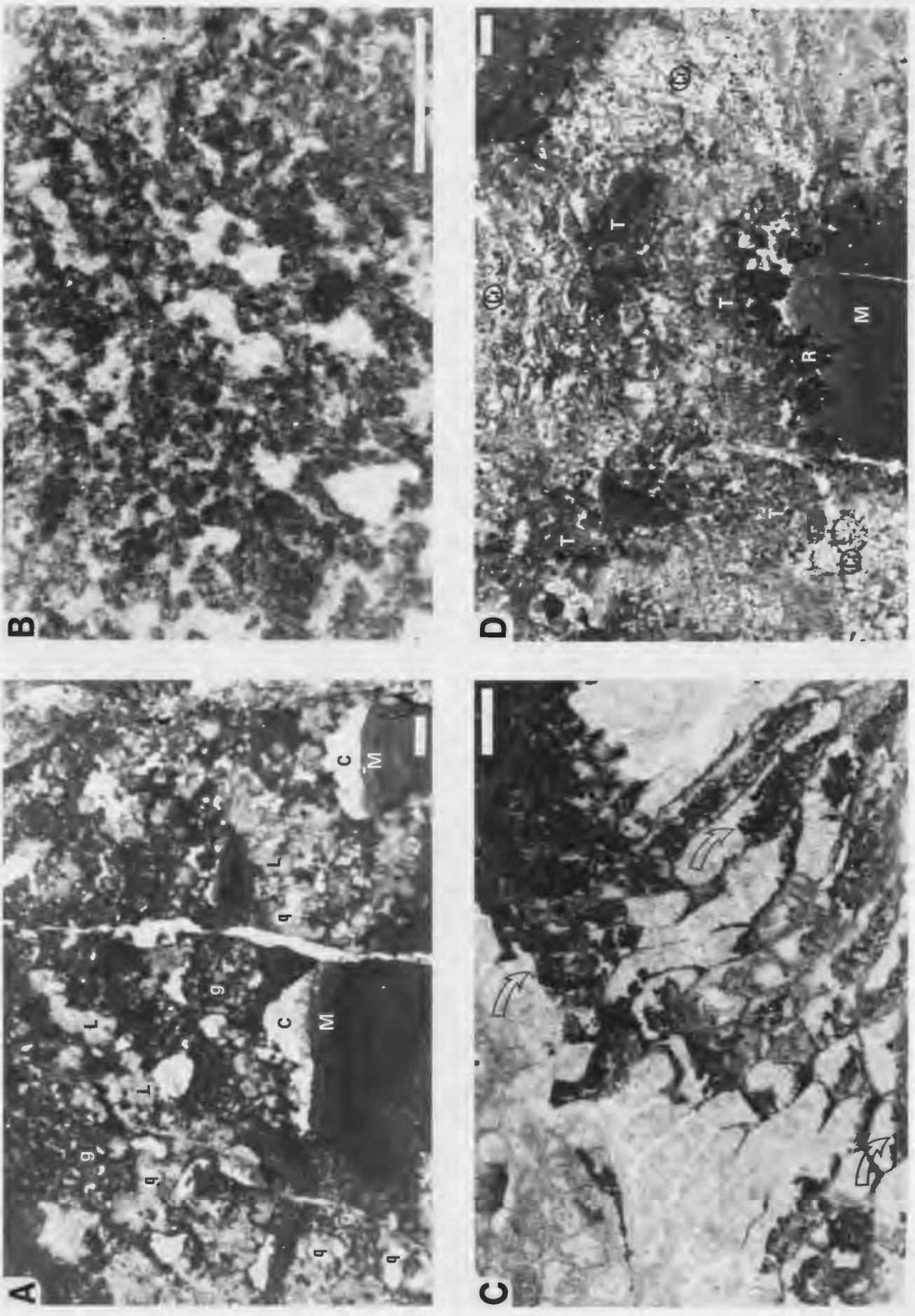
A
B
C
D
M
T
R
L

PLATE 49

Green Head microbial-metazoan complex
Horizon L, Port au Port Peninsula

Microstructure - Unit 5

A - Composite *Renalcis* and spongeous grumous microstructure of thrombolitic *Renalcis* boundstone. Note random to prostrate orientation of chambered and saccate *Renalcis*, and pelletal sediment (arrows) within irregular fenestrae. Sample GH-E-1A.

B - Poorly defined chambered, saccate and clotted *Renalcis* (arrows) surrounded by, and intergradational with, spongeous grumous microstructures. Note pelletal sediment within fenestrae, and euhedral dolomite (D). Sample GH-E-1A.

C - Spongeous microcrystalline lobate (L) and grumous (g) grading to clotted *Renalcis* microstructures. Note pendant form of grumous grading to clotted *Renalcis* structures at roof of cavity occluded by pelletal sediment (P) and blocky cement (C). Fenestrae between microcrystalline lobes are also filled by similar pelletal sediment (arrows). Sample GH-C-1A.

D - Abundant brachiopod and trilobite debris within packstone that surrounds free-standing thrombolitic *Renalcis* boundstone heads. Sample GH-C-1B.

Scale bars 1 mm.

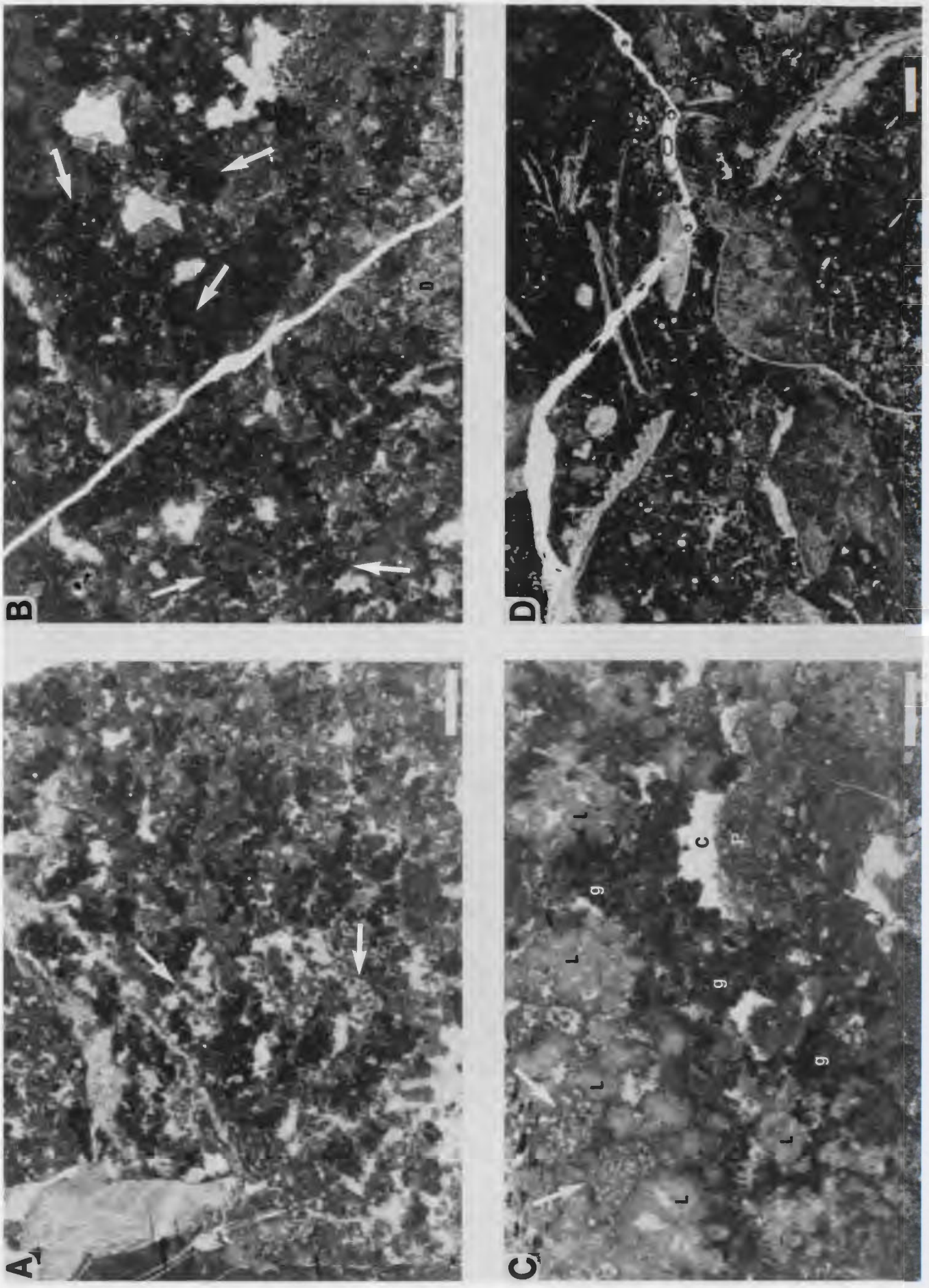
A
B
C
D
L
g
c
p

PLATE 50

Horizon M, Port au Port Peninsula

Megastructure and mesostructure - Beds A and B

A - Domed bioherm flanked and overlain by peloid-intraclast grainstone; Bed A. Basal cryptomicrobial Zone A1 is overlain by zone of aberrant digitate and cup-like stromatoids (Zone A2). Scale rule 10 cm.

B - Cryptomicrobial boundstone comprised of irregular mottled light coloured mudstone, wackestone and dolomite patches, and dark cryptomicrobial fabrics; Zone A1.

C,D - Aberrant boundstone comprised of dark conical and cup-like stromatoids encrusting light coloured elongate axial areas of coarse sparry calcite, dolomite and lime-mudstone; Zone B2. Note edgewise pebble (arrows in C) lodged between and overlying aberrant structures.

E - Digitate cryptomicrobial boundstone, Zone B4. Light coloured dolomitic and dark coloured silicified cryptomicrobial digits are encased in peloid grainstone. Lens cap 5 cm.

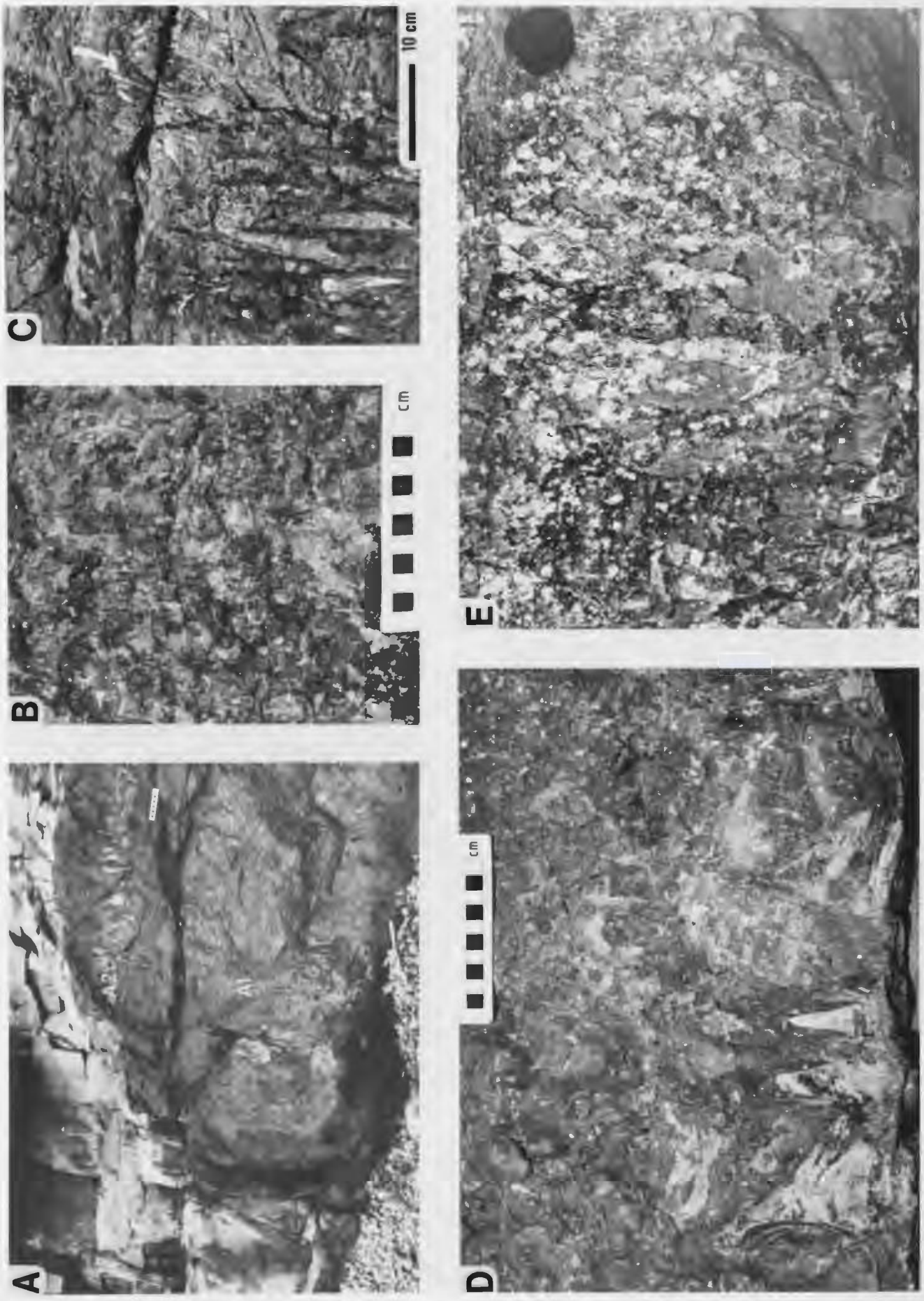
A
A1
A2
B
cm
C
10 cm
D
cm
E

PLATE 51

Horizon M, Port au Port Peninsula

Megastructure and mesostructure - Bed C

A - Domed bioherms flanked and draped by dolo-grainstone. Irregular, upward and outward radiating, sub-digitate stromatoid columns are evident at the crest of the bioherms. Note pocket of pebbly conglomerate between the bioherms. Scale rule 10 cm.

B - Plan view of upper surface of bioherm showing cerebroid pattern of interconnected dark stromatoid columns, and light coloured dolomitic inter-framework sediment. Scale rule 10 cm.

C - Vertical slab of digitate stromatolite showing irregular, weakly laminated stromatoid columns (S), and selectively dolomitized inter-framework packstone. The columns have an indistinct dark selvage, and numerous column fragments are evident in the inter-framework sediment. Sample WB-5A.

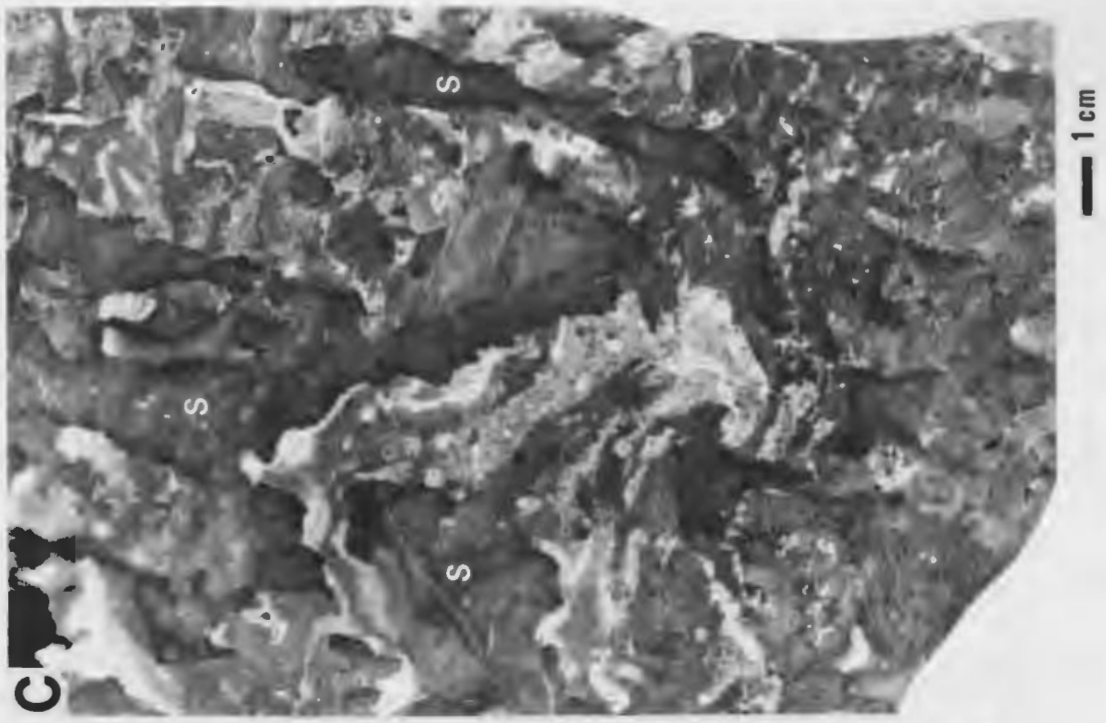
C
S
S
S
1 cm


A

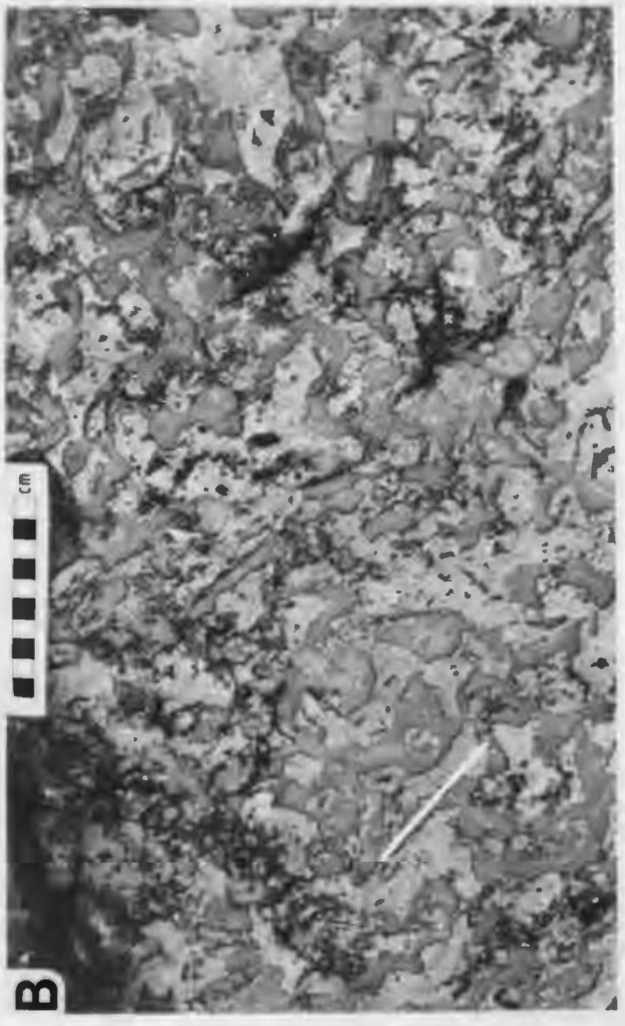
B
cm

PLATE 52

Horizon M, Port au Port Peninsula

Microstructure of stromatoids - Zones A1 and C

A - Spongeous *structure grumeleuse* microstructure of crudely laminated stromatoid column; Bed C. Irregular fenestrae commonly contain pelletal sediment (arrows) that is virtually indistinguishable from the microclotted fabric of the stromatoids. The column has a discontinuous vermiform selvage (V) in which sinuous filament moulds are oriented parallel to the margins of the columns. The column is flanked to the left by poorly sorted peloidal grainstone and packstone (P). Sample WB-5A-1.

B - Spongeous *structure grumeleuse* microstructure with cluster of spherical cellular bodies or "calcispheres" of uncertain origin; stromatoid column, Bed C. Sample WB-5B-H1, horizontal section.

C - Spongeous, diffuse *structure grumeleuse* microstructure of crudely laminated stromatoid column; Bed A, Zone 1. Pellet-filled fenestrae are difficult to distinguish from microclotted stromatoids. Sample WB-1A.

D - Spongeous *structure grumeleuse* microstructure with well defined silt-sized microclots or pellets; stromatoid column, Bed C. Sample WB-5A-3.

Scale bars 1 mm.

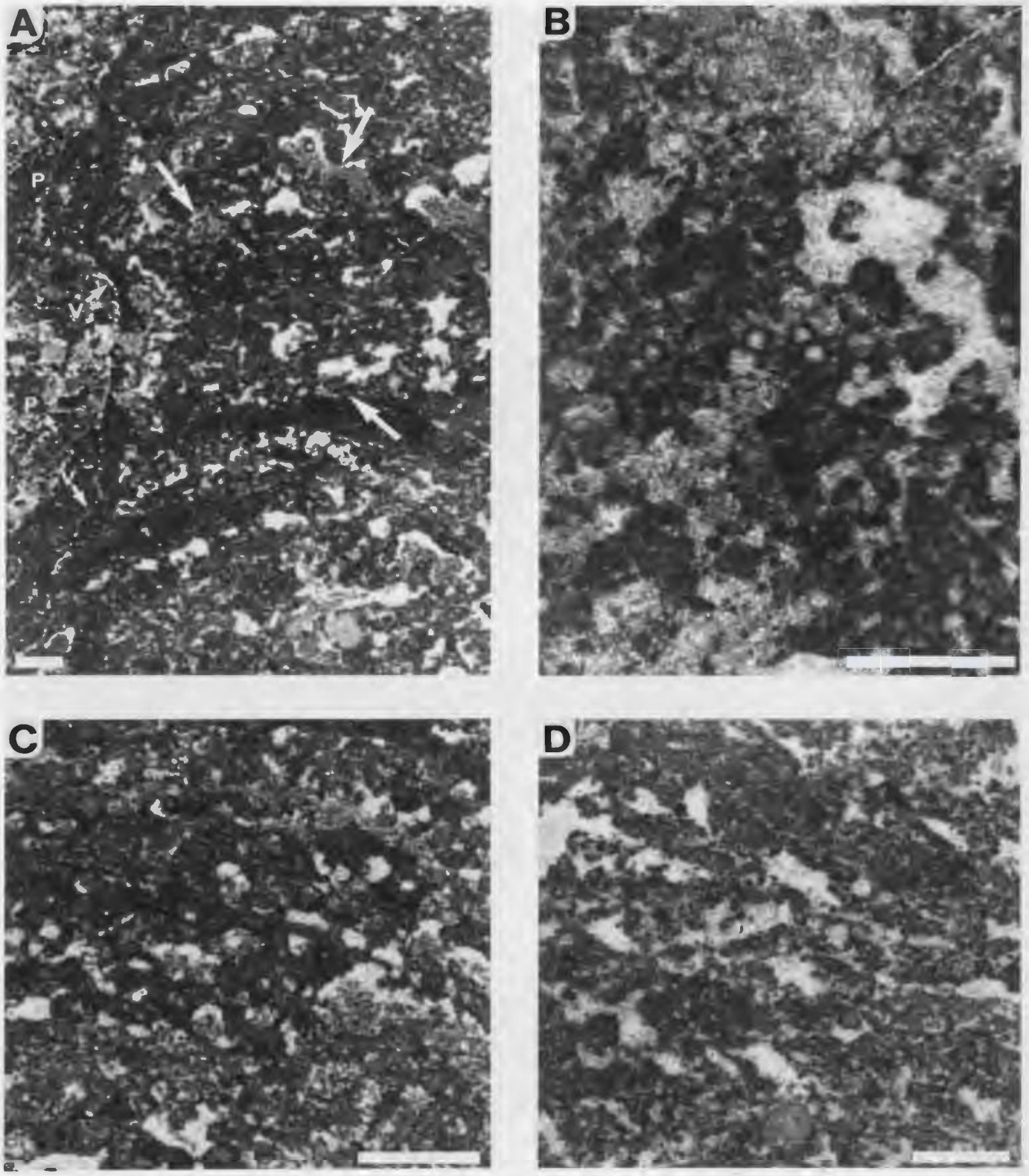
A
P
V
P
B
C
D

PLATE 53

Horizon M, Port au Port Peninsula

Microstructure of stromatoids and cryptomicrobial fabrics - Beds A and B.

A - Weakly striated peloidal and massive microstructure of planar stromatoids; Zone B1. Note lenticular nature of peloidal laminae (P), and bound gastropod shell (top right) filled with peloidal sediment. Sample WB-3A.

B - Well defined striated peloidal and massive microstructure of aberrant cup-shaped stromatoid; Zone B2. Lenticular peloidal laminae are laterally discontinuous. Sample WB-3F.

C - Mottled microstructure of dolomitic sub-digitate cryptomicrobial framework (C) flanked on the left by inter-framework peloidal-intraclast grainstone; Zone B3. Lighter coloured micritic and white sparry dolomite patches may represent sediment and cement-filled burrows, respectively, within the framework. Sample WB-3B.

D - Extensively dolomitized cryptomicrobial framework with relict massive cryptocrystalline microstructure; Zone B4. Sample WB-4A.

Scale bars 1 mm.

PLATE 53

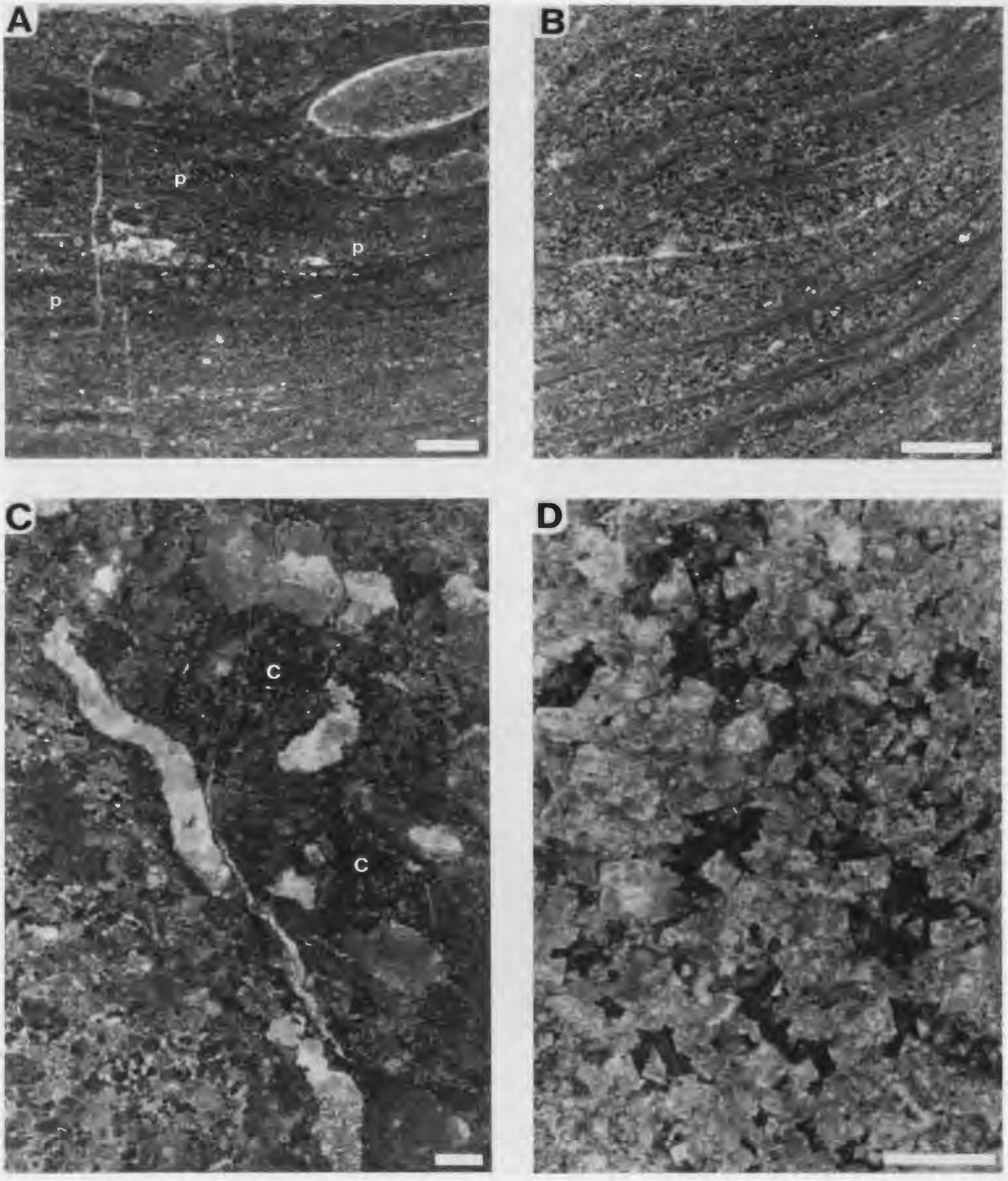

PLATE 54

Horizon N, Port au Port Peninsula

Megastructure and mesostructure

A - Elongate composite bioherm composed of several coalesced domes; Bed A. Hammer 30 cm.

B - Undulose to wavy stromatoids within stratiform stromatolite, Zone B1. Note light coloured ooid laminae and lenses (arrows).

C - Thrombolite bioherm (Zone B2) developed on stratiform stromatolite (S) of Zone B1. The thrombolite bioherm is encased in peloid-intraclast grainstone.

D - Margin of thrombolite bioherm illustrated in C, showing dark sub-digitate to arborescent thromboids and lighter coloured inter-framework sediment. The bioherm is flanked by coarse grained peloid-intraclast grainstone which dips steeply away from the bioherm, and contains reworked dark fragments\peloids of thromboids (arrow). Note grainstone filled crevice at surface of bioherm (g).

E - Magnified view of crest of thrombolite bioherm illustrated in C and D. Dark thromboids are encased in peloid-skeletal packstone (p), and light coloured lime-mudstone (m) and white sparry calcite occlude framework supported cavities. Note small weakly laminated stromatoid columns (s) at base of photo, and grainstone filled crevice (g).

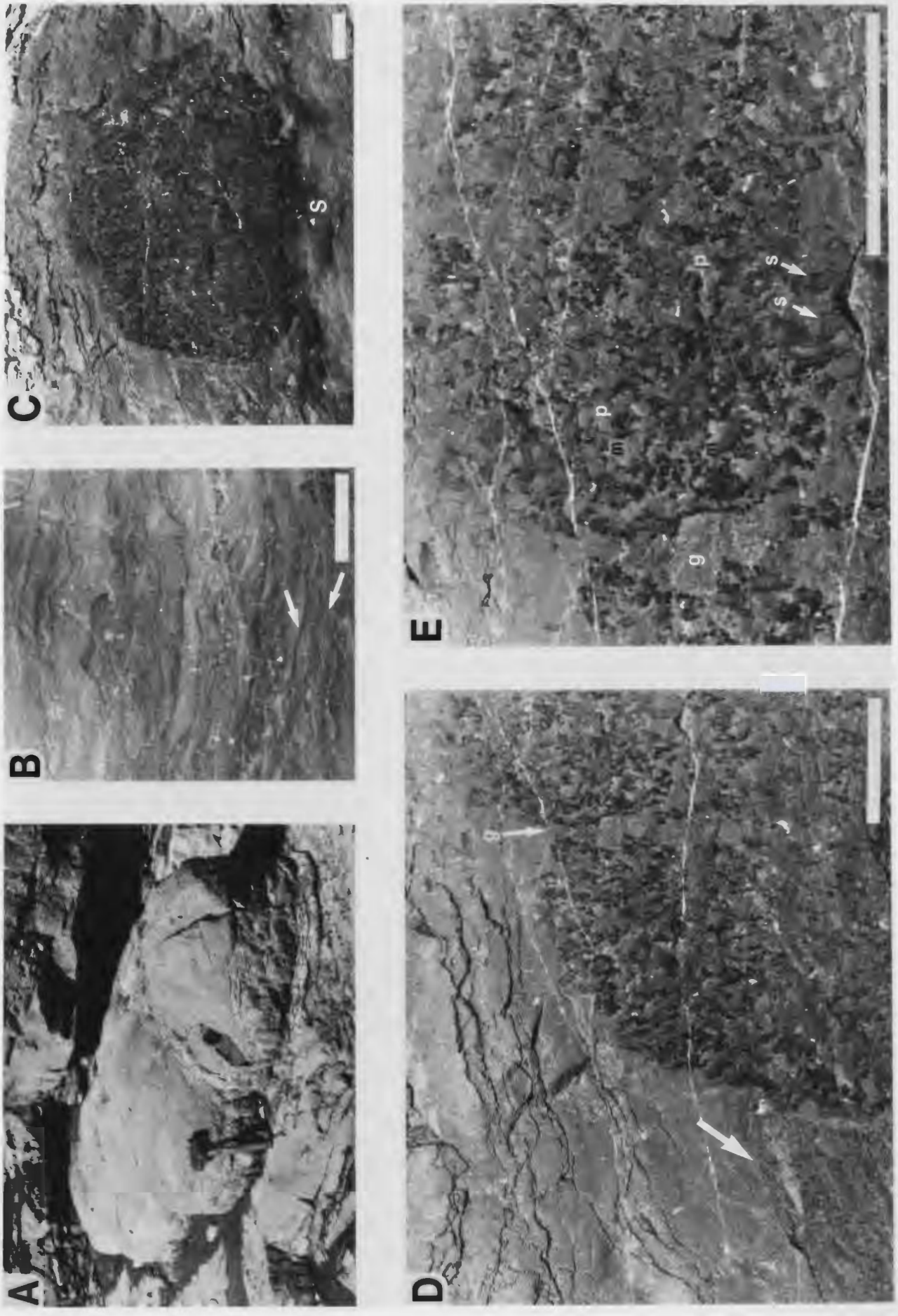
A
B
C
D
E
s
p
g
s

PLATE 55

Horizon N, Port au Port Peninsula

Mesostructure and microstructure - Zone B2

A - Vertical slab of thrombolite Zone B2 showing dark thromboids encased in inter-framework packstone (P), and light coloured cavity-filling mudstone (M). Note pendant grape like clusters of lobate thromboids at roof of mud-filled cavities. and numerous gastropod shells (arrows) within inter-framework sediment. Sample BH-10C.

B - Variegated spherulitic lobate (L), grumous (G) and vermiform-grumous grading to vermiform-peloidal (V) microstructure of thromboid; Zone B1. Note pelletal sediment within bound gastropod shells (arrows), and poorly defined gradational contact between thromboid and inter-framework peloidal grainstone (g). Sample BH-10C.

C - Variegated spherulitic lobate (L), grumous (G), vermiform (V), and massive (M) micro-structure of thromboid, Zone B2. Note bound gastropod shell (arrow), former cavity occluded by wackestone (W), and burrow (B).
Sample BH-10C-H, horizontal section.

D - Filamentous microfossils encased in sparry calcite within thromboid; Zone B2.
Sample BH-10A-C1.

Scale bars 1 mm (except A).

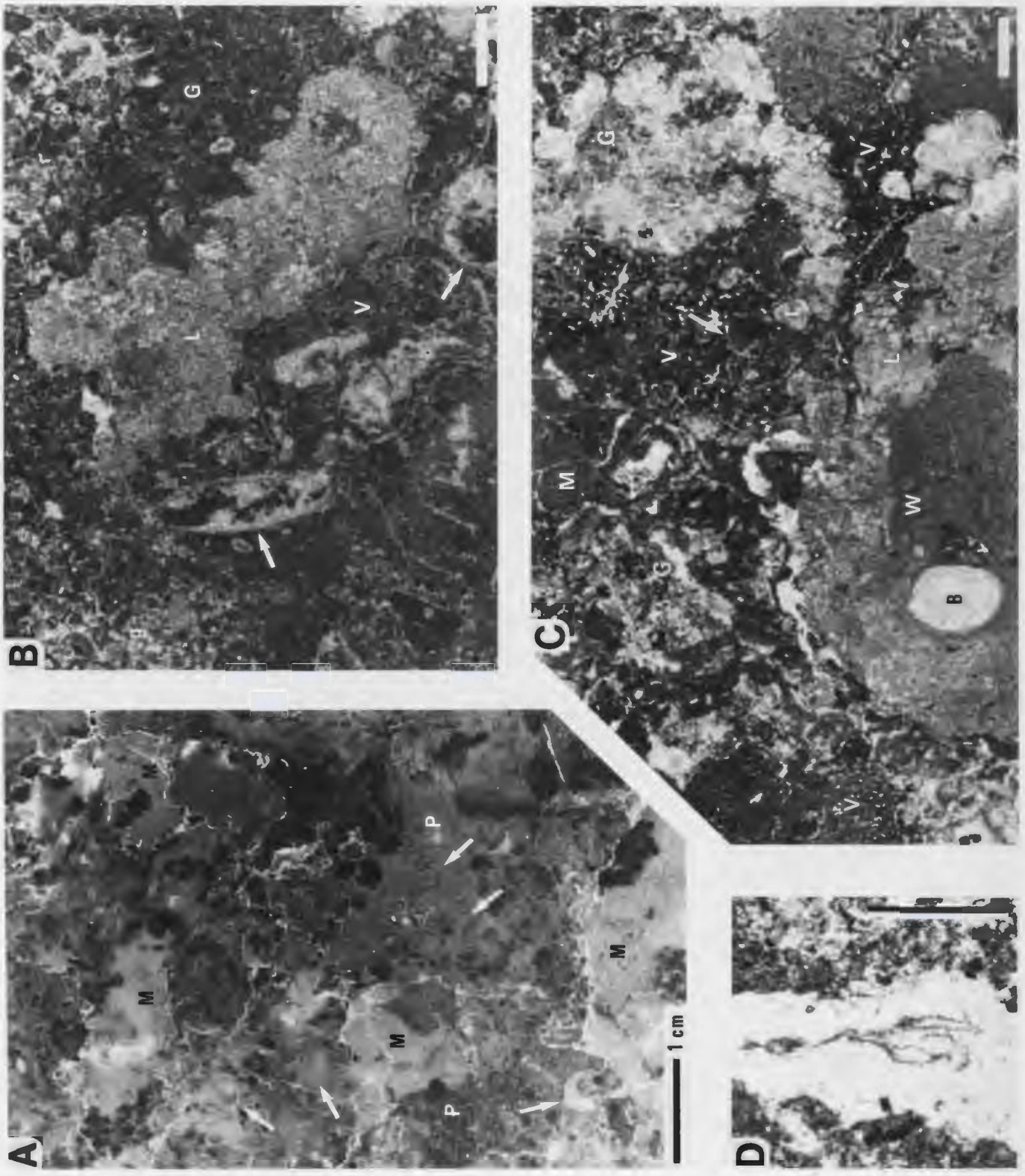
A
M
P
M
P
M
1 cm
B
G
V
L
C
G
M
V
L
W
B
V
D

PLATE 56

Horizon N, Port au Port Peninsula

Microstructure - Zone A and B2

A - Composite tubiform-grumous microstructure flanked to the left and right by spherulitic lobate microstructure (L); thromboid, Zone B2. Sub-linear tubular burrows (arrows) disrupt grumous material, and have weakly defined walls. Sample BH-10A.

B - Banded vermiform-peloidal and massive microstructure of stromatoid column; Bed A. Note prostrate vermiform tubules at base of vermiform-peloidal laminae (arrows), thick peloidal lens (P), sediment-filled burrows (B) and spar-filled borings (b). Sample BH-7.

C - Detail of composite vermiform-peloidal stromatoid in which individual peloids, groups of peloids, and small patches of diffuse peloidal micrite are separated by sparry tubules (filament moulds). Note overlying weakly banded crypto-crystalline stromatoid. Sample BH-7.

D - Massive to diffuse grumous thromboids (T) encased in vermiform-peloidal microstructure; diffusely clotted larger bioherms, Bed A. Sample BH-8B.

Scale bars 1 mm.

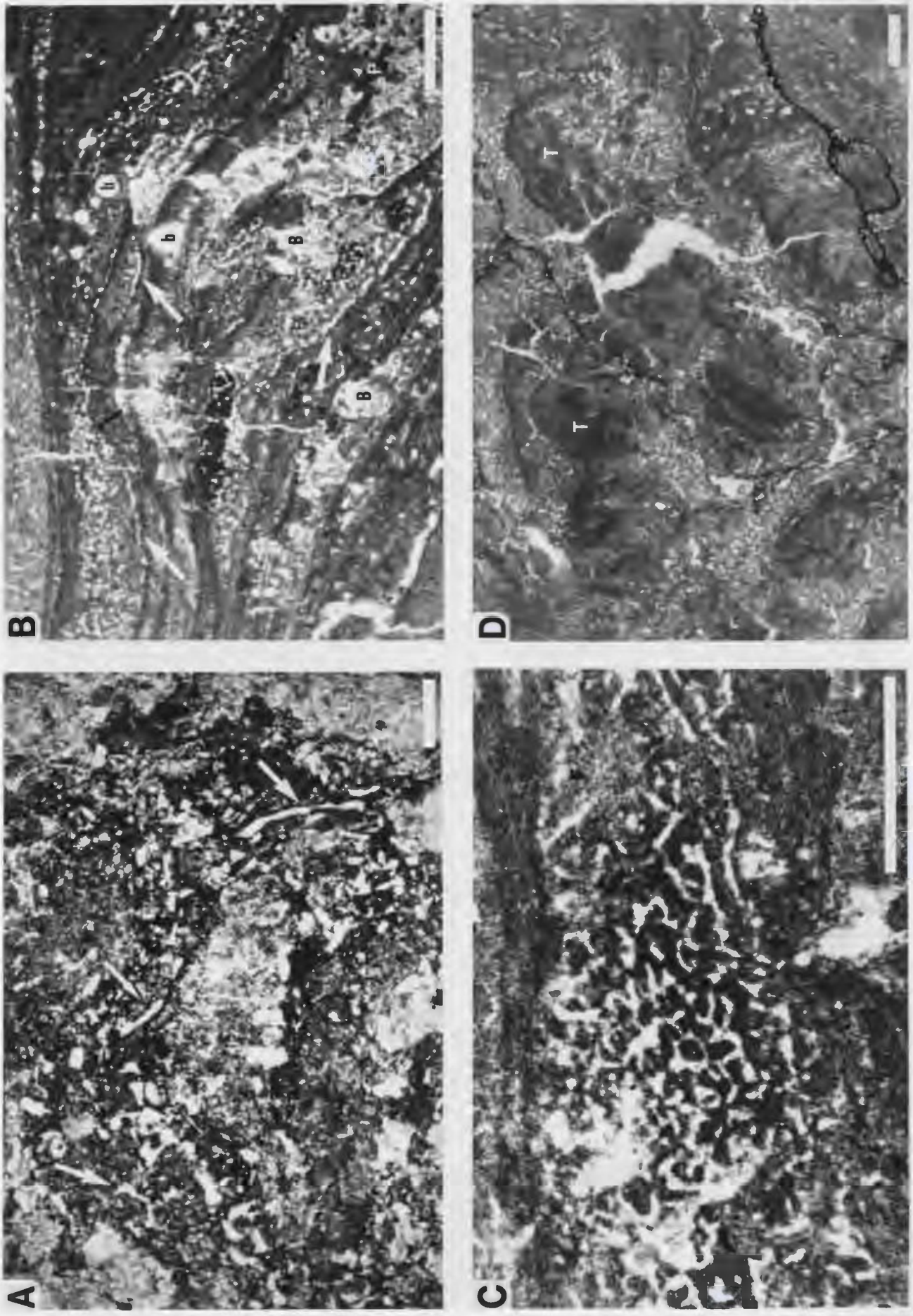
A
B
b
B
B
D
T
T
C

PLATE 57

Horizon O, Port au Port Peninsula

Megastructure and mesostructure

A - Karst eroded thrombolite mounds (T) encased in grainstone (G) and overlain by pebble conglomerate (C). Thrombolites are established on eroded lime-mudstone substrate (S1), and are truncated by two subsequent erosion surfaces (S2 and S3), each phase of erosion being preceded by the deposition of inter-biohermal grainstones (G1 and G2). See corresponding field sketch shown in Fig 4-37. Scale rule 10 cm.

B - Vertical slab of thrombolite bioherm showing dark prostrate and pendant thromboids, inter-framework grainstone and wackestone (W), and flanking skeletal-peloid-ooid grainstone G2. Former framework cavities are roofed by pendant thromboids, and filled with mudstone (M) and white sparry cement. Sample BH-12.

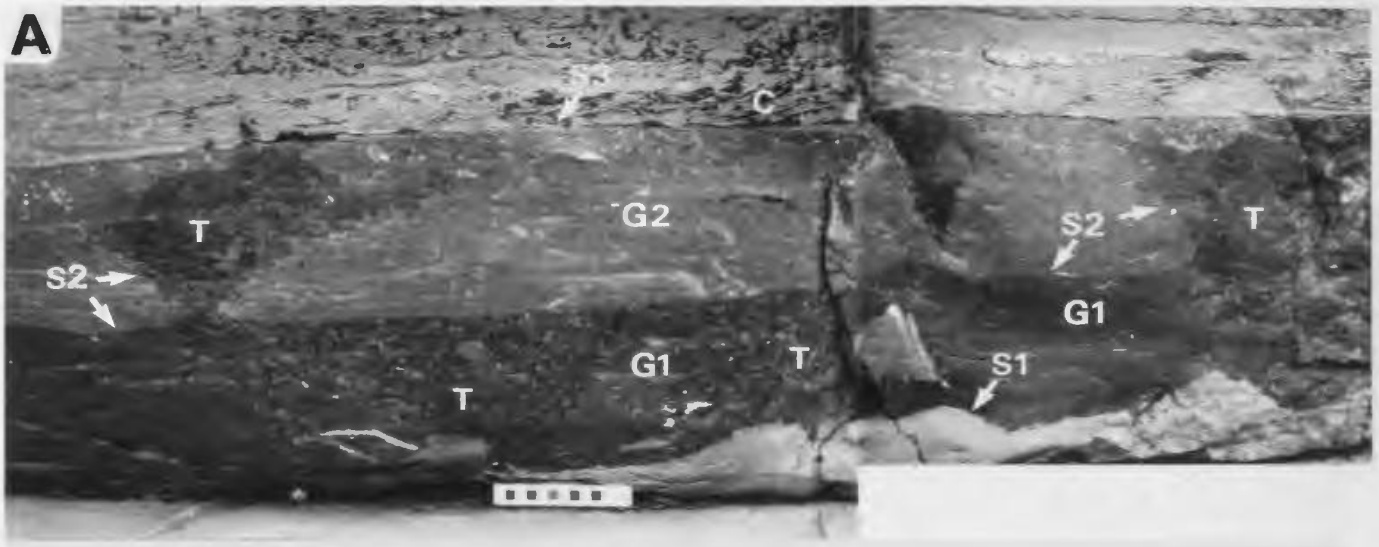
A
C
T
G2
S2
T
S2
T
G1
G1
T
S1

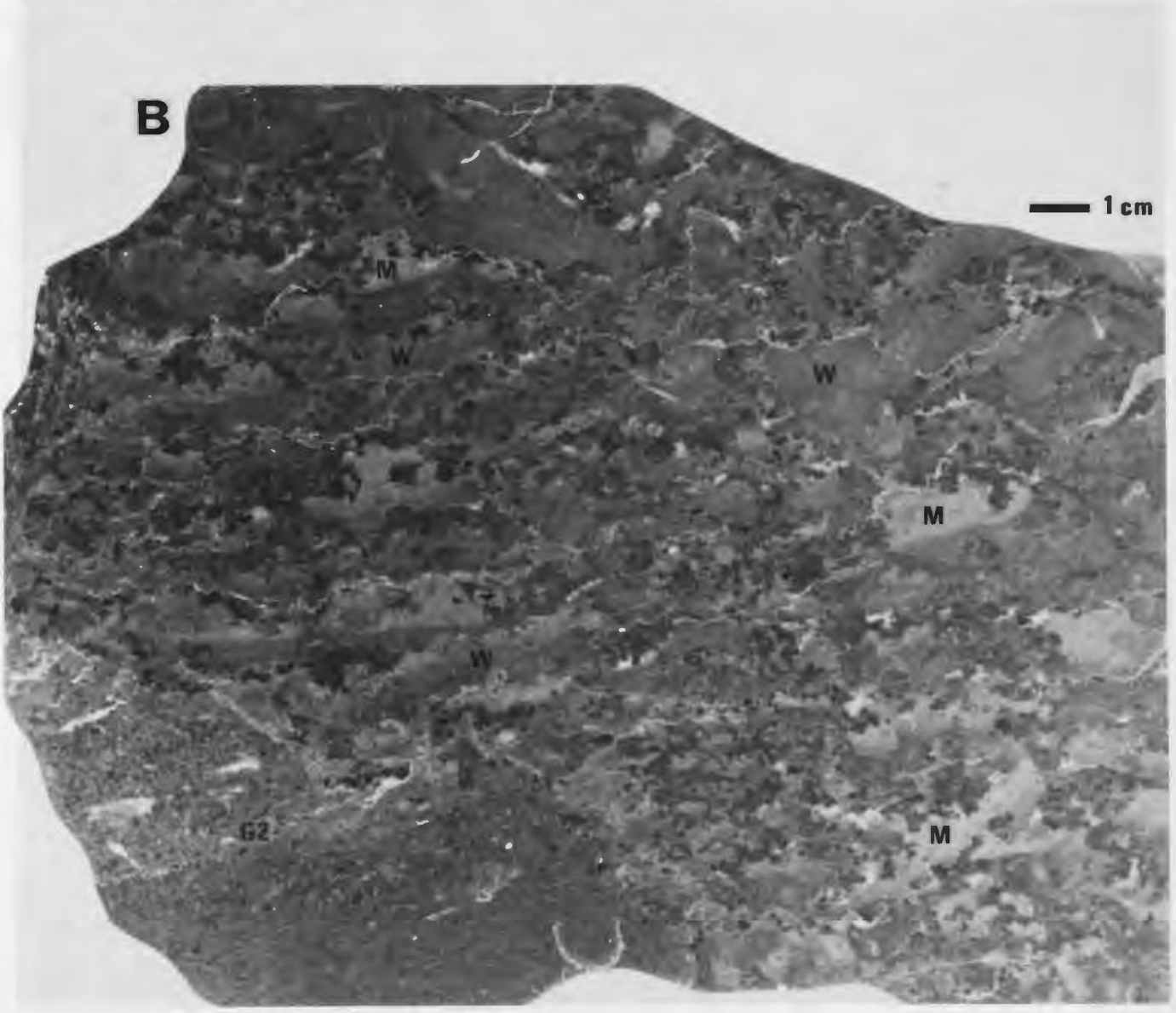
B
1 cm
M
W
W
M
W
G2
M

PLATE 58

Horizon O, Port au Port Peninsula

Microstructure

A - Variegated saccate lobate (L), spongeous grumous (g), peloidal (P), and vermiform-peloidal (V) microstructure of thromboid overlain by inter-framework grainstone and wackestone (W). Note discontinuous cryptocrystalline wall around turbid microspar lobes, and gradational contact between thromboid and inter-framework sediment. Thromboid is disrupted by relatively large burrow (B). Sample BH-12A.

B - Magnified view of A, showing saccate lobate microstructures (L) encased in grumous (g) grading to peloidal (P) and vermiform-peloidal (V) microstructures. Note former framework cavity (far right) floored with peloids and occluded by blocky spar cement (C), and peloid-filled ?burrow (B). Sample BH-12A.

C - Variegated spongeous, lobate (L), and grumous (g) grading to peloidal (P) microstructure of thromboids, and pockets of inter-framework weakly peloidal mudstone (M). Note infiltrated peloids within irregular fenestrae between lobate microstructures (arrows), and sediment\cement filled burrow (B). Sample BH-12A.

D - Spongeous, grumous grading to peloidal microstructure of thromboid (lower two thirds of photo), overlain by inter-framework peloidal grainstone (upper third). Contact between thromboid and inter-framework (arrows) is indistinct. Sample BH-12A.

Scale bars 1 mm.

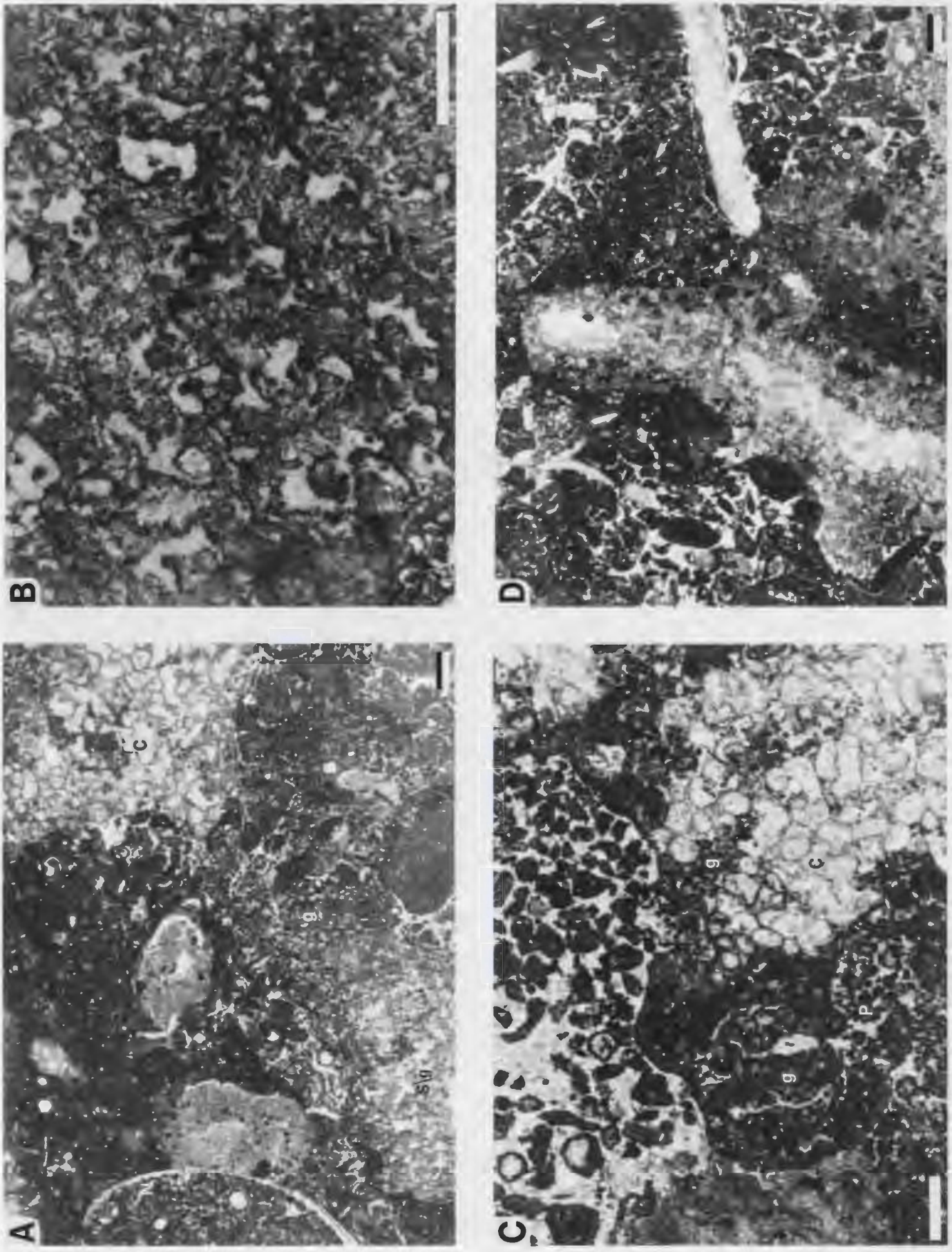
A
B
C
D
c
g
p
slg

PLATE 59

Horizon P, Port au Port Peninsula

Microstructure

A - Poorly differentiated fabric of thrombolite, showing spongeous grumous (S\g), grumous (g), and *Lichenaria* coral (C) framework, encased in inter-framework grainstone (lower right) and wackestone (upper left). Note sediment-filled nautiloid shell (N). Sample BH-13-B1.

B - Spongeous grumous microstructure of cryptomicrobial framework. Note diffuse peloids within irregular fenestrae. Sample BH-13-B1.

C - *Lichenaria* coral (C) encrusted by diffuse grumous (g) and peloidal (P) cryptomicrobial microstructures, and overlain by inter-framework peloid grainstone. Micrite-rimmed grains within inter-framework grainstone are probably fragments of corallites that have been micritized by endolithic microbes. Sample BH-13B.

D - Dolomite patches encased in poorly differentiated grumous and peloidal fabrics. The geometric shape of these and other dolomite patches is consistent with the gross morphology of sponges; they may be dolomitized sponges.

Scale bars 1 mm.

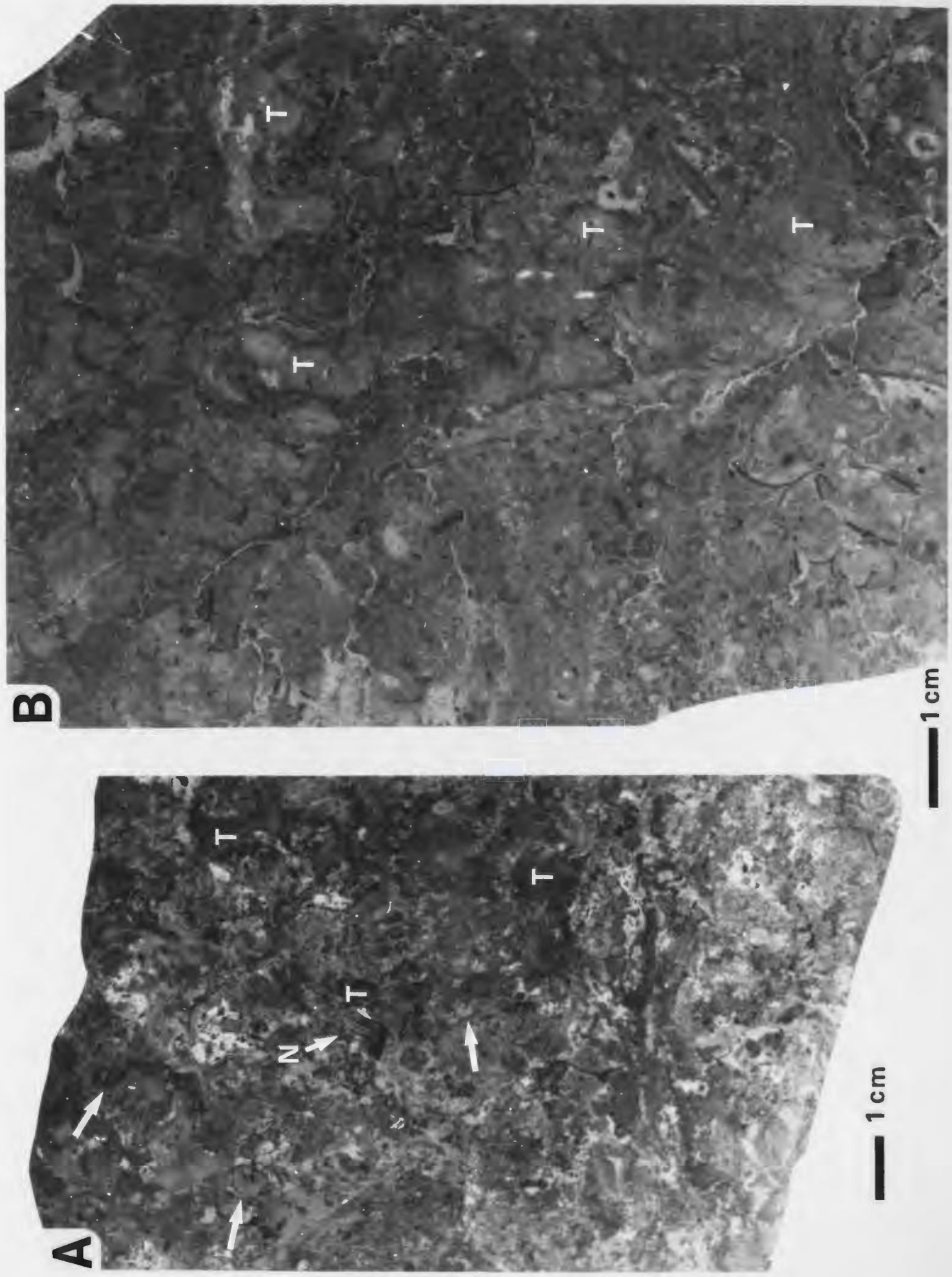
B
T
T
T
T
1 cm
A
T
T
T
N
1 cm

PLATE 60

Horizon Q, Port au Port Peninsula

Mesostructure

A - Vertical slab of thrombolite Bed C showing poorly differentiated ragged thromboids (T) encased in burrow mottled peloid-skeletal packstone. Note nauliloid (N) and gastropods (arrows). Sample BH-31B.

B - Vertical slab of thrombolite Bed A showing poorly differentiated, light coloured, amoeboid and sub-digitate thromboids (T) encased in burrow-mottled peloid-skeletal wackestone. Sample BH-14.

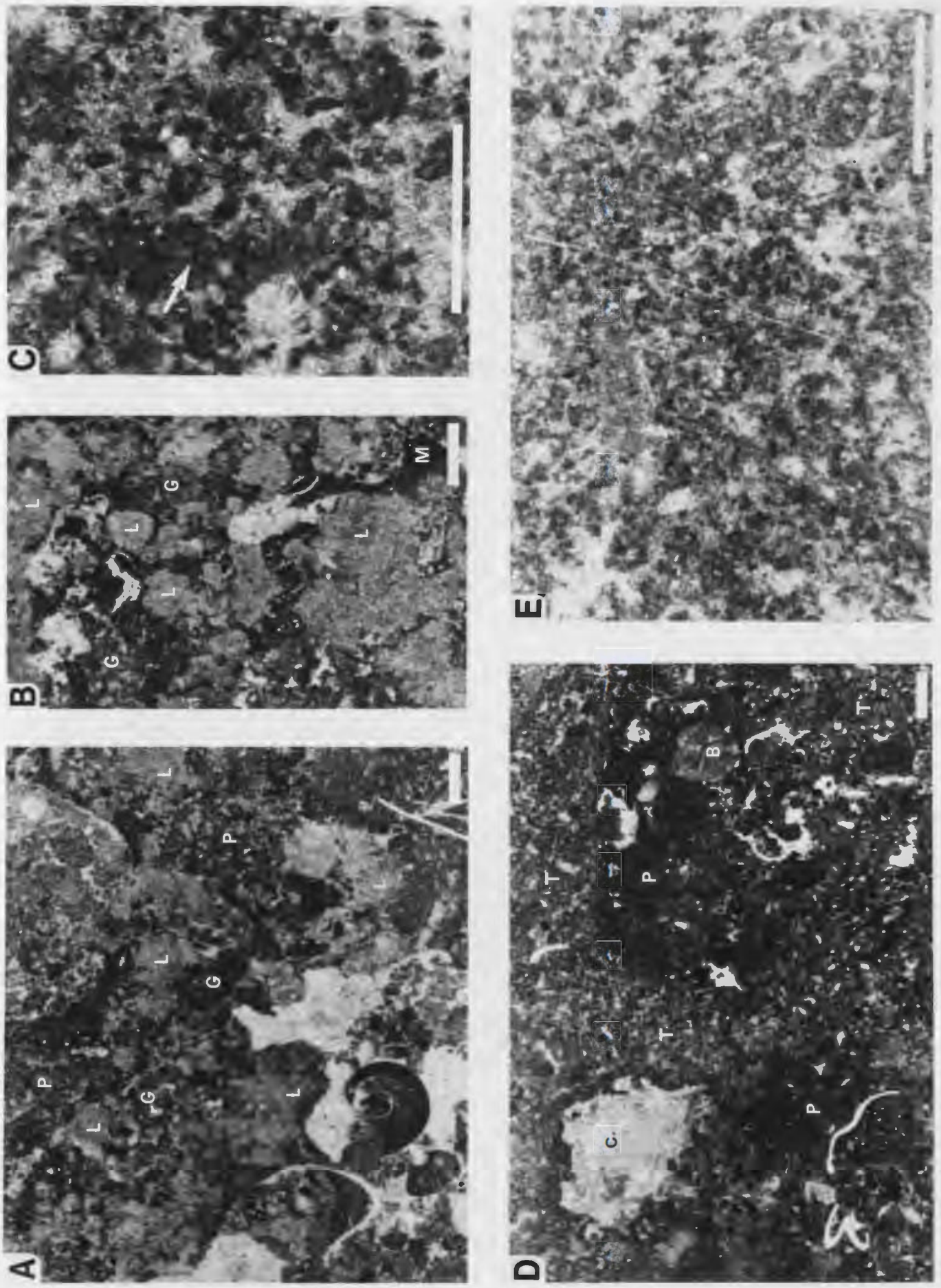
A
P
L
G
L
L
G
L
P
L
L
L
B
G
L
L
L
L
M
C
D
C
P
T
T
P
B
T
E

PLATE 61

Horizon Q, Port au Port Peninsula

Microstructure

A - Variegated diffuse lobate (L), grumous (G) and diffuse peloidal (P) microstructure of thromboid encased in inter-framework gastropod packstone (lower left) and peloid-intraclast grainstone (upper right). Note pelletal sediment within gastropod shell, and blocky spar cement within shelter cavities. Bed C, Sample BH-31A.

B - Variegated lobate (L), grumous (G) and massive (M) microstructutre of thromboid. Bed C, Sample BH-31A.

C - Grumous grading to peloidal microstructure of thromboid with tubular *Girvanella*-like fragment (arrow). Bed C, Sample BH-31A.

D - Spongeous, grumous grading to diffuse peloidal microstructure of thromboids (T), encased in skeletal-peloid packstone (P) and wackestone (W). Note intergradation of thromboids and inter-framework sediment, blocky cement within shelter cavity (C), and mud-filled burrow (B). Bed A, Sample BH-14.

E - Spongeous, grumous grading to diffuse peloidal microstructure of thromboid. Bed A, Sample BH-14.

Scale bars 1 mm.

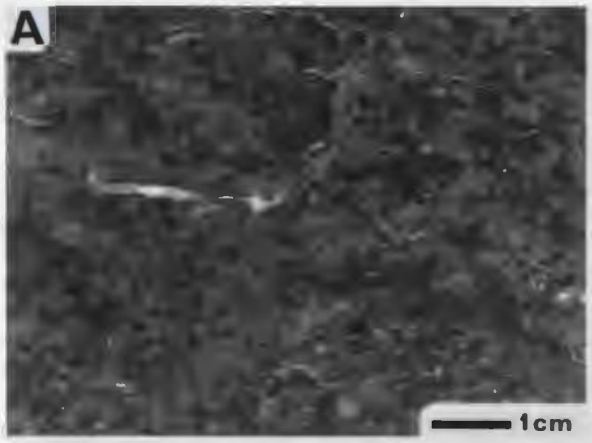
A
1cm

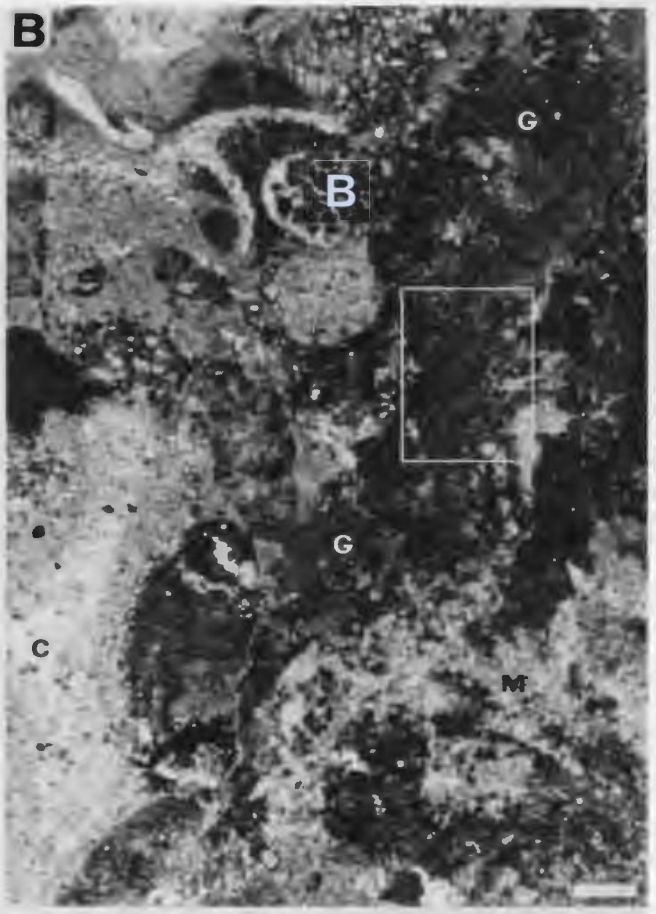
B
G
B
G
C
M

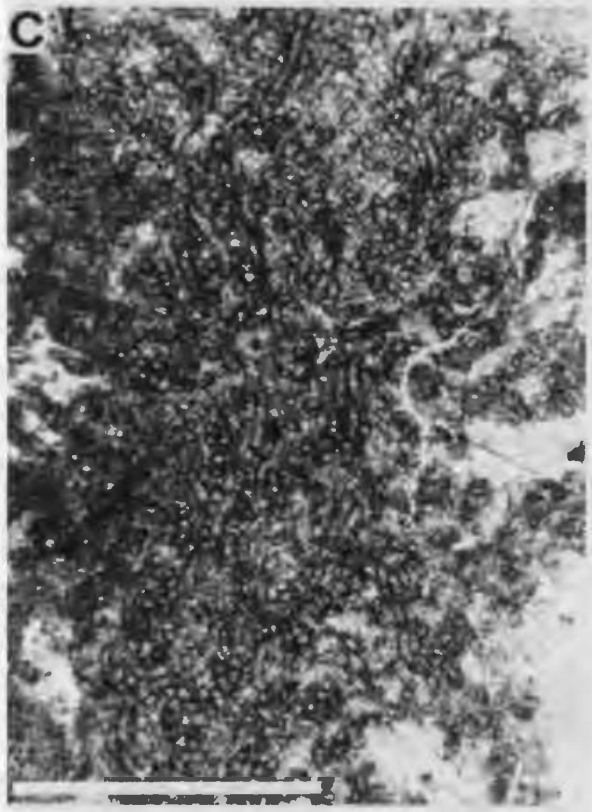
C

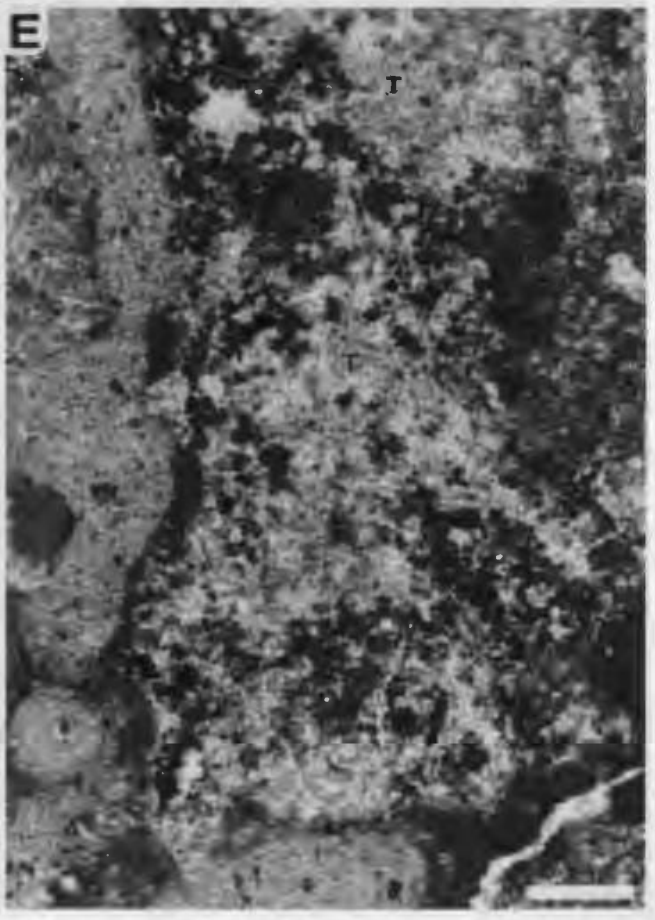
E
T
T

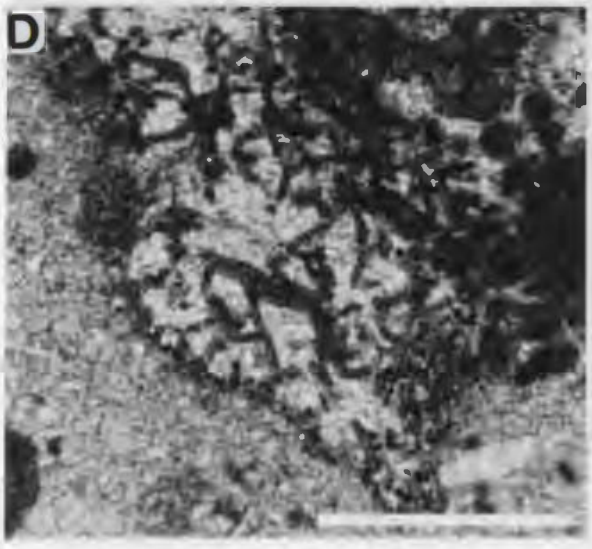
D

PLATE 62

Horizon R, Port au Port Peninsula

Mesostructure and microstructure

A - Vertical slab of thrombolite showing small dark subrounded and amoeboid thromboids encased in skeletal wackestone. Sample CAT-1.

B - Thromboid with well preserved *Girvanella* (outlined area) grading to diffuse grumous microstructure (G). The lower portion of the thromboid has been extensively replaced by massive microspar (M). The thromboid is flanked on the left by slightly dolomitic skeletal wackestone and block cement (C). Note peloid-filled burrow (B). Sample CAT-1.

C - Magnified view of area outlined in B showing dense network of *Girvanella* tubules. Sample CAT-1.

D - Framework fragment (intraclast) comprised of open network of *Girvanella* tubules and interstitial microspar; inter-biostromal packstone. Sample CAT-2.

E - Relict grumous and *Girvanella* (not visible at this magnification) microstructure of extensively neomorphosed, microsparitic thromboid (T). Thromboid is encased in burrowed mudstone (microspar). Sample CAT-1.

Scale bars 0.5 mm.

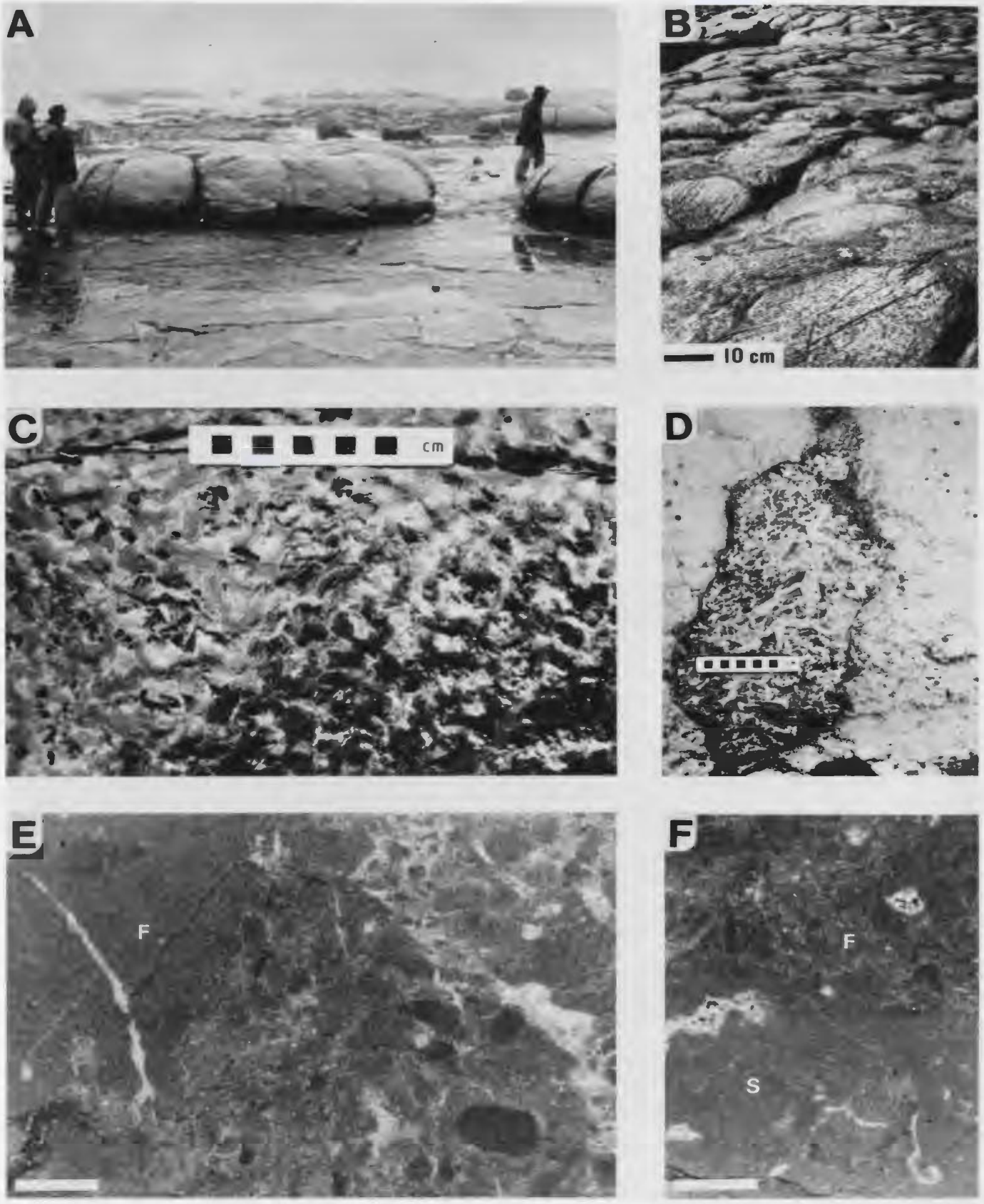
A
B
10 cm
C
cm
D
E
F
F
F
S

PLATE 63

Great Northern Peninsula - Horizon 1
Petit Jardin Formation, Flowers Cove

Mesostructure and microstructure

A - Large discoidal bioherms, each composed of several coalesced dome-shaped mounds. Inter-biohermal sediments have been selectively eroded, such that the bioherms now appear just as they grew on the Cambrian sea-floor.

B - Laterally continuous biostrome formed by the coalescence of discoidal bioherms. The biostrome and the constituent dome-shaped mounds are truncated by a planar erosion surface riddled with tiny solution pits (visible in foreground).

C - Anastomosing 3-tone cerebroid fabric of bioherm; vertical section. Dark coloured mottles are rimmed by medium toned selvages, and probably represent frame-building microbial components. Scale rule 10 cm.

D - Brecciated slump lobe of draping sediments on the flank of a large discoidal bioherm. Scale rule 10 cm.

E - Massive microcrystalline microstructure of dark ?framework component (F), encased in peloidal inter-framework sediment. Note wedge-shaped crack restricted to ?framework component, and finely disseminated pyrite that imparts dark tone to this component. Scale bar 1 mm. Sample FC-1.

F - Diffuse grumous microstructure of dark pyritic ?framework component (F), rimmed by medium toned, non-pyritic, massive micro-crystalline selvage (S) with trilobite fragment. Scale bar 1 mm. Sample FC-1.

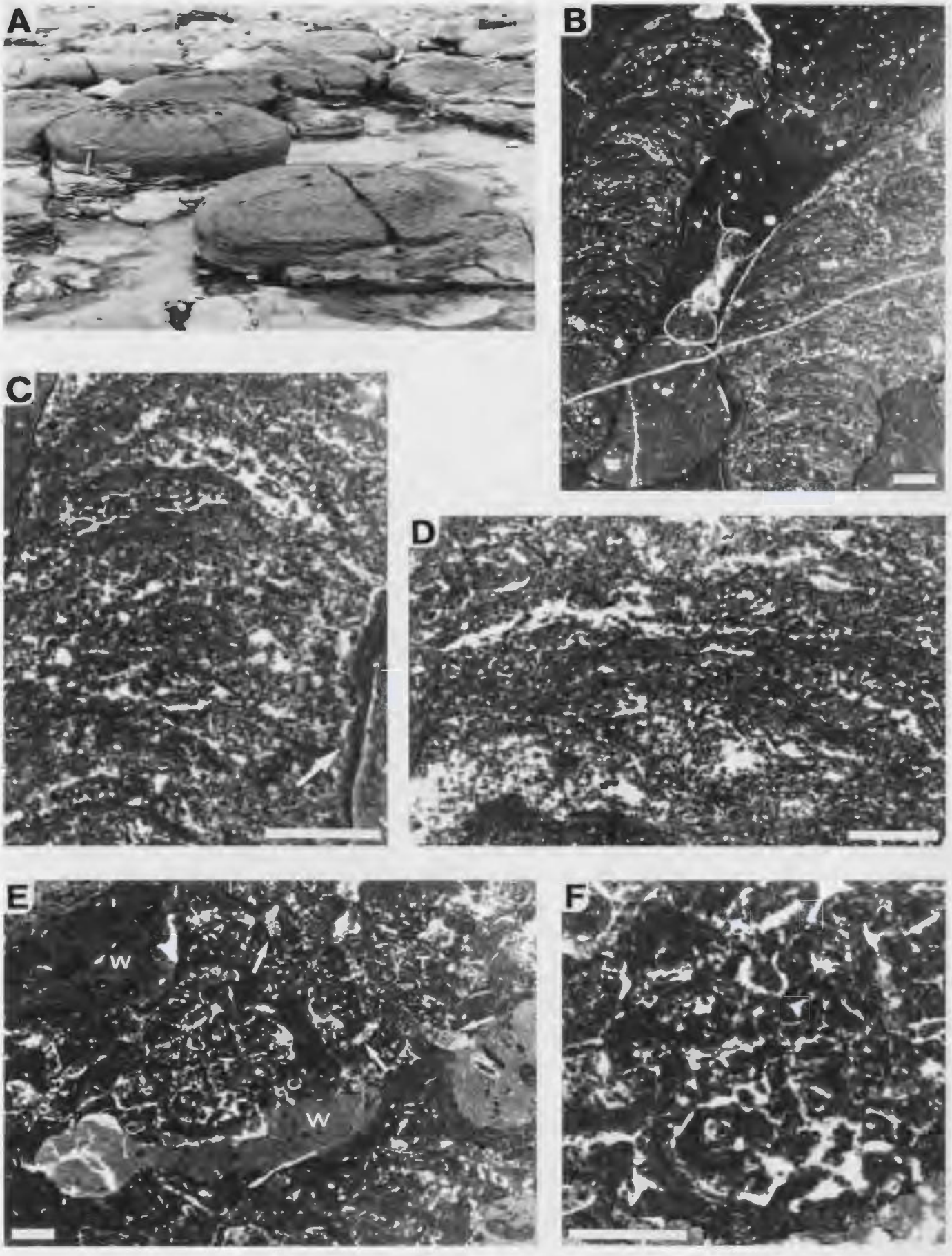
A
B
C
D
E
W
W
F

PLATE 64

Great Northern Peninsula - Horizon 2
Boat Harbour Formation, Eddies Cove West A

Megastructure and microstructure

A - Domed bioherms appearing much the same as they grew on the Ordovician sea-floor. Hammer 30 cm.

B - Striated, spongeous grading to vermiform, peloidal microstructure of stromatoid columns; Zone 3. Note gastropod shell lodged between adjacent columns. Sample BH-18B.

C,D - Magnified view of striated, spongeous grading to vermiform peloidal microstructure of stromatoid column shown in B. Striation results from alternating laminae and lenses of partially merged diffuse peloids (cf. grumous micro-structure), and relatively well defined peloids separated by a network of irregular to tubular micro-fenestrae. Note cryptocrystalline selvage (arrow) at margin of column in C. Zone 3, Sample BH-18B.

E - Spongeous grading to vermiform, diffuse peloidal microstructure of thromboids (T) separated by patches of inter-framework peloid-skeletal wackestone (W). Much of the thromboid appears to be burrowed (arrows). Zone 4, Sample BH-19A.

F - Magnified view of spongeous grading to vermiform, diffuse peloidal microstructure of thromboid shown in E. Poorly sorted peloids and groups of partially merged peloids are separated by irregular to tubular micro-fenestrae. Zone 4, Sample BH-19A.

Scale bars 1 mm.

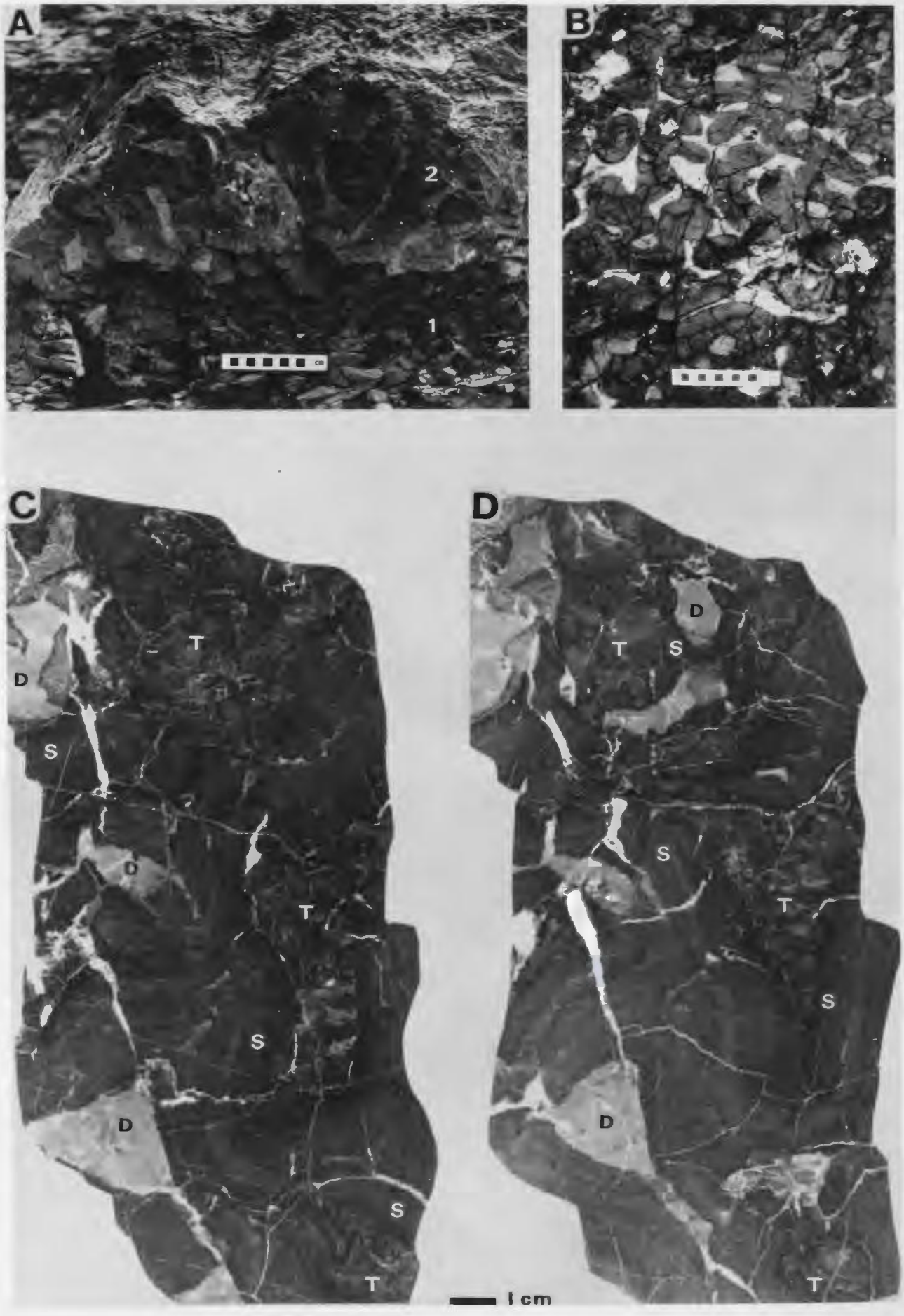
A
2
1
B
C
T
D
S
D
T
S
D
D
S
T
D
S
T
D
T
S
D
T
1 cm

PLATE 65

Great Northern Peninsula - Horizon 3
Boat Harbour Formation, Eddies Cove West B

Mesostructure

A - Mound-like head at top of biostrome showing transition from basal rubbly weathering thrombolite (Zone 1) to aberrant thrombolitic and stromatolitic Zone 2 (thrombolite Zone 3 has been eroded from the mound crest). The dark coloured cerebroid framework of Zone 2 is infilled by light coloured dolostone. Scale rule 10 cm.

B - Plan view of aberrant stromatolitic and thrombolitic Zone 2, showing dark cerebroid framework infilled by light coloured inter-framework dolostone. Scale rule 10 cm.

C,D - Vertical serial slabs of aberrant thrombolitic and stromatolitic Zone 2. An axial clotted coral-thromboid framework (T) is encrusted by relatively thick, vertical to steeply convex and conical laminated, stromatoid walls (S). Inter-framework spaces are filled with light coloured dolo-grainstone (D), and fractures are occluded by white spar cement. Sample BH-25.

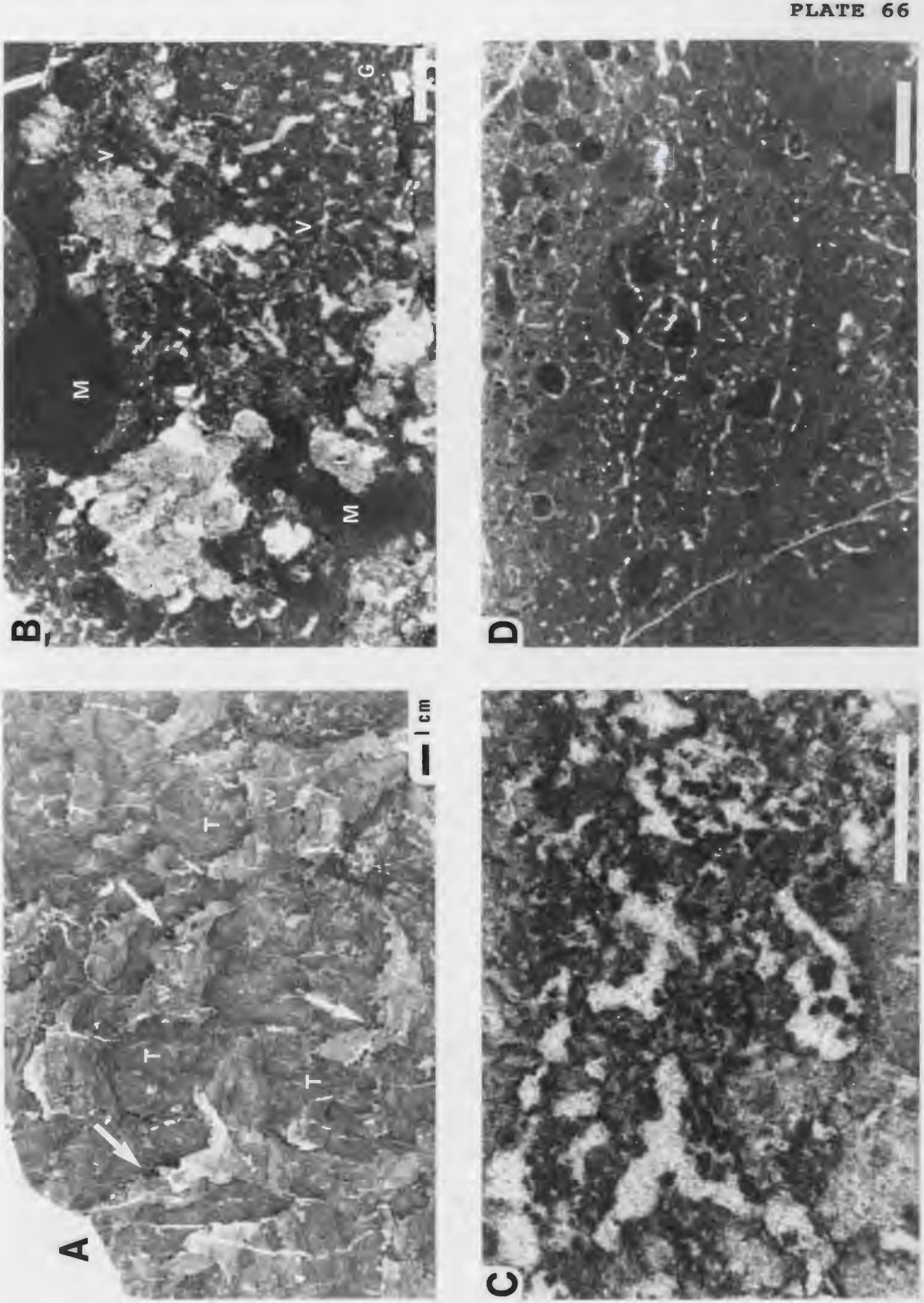
A
T
T
T
1 cm
B
M
V
V
M
G
C
D

PLATE 66

Great Northern Peninsula - Horizon 3
Boat Harbour Formation, Eddies Cove West B

Mesostructure and microstructure - Zones 1 and 3

A - Vertical slab of thrombolite Zone 3, showing dark coloured anastomosing thromboid framework (T), in part crudely laminated, infilled by light coloured and burrow-mottled, peloid-skeletal wackestone (W). Note small pendant lobate and saccate bodies at underside of prostrate thromboid framework (arrows). Sample BH-27.

B - Variegated spherulitic lobate (L), diffuse vermiform (V), spongeous grumous (G), and massive (M) microstructure of thromboid. Sample BH-27A.

C - Spongeous *structure grumeleuse* microstructure of thromboid. Note silt-size pellets within irregular fenestrae. Sample BH-27A.

D - Vermiform and vermiform-peloidal microstructure of crudely laminated thromboid. Vermiform tubules (filament moulds) are generally prostrate, and partially envelop well defined peloids. Sample BH-27C.

Scale bars 1 mm (except A).

A
T
T
T
W
1 cm
B
M
V
V
M
G
C
D

PLATE 67

Great Northern Peninsula - Horizon 3
Boat Harbour Formation, Eddies Cove West B

Microstructure - Zone 2

A - Intergrown coral-thromboid framework with inter-framework spiculitic mudstone (m). Individual corallites within the coral colonies (C) contain infiltered silt-sized peloids (arrows) which are indistinguishable from cryptocrystalline microclots within the encasing *structure grumeleuse* material (G). Note microcrystalline lobate (L) and massive to diffuse grumous (g) microstructures within thromboids, and peloids within burrows (B) in framework and inter-framework sediment. Sample BH-26B.

B - *Lichenaria* coral (C) encased in spongeous *structure grumeleuse* and *Renalcis*-rich (R) thromboid. Many corallites contain irfiltered pellets (arrows) indistinguishable from microclots within surrounding *structure grumeleuse* thromboid. Note pendant growth form of *Renalcis*. Sample BH-25A.

C - Margin of coral-thromboid framestone head showing outward growing, prostrate to pendant *Renalcis* encased in spongeous *structure grumeleuse*, and encrusting weakly vertically laminated, spongeous grading to vermiform, *structure grumeleuse* stromatoid wall (S) (base of encrusting stromatoid wall delineated by arrows). Sample BH-25A.

D - Magnified view of spongeous grading to vermiform, *structure grumeleuse* microstructure of weakly horizontally laminated stromatoid crust that envelops coral-thromboid framework shown in A. Sample BH-25B.

Scale bars 1 mm.

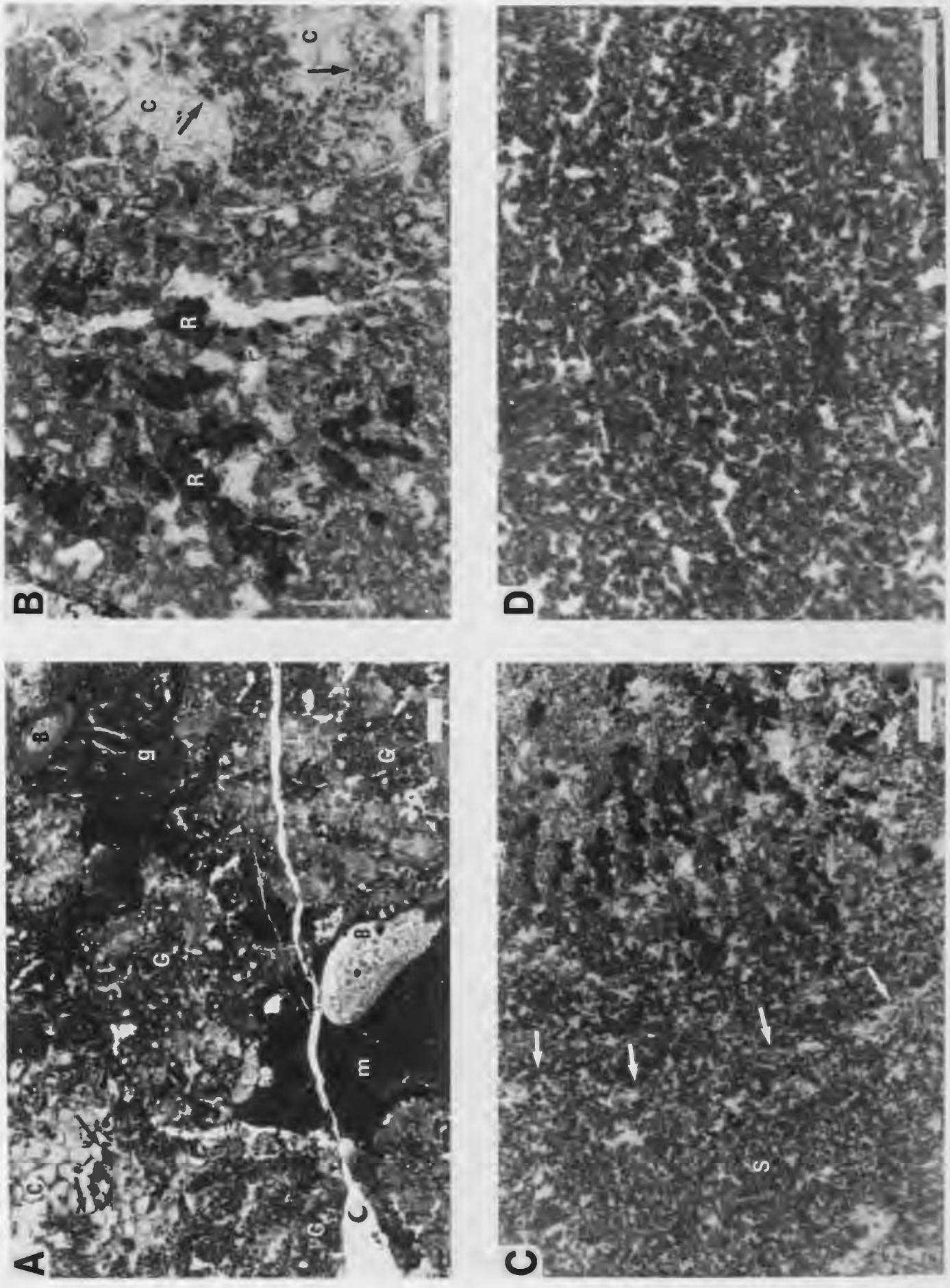
A
B
C
D
B
g
G
m
S
C
R

PLATE 68

Southern Canadian Rocky Mountains
Waterfowl and Sullivan Formations
Upper Cambrian

Megastructure, mesostructure, microstructure

A - Small domed and subspherical, "deep water" thrombolite bioherms (T) rooted in allodapic ooid-skeletal grainstone (G), and buried by shale. Sullivan Formation, Totem Creek, Mount Murchison.

B - Vertical slab of thrombolite composed of small arborescent, "*Epiphyton*-like", thromboids encased in mottled peloid-skeletal packstone. Waterfowl Formation, Totem Creek, Mount Murchison, Sample WTF-3.

C - Silty diffuse grumous microstructure of subdigitate thromboids (T) encased in silt-rich peloid-skeletal packstone (P). "Deep water" thrombolite, Sullivan Formation, Totem Creek, Mount Murchison, Sample SUL-2.

D - Massive to diffuse grumous microstructure of thromboid, with poorly preserved *Girvanella* (arrow) (tubules are best seen as the microscope is racked in and out of focus, and are difficult to identify in photomicrographs). Note sediment-filled burrow top left. Sullivan Formation, Windy Point, Sample SUL-1H, horizontal section.

E - Spongeous, silty diffuse peloidal microstructure of thrombolid\cryptomicrobial fabric, with scattered *Girvanella* tubules (arrows). Waterfowl Formation, Totem Creek, Mount Murchison, Sample WTF-1.

F - Diffuse cellular lobate microstructure (L) of arborescent thromboids (as shown in B), encased in silty peloid-ooid-skeletal packstone. Waterfowl Formation, Totem Creek, Mount Murchison, Sample WTF-3.

Scale bars 1 mm (except A,B).

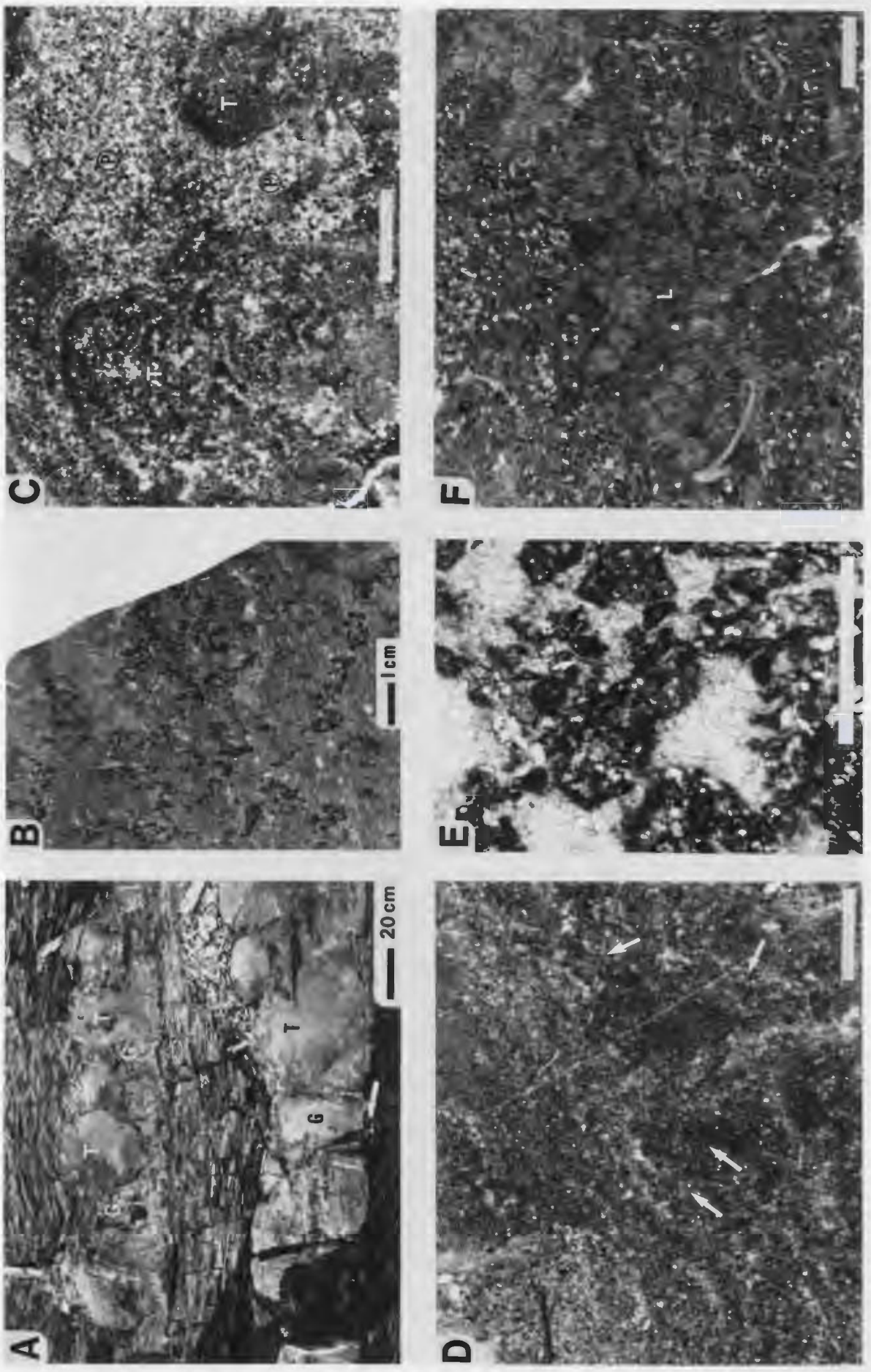
A
20 cm
T
G
B
1 cm
C
T
P
F
L
D
E

PLATE 69

Central Appalachians, eastern U.S.A.
Elbrook and Conococheague Formations
Middle and Upper Cambrian

Mesostructure and microstructure

A - Vertical slab of thrombolite comprised of small dark lobate and medium tone amoeboid thromboids (T), and light coloured inter-framework mudstone and wackestone. Elbrook Formation, Sample CLB-1.

B - Diffuse, weakly spherulitic, microcrystalline lobate microstructure of dark lobate thromboids shown in A. Thromboids are separated by thin seams of silty and dolomitic inter-framework mudstone (m) and sparry cement (C). Elbrook Formation, Sample CLB-1.

C,D - Diffuse spherulitic lobate microstructure of dark lobate thromboid as shown in A; C) plane polarized light, D) crossed polarized light. Note sweeping radial extinction pattern of individual lobes\spherulites. Elbrook Formation, Sample CLB-1.

E - Spongeous grumous microstructure of medium tone thromboid as shown in A. Note silt sized pellets within irregular fenestrae (arrows) and burrow (B); they are commonly indistinguishable from cryptocrystalline microclots. Elbrook Formation, Sample CLB-2.

F - Variegated diffuse microcrystalline lobate (L) and massive to diffuse grumous (G) micro-structure of thromboid with scattered dolomite rhombs. Conococheague Formation, Sample CON-1.

Scale bars 1 mm (except A).

A
T
T
1 cm
B
m
c
c
m
C
D
E
B
F
G
L
L
L

PLATE 70

Great Basin, western U.S.A.
Wheeler Formation
Middle Cambrian

Mesostructure and microstructure - Unit 2

A - Vertical slab of stromatolitic thrombolite (*Renalcis* boundstone) showing arborescent clusters of small dark thromboids which are encrusted by crenulate stromatoids (S) in the lower half of the slab. Light coloured mudstone and peloid-skeletal wackestone occur between the thromboid-stromatoid framework, and occlude shelter cavity (C) in which a trilobite carapace (arrow) is lodged. Sample WHL-1.

B - Chambered *Renalcis* encased in turbid microspar. Sample NJ-79-113-A2.

C - Mutually encrusting colonies of chambered (arrows) and clotted (c) *Renalcis* encased in turbid microspar. Sample NJ-79-113-A2.

Scale bars 1 mm (except A).

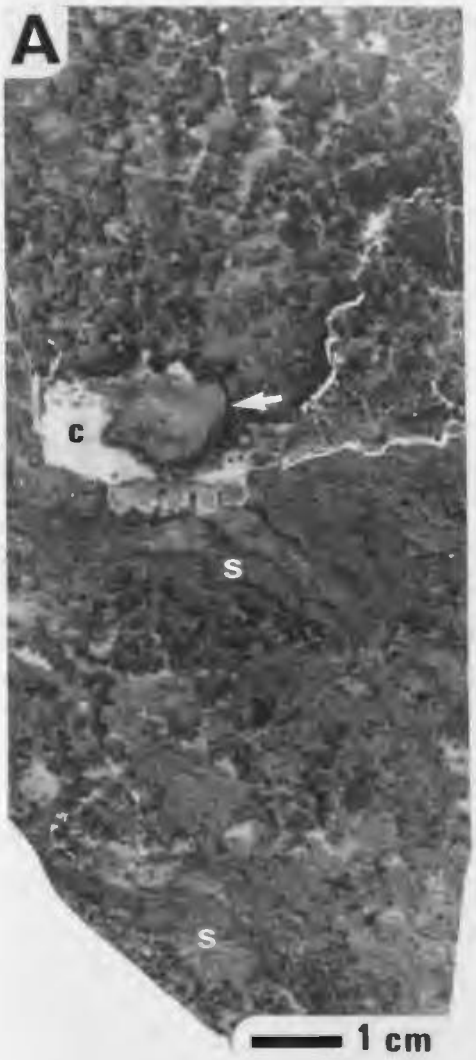
A
c
s
s
1 cm

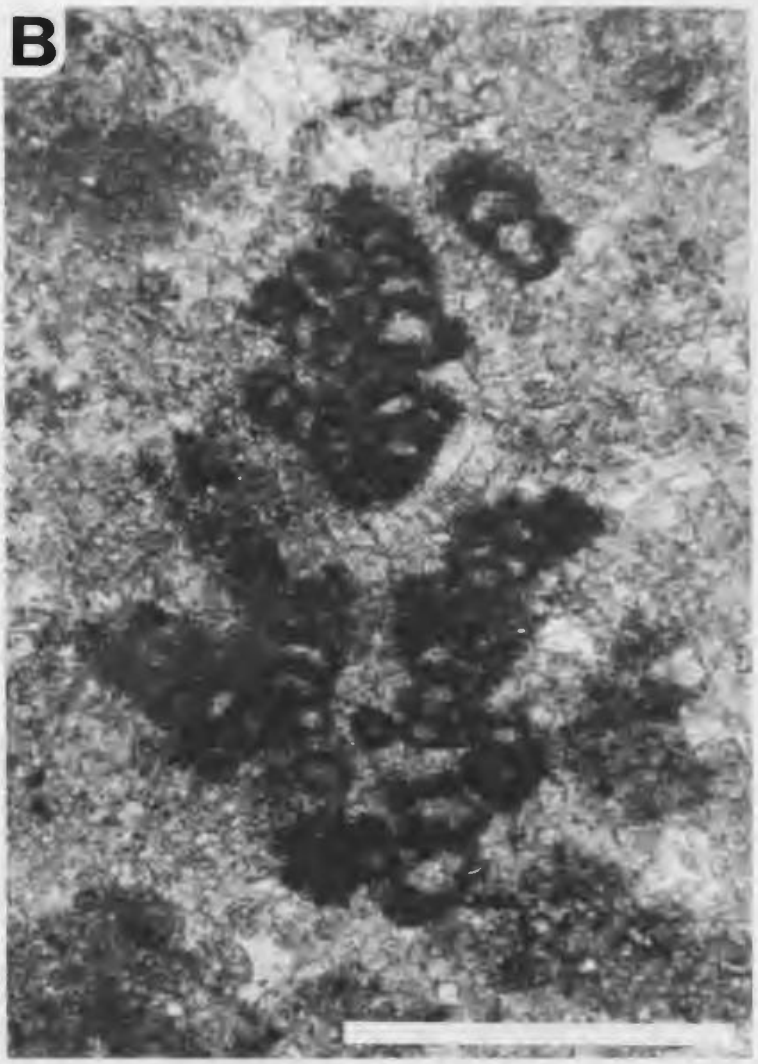
B

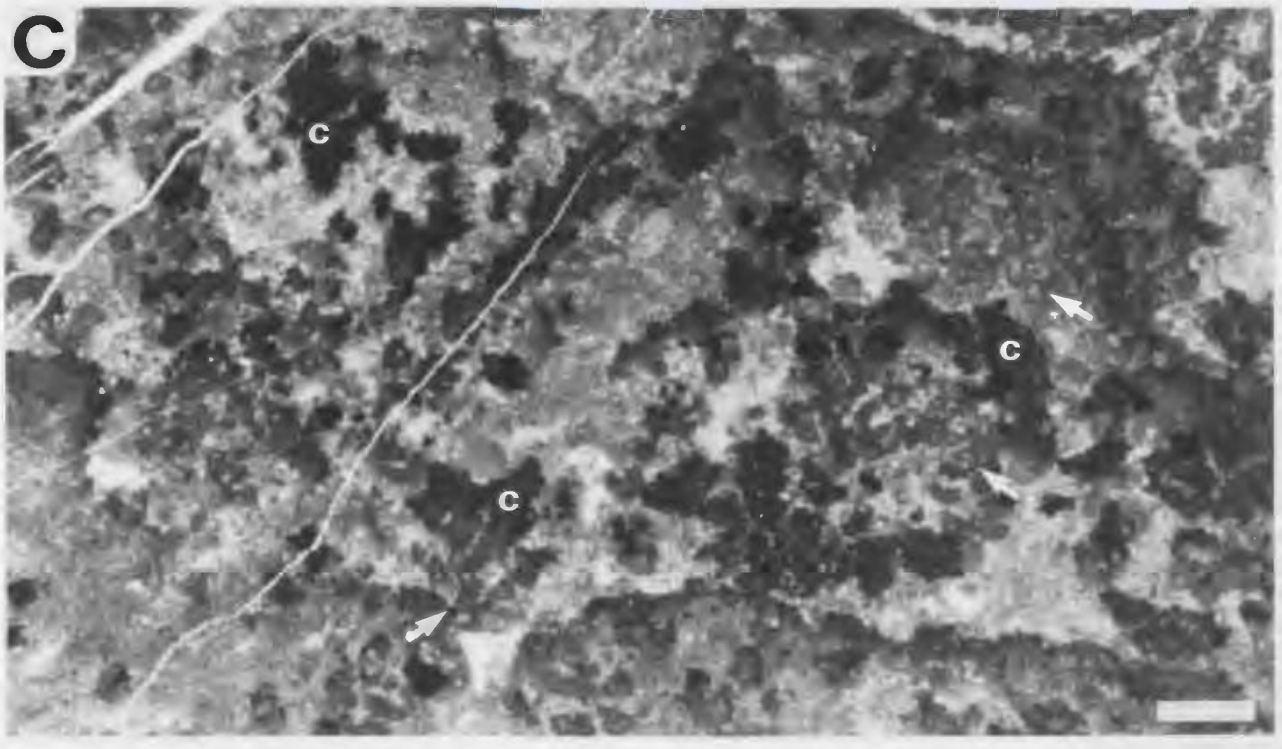
C
c
c
c

PLATE 71

Great Basin, western U.S.A.
Wheeler Formation
Middle Cambrian

Microstructure - Unit 2

A - Alternating bands of chambered *Renalcis* (R), and encrusting streaky, crypto- and micro-crystalline, stromatoids (S). Note gradation from diffuse *Renalcis* to diffuse lobate microstructures (L), and local clotted (grumous) microstructure of cryptocrystalline stromatoids (arrows). Sample NJ-79-113-A2.

B - Streaky crypto- and micro-crystalline microstructure of pseudo-columnar and columnar stromatoids. Note clotted *Renalcis* colonies within stromatoid, local clotted grumous microstructure of cryptocrystalline stromatoids, and scattered quartz silt within stromatoids. Sample NJ-79-113-A.

C - Streaky, grumous and microcrystalline microstructure of crenulate stromatoids. Grumous laminae resemble a prostrate form of clotted *Renalcis*. Note clotted *Renalcis* colonies that encrust stromatoid sheet (arrow at top), and diffuse lobate *Renalcis* (R) that is encrusted by the stromatoids. Sample NJ-79-113-A2.

Scale bars 1 mm.

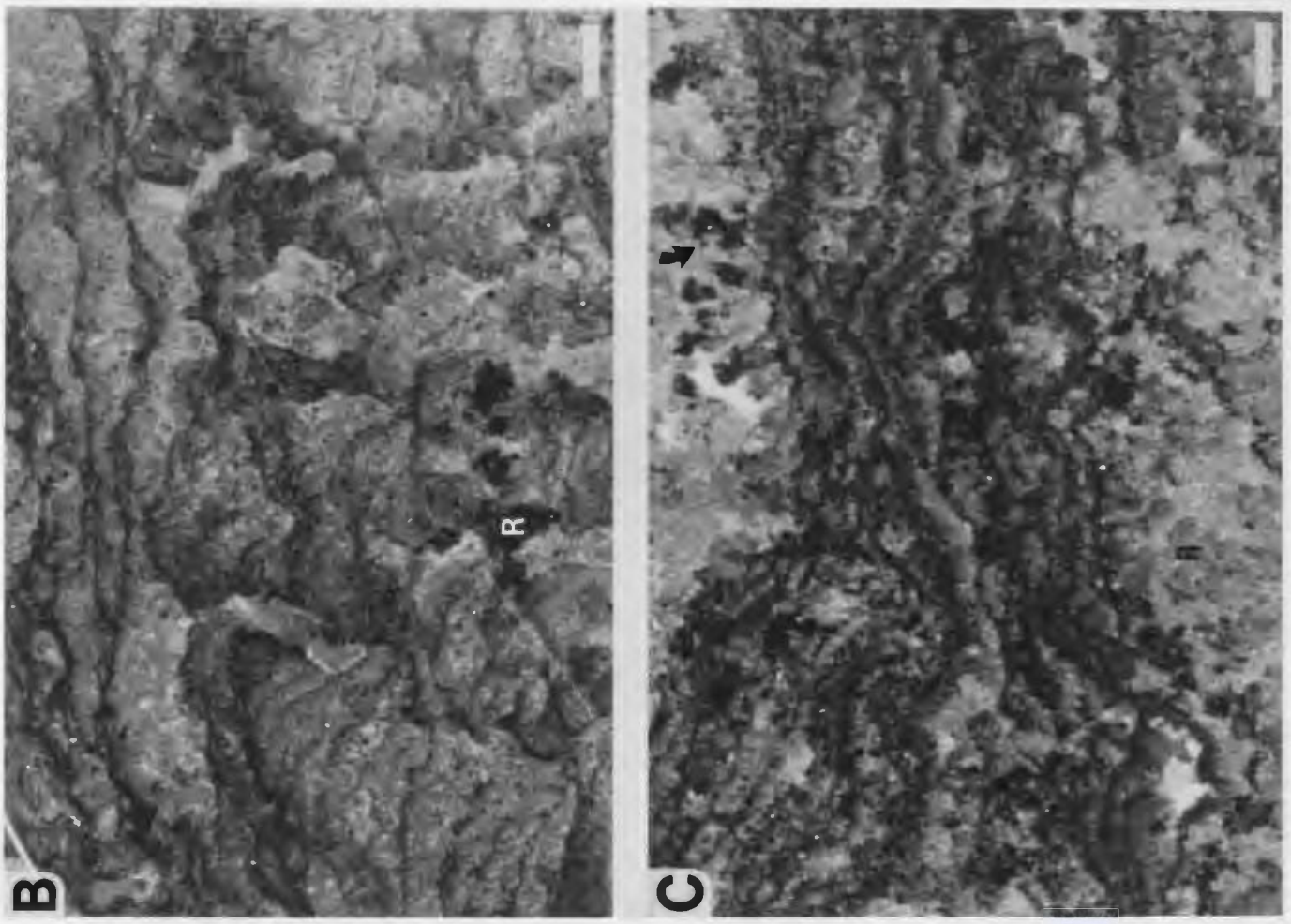
B
R
C
R

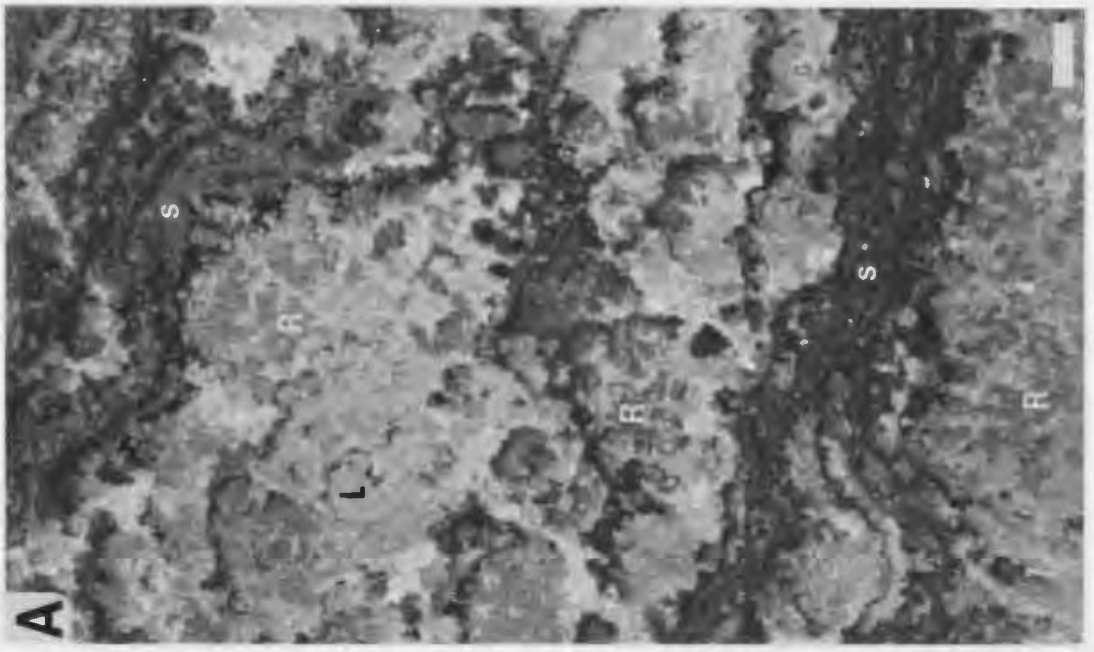
A
S
R
L
S
R
S
R

PLATE 72

Great Basin, western U.S.A.
Wheeler Formation
Middle Cambrian

Microstructure - Units 2 and 3

A - Dendritic *Epiphyton* encased in turbid microspar. Unit 2, Sample WHL-1A.

B - Dendritic *Epiphyton* colonies at margin of former crevasse-like cavity between vertical hummocky laminae. Remainder of cavity is filled with ooid-skeletal wacketone (W). Hummocky microspar laminae may represent marine cement and\or stromatoid crusts.
Unit 3, Sample RR-79-33.

C - Walled tubular structures cf. *Microtubus communis* Flügel 1964 occurring in close association with dendritic *Epiphyton* (E) (seen here in transverse section).
Unit 3, Saple RR-79-33

Scale bars 1 mm.

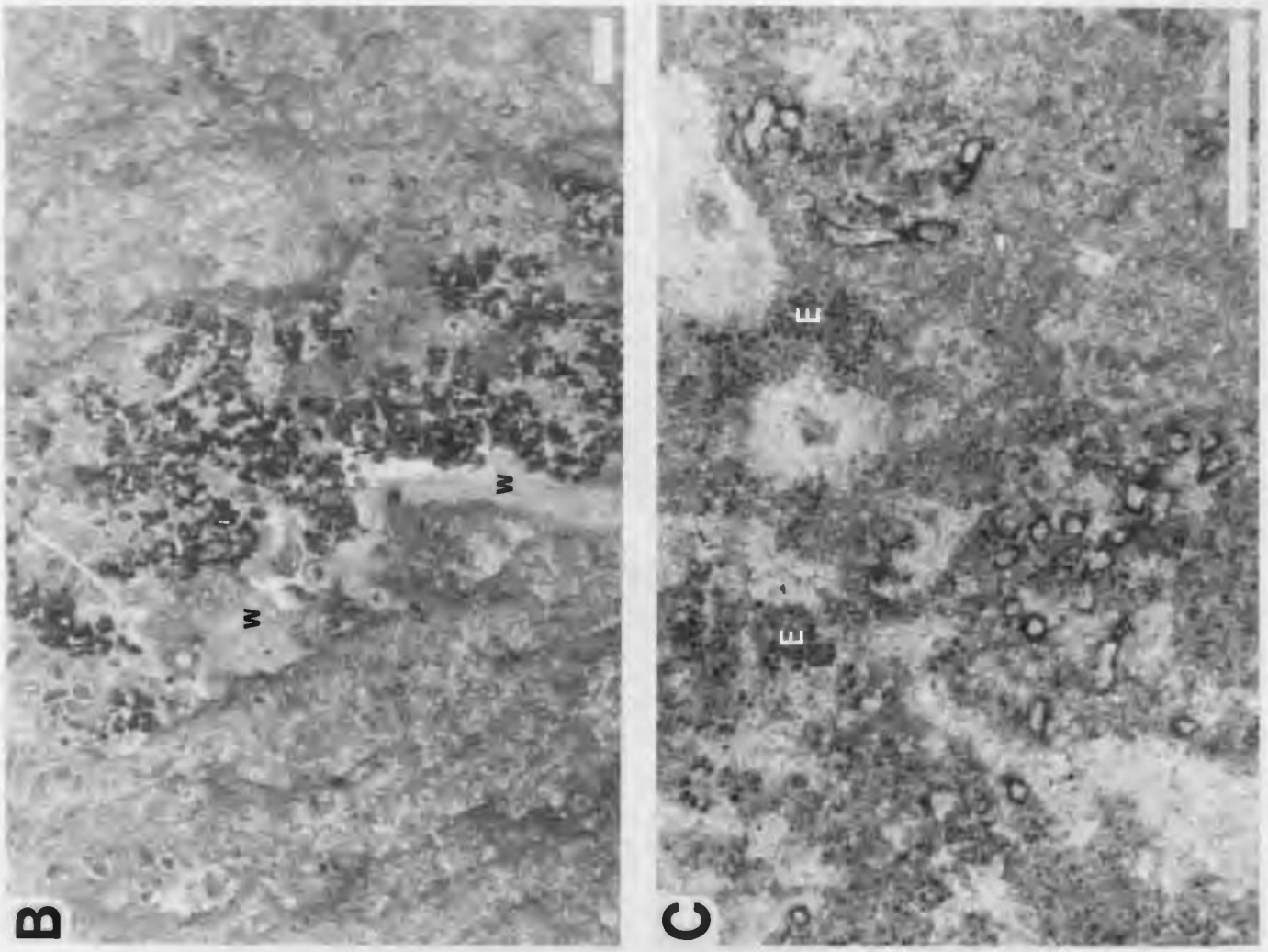
B
W
W
C
E
E

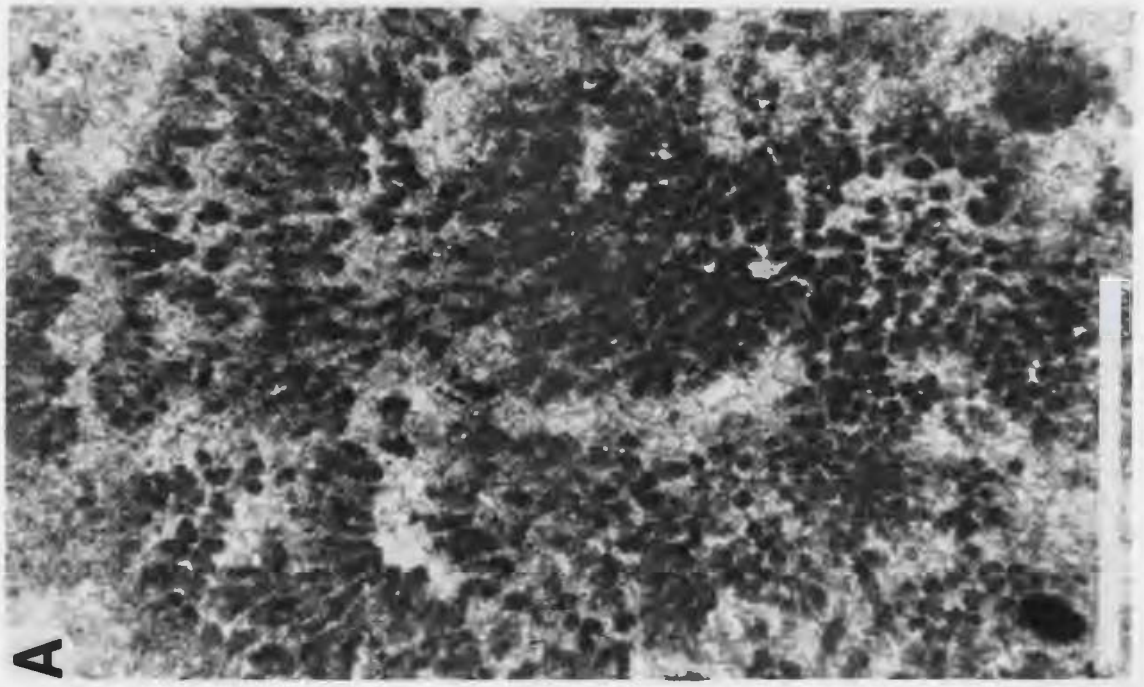
A

PLATE 73

Great Basin, western U.S.A.
Wheeler Formation
Middle Cambrian

Microstructure - Units 4 and 5

A - Streaky cryptocrystalline and microcrystalline microstructure of columnar-layered stromatoids, Unit 4. Laminae are commonly separated by laminoid, spar-filled fenestrae (F). Sample WHL-4.

B - Mottled tubiform microstructure of poorly laminated, extensively bioturbated, stromatoid column; Unit 4. Note tubular burrows (arrows) and trilobite fragment (lower left). Sample NJ-79-113-B2.

C - Diffuse streaky grumous microstructure of undulose stromatoids, Unit 5. Note alternating thin massive and thicker grumous laminae at top, and possible burrow (arrow). Sample NJ-79-113-C.

D - Streaky microstructure comprised of alternating thin cryptocrystalline and thick grumous laminae; undulose stromatoid, Unit 5. Sample NJ-79-113-C.

Scale bars 1 mm.

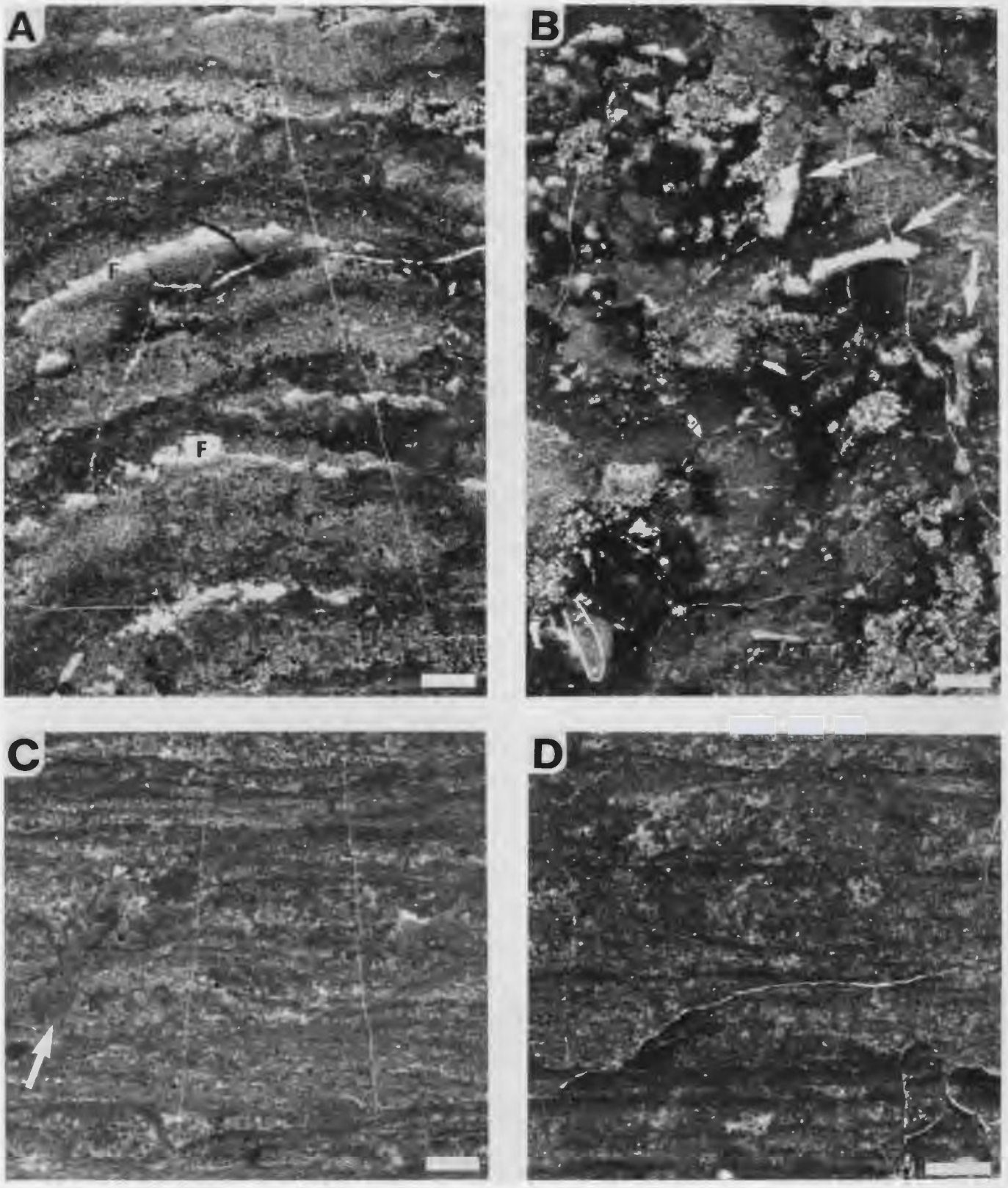
A
F
F
B
C
D

PLATE 74

Great Basin, western U.S.A.
Wheeler Formation
Middle Cambrian

Microstructure - Unit 6

A - Alternating bands of light coloured chambered, and dark coloured clotted, *Renalcis*. Note selective occurrence of euhedral authigenic quartz within clotted *Renalcis*.
Sample NJ-79-113-C1.

B - Intergrown chambered and clotted *Renalcis* colonies encased in turbid microspar. Note selective occurrence of authigenic quartz within clotted *Renalcis*. Sample NJ-79-113-C1.

C,D - Intergradation of chambered and clotted *Renalcis* morphotypes, encased in fibrous turbid marine cement (MC) and microspar; C) plane polarized light, D) crossed polarized light.
Sample NJ-79-113-D.

Scale bars 1 mm.

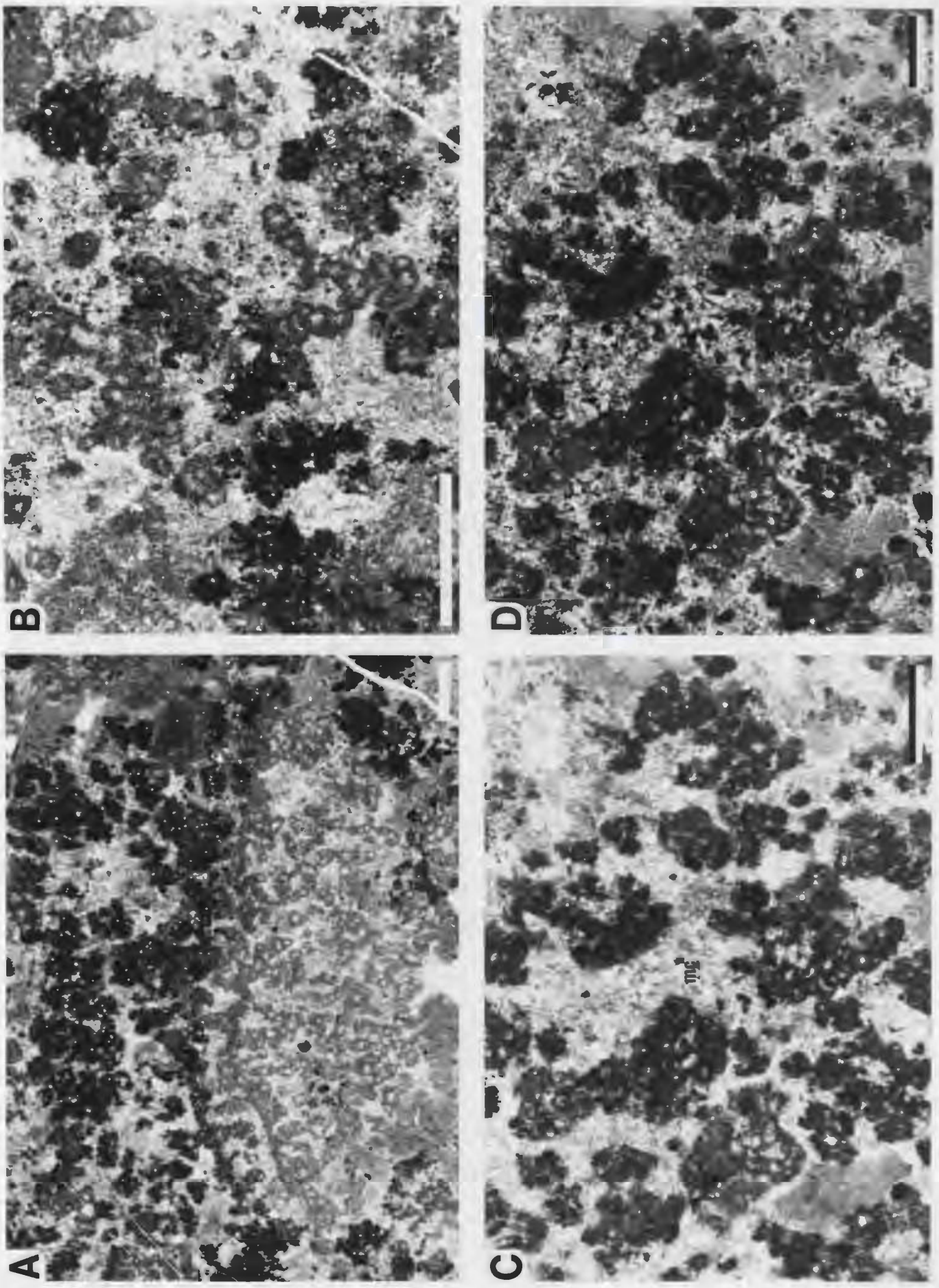
A
B
C
D

PLATE 75

Great Basin, western U.S.A.
Orr Formation
Upper Cambrian

Horizon 1: lower Big Horse Limestone Member
Microstructure

A - Massive to diffuse grumous microstructure of thromboid encased in silty peloid-skeletal packstone. Note diffuse *Epiphyton* colony (E) which appears as a cluster of dark subrounded microclots in transverse section, and spar-filled burrows (arrows) within thromboid. Sample COB-1B.

B - Mottled grumous microstructure of thromboid with numerous dark clusters of diffuse *Epiphyton* (E) colonies. Note trilobite within inter-framework grainstone (arrow lower left). Sample COB-3.

C,D,E - Spectrum of C) diffuse grumous, grading to D) distinct grumous, and E) *Epiphyton* microstuctures within thromboids. With increasing neomorphism and\or *in situ* fragmentation and collapse of the delicate dendritic "thalli", the colonies appear as clusters of diffuse subrounded cryptocrystalline microclots. Note isopachous microspar rims around microclots in C (arrows; these rims are probably former marine cement), and juxtaposition of well preserved dendritic *Epiphyton* (E) and poorly preserved microclotted (diffuse grumous) colony (g) in E. Samples COB-1A, COB-1A and COB-3, respectively.

Scale bars 0.5 mm.

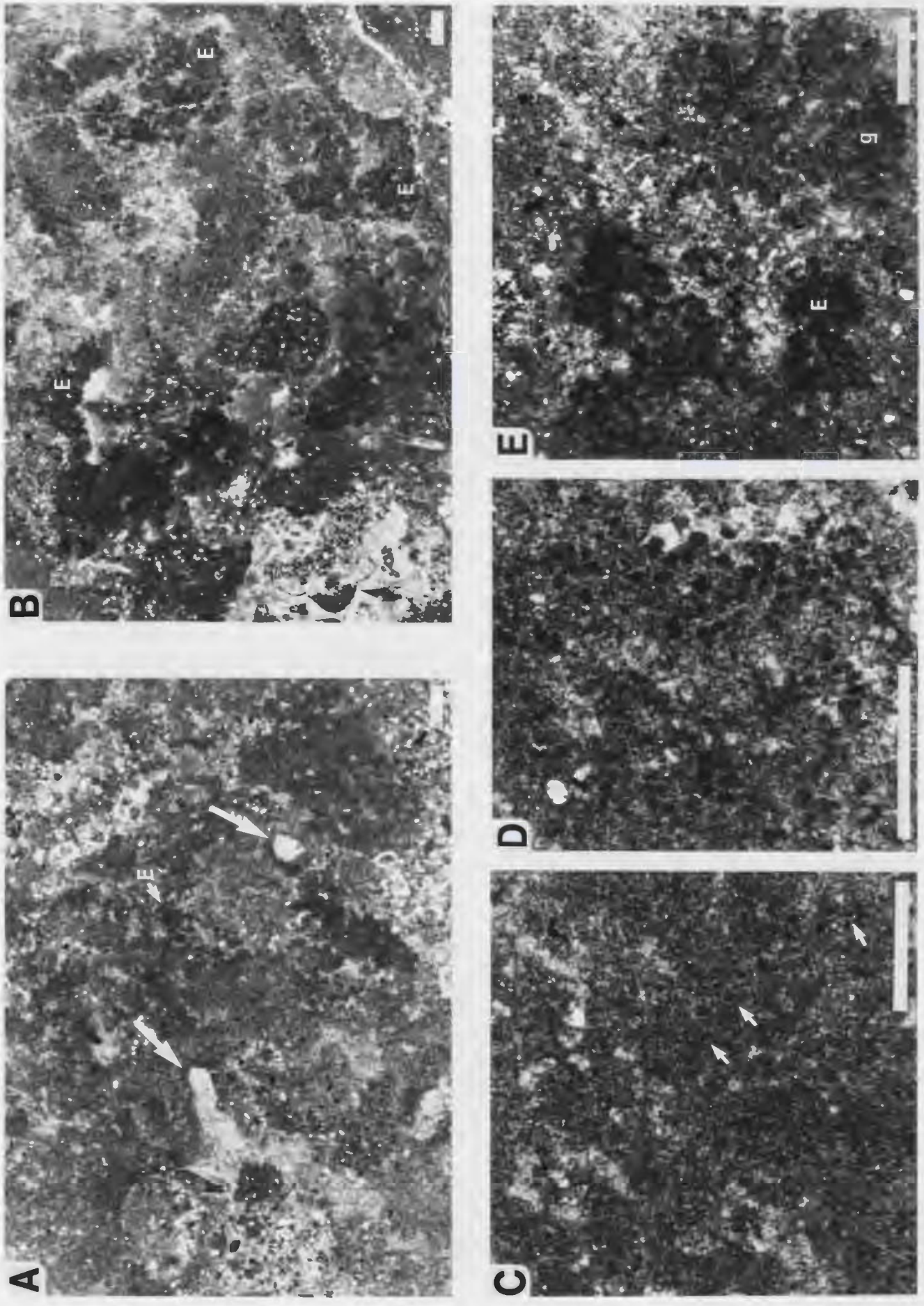
A
B
C
D
E
E
E
E
E
b

PLATE 76

Great Basin, western U.S.A.
Orr Formation
Upper Cambrian

Horizon 2: upper Big Horse Limestone Member
Microstructure - Unit 1

A - Mottled grumous (g) and tubular microstructure (tubular burrows within dark micrite) of thromboid. Sample COB-6.

B - Variegated massive (m) and grumous (g) microstructure of thromboid. Note spar-filled burrow in massive micrite top left. Sample COB-6.

C - Magnified view of upper right portion of B showing open network of wispy elongate microclots (arrows) within grumous thromboid. This microstructure is intermediate between grumous and filamentous microstructures. Sample COB-6.

Scale bars 1 mm.

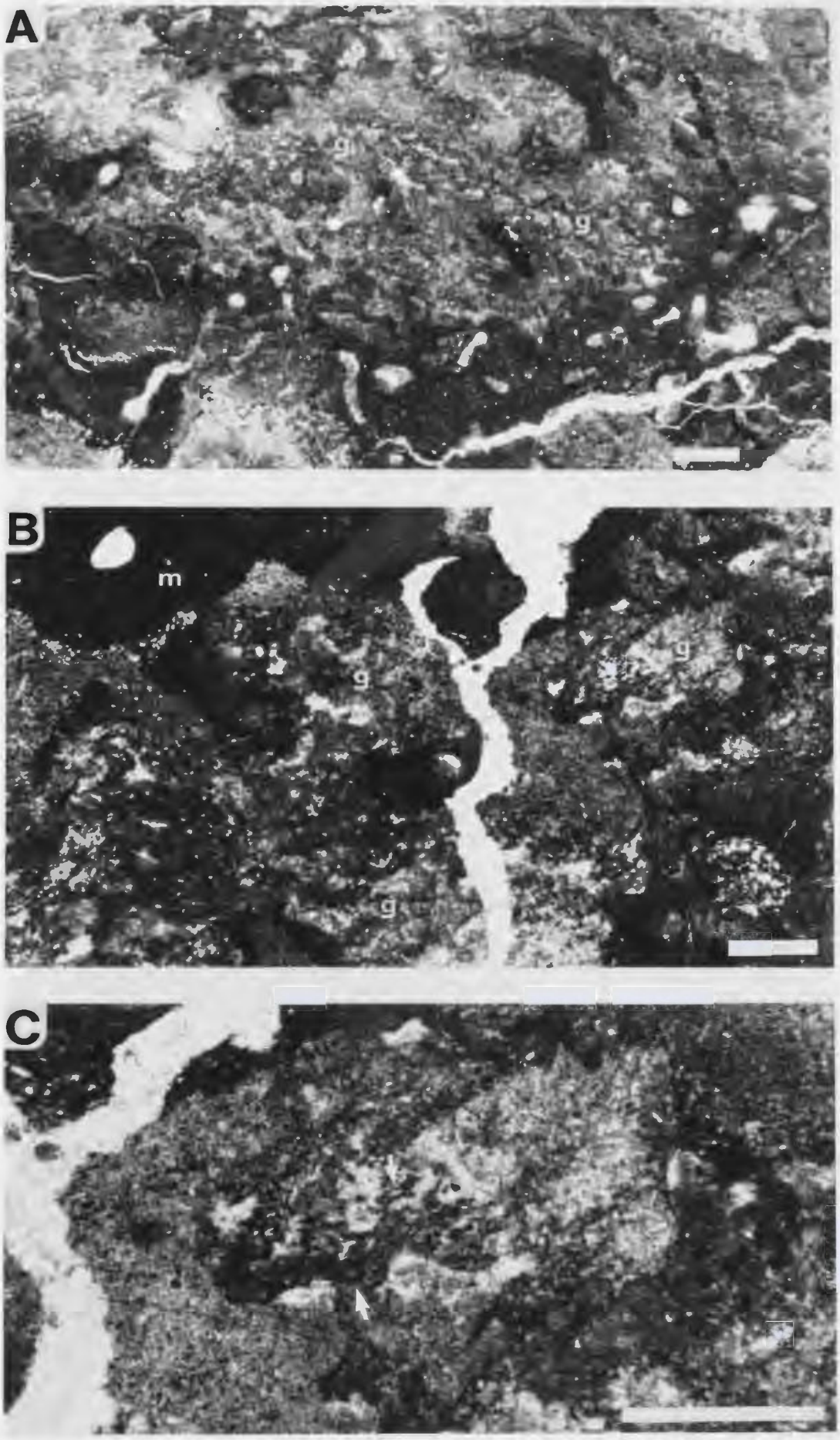
A
g
g
B
m
g
g
g
C

PLATE 77

Great Basin, western U.S.A.
Orr Formation
Upper Cambrian

Horizon 2: upper Big Horse Limestone Member
Mesostructure and microstructure - Unit 2

A,B - Closely packed, club-shaped, stromatolite columns separated by narrow grainstone wedges, and encrusted by dark thrombolitic rims (arrows in B); A) natural vertical exposure, B) natural horizontal exposure. Scale rule 10 cm.

C - Spongeous grumous microstructure of weakly laminated stromatoid column. Sample COB-7B.

D - Grumous grading to diffuse filamentous microstructure of gently convex stromatoid. Cryptocrystalline microclots have an elongate thread-like form (arrows) and are arranged perpendicular to the laminae. Note burrows (B) in overlying dolomitic lamina. Sample COB-7B.

E - Dendritic *Epiphyton* within thrombolitic crust at margin of stromatoid column. Note outward (towards left) and pendant growth form of colonies. Sample COB-7A.

F - Magnified view of *Epiphyton* colony in area outlined in E. Sample COB-7A.

Scale bars 1 mm (except A,B).

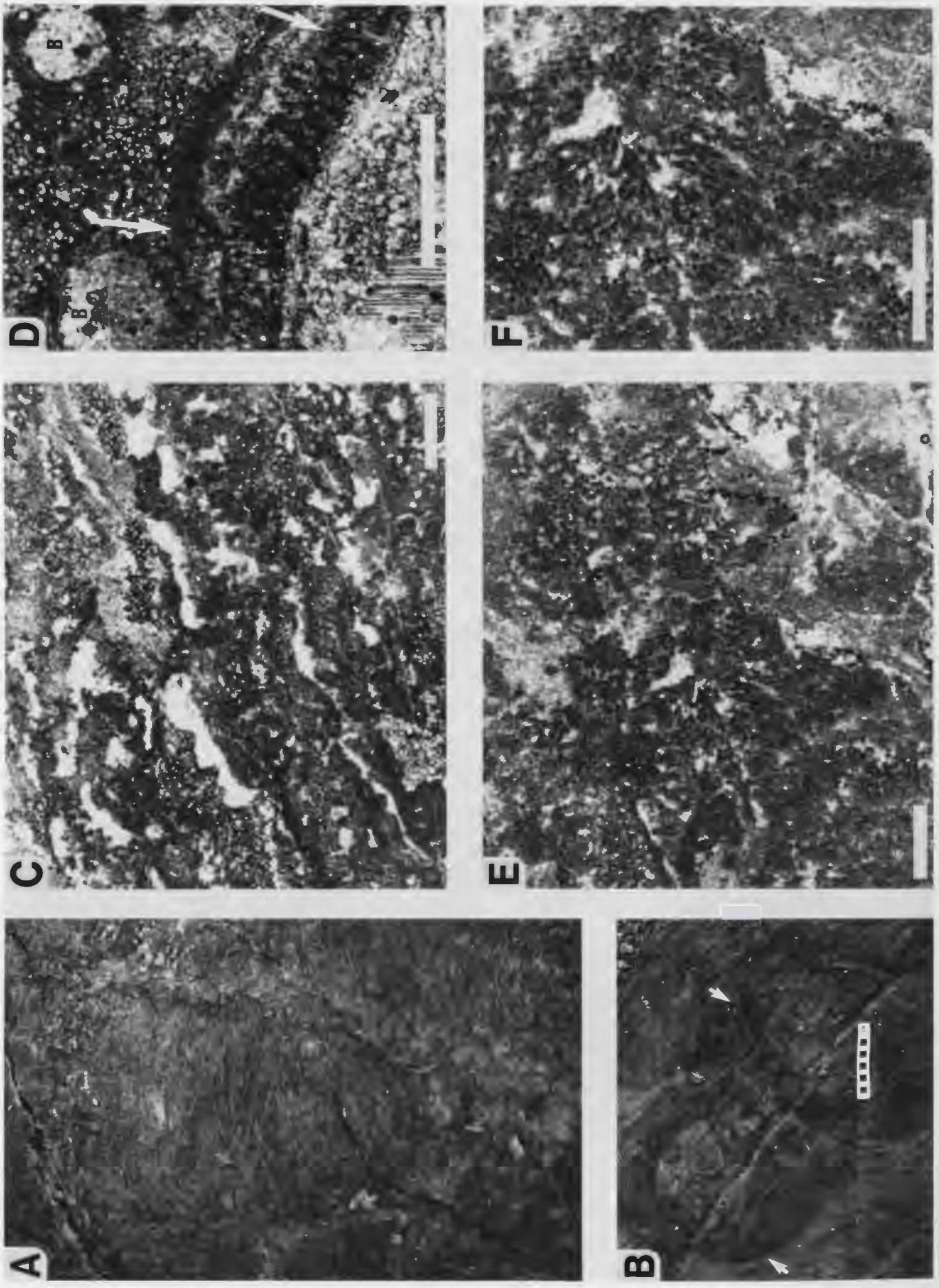
A
B
C
D
E
F

PLATE 78

Great Basin, western U.S.A.
Orr Formation
Upper Cambrian

Horizon 2: upper Big Horse Limestone Member
Microstructure - Unit 2
Mesostructure and microstructure - Unit 3

A,B - *Epiphyton* colonies encased in turbid microspar and burrowed mudstone; thrombolitic crust at margin of stromatoid column, Unit 2. Note former cavities filled with mudstone and sparry cement (C). Sample COB-8.

C - Dark knobbly crust of *Epiphyton* boundstone at crest of club-shaped stromatolite columns; Unit 3. Scale bar 10 cm.

D - *Epiphyton* colonies encased and overlain by relatively coarse and poorly sorted peloid packstone; knobbly *Epiphyton* crust, Unit 3. Sample COB-9.

Scale bars 1 mm (except C).

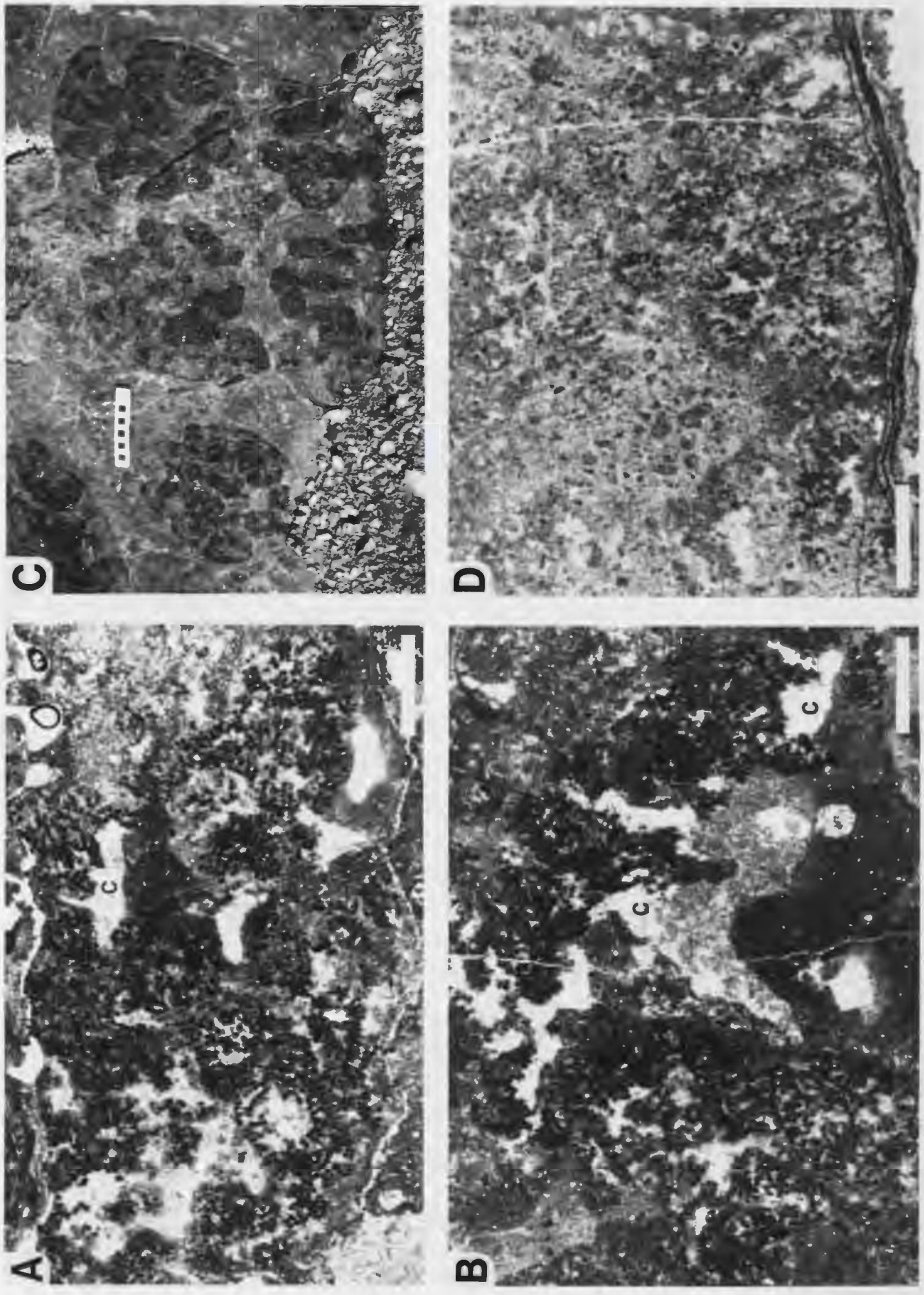
A
B
C
D
c
c
c

PLATE 79

Great Basin, western U.S.A.
Orr Formation
Upper Cambrian

Horizon 3: lower Candland Shale Member
Microstructure

A - Sub-digitate thromboid (T) encased in trilobite-pelmatozoan-brachiopod packstone. Note pocket of skeletal debris within thromboid (arrow), and possible burrow (B). Sample COB-10.

B - Magnified view of thromboid in A, showing lobate (L) and grumous (g) microstructures. Some lobes have a diffuse cryptocrystalline wall (diffuse saccate microstructure). Sample COB-10.

C - Saccate lobate microstructure of thromboid surrounded by pelmatozoan-trilobite wackestone. Sample COB-10B.

Scale bars 1 mm.

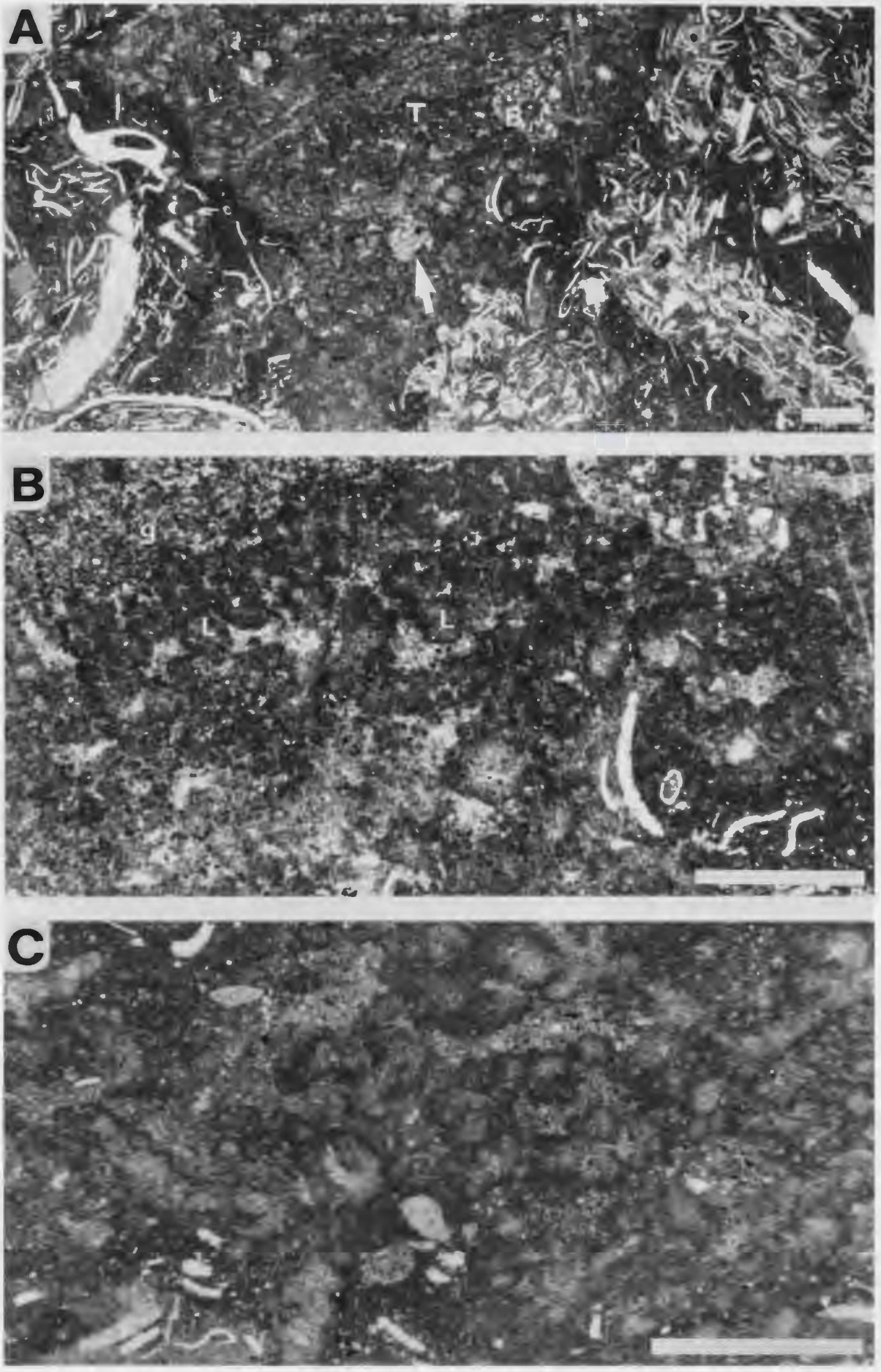
A
T
B
B
g
L
L
C

PLATE 80

Great Basin, western U.S.A.
Orr Formation
Upper Cambrian

Horizon 4: upper Candland Shale Member
Microstructure

A - Arcuate micritic sheets encrusted by turbid marine cement (MC) and pendant *Epiphyton* colonies (E), and encased in mudstone (M). Sample COC-1.

B - Magnified view of arcuate micritic sheets shown in upper right portion of A. Note isopachous fibrous marine cement on convex surface of uppermost sheet (arrow), and masses of turbid microcrystalline marine cement (MC) beneath micritic sheets. Sample COC-1.

C - Horizontal section of micritic sheet showing network of randomly oriented micitic filaments. Sample COC-1.

D - Micritic sheet that appears to bifurcate. Note relatively thick mass of turbid, poorly fibrous, microcrystalline marine cement (MC) beneath sheet, whereas upper surface of sheet is directly overlain by microsparitic lime-mud. Sample COC-1.

Scale bars 1 mm.

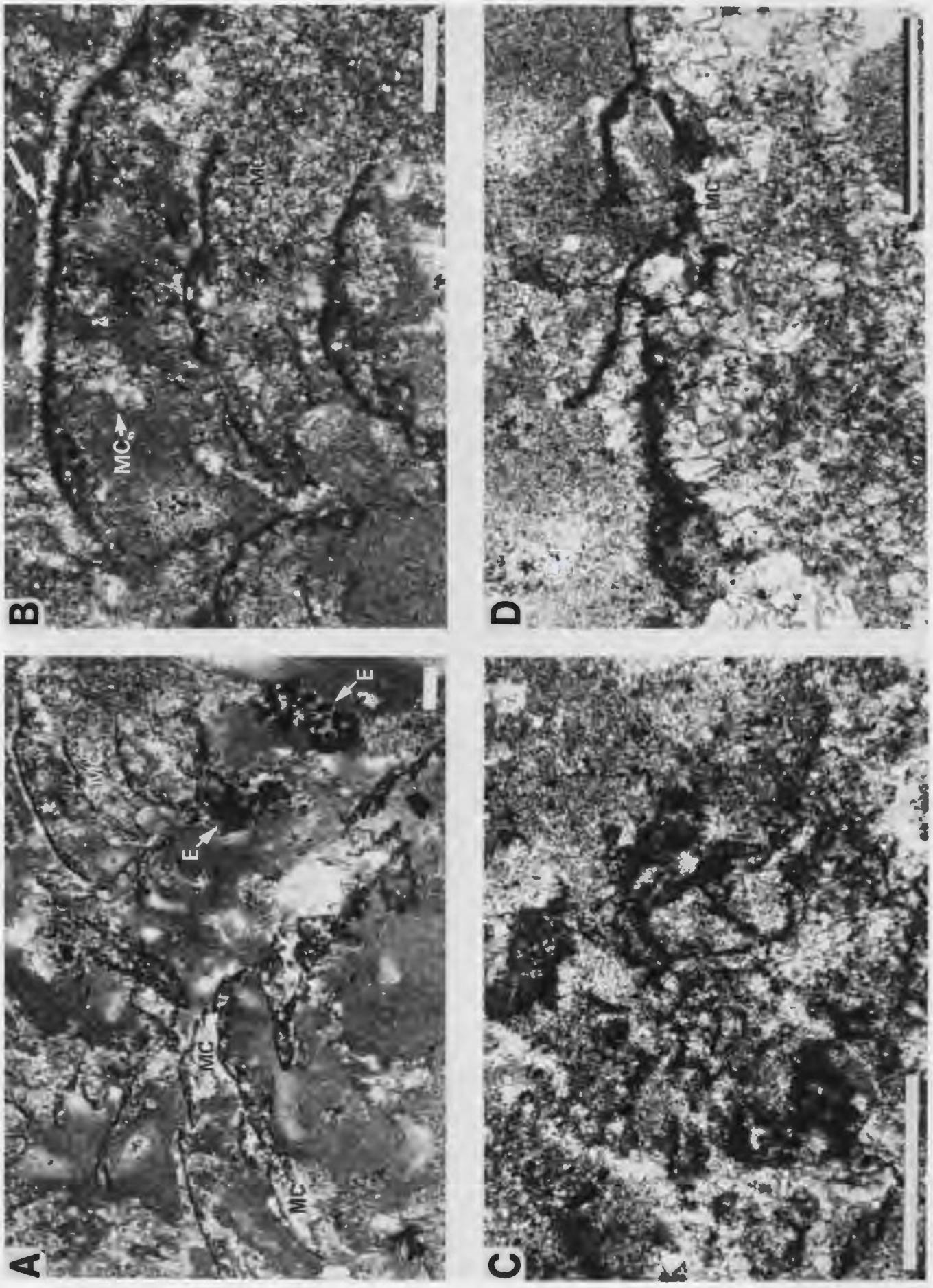
A
MC
E
E
MC
MC
B
MC
MC
C
D
MC

Plate 81

Amadeus Basin, central Australia
Shannon Formation
Middle-Upper Cambrian

Carbonate cycles in lower and upper units

A - Stromatolite dominated carbonate cycle, lower unit. Recessive mudrock is overlain by (1) grainstone with dolo-mudstone lenses, (2a) wavy and (2b) hemispherical stromatolite, and (3) undulose stromatolite.

B - Wave-rippled ooid grainstone with lenticular and wavy dolo-mudstone drapes; basal portion of a carbonate cycle, lower unit.

C - Cubic and pagoda halite pseudomorphs within dolo-mudstone at the top of a carbonate cycle, lower unit.

D - Thin transgressive sequence at the base of a carbonate cycle in the upper unit. (1) Karst eroded dolo-mudstone, (2) stromatolite, (3) thrombolite, and (4) grainstone.

PLATE 81

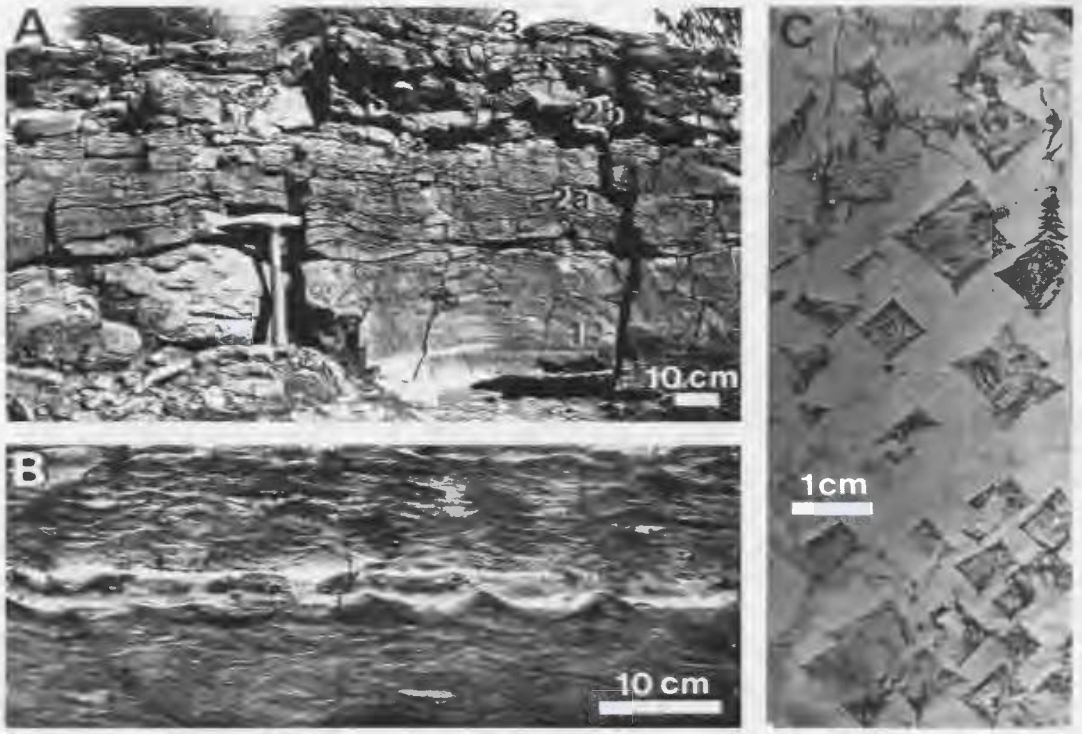

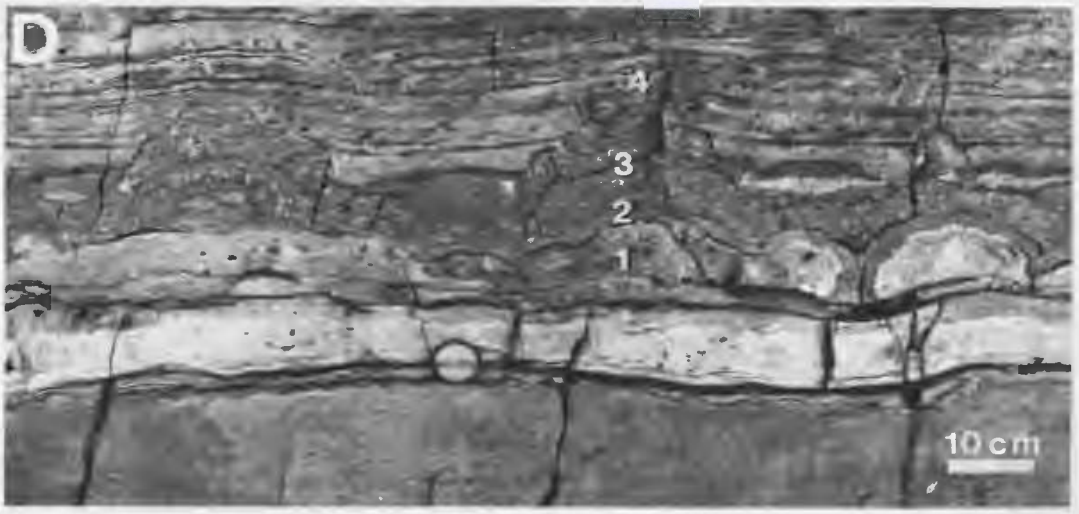

Plate 82

Amadeus Basin, central Australia
Shannon Formation
Middle-Upper Cambrian

Carbonate cycles in upper unit

A,B - Thrombolite dominated cycles. Recessive mudrock is overlain by (1) grainstone, (2) thrombolite bioherms, (3) inter-biohermal grainstone, (4a) columnar and (4b) wavy stromatolite, (5) intraclast conglomerate, (6) wave-rippled grainstone, and (7) dolo-mudstone and undulose stromatolite.

C - Columnar stromatolite capping thrombolite bioherms shown in A.

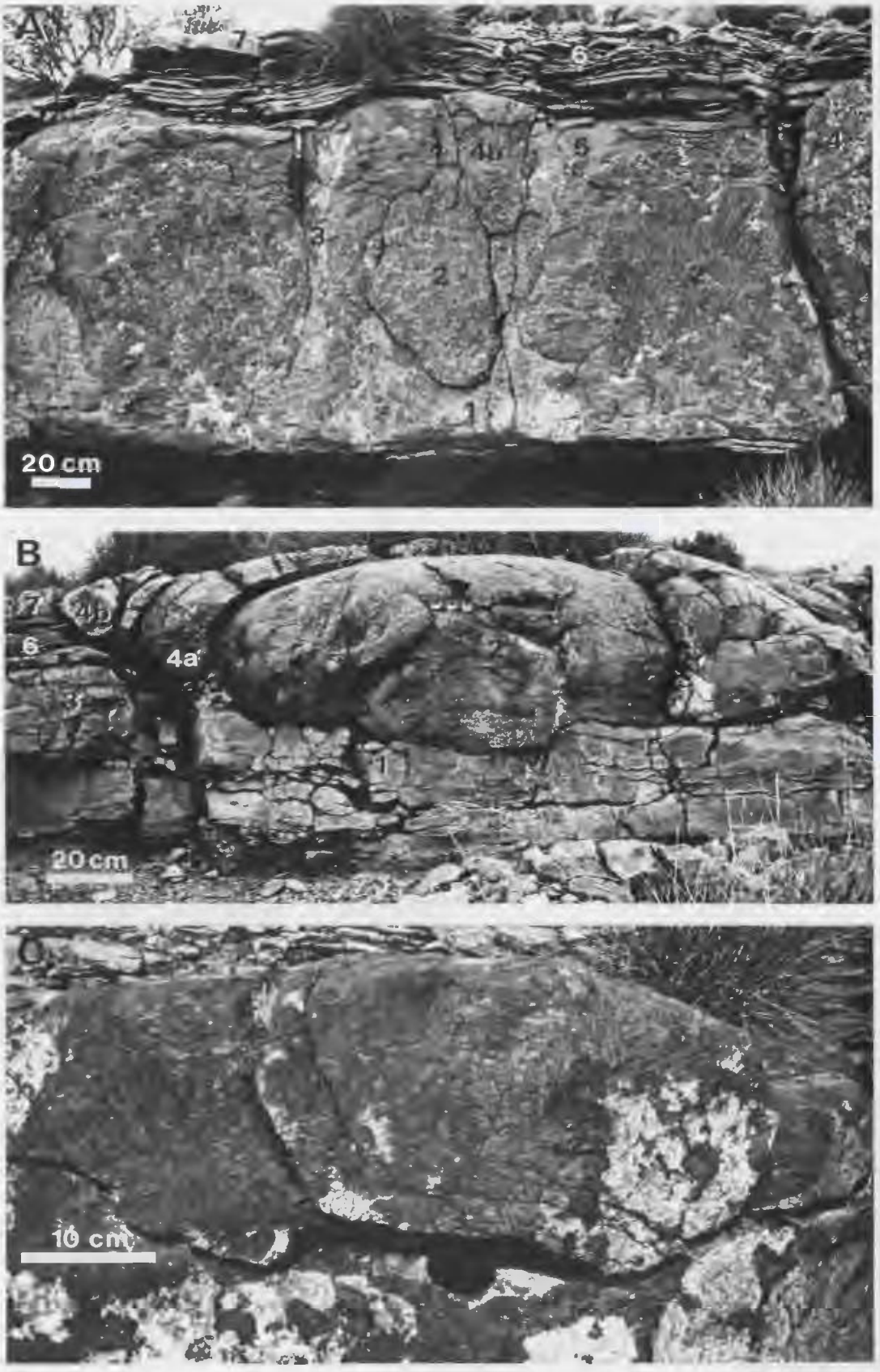
A
7
6
5
4
3
2
1
20 cm
B
7
6
4a
3
1
20 cm
C
10 cm

Plate 83

Amadeus Basin, central Australia
Shannon Formation
Middle-Upper Cambrian

Mesostructure of thrombolites

A - Digitate and arborescent thromboids at crest of bioherm; Type 1 thrombolite. Note capping columnar stromatolite (above hammer head). Hammer 30 cm.

B - Basal portion of bioherm showing prostrate and pendant thromboids (variegated black and medium grey), spar-filled shelter cavities (white) and dolomitic inter-framework sediment (light grey); Type 1 thrombolite. Natural exposure surface. Scale rule 5 cm.

C - Vertical slab of crestal portion of bioherm showing arborescent thromboids and dolomitic inter-framework grainstone with numerous intraclast; Type 1 thrombolite. Sample CS-B-1.

D - Vertical slab of basal portion of bioherm showing amoeboid thromboids encased in dolomitic packstone (p); Type 1 thrombolite. Thromboids are disrupted by burrows (arrows), and support small shelter cavities occluded by white sparry calcite (s). Sample CS-A-11B.

E - Relatively large lobate and saccate thromboids encased in dolomitic wackestone; Type 2 thrombolite. Natural exposure surface.

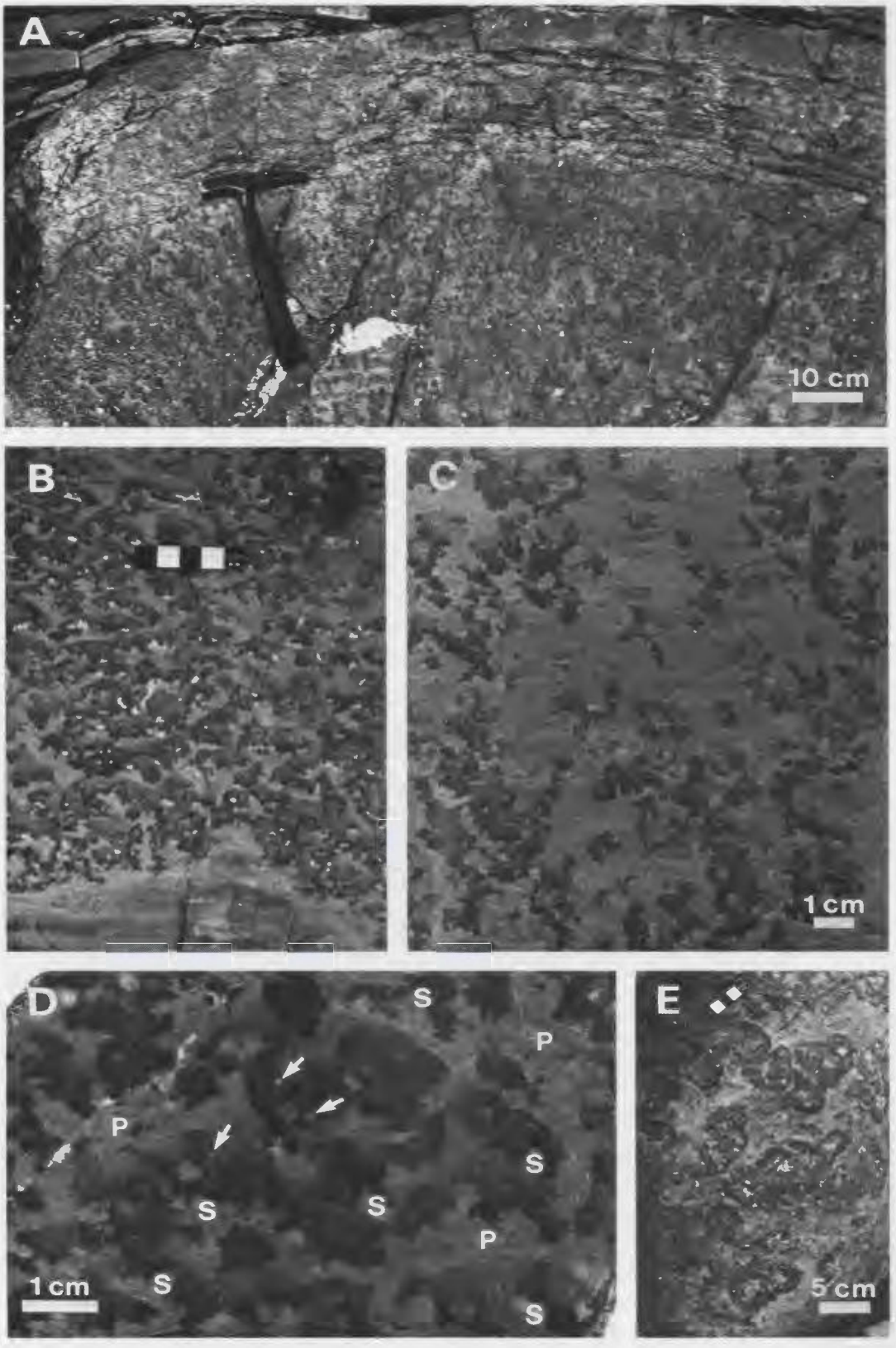
A
10 cm
B
C
1 cm
D
S
P
P
S
S
S
P
S
1 cm
S
E
5 cm

Plate 84

Amadeus Basin, central Australia
Shannon Formation
Middle-Upper Cambrian

Microstructure of thrombolites - 1

A - Variegated microcrystalline lobate (L) and cryptocrystalline massive (M) microstructure of sub-digitate thromboids encased in peloid grainstone (G). Sample CS-A-12.

B - Mesoclot with multiply saccate lobate microstructure (cryptocrystalline rims of lobes are arrowed). Inter-framework peloid-skeletal grainstone (G) and wackestone (W). Note trilobite fragment top left. Sample CS-1.

C,D - Saccate lobate microstructure of thromboid; C) plane polarized light, D) cross polarized light. Note sweeping extinction of poorly defined spherulites within microcrystalline lobes. Sample CS-A-11B.

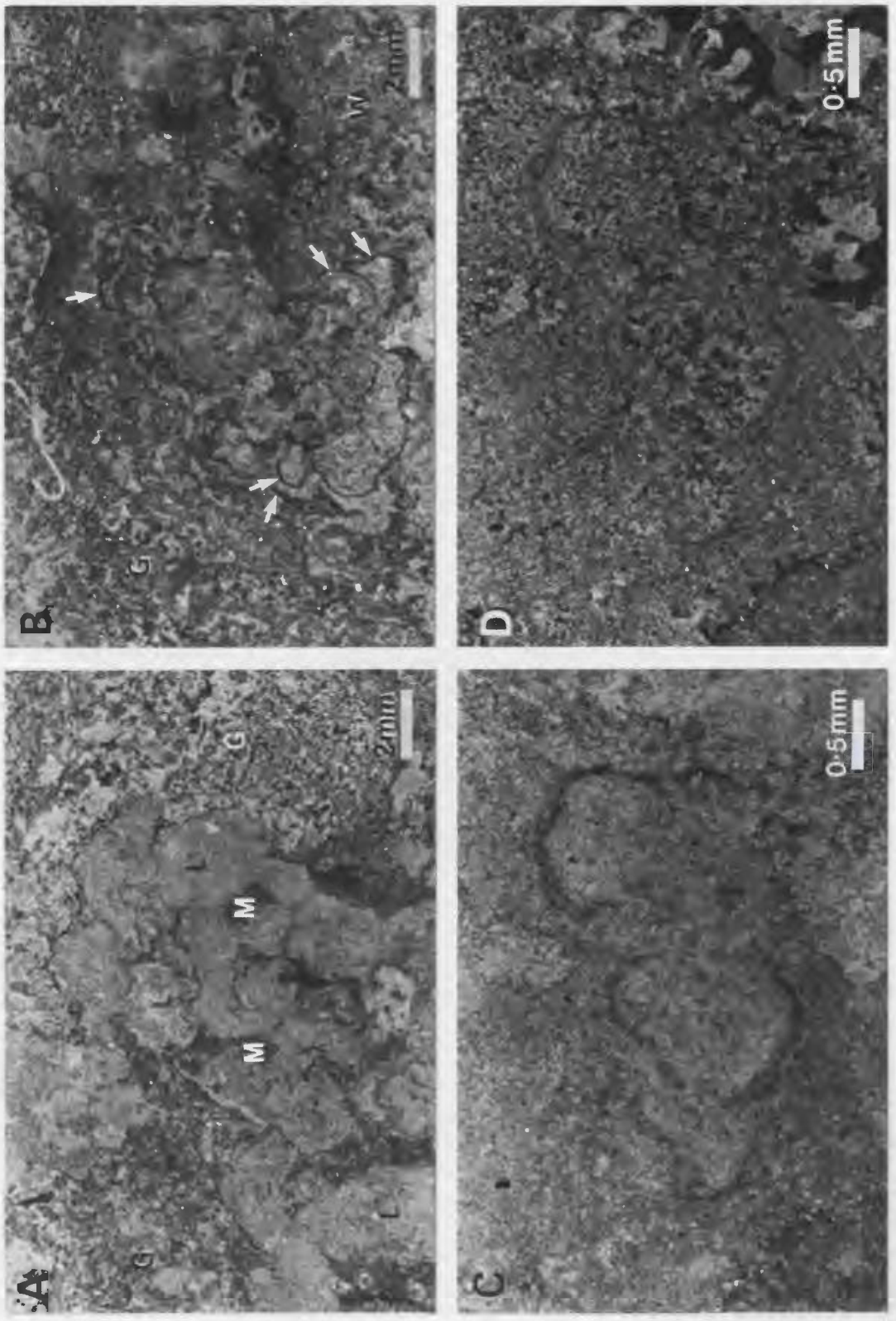
A
G
M
M
G
2mm
B
G
W
2mm
C
0·5mm
D
0·5mm

Plate 85

Amadeus Basin, central Australia
Shannon Formation
Upper Cambrian

Microstructure of thrombolites - 2

A,B - Weakly spherulitic lobate microstructure of thromboid; A) plane polarized light, B) cross polarized light. Sample CS-A-12B-2.

C - Variegated microcrystalline lobate (L) and silty cryptocrystalline massive (M) microstructure of relatively large thromboid encased in inter-framework silty peloid wackestone (W); Type 2 thrombolite. Sample CS-A-21.

D - Radiating tuft of poorly preserved calcified filaments cf. *Girvanella* (arrows) within interbiohermal grainstone. Note diffuse silt-sized peloids trapped between filaments, reworked fragments of turbid microcrystalline lobate thromboids (L), and metazoan fragments (lower right). Sample CS-A-15.

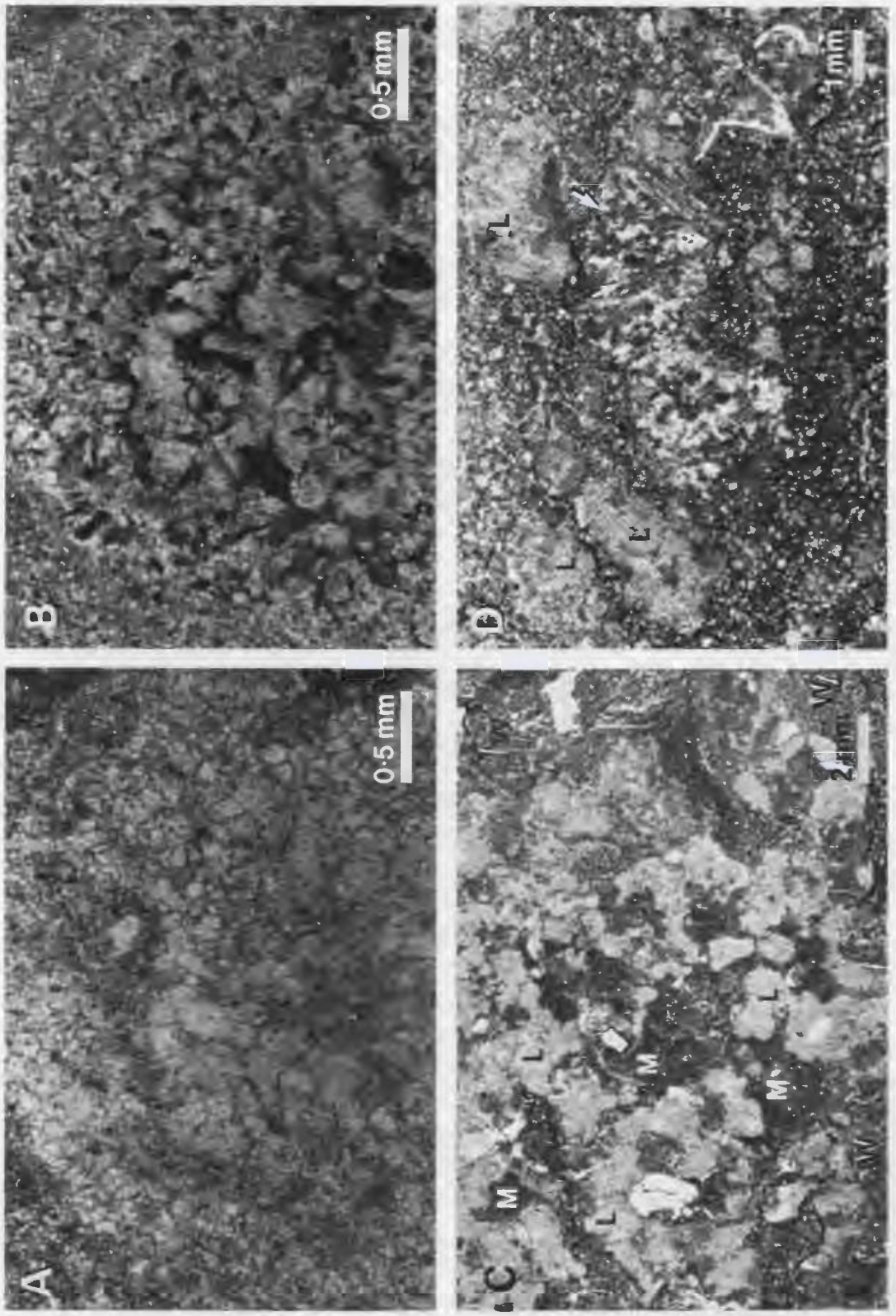
A
0·5 mm
B
0·5 mm
C
M
L
M
L
M
L
M
W
2 mm
D
L
M
1 mm

Plate 86

Amadeus Basin, central Australia
Shannon Formation
Upper Cambrian

Mesostructure of stromatolites

A - Vertical slab of columnar stromatolite (*Madiganites mawsoni* Walter 1972). Columns are encased in peloid-intraclast packstone. Sample CS-A-25.

B - Vertical slab of columnar grading to wavy stromatolite. Sample CS-B-12.

C - Linked hemispherical stromatolite capped by undulose stromatolite. Hammer 30 cm.

D - Wavy grading to hemispherical (left of hammer) and undulose stromatolite. Hammer 30 cm.

E - Alternating wavy and planar stromatolite capped by vuggy undulose stromatolite. Lens cap 5 cm.

PLATE 86

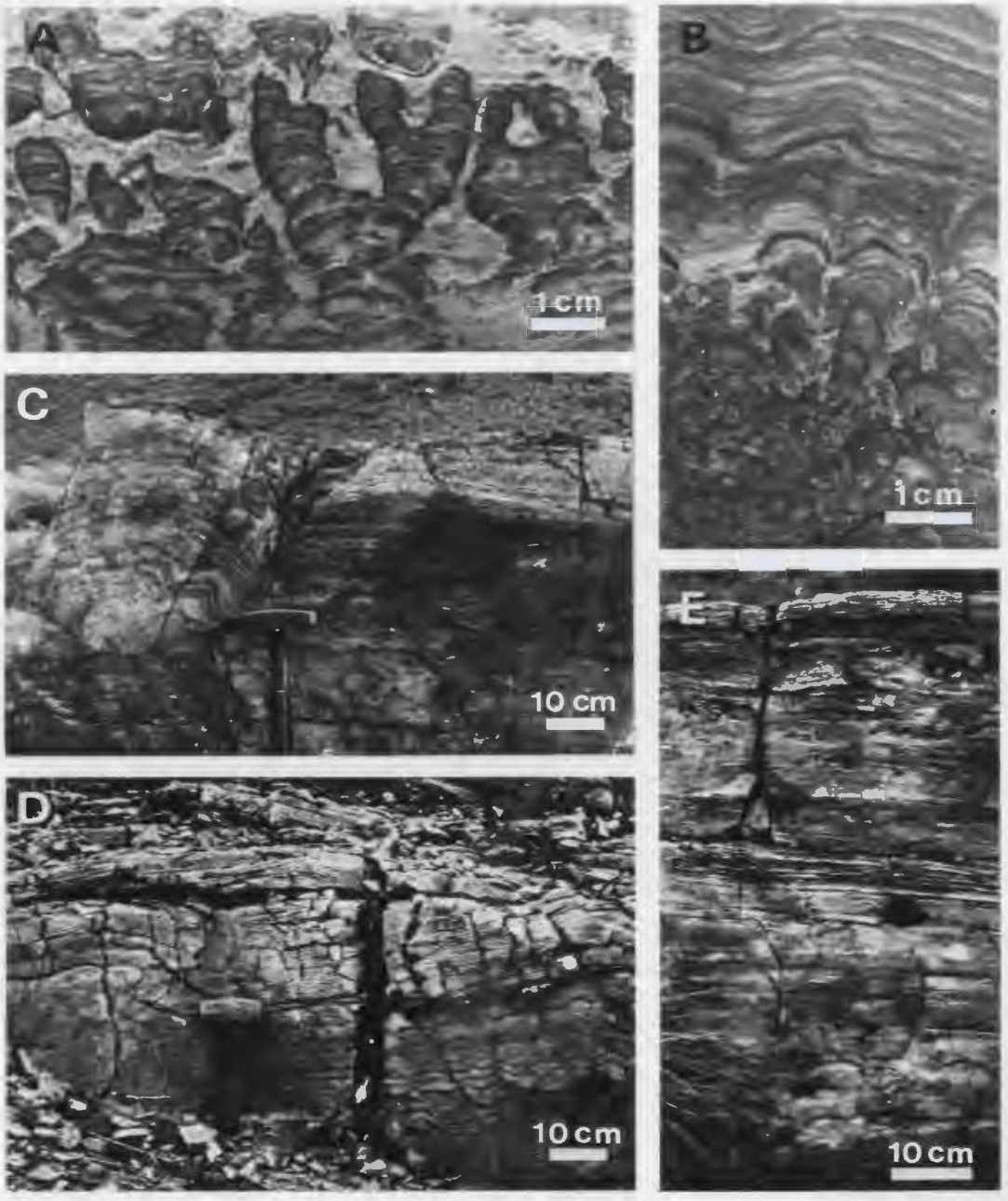

Plate 87

Amadeus Basin, central Australia
Shannon Formation
Upper Cambrian

Microstructure of columnar stromatolites

A - Columnar stromatoids with streaky vermiform microstructure. Vermiform laminae are disrupted by metazoan burrows (arrows), and columns are rimmed by a thin cryptocrystalline wall. Columns are encased in peloid-intraclast grainstone. Sample CS-A-25.

B - Alternating vermiform and massive cryptocrystalline laminae within pseudo-columnar stromatoid. Sample CS-A-25.

C - Vermiform microstructure of columnar stromatoid. Note reticulate network of sinuous tubules (cf. *Spongiostroma maeandrinum* Gürich, 1906). Sample CS-B-10.

D - Vermiform grading to grumous microstructure of stromatoid column. Sample CS-B-18.

PLATE 87

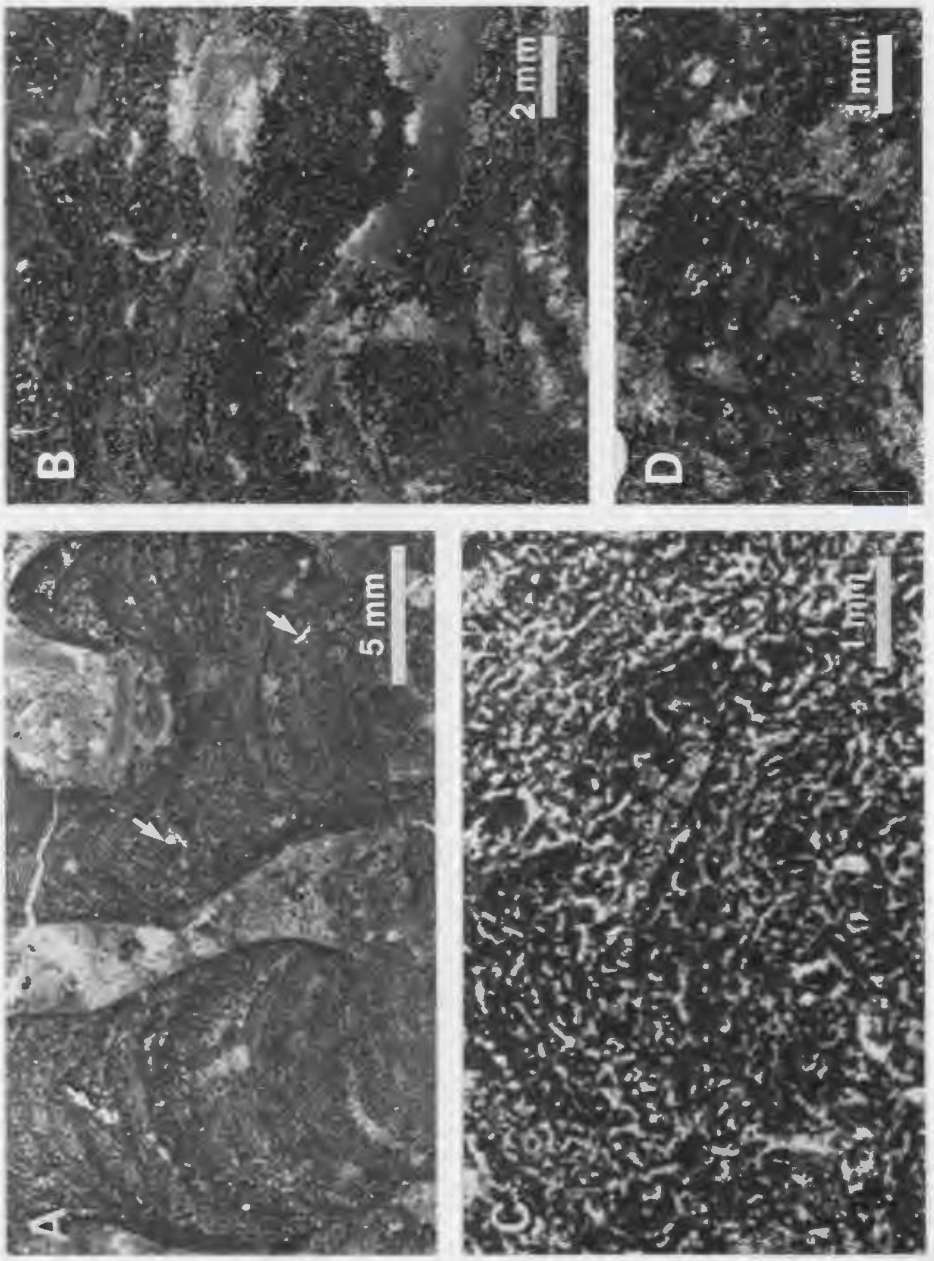

Plate 88

Amadeus Basin, central Australia
Shannon Formation
Upper Cambrian

Microstructure of planar and undulose stromatolites, and cryptomicrobial boundstones

A - Banded microcrystalline and cryptocrystalline microstructure of planar stromatolite. Sample CS-A-27.

B - Irregular streaky microstructure of undulose stromatolite. Sample CS-A-5.

C - Crudely laminated digitate column with mottled and diffuse vermiform grading to grumous microstructure; cryptomicrobial boundstone. Note abundant mollusc fragments in inter-column sediments, and embayed, probably bioeroded, margins of column. Sample CS-B-9.

D - Tubiform microstructure of bioturbated cryptomicrobial boundstone. Sample CS-F-5.

PLATE 88

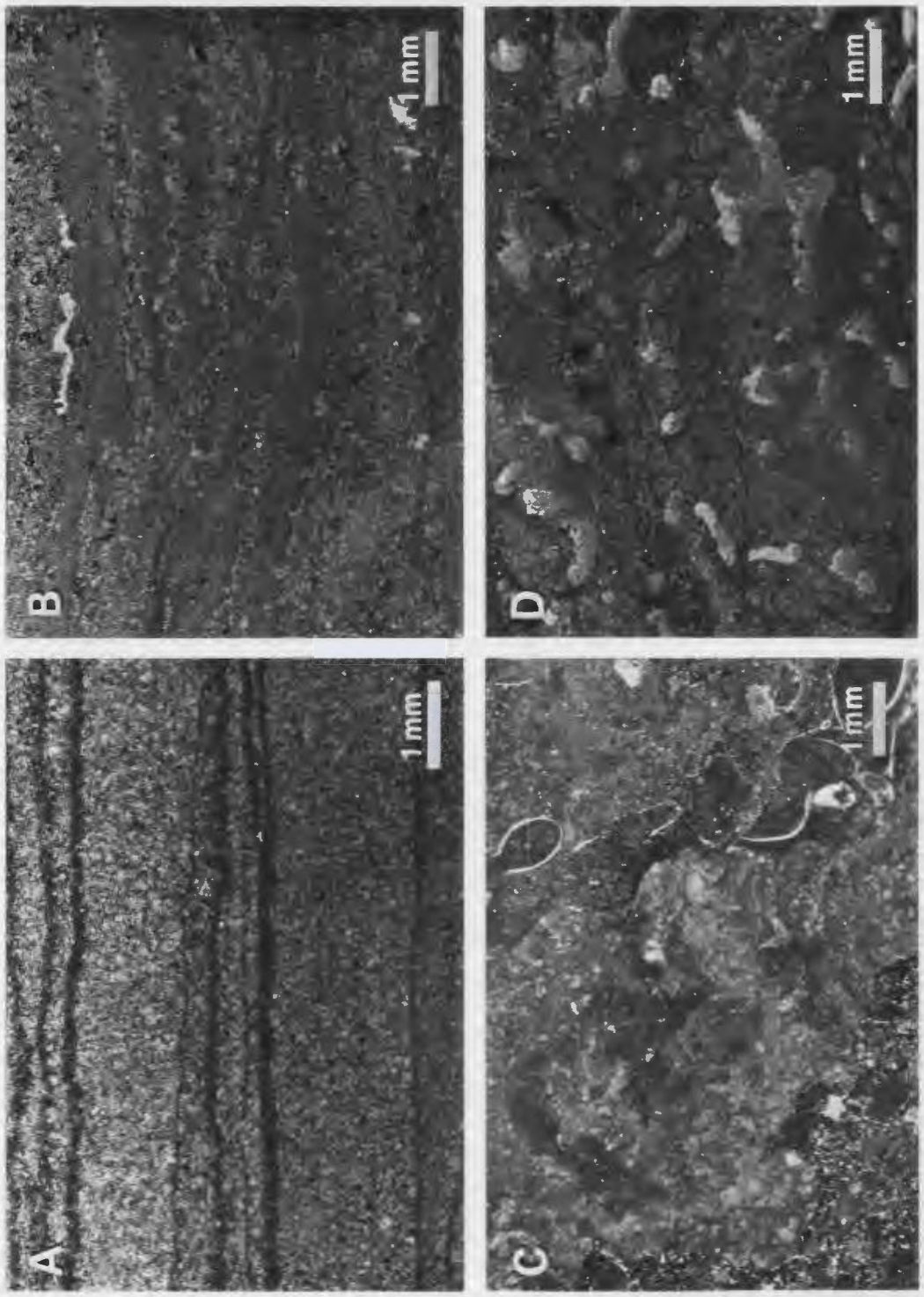

APPENDIX A

SYMBOLS USED ON SCHEMATIC RECONSTRUCTIONS

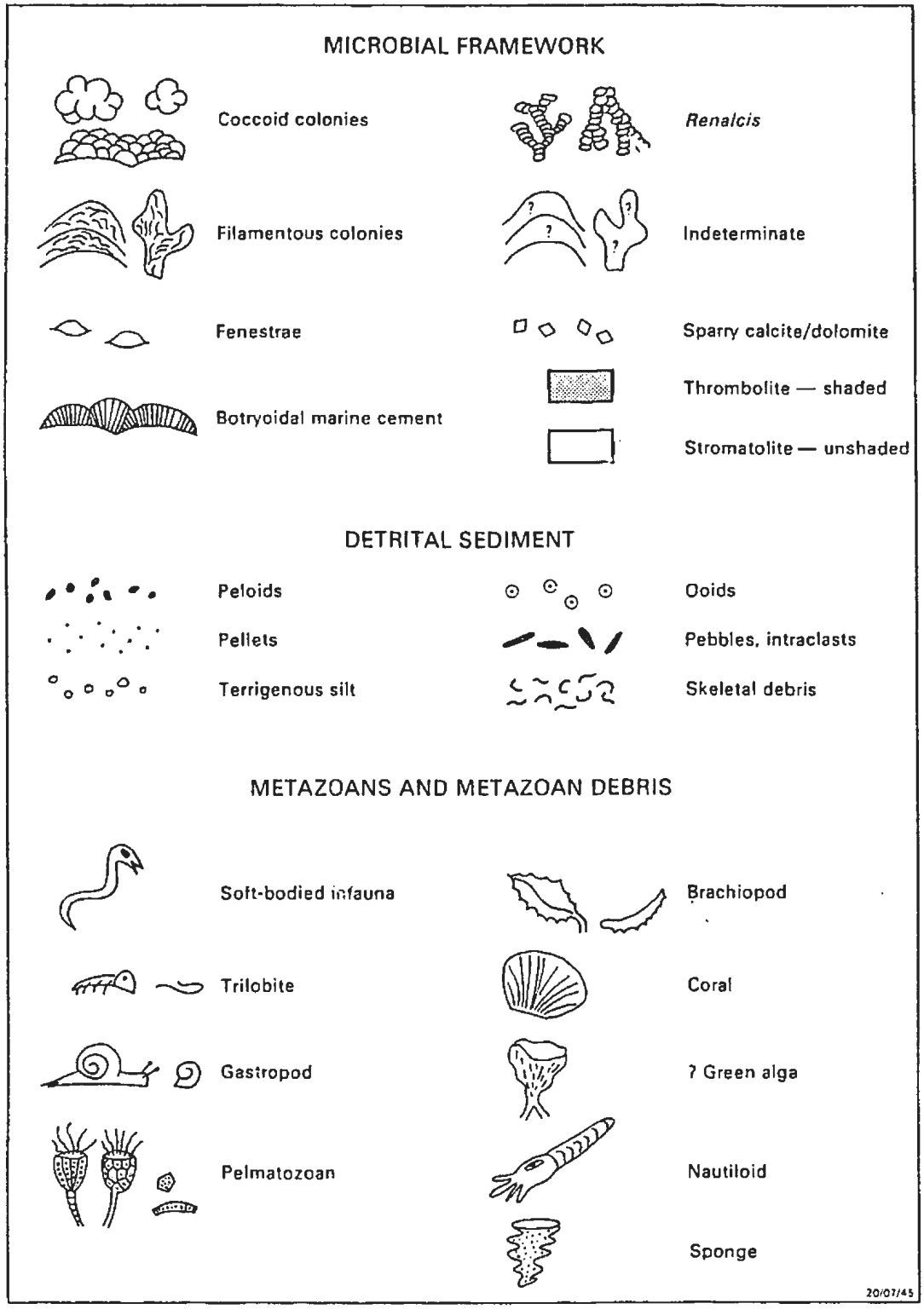

APPENDIX B

CLASSIFICATION, STRUCTURE, VOLUMETRIC COMPOSITION AND INTERPRETED ORIGIN OF ANALYSED SAMPLES

LEGEND FOR COLUMNS IN FOLLOWING TABLES

1 Zone — Zone of horizon

2 Sample — Sample number

3 Classification

T-thrombolite — ST-stromatolitic thrombolite
S-stromatolite — TS-thrombolitic stromatolite
Crypt-cryptomicrobial boundstone
Cmt-marine cement — Pbl-pebble aggregate
Cr-coral — R-*Renalcis*
Sp-sponge — Bnd-boundstone

4 Megastructure

Bh-bioherm — Bs-biostrome
T-tabular — D-domed — M-mounded
P-pedestal — C-club — Egg-egg shape
S-spherical — E-ellipsoidal — Ds-discoidal
Tng-tonguing — Br-bridging

5 Volume — Volume percent thromboids

6 Geometry — Geometry of thromboids

R-rounded — L-lobate — S-saccate
G-grape like — Am-amoeboid — D-digitate
Ar-arborescent — Pr-prostrate — Pn-pendant
Crb-cerebroid — Arc-arcuate

7 Microstructure of Thromboids

1 Calcified "microfossils"
1a-*Renalcis* 1b-*Girvanella* 1c-*Epiphyton*
1d-*Nuia* 1e-Calcispheres
2 Lobate microstructure
2a-saccate 2b-cellular 2c-spherulitic
2d-massive
3 Grumous microstructure
3a-*structure grumeleuse*
4 Peloidal microstructure
4a-silty 4b-oolitic 4c-bioclastic
5 Vermiform microstructure
6 Filamentous microstructure
7 Spongeous microstructure
8 Tubiform microstructure
9 Mottled microstructure
10 Massive microstructure
/ denotes compound microstructure
- denotes gradational microstructure

8 Coccoid	coccoid microbes	# dominant
9 Filamentous	filamentous microbes	+ minor
10 Calcification	inorganic calcification	- absent
11 Trapping	sediment trapping	\ indeterminant

12 Volume — Volume percent stromatoids

13 Geometry — Geometry of stromatoids
C-columnar C/L-columnar layered
Cn-conical H-hemispherical
W-wavy Pst-pustular
Cr-crenulate U-undulose
P-planar Cps-pseudocolumnar
Cp-cup like

14 Microstructure of Stromatoids
11 Laminated
11a-film 11b-banded 11c-streaky
11d-striated 11e-tussock
/ denotes compound
- denotes gradational
other codes as for microstructure of thromboids

15 Coccoid	coccoid microbes	# dominant
16 Filamentous	filamentous microbes	+ minor
17 Calcification	inorganic calcification	- absent
18 Trapping	sediment trapping	\ indeterminant

19 Volume — Volume percent cryptic fabrics

20 Microstructure of cryptic fabrics
codes as for thromboids and stromatoids

21 Marine cement — Volume percent frame-building marine cement

22 Pebbles — Volume percent frame-building pebbles

23 Skeletal — Volume percent frame-building metazoans and calcareous algae
Cr-coral R-*Renalcis* Sp-sponge

24 Volume — Volume percent inter-framework sediment

25 Texture — Texture of inter-framework sediment
G-grainstone P-packstone
W-wackestone M-mudstone

26 Peloids/ooids/clasts
27 Bioclasts
28 Terrigenous
29 Spar cement
30 Dolomite
31 Stylolites
32 Bioturbation

A-abundant
C-common
M-minor
R-rare

Zone	Sample	Classification	Megastructure	FRAMEWORK COMPONENTS: THROMBOIDS: Volume	Geometry	Microstructure	Coccoid Filamentous Calcification Trapping	FRAMEWORK COMPONENTS: STROMATOIDS: Volume	Geometry	Microstructure	Coccoid Filamentous Calcification Trapping	FRAMEWORK COMPONENTS: CRYPTIC: Volume	Microstructure	Marine cement	Pebbles	Skeletal	INTER-FRAMEWORK: Volume	Texture	Peloids/ooids/clasts Bioclasts Terrigenous	DIAGENETIC: Spar cement Dolomite Stylolites	Bioturbation
WESTERN NEWFOUNDLAND, PORT AU PORT PENINSULA																						
HORIZON A: CAPE ANN MEMBER, PETIT JARDIN FORMATION																						
D2	CA-17	S	TBs	-				90	CH	11c\3-10	\ \ \ \	-		-	-	-	10	W	C - -	M - C	C
D1	CA-16	ST	TBs	35	DArb	2ad,3	# - # -	30	CU	11c\3-9	- ? - #	-		R	5	-	30	WP	A M C	R M M	A
3	CA-15	CmtS	Bs	-				70	W	11c\4a	- ? - #	-		15	-	-	15	P	A A A	M - M	-
3	CA-13	S	DBs	-				10	W	11c\4,10	- ? - #	-		-	-	-	90	G	A M M	R R C	M
3	CA-12	TS	DBs	10	L	2ad	# - # -	90	W	11c\9,3,4a,6	- # # #	-		-	-	-	-	-	- - -	C M A	M
2	CA-2	TS	BrBs	15	LSG	2a	# - # -	20	CP	11c-d\3	\ \ \ +	-		5	-	-	60	W	C M M	R A A	C
2	CA-1B	TS	BrBs	15	LSG	2ab	# - # -	35	CHP	11c	\ \ \ +	-		5	-	-	45	W	C R M	M A C	C
2	CA-1A	ST	BrBs	25	LSG	2a	# - # -	20	CHP	11c	\ \ \ +	-		5	-	-	50	W	C R M	M A A	M
1	CA-3	CmtS	EBh	-				5\40	Cps	11c\4a	\ \ \ +	-		40\25	-	-	20	M	- - M	- - C	M
1	CA-10A	Cmt	EBh	-				-						70	-	-	30	W	M - C	M M C	C
1	CA-10B	CmtT	EBh	35	L	10	\ \ \ \	-				-		25	-	-	40	W	M - C	M M C	C
1	CA-11	CmtT	PBh	45	LPnG	10	\ \ \ \	5	H	11c	\ \ \ \	-		30	-	-	20	M	- - M	R M C	-
1	CA-6	CmtT	SBh	35	LPnG	2	# - # -	10	H	11c\4a	\ \ - #	-		20	-	-	35	M	- - R	R M C	-
C	CA-8,9	T	T-EBh	40	AmDPrPn	3-11c\9,2	# + # -	10	C	11c	\ \ \ \	-		-	-	-	50	WP	A A C	R C A	A
C	CA-4	T	TBs,SBh	50	AmDPrPn	3-11c\9,2	# + # -	-				-		-	-	-	50	WP	A A C	R A C	A
B3	CA-5C	T	TBh	-				95	H	11c\4a	- ? - #	-		-	5	-	-	-	- - -	- C C	-
B2	CA-5B	PblS	TBh	-				35	CCps	11c\4a	- ? - #	-		-	30	-	35	WG	C C A	C C C	-
B1	CA-5A	Pbl	TBh	-				-							60	-	40	WG	C C A	C C C	-
A	CA-7	TS	DBh	10	LS	2	# - # -	30	C	10,11c\9-3	# - # -	-		R	-	-	60	W	M R R	M M -	C
HORIZON B: CAMPBELLS MEMBER, PETIT JARDIN FORMATION																						
2	CMB-1AB	T	MBs-SBh	40	DLS	10-11c,2a,3	+ - # -	-				-		-	-	-	60	WP	C A C	C M A	A
1	CMB-2	T	TBs	45	AmL	6-3,2c,10,9	# # # -	R		11c\10-3	\ \ ? #	-		-	-	-	55	M	M R M	C M C	A

Zone	Sample	Classification	Megastructure	FRAMEWORK COMPONENTS: THROMBOIDS: Volume	Geometry	Microstructure	Coccoid Filamentous Calcification Trapping	STROMATOIDS: Volume	Geometry	Microstructure	Coccoid Filamentous Calcification Trapping	CRYPTIC: Volume	Microstructure	Marine cement	Pebbles	Skeletal	INTER-FRAMEWORK: Volume	Texture	Peloids/ooids/clasts Bioclasts Terrigenous	DIAGENETIC: Spar cement Dolomite Stylolites	Bioturbation
HORIZON C: CAMPBELLS MEMBER, PETIT JARDIN FORMATION																					
B7	CMB-6D	CmtS	DBh	-				90	PCr	11b\3,4b-c	# # # #	-		10	-	-	-	-	- - -	- C	- -
B6	CMB-6C	CmtS	DBh	R				90	CPst	11b\3,4b-c	# # # #	-		10	-	-	-	-	- - -	- C	- -
B5	CMB-6B	CmtS	DBh	-				70	H	11b\3,4b-c	# # # #	-		5	-	-	25	P	A - -	M M M	-
B4	CMB-6A	TS	DBh	5	L	2d	# - # -	15	C	11c\3,2d	# - # -	-		R	-	-	80	P	C A C	M C C	M
B3	CMB-5C	CmtS	DBh	-				90	CpsC/L	11b\10,4a,3	? # ? #	-		5	-	-	5	G	A - A	M A C	-
B2	CMB-5A	Crypt	DBh	5	L	10	\ \ \ \	-				45	10	-	-	-	50	P	M A M	M A A	C
B1	CMB-5B	DspT	DBh	30	LArb	10	\ \ \ \	-				35	10	-	-	-	35	W	M C M	M A A	A
A2	CMB-4B	S	BDh	-				50	C	11c\4a,3	\ \ # #	-		-	-	-	50	P	C A M	C M C	A
A1	CMB-4A	T	DBh	65	LG	2a-b	# - # -	-				-		-	-	-	35	P	C A M	C M C	A
HORIZON D: CAMPBELLS MEMBER, PETIT JARDIN FORMATION																					
C	CMB CK-1	T	DBh	65	PrD	9-3,2c,(6)	# + # #	-				-		R	-	-	45	MW	C C M	C M A	A
B	CMB CK-5	TS	DBh,TBs	10	L	1a	# - # -	40	CP	11c-d\3,4a,9,1a	\ \ - +	-		-	-	-	50	PG	A C C	C - M	C
B	CMB CK-6	S	DBs	R	LArb	1a	# - # -	45	CP	11c-d\3,4a,9,1a	\ \ - +	-		R	-	-	55	WP	C A C	C R M	C
A	CMB CK-4	TS	EBh	20	LArbG	1a,1b	# # # -	50	CP	11c-d\3,4a,9,1ab	\ \ - +	-		R	-	-	30	WP	C C C	M - M	C
HORIZON E: BIG COVE MEMBER, PETIT JARDIN FORMATION																					
3	BCB-1B	T	DBs	50	Am	3,1b	- # # -	-				-		-	-	-	50	W	C C C	M M A	A
2	BCB-1A	PblT	DBs	25	D	9,1b,(6)	\ + # -	-				-		-	-	-	70	WP	A A M	C M C	C
1	BCB-1	Pbl	DBs	-				-				-		-	-	-	60	WP	A A M	C M C	-
HORIZON F: FELIX MEMBER, PETIT JARDIN FORMATION																					
	FLX-1	S	DBh	-				55	C	10	\ \ \ \	-		-	-	-	45	M	M R C	- M -	R

Zone	Sample	Classification	Megastructure	FRAMEWORK COMPONENTS: THROMBOIDS: Volume	Geometry	Microstructure	Coccoid Filamentous Calcification Trapping	FRAMEWORK COMPONENTS: STROMATOIDS: Volume	Geometry	Microstructure	Coccoid Filamentous Calcification Trapping	FRAMEWORK COMPONENTS: CRYPTIC: Volume	Microstructure	Marine cement	Pebbles	Skeletal	INTER-FRAMEWORK: Volume	Texture	Peloids/ooids/clasts	Bioclasts	Terrigenous	DIAGENETIC: Spar cement	Dolomite	Stylolites	Bioturbation
HORIZON G: FELIX MEMBER, PETIT JARDIN FORMATION																									
2	MOW-2	Crypt	DBs	-				-				100	10	-	-	-	-	-	-	-	-	-	-	A	M	-
1	MOW-1	Crypt	DBh	-				-				100	10	-	-	-	-	-	-	-	-	-	-	A	M	-
HORIZON H: MAN O' WAR MEMBER, PETIT JARDIN FORMATION																									
3	MOW-23	T	TBh	45	AmD	7\3	\ \ \ \	-				-		-	-	-	55	W	A	A	R	C	C	A	C
2	MOW-24,25	PblT	TBh	25	AmD	3,10,1a	# - # +	-				-		R	20	-	55	P	A	A	M	C	M	A	A
1	MOW-P	Pbl	TBh	-								-		-	50	-	50	P	A	A	M	C	M	-	-
HORIZON I: MAN O' WAR MEMBER, PETIT JARDIN FORMATION																									
B3	MOW-18	S	EBh	-				100	U	11	\ \ \ \	-		-	-	-	-	-	\	\	\	\	\	\	\
B2	MOW-17,19	S	EBh	-				95	PstCps	11c\3,10,2,4	# # # #	-		-	-	-	5	W	C	-	R	M	-	M	M
B1	MOW-27	S	EBh	-				50	C	11c\3,10,2b	# + # -	-		-	-	-	50	W	A	A	M	M	A	M	A
B1	MOW-16	S	EBh	-				50	C	11c\3,5,10,2ab	# + # -	-		-	-	-	50	W	M	A	M	M	C	M	A
A	MOW-21	S	TBh	-				50	C	11c\3,10,2ab	# + # -	-		-	-	-	50	W	C	-	R	M	M	A	C
HORIZON J: MAN O' WAR MEMBER, PETIT JARDIN FORMATION																									
B4	MOW-11	S	D-SBh	-				100	H	11b\7,3-6,10	- # # -	-		-	-	-	-	-	-	-	-	C	-	M	M
B3	MOW-10	T	TBs	40	L	2c	# - # -	-				-		-	-	-	60	G	A	C	C	C	C	C	-
B2	MOW-8,9	S	CbH	-				45	C	11c-d\3,4a	- # # #	-		-	-	-	55	WP	A	M	M	C	A	M	A
B1	MOW-6	T	DBh	70	AmD	2c,3-11c	# - # +	-				-		-	-	-	30	M	-	-	M	M	M	M	M
A2	MOW-13	S	DBh	-				90	CpsC	11c-d\4a,8	# + # #	-		-	-	-	10	WP	A	R	C	M	M	M	C
A1	MOW-12	T	TBs	45	DAm	2c,3-6,5,10 4,1d	# # # +	-				-		-	-	-	55	WP	C	R	R	M	A	M	A

Zone	Sample	Classification	Megastructure	FRAMEWORK COMPONENTS: THROMBOIDS: Volume	Geometry	Microstructure	Coccoid Filamentous Calcification Trapping	STROMATOIDS: Volume	Geometry	Microstructure	Coccoid Filamentous Calcification Trapping	CRYPTIC: Volume	Microstructure	Marine cement	Pebbles	Skeletal	INTER-FRAMEWORK: Volume	Texture	Peloids/ooids/clasts Bioclasts Terrigenous	DIAGENETIC: Spar cement	Dolomite Stylolites	Bioturbation
HORIZON K: BERRY HEAD FORMATION																						
2	BEH-3	S	TBs	-				100	PU	11b\10,3a	- # - #	-		-	-	-	-	-	- - -	-	- C	-
1	BEH-1,2	S	TBs	-				50	C	11c\5,10	- # # +	-		-	-	-	50	PG	A C -	C	- A	A
HORIZON L: WATTS BIGHT FORMATION (GREEN HEAD COMPLEX)																						
5	GH-E-2	T	TBs	40	LGPn	7,1a,2	# - # -	-				-		-	-	-	60	W	C A -	M	A C	C
5	GH-E-1	T	TBs	50	LSG	1a,2,7	# - # -	-				-		-	-	-	50	WP	A A -	M	A C	A
3	GH-C-2	CrR-T	TngBh	40	LGPn	3,7,2,1a	# - # -	-				-		-	-	Cr20	40	W	M M -	-	C M	C
3	GH-C-1C	CrR-T	TngBh	10	LGPn	2,3,1a	# - # -	-				-		-	-	Cr50	40	M	R - -	M	C M	C
3	GH-C-1D	CrR-T	TngBh	30	LGPn	3,1a,7,2	# - # -	-				-		-	-	Cr30	40	M	R R -	M	C M	C
3	GH-C-1A,B	T	TngBh	60	LGPn	2,3,7,1a	# - # -	-				-		-	-	-	40	W	M M -	M	C M	C
2	GH-B	T	TBh	45	D	7,3-10	\ \ ? -	-				-		-	-	-	55	WP	A C -	-	A A	C
1	GH-A-2,3	R-T	TBs	60	LArbAm	1a,2,3,7	# - # -	-				-		-	-	?Cr	40	W	C M -	M	C M	C
1	GH-A-1	R-T	TBs	50	LArbAm	1a,2da,3,7	# - # -	R				-		-	-	?Cr	50	PG	A A -	M	- M	C
HORIZON M: WATTS BIGHT FORMATION																						
C	WB-5	S	DBh	-				40	C	11c\7,3a,2b,5,1e	+ # - #	-		-	-	-	60	P	A R -	C	A -	C
B4	WB-A	Crypt	D-DsBh	-				-				40	10	-	-	-	60	G	A - -	M	A M	M
B3	WB-C,D,E	Crypt	D-DsBh	-				-				50	10,9,3	-	-	-	50	P	A M -	C	A C	A
B2	WB-3B,F	?Sp-S	D-DsBh	-				20	CnCp	11b-d\4,10	- # - #	-		-	-	?Sp20	60	P	A M -	A	A C	C
B1	WB-3A	PblS	D-DsBh	-				40	P	11d\4,10	# - # -	-		-	20	-	30	P	A M -	M	- -	-
A1	WB-1	DspS	DBh	-				30	CH	11c\7,3a	? - ? #	10\40	10	-	-	-	60	W	C C -	M	A A	A

Zone	Sample	Classification	Megastructure	FRAMEWORK COMPONENTS: THROMBOIDS: Volume	Geometry	Microstructure	Coccoid Filamentous Calcification Trapping	STROMATOIDS: Volume	Geometry	Microstructure	Coccoid Filamentous Calcification Trapping	CRYPTIC: Volume	Microstructure	Marine cement	Pebbles	Skeletal	INTER-FRAMEWORK: Volume	Texture	Peloids/ooids/clasts Bioclasts Terrigenous	DIAGENETIC: Spar cement Dolomite Stylolites	Bioturbation
HORIZON N: BOAT HARBOUR FORMATION																					
B2	BH-10	T	S-EBh	50	ArbD	2c,1a,3a,4,8,5	# # # #	-				-		-	-	-	50	WP	A A -	A - C	A
B1	BH-9	S	TBs	-				90	UWH	11c\5,4,10	- # - #	-		-	-	-	10	G	A - -	- - A	-
A	BH-7	S	D-Ds8h	-				70	CpsCH	11c\5,4,10	- # - #	10	10	-	S	-	15	M	- - -	M - C	A
A	BH-8	T	D-Ds8h	50	RL	10,3,2a,5,4	# # # #	-				50	10	-	-	-	-	-	- - -	- - -	-
HORIZON O: BOAT HARBOUR FORMATION																					
	BH-12	T	C-DBh	50	PrPn	2c,3a-4	# ? # #	-				-		-	-	-	50	WG	A M -	C M C	A
HORIZON P: BOAT HARBOUR FORMATION																					
	H-13	Cr-Crypt ?Sp	DBh\MBs	10°Am		7,3a,10	\ \ \ \	-				25°10		-	-	Cr15	50°WP	A A - ?Sp	M C M	A	
HORIZON Q: BOAT HARBOUR FORMATION																					
C	BH-31	DspT	D-CBh	30°Am	D	2c,3-4,1e,(5,5)	# + # #	-				30°10		-	-	-	40°PG	A A R	C M M	A	
A	BH-14	DspT	DBh,DBs	30°Am	D	3a,2c,1e	# + # #	-				20°10		-	-	-	50°WP	A A M	M R C	A	
HORIZON R: CATOCHE FORMATION																					
	CAT-1	T	T-DBs	45	RAm	1b,3,(1e)	- # # -	-				-		-	-	-	55	W	C A -	M - M	C

Zone	Sample	Classification	Megastructure	FRAMEWORK COMPONENTS: THROMBOIDS: Volume	Geometry	Microstructure	Coccoid Filamentous Calcification Trapping	STROMATOIDS: Volume	Geometry	Microstructure	Coccoid Filamentous Calcification Trapping	CRYPTIC: Volume	Microstructure	Marine cement	Pebbles	Skeletal	INTER-FRAMEWORK: Volume	Texture	Pelojds/ooids/clasts	Bioclasts	Terrigenous	DIAGENETIC: Spar cement	Dolomite	Stylolites	Bioturbation
GREAT NORTHERN PENINSULA, WESTERN NEWFOUNDLAND																									
PETIT JARDIN FORMATION, FLOWERS COVE																									
FC-1,5	Crypt	OsBh-TBs	-				-				45	10	-	-	-	55	W	M	R	R	M	A	C	?
BOAT HARBOUR FORMATION, EDDIES COVE WEST - A																									
5	BH-24	T	DBh	50	DLS	2c,3a,7,5	# # # #	-				-		-	-	-	50	W	C	A	-	M	-	M	A
4	BH-19	T	DBh	75	Am	4,5,7	- # - #	-				-		-	-	-	25	W	A	A	-	M	-	A	A
3	BH-18	S	DBh	-				75	C	11c\4,5,7,1e	- # - #	-		-	-	-	25	W	C	C	-	M	-	-	C
2	BH-22,23	S	DBh	-				50	C	11c\4,7,1e	- # - #	-		-	-	-	50	P	A	A	-	M	-	C	C
BOAT HARBOUR FORMATION, EDDIES COVE WEST - B																									
3	BH-27	T	MBS	70	PrPnD	9,4\5,,2c,3a	+ # + #	-				-		-	-	-	30	W	C	M	-	-	M	C	A
3	BH-26	Cr-ST	MBs	50	Crb	2d,3a,7	# ? # #	20	CHP	11c\4,10,5	- # - #	-		-	-	Cr10	20	M	R	R	-	M	-	M	A
2	BH-25	Cr-R-TS	MBs	25	Crb	1a,3a,7	# ? # #	40	CnC	11c\3a,5,7	- # - #	-		-	-	Cr10	25	W	M	M	-	A	C	C	C

Zone	Sample	Classification	Megastructure	FRAMEWORK COMPONENTS: THROMBOIDS: Volume	Geometry	Microstructure	Coccoid Filamentous Calcification Trapping	STROMATOIDS: Volume	Geometry	Microstructure	Coccoid Filamentous Calcification Trapping	CRYPTIC: Volume	Microstructure	Marine cement	Pebbles	Skeletal	INTER-FRAMEWORK: Volume	Texture	Peloids/ooids/clasts Bioclasts Terrigenous	DIAGENETIC: Spar cement	Dolomite	Stylolites	Bioturbation
SOUTHERN CANADIAN ROCKY MOUNTAINS																							
SULLIVAN FORMATION, WINDY POINT, SASKATCHEWAN RIVER																							
	SUL-2	T	EBh	70	Am	3	? - # +	-				-		-	-	-	30	W	C C C	M M C	C
	SUL-1	T	EggBh	70	LAm	3	? - # +	-				-		-	-	-	30	W	? C C	M M C	C
SULLIVAN FORMATION, TOTEM CREEK, MT. MURCHISON																							
	SUL-4	T	DBh	60	AmD	10	\ \ \ \	-				-		-	-	-	40	W	- C -	- M M C			
	SUL-3	T	DBh	60	AmD	10,(9)	\ \ # -	-				-		-	-	-	40	W	- C -	- M M C			
WATERFOWL FORMATION, TOTEM CREEK, MT. MURCHISON																							
	WTF-3	T	DBh	35	ArbS	2dbc	# - # -	R				-		-	-	-	65	P	C C A	M M -	?		
	WTF-2	Crypt	DBh	-				-				100	7,10-3,(1b)	-	-	-	-	-	- - -	M C M	?		
	WTF-1	Crypt	DBh	-				-				100	7,4ac,2b	-	-	-	-	-	- - -	C C M	?		
EASTERN UNITED STATES OF AMERICA																							
CONOCOCHEAGUE FORMATION, INTERSECTION OF INTERSTATE HIGHWAYS 77/81																							
	CON-2	T	DBh	40	L	9,3,2d,4a	# # # +	-				-		-	-	-	60	P	A M C	M A A	A		
	CON-1	T	DBh	45	AmDL	9,3,2d,(8)	# - # -	-				-		-	-	-	55	P	A M C	M A A	A		
ELBROOK FORMATION, INTERSTATE HIGHWAY 81, CLAYFOR LAKE TURNOFF																							
	ELS-1,2	T	DBh	55	L	2c,7,3a	# - # -	-				-		-	-	-	45	WM	M - M	C C M	M		

Zone	Sample	Classification	Megastructure	FRAMEWORK COMPONENTS: THROMBOIDS: Volume	Geometry	Microstructure	Coccoid Filamentous Calcification Trapping	STROMATOIDS: Volume	Geometry	Microstructure	Coccoid Filamentous Calcification Trapping	CRYPTIC: Volume	Microstructure	Marine cement Pebbles Skeletal	INTER-FRAMEWORK: Volume	Texture	Peloids/ooids/clasts Bioclasts Terrigenous	DIAGENETIC: Spar cement Dolomite Stylolites Bioturbation
WESTERN UNITED STATES OF AMERICA. THE GREAT BASIN																		
WHEELER FORMATION, DRUM MOUNTAINS																		
6	NJ-113C1,D	RBnd	DBh	40	Arb	1a	# - # -	-				-		- - -	60	M	- R -	A R - -
5	NJ-113C	S	DBs	-				90	UCr	11c\10,3	\ \ # -	-		- - -	10	W	M R R	- - - -
4	NJ-113B	S	CBh	-				90	U	11c\10,9,8	? - # -	-		- - -	10	W	C R -	C A - C
4	WHL-4	S	CBh	-				70	C/L	11c\10,9,8	? - # -	-		- - -	30	W	C R -	C C - C
3	RR-79-33	E-S	TBs	20	Arb	1c	# - # -	60	H	11\10,3,9	\ \ \ \	-		?30 - -	20	W	M M R	M - - M
3	WHL-2	R-E-Bnd	TBs	60	LArb	1ac	# - # -	R	H	11\10	\ \ \ \	-		? - -	40	M	- - -	A - - -
2	NJ-113A	R-S	DBh	25	Arb	1a	# - # -	50	UCps	11c\10,3,1a	# - # -	-		- - -	25	M	M - R	A M - -
2	RR-79-30	R-Bnd	DBh	40	Arb	1a	# - # -	10	PCps	11c	? - # -	-		- - -	50	M	M M R	A M M -
2	WHL-1	S-R-E-Bnd	DBh	35	Arb	1ac	# - # -	25	Cps	11C\10,3,(1ac)	? - # -	-		- - -	40	M	- R -	A - M -
ORR FORMATION, HOUSE RANGE																		
HORIZON 1: BIG HORSE LIMESTONE MEMBER, LOWER																		
	COB-3	E-Bnd	DBh	30	LSPn	10,3,1c	# - # -	-				-		- - -	70	P	A C C	M M C A
	COB-2	S	DBh	-				30	C	11C\10,9	\ \ ? \	-		- - -	70	P	A C C	C C M C
	COB-1	E-Bnd	DBh	35	LPrPn	10,3,1c	# + # -	-				-		- - -	65	PM	A A A	C - C A
HORIZON 2: BIG HORSE LIMESTONE MEMBER, UPPER																		
3	COB-9	E-Bnd	DBh	50	LArb	1c,3,10	# - # -	-				-		- - -	50	P	A M -	M - - -
2	COB-7B	S	PBh	-				85	C	11c\ 7\3,(5)	\ + # \	-		- - -	15	G	A C ?	M A - C
1B	COB-8	E-Bnd	PBh	45	ArbPn	1c,3,10,	# - # -	-				-		- - -	55	M	- R -	C - M C
1B	COB-7A	E-Bnd	PBh	40	LPn	1c,3	# - # -	-				-		- - -	60	M	- - -	C - - C
1A	COB-6	T	DBh	40	PrAmL	9,8,3,10,(6)	# + # -	-				-		- - -	60	MP	C M -	C C C A
HORIZON 3: CANDLAND SHALE MEMBER, LOWER																		
	COB-10	T	TBs	45	LArb	2ad,3	# - # -	-				-		- - -	55	P	- A R	C - - C
HORIZON 4: CANDLAND SHALE MEMBER, UPPER																		
	COC-1	G-E-Bnd	DBh	35	ArcPn	1bc	# # - -	-				-		- - -	65	M	- - -	A - C -

Zone	Sample	Classification	Megastructure	FRAMEWORK COMPONENTS												INTER-FRAMEWORK				DIAGENETIC			
				THROMBOIDS				STROMATOIDS				CRYPTIC											
				Volume	Geometry	Microstructure	Coccoid Filamentous Calcification Trapping	Volume	Geometry	Microstructure	Coccoid Filamentous Calcification Trapping	Volume	Microstructure	Marine cement	Pebbles	Skeletal	Volume	Texture	Peloids/ooids/clasts Bioclasts Terrigenous		Spar cement Dolomite Stylolites	Bioturbation		
AMADEUS BASIN, CENTRAL AUSTRALIA																							
SHANNON FORMATION																							
	A-1	S	MBs	-				100	W	11b\10	- ? \ \	-		-	-	-	-	-	- - - -		-	A	C	-
	A-2	S	TBs	-				100	W	11b\10	- ? \ \	-		-	-	-	-	-	- - - -		-	A	M	-
	A-4	S	TBs	-				100	W	11b\10	- ? - ?	-		-	-	-	-	-	- - - -		-	A	-	-
	A-5	S	TBs	-				100	U	11c	? - ? -	-		-	-	-	-	-	- - - -		C	A	-	-
	A-11	T	CBh	45	LSArb	2acd,10	# - # -	-				-		-	-	-	55	GP	C R M		A	M	C	C
	A-12	T	CBh	35	ArbLS	2cd,3,10	# - # -	-				-		-	-	-	65	G	A M R		M	C	C	C
	A-13	S	DBh	-				45	C	11c\5	- * ? -	-		-	-	-	55	G	A - -		M	M	M	-
	A-16	T(2)	DBh	40	AmS	2d	# - # #	-				-		-	-	-	60	PW	C C M		C	C	C	C
	A-19	T	EBh	40	AmPrS	2d	# - # -	-				-		-	-	-	60	GP	A M C		M	C	A	C
	A-21	T(2)	DBh	40	AmL	2cd,10	# - # #	-				-		-	-	-	60	W	C M C		C	C	C	C
	A-22	S	TBh	-				100	W	11b\10	- ? \ \	-		-	-	-	-	-	- - - -		R	-	C	-
	A-24	Crypt	EBh	-				-				100	9,11c.5,3.2	-			?	GPW	C C C		C	R	C	A
	A-25	S	DBh	-				50	C	11c\5.(3)	- # ? +	-		-	-	-	50	P	A - -		R	C	M	M
	A-26	S	DBh	-				100	W	11b\10	- ? \ \	-		-	-	-	-	-	- - - -		-	A	M	-
	A-27	S	TBs	-				100	P	11b\10	- # - #	-		-	-	-	-	-	- - - -		-	-	M	-
	CS-1	T	CBh	40	PrLS	2d,10	# - # -	-				-		-	-	-	60	G	C C C		C	C	C	C
	CS-2	T	CBh	35	LD	2ac,4	# ? # #	-				-		-	-	-	65	G	A M M		C	M	C	M

Zone	Sample	Classification	Megastructure	FRAMEWORK COMPONENTS: THROMBOIDS: Volume	Geometry	Microstructure	Coccoid Filamentous Calcification Trapping	STROMATOIDS: Volume	Geometry	Microstructure	Coccoid Filamentous Calcification Trapping	CRYPTIC: Volume	Microstructure	Marine cement	Pebbles	Skeletal	INTER-FRAMEWORK: Volume	Texture	Peloids/ooids/clasts Bioclasts Terrigenous	DIAGENETIC: Spar cement Dolomite Stylolites	Bioturbation
SHANNON FORMATION (ctd)																				
	B-1	T	EBh	40	Arb	2cd,10	# - # +	-				-		-	-	-	60	G	A M M	C C C	C
	B-2	T(2)	DBh	40	AmL	2acd,10	# - # +	-				-		-	-	-	60	W	C C M	C C M	C
	B-4	S	TBs	-				100	W	11b\10	- ? \ \	-		-	-	-	-	-	- - -	- - M	-
	B-7	T	CBh	45	L	2acd,10	# - # +	-				-		-	-	-	55	G	A C C	C C M	C
	B-8	S	DBh	-				60	WC	11c\10,3	\ \ \ \	-		-	-	-	40	P	C M C	M C C	-
	B-9	T	DBh	40	D	2cd,10,9,3	# - # +	-				-		-	-	-	60	GP	C C -	R C -	C
	B-10	S	DBh	-				70	CW	11c\5	- # \ \	-		-	-	-	30	G	C - C	- A -	-
	B-12	S	Ds8h	-				80	CW	11c\5,3	- # \ \	-		-	-	-	20	G	A - -	M - M	-
	B-18	S	DBh	-				70	C	11c\10,5	- # \ +	-		-	-	-	30	G	A - C	- C C	-
	B-21B	S	DBs	-				100	W	11b\10	- ? \ \	-		-	-	-	-	-	- - -	- M C	-
	B-26	T	DBh	45	LAm	2d	# - # -	-				-		-	-	-	55	G	A M M	M A C	M
	B-28	T	DBh	45	PrAm	2acd,10	# - # -	-				-		-	-	-	55	P	A - C	M C C	C
	C-1	DspT	EBh	20	AmL	2cd	# - # -	-				20	11c	-	-	-	60	P	A R C	C M C	R
	C-3-1	DspT	DBh	20	AmD	2cd,10	# - # -	-				25	11c,5	-	-	-	55	PW	C C C	C M C	C
	C-3-2	S	DBh	-				50	C	11c5,4a,10	- # - #	-		-	-	-	50	G	A - C	A C C	-
	C-4	S	DBh	-				90	MW	11b\3	\ \ \ \	-		-	-	-	10	G	C - M	- A M	-
	D-3	DspS	DBh	-				30	M	11c\10,2cd	# + # +	10	11c\10,2cd	-			60	GP	C A -	M - C	M
	D-4	DspT	EBh	30	AmD	2d	# - # -	-				10	2d	-	-	-	60	G	C C C	M - C	M

APPENDIX C

CAMBRO-ORDOVICIAN THROMBOLITE-BEARING FORMATIONS

1 LOWER CAMBRIAN

FORMATION	LOCATION	REFERENCE
Peyto Lst Mbr (Gog Gp)	Alberta	Aitken & others (1972) Aitken (1981a)
Serie lie de vin	Anti-Atlas, Morocco	Schmitt & Monninger (1977) Schmitt (1979) Monninger (1979) Bertrand-Sarfati (1981)
Unnamed	Southern Spain	Zamarreno (1977)

2 MIDDLE CAMBRIAN

FORMATION	LOCATION	REFERENCE
Arctomys	Alberta	This study
Bonanza King	California	Kepper (1976)
March Point (Cape Anne Mbr)	Western Newfoundland	James & Stevens (1982) Chow (1986) This study
Carrara (Jangle Lst Mbr)	California	Personal observation (1984)
Elbrook	Virginia	Markello & Read (1982) Koerschner (1983) Read (1983)
Eldon	Alberta	Aitken (1978, 1981a) Aitken & others (1972)
Honaker	Virginia	Markello & Read (1982) Read (1983)
Karsha	Northern India	Garzanti & others (1986)
Mt White	Alberta	Aitken (1967, 1978, 1981a)
Shady (upper)	Virginia	Read & Pfeil (1983)
Stephen	Alberta	Aitken (1966, 1981a) Aitken & others (1972)
Teutonic	Utah	Pratt (1982a)
Wheeler	Utah	Robison & Rees (1981) Rees (unpublished)
Wirrealpa	South Australia	Young (1978)

3 UPPER CAMBRIAN

FORMATION	LOCATION	REFERENCE
Arrinthrunga	Central Australia	Kennard (1981)
Berry Head	Western Newfoundland	Chow (1986)
		This study
Bison Creek	Alberta	Aitken (1966b, 1967)
		Aitken & others (1972)
Bonneterre	Missouri	Howe (1966)
		Aitken (1967)
Cass Fjord	Ellesmere Island	Packard (1987a)
Conococheague	Maryland-Virginia	Bova & others (1982)
		Koerschner (1983)
		Demicco (1981, 1983, 1985)
		Demicco & Hardie (1981)
Copper Ridge	Virginia	Read (1983)
Derby-Doerun	Missouri	Howe (1966)
		Aitken (1967)
Eminence	Missouri	Howe (1966)
		Aitken (1967)
Hoyt	New York	Owen & Friedman (1984)
Jay Creek Lst	Central Australia	Mawson & Madigan (1930)
		This study
La Flecha	Argentina	Baldis & others (1984)
		Armella (1988a,1988b)
Lyell	Alberta	Aitken (1966, 1967, 1978)
		Aitken (1981a)
		Aitken & others (1972)
Lynx Gp	Alberta	Aitken (1967)
Mistaya	Alberta	Aitken (1967, 1981a)
Ninmaroo	Central Australia	Radke (1980, 1981)
Nolichuchy	Virginia	Markello (1979)
		Markello & Read (1981, 1982)
Nopah	Nevada	Cooper & others (1981)
Orr	Utah	Lohmann (1975, 1976, 1977)
Potosi	Missouri	Howe (1966)
		Aitken (1967)
Pilgram	Montana	Sepkoski (1982)
Petit Jardin	Western Newfoundland	Chow (1986)
		This study
Richland	Pennsylvania	Moshier (1986)
Shannon	Central Australia	Kennard (1986)
		This study
St Charles	Utah-Idaho	Taylor & others (1981)
		Taylor & Repetski (1985)
Sullivan	Alberta	Aitken (1966, 1967, 1978)
		Aitken (1981a)
		Aitken & others (1972)
Waterfowl	Alberta	Aitken (1967, 1981a)
		Aitken & others (1972)
Whitehall	New York	Rubin & Friedman (1977)
Wilberns	Texas	Ahr (1971)
		Chafetz (1973)
Unnamed	North China	Meng & others (1986)

4 LOWER ORDOVICIAN

FORMATION	LOCATION	REFERENCE
Aguathuna	Western Newfoundland	Pratt (1979) Pratt & James (1982, 1986) Knight & James (1987)
Boat Harbour (Isthmus Bay)	Western Newfoundland	Pratt (1979) Pratt & James (1982, 1986) Knight & James (1987)
Catoche	Western Newfoundland	Pratt (1979) Pratt & James (1982, 1986) Knight & James (1987) Stevens & James (1976)
Chepultepec	Virginia	Bova (1982) Bova & others (1982) Bova & Read (1987)
Christian Elv	Ellesmere Island	Packard (1987b)
Garden City	Utah-Idaho	Taylor & Repetski (1985)
Gasconade	Missouri	Howe (1966) Aitken (1967)
Great Meadows (Cutting)	New York	Fisher & Mazzullo (1976)
Jefferson City	Missouri	Howe (1966) Aitken (1967)
Romaine	Quebec	Desrochers (1984, 1986)
Roubidoux	Missouri	Howe (1966) Aitken (1967)
Sailmhor	Scotland	Wright (1984)
Survey Peak	Alberta	Aitken (1967, 1978, 1981a) Aitken & others (1972) Barnes (1984)
Watts Bight (Isthmus Bay)	Western Newfoundland	Pratt (1979) Pratt & James (1982, 1986) Knight & James (1987)

APPENDIX D

POST EARLY ORDOVICIAN THROMBOLITIC METAZOAN-ALGAL BUILDUPS

AGE	FORMATION	LOCATION	REFERENCE
Late Jurassic	Mullersfelsen	West Germany	Flügel & Steiger (1981)
Late Jurassic	Abenaki	Nova Scotian Shelf	Jansa & others (1983) Ellis & others (1985)
Early Permian	Laborcita	New Mexico	Toomey & Cys (1979) Toomey & Babcock (1983)
Pennsylvanian	Holder	New Mexico	Toomey & others (1977) Toomey & Babcock (1983)
Mississippian	Codroy Gp	Western Newfoundland	Dix (1982) Dix & James (1987)
Mississippian	Pitkin	Arkansas	Webb (1987)
Early Carboniferous	Red Hill Oolite	NW England	Adams (1984)
Late Silurian - Early Devonian	Holitna Gp	Alaska	Clough & Blodgett (1985)
Late Silurian	Petit Kocher	New Brunswick	Noble (1985)
Late Silurian	Glenbower	SE Australia	Feary (1986)
Late Silurian	West Point	Quebec	Bourque (1987)
Early Silurian	La Vieille	Quebec	Bourque & others (1987)
Early Silurian	Sayabec	Quebec	Bourque & others (1987)
Early Silurian - Late Ordovician	Red Head Rapids	Southampton Island, N.W.T.	Heywood & Sandford (1976) Dewing & Copper (1987)